

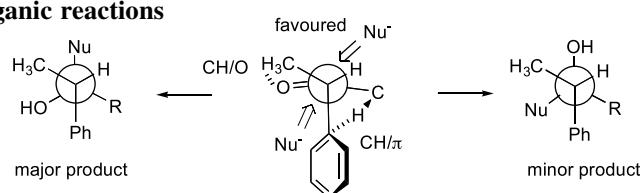
## Contents

## REPORT

**CH/π hydrogen bonds in organic reactions**

M. Nishio

pp 6923–6950



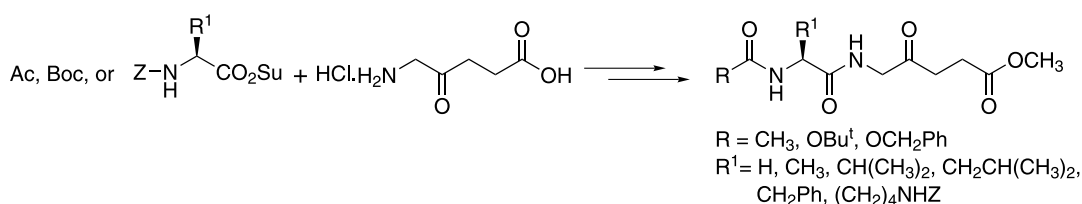
The origin of the stereoselectivity of organic reactions such as Diels–Alder reactions, topochemical photoreactions, diastereoface- and enantioface-discriminating reactions and enantioselective catalytic reactions with transition metal complexes has been explored in the context of the CH/π hydrogen bond. The ground-state conformation of the reacting molecules, where CH/π hydrogen bonds play the central role, has been suggested to be the most important factor in controlling the stereoselectivity of the reactions. The underlying concept of the Cram and the Prelog rule was critically examined and a hypothesis has been presented that the π-facial selectivity is understood in terms of the conformational preference of the substrates. The contribution from the CH/π and CH/O hydrogen bonds has been suggested to be indispensable.

## ARTICLES

**An efficient synthesis of 5-aminolaevulinic acid (ALA)-containing peptides for use in photodynamic therapy**

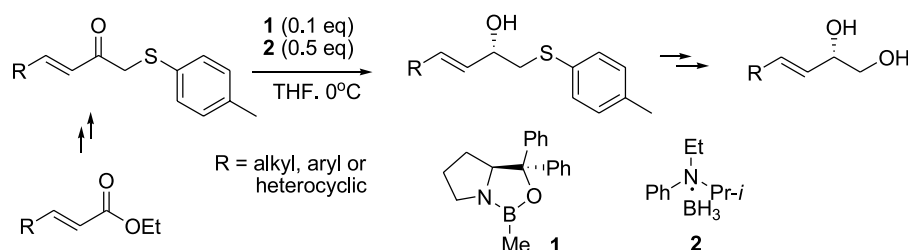
pp 6951–6958

Louis M.-A. Rogers, Philip G. McGivern, Anthony R. Butler, Alexander J. MacRobert and Ian M. Eggleston\*


**Highly enantioselective synthesis of multifunctionalized allylic building blocks via oxazaborolidine-catalyzed borane reduction**

pp 6959–6966

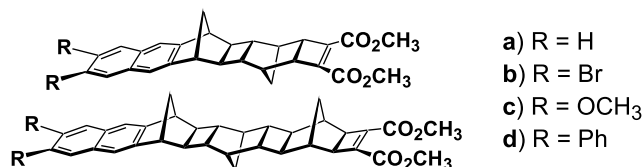
Byung Tae Cho\* and Sung Hye Shin



**Photoinduced electron transfer across linearly fused oligo-norbornyl structures**

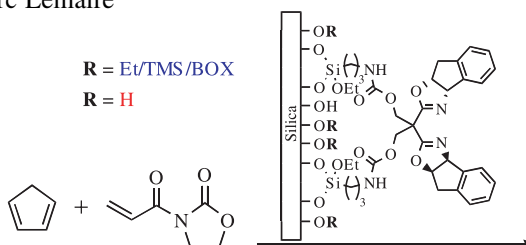
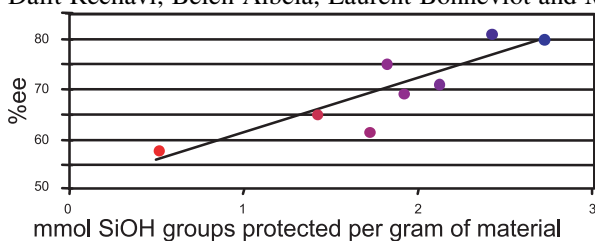
pp 6967–6975

Tahsin J. Chow,\* Yan-Ting Pan, Yu-Shan Yeh, Yuh-Sheng Wen, Kew-Yu Chen and Pi-Tai Chou

**Understanding the enantioselectivity of a heterogeneous catalyst: the influence of ligand loading and of silica passivation**

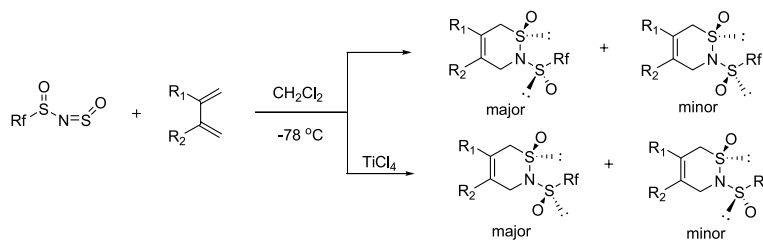
pp 6976–6981

Dalit Rechavi, Belén Albela, Laurent Bonneviot and Marc Lemaire\*

**Diastereoselectivity-switchable and regiospecific hetero Diels–Alder reaction of N-sulfinylper(poly)fluoroalkanesulfinamides with dienes**

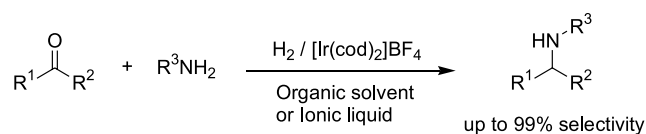
pp 6982–6987

Xiao-Jin Wang and Jin-Tao Liu\*

**Effective reductive amination of carbonyl compounds with hydrogen catalyzed by iridium complex in organic solvent and in ionic liquid**

pp 6988–6992

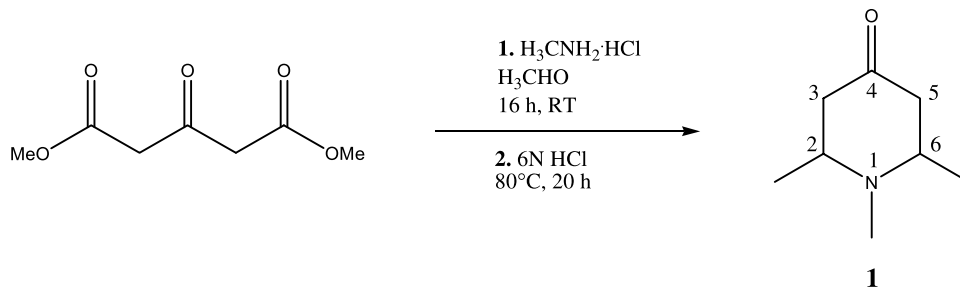
Daisuke Imao, Shoichiro Fujihara, Takeshi Yamamoto, Tetsuo Ohta\* and Yoshihiko Ito



**Studies on the stereochemistry of 1,2,6-trimethyl-4-piperidone**

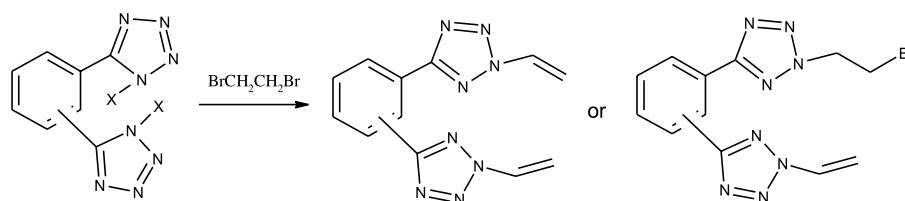
pp 6993–7001

Florian Diwischek, Mario Arnone, Bernd Engels\* and Ulrike Holzgrabe\*

**Reactions of bis(tetrazole)phenylenes. Surprising formation of vinyl compounds from alkyl halides**

pp 7002–7011

Adrienne Fleming, Fintan Kelleher, Mary F. Mahon, John McGinley\* and Vipra Prajapati

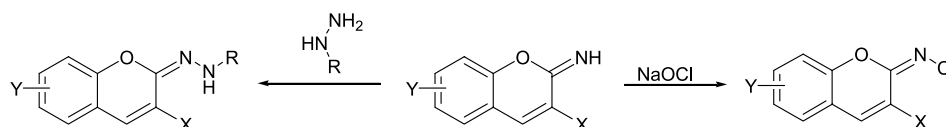


Reactions of either  $1,n\text{-(HN}_4\text{C)}_2\text{C}_6\text{H}_4$  or  $1,n\text{-(Bu}_3\text{SnN}_4\text{C)}_2\text{C}_6\text{H}_4$  ( $n=2, 3, 4$ ) with 1,2-dibromoethane yields compounds containing pendant bromoethyl or vinyl groups with substitution occurring at either 1- $N,2\text{-}N'$  or 2- $N,2\text{-}N'$ , respectively.

**Synthesis of new iminocoumarins and their transformations into *N*-chloro and hydrazono compounds**

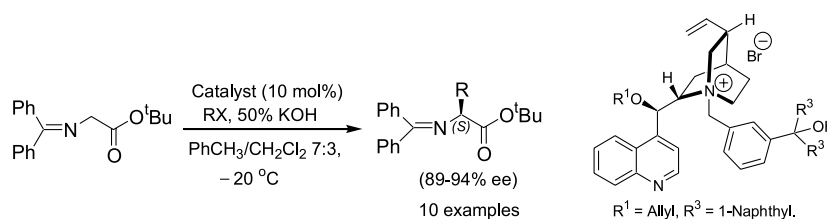
pp 7012–7021

Julija Volmajer, Renata Toplak, Ivan Leban and Alenka Majcen Le Marechal\*

**Cinchona alkaloid phase-transfer catalysts revisited: influence of substituted aryl groups on the enantioselectivity of glycine ester enolate alkylation**

pp 7022–7028

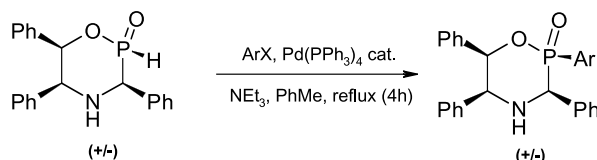
Sanjeev Kumar and Uma Ramachandran\*



**Pallado-catalysed *P*-arylations and *P*-vinylation of 2-hydrogeno-2-oxo-1,4,2-oxazaphosphinanes**

pp 7029–7036

Jean-Luc Pirat,\* Jérôme Monbrun, David Virieux and Henri-Jean Cristau\*



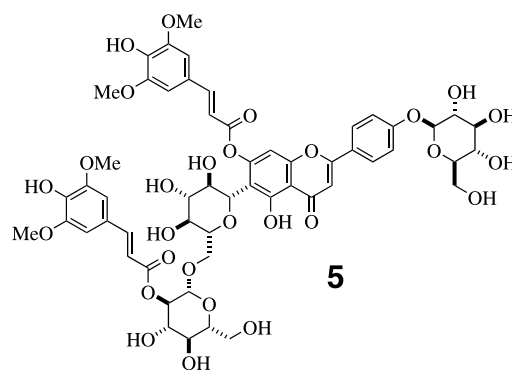
A simple and effective preparation of 2-aryl- (or 2-vinyl)-1,4,2-oxazaphosphinanes, phosphorus analogues of aryl-morpholinols has been developed, involving palladium catalysed coupling of aryl (or vinyl)-halides with 2-*H*-1,4,2-oxazaphosphinane in presence of triethylamine. A deprotection step was also proposed to afford the corresponding *P*-aryl- $\alpha$ -aminobenzylphosphinic acid.

**Five novel flavonoids from *Wasabia japonica***

pp 7037–7044

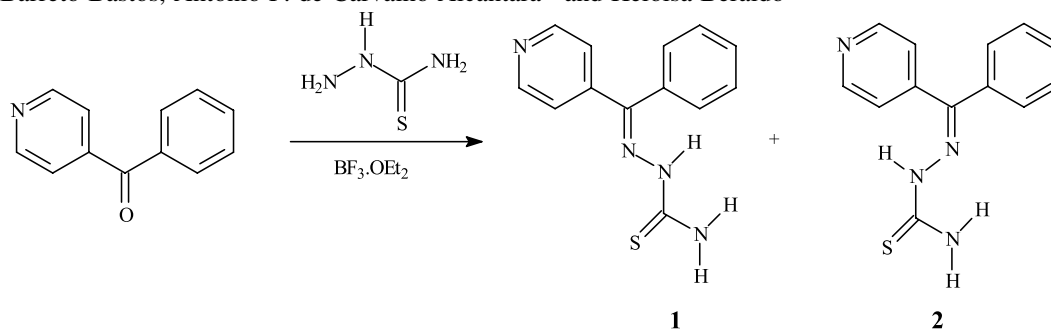
Takahiro Hosoya, Young Sook Yun and Akira Kunugi\*

From the fresh leaves of *Wasabia japonica* Matsum., five novel flavonoids **1–5**, isovitexin derivatives having a *trans*-sinapoyl group at C-7, were isolated, and their structures were elucidated on the basis of their spectroscopic data (NMR, MS, UV, and IR) and chemical evidence.

**Structural analyses of 4-benzoylpyridine thiosemicarbazone using NMR techniques and theoretical calculations**

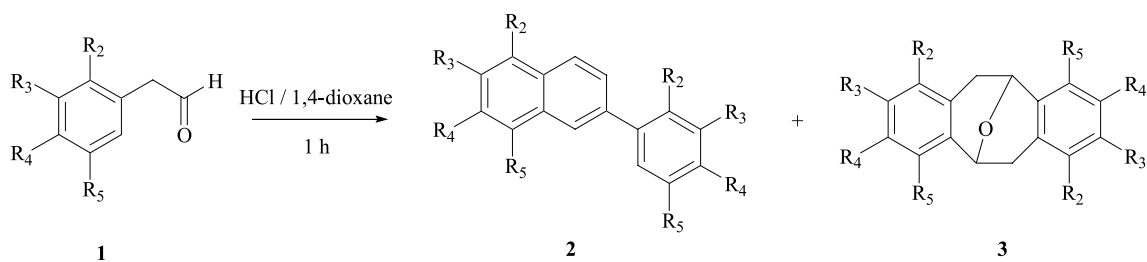
pp 7045–7053

Ana Mena Barreto Bastos, Antônio F. de Carvalho Alcântara\* and Heloisa Beraldo\*

**Facile access to methoxylated 2-phenylnaphthalenes and epoxydibenzocyclooctenes**

pp 7054–7058

Cédric Maurin, Fabrice Bailly and Philippe Cotelle\*




**OTHER CONTENTS**

**Contributors to this issue**  
**Instructions to contributors**

**p I**  
**pp III–VI**

\*Corresponding author

 Supplementary data available via ScienceDirect



Full text of this journal is available, on-line from **ScienceDirect**. Visit [www.sciencedirect.com](http://www.sciencedirect.com) for more information.

---

**CONTENTS**  
**Direct**

This journal is part of **ContentsDirect**, the *free* alerting service which sends tables of contents by e-mail for Elsevier books and journals. You can register for **ContentsDirect** online at: <http://contentsdirect.elsevier.com>

---

Indexed/Abstracted in: AGRICOLA, Beilstein, BIOSIS Previews, CAB Abstracts, Chemical Abstracts, Chemical Engineering and Biotechnology Abstracts, Current Biotechnology Abstracts, Current Contents: Life Sciences, Current Contents: Physical, Chemical and Earth Sciences, Current Contents Search, Derwent Drug File, Ei Compendex, EMBASE/Excerpta Medica, Medline, PASCAL, Research Alert, Science Citation Index, SciSearch



ISSN 0040-4020

Tetrahedron report number 724

# CH/ $\pi$ hydrogen bonds in organic reactions

M. Nishio\*

*The CHPI Institute, 3-10-7 Narusedai, Machida-shi, Tokyo 194-0043, Japan*

Received 7 April 2005

Available online 6 June 2005

## Contents

1. Introduction . . . . .	6924
1.1. CH/ $\pi$ hydrogen bonds . . . . .	6924
1.2. Stereoselectivity in organic reactions . . . . .	6924
2. Selectivity in coupling reactions . . . . .	6924
2.1. Diels–Alder reactions . . . . .	6924
2.1.1. Cycloaddition of cyclopropene to butadiene . . . . .	6924
2.1.2. Hetero-Diels–Alder reaction of <i>o</i> -xylylene with aldehydes . . . . .	6925
2.1.3. Diels–Alder reactions of cyclopentadiene with dienophiles . . . . .	6926
2.1.4. Diels–Alder reactions of dienophiles with [3,3]orthoanthracenophanes . . . . .	6926
2.2. Other coupling reactions . . . . .	6927
2.2.1. Formation of cyclopropanes by addition of carbenes to alkenes . . . . .	6927
2.2.2. Medium-sized cyclophanes . . . . .	6928
2.3. Topochemical photoreactions . . . . .	6928
2.3.1. Photocycloadditions in the solid state . . . . .	6929
2.3.2. Topochemical polymerization . . . . .	6930
3. Diastereoface-discriminating reactions . . . . .	6930
3.1. Cram rule revisited . . . . .	6930
3.1.1. Felkin model and hypothesis . . . . .	6930
3.1.2. Alternative explanation to Cram rule . . . . .	6931
3.2. Prelog rule revisited . . . . .	6933
3.3. Other $\pi$ -facial selections . . . . .	6935
4. Enantioface-discriminating reactions . . . . .	6936
5. Stereoselective reactions involving transition metals . . . . .	6937
5.1. Stereoselective formation of transition metal complexes . . . . .	6937
5.2. Catalytic enantioselective reactions . . . . .	6939
6. Other reactions . . . . .	6946
7. Summary and prospects . . . . .	6947
Acknowledgements . . . . .	6947
References and notes . . . . .	6947

**Keywords:** Stereoselectivity; Diels–Alder reactions; Topochemical photoreactions; Diastereoface-discriminating reactions; Cram rule; Felkin–Anh model; Prelog rule; Enantioface-discriminating reactions; Catalytic enantioselective reactions.

\* Tel.: +81 42 427 5956; fax: +81 42 427 5956; e-mail: [dionisio@tim.hi-ho.ne.jp](mailto:dionisio@tim.hi-ho.ne.jp)

## 1. Introduction

### 1.1. CH/ $\pi$ hydrogen bonds

The CH/ $\pi$  interaction<sup>1,†</sup> is the weakest extreme of hydrogen bonds<sup>2,3</sup> that occurs between a soft acid (CH) and a soft base ( $\pi$ -system)<sup>4,5</sup> in the context of Pearson's HSAB principle. The other hydrogen bonds are the conventional hydrogen bonds, XH/ $\pi$  and CH/ $n$  interactions.<sup>6–8</sup> The XH/ $\pi$  interactions (X=O, N, etc.) are hydrogen bonds between hard acids and soft bases, while the CH/ $n$  interactions (CH/O, CH/N, etc.) are hydrogen bonds between soft acids and hard bases.<sup>1,4,8</sup>

Evidence for the CH/ $\pi$  hydrogen bond has been obtained from various experiments, including thermodynamic, spectroscopic and crystallographic studies of the interacting species.<sup>9,10</sup> Crystallographic database<sup>11,12</sup> and bond critical point analyses<sup>13,14</sup> have provided evidence for the hydrogen bond nature of the CH/ $\pi$  interaction. The results of recent molecular orbital calculations<sup>15–18</sup> are compatible with the experimental data,<sup>19–23</sup> with respect to the estimation of energies. Table 1 compares the energy components of CH/ $\pi$  and related weak hydrogen bonds<sup>24,25</sup> calculated at high levels of theory with large basis sets.

According to Table 1, the energy of a typical CH/ $\pi$  hydrogen bond, where alkyl or aromatic groups are involved as the CH donor, is ca. 0.5–2.5 kcal mol<sup>-1</sup>. Stabilization of the CH/ $\pi$  hydrogen bond largely comes from the correlation term (dispersion force). The electrostatic contribution is < 20% of the total energy when nonpolar CHs and the benzene  $\pi$ -system are concerned. The electrostatic interaction, however, is important in determining the directionality of the CH/ $\pi$  bond. The proportion of the electrostatic energy increases on going from sp<sup>3</sup>-CH to sp<sup>2</sup>-CH and then to sp-CH.<sup>1,10</sup> A similar trend is observed by introducing an electron-withdrawing atom or group and the energetic feature of the CH/ $\pi$  hydrogen bond is summarized as follows: the stronger the proton-donating ability of a CH, the stronger the stabilizing effect and the larger the contribution from the electrostatic interaction. The interaction energy becomes larger when the electron density of a  $\pi$ -system increases.<sup>19,26</sup>

### 1.2. Stereoselectivity in organic reactions

A hypothesis was presented, in the late 1970s, that this type of attractive force plays significant roles in chemistry and biology.<sup>27–29</sup> In previous *Tetrahedron Reports*, we discussed the consequence of the CH/ $\pi$  interaction in chiroptical properties, conformation of organic molecules<sup>4</sup> and molecular recognition.<sup>5</sup> Now that the importance of this weak hydrogen bond has been recognized in a variety of molecular interactions, it seems timely to summarize the progress in more dynamic aspects of organic chemistry.

To begin with, it should be remembered that the difference in the Gibbs energy ( $\Delta\Delta G^\ddagger$ ) of the transition states of two competing reactions needs not be very large in order to

achieve an acceptable selectivity. For instance, a 99:1 selectivity (98% ee in an enantioselective reaction) may result from a  $\Delta\Delta G^\ddagger$  of ca. 2.8 kcal mol<sup>-1</sup> in a kinetically controlled organic reaction. Another important point is that the direction of the intermolecular forces involved in the transition geometry is critical for effective discrimination. Further, in order to be practical in a dynamically interacting molecular system, the energy of a one-unit interaction should not be too large. Both the above requisites are fulfilled by the CH/ $\pi$  hydrogen bond. Combinations of a few such interactions are sufficient to bring about a satisfactory result, with regard to stereoselective synthesis.

A number of discussions have been raised as to the role of CH/ $\pi$  hydrogen bonds in the stereoselectivity of organic reactions. These include Diels–Alder reactions, diastereoface- and enantioface-discriminating reactions and catalytic enantioselective reactions, etc. The role of CH/ $\pi$  interactions in these reactions is discussed below.

## 2. Selectivity in coupling reactions

### 2.1. Diels–Alder reactions

Preferential formation of the *endo* product (vs *exo*) has often been reported for the Diels–Alder reaction and various interpretations have been presented for the *endo* selectivity. The suggestions include the steric effect, the differential volumes of activation, the different polarities of the transition state and the secondary orbital interaction.<sup>‡</sup> Despite this, there is no agreement among the scientific community on the factors governing the selectivity of the reactions. In a recent review, García, Mayoral and Salvatella<sup>30</sup> critically examined the mechanism of Diels–Alder reactions, where the origin of the *endo* preference was attributed to the secondary orbital interactions. They concluded that the high *endo* selectivity is more reasonably explained in the context of well-known concepts including steric effects, hydrogen bonds and electrostatic interactions. Here, we examine the possibility of the CH/ $\pi$  hydrogen bond.

**2.1.1. Cycloaddition of cyclopropene to butadiene.** The reaction of butadiene with cyclopropene (Fig. 1a) proceeds with a virtually perfect *endo* selectivity. Sodupe et al. studied the mechanism by the ab initio MO method and attributed the origin of the stereoselectivity to the CH/ $\pi$  hydrogen bond operating between a CH of cyclopropene and the central C–C bond of the diene (Fig. 1b).<sup>31</sup> The difference in energy of the transition geometries ( $\Delta\Delta H^\ddagger$ ) was calculated, at the QCISD(T)/D95V\*//CASSCF/D95V\* level, to be 1.88 kcal mol<sup>-1</sup> in favour of the *endo* transition state (TS). Consistent with this result, in the TS leading to the *endo* product, the C–H bond in cyclopropene pointing to the central C–C bond of butadiene was found the longer of the two methylene C–H bonds. The methylene group of a three-membered ring such as cyclopropene is known to be an effective CH donor by a crystallographic database study.<sup>32</sup>

<sup>†</sup> A comprehensive literature list of CH/ $\pi$  hydrogen bonds is available in the literature list on the website: <http://www.tim.hi-ho.ne.jp/dionisio>

<sup>‡</sup> The importance of the secondary orbital effect was proposed on few experimental data, the reliability of which was far from satisfactory.<sup>30</sup>

**Table 1.** Energy components of CH/ $\pi$  and related weak hydrogen bonds (energies in kcal mol<sup>-1</sup>)

	Acid/base	Total <sup>a</sup>	ES <sup>b</sup>	ER <sup>c</sup>	CORR <sup>d</sup>	CORR/total	ES/total
CH/ $\pi$	CH <sub>4</sub> /C <sub>2</sub> H <sub>4</sub> <sup>e</sup>	-0.49	-0.24	0.61	-0.86	1.76	0.49
CH/ $\pi$	CH <sub>4</sub> /C <sub>6</sub> H <sub>6</sub> <sup>f</sup>	-1.45	-0.25	1.10	-2.30	1.59	0.17
CH/ $\pi$	C <sub>2</sub> H <sub>4</sub> /C <sub>6</sub> H <sub>6</sub> <sup>f</sup>	-2.06	-0.65	1.82	-3.22	1.56	0.32
CH/ $\pi$	C <sub>2</sub> H <sub>2</sub> /C <sub>6</sub> H <sub>6</sub> <sup>f</sup>	-2.83	-2.01	1.44	-2.26	0.80	0.71
CH/ $\pi$	C <sub>6</sub> H <sub>6</sub> /C <sub>6</sub> H <sub>6</sub> <sup>g</sup>	-2.46	-0.55	1.57	-3.48	1.41	0.16
CH/ $\pi$	CH <sub>2</sub> Cl <sub>2</sub> /C <sub>6</sub> H <sub>6</sub> <sup>h</sup>	-4.5	-1.8	2.4	-5.1	1.13	0.40
CH/ $\pi$	CHCl <sub>3</sub> /C <sub>6</sub> H <sub>6</sub> <sup>h</sup>	-5.6	-2.4	4.6	-7.9	1.41	0.43
NH/ $\pi$	NH <sub>3</sub> /C <sub>6</sub> H <sub>6</sub> <sup>i</sup>	-2.22	-1.01	1.14	-2.36	1.06	0.45
OH/ $\pi$	H <sub>2</sub> O/C <sub>6</sub> H <sub>6</sub> <sup>i</sup>	-3.02	-1.86	1.07	-2.23	0.74	0.62
CH/O	CH <sub>4</sub> /H <sub>2</sub> O <sup>j</sup>	-0.29	-0.42	0.38	-0.08	0.28	1.45
CH/O	CHF <sub>3</sub> /H <sub>2</sub> O <sup>k</sup>	-3.70	-7.06	4.14	-0.25	0.07	1.91

<sup>a</sup> Estimated by CCSD(T) level interaction energy at the basis set limit, unless otherwise noted.

<sup>b</sup> Electrostatic.

<sup>c</sup> Exchange repulsion.

<sup>d</sup> Correlation energy.

<sup>e</sup> Ref. 15.

<sup>f</sup> Ref. 16.

<sup>g</sup> Ref. 17.

<sup>h</sup> Ref. 18.

<sup>i</sup> Ref. 24.

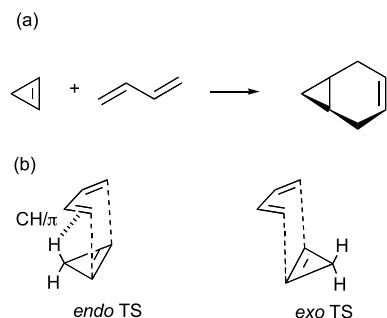
<sup>j</sup> Ref. 25 (MP2/6-31+G\*\*): -0.13 and -0.11 kcal mol<sup>-1</sup>, respectively, for polarization and charge-transfer terms by Morokuma partitioning analysis).

<sup>k</sup> Ref. 25 (MP2/6-31+G\*\*): -0.69 and -0.97 kcal mol<sup>-1</sup>, respectively, for polarization and charge-transfer terms). Contribution from the charge-transfer energy is the subject of current controversy (Refs. 13,14).

**2.1.2. Hetero-Diels–Alder reaction of *o*-xylylene with aldehydes.** Cycloaddition reactions between *o*-xylylene derivatives **1** and alkenes (Diels–Alder reaction) or aldehydes (hetero-Diels–Alder reaction) show high *endo* selectivity. Houk and co-workers have provided evidence for the involvement of CH/ $\pi$  hydrogen bonds in the *endo* selectivity of the hetero-Diels–Alder reaction (Fig. 2a).<sup>33</sup>

They found, by *ab initio* calculations at the MP2/6-31G(d) level, the activation energies of the *endo* and *exo* pathways to be 3.6 and 4.7 kcal mol<sup>-1</sup>, respectively, in the reaction of acetaldehyde with **1** (R'=OH). The *endo* TS was more stable by 1.1 kcal mol<sup>-1</sup> than the *exo* TS (Fig. 2b). The calculated TS energies of the relevant molecules are summarized in Table 2 and Table 3 lists the atomic distances at the transition geometries of the cycloaddition reactions.

The activation energy is smaller in the *endo* TS than in the *exo* TS in every case. The atomic distances *d*<sub>1</sub>–*d*<sub>3</sub> at the *endo* transition geometries are very short. The above computational data are consistent with the experimental result that the *endo* product is preferentially formed. Houk et al. argued for the above finding in the context of the CH/ $\pi$  hydrogen bond; the preference for the *endo* product was ascribed to the stabilizing methyl/ $\pi$  or phenyl/ $\pi$  interactions, which can

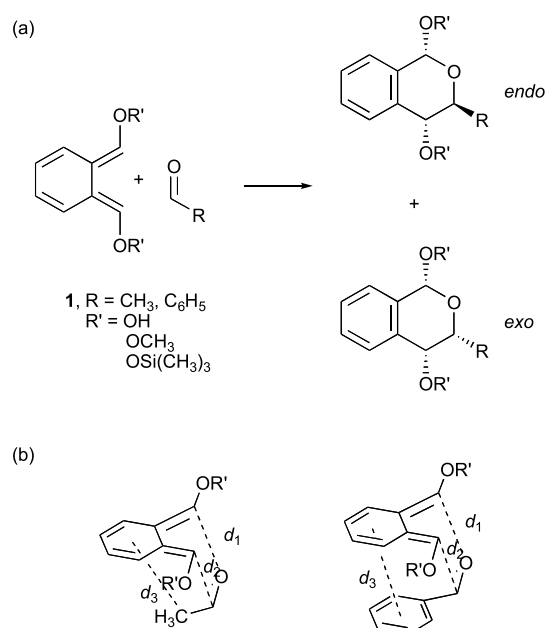


**Figure 1.** (a) Reaction of butadiene and cyclopropene. (b) *Endo* and *exo* transition states of the Diels–Alder reaction.

**Table 2.** Activation energies (kcal mol<sup>-1</sup>) of cycloaddition reactions between *o*-xylylene derivatives **1** and aldehydes calculated at the MP2/6-31G(d) level

R	R'	<i>endo</i> TS	<i>exo</i> TS	$\Delta\Delta H_{exo-endo}$
CH <sub>3</sub>	OH	3.6	4.7	1.1
	OCH <sub>3</sub>	3.9	5.2	1.3
	OSi(CH <sub>3</sub> ) <sub>3</sub>	0.1	1.9	1.8
C <sub>6</sub> H <sub>5</sub>	OH		0.4	
	OCH <sub>3</sub>		2.2	
	OSi(CH <sub>3</sub> ) <sub>3</sub>		1.9	

only occur in the *endo* transition geometry. Thus, the virtually complete *endo* selectivity of the reactions of **1** with acetaldehyde and benzaldehyde is a consequence of the



**Figure 2.** (a) Hetero-Diels–Alder reactions of *o*-xylylene derivatives. (b) Transition states of *o*-xylylene with acetaldehyde and benzaldehyde leading to the *endo* products.



**Table 3.** Atomic distances (Å) at the *endo* transition geometries of cycloaddition reactions between *o*-xylylene derivatives **1** and aldehydes calculated at the MP2/6-31G(d) level

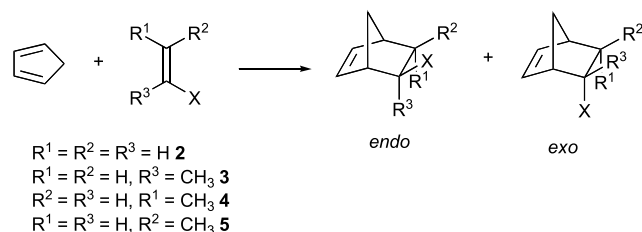
R	R'	$d_1$	$d_2$	$d_3$
CH <sub>3</sub>	OH	2.297	2.203	3.794
	OCH <sub>3</sub>	2.282	2.226	3.910
	OSi(CH <sub>3</sub> ) <sub>3</sub>	2.356	2.194	3.778
C <sub>6</sub> H <sub>5</sub>	OH	2.253	2.264	3.639
	OCH <sub>3</sub>	2.258	2.278	3.650
	OSi(CH <sub>3</sub> ) <sub>3</sub>	2.291	2.251	3.728

CH/ $\pi$  hydrogen bonds. As to the substituent effect [Table 2: R' = OH vs OCH<sub>3</sub>, OSi(CH<sub>3</sub>)<sub>3</sub>], they argued for the possibility of an unfavourable steric effect. The observed trend may be interpreted in view of the differing strengths of the CH/ $\pi$  hydrogen bonds brought about by the substitution.

**2.1.3. Diels–Alder reactions of cyclopentadiene with dienophiles.** In 1970, Kobuke et al. studied the stereochemistry of Diels–Alder reactions of cyclopentadiene with dienophiles CH<sub>2</sub>=CHX **2**, CH<sub>2</sub>=CH(CH<sub>3</sub>)X **3**, *trans*-**4** and *cis*-CH<sub>3</sub>CH=CHX **5** (Fig. 3: X = CN, COCH<sub>3</sub>, CHO, COOH, COOR).<sup>34</sup> Table 4 lists part of their data. It is remarkable that, in every case, the introduction of a methyl group at positions  $\alpha$  or *trans* to the group X increased the proportion of the *endo* product, whereas replacement of H by CH<sub>3</sub> at positions *cis* to X did not show such an effect. They attributed the results to an attractive interaction between the methyl group and the diene  $\pi$ -system. The results are comprehensible if the CH/ $\pi$  hydrogen bonds contribute to stabilizing the transition structure, leading to the *endo* product. Unfavourable electrostatic interactions between X and the diene moiety may also be important.

**2.1.4. Diels–Alder reactions of dienophiles with [3,3]orthoanthracenophanes.** Mataka et al. studied the stereoselectivity in Diels–Alder reactions of a series of dienophiles with [3,3]orthoanthracenophanes **6** and **7** (Fig. 4a).<sup>35</sup> A dienophile may approach the anthracene ring from three directions: inside, outside-*endo* and outside-*exo*. On treatment with maleic anhydride and maleimide, naphthophane **7** exhibited a preference for the inside addition (inside/outside = 5/1). The inside/outside ratio was found to be smaller for benzophane **6** (4/3). The authors explained the result in the context of the attractive  $\pi/\pi$  or CH/ $\pi$  interactions, which may operate between the aromatic rings of the reagents.

They further studied the substituent effect on the selectivity of the addition of *N*-(*p*-substituted phenyl)maleimides **8** to **6** and **7** (Fig. 4b)<sup>36</sup> and Table 5 summarizes the results. The

**Figure 3.** Diels–Alder reactions of cyclopentadiene with various dienophiles CH<sub>2</sub>=CHX.**Table 4.** Proportion of the *endo* product (%) in the Diels–Alder reactions of cyclopentadiene with various dienophiles **2–5** (adapted from Table 1 of Ref. 34. The *endo*–*exo* notation is inverted from the original paper)

X	<b>2</b>	<b>3</b>	<b>4</b>	<b>5</b>
CN	42.5	88.0	71.9	20.5
COCH <sub>3</sub>	20.6	53.0	35.4	25.3
COOCH <sub>3</sub>	25.7	69.9	49.1	—
COOC <sub>4</sub> H <sub>9</sub> ( <i>sec</i> )	—	—	50.7	20.4
CHO	25.6	83.0	36.9	—
COOH	19.8	70.8	37.6	16.4

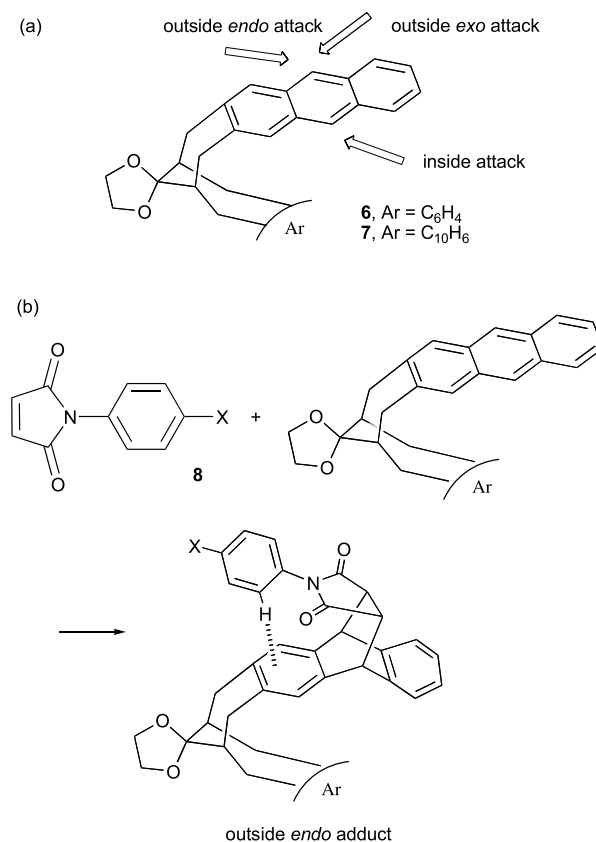
**Table 5.** Stereoselectivity in the Diels–Alder reactions of [3,3]orthoanthracenophanes **6** and **7** and various dienophiles **8** (adapted from Table 1 in Ref. 36)

	X in <b>8</b>	Yield	Ratio 1 (%) <sup>a</sup>	Ratio 2 (%) <sup>b</sup>
<b>6</b>	OCH <sub>3</sub>	80	43/57	60/40
	H	96	50/50	60/40
	Cl	87	48/52	67/33
	NO <sub>2</sub>	90	45/55	75/25
<b>7</b>	OCH <sub>3</sub>	82	45/55	83/17
	H	96	50/50	100/0
	Cl	87	53/47	100/0
	NO <sub>2</sub>	86	33/67	100/0

<sup>a</sup> Inside/outside.

<sup>b</sup> Outside-*endo*/outside-*exo*.

inside/outside ratio does not significantly differ on substitution. On the other hand, in every case, the *endo* is preferred over the *exo* adduct. In **6**, the *endo*/*exo* ratio

**Figure 4.** (a) Diels–Alder reactions of dienophiles with [3,3]orthoanthracenophanes. (b) Addition reactions of maleimide derivatives **8** to benzophane **6** and naphthophane **7**.

increased from  $X=\text{OCH}_3$  and H to Cl, and then to  $\text{NO}_2$ . In 7, the *endo* adduct was exclusively produced, except for  $R=\text{OCH}_3$  (*endo/exo* = 83/17). Introduction of an electron-withdrawing group on the phenyl ring is accompanied by an increase in the *endo* adduct. This result seems reasonable, since the electron-withdrawing substituent increases the activity of the CHs on the phenyl ring, thereby enhancing the effect of the  $\text{CH}/\pi$  bond.

## 2.2. Other coupling reactions

### 2.2.1. Formation of cyclopropanes by addition of carbenes to alkenes.

In 1964, Closs and Moss studied the stereochemistry of the reactions of benzal bromide (a carbene precursor) with allyllithium in the presence of alkenes (Fig. 5). Table 6 shows that the *syn/anti* ratio of the product arylcyclopropanes **9** is more than unity in every case.<sup>37</sup> Of particular interest is that the thermodynamically less stable *syn* isomers were preferred to the *anti* isomers. The influence of the aryl substituent X was reported to follow the sequence of diminishing stereoselectivity  $p\text{-OCH}_3 > p\text{-CH}_3 > p\text{-Cl} > m\text{-Cl} > \text{H}$ .

They explained the above results in terms of the electrostatic attraction and the London dispersion force operating between the olefinic  $\text{C}=\text{C}$  moiety and the carbene substituent; the possibility of the charge transfer interaction was also suggested. The result may be more reasonably understood in the context of the  $\text{CH}/\pi$  hydrogen bond (Fig. 6). In support of this hypothesis, the stereoselectivity of the reaction with *cis*-2-butene ( $R=\text{CH}_3$ ) is larger than that with propene ( $R=\text{H}$ ). The *syn/anti* isomer ratio is larger when  $X=p\text{-OCH}_3$  or  $p\text{-CH}_3$ . This is consistent with the  $\text{CH}/\pi$  interaction working more effectively when the electron density of the aromatic ring increases.

Moss has studied the stereoselectivity of reactions of propene, 1-butene, isopropylethene and *t*-butylethene with *p*-tolyl carbenoid (Fig. 7).<sup>38</sup>

The relative rate of formation of the cyclopropanes **10** was found to be larger for the *syn* product and the maximum preference was recorded in the case of propene ( $R=\text{CH}_3$ ). Successive replacement of the  $\text{CH}_3$  hydrogen of propene by a methyl group resulted in a decrease in the *syn/anti*-ratio from 3.1 (propene) to 2.1 for 1-butene and to 1.4 for isopropylethene. For *t*-butylethene, the *anti* isomer was the preferred product. Moss explained the result in terms of the steric effect (Table 7). Another, more plausible, interpretation is possible in the context of the  $\text{CH}/\pi$  hydrogen bond. The number of CH groups, which can interact with the

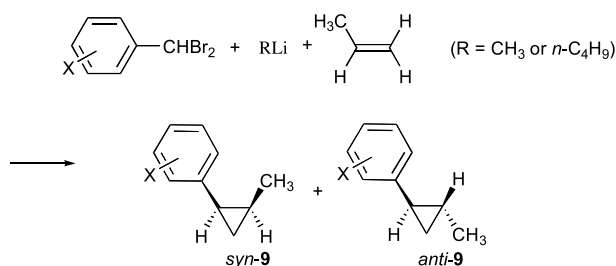


Figure 5.

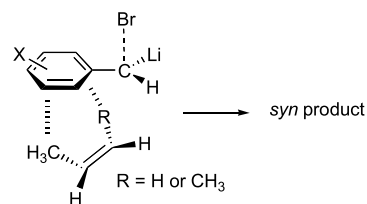


Figure 6.

aromatic ring is three in propene ( $R^1=R^2=\text{H}$  in Fig. 8), whereas the number of CH groups decreases to two and one, respectively, in 1-butene ( $R^1=\text{H}$ ,  $R^2=\text{CH}_3$ ) and isopropylethene ( $R^1=R^2=\text{CH}_3$ ). In *t*-butylethene, there is no CH group to interact.

Casey et al. studied the reaction of  $(\text{CO})_5\text{WCHC}_6\text{H}_5$  **11** (a carbene precursor) with a series of alkenes (Fig. 9).<sup>39</sup> Table 8 summarizes the relative reactivity of the alkenes with **11** to give **12** and the product stereoselectivity (*syn/anti* ratio).

They noticed several interesting points: (1) ethene did not react, (2) for alkyl-substituted alkenes  $\text{CH}_2=\text{CH-R}$ , there was a progressive change in the *syn/anti* ratio to lower values as R became larger, [this tendency is the same as Moss observed in the reactions of alkenes with *p*-tolyl carbenoid (vide supra)] and (3) the reactivity of the alkenes is determined by the number of methyl groups attached to the more substituted end of the  $\text{C}=\text{C}$  bond. They explained the stereochemistry of cyclopropane formation by the mode of approach of the alkenes towards the phenyl carbene complex.

Our own hypothesis is that the TS geometry is stabilized by  $\text{CH}/\pi$  hydrogen bonds operating between the aromatic group of the intermediate carbenoid and the groups attached to the carbon-carbon double bond. Thus, the constant decrease in the *syn/anti* ratio from  $R=\text{CH}_3$  to *t*-butyl is rationalized by a decline, along this series, in the number of CH hydrogens, which are capable of interacting with the phenyl group. That this is not the effect of the size of the substituent is apparent, because the relative reactivity of styrene is very large (11 for  $R=\text{CH}_3$  vs 410 for  $R=\text{C}_6\text{H}_5$ ). In this case, aromatic CHs are involved. The aromatic  $\text{CH}/\pi$  hydrogen bond is larger than those involving aliphatic CHs. The relative reactivity of  $\text{CH}_2=\text{C}(\text{CH}_3)_2$  and  $\text{CH}_3\text{-CH}=\text{C}(\text{CH}_3)_2$  is 3500 and 820, respectively. Introduction of a second methyl group as  $R^3$  significantly increased the

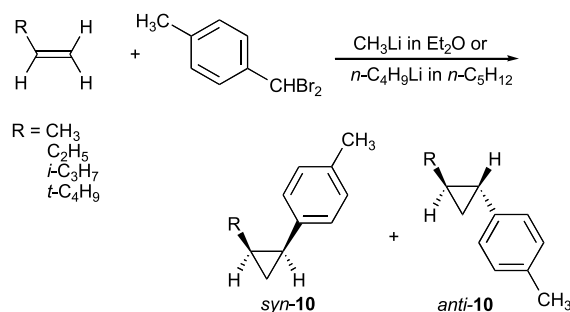
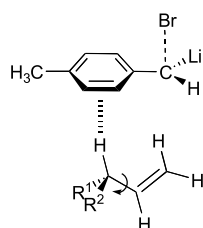
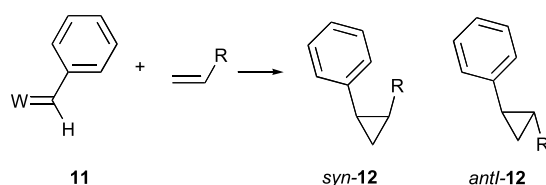
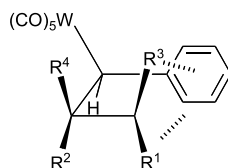


Figure 7. Reactions of propene, 1-butene, isopropylethene and *t*-butylethene with *p*-tolyl carbenoid.

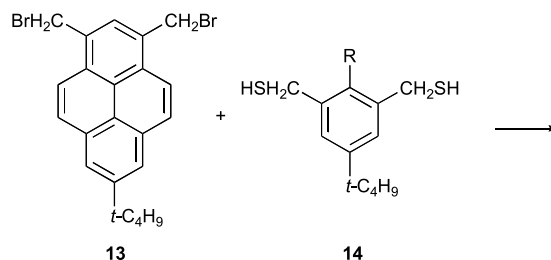
**Table 6.** Isomer ratios (*syn/anti*) of arylcyclopropanes **9** obtained from benzal bromide at  $-10\text{ }^{\circ}\text{C}$  in hydrocarbon medium

X	H	<i>p</i> -Cl	<i>m</i> -Cl	<i>p</i> -CH <sub>3</sub>	<i>p</i> -OCH <sub>3</sub>
1-Butene	2.1	2.1	2.5	2.7	3.0
<i>cis</i> -2-Butene	2.4	2.9	3.7	4.5	8.1

**Figure 8.** Suggested TS geometry for reactions of alkenes with *p*-tolyl carbenoid.**Figure 9.** Reactions of  $(\text{CO})_5\text{WCHC}_6\text{H}_5$  **11** with alkenes.**Figure 10.**

reaction rate. The genesis of this effect may be explained as illustrated in **Figure 10**. Two methyl groups ( $\text{R}^1$  and  $\text{R}^3$ ) are cooperating in stabilizing the TS, with the use of  $\text{CH}/\pi$  bonds.

**2.2.2. Medium-sized cyclophanes.** Tashiro et al. found that coupling of 1,3-bis(bromomethyl)-7-*t*-butylpyrene **13** with a series of 1,3-bis(mercaptomethyl)benzenes **14**, under high-dilution conditions, give *syn* or *anti* 2,11-dithia[3]metacyclo(1,3)pyrenophane derivatives (**Fig. 11**).<sup>40</sup> The *syn* isomer was obtained as a single product in the cases of the 9-methyl and 9-ethyl compounds, whereas the *anti* conformer was exclusively formed for  $\text{R} = \text{OCH}_3$  and  $\text{F}$  (**Table 9**). They attributed this to a compromise between attractive ( $\text{CH}/\pi$ ) and repulsive (electrostatic, as well as steric) interactions.

**Figure 11.** Coupling reactions of 1,3-bis(bromomethyl)-7-*t*-butylpyrene with 1,3-bis(mercaptomethyl)benzenes.

The interaction of  $\text{CH}_3$  or  $\text{CH}_2\text{CH}_3$  with the pyrene aromatic ring is favourable in terms of the  $\text{CH}/\pi$  hydrogen bond to give the *R*/pyrene-*syn* isomer as the sole product, while the interaction of  $\text{OCH}_3$  and  $\text{F}$  versus the pyrene moiety is unfavourable in view of the dipolar interaction and leads to the exclusive formation of the *anti* product.

### 2.3. Topochemical photoreactions

Recently, a great deal of attention has been focused on solvent-free reactions, because of social demands for clean chemistry. These reactions give excellent regio-, stereo- and enantio-selectivity, as compared to reactions in the homogeneous phase. The excellent conversion efficiency and stereoselectivity are due to restriction of the topology of the reacting molecules in the crystallographic environment. The manner in which the  $\text{CH}/\pi$  hydrogen bonds determine the transition geometry of these reactions will now be examined.

**Table 7.** Isomer ratios (*syn/anti*) of formation of arylcyclopropanes **10** obtained in reactions of propene, 1-butene, isopropylethene and *t*-butylethene with *p*-tolyl carbenoid

R	$n\text{-C}_4\text{H}_9\text{Li}/n\text{-C}_5\text{H}_{12}$			$\text{CH}_3\text{Li}/(\text{C}_2\text{H}_5)_2\text{O}$		
	<i>syn</i>	<i>anti</i>	<i>syn/anti</i>	<i>syn</i>	<i>anti</i>	<i>syn/anti</i>
$\text{CH}_3$						3.1
$\text{C}_2\text{H}_5$	1.3	0.50	2.6	0.75	0.35	2.1
<i>i</i> - $\text{C}_3\text{H}_7$	0.51	0.27	1.9	0.33	0.23	1.4
<i>t</i> - $\text{C}_4\text{H}_9$	0.13	0.17	0.72	0.086	0.19	0.45

**Table 8.** Relative reactivity of alkenes with (CO)<sub>5</sub>WCHC<sub>6</sub>H<sub>5</sub> **11** to give *syn* and *anti* cyclopropanes **12**

Alkene	R <sup>1</sup>	R <sup>2</sup>	R <sup>3</sup>	R <sup>4</sup>	Reactivity	<i>syn</i>	<i>anti</i>	<i>syn/anti</i>
CH <sub>2</sub> =CH <sub>2</sub>	H	H	H	H	0			
CH <sub>2</sub> =CHCH <sub>3</sub>	CH <sub>3</sub>	H	H	H	11	7.0	3.9	1.8
CH <sub>2</sub> =CHCH <sub>2</sub> CH <sub>3</sub>	CH <sub>2</sub> CH <sub>3</sub>	H	H	H	5.6	2.7	2.9	0.9
CH <sub>2</sub> =CHCH(CH <sub>3</sub> ) <sub>2</sub>	CH(CH <sub>3</sub> ) <sub>2</sub>	H	H	H	2.4	0.64	1.7	0.36
CH <sub>2</sub> =CHC(CH <sub>3</sub> ) <sub>3</sub>	C(CH <sub>3</sub> ) <sub>3</sub>	H	H	H	1.0	0	1.0	0.01
CH <sub>2</sub> =CHC <sub>6</sub> H <sub>5</sub>	C <sub>6</sub> H <sub>5</sub>	H	H	H	410	371	38	9.7
<i>cis</i> -CH <sub>3</sub> CH=CHCH <sub>3</sub>	CH <sub>3</sub>	CH <sub>3</sub>	H	H	7.6	7.4	0.2	41
<i>trans</i> -CH <sub>3</sub> CH=CHCH <sub>3</sub>	CH <sub>3</sub>	H	CH <sub>3</sub>	H	3.5			
CH <sub>2</sub> =C(CH <sub>3</sub> ) <sub>2</sub>	H	CH <sub>3</sub>	CH <sub>3</sub>	H	3500			
CH <sub>3</sub> CH=C(CH <sub>3</sub> ) <sub>2</sub>	CH <sub>3</sub>	CH <sub>3</sub>	CH <sub>3</sub>	H	820	811	9	94
Cyclopentene	H	H	CH <sub>2</sub>	CH <sub>2</sub>	6.0	4.3	1.7	2.6

**2.3.1. Photocycloadditions in the solid state.** Honda found that a single crystal-to-single crystal photodimerization took place when 2-benzyl-5-benzylidenecyclopentanone **15** was irradiated by UV light (Fig. 12).<sup>41,42</sup> From 117 to 200 K, the reaction rate increased, gradually. This was expected, but the rate constant was slightly reduced at higher temperatures. Below 200 K, the intermolecular distance of the two reacting atoms was found to remain almost constant (4.15 Å). The distance *d* gradually increased after the temperature reached 200 K (4.19 Å at 330 K). No crystal phase transition was observed around the threshold temperature. It seems clear that CH/ $\pi$  hydrogen bonds between a methylene CH in a molecule and an aromatic ring of a nearby molecule hold the reacting species at the correct distance and orientation. Short CH/ $\pi$  distances (3.03–3.36 Å) were found between a benzylic CH and the six aromatic carbon atoms.

Hasegawa et al. found, on irradiation of 2-(dibenzylamino)ethyl 3-benzoylacrylate **16** in the solid state, that a [2+2] cycloaddition took place to give a head-to-tail dimer **17** in quantitative yield with a perfect stereoselectivity (Fig. 13).<sup>43</sup> Analysis of the crystal structure of **17** disclosed a number of CH/ $\pi$  short contacts between the aliphatic and aromatic CHs and the benzene rings. They concluded that the dipolar interactions between the ester C=O and N and the CH/ $\pi$  hydrogen bonds are crucial driving forces of the crystal packing and of the suitable orientation of the molecules for efficient cycloaddition. The exclusive formation of the *cis* product was attributed to the CH/ $\pi$  hydrogen bond (2.86 Å) operating between a methylene CH and a benzoyl aromatic ring.

Sakamoto et al. presented an interesting example of an absolute asymmetric synthesis, where CH/ $\pi$  hydrogen bonds play an important part.<sup>44</sup> A series of *N*-tigloylbenzoylformamides **18** was prepared and their photoreactions in the solid state were studied (Fig. 14).

**Table 9.** Yields (%) of the coupling reactions of 1,3-bis(bromomethyl)-7-*t*-butylpyrene **13** with 1,3-bis(mercaptomethyl)benzenes **14**

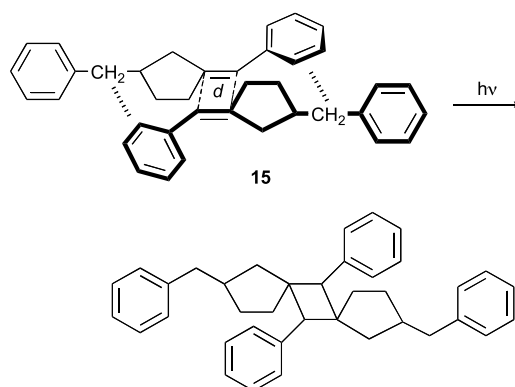
R	<i>syn</i> <sup>a</sup>	<i>anti</i> <sup>a</sup>
CH <sub>3</sub>	35	0
C <sub>2</sub> H <sub>5</sub>	44	0
OCH <sub>3</sub>	0	25
F	0	41

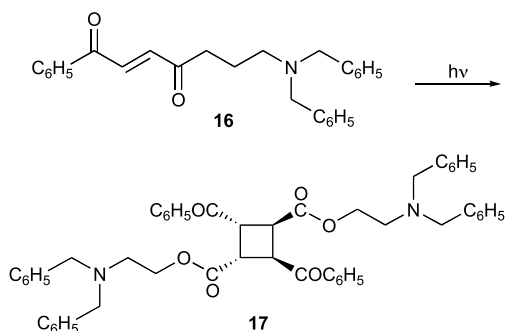
<sup>a</sup> *syn/anti* notation given with respect to R versus pyrene.

By the X-ray method, the crystal conformation of **18** was shown to be *E,E*, except for **18c**, for which the *E,Z* conformation was attributed. Methacryloyl compounds, lacking the terminal  $\beta$ -methyl group, are in the *E,Z* conformation in every case. In compounds with the *E,E* conformation, the distance between the  $\beta$ -methyl of the *N*-tigloyl moiety and the centre of the benzoyl aromatic ring was found to be very short, as illustrated in Ref. 44. (Crystal conformation of **18a** (R = *i*-C<sub>3</sub>H<sub>7</sub>)).

*N*-Isopropyl- **18a** and *N*-benzyl-*N*-tigloylbenzoylformamide **18b** yielded crystals with a chiral space group (*P*<sub>2</sub><sub>1</sub>), by spontaneous resolution. On photolysis in the solid state, **18a**, **18b**, **18d** and **18e** gave the oxetanes **19** (Fig. 15) in excellent yields, whereas for **18c** and methacryloyl compounds, only *cis/trans* isomerization occurred (Table 10). It is remarkable that **18a** and **18b** afforded *syn*-**19a** and **19b**, respectively, in an optically active form (Fig. 15). This is probably a consequence of the CH/ $\pi$  hydrogen bonds, which restrict the motion of the molecules. On the contrary, oxetanes with the *anti* configuration were obtained in racemic mixtures. The *syn/anti* ratio varied from 3.7 to 60, depending on the substituent R and the reaction temperature.

Somekawa et al. have reported a remarkable effect of molecular packing on site- and stereo-selectivity in the [2+2] photocycloaddition of 2-pyrones with maleimide in the solid state. Irradiation of the 1:1 complexes of 4-( $\omega$ -arylalkoxy)-6-methyl-2-pyrones **20** with maleimide gave the cycloadducts **21** with perfect stereoselectivity (Fig. 16).<sup>45</sup>

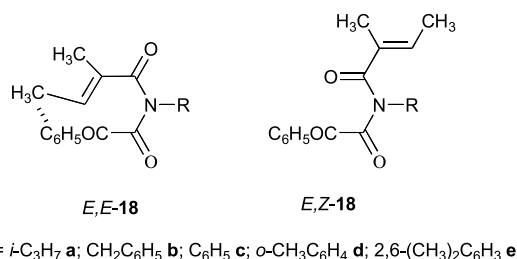
**Figure 12.** Single crystal-to-single crystal photodimerization of 2-benzyl-5-benzylidenecyclopentanone.



**Figure 13.** [2+2] Cycloaddition of 2-(dibenzylamino)ethyl 3-benzoylacrylate **16**, giving rise to a head-to-tail dimer **17**.

The high reactivity and stereoselectivity were understood by X-ray structure analyses of the 1:1 complexes **21** of **20** and maleimides (see Fig. 4 of Ref. 45 – Crystal structure of the 1:1 complexes of **20** and maleimide **21**). The importance of ordinary hydrogen bonds, CH/O and CH/ $\pi$  hydrogen bonds and/or  $\pi/\pi$  stacking has been suggested.

**2.3.2. Topochemical polymerization.** Matsumoto has reviewed the topochemical polymerization of 1,3-dienes.<sup>46</sup> Polymerizable diene molecules include muconate esters<sup>47</sup> and ammonium salts (*ZZ* and *EE*),<sup>48</sup> sorbates (*EE*), etc. For the construction of polymerizable 3D structures, the formation of a robust 2D hydrogen-bond network was indispensable. The molecules were found to closely pack by  $\pi/\pi$  stackings, CH/ $\pi$  hydrogen bonds and halogen/halogen interactions, forming a columnar structure. The structure of the polymerizable monomers was characterized by a  $\pi/\pi$  distance of 4.9–5.2 Å along the columns and the angle between the stacking direction and the molecular plane was ca. 45° (see Figures 7 and 8 of Ref. 47). A disyndiotactic polymer was prepared using di(4-methoxybenzyl)muconate as the monomer, the alternate molecular stacking in a

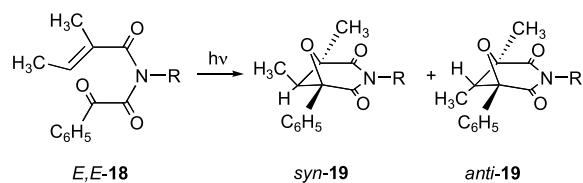


**Figure 14.** *E,E* and *E,Z* conformation of *N*-tigloylbenzoylformamides **18**.

**Table 10.** Structural parameters of *N*-tigloylbenzoylformamides **18** and stereochemical outcome of the photolysis in the solid state

	Configur- ation	Tortion (°)	$d_{C\beta\pi/ring}$	$d_{C/O}$	$d_{C/C}$	Temperature (°C)	Yield (%)	<i>syn/anti</i>	ee (%)
<b>18a</b>	<i>E,E</i>	150.4	3.37	2.98	2.99	0	84	3.7	35
<b>18b</b>	<i>E,E</i>	nd <sup>a</sup>	nd <sup>a</sup>	nd <sup>a</sup>	nd <sup>a</sup>	−78	89	6.7	99
						15	100	60	91
						−78	100	60	91
<b>18c</b>	<i>E,Z</i>	15.5		3.79	4.75	0	0	-	-
<b>18d</b>	<i>E,E</i>	155.5	2.98	2.68	2.70	15	100	27	0
<b>18e</b>	<i>E,E</i>	157.9	3.16	2.98	2.98	15	100	20	0

<sup>a</sup> Not determined.



**Figure 15.** Photoreactions in the solid state of *E,E*-**18** to give **19**.

column formed in the crystals with the aid of CH/ $\pi$  and CH/O hydrogen bonds (see Figure 2c of Ref. 49).

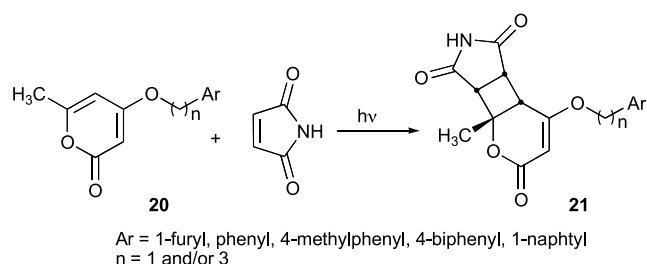
### 3. Diastereoface-discriminating reactions

#### 3.1. Cram rule revisited

In this section, the  $\pi$ -facial discrimination of nucleophiles to carbonyl compounds is discussed. This includes the Cram rule and various models proposed for explaining the genesis of this rule (1,2-asymmetric induction). The underlying concept of these models has, however, remained unclear. Here, possible implications of the CH/O and CH/ $\pi$  hydrogen bonds will be presented.

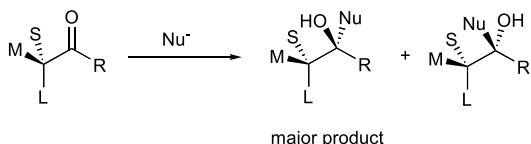
**3.1.1. Felkin model and hypothesis.** In 1952, Cram proposed an empirical rule for the stereoselective addition of nucleophiles to chiral carbonyl compounds (Fig. 17).<sup>50</sup>

Various models have since appeared to explain the origin of the  $\pi$ -facial selectivity including the Cram open-chain model, Cram chelate (or cyclic) model, Cornforth dipolar model,<sup>51</sup> Karabatsos model<sup>52</sup> and Felkin (or Felkin–Anh) model.<sup>53</sup> Of these, the mechanism is well elucidated for the Cram chelate model and the Cornforth model. The predictive power of these models is satisfactory and the



**Figure 16.** [2+2] Photocycloaddition of 2-pyrones **20** with maleimide in the solid state.





**Figure 17.** Cram rule (open-chain model); L: largest, M: medium (often CH<sub>3</sub>), S: smallest (mostly H), Nu<sup>-</sup>: nucleophile.

selectivity of the reactions is generally good,<sup>54</sup> probably because this is founded on a sound physicochemical basis that the geometry of the transition state is rather fixed by the chelation or dipolar interaction (Fig. 18).<sup>55,56</sup>

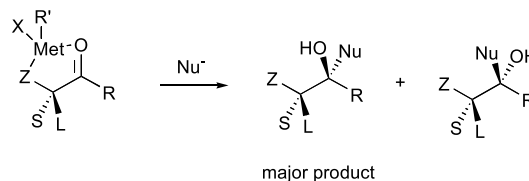
The influence of the chiral atom on the nearby reaction centre in typical carbonyl compounds, however, has remained unclear. In other words, this is one of the most important, yet unanswered, issues in stereochemistry.<sup>57</sup> Felkin hypothesized that the L–C bond is orthogonal to C=O. The approach of the nucleophile to the substrate was presumed to occur *anti* to L, avoiding the unfavourable steric interaction (Fig. 19). From steric reasoning, TS1 was considered more favourable than TS2, giving rise to the differential formation of diastereomeric alcohols. In most cases, this model predicts the correct configuration of the major product.

Despite the wide acceptance of the Felkin model, the reason why the L–C bond is orthogonal to C=O has remained unsettled, although this premise was supported by the computational result of Anh and Eisenstein.<sup>58</sup> Their conclusion was derived from *ab initio* calculations at the STO-3G level of the hydride attack on 2-chloropropanal and 2-methylbutanal, where the H<sup>-</sup>/C(C=O) distance and the H<sup>-</sup>–C–O angle were kept constant at 1.5 Å and 90°, respectively. The computational data matched the Felkin hypothesis in that the group regarded as L is perpendicular to the C=O plane (Fig. 20).<sup>§</sup>

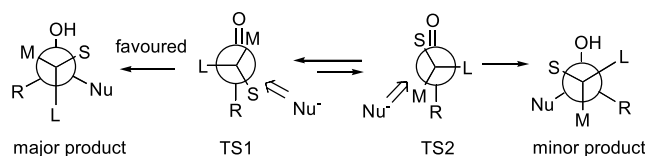
Wu and Houk reported computational data (6-31G\*/3-21G) for the hydride and NaH additions to propanal (Fig. 21).<sup>59</sup> Their results suggested that the TS in the NaH addition to propanal is stabilized at a conformation with the smallest group (H, rather than CH<sub>3</sub>) *anti* to the approaching hydride anion; this is inconsistent with the result of Anh and Eisenstein.

The mechanism of the  $\pi$ -facial diastereoselectivity may include various factors such as conformational, electrostatic, steric,<sup>60,61</sup> anisotropic inductive<sup>62</sup> or electronic effects. Wong and Paddon-Row studied, by MP2/6-31G\*\*/HF/3-21G level calculations, the TS energy for the addition of cyanide anion to 2-fluoropropanal.<sup>63</sup> The most stable TS structure was suggested to bear the C–F bond antiperiplanar to the approaching CN<sup>-</sup> (Fig. 22a). The TS structure for the addition of lithium hydride to 2-fluoropropanal was also calculated [MP2/6-31+G\*\*/HF/6-31G(d)].<sup>64</sup> The authors argued that the most stable TS structure, represented by Figure 22b, was dominated by electrostatic attraction between Li<sup>+</sup> and F. Another TS geometry, such as Figure

<sup>§</sup> This may be a fortuitous coincidence of the ‘theory’ in Felkin’s premise.



**Figure 18.** Cram chelate model; Z=OR, NR<sub>2</sub>, etc., Met=metal.

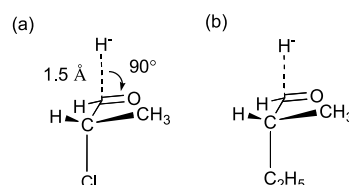


**Figure 19.** Felkin–Anh model; L: largest, M: medium, S: smallest, Nu<sup>-</sup>: nucleophile.

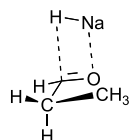
22c, was also found favourable; this was the most stable when the lithium ion was removed in the calculation.

Frenking, Köhler and Reetz calculated, at the MP2/6-31G(d)//HF/6-31G(d) level, the TS energy for the addition of LiH to propanal and 2-chloropropanal.<sup>65,66</sup> They showed that the relative Gibbs energy of the TS was determined, primarily, by the conformational energy of propanal and 2-chloropropanal (Fig. 23a and b). They also calculated the TS energies of the cyanide addition to 2-chloropropanal. Again, the conformation of the substrate was found to be important in determining the most stable geometry of the TS (Fig. 23c). Fleming et al. calculated the TS energy for the LiH addition to 2-silylpropanal and 2-trimethylsilylpropanal (MP2/6-31G\*\*/HF/6-31G\*\*).<sup>67</sup> They concluded that the diastereoselectivity of the nucleophilic attack on a carbonyl group is largely controlled by the size of the substituent (Fig. 23d); the importance of an attractive interaction between CH<sub>3</sub> and the carbonyl oxygen atom was also suggested. It should be noted that the stable geometry bears C–CH<sub>3</sub> nearly eclipsed to the C=O bond in all of the above cases, except for Figure 22b (Figs. 20, 21, 22a and c, and 23a–d). This may indicate that a CH/O hydrogen bond is an important factor in stabilizing the TS geometry. In support of this suggestion, a literature survey showed that the group attributed to M is usually aliphatic, bearing at least a  $\beta$ -CH group.<sup>68</sup> In fact, the CH/O hydrogen bond<sup>69,70</sup> has been shown to operate in stabilizing the *gauche* conformation of simple organic molecules.<sup>71–76</sup>

### 3.1.2. Alternative explanation to Cram rule. Chérest and Prudent reported that the hydride reductions of ketones



**Figure 20.** Stable TS geometries for the H<sup>-</sup> addition to (a) 2-chloropropanal and (b) 2-methylbutanal, calculated by Anh and Eisenstein at the STO-3G level. H<sup>-</sup>/C distance 1.5 Å, H<sup>-</sup>–C–O angle 90°.



**Figure 21.** Stable TS geometry in the NaH addition to propanal suggested by Wu and Houk (6-31G\*/3-21G).

LCHCH<sub>3</sub>COR gave diastereomeric alcohols in differing yields (Table 11).<sup>77</sup> When L=C<sub>6</sub>H<sub>5</sub>, a gradual increase of the product ratio in the lower alkyl homologues was followed by an abrupt jump at R=*t*-C<sub>4</sub>H<sub>9</sub>. The ratio of the product alcohols did not obey this pattern, however, when L was an aliphatic group (cyclohexyl).

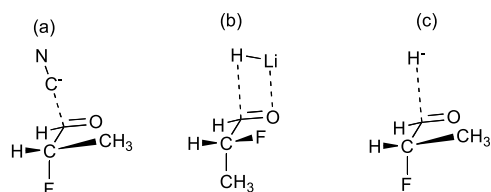
Recently, we presented a model for the nucleophilic addition to a series of ketones C<sub>6</sub>H<sub>5</sub>CHCH<sub>3</sub>COR **22** (Fig. 24).<sup>78</sup> The contribution from the CH/O and CH/ $\pi$  hydrogen bonds has been suggested to be crucial in stabilizing the TS geometry, leading to the preferred product. The experimental result reported by Felkin et al.<sup>53</sup> was reproduced on the grounds of the rotamer distribution estimated by the MO method.

Table 12 summarizes the Gibbs energy of the possible rotamers of C<sub>6</sub>H<sub>5</sub>CHCH<sub>3</sub>COR, calculated at the MP2/6-311G(d,p)/MP2/6-31G(d) level of approximation.

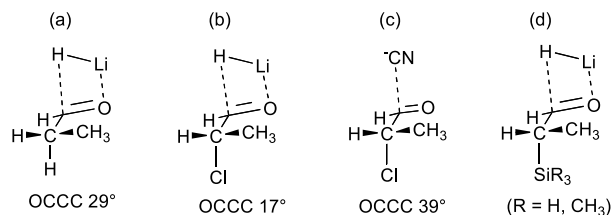
The relative stability of the rotamers **a** and **a'** (vs **b**, Fig. 25) has been attributed to CH/O hydrogen bonds, since this type of interaction can occur only in these geometries. The more stable **a** bears an  $\alpha$ -CH pointing toward C<sub>ipso</sub>, forming a five-membered CH/ $\pi$  hydrogen bond, while rotamer **a'** bears a six-membered CH/ $\pi$  bond.<sup>79</sup>

In Table 13 are listed the abundances of these rotamers (Fig. 26). The population of rotamers **a** and **b** decreases on going from R=CH<sub>3</sub> to R=C<sub>2</sub>H<sub>5</sub> and *i*-C<sub>3</sub>H<sub>7</sub>. The population of rotamer **a'** increases in the same order; the *t*-butyl homologue exists only in geometry **a'**. The rotamer corresponding to **c** has not been found, probably because of the unfavorable electrostatic interaction (C=O vs Ph).

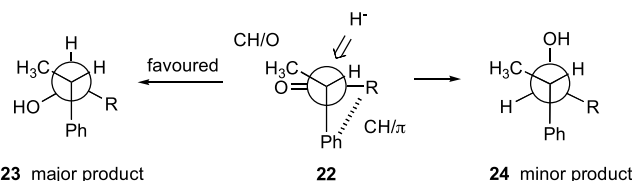
The experimental data by Felkin et al.<sup>53</sup> were reproduced if the geometry of the transition state is similar to the ground-state conformation (reactant like) and the reagent approaches from the less-hindered side of the prevalent conformer (Fig. 27). The approach of the nucleophile to **22** may take place more easily from the less-hindered side of the carbonyl  $\pi$ -face. Rotamers **a** and **a'** will give **23** as the predominant product and rotamer **b** will give **23** and **24** in



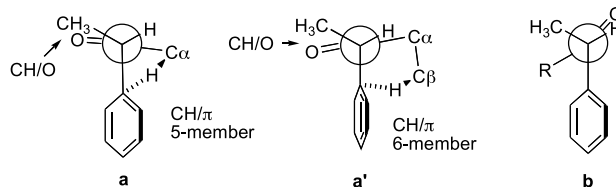
**Figure 22.** Stable TS geometries in (a) CN<sup>-</sup>, (b) LiH and (c) H<sup>-</sup> addition to 2-fluoropropanal.



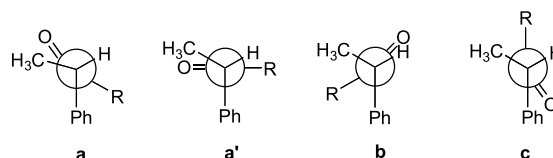
**Figure 23.** Transition geometries of (a) addition of LiH to propanal, (b) addition of LiH to 2-chloropropanal, (c) cyanide addition to 2-chloropropanal and (d) LiH addition to 2-silylpropanal and 2-trimethylsilylpropanal. The numbers refer to the O–C–C–CH<sub>3</sub> torsion angle.



**Figure 24.** Suggested model for addition of nucleophiles to alkyl 1-phenylethyl ketones C<sub>6</sub>H<sub>5</sub>CHCH<sub>3</sub>COR.



**Figure 25.** CH/O and CH/ $\pi$  hydrogen bonds suggested for rotamers **a** and **a'** of alkyl 1-phenylethyl ketones C<sub>6</sub>H<sub>5</sub>CHCH<sub>3</sub>COR.



**Figure 26.** Possible rotamers of alkyl 1-phenylethyl ketones C<sub>6</sub>H<sub>5</sub>CHCH<sub>3</sub>COR.

equal amounts. According to Table 12, the torsion angle  $\phi$  in rotamer **a'** is larger than that in rotamer **a**. Hence, it is reasonable to envisage a differing  $\pi$ -facial selection for the approach of the reagent in the cases of rotamers **a** and **a'**. In rotamer **a'**, the phenyl group must rotate to make an effective six-membered CH/ $\pi$  bond. One of the two *ortho* hydrogens, consequently, orients itself towards the carbonyl  $\pi$ -face. The torsion angle defined by C<sub>ortho</sub>–C<sub>ipso</sub>–C(=O) in rotamer **a'** has, in fact, been found to be smaller than that in rotamer **a**.<sup>78</sup>

**Table 11.** Diastereomeric ratios of alcohols produced by hydride reductions of ketones LCHCH<sub>3</sub>COR

R	L=C <sub>6</sub> H <sub>5</sub>		L=cyclo-C <sub>6</sub> H <sub>11</sub>	
	LiAlH <sub>4</sub>	NaBH <sub>4</sub>	LiAlH <sub>4</sub>	NaBH <sub>4</sub>
CH <sub>3</sub>	2.8	1.6	1.6	1.2
C <sub>2</sub> H <sub>5</sub>	3.2	2.0	2.0	1.6
<i>i</i> -C <sub>3</sub> H <sub>7</sub>	5.0	2.7	4.1	3.2
<i>t</i> -C <sub>4</sub> H <sub>9</sub>	49.0	7.3	1.6	3.5

**Table 12.** Relative Gibbs energy (kcal mol<sup>-1</sup>) at 298.15 K and 1 atm. In parentheses are given C<sub>6</sub>H<sub>5</sub>-C-C-R torsion angles  $\phi$  (°). Adapted from Ref. 78

R	a and a'	b and b'
CH <sub>3</sub>	0.00 (77) <b>a</b>	2.51 (-77) <b>b</b>
C <sub>2</sub> H <sub>5</sub>	0.00 (79) <b>a</b> 1.05 (77) <b>a'</b>	2.30 (-40) <b>b</b> 2.57 (-78) <b>b'</b>
<i>i</i> -C <sub>3</sub> H <sub>7</sub>	0.00 (71) <b>a</b> 1.55 (96) <b>a'</b>	2.45 (-63) <b>b</b>
<i>t</i> -C <sub>4</sub> H <sub>9</sub>	0.00 (93) <b>a'</b>	5.25 (-71) <b>b'</b>

**Table 13.** Rotameric abundance (%) of alkyl 1-phenylethyl ketones C<sub>6</sub>H<sub>5</sub>CHCH<sub>3</sub>COR

R	a	a'	b	c
CH <sub>3</sub>	95.9	—	4.1	0.0
C <sub>2</sub> H <sub>5</sub>	94.3	2.6	3.1	0.0
<i>i</i> -C <sub>3</sub> H <sub>7</sub>	90.2	8.4	1.4	0.0
<i>t</i> -C <sub>4</sub> H <sub>9</sub>	—	100.0	0.0	0.0

In rotamer **a'**, the approach of the reagent from the lower side of the C=O  $\pi$ -face will be much more disturbed. By assuming  $x = 4y^{\text{II}}$  for rotamer **a** and  $x = 49y^{\text{II}}$  for rotamer **a'**, proportion of the diastereomeric products **23/24** was predicted to be 3.7, 3.9, 4.3 and 49 for R=CH<sub>3</sub>, C<sub>2</sub>H<sub>5</sub>, *i*-C<sub>3</sub>H<sub>7</sub> and *t*-C<sub>4</sub>H<sub>9</sub>, respectively. Agreement of the calculated with the experimental data is satisfactory.

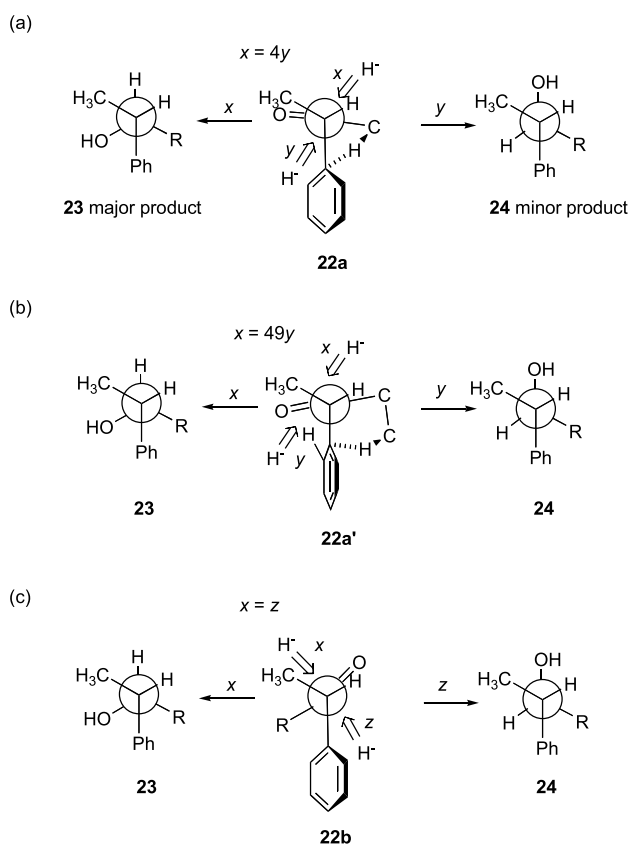
Calculations were also carried out for the transition states of a model reaction. The geometry of the diastereomeric TS (C<sub>6</sub>H<sub>5</sub>CHCH<sub>3</sub>COR + LiH) was optimized, at the MP2/6-311G(d,p)//MP2/6-31G(d) level, starting from the ground-state conformations **a** and **a'**. The difference in the Gibbs energies TS1 and TS2, leading to products **23** and **24**, was estimated to be 1.37 kcal mol<sup>-1</sup> for R=CH<sub>3</sub> and 4.13 kcal mol<sup>-1</sup> for R=*t*-butyl. Table 14 summarizes the geometrical data.

The transition-state geometries TS1, which lead to the predominant product, are not much different from those of the ground-state conformation. In TS2, on the contrary, the torsion angles  $\psi$  and  $\alpha$  twisted considerably to avoid unfavorable steric constraints (see Figure 4 of Ref. 78 – Transition-state geometries TS1 and TS2). Notice that the CH/ $\pi$  and CH/O distances are very short in these geometries. The results suggest that these weak hydrogen bonds are operating in stabilizing the transition structures.

The origin of the diastereofacial selection was also studied for the oxidation of alkyl 1-phenylethyl sulfides C<sub>6</sub>H<sub>5</sub>CHCH<sub>3</sub>-S-R to sulfoxides C<sub>6</sub>H<sub>5</sub>CHCH<sub>3</sub>-SO-R (Fig. 28).<sup>80</sup> A similar argument (*vide supra*) has provided an estimate of the diastereomeric ratio: 3.0, 3.2, 3.4 and 49.1 for R=CH<sub>3</sub>, C<sub>2</sub>H<sub>5</sub>, *i*-C<sub>3</sub>H<sub>7</sub> and *t*-C<sub>4</sub>H<sub>9</sub>, respectively. This result compares with the experimental data: major/minor = 3.0, 3.2, 3.6 and 49, respectively, in the same order.<sup>81</sup> The

<sup>I</sup> The assumption was made in view of the experimental data reported for the reduction of bicyclic ketones (Ref. 60).

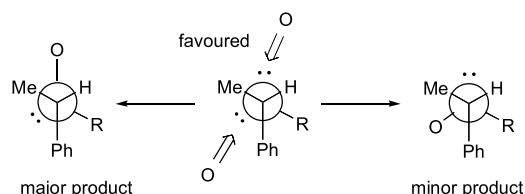
<sup>II</sup> This assumption was arbitrarily made to obtain an acceptable fit with the experimental data.

**Figure 27.** Mechanism suggested for the diastereoselective addition of hydride anion to alkyl 1-phenylethyl ketones C<sub>6</sub>H<sub>5</sub>CHCH<sub>3</sub>COR **22**.

coincidence of the above result with that obtained for the hydride reductions of C<sub>6</sub>H<sub>5</sub>CHCH<sub>3</sub>COR is impressive. The ground-state conformation seems to be of central importance in the mechanism of the diastereofacial selection.

### 3.2. Prelog rule revisited

Prelog's generalization covers the relationship between the configuration of the optically active alcohol of an  $\alpha$ -keto ester and the steric course of asymmetric reactions (Fig. 29). Prelog assumed that two carbonyl groups in the  $\alpha$ -keto ester of a secondary alcohol RCOCOOCHR<sup>L</sup>R<sup>M</sup> are anticoplanar. He also postulated the largest group R<sup>L</sup> to occupy the same plane of the carbonyl C=O and the ester oxygen, so that the remaining two smaller groups (R<sup>M</sup> and H) are staggered on either side of the ester carbonyl group. A nucleophilic reagent will approach the keto carbonyl function from the side of H. Subsequent hydrolysis will give the  $\alpha$ -hydroxy acid, with the indicated enantiomer in excess. The configuration of the secondary alcohols can be deduced by examining the configuration of the  $\alpha$ -hydroxy acid

**Figure 28.** Diastereoselective oxidation of alkyl 1-phenylethyl sulfides C<sub>6</sub>H<sub>5</sub>CHCH<sub>3</sub>-S-R to sulfoxides.



**Table 14.** Torsion angles defined by  $C_{ortho}-C_{ipso}-C-C(O)$   $\alpha$  ( $^\circ$ ) and  $CH_3-C-C=O$   $\psi$  ( $^\circ$ ) and distances  $d_{H_{ortho}/C}$ ,  $d_{CH/\pi}$  and  $d_{CH/O}$  ( $\text{\AA}$ ) at the transition-state structures. TS1 and TS2 correspond, respectively, to the transition structures leading to **23** and **24**. Starting geometry: **a** for  $R=CH_3$ , **a'** for  $R=t-C_4H_9$

R		$\alpha$	$\psi$	$d_{H_{ortho}/C}^a$	$d_{CH/\pi}^b$	$d_{CH/O}^c$
CH <sub>3</sub>	TS1	59	27	2.822	2.826	2.633
	TS2	73	-39	3.187	2.600	2.587
<i>t</i> -C <sub>4</sub> H <sub>9</sub>	TS1	58	29	2.836	2.599	2.599
	TS2	71	-33	3.194	2.473	2.497

<sup>a</sup> Distance between  $H_{ortho}$  and carbonyl carbon atom.

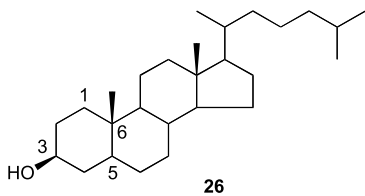
<sup>b</sup> Distance between CH ( $\alpha$ -CH for **a**,  $\beta$ -CH for **a'**) and  $C_{ipso}$ .

<sup>c</sup> Distance between one of the three CHs in the benzylic methyl group and the carbonyl oxygen atom.

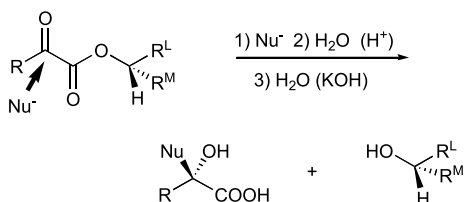
preferentially produced. The genesis of the rule is based on the difference in the effective bulk of the two groups  $R^L$  and  $R^M$ . More specifically, the steric requirement of groups close to the chiral centre is considered to be the most important factor in controlling the extent of the asymmetric synthesis.

In the application of Prelog's generalization to the determination of the configuration of chiral alcohols, the reaction of benzoylformic esters with methylmagnesium iodide is used (Fig. 30). The configuration of a secondary alcohol is predicted to be *S* when the product atrolactic acid **25** with the *S* configuration is produced in excess. In spite of this simplicity, the predictive power of the rule is amazing. Of the 120 examples listed in Tables 2–7 in the textbook of Morrison and Mosher,<sup>82</sup> only four cases were reported as exceptions to the Prelog rule.

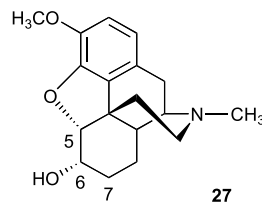
As one of the rare exceptions, 3- $\beta$ -cholesterol **26** gave *R*-**25** with 1.7% ee when subjected to the atrolactic acid synthesis. In a formal sense, the greater branching at  $C^5$  (vs  $C^1$ ) may be used in designing the chiral centre at  $C^5$  to be *S*. This would lead to the prediction that *S*-**25** will be preferentially produced. This, however, was not borne out by the experiment.



Another exception was noted for the atrolactic acid synthesis starting from dihydrocodeine **27**. The configuration at  $C^6$  is known to be *S*. If one were to designate  $C^5$  as  $R^L$  and  $C^7$  as  $R^M$  and applied the Prelog rule in a formal manner, it would be expected that *S*-**25** is the preferred product. *R*-**25** was obtained in 15% ee, however, contrary to the prediction.



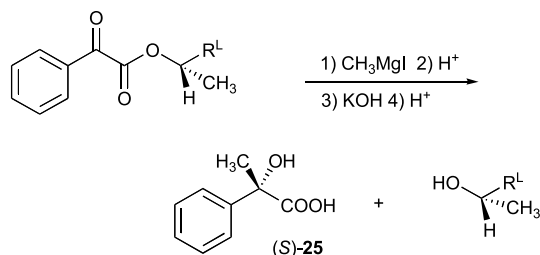
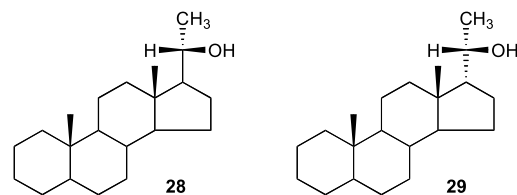
**Figure 29.** Prelog rule:  $R^L$ =largest,  $R^M$ =medium,  $Nu^-$ =nucleophile.



Our hypothesis is that the number and probability of CH/ $\pi$  interactions involved in the TS are additionally important in determining the stereoselectivity. As illustrated in Figure 31, the benzoylformate moiety of **26** may curl back to make contact with the 6-methyl and  $\beta$ -axial CHs in the steroid. Similarly, the methoxy group of **27** may interact with the benzoyl group at the terminus of the molecule, giving rise to the preferential formation of *R*-**25**.

Table 15 summarizes the effect of variations in the alcohol moiety on the atrolactic acid synthesis. It is noted that the enantioselectivity is greater for the 2-octyl ester ( $R^L=n-C_8H_{17}$ : 18% ee) than for the phenyl (3% ee) and  $\alpha$ -naphthyl (12% ee) esters. According to Morrison and Mosher, this is surprising because an increase in the stereoselectivity should follow the increase in steric requirement of  $R^L$ . In the context of the above hypothesis, the result is understandable, since the *n*-hexyl group may be more effective, in view of its flexibility, in forming CH/ $\pi$  hydrogen bonds with the benzoylformate group.

The outcome of the asymmetric synthesis is significantly different in two steroids of similar structure, namely 52% ee for **28** and 18% ee for **29**.



**Figure 30.** Atrolactic acid asymmetric synthesis.

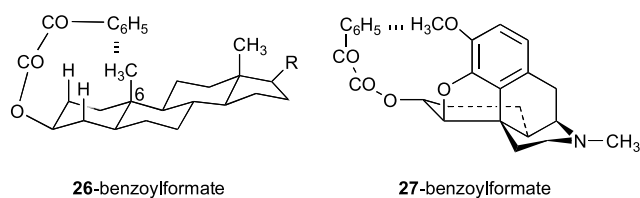


Figure 31.

The difference in the % ee may be understood on the ground of the above CH/ $\pi$  hypothesis. Thus, the TS leading to *S*-**25** may be more effectively stabilized by the CH/ $\pi$  hydrogen bonds in **28** than in **29** (Fig. 32).

Table 16 compares the extent of asymmetric synthesis for benzoylformate and pyruvate esters. The enantioselectivity is uniformly higher for benzoylformate ( $R = \text{Ar}$ ) than for pyruvate esters ( $R = \text{CH}_3$ ). This may be comprehensible if CH/ $\pi$  interactions are operating in the former cases, between the chiral alkyl moiety and the benzoyl group, in determining the TS geometry of the competitive reaction.

Table 17 lists the results obtained by the Grignard reaction of esters in which the two C=O groups are separated by two or three methylene groups. A considerable stereoselectivity was still recorded. This is surprising, since attack of the nucleophile occurs at positions very distant from the stereogenic centre: five and six covalent bonds are present for the  $\gamma$ -keto ( $n = 2$ ) and  $\delta$ -keto ( $n = 3$ ) esters, respectively, between the benzoyl carbon and the menthyl group. This result can hardly be explained without invoking a folded or coiled conformation of the esters. In the above cases, formation of CH/ $\pi$  and CH/O hydrogen bonds may be possible between the acetyl- or benzoylformate moiety and the menthyl group.

### 3.3. Other $\pi$ -facial selections

Corey and co-workers reported that the stereoselective reduction by borohydrides of a prostaglandin precursor was better accomplished when they used esters with an aromatic substituent as R (Fig. 33).<sup>83</sup> For instance, the *S*-isomer was obtained in a 92:8 diastereomeric excess when  $R = \text{NHC}_6\text{H}_4\text{C}_6\text{H}_5(p)$ , while no selectivity was noted for  $R = \text{CH}_3$ . It should be noted that there is an aliphatic ( $n\text{-C}_5\text{H}_{11}$ ) group at the other terminus of the molecule. A folded conformation of the substrate will prevent the reagent approaching from

**Table 15.** The effect of the size of the ligands, attached to the chiral alcohol centre, on the extent of asymmetric synthesis (adapted from Table 2.1 of Ref. 82)

$R^L$	% ee	Yield	Configuration <sup>a</sup>
$\text{C}_5\text{H}_6$	3	78	<i>S</i>
$\alpha\text{-C}_{10}\text{H}_7$	12	90	<i>S</i>
$n\text{-C}_6\text{H}_{13}$	18	43	<i>S</i>
$t\text{-C}_4\text{H}_9$	24	82	<i>S</i>
$2,4,6\text{-(CH}_3)_3\text{C}_5\text{H}_2$	30	80	<i>S</i>
$\text{C}(\text{C}_6\text{H}_5)_3$	49	—	<i>S</i>
(-)-Bornyl	54	90	<i>S</i>
Steroid <b>7</b>	52	91	<i>S</i>
Steroid <b>8</b>	18	85	<i>S</i>

<sup>a</sup> Product secondary alcohol.

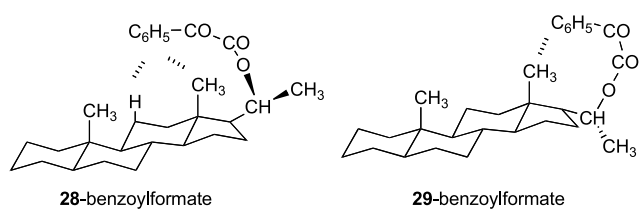


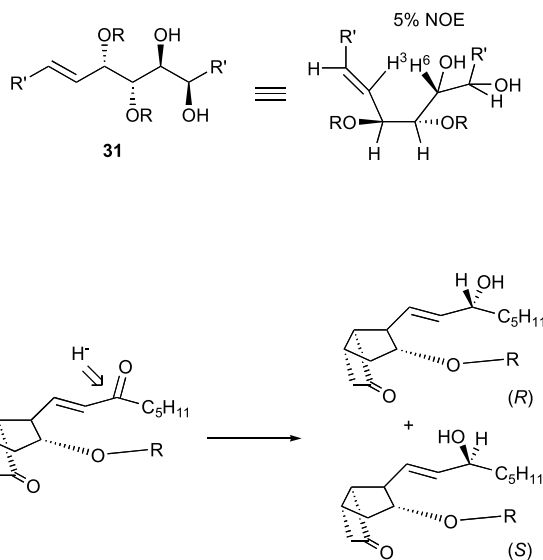
Figure 32.

the inner side of the carbonyl group, giving rise to the preferential formation of the *S*-isomer.

The osmium tetroxide-catalyzed hydroxylation of C=C double bonds is useful for introducing vicinal hydroxyl groups in a stereochemically predictable manner. The stereochemical bias of the reactions, however, is not high enough in the most commonly used examples. Saito et al. reported a remarkable diastereoselectivity in the  $\text{OsO}_4$ -catalyzed dihydroxylation of bis-allylic compounds.<sup>84</sup> Diethyl *E,E*-4,4-bis(*t*-butyldimethylsiloxy)octadiendioates **30**, for example, gave rise to 2,3,6,7-tetrahydroxylated products **32** (via **31**) as single isomers for  $R' = \text{CO}_2\text{Et}$ ,  $\text{CH}_2\text{OAc}$  and  $\text{CH}_2\text{OBz}$  (Fig. 34).

This result implies that the two C=C double bonds mutually shield two diastereofaces, leaving the outer two faces only available for the approach of the reagent. To account for the unusually high diastereoselectivity, Saito proposed a folded conformation involved in the transition state. Figure 35 illustrates this for the *E,E*-isomer, but the situation is the same for the *E,Z* and *Z,Z* isomers. Later, this proposal has been supported by MO calculations on a model compound, 1,5-hexadiene (vide infra).

The above proposal has been shown to be correct, since a significant NOE enhancement (5%) was recorded for  $\text{H}^3$  when  $\text{H}^6$  of **31** was irradiated. Further, the reaction did not proceed to any extent on treatment with NBS; unchanged **30** was quantitatively recovered. The crucial role of the CH/ $\pi$  hydrogen bonds in keeping this conformation stable is evident.



**Figure 33.** Stereoselective reduction of a prostaglandin precursor.

**Table 16.** Comparison of asymmetric synthesis for benzoylformate esters and pyruvate esters (adapted from Table 2.2 of Ref. 82)

R	R'	R*	Configuration <sup>a</sup>	ee (%)	Yield (%)
CH <sub>3</sub>	C <sub>6</sub> H <sub>5</sub>	(-)-Menthyl	S	14, 18	79, 50
C <sub>6</sub> H <sub>5</sub>	CH <sub>3</sub>	(-)-Menthyl	R	22–30	77–97
CH <sub>3</sub>	CH <sub>3</sub> C <sub>6</sub> H <sub>4</sub>	(-)-Menthyl	S	13	
CH <sub>3</sub> C <sub>6</sub> H <sub>4</sub>	CH <sub>3</sub>	(-)-Menthyl	R	25	91
CH <sub>3</sub>	CH <sub>3</sub> OC <sub>6</sub> H <sub>4</sub>	(-)-Menthyl	S	15	30
CH <sub>3</sub> OC <sub>6</sub> H <sub>4</sub>	CH <sub>3</sub>	(-)-Menthyl	R	26	60
CH <sub>3</sub>	C <sub>6</sub> H <sub>5</sub>	(+)-2-Octyl	S	9, 13	38, 20
C <sub>6</sub> H <sub>5</sub>	CH <sub>3</sub>	(+)-2-Octyl	R	18	43
CH <sub>3</sub>	CH <sub>3</sub> C <sub>6</sub> H <sub>4</sub>	(-)-Bornyl	R	0	
CH <sub>3</sub> C <sub>6</sub> H <sub>4</sub>	CH <sub>3</sub>	(-)-Bornyl	S	10	36

<sup>a</sup> Product  $\alpha$ -hydroxy acid.

Saito also showed the Diels–Alder reaction of cyclopentadiene and of amine conjugate addition of **30** to proceed with exclusive diastereoselectivity (Fig. 36).<sup>85</sup>

A diastereoselective intramolecular cycloaddition of nitrones to alkenes was reported by the same authors.<sup>86</sup> Thus, a hydroxy carbonyl compound **33** was converted, via an *O*-diphenylvinylsilyl derivative, into a cycloadduct of a bicyclo[4.3.0] framework with 96% de. They attributed the remarkable diastereoselectivity to the CH/ $\pi$  hydrogen bond (Fig. 37).

Gung et al. examined the conformational energy of 1,5-hexadiene by the MO method. The global minimum has been found, by ab initio calculations at the MP2/6-31G\* level, at the *gauche* conformations (Fig. 38 and Table 18, **d** and **f**).<sup>87</sup>

Note that the vinylic hydrogen in conformer **d** (=f) of 1,5-hexadiene may be involved in a five-membered CH/ $\pi$  hydrogen bond (Fig. 39). Gung attributed the origin of the diastereoselectivity in the reactions reported by Saito (vide supra) to the CH/ $\pi$  interaction.

From discussions raised in this and previous sections, it now seems apparent that the ground-state conformation of the reacting molecule is important in bringing about a significant stereoselectivity. For instance, the remarkable enantioselectivity recorded in the atrolactic acid synthesis (1,4-asymmetric induction) cannot be accommodated

**Table 17.** Comparison of asymmetric synthesis for  $\alpha$ -keto ( $n=0$ ),  $\gamma$ -keto ( $n=2$ ) and  $\delta$ -keto ( $n=3$ ) esters (adapted from Table 2.7 of Ref. 82)

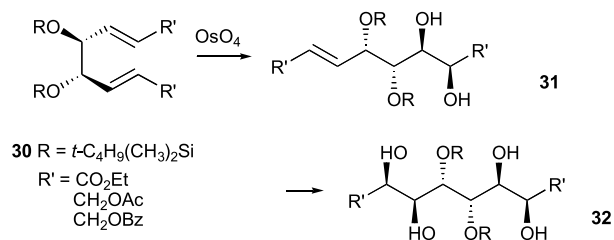
R	$n$	R'	ee (%)	Yield (%)
CH <sub>3</sub>	0	C <sub>6</sub> H <sub>5</sub>	14, 18	79, 50
C <sub>6</sub> H <sub>5</sub>	0	CH <sub>3</sub>	22–30	77–97
CH <sub>3</sub>	2	C <sub>6</sub> H <sub>5</sub>	5–13	40–60
C <sub>6</sub> H <sub>5</sub>	2	CH <sub>3</sub>	10–17	40
CH <sub>3</sub>	3	C <sub>6</sub> H <sub>5</sub>	1.6–16	70
C <sub>6</sub> H <sub>5</sub>	3	CH <sub>3</sub>	13–19	86–96

without taking into account extensive curling back of the chiral group to the reaction centre. According to recent database<sup>88–90</sup> and MO studies,<sup>91,92</sup> the alkyl/aromatic folded conformation of organic molecules seems to be the rule rather than the exception. To cite other possible examples, in the remote functionalization of steroidal compounds reported by Breslow et al. (Fig. 40a), significant regioselectivities were brought about when an aromatic group was incorporated, as in **34**.<sup>93–96</sup> The TS geometry for the intramolecular reagent (PhICl<sub>2</sub>) attack might have been stabilized by attractive interactions between the benzene  $\pi$ -ring and the axial CHs of the steroidal part. In order to account for the selectivity in the functionalization of the long-chain aliphatic groups of **35**, Breslow invoked the involvement of an extensively coiled structure of the reacting molecule (Fig. 40b).<sup>97</sup> Terpene compounds such as farnesol **36** and geranylgeraniol derivatives **37** were found extensively coiled in the process of their regioselective epoxidation reactions (Fig. 40c).<sup>98</sup>

Fish and Johnson reported that the non-enzymatic cyclization of a squalene derivative proceeded with 49% yield in a one-pot synthesis (Fig. 41).<sup>99</sup> Such a remarkable result can hardly be anticipated without considering effective coiling of the long-chain squalene molecule. Gung argued this in the context of the CH/ $\pi$  hydrogen bond.<sup>87</sup>

#### 4. Enantioface-discriminating reactions

This topic was dealt with in our previous Report.<sup>100</sup> The following is therefore a brief summary. Morrison and Mosher studied the enantioface-discriminating reaction of alkyl phenyl ketones RCOC<sub>6</sub>H<sub>5</sub> with chiral Grignard

**Figure 34.** Highly diastereoselective hydroxylation of bis-allylic compounds.

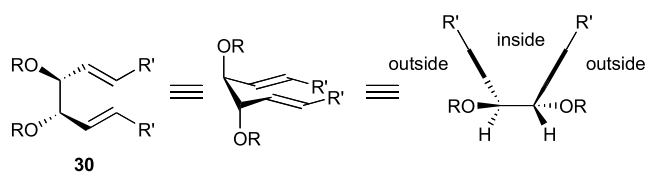


Figure 35. Folded conformation of *E,E*-30.

reagents prepared from (+)-1-chloro-2-methylbutane (Fig. 42). The reduction gave rise to the preferential formation of alcohols with the (*S*)-configuration. The enantiomeric excess (% ee) was 4, 6, 24 and 16, respectively, for R = CH<sub>3</sub>, C<sub>2</sub>H<sub>5</sub>, *i*-C<sub>3</sub>H<sub>7</sub> and *t*-C<sub>4</sub>H<sub>9</sub>.<sup>101</sup>

In the reduction with (+)-1-chloro-2-phenylbutane, the stereoselectivity (% ee) was 47, 52, 82 and 16, respectively, for R = CH<sub>3</sub>, C<sub>2</sub>H<sub>5</sub>, *i*-C<sub>3</sub>H<sub>7</sub> and *t*-C<sub>4</sub>H<sub>9</sub>. Note that the extent of the asymmetric synthesis is much greater where a phenyl group was incorporated in both the ketones and the Grignard reagent. This is understandable if the CH/π hydrogen bonds are assumed to operate between the alkyl and the phenyl group at two points (Fig. 43).

Capillon and Guetté<sup>102</sup> have reported the asymmetric reduction of ethyl *p*-substituted phenyl ketones by chiral Grignard reagents (Fig. 44). They found that the optical yield was decreased by the introduction of an electron-withdrawing group on the aromatic ring of the ketones or Grignard reagents (Table 19). This is reasonable because the CH/π interaction will decrease on substitution of H by CF<sub>3</sub> or Cl.

## 5. Stereoselective reactions involving transition metals

### 5.1. Stereoselective formation of transition metal complexes

Selective formation of one of the possible stereoisomers has often been noted in coordination and organometallic chemistry. Careful examinations have revealed that an

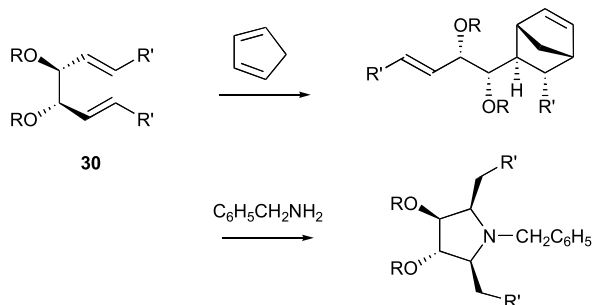


Figure 36. Highly stereoselective Diels–Alder reaction of cyclopentadiene and amine conjugate addition to 30.

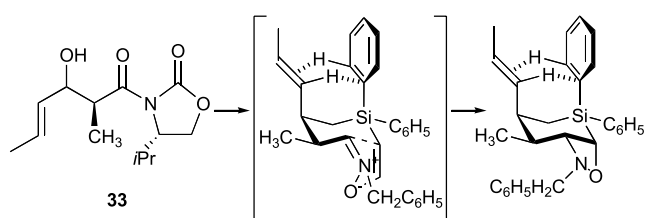


Figure 37. Diastereoselective intramolecular cycloaddition of nitrones to alkenes.

attractive interaction between CHs and an aromatic ring in a nearby ligand exists whenever a significant stereoselectivity was obtained.

Okawa reported that the CH/π interaction is important in the stereoselective formation of coordination compounds.<sup>103</sup> A cobalt complex **38** [ $\Delta$ -*cis*-β<sub>1</sub>-Co(SB)(*l*-moba)] (SB = *N,N'*-disalicylideneethylenediamine, moba = 1-*l*-menthyloxy-3-benzoylacetone) was preferentially produced, among the possible isomers in the mixed chelate compounds (Fig. 45).<sup>104</sup> He attributed the stereoselective formation of **38** to the CH/π hydrogen bonds, operating between the *l*-menthyl group and an aromatic ring of the SB ligand. This interaction may occur only in this stereoisomer.

A similar phenomenon was reported by the same authors for the selective formation of the *cis*-Δ isomer of [M(*l*-moba)<sub>3</sub>] **39**.<sup>105,106</sup> Okawa attributed the stability of **39** to CH/π hydrogen bonds working between the three *l*-menthyloxy groups and the phenyl ring (Fig. 46). Replacement of the phenyl group by the naphthyl group increased the stereoselectivity.<sup>107</sup> Substitution of the *para*-hydrogen X by CH<sub>3</sub> and Br increased and decreased, respectively, the selectivity.<sup>108</sup> They also demonstrated that lanthanide complexes of **39** (M = La, Pr, Gd, Er) could be used in the enantioselective hydride reduction of various ketones.<sup>109</sup>

Yamanari reported the stabilizing role of a methyl group in the stereoselective formation of linkage isomers, *fac* and *mer*, in cobalt and ruthenium complexes containing pyrimidine-2-thione derivatives.<sup>110</sup> The crystal structures of linkage isomers of [Co(4,6-dimethyl-pyrimidine-2-thione)<sub>3</sub>] and [Ru(4-methyl-pyrimidine-2-thione)(2,2'-

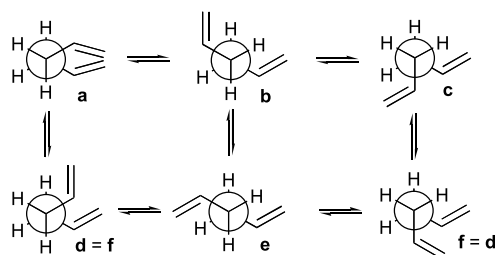


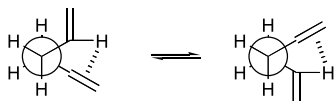
Figure 38. Stable conformers of 1,5-hexadiene (adapted from Ref. 87).

Table 18. Relative steric energy of conformers of 1,5-hexadiene calculated by the ab initio method (adapted from Ref. 87)

	a	b	c	d = f	e
MP2/6-31G*//HF/6-31G*	0.36	1.01	0.55	0.0	0.13
MP4/6-31G*//HF/6-31G*	0.30	0.05	0.57	0.0	0.10

**Table 19.** Effect of substituents in the asymmetric reduction of ethyl *p*-substituted phenyl ketones by chiral Grignard reagents (adapted from Tables 1 and 2 of Ref. 102)

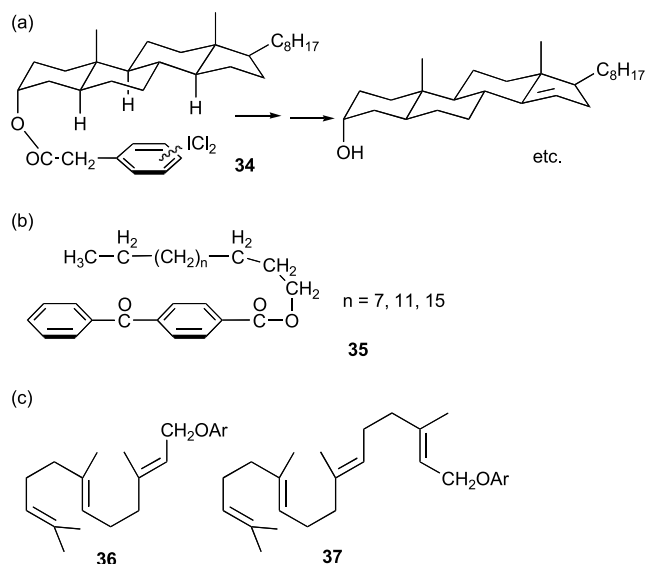
X	Y		
	OCH <sub>3</sub>	H	CF <sub>3</sub>
OCH <sub>3</sub>	51	51	
CH <sub>3</sub>	54	52	10
H	57	50	22
Cl	36	43	
CF <sub>3</sub>	22	22	10



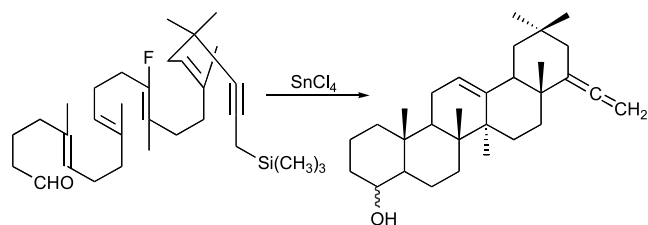
**Figure 39.** Five-membered CH/π hydrogen bond in 1,5-hexadiene.

bipyridyl)<sub>2</sub>] were determined.<sup>111</sup> The difference in the stability of the adjacent and remote isomers has been attributed to CH<sub>3</sub>/π hydrogen bonds occurring between the ligands (Fig. 47).

In order to investigate the effect of non-covalent forces in regulating the stereochemistry of coordination compounds, Kojima and co-workers synthesized a series of ruthenium complexes bearing bisamide-TPA as ligands [TPA = tris(2-pyridylmethyl)amine].<sup>112</sup> When the complex [RuCl(1-Naph<sub>2</sub>-TPA)]PF<sub>6</sub> was reacted with benzoylacetone C<sub>6</sub>H<sub>5</sub>-COCH<sub>2</sub>COCH<sub>3</sub> (Fig. 48: R<sup>1</sup>=CH<sub>3</sub>, R<sup>2</sup>=C<sub>6</sub>H<sub>5</sub>), a 1.8:1 mixture of two isomers (**40**<sub>Me</sub> and **40**<sub>Ph</sub>) was obtained. Structural elucidation, by NMR and crystallographic determinations, of the products revealed that the methyl group of the major product **40**<sub>Me</sub> was sandwiched between the naphthyl rings. Prolonged reaction in ethylene glycol at 100 °C afforded only the methyl-included isomer **40**<sub>Me</sub> as the sole product. It therefore follows that the CH/π-interacted isomer is the thermodynamically more stable. The reaction was found to involve an intramolecular rearrangement from **40**<sub>Ph</sub> to **40**<sub>Me</sub> without rupture of the



**Figure 40.** Remote functionalization reactions giving rise to significant regioselectivities.<sup>93–98</sup>

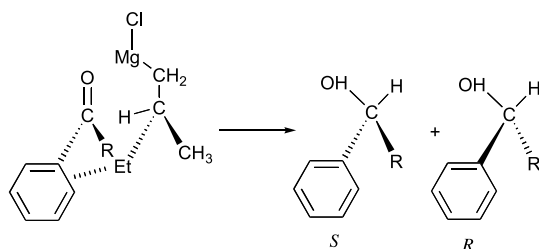


**Figure 41.** Non-enzymatic one-pot cyclization of a squalene derivative.

Ru-β-diketonato coordination bonds (Proposed reaction mechanism of the intramolecular rearrangement of the phenyl-included complex to the methyl-included complex in ethylene glycol (adapted from Figure 9 of Ref. 112). The result has been argued to indicate that CH/π hydrogen bonds are more effective than the π/π interactions in this molecular environment.

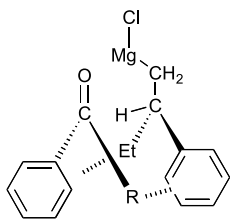
Brunner first recognized that, in half-sandwich transition metal complexes with a cyclopentadienyl (Cp) group as ligand, one of the diastereomers where a hydrogen atom of the η<sup>5</sup>-Cp moiety points toward the phenyl group in a neighboring ligand is more stable than its diastereomeric congener.<sup>113–115</sup> The Cp and phenyl rings are mutually perpendicular and form a T-shaped arrangement. Fig. 49 illustrates the situation for the square pyramidal complex. Brunner termed this the ‘β-phenyl effect’, because the position of the phenyl group, which plays an important part in the stabilization, is β to the central metal atom. This phenomenon is now understood in the context of the CH/π hydrogen bond<sup>116</sup> and is not limited to Cp complexes.<sup>117,118</sup>

Gladysz and co-workers studied the reaction of a dibenzyl sulfide complex [(η<sup>5</sup>-Cp)Re(NO)(PPh<sub>3</sub>)(S(CH<sub>2</sub>Ph)<sub>2</sub>)]<sup>+</sup>TfO<sup>-</sup> with *t*-BuOK.<sup>119</sup> A thiolate compound [(η<sup>5</sup>-Cp)Re(NO)(PPh<sub>3</sub>)(S(CH(*o*-C<sub>6</sub>H<sub>4</sub>CH<sub>3</sub>)Ph))] **41** was produced as a 96:4 mixture of *SR,RS/SS,RR* Re:C diastereomers. The crystal structure of the more stable diastereomer, *SR,RS-41*, was determined, as shown in Crystal structure of the *SR* enantiomer of *SR,RS-[(η<sup>5</sup>-Cp)Re(NO)(PPh<sub>3</sub>)(S(CH(*o*-C<sub>6</sub>H<sub>4</sub>CH<sub>3</sub>)Ph))] **41** (see Ref. 119). They considered the structure to be stabilized by an attractive interaction. In view of these findings, they presumed that the reaction involved the initial formation of an ylide, followed by a [2,3]-sigmatropic rearrangement. This would yield an intermediate with a de-aromatized ring, which could then undergo a [1,3]-hydrogen migration to give the final product [(η<sup>5</sup>-Cp)Re(NO)(PPh<sub>3</sub>)(S(CH(*o*-C<sub>6</sub>H<sub>4</sub>CH<sub>3</sub>)Ph))] **41**. The presumed pathway is shown in Scheme 4 of Ref. 119 – Proposed mechanism of the highly diastereoselective reaction of a rhenium complex [(η<sup>5</sup>-*



**Figure 42.** Asymmetric reduction of alkyl phenyl ketones by a chiral Grignard reagent.





**Figure 43.** Asymmetric reduction of alkyl phenyl ketones by a chiral Grignard reagent.

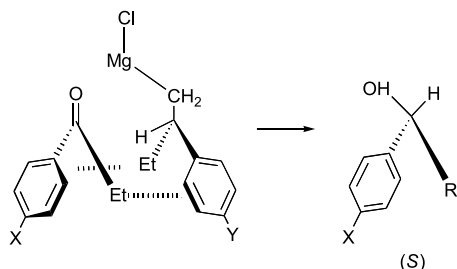
$(Cp)Re(NO)(PPh_3)(S(CH_2Ph)_2)^+TfO^-$  to give  $[(\eta^5-Cp)Re(NO)(PPh_3)(S(CH(o-C_6H_4CH_3)Ph))] \mathbf{41}$ . Note that the migration can only occur from the *si*-side of the intermediate carbanion (when the configuration at rhenium is *S*).

## 5.2. Catalytic enantioselective reactions

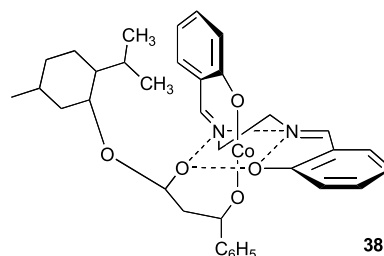
In 1979, Brunner suggested that transition metal complexes that are configurationally stable at the central atom could be used as optically active auxiliaries in enantioselective synthesis.<sup>120</sup> This idea was further put forward in two subsequent reviews.<sup>114,121</sup> The importance of the CH/ $\pi$  hydrogen bond in stabilizing the structure of the TS has since been demonstrated in a number of reactions that use enantioselective catalysts.

Noyori et al. reported that a combined reaction system of a chiral ruthenium complex  $[RuCl\{YCH(C_6H_5)CH(C_6H_5)-NH_2\}\eta^6\text{-arene}]$  ( $Y=O$  or  $NR$ ) and an alkaline base in 2-propanol or formic acid catalyzes the transfer hydrogenation of aromatic ketones or aldehydes to give chiral alcohols with high enantiomeric purity (Fig. 50).<sup>122,123</sup>

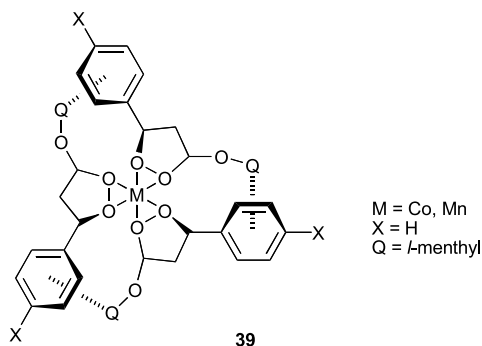
Deuteriobenzaldehydes  $XC_6H_4CDO$ , for example, when treated with a chiral catalyst  $\mathbf{42}$  ( $Y=NTs$ ;  $\eta^6\text{-arene}=\text{benzene}$ , *p*-cymene, hexamethylbenzene, etc.), gave the corresponding chiral alcohols; the enantioselectivity of the reaction is excellent (97–99% ee). In the reactions with a less effective catalyst ( $Y=O$ ;  $\eta^6\text{-arene}=\text{C}_6\text{H}_6$ ), the stereoselectivity decreased from 61% ee for  $X=\text{OCH}_3$  to 49% ( $\text{CH}_3$ ), 45% ( $\text{H}$ ), 37% ( $\text{Br}$ ) and then to 20% for  $X=\text{CF}_3$  (Table 20).<sup>124</sup> The result is consistent with the effect of the CH/ $\pi$  hydrogen bonds decreasing with the decrease of the  $\pi$ -electron density of the aromatic ring. It is noteworthy that the reaction of 4-cyano-4'-methoxybenzophenone catalyzed by *R,R*- $\mathbf{42}$  ( $\eta^6\text{-arene}=\text{benzene}$ ) gave 4-cyano-4'-methoxybenzhydrol in an *R/S* ratio of 67/33, a result highlighting the effect of the CH/ $\pi$  hydrogen bonds.



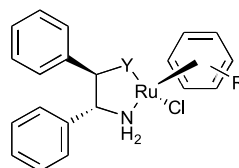
**Figure 44.** Asymmetric reduction of ethyl *p*-substituted phenyl ketones by chiral Grignard reagents.



**Figure 45.** Proposed structure of  $[\Lambda\text{-cis-}\beta_1\text{-Co(SB)(l-moba)}] \mathbf{38}$ : SB = *N,N'*-disalicylideneethylenediamine; moba = 1-*l*-menthyloxy-3-benzoylacetone.

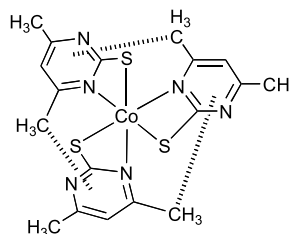


**Figure 46.** CH/ $\pi$  hydrogen bonds working between *l*-menthyloxy groups and the phenyl ring in *cis*- $\Delta$   $[M(l-moba)_3] \mathbf{39}$ .

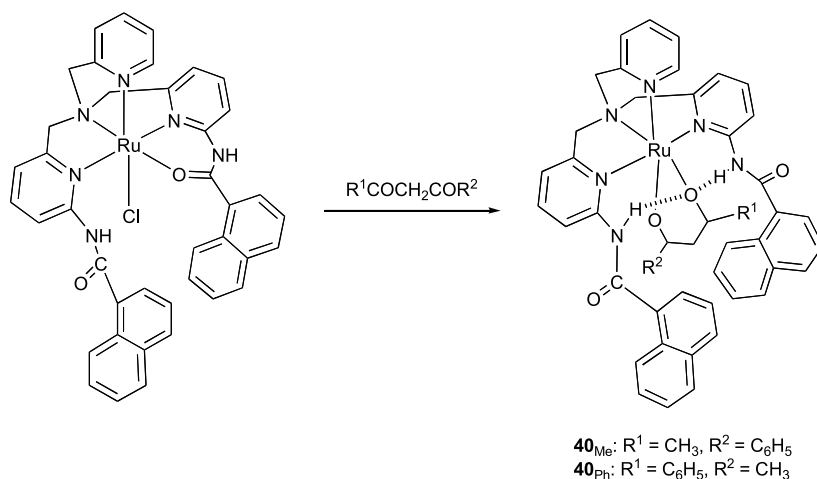


**42.**  $Y=O$  or  $NTs$   
 $\eta^6\text{-arene}=\text{benzene}$ , *p*-cymene, etc.

Noyori concluded that the enantioselectivity emerged not only from the chiral geometry of the five-membered chelate ring, but also by the contribution from the CH/ $\pi$  hydrogen bond.<sup>125</sup> The geometry of the diastereomeric transition structure of the model reactions,  $RuH(OCH_2CH_2NH_2)(\eta^6\text{-arene})+C_6H_5CHO$ , was optimized by MO calculations at the RMP2/BS-III//B3LYP/BS-I level. For the  $\eta^6\text{-benzene}$  *R,R*-catalyst, the activation energy ( $E_a$ ) leading to the preferred *R*-alcohol (Fig. 51a) was calculated as ca.  $9.5 \text{ kcal mol}^{-1}$ , whereas the  $E_a$  leading to the *S*-alcohol (Fig. 51b) was  $12.5 \text{ kcal mol}^{-1}$  ( $\Delta E_a=2.9 \text{ kcal mol}^{-1}$ ). The distance from an arene CH to the nearest phenyl carbon was found to be  $2.86 \text{ \AA}$ . For hexamethylbenzene as the  $\eta^6\text{-arene}$  ligand,  $\Delta E_a$  was estimated to be ca.  $1.7 \text{ kcal mol}^{-1}$ , in favour of the *R*-alcohol (Fig. 51c). The results imply that the



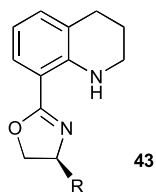
**Figure 47.** CH/ $\pi$  hydrogen bonds in a linkage isomer of a cobalt complex containing 4,6-dimethyl-pyrimidine-2-thione.



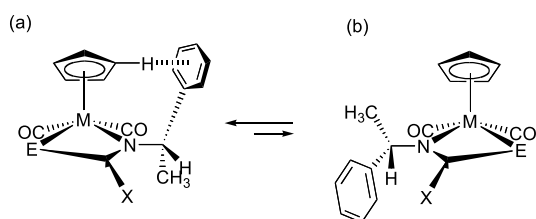
**Figure 48.** Reaction of [RuCl(1-Naph<sub>2</sub>-TPA)]PF<sub>6</sub> and benzoylacetone giving rise to a mixture of **40<sub>Me</sub>** and **40<sub>Ph</sub>**.

aliphatic CHs in the η-arene ligand are as effective as the aromatic CHs in stabilizing the structure of the intermediate.

Zhou et al. reported the stereoselectivity in the transfer hydrogenation of various ketones using [Ru(*p*-cymene)Cl<sub>2</sub>]<sub>2</sub> and *S*-1,2,3,4-tetrahydroquinolinyl-oxazolines **43**.<sup>126</sup> Good enantioselectivity was obtained when a phenyl group was introduced on the oxazoline ring of **43**, while, in the cases of R=isopropyl or benzyl, the enantioselectivity decreased considerably (Table 21). This may indicate that, for R=phenyl, the CH/π hydrogen bonds stabilize the TS, leading to the preferred isomer, as shown in Figure 52. In fact, short CH/π distances were observed between *p*-cymene and a phenyl group in the crystal structure of ruthenium complexes bearing *p*-cymene as the η<sup>6</sup>-arene ligand (see Figure 1 of Ref. 127 – Crystal structure of [Ru(η<sup>6</sup>-cymene)(2-(dimethylamino)-3-phenylpropyl)]-diphenylphosphine]; and see Figure 2 of Ref. 128 – crystal structure of [Ru(η<sup>6</sup>-cymene)(α-methylbenzyl-3,5-di-*t*-butylsalicylamidine)Cl]).<sup>127,128</sup>

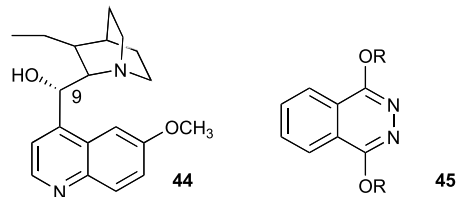


The osmium-catalyzed asymmetric dihydroxylation reaction has attracted much attention, in view of its high enantioselectivity and usefulness for various synthetic purposes.<sup>129,130</sup> A dihydroquinidine derivative **44** with a phthalazine substituent **45** at C<sup>9</sup> has been found to be one of the most effective ligands, giving high enantioselectivity for

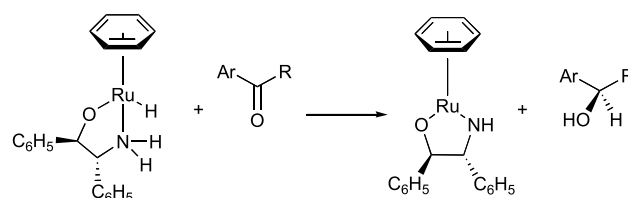


**Figure 49.** β-Phenyl effect: (a) more stable isomer; (b) less stable isomer.

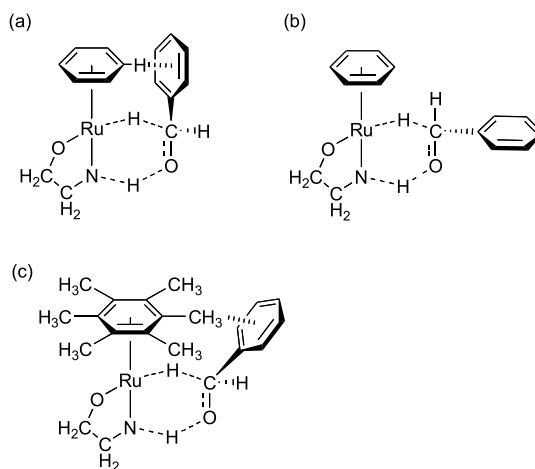
olefins with aromatic substituents. Table 22 lists a part of the data reported by Sharpless and his group.<sup>131</sup>



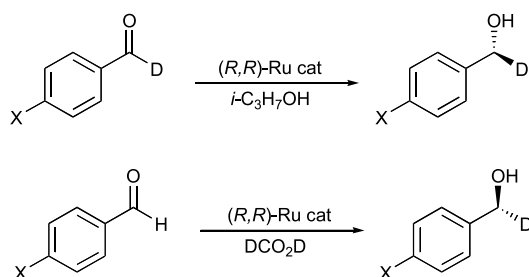
In order to rationalize the high enantioselectivity of the reactions using bis-cincona alkaloids, Sharpless proposed a



**Figure 50.** Enantioselective transfer hydrogenation of aromatic ketones or aldehydes.

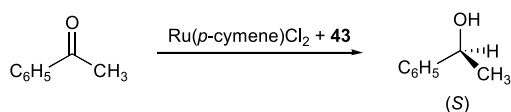


**Figure 51.** Suggested geometries of: (a) the TS leading to the preferred product; (b) the minor product (η<sup>6</sup>-arene=benzene); and (c) the more favourable TS for η<sup>6</sup>-arene=hexamethylbenzene, as suggested by DFT calculations.

**Table 20.** Enantioselective synthesis of optically active deuteriobenzyl alcohol by transfer hydrogenation catalyzed by a chiral ruthenium complex [RuCl{YCH(C<sub>6</sub>H<sub>5</sub>)CH(C<sub>6</sub>H<sub>5</sub>)NH<sub>2</sub>}η<sup>6</sup>-arene]

Y	η <sup>6</sup> -Arene	Aldehyde	H-source	ee (%)	Yield (%)	Configuration
NTs	<i>p</i> -Cymene	C <sub>6</sub> H <sub>5</sub> CDO	<i>i</i> -C <sub>3</sub> H <sub>7</sub> OH	98	100	<i>R</i>
NTs	Benzene	C <sub>6</sub> H <sub>5</sub> CDO	<i>i</i> -C <sub>3</sub> H <sub>7</sub> OH	97	100	<i>R</i>
NTs	<i>p</i> -Cymene	<i>p</i> -CH <sub>3</sub> OC <sub>6</sub> H <sub>4</sub> CHO	DCO <sub>2</sub> D	98	93	<i>S</i>
NTs	<i>p</i> -Cymene	<i>p</i> -CH <sub>3</sub> C <sub>6</sub> H <sub>4</sub> CHO	DCO <sub>2</sub> D	98	92	<i>S</i>
NTs	<i>p</i> -Cymene	C <sub>6</sub> H <sub>5</sub> CHO	DCO <sub>2</sub> D	99	97	<i>S</i>
NTs	<i>p</i> -Cymene	<i>p</i> -BrC <sub>6</sub> H <sub>4</sub> CHO	DCO <sub>2</sub> D	99	99	<i>S</i>
NTs	<i>p</i> -Cymene	<i>p</i> -CF <sub>3</sub> C <sub>6</sub> H <sub>4</sub> CHO	DCO <sub>2</sub> D	97	95	<i>S</i>
O	Benzene	<i>p</i> -OCH <sub>3</sub> C <sub>6</sub> H <sub>4</sub> CDO	<i>i</i> -C <sub>3</sub> H <sub>7</sub> OH	61		<i>R</i>
O	Benzene	<i>p</i> -CH <sub>3</sub> C <sub>6</sub> H <sub>4</sub> CDO	<i>i</i> -C <sub>3</sub> H <sub>7</sub> OH	49		<i>R</i>
O	Benzene	C <sub>6</sub> H <sub>5</sub> CDO	<i>i</i> -C <sub>3</sub> H <sub>7</sub> OH	45		<i>R</i>
O	Benzene	<i>p</i> -BrC <sub>6</sub> H <sub>4</sub> CDO	<i>i</i> -C <sub>3</sub> H <sub>7</sub> OH	37		<i>R</i>
O	Benzene	<i>p</i> -CF <sub>3</sub> C <sub>6</sub> H <sub>4</sub> CDO	<i>i</i> -C <sub>3</sub> H <sub>7</sub> OH	20		<i>R</i>

TS model for the osmium-catalyzed asymmetric dihydroxylation. <sup>132</sup> He suggested that the  $\pi/\pi$  stacking (substrate vs aromatic ring of **45**) and CH/ $\pi$  interaction (substrate vs aromatic ring of **44**) is responsible for stabilizing the transition-state, leading to the preferred product. In this model, the ligand forms a chiral L-shaped cleft to be nestled in by the aromatic or aliphatic group of the substrates; the pro-*R* conformer can be stabilized more readily than the pro-*S* conformer. In support of this suggestion, the introduction

**Table 21.** Stereoselectivity in the transfer hydrogenation of various ketones catalyzed by [Ru(*p*-cymene)Cl<sub>2</sub>]<sub>2</sub> and *S*-1,2,3,4-tetrahydroquinolinyl-oxazolines **43**

R in <b>43</b>	Temperature (°C)	Time (h)	ee (%)	Yield (%)
C <sub>6</sub> H <sub>5</sub>	82	1	44	71
C <sub>6</sub> H <sub>5</sub>	25	2	73	56
C <sub>6</sub> H <sub>5</sub>	0	5	75	50
C <sub>6</sub> H <sub>5</sub>	-20	21	83	46
CH <sub>2</sub> C <sub>6</sub> H <sub>5</sub>	82	1	12	43
CH(CH <sub>3</sub> ) <sub>2</sub>	82	1	16	40

**Table 22.** Osmium-catalyzed asymmetric dihydroxylation reactions of olefins with aromatic substituents

R	Temperature (°C)	Rate <sup>a</sup>	ee (%)	Configuration
<i>n</i> -C <sub>8</sub> H <sub>17</sub>	0	1065	84	<i>R</i>
C <sub>6</sub> H <sub>5</sub>	0	7320	97	<i>R</i>
C <sub>6</sub> H <sub>5</sub>	rt <sup>b</sup>		94	<i>R</i>
2-C <sub>10</sub> H <sub>8</sub>	0	35,600	98	<i>R</i>
2-C <sub>10</sub> H <sub>8</sub>	rt		98	<i>R</i>

<sup>a</sup> Ceiling rate constant  $k_c$  [L/(mol min)] measured in *t*-BuOH at 25 °C.

<sup>b</sup> Room temperature.

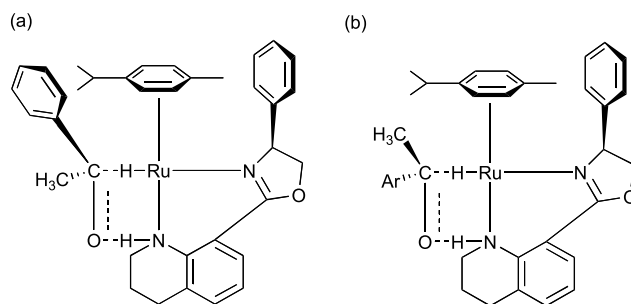
of a *t*-butyl group at R<sup>2</sup> of styrene barely affected the stereochemical result, whereas the substitution at R<sup>1</sup> significantly decreased the enantioselectivity (Table 23). This result is reasonable, since, in the latter case, the *t*-butyl group is forced to reside at position B, thus disturbing entry into the cleft (see Ref. 132 – Sharpless model leading to the preferred dihydroxylation product with the *R*-configuration (stereoview)).

The reaction mechanism of the OsO<sub>4</sub>-complex catalyzed asymmetric dihydroxylation of terminal aliphatic *n*-alkenes (from propene to 1-decene) has been studied by the hybrid quantum mechanics (Becke3LPY) and molecular mechanics (MM3) method. <sup>133</sup> The experimental features, namely

**Table 23**

R <sup>1</sup>	R <sup>2</sup>	ee (%) (273 K)	$\Delta\Delta G^a$
H	H	97	2.3
H	<i>t</i> -C <sub>4</sub> H <sub>9</sub>	95	2.0
<i>t</i> -C <sub>4</sub> H <sub>9</sub>	<i>t</i> -C <sub>4</sub> H <sub>9</sub>	49	0.6

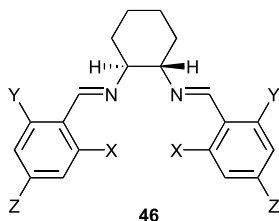
<sup>a</sup> kcal mol<sup>-1</sup> (273 K).

**Figure 52.** Proposed transition geometries of the transfer hydrogenation of acetophenone using [Ru(*p*-cymene)Cl<sub>2</sub>]<sub>2</sub> and chiral 1,2,3,4-tetrahydroquinolinyl-oxazoline **43** (R=C<sub>6</sub>H<sub>5</sub>) as precatalyst: (a) more stable TS; and (b) less stable TS.



the selectivity leading to the *R* product and the dependence of the enantiomeric excess on the length of the aliphatic chain, have been satisfactorily reproduced. These workers attributed the origin of the enantioselectivity to the CH/ $\pi$  hydrogen bonds operating between the aliphatic CHs of the substrate and the aromatic rings of the chiral ligand [bis(dihydroquinidine)pyridazine] in the osmium complex. The selectivity has increased with the elongation of the aliphatic chain until a ceiling value (79% ee with 1-pentene, by experiments; 82% ee for 1-hexene, by the calculations) is reached, with further elongations giving little effect on the enantiomeric excess. This apparently peculiar phenomenon may be ascribed to the difference in the stability of the conformation involved in the transition states.

Asymmetric alkene aziridination is a reaction that holds considerable potential as a synthetic tool (Fig. 53). Jacobsen et al. reported that benzylidene derivatives of 1,2-diaminocyclohexane **46** are effective ligands for copper-catalyzed enantioselective aziridination.<sup>134</sup> A significant improvement in enantioselectivity was observed when substituents were introduced at positions 2 and 6 of the benzal moiety in **46**. Table 24 summarizes their results in the asymmetric aziridination of 6-cyano-2,2-dimethylchromene as substrate. A similar result was obtained for the asymmetric cyclopropanation with the same catalysts.<sup>135</sup>



The crystal structure of a Cu(I) complex of **46** (X=Y=Z = *t*-C<sub>4</sub>H<sub>9</sub>) bound to styrene was determined (Fig. 54).<sup>136</sup> Two 1,3,5-tri-*t*-butylphenyl groups in the ligand are orthogonal to each other, with the phenyl group of styrene lying squarely in the resulting cleft. One of the aromatic *ortho*-CHs and *cis*- $\beta$ -hydrogens of the substrate styrene were found to stabilize the structure of the complex. A preferential binding, in solution, of one enantioface of the alkene to the chiral complex has been shown from inspection of the relevant <sup>1</sup>H and <sup>13</sup>C NMR signals at low temperature.

Scott and co-workers found that diiminocyclohexane derivatives **47** were effective in the asymmetric aziridination of alkenes including styrene derivatives and cinnamate esters.<sup>137</sup> They assessed the performance of the different ligands in a test reaction using chromene **48** (Fig. 55) and discussed the structural origin of a variation in the catalyst efficiency in the enantioselective aziridination (Table 25).

The introduction of groups at positions 2 and 6 increased the enantioselectivity. This suggests that twisting of the axial ligand constitutes an essential part of the mechanism of enantioselection. Scott et al. also studied the aziridination of cinnamate esters, which may allow access to phenylalanine analogs (Table 26).

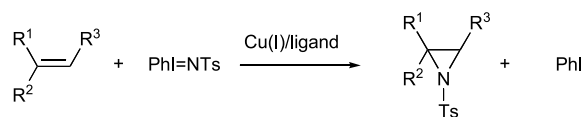


Figure 53.

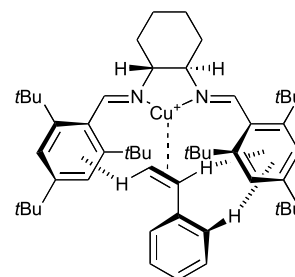


Figure 54. TS geometry of the reaction of styrene with a copper complex of **46**.

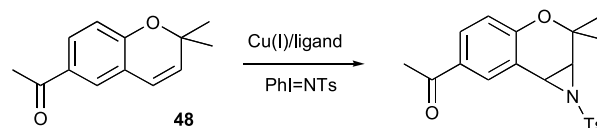
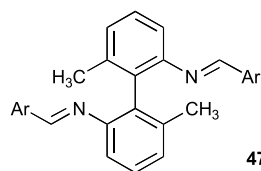
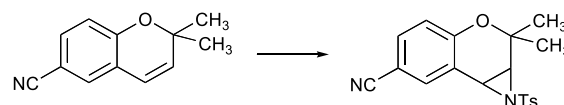


Figure 55. Asymmetric aziridination of chromene **48**.

The crystal structures were determined for the complexes [CuL(CH<sub>3</sub>CN)<sub>2</sub>][BF<sub>4</sub>] (L = **47**, X = Y = Cl, Z = H) and [CuL<sub>2</sub>][OTf]<sub>2</sub> (L = **47**, X = Y = H, Z = *t*-C<sub>4</sub>H<sub>9</sub>).<sup>138</sup> A short CH/ $\pi$  contact was noted in the former complex between a

Table 24.



X	Y	Z	% ee	Turnover
H	H	H	50	10
F	H	H	64	3.6
Cl	H	H	72	3.6
Br	H	H	81	8.2
H	H	Br	42	3.6
Cl	Cl	H	> 98	16
CH <sub>3</sub>	CH <sub>3</sub>	CH <sub>3</sub>	92	6.1

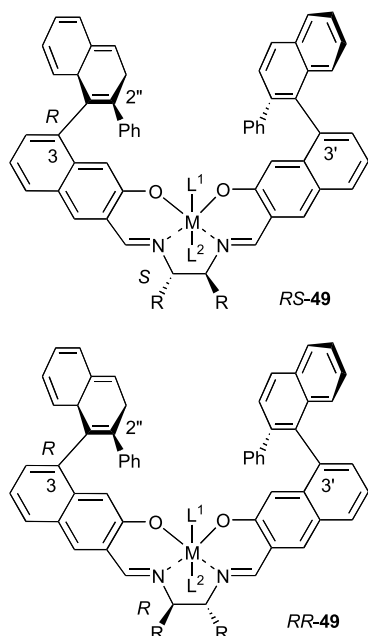
Table 25

Ligand	Temperature (°C)	ee (%)	Yield (%)
4-C <sub>6</sub> H <sub>4</sub> - <i>t</i> Bu	rt <sup>a</sup>	13	53
2-Naphthyl	rt	16	75
2,6-C <sub>6</sub> H <sub>3</sub> Cl <sub>2</sub>	rt	86	83
2,6-C <sub>6</sub> H <sub>3</sub> Cl <sub>2</sub>	-40	85	80
2,4,6-C <sub>6</sub> H <sub>2</sub> Me <sub>3</sub>	rt	94	79
10-Anthryl	rt	55	56
4-C <sub>6</sub> H <sub>4</sub> -NO <sub>2</sub>	rt	65	0

<sup>a</sup> Room temperature.

CH in CH<sub>3</sub>CN and the aromatic part of the pre-catalyst. In the latter crystal, CH/ $\pi$  contacts were found between the *t*-butyl group and the aromatic ring. They concluded that these interactions play a role in stabilizing the structure of the complexes.

Katsuki achieved high enantioselectivity in various oxidation reactions by using (salen)manganese complexes such as **49** (M=Mn; R=Ph) bearing asymmetric components in their ethylenediamine and salicylaldehyde moieties.



They found that *RS-49* was more effective in the catalytic enantiomeric epoxidation, whereas *RR-49* was more effective in the C–H hydroxylation. The enantioselectivity was also affected by the presence and absence of the apical donor ligands. The addition of 4-phenylpyridine *N*-oxide in the *RS-49*-catalyzed epoxidation increased the enantioselectivity, whereas the selectivity of the *RR-49*-catalyzed hydroxylation was decreased by the addition of the donor. In order to clarify the reason for this peculiar phenomenon, they determined the crystal structures of four complexes (Fig. 56).<sup>139</sup>

Table 26.

X	R	ee (%)	Yield (%)
H	CH <sub>3</sub>	69	70
H	C <sub>2</sub> H <sub>5</sub>	75	63
H	<i>t</i> -C <sub>4</sub> H <sub>9</sub>	77	59
<i>p</i> -CH <sub>3</sub>	<i>t</i> -C <sub>4</sub> H <sub>9</sub>	60	59
<i>p</i> -OCH <sub>3</sub>	<i>t</i> -C <sub>4</sub> H <sub>9</sub>	87	51
<i>p</i> -F	<i>t</i> -C <sub>4</sub> H <sub>9</sub>	92	66
<i>p</i> -Cl	<i>t</i> -C <sub>4</sub> H <sub>9</sub>	85	69
<i>p</i> -Br	<i>t</i> -C <sub>4</sub> H <sub>9</sub>	96	45
<i>p</i> -NO <sub>2</sub>	<i>t</i> -C <sub>4</sub> H <sub>9</sub>	0	0
<i>m</i> -NO <sub>2</sub>	<i>t</i> -C <sub>4</sub> H <sub>9</sub>	61	28

It is clear from Figure 56 that the basal salen ligands are in a slightly distorted square planar geometry with a stepped conformation. The sense of the folding of the chelate ring is opposite in *RS-49* and *RR-49*. In every case, the 2''-phenyl group is very close and almost perpendicular to the C3'-naphthalene ring. This is attributable to the aromatic CH/ $\pi$  hydrogen bonds. Further, OH/ $\pi$  interactions between the aqua ligands and the 2'-phenyl groups on the naphthyl substituents stabilize the structure of the complexes. The degree of folding of the salen ligands in these four complexes is, however, considerably different. *RS-49a* takes a shallow stepped conformation, while *RR-49a* takes a deeply folded stepped conformation. In *RS-49a*, the OH/ $\pi$  interactions work to pull up the left half of the salen and down the right half, while the chelation effect moves down the left half of the ligand and up the right half. These two effects cancel each other and *RS-49a* takes a shallow stepped conformation, accordingly. In *RR-49a*, however, the two factors cooperatively work to increase the ligand folding. In the case of *RS-49*, replacement of one of the two aqua ligands by cyclopentene oxide is accompanied by an increase of the ligand folding. On the contrary, in *RR-49*, the folding of the ligand decreased on substitution of L<sup>1</sup> from H<sub>2</sub>O to C<sub>5</sub>H<sub>8</sub>O. The conformational change of the complexes brought about by the ligand exchange is attributed to the CH/ $\pi$  hydrogen bonds (C<sub>5</sub>H<sub>8</sub>O/2''-Ph), which disturb the formation of one of the two OH/ $\pi$  bonds. Sufficient twisting of the axially chiral ligand seems to be essential for the effective enantioselectivity.

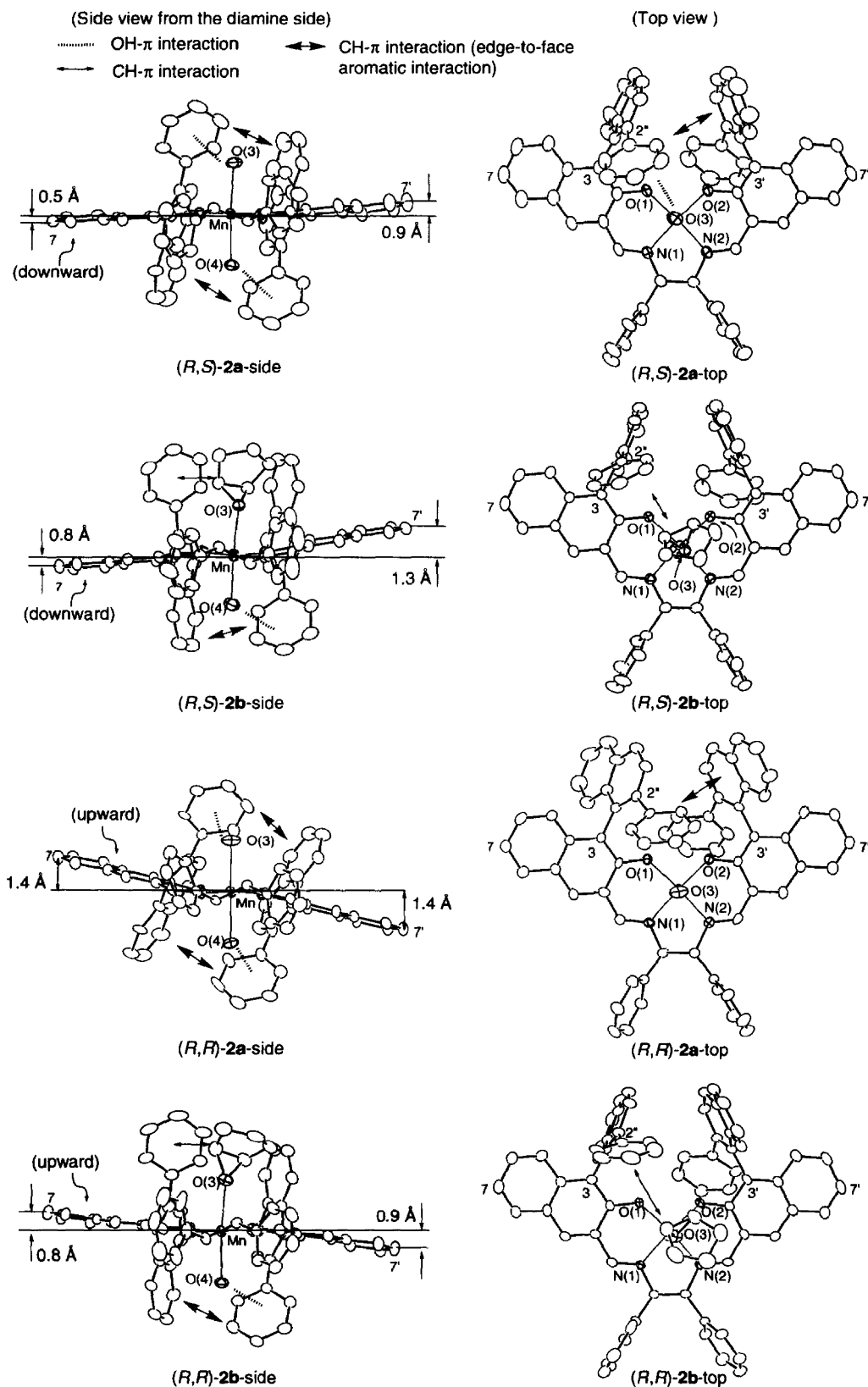
The same workers also reported the hafnium(salen) complex-catalyzed addition of benzenethiol to *N*-(2-alkenoyl)-oxazolidinones. Good enantioselectivity was obtained only when a primary alkyl group was introduced as R (Table 27).<sup>140</sup>

The crystal structure of the hafnium complex (**49**, M=Hf; R=H; L=OPh) was determined. The complex adopted a slightly distorted pentagonal bipyramidal structure, in which two phenoxy ligands occupied the axial positions and one water molecule was equatorially coordinated (Fig. 57). The complex was stabilized by OH/ $\pi$  (H<sub>2</sub>O/naphthalene ring) and CH/ $\pi$  (2'-Ph/OPh) hydrogen bonds, benzenethiol attacking the *si*-face of the  $\beta$ -carbon of the alkenoyl group to give the *S*-adduct, preferentially. This model explains why the good substrates are limited to *N*-(2-alkenoyl)-oxazolidinones bearing a primary alkyl group. Katsuki suggested that the enantioselective Bayer–Villiger

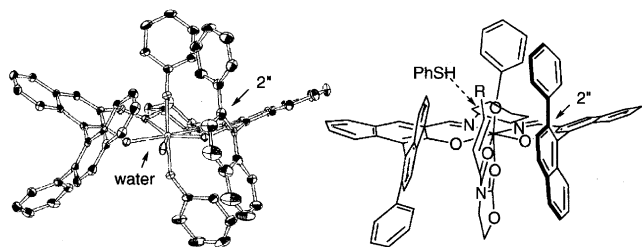
Table 27.

	ee (%)	Yield (%)
CH <sub>3</sub>	92–93	75–81
C <sub>2</sub> H <sub>5</sub>	87	77
<i>n</i> -C <sub>5</sub> H <sub>11</sub>	84	73
<i>i</i> -C <sub>3</sub> H <sub>7</sub>	59	31
C <sub>6</sub> H <sub>5</sub>	59	10
<i>t</i> -C <sub>4</sub> H <sub>9</sub>		NR <sup>a</sup>

<sup>a</sup> No reaction.



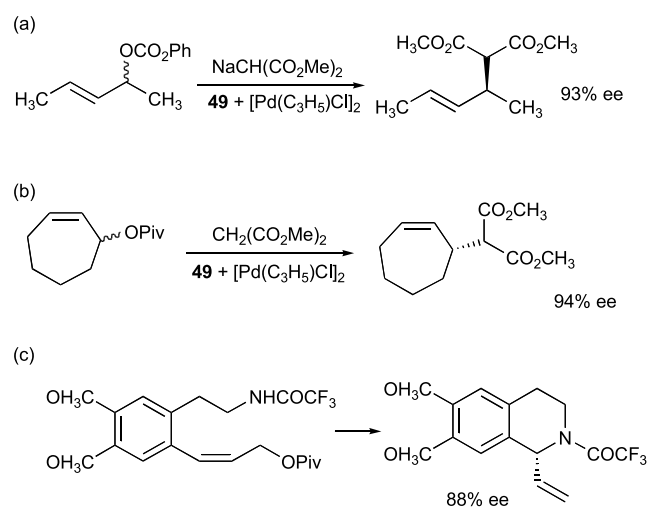
**Figure 56.** Crystal structures of (salen)manganese(III) complexes: (a) *RS*-49a:  $L^1=L^2=H_2O$ ; (b) *RS*-49b:  $L^1$ =cyclopentene oxide;  $L^2=H_2O$ ; (c) *RR*-49a:  $L^1=L^2=H_2O$ ; and (d) *RR*-49b:  $L^1$ =cyclopentene oxide;  $L^2=H_2O$  (adapted from Figure 3 of Ref. 139).



**Figure 57.** X-ray structure of a hafnium complex **49** (M=Hf; R=H; L=OC<sub>6</sub>H<sub>5</sub>) and the proposed structure of 9-N-(2-alkenoyl)-oxazolidinone adduct (Figure 2 of Ref. 140).

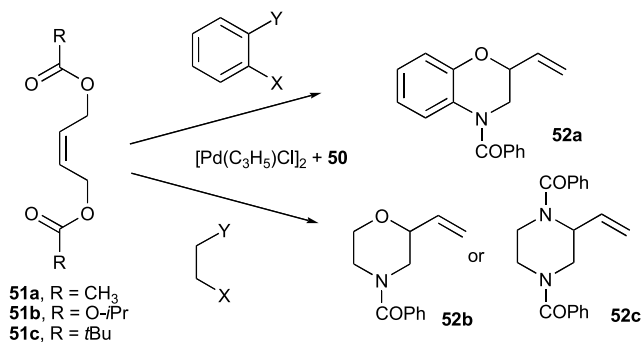
oxidation, catalyzed by a zirconium complex (**49**, M=Zr),<sup>141</sup> proceeds with a similar mechanism.

Katsuki et al. also reported that a 2-(phosphinophenyl)-



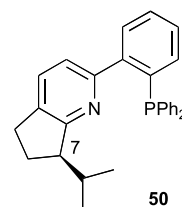
**Figure 58.** Palladium-catalyzed allylic alkylation reactions (a) and (b) and asymmetric intramolecular allylic amination (c).

**Table 28.**



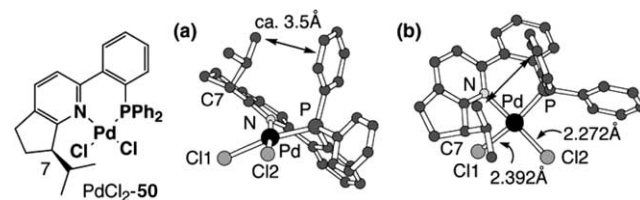
Substrate	Nucleophile	Product	Temperature (°C)	Time (h)	ee (%)	Yield (%)
<b>51a</b>	2-(Benzylamino)phenol	<b>52a</b>	rt	24	66	98
<b>51b</b>	2-(Benzylamino)phenol	<b>52a</b>	rt	24	72	89
<b>51b</b>	2-(Benzylamino)phenol	<b>52a</b>	0	72	86	96
<b>51c</b>	2-(Benzylamino)phenol	<b>52a</b>	rt	24	67	92
<b>51a</b>	2-(Benzylamino)ethanol	<b>52b</b>	rt	24	69	67
<b>51c</b>	2-(Benzylamino)ethanol	<b>52b</b>	0	72	81	74
<b>51a</b>	15-Bis(benzylamino)ethane	<b>52c</b>	rt	24	54	85
<b>51b</b>	15-Bis(benzylamino)ethane	<b>52c</b>	rt	24	76	81
<b>51c</b>	15-Bis(benzylamino)ethane	<b>52c</b>	0	72	86	88

pyridine complex **50** bearing an isopropyl group is an efficient chiral auxiliary for palladium-catalyzed allylic alkylation reactions (Fig. 58a and b)<sup>142,143</sup> and an asymmetric intramolecular allylic amination (Fig. 58c).<sup>144</sup>



The selectivity was also examined for the Pd-catalyzed tandem allylic substitution of *Z*-1,4-dialkoxy- and *Z*-1,4-bis(alkoxycarbonyloxy)-2-butene **51** using the 2-(phosphinophenyl)pyridine **50** as a chiral ligand. Good enantiomeric selectivity was observed, in every case, affording **52a-52c** (Table 28).

The precatalyst **50** was designed with the expectation that the isopropyl group at position 7 may regulate the coordination sphere around the palladium ion and induce high enantioselectivity. The result was as expected.<sup>145</sup> As shown in Figure 59, the six-membered chelate ring in the crystal of **50** adopts an envelope-like form and the palladium atom is out of the plane. One methyl in the



**Figure 59.** Structure of **50**-PdCl<sub>2</sub> complex: (a) front view from a Cl ligand; and (b) top view from the isopropyl group (Figure 1 of Ref. 145).

isopropyl group has been found to be oriented to the pseudoaxial phenyl group, probably due to the CH/ $\pi$  attraction. The other methyl group is enforced, accordingly, to locate above the Cl<sup>1</sup> atom that constitutes an asymmetric coordination sphere.

## 6. Other reactions

Guthrie has studied the base-catalyzed  $\beta$ -elimination and ester hydrolysis with a steroidal enzyme model (Fig. 60). The rate of the catalytic reactions was found to enhance regularly on replacing the phenyl group (9) in the substrate by a naphthyl (27) and then by a phenanthryl group (110).<sup>146</sup> A similar result was found for the hydrolysis of ArCH<sub>2</sub>-CH<sub>2</sub>COOR, where the rate increased from Ar = phenyl (4.5) to naphthyl (11.8) and then to phenanthryl (24.0).<sup>147</sup> The surface area of the aromatic  $\pi$ -plane, capable of interacting with the axial CHs in the steroid, becomes larger in the above order.

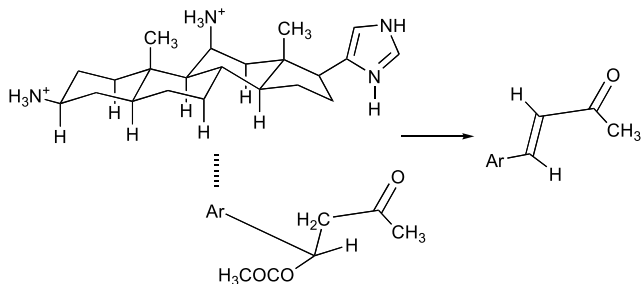


Figure 60.

Endo<sup>148</sup> studied the oxidative coupling of sulphides, XSH and YSH, to disulphides (Fig. 61). The ratio of the products,  $r = \text{XSSY}/\text{XSSX}$  (or  $\text{YSSY}$ ), represents the extent of molecular recognition of the interacting species. The recognition was found to be most specific when a branched alkyl group [X = (CH<sub>3</sub>)<sub>2</sub>CH(CH<sub>2</sub>)<sub>n</sub>CONHCONHCH<sub>2</sub>CH<sub>2</sub>] and an aromatic group [Y = (CH<sub>3</sub>)<sub>2</sub>NC<sub>6</sub>H<sub>4</sub>-CONHCONHCH<sub>2</sub>] were used. In the case of  $n=2$  (*i*-C<sub>5</sub>H<sub>11</sub>),  $r$  reached maximal, but decreased on substitution of the alkyl with a longer group. Molecular models suggested that the intermediate complex of the reacting species could be stabilized by CH/ $\pi$  bonds. The interaction would be most effective if XSH bears a branched alkyl group of an appropriate length; a face-to-face arrangement of the relevant groups seems to be essential for an effective recognition to occur. In support of this suggestion, the C(CH<sub>3</sub>)/C(phenyl) distance in a 1:1 complex of C<sub>6</sub>H<sub>5</sub>CH<sub>2</sub>-

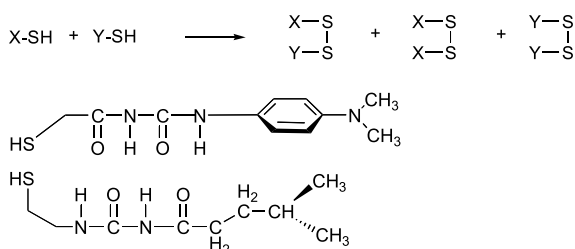


Figure 61.

(CONH)<sub>2</sub>C<sub>6</sub>H<sub>4</sub>N(CH<sub>3</sub>)<sub>2</sub> and *i*-C<sub>4</sub>H<sub>9</sub>(NHCO)<sub>2</sub>C<sub>6</sub>H<sub>4</sub>NO<sub>2</sub> has been found very short (3.60 Å).<sup>149</sup>

An optical activation of ( $\pm$ )-3-(*p*-cumyl)-2-methylpropanal through the enamine intermediate was studied.<sup>150</sup> (*S*)-(+)-3-(*p*-cumyl)-2-methylpropanal was preferentially produced, when (*S*)-3-isopropyl-1-methylpiperazine was used as the amine component. The result was interpreted based on the CH/ $\pi$  hydrogen bonds occurring between the isopropyl group of the piperazine moiety and the aromatic part of the *p*-cumyl-propanal (Fig. 62).

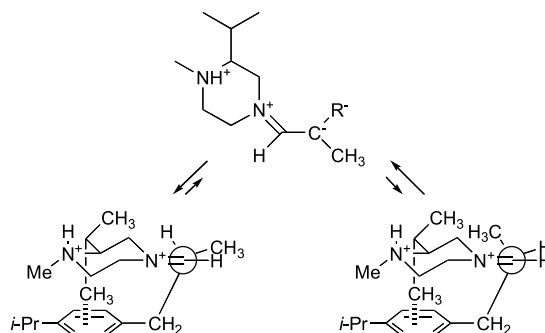


Figure 62.

Thermolysis of sulfoxides bearing at least a  $\beta$ -hydrogen atom proceeds via an intramolecular *cis*-elimination mechanism, affording olefins and sulfenic acids. Yoshimura studied the thermolysis of a series of sulfoxide diastereomers C<sub>6</sub>H<sub>5</sub>SOCHCH<sub>3</sub>C<sub>6</sub>H<sub>4</sub>-X (X = OCH<sub>3</sub>, H, Cl, NO<sub>2</sub>).<sup>151</sup> The pyrolytic rate of the *erythro* isomers was found to be 2- to 3-fold faster than that of the *threo* isomers, irrespective of the reaction conditions and the nature of X. The stable conformer of the *erythro* isomer was suggested to be advantageous for the Ei reaction to take place since the methyl and S-O groups are closer to each other in the *erythro* relative to the *threo* isomers (Fig. 63);<sup>151</sup> the CH/O and CH/ $\pi$  hydrogen bonds play an important role in stabilizing the conformation of the *erythro* sulfoxides.

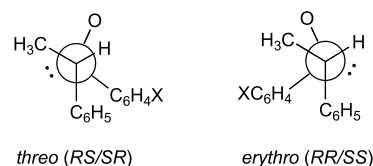


Figure 63.

The involvement of CH/ $\pi$  bonds in reaction selectivity has been argued for the substituent effect on the cyclization of conformationally constrained 1,3-dioxolanyl radicals (Fig. 64).<sup>152</sup> An opposed stereoselectivity was obtained when the phenyl group was replaced by methyl.

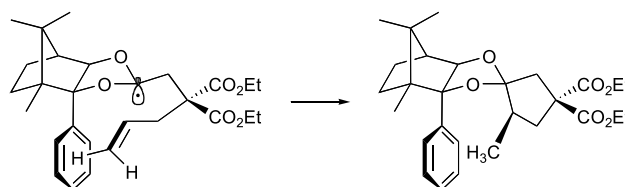


Figure 64.

## 7. Summary and prospects

The energy of the CH/ $\pi$  interaction is the smallest among weak hydrogen bonds. The total stabilization may, however, become significant by cooperation of a number of weak interactions. In addition, the CH/ $\pi$  hydrogen bond is advantageous in view of entropy. As has been demonstrated in every part of the previous sections, the above situation is commonly met in the dynamically interacting molecular systems. In other words, the circumstance for the operation of CH/ $\pi$  hydrogen bonds is pre-arranged in many cases, given that the interacting system bears at least a  $\pi$ -group. The topics cited in this *Report* are limited only to those in papers found by the author; it is probable that many papers have escaped his attention. He is afraid that the discussions raised in the text are too speculative and, therefore, appreciates any criticisms from interested readers. It is hoped that this treatise will stimulate organic chemists seeking efficient and selective methods of synthesizing useful materials.

## Acknowledgements

The author wishes to express his deep gratitude to Emeritus Professor Minoru Hirota (Yokohama National University), Drs Ken Nishihata, Yoshio Kodama, Shoji Zushi (Meiji Seika Kaisha, Ltd.), Sei Tsuboyama, Jun Uzawa (RIKEN), Yoji Umezawa (Microbial Chemistry Research Center), Kazumasa Honda (National Institute of Advanced Industrial Science and Technology), Hiroko Suezawa (Ministry of Education, Culture, Sports, Science and Technology), Osamu Takahashi (Hiroshima University) and Yuji Kohno (Tohoku University) for their cooperation in a long-term pursuit of the CH/ $\pi$  hydrogen bond. He also thanks Professors Tsutomu Katsuki (Kyushu University), Kendall N. Houk (UCLA), Masami Sakamoto (Chiba University), Drs Takahiko Kojima (Kyushu University) and Seiji Tsuzuki (National Institute of Advanced Industrial Science and Technology) for reading the relevant parts of the original manuscript. Many thanks are also due to Professors Takayuki Shioiri (Meijo University) and William B. Motherwell (University College, London), who kindly provided the author the opportunity to write this *Report*, and for their encouragement. It is a privilege of the author to dedicate this *Report* to the memory of Sir Derek H. R. Barton, to whose foresighted work we owe much for the progress of stereochemistry in organic reactions.

## References and notes

- Nishio, M.; Hirota, M.; Umezawa, Y. *The CH/ $\pi$  Interaction. Evidence, Nature, and Consequences*; Wiley-VCH: New York, 1998.
- Jeffrey, G. A. *An Introduction to Hydrogen Bonding*; Oxford University Press: Oxford, 1997.
- Steiner, T. *Angew. Chem., Int. Ed.* **2002**, 48–76.
- Nishio, M.; Hirota, M. *Tetrahedron* **1989**, 45, 7201–7245.
- Nishio, M.; Umezawa, Y.; Hirota, M.; Takeuchi, Y. *Tetrahedron* **1995**, 51, 8665–8701.

- Desiraju, G. R.; Steiner, T. *The Weak Hydrogen Bond in Structural Chemistry and Biology*; Oxford University Press: Oxford, 1999.
- Desiraju, G. R. *Acc. Chem. Res.* **2002**, 35, 565–573.
- Nishio, M. Weak Hydrogen Bonds. In *Encyclopedia of Supramolecular Chemistry*; Atwood, J. L., Steed, J. W., Eds.; Marcel Dekker: New York, 2004; pp 1576–1585.
- Nishio, M.; Hirota, M.; Umezawa, Y. *The CH/ $\pi$  Interaction. Evidence, Nature, and Consequences*; Wiley-VCH: New York, 1998; Chapter 2.
- Nishio, M. *CrystEngComm* **2004**, 6, 130–158.
- Takahashi, O.; Kohno, Y.; Iwasaki, S.; Saito, K.; Iwaoka, M.; Tomoda, S.; Umezawa, Y.; Tsuboyama, S.; Nishio, M. *Bull. Chem. Soc. Jpn.* **2001**, 74, 2421–2430.
- Suezawa, H.; Yoshida, T.; Ishihara, S.; Umezawa, Y.; Nishio, M. *CrystEngComm* **2003**, 5, 514–518.
- Novoa, J. J.; Mota, F. *Chem. Phys. Lett.* **2000**, 318, 345–354.
- Takahashi, O.; Kohno, Y.; Saito, K. *Chem. Phys. Lett.* **2003**, 378, 509–515.
- Tsuzuki, S.; Honda, K.; Uchimaru, T.; Mikami, M.; Tanabe, K. *J. Phys. Chem. A* **1999**, 103, 8265–8271.
- Tsuzuki, S.; Honda, K.; Uchimaru, T.; Mikami, M.; Tanabe, K. *J. Am. Chem. Soc.* **2000**, 122, 3746–3753.
- Tsuzuki, S.; Honda, K.; Uchimaru, T.; Mikami, M.; Tanabe, K. *J. Am. Chem. Soc.* **2002**, 124, 104–112.
- Tsuzuki, S.; Honda, K.; Uchimaru, T.; Mikami, M.; Tanabe, K. *J. Phys. Chem. A* **2002**, 106, 4423–4428.
- Ehama, R.; Yokoo, A.; Tsushima, M.; Yuzuri, T.; Suezawa, H.; Hirota, M. *Bull. Chem. Soc., Jpn.* **1993**, 66, 814–818.
- Adams, H.; Carver, F. J.; Hunter, C. A.; Morales, J. C.; Seward, E. M. *Angew. Chem., Int. Ed.* **1996**, 35, 1542–1544.
- Kim, E.-I.; Paliwal, S.; Wilcox, C. S. *J. Am. Chem. Soc.* **1998**, 120, 11192–11193.
- Caciuffo, R.; Galeazzi, R.; Horsewill, A. J.; Ikram, A.; Ugozzoli, F. *Phys. Rev. B* **1999**, 60, 11867–11870.
- Arena, G.; Contino, A.; Magri, A.; Sciotto, D.; Arduini, A.; Pochini, A.; Secchi, A. *Supramol. Chem.* **2001**, 13, 379–386.
- Tsuzuki, S.; Honda, K.; Uchimaru, T.; Mikami, M.; Tanabe, K. *J. Am. Chem. Soc.* **2000**, 122, 11450–11458.
- Gu, Y.; Kar, T.; Scheiner, S. *J. Am. Chem. Soc.* **1999**, 121, 9411–9422.
- Fujii, A.; Morita, S.; Miyazaki, M.; Ebata, T.; Mikami, N. *J. Phys. Chem. A* **2004**, 108, 2652–2658.
- Nishio, M. *Kagaku no Ryoiki*, **1977**, 31, 998–1006; **1979**, 33, 422–432; **1983**, 37, 243–251.
- Kodama, Y.; Nishihata, K.; Nishio, M.; Uzawa, J.; Sakamoto, K.; Iwamura, H. *Bull. Chem. Soc. Jpn.* **1979**, 52, 2661–2669.
- Zushi, S.; Kodama, Y.; Nishihata, K.; Umemura, K.; Nishio, M.; Uzawa, J.; Hirota, M. *Bull. Chem. Soc. Jpn.* **1980**, 53, 3631–3640.
- García, J. I.; Mayoral, J. A.; Salvatella, L. *Acc. Chem. Res.* **2000**, 33, 658–664.
- Sodupe, M.; Rios, R.; Branchadell, V.; Nicholas, T.; Oliva, A.; Dannenberg, J. J. *J. Am. Chem. Soc.* **1997**, 119, 4232–4238.
- Allen, F. H.; Lommerse, J. P. M.; Hoy, V. J.; Howard, J. A. K.; Desiraju, G. R. *Acta Crystallogr. Sect. B* **1996**, 52, 734–735.
- Ujaque, G.; Lee, P. S.; Houk, K. N.; Hentemann, M. F.; Danishefsky, S. J. *Chem. Eur. J.* **2002**, 8, 3423–3430.
- Kobuke, Y.; Fueno, T.; Furukawa, J. *J. Am. Chem. Soc.* **1970**, 92, 6548–6553.



35. Mataka, S.; Ma, J.; Thiemann, T.; Rudzinski, J. M.; Tsuzuki, H.; Sawada, T.; Tashiro, M. *Tetrahedron* **1997**, *53*, 885–902.
36. Mataka, S.; Ma, J.; Thiemann, T.; Miura, T.; Sawada, T.; Tashiro, M. *Tetrahedron* **1997**, *53*, 6817–6824.
37. Closs, G. L.; Moss, R. A. *J. Am. Chem. Soc.* **1964**, *86*, 4042–4053.
38. Moss, R. A. *J. Org. Chem.* **1965**, *30*, 3261–3265.
39. Casey, C. P.; Polichnowski, S. W.; Shusterman, A. J.; Jones, C. R. *J. Am. Chem. Soc.* **1979**, *101*, 7282–7292.
40. Yamato, T.; Miyazawa, A.; Tashiro, M. *J. Chem. Soc., Perkin Trans. I* **1993**, 3127–3137.
41. Honda, K.; Nakanishi, F.; Feeder, N. *J. Am. Chem. Soc.* **1999**, *121*, 8246–8250.
42. Honda, K.; Nakanishi, F.; Lee, S.-A.; Mikami, M.; Tsuzuki, S.; Yamamoto, T.; Feeder, N. *Mol. Cryst. Liq. Cryst.* **2001**, *356*, 413–422.
43. Hasegawa, T.; Ikeda, K.; Yamazaki, Y. *J. Chem. Soc., Perkin Trans. I* **2001**, 3025–3028.
44. Sakamoto, M.; Takahashi, M.; Fujita, T.; Watanabe, S.; Nishio, T.; Iida, I.; Aoyama, H. *J. Org. Chem.* **1997**, *62*, 6298–6308.
45. Obata, T.; Shimo, T.; Yasutake, M.; Shinmyozu, T.; Kawaminami, M.; Yoshida, R.; Somekawa, K. *Tetrahedron* **2001**, *57*, 1531–1541.
46. Matsumoto, A. *Polym. J.* **2003**, *35*, 93–121.
47. Matsumoto, A.; Tanaka, T.; Tsubouchi, T.; Tashiro, K.; Saragai, S.; Nakamoto, S. *J. Am. Chem. Soc.* **2002**, *124*, 8891–8902.
48. Nagahama, S.; Inoue, K.; Sada, K.; Miyata, M.; Matsumoto, A. *Cryst. Growth Des.* **2003**, *3*, 247–256.
49. Tanaka, T.; Matsumoto, A. *J. Am. Chem. Soc.* **2002**, *124*, 9676–9677.
50. Cram, D. J.; Abd Elhafez, F. A. *J. Am. Chem. Soc.* **1952**, *74*, 5828–5835.
51. Cornforth, J. W.; Cornforth, R. H.; Mathew, K. K. *J. Chem. Soc.* **1959**, 112–121.
52. Karabatsos, G. J. *J. Am. Chem. Soc.* **1967**, *89*, 1367–1371.
53. Chérest, M.; Felkin, H.; Prudent, N. *Tetrahedron Lett.* **1968**, 2199–2204.
54. Mengel, A.; Reiser, O. *Chem. Rev.* **1999**, *99*, 1191–1223.
55. Eliel, E. L.; Frye, S. V.; Hortelano, E. R.; Chen, X.; Bai, X. *Pure Appl. Chem.* **1991**, *63*, 1591–1598.
56. Reetz, M. T. *Acc. Chem. Res.* **1993**, *26*, 462–468.
57. Eliel, E. L.; Wilen, S. H.; Mander, L. N. *Stereochemistry of Organic Compounds*; Wiley-Interscience: New York, 1994; pp 876–880.
58. Anh, N. T.; Eisenstein, O. *Tetrahedron Lett.* **1976**, 155–158.
59. Wu, Y.-D.; Houk, K. N. *J. Am. Chem. Soc.* **1987**, *109*, 908–910.
60. Varech, D.; Jacques, J. *Tetrahedron Lett.* **1973**, 4443–4446.
61. Brienne, M. J.; Varech, D.; Jacques, J. *Tetrahedron Lett.* **1974**, 1233–1236.
62. Chérest, M.; Felkin, H.; Tacheau, P.; Jacques, J.; Varech, D. *J. Chem. Soc., Chem. Commun.* **1977**, 372–373.
63. Wong, S. S.; Paddon-Row, M. N. *J. Chem. Soc., Perkin Trans. 2* **1990**, 456–458.
64. Wong, S. S.; Paddon-Row, M. N. *J. Chem. Soc., Chem. Commun.* **1991**, 327–330.
65. Frenking, G.; Köhler, K. F.; Reetz, M. T. *Tetrahedron* **1991**, *47*, 8991–9004.
66. Frenking, G.; Köhler, K. F.; Reetz, M. T. *Tetrahedron* **1991**, *47*, 9005–9018.
67. Fleming, I.; Hrovat, D. A.; Borden, W. T. *J. Chem. Soc., Perkin Trans. 2* **2001**, 331–338.
68. Table 1 in Mengel, A.; Reiser, O. *Chem. Rev.* **1999**, *99*, 1191–1223.
69. Desiraju, G. R.; Steiner, T. *The Weak Hydrogen Bond in Structural Chemistry and Biology*; Oxford University Press: Oxford, 1999; Chapter 2.
70. Novoa, J. J.; Mota, F. *Chem. Phys. Lett.* **1997**, *266*, 23–30.
71. Tsuzuki, S.; Uchimaru, T.; Tanabe, K.; Hirano, T. *J. Phys. Chem.* **1993**, *97*, 1346–1350.
72. Yoshida, H.; Tanaka, T.; Matsuura, H. *Chem. Lett.* **1996**, 637–638.
73. Tsuzuki, S.; Houjou, H.; Nagawa, Y.; Hiratani, K. *J. Chem. Soc., Perkin Trans. 2* **2001**, 1951–1955.
74. Takahashi, O.; Yasunaga, K.; Gondoh, Y.; Kohno, Y.; Saito, K.; Nishio, M. *Bull. Chem. Soc. Jpn.* **2002**, *75*, 1777–1783.
75. Takahashi, O.; Kohno, Y.; Gondoh, Y.; Saito, K.; Nishio, M. *Bull. Chem. Soc. Jpn.* **2003**, *76*, 369–374.
76. Matsuura, H.; Yoshida, H.; Hieda, M.; Yamanaka, S.; Harada, T.; Kei, S.; Ohno, K. *J. Am. Chem. Soc.* **2003**, *125*, 13910–13191.
77. Chérest, M.; Prudent, N. *Tetrahedron* **1980**, *36*, 1599–1606.
78. Takahashi, O.; Saito, K.; Kohno, Y.; Suezawa, H.; Ishihara, S.; Nishio, M. *New J. Chem.* **2004**, *28*, 355–360.
79. Nishio, M.; Hirota, M.; Umezawa, Y. *The CH/π Interaction. Evidence, Nature, and Consequences*; Wiley-VCH: New York, 1998; pp 66–67, 84–85.
80. Takahashi, O.; Gondoh, Y.; Saito, K.; Kohno, Y.; Suezawa, H.; Yoshida, T.; Ishihara, S.; Nishio, M. *New J. Chem.* **2003**, *27*, 1639–1643.
81. Nishihata, K.; Nishio, M. *Tetrahedron Lett.* **1977**, 1041–1044.
82. Morrison, J. D.; Mosher, H. S. *Asymmetric organic reactions*; Prentice-Hall: NJ, 1971.
83. Corey, E. J.; Becker, K. B.; Varma, R. K. *J. Am. Chem. Soc.* **1972**, *94*, 8616–8618.
84. Saito, S.; Morikawa, Y.; Moriwake, T. *J. Org. Chem.* **1990**, *55*, 5424–5426.
85. Saito, S.; Narahara, O.; Ishikawa, T.; Asahara, M.; Moriwake, T.; Gawronski, J.; Kazmierczak, F. *J. Org. Chem.* **1993**, *58*, 6292–6302.
86. Ishikawa, T.; Kudo, T.; Shigemori, K.; Saito, S. *J. Am. Chem. Soc.* **2000**, *122*, 7633–7637.
87. Gung, B. J.; Zhu, Z.; Fouch, R. A. *J. Am. Chem. Soc.* **1995**, *117*, 1783–1788.
88. Takahashi, H.; Umezawa, Y.; Tsuboyama, S.; Uzawa, J.; Nishio, M. *Tetrahedron* **1999**, *55*, 10047–10056.
89. Umezawa, Y.; Tsuboyama, S.; Takahashi, H.; Uzawa, J.; Nishio, M. *Bioorg. Med. Chem.* **1999**, *7*, 2021–2026.
90. Suezawa, H.; Ishihara, S.; Takahashi, O.; Saito, K.; Kohno, Y.; Nishio, M. *New J. Chem.* **2003**, *27*, 1609–1613.
91. Takahashi, O.; Kohno, Y.; Gondoh, Y.; Saito, K.; Nishio, M. *Chem. Eur. J.* **2003**, *9*, 756–762.
92. Takahashi, O.; Saito, K.; Kohno, Y.; Suezawa, H.; Ishihara, S.; Nishio, M. *Bull. Chem. Soc. Jpn.* **2003**, *76*, 2167–2173.
93. Breslow, R.; Corcoran, R.; Dales, J. A.; Liu, S.; Kalicky, P. *J. Am. Chem. Soc.* **1974**, *96*, 1973–1974.
94. Breslow, R.; Corcoran, R. J.; Snider, B. B. *J. Am. Chem. Soc.* **1974**, *96*, 6791–6792.
95. Breslow, R.; Snider, B. B.; Corcoran, R. J. *J. Am. Chem. Soc.* **1974**, *96*, 6792–6794.
96. Snider, B. B.; Corcoran, R. J.; Breslow, R. *J. Am. Chem. Soc.* **1975**, *97*, 6580–6581.

97. Breslow, R.; Rothbard, J.; Herman, F.; Roderiguez, M. *J. Am. Chem. Soc.* **1978**, *100*, 1213–1217.
98. Breslow, R.; Maresca, L. M. *Tetrahedron Lett.* **1978**, 887–890.
99. Fish, P. V.; Johnson, W. S. *J. Org. Chem.* **1994**, *59*, 2324.
100. Nishio, M.; Umezawa, Y.; Hirota, M.; Takeuchi, Y. *Tetrahedron* **1995**, *51*, 8665–8701. Section 4.1.
101. Birwistle, J. S.; Lee, J.; Morrison, J. D.; Sanderson, W. A.; Mosher, H. S. *J. Org. Chem.* **1964**, *29*, 37–40.
102. Capillon, J.; Guetté, J. P. *Tetrahedron* **1979**, *35*, 1817–1820.
103. Okawa, H.; Numata, Y.; Mio, A.; Kida, S. *Bull. Chem. Soc. Jpn.* **1980**, *53*, 2248–2251.
104. Nakamura, M.; Okawa, H.; Inazu, T.; Kida, S. *Bull. Chem. Soc. Jpn.* **1982**, *55*, 2400–2403.
105. Okawa, H.; Ueda, K.; Kida, S. *Inorg. Chem.* **1982**, *21*, 1594–1598.
106. Okawa, H. *Coord. Chem. Rev.* **1988**, *92*, 1–28.
107. Nakamura, M.; Okawa, H.; Kida, S. *Inorg. Chim. Acta* **1984**, *96*, 111.
108. Nakamura, M.; Okawa, H.; Kida, S. *Bull. Chem. Soc. Jpn.* **1985**, *58*, 3377–3378.
109. Okawa, H.; Katsuki, T.; Nakamura, N.; Kumagai, N.; Shuin, Y.; Shimmyozu, T.; Kida, S. *Chem. Commun.* **1989**, 139–140.
110. Yamanari, K.; Dogi, S.; Okubo, K.; Fujihara, T.; Fuyuhiko, A.; Kaizaki, S. *Bull. Chem. Soc. Jpn.* **1994**, *67*, 3004–3008.
111. Yamanari, K.; Nozaki, T.; Fuyuhiko, A.; Kushi, Y.; Kaizaki, S. *J. Chem. Soc., Dalton Trans.* **1996**, 2851–2856.
112. Kojima, T.; Miyazaki, S.; Hayashi, K.; Shimazaki, Y.; Tani, F.; Naruta, Y.; Matsuda, Y. *Chem. Eur. J.* **2004**, *10*, 6402–6410.
113. Brunner, H.; Bauer, I.; Lukas, R. *Z. Naturforsch* **1979**, *34b*, 1418–1423.
114. Brunner, H.; Rastogi, D. K. *Inorg. Chem.* **1980**, *19*, 891–895.
115. Brunner, H.; Aglifoglio, G.; Bernal, I.; Creswick, M. W. *Angew. Chem., Int. Ed.* **1980**, *19*, 647–642.
116. Brunner, H. *Angew. Chem., Int. Ed.* **1999**, *38*, 1195–1208.
117. Brunner, H.; Oeschey, B. R.; Nuber, B. *Angew. Chem., Int. Ed.* **1994**, *33*, 866–868.
118. Brunner, H.; Oeschey, B. R.; Nuber, B. *J. Chem. Soc., Dalton Trans.* **1996**, 1499–1508.
119. Cagle, P. C.; Meyer, O.; Vichard, D.; Weickhardt, K.; Arif, A. M.; Gladysz, J. A. *Organometallics* **1996**, *15*, 194–204.
120. Brunner, H. *Acc. Chem. Res.* **1979**, *12*, 250–257.
121. Brunner, H. *Angew. Chem., Int. Ed.* **1983**, *22*, 987–1012.
122. Noyori, R.; Hashiguchi, S. *Acc. Chem. Res.* **1997**, *30*, 97–102.
123. Yamakawa, M.; Ito, H.; Noyori, R. *J. Am. Chem. Soc.* **2000**, *122*, 1466–1478.
124. Yamada, I.; Noyori, R. *Org. Lett.* **2001**, *2*, 3425–3427.
125. Yamakawa, M.; Yamada, I.; Noyori, R. *Angew. Chem., Int. Ed.* **2001**, *40*, 2818–2821.
126. Zhou, Y.-B.; Tang, F.-Y.; Xu, H.-D.; Wu, X.-Y.; Ma, J.-A.; Zhou, Q.-L. *Tetrahedron: Asymmetry* **2002**, *13*, 469–473.
127. Arena, C. G.; Calamia, S.; Faraone, F.; Graiff, C.; Tiripicchio, A. *J. Chem. Soc., Dalton Trans.* **2000**, 3149–3157.
128. Rath, R. K.; Nethaji, M.; Chakravarty, A. R. *Polyhedron* **2002**, *21*, 1929–1934.
129. Sharpless, K. B.; Amberg, W.; Bennani, Y. L.; Crispino, G. A.; Hartung, J.; Jeong, H.-L.; Morikawa, K.; Wang, Z.-M.; Xu, D.; Zhang, X.-L. *J. Org. Chem.* **1992**, *57*, 2768.
130. Corey, E. J.; Noe, M. C. *J. Am. Chem. Soc.* **1993**, *115*, 12579–12580.
131. Kolb, H. C.; Andersson, P. G.; Sharpless, K. B. *J. Am. Chem. Soc.* **1994**, *116*, 1278–1291.
132. Becker, H.; Hou, P.-T.; Kolb, H. C.; Loren, S.; Norrby, P.-O.; Sharpless, K. B. *Tetrahedron Lett.* **1994**, *35*, 7315–7318.
133. Drudis-Solé, G.; Ujaque, G.; Maseras, F.; Lledós, A. *Chem. Eur. J.* **2005**, *11*, 1017–1029.
134. Li, Z.; Conser, K. R.; Jacobsen, E. N. *J. Am. Chem. Soc.* **1993**, *115*, 5326–5327.
135. Li, Z.; Quan, R. W.; Jacobsen, E. N. *J. Am. Chem. Soc.* **1995**, *117*, 5889–5890.
136. Quan, R. W.; Li, Z.; Jacobsen, E. N. *J. Am. Chem. Soc.* **1996**, *118*, 8156–8157.
137. Sanders, C. J.; Gillespie, K. M.; Bell, D.; Scott, P. *J. Am. Chem. Soc.* **2000**, *122*, 7132–7133.
138. Gillespie, K. M.; Sanders, C. J.; O’Shaughnessy, P.; Westmoreland, I.; Thickitt, C. P.; Scott, P. *J. Org. Chem.* **2002**, *67*, 3450–3458.
139. Hashihayata, T.; Punniyamurthy, T.; Irie, R.; Katsuki, T.; Akita, M.; Morooka, Y. *Tetrahedron* **1999**, *55*, 14599–14610.
140. Matsumoto, K.; Watanabe, A.; Uchida, T.; Ogi, K.; Katsuki, T. *Tetrahedron Lett.* **2004**, *45*, 2385–2388.
141. Watanabe, A.; Uchida, T.; Ito, K.; Katsuki, T. *Tetrahedron Lett.* **2002**, *43*, 4481–4485.
142. Ito, K.; Kashiwagi, R.; Iwasaki, K.; Katsuki, T. *Synlett* **1999**, 1563–1566.
143. Ito, K.; Kashiwagi, R.; Iwasaki, K.; Hayashi, S.; Uchida, T.; Katsuki, T. *Synlett* **2001**, 284–286.
144. Ito, K.; Akashi, S.; Saito, B.; Katsuki, T. *Synlett* **2003**, 1809–1812.
145. Ito, K.; Imahayashi, Y.; Kuroda, T.; Eno, S.; Saito, B.; Katsuki, T. *Tetrahedron Lett.* **2004**, *45*, 7277–7281.
146. Guthrie, J. P.; O’Leary, S. *Can. J. Chem.* **1975**, *53*, 2150–2156.
147. Guthrie, J. P.; Ueda, Y. *Can. J. Chem.* **1976**, *54*, 2745–2758.
148. Endo, T.; Kuwahara, A.; Tasai, H.; Murata, T.; Hashimoto, M.; Ishigami, T. *Nature* **1977**, *268*, 74–76.
149. Endo, T.; Miyazawa, K.; Endo, M.; Uchida, A.; Ohashi, Y.; Sasada, Y. *Chem. Lett.* **1982**, 1989.
150. Yokoo, Y.; Sakurai, T.; Saburi, M.; Yoshikawa, S. *Nippon Kagaku Kaishi* **1981**, 1904–1910.
151. Yoshimura, T.; Tsukurimichi, E.; Iizuka, Y.; Mizuno, H.; Isaji, H.; Shimasaki, C. *Bull. Chem. Soc. Jpn.* **1989**, *62*, 1891–1899.
152. Stien, D.; Crich, D.; Bertrand, M. P. *Tetrahedron* **1998**, *54*, 10779–10788.



**Biographical sketch**

**Motohiro Nishio** was born in 1936 in Kobe, Japan. In 1959, he graduated from the Faculty of Pharmaceutical Sciences, the University of Tokyo. After spells at the Laboratory of Organic Chemistry, Department of Agricultural Chemistry, University of Tokyo (Professor Masanao Matsui, 1961–1963) and Faculté de Pharmacie, Université de Paris (1965–1966) he obtained his PhD in physical organic chemistry from the University of Tokyo under the supervision of Professor Shoji Shibata. From 1959 to 1996 he worked at Meiji Seika Kaisha, R&D Division; after which he was a Visiting Professor from 1996 to 1999 at Chiba University. He also acted as a Visiting Scientist at the Institute of Physical and Chemical Research (RIKEN, 1996–1999) and at Yokohama National University as a Lecturer (1997–1999). In 1999, he founded the CHPI Institute in his home address. He has published 79 papers (69 in English, 3 in French, 7 in Japanese), 16 reviews (4 in English, 12 in Japanese) and 4 books (1 in English, 3 in Japanese). His research interests include stereochemistry, CH/ $\pi$  hydrogen bonds in chemistry and structural biology.

# An efficient synthesis of 5-aminolaevulinic acid (ALA)-containing peptides for use in photodynamic therapy

Louis M.-A. Rogers,<sup>a</sup> Philip G. McGivern,<sup>b</sup> Anthony R. Butler,<sup>c</sup> Alexander J. MacRobert<sup>d</sup>  
and Ian M. Eggleston<sup>b,\*</sup>

<sup>a</sup>Centre for Biomolecular Sciences, University of St. Andrews, North Haugh, St. Andrews, KY16 9ST Fife, Scotland, UK

<sup>b</sup>Division of Biological Chemistry and Molecular Microbiology, School of Life Sciences, Carnelley Building, University of Dundee, Dundee DD1 4HN, UK

<sup>c</sup>Bute Medical School, University of St. Andrews, St. Andrews KY16 9TS, UK

<sup>d</sup>National Medical Laser Centre, Division of Surgical Specialities, Royal Free and University College Medical School, University College London, Charles Bell House, 67-73 Riding House Street, London W1P 7PN, UK

Received 25 February 2005; revised 14 April 2005; accepted 12 May 2005

**Abstract**—An efficient and cost-effective procedure has been devised for the preparation of urethane-protected 5-aminolaevulinic acid (5-ALA) dipeptide ester derivatives which avoids problems associated with the instability of 5-ALA under basic conditions. The procedure is also applicable to the direct synthesis of *N*-( $\alpha$ )-acetyl amino acid-ALA dipeptides in high enantiomeric purity as potential novel prodrugs for photodynamic therapy (PDT).

© 2005 Elsevier Ltd. All rights reserved.

## 1. Introduction

Photodynamic therapy (PDT) is a non-thermal technique for inducing tumour destruction with light following administration of a light-activated photosensitising drug.<sup>1,2</sup> Provided that the drug may be selectively introduced and retained in cancerous cells relative to normal adjacent tissue, necrosis is selective. A promising approach in PDT involves the exogenous administration of 5-aminolaevulinic acid (ALA), a naturally occurring compound present in mammalian cells which can be metabolised to a porphyrin photosensitiser, protoporphyrin IX (PpIX) via the haem biosynthetic pathway (Fig. 1).<sup>3</sup> Following accumulation of PpIX within the affected tissue, PDT treatment is then carried out using red laser light, activating PpIX and leading to the production of cytotoxic reactive oxygen species. The main clinical application of ALA-PDT at present is for the treatment of skin cancers via topical application of ALA at the appropriate place on the skin,<sup>4</sup> but the technique is also particularly suited to the visualization and treatment of early tumours in hollow organs where damage to underlying muscle must be minimized.

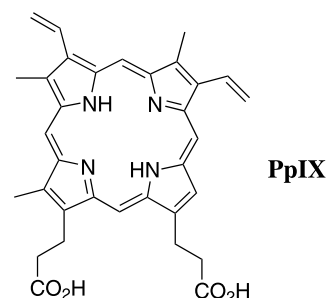


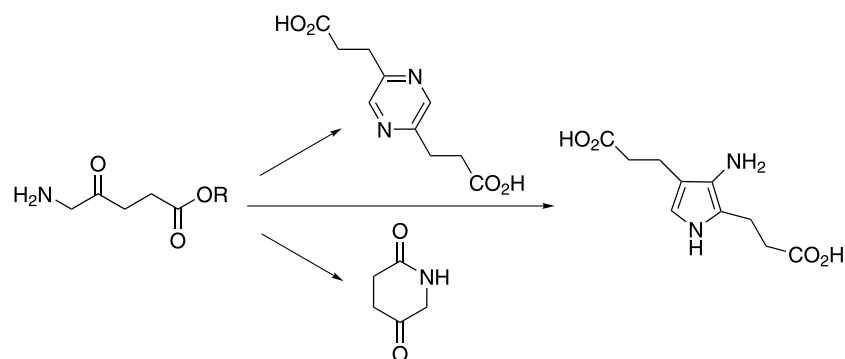
Figure 1.

A significant drawback to ALA-PDT is the fact that ALA is a zwitterion at physiological pH resulting in low lipid solubility and limiting passage through biological barriers such as cellular membranes. To overcome this problem, various lipophilic ALA ester derivatives or other novel prodrugs and formulations have been investigated. In this regard, we<sup>5</sup> and others<sup>6</sup> have conjectured that incorporation of 5-ALA into a short peptide derivative, would provide a suitable means of both facilitating transdermal delivery and also improved targeting into cancerous cells. Release of ALA once incorporated would then be mediated by intracellular peptidase and esterase activities.

We report herein an efficient route for the synthesis of a

**Keywords:** Aminolaevulinic acid; Peptide; Prodrug; Photodynamic therapy.

\* Corresponding author. Tel.: +44 1382 344319; fax: +44 1382 345517; e-mail: [i.m.eggleston@dundee.ac.uk](mailto:i.m.eggleston@dundee.ac.uk)



**Figure 2.** Possible degradation products of 5-ALA derivatives at neutral or basic pH.

range of 5-ALA peptide prodrug derivatives, suitable for evaluation in skin explant and cellular assays.

## 2. Results and discussion

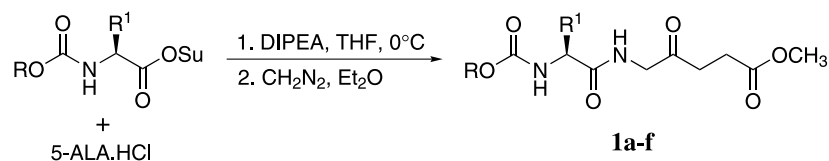
Although Bertozzi et al.<sup>7</sup> have reported the solid phase synthesis of peptides containing 2-ALA, the preparation of 5-ALA-containing peptides is non-trivial. Acylation of 5-ALA derivatives is fraught with potential difficulties, chiefly associated with the instability of ALA in solution above pH 4.<sup>8</sup> It has been shown that around pH 7, 5-ALA dimerises to give pyrazine derivatives,<sup>9</sup> while at higher pH, pseudo-porphobilinogen may be formed.<sup>10</sup> Conversion to ester derivatives appears to exacerbate these problems of instability, introducing the potential for formation of lactam-type derivatives (Fig. 2).

All these processes are typically associated with a significant darkening of the ALA solution, and indeed we have found that using conventional peptide synthesis methodology, coupling of equimolar quantities of *N*-( $\alpha$ )-protected amino acids to esters of ALA via carbodiimide/1-hydroxybenzotriazole (HOBt) activation generally leads to complex mixtures and uniformly low yields of the desired peptides.<sup>11</sup>

Berger et al.<sup>6</sup> have reported two separate approaches for the preparation of 5-ALA-containing peptides, however both employ either an excess of the activated amino acid

components or a 5-ALA derivative. In the first case,<sup>6a</sup> 1 equiv of a Boc-protected amino acid was preactivated with 5 equiv each of *N*-(3-dimethylaminopropyl)-*N*-ethylcarbodiimide hydrochloride (EDC·HCl) and HOBt and coupled with 5 equiv of an ester derivative of 5-ALA. Although apparently effective, the expense of 5-ALA makes this approach less attractive for large scale preparations of such 5-ALA-containing dipeptides. In a more recent report,<sup>6b</sup> 5-ALA containing peptides were obtained via reaction of in situ formed symmetrical anhydrides of di- or tripeptide derivatives, necessitating the use of 2 equiv of the latter relative to the 5-ALA component.

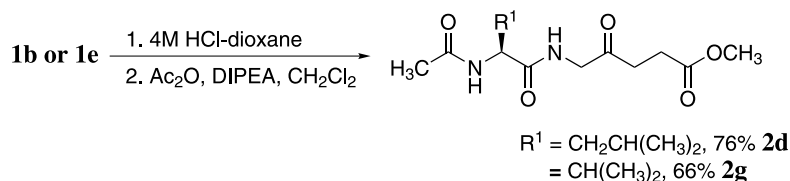
For our studies in this area, we have developed an alternative approach that provides access to various orthogonally protected ALA dipeptides, derivatisable at either N- or C-terminus, once the key ALA pseudopeptide bond is formed, but crucially employing only 1 equiv of both 5-ALA and the activated amino acid derivative. To achieve this, and avoid competing decomposition of 5-ALA, we chose to react the latter, in the form of its hydrochloride salt, with a urethane-protected amino acid active ester in THF solution (in which 5-ALA hydrochloride is insoluble). Initiation of the coupling reaction is then effected by slow addition of base (DIPEA) such that any 5-ALA released into solution is immediately intercepted by the acylating agent (in excess) before competing side reactions can intervene (Scheme 1). This general strategy of simultaneous deprotection and coupling has been utilized previously in peptide chemistry to overcome the problem of



**Scheme 1.**

**Table 1.** Urethane-protected 5-ALA dipeptide derivatives

	R	R <sup>1</sup>	Yield/%	Name
<b>1a</b>	Bu <sup>t</sup>	CH <sub>3</sub>	65	Boc-Ala-ALA-OCH <sub>3</sub>
<b>1b</b>	Bu <sup>t</sup>	CH <sub>2</sub> CH(CH <sub>3</sub> ) <sub>2</sub>	87	Boc-Leu-ALA-OCH <sub>3</sub>
<b>1c</b>	Bu <sup>t</sup>	(CH <sub>2</sub> ) <sub>4</sub> NH <sub>2</sub>	85	Boc-Lys(Z)-ALA-OCH <sub>3</sub>
<b>1d</b>	Bu <sup>t</sup>	CH <sub>2</sub> Ph	79	Boc-Phe-ALA-OCH <sub>3</sub>
<b>1e</b>	Bu <sup>t</sup>	CH(CH <sub>3</sub> ) <sub>2</sub>	32	Boc-Val-ALA-OCH <sub>3</sub>
<b>1f</b>	CH <sub>2</sub> Ph	H	80	Z-Gly-ALA-OCH <sub>3</sub>



Scheme 2.

diketopiperazine formation on coupling to an Xaa-Pro-OMe dipeptide<sup>12</sup> and has also been exploited more recently as part of a highly efficient tandem deprotection-coupling methodology using *N*-( $\alpha$ )-allyloxycarbonyl protected amino acid derivatives.<sup>13</sup>

As shown in Table 1, when a variety of amino acid succinimidyl ester derivatives, were coupled with 5-ALA as described above, the corresponding dipeptides were isolated in generally very good yields, via conversion to the methyl esters by treatment with ethereal diazomethane to facilitate isolation. The sole exception was the Boc-Val derivative which coupled rather slowly and ultimately gave a modest yield of 32%. These results compare very favourably with those reported by Berger et al.<sup>6</sup> for the preparation of similar dipeptides on the same scale of synthesis (e.g., **1a**, **1d**<sup>6a</sup>) and it should be noted again that they provide a significant economy in terms of the use of 5-ALA. All the dipeptides were obtained in analytically pure form following isolation by chromatography or crystallization.

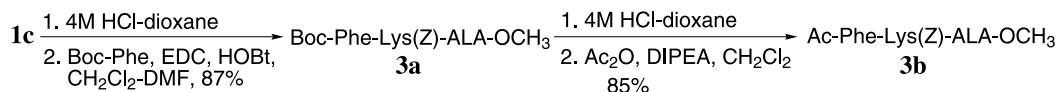
We have found that the most appropriate 5-ALA dipeptide substrates for PDT studies are those in which 5-ALA is coupled to an *N*-( $\alpha$ )-acetyl amino acid derivative, since they provide a useful balance of lipophilicity and water solubility.<sup>14</sup> As expected, Boc-protected derivatives such as **1b** and **1e**, were readily transformable into novel prodrug entities as illustrated in Scheme 2. Treatment of **1b** or **1e** with 4 M HCl–dioxane provided the corresponding hydrochloride salts which were then treated with acetic anhydride in the presence of DIPEA to give the corresponding acetylated peptides in good yield. No degradation of the

5-ALA peptides was observed under these conditions with the key acylation step having already been performed.

To confirm that suitably protected 5-ALA dipeptides may be further elaborated by standard peptide chemistry, the lysine-containing derivative **1c** was transformed into the corresponding pseudotripeptides **3a** and **3b** as shown in Scheme 3. Once again, no degradation of the 5-ALA unit was observed either during acidolytic cleavage of *N*-( $\alpha$ )-Boc protection or subsequent acylation reactions in the presence of tertiary amine. The dipeptide fragment Ac-Phe-Lys has previously been employed to create lysosomally-cleavable prodrugs of the anticancer agent doxorubicin<sup>15</sup> showing the potential value of expedient access to building blocks such as **1a–f** for the preparation of peptide prodrugs that are susceptible to cleavage by specific proteases or targeted to particular cellular transporters.<sup>16</sup>

In view of the effectiveness of our protocol for the coupling of Boc or Z-protected amino acids to 5-ALA we were interested to explore the possibility of the direct synthesis of *N*-( $\alpha$ )-acetylated derivatives by this method in order to facilitate rapid biochemical screening of such prodrugs. When the *N*-( $\alpha$ )-acetyl succinimidyl ester derivatives of Gly, D- or L-Ala, D- or L-Phe, and L-Val were reacted with 5-ALA hydrochloride as before, followed by esterification (Scheme 4), the desired dipeptides were obtained in moderate yields (26–43%, Table 2, entries 1, 2, 4, 8–10) and with surprisingly good optical purity.

Coupling with activated *N*-( $\alpha$ )-acetyl amino acids is rarely used in peptide synthesis since the former are highly prone



Scheme 3.

Table 2. Direct preparation of Ac-Xaa-ALA-OCH<sub>3</sub> derivatives

	Entry	L OR D	R <sup>1</sup>	Dilute base	ee <sup>a</sup> /%	Yield/%
<b>2a</b>	1	—	H	N	—	32
<b>2b</b>	2	L	CH <sub>3</sub>	N	46	26
	3	L	CH <sub>3</sub>	Y	>98	51
<b>2c</b>	4	D	CH <sub>3</sub>	N	41	47
	5	D	CH <sub>3</sub>	Y	>98	73
<b>2d</b>	6 <sup>b</sup>	L	CH <sub>2</sub> CH(CH <sub>3</sub> ) <sub>2</sub>	N	0	37
	7	L	CH <sub>2</sub> CH(CH <sub>3</sub> ) <sub>2</sub>	Y	90	47
<b>2e</b>	8	L	CH <sub>2</sub> Ph	N	>98	43
<b>2f</b>	9	D	CH <sub>2</sub> Ph	N	>98	41
<b>2g</b>	10	L	CH(CH <sub>3</sub> ) <sub>2</sub>	N	64	33
	11	L	CH(CH <sub>3</sub> ) <sub>2</sub>	Y	>98	38

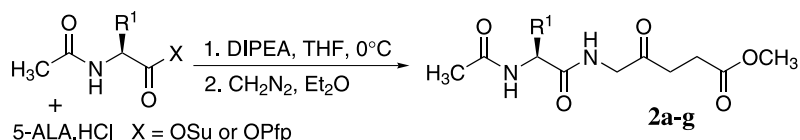
<sup>a</sup> ee determined by <sup>1</sup>H NMR with the chiral shift reagent Eu(hfc)<sub>3</sub> (hfc, 3-(heptafluoropropylhydroxy-methylene)-(+)–camphorate).

<sup>b</sup> Coupling via the pentafluorophenyl ester.

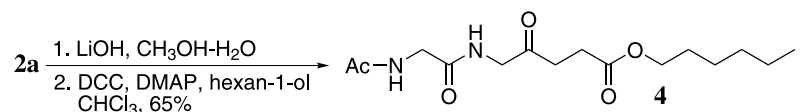
to racemisation via oxazolone formation in the presence of base,<sup>17</sup> but for the Phe derivatives **2e** and **2f** (entries 8 and 9) the desired peptide was obtained essentially as a single enantiomer. Enantiomeric purities were assessed using chiral shift <sup>1</sup>H NMR with Eu(hfc)<sub>3</sub>; addition of the reagent led to a splitting of the resonance corresponding to the ester methyl group, presumably via diastereoisomeric chelate formation involving the ester and keto carbonyls of the ALA residue. Integration of these signals then gave a direct estimation of the enantiomeric purity of the peptide.

The direct acylation of 5-ALA with *N*-( $\alpha$ )-acetyl derivatives offers some advantages in terms of speed and economy, particularly for cases such as Val, where coupling of the Boc-protected derivative proceeds in a somewhat lower yield (see Table 1). As anticipated, when the rate of addition of base was carefully controlled (in dilute THF solution), not only the yield but also the optical purity of the peptides (Table 2, entries 3, 5, 7, 11) was significantly improved, since controlled base addition limits the concentration of free 5-ALA, the species required for coupling which may also participate in polymerization or dimerisation reactions etc (see above),<sup>8–10</sup> but moreover minimises the amount of base available to promote oxazolone formation and racemisation. Preliminary studies with other active esters such as pentafluorophenyl (entry 6) and 4-nitrophenyl (not shown), did not suggest any significant advantage in terms of yield relative to the readily available succinimidyl esters which formed the basis of our study, however racemisation appeared to be much more significant with these species.

Once again, derivatives such as **2a** were readily transformable into other potential prodrugs by standard chemistry with the key Xaa-ALA peptide bond now in place. For example (Scheme 5), saponification of **2a** with aq LiOH proceeded in quantitative yield whereupon the dipeptide acid was converted to the corresponding hexyl ester in 65% yield by DMAP-catalysed esterification<sup>18</sup> with DCC. This further emphasizes the potential of derivatives such as **1a–f** and **2a–g** as synthons for the preparation of more elaborate 5-ALA-containing peptides and also highlights the possibility of employing other chemistries in the esterification stage of our general procedure once the critical acylation has been achieved.



Scheme 4.



Scheme 5.

### 3. Conclusion

We have developed highly efficient and economic preparations of 5-ALA peptides that overcome the known instability of the amino acid under basic conditions. The derivatives obtained may be elaborated into a wide range of 5-ALA prodrug derivatives using conventional peptide chemistry for use as novel PDT agents. Details of these studies will be reported shortly.<sup>14</sup>

### 4. Experimental

#### 4.1. General

Melting points were recorded on an Electrothermal IA9000 series digital melting point apparatus and are quoted uncorrected. NMR spectra were recorded on a Varian Gemini 300 (<sup>1</sup>H, 300 MHz; <sup>13</sup>C, 75.4 MHz;) or Bruker Avance DPX 300 FT-spectrometers. Chemical shifts ( $\delta$ ) are expressed in ppm and coupling constants (*J*) are given in Hz. Mass spectra were recorded on a VG AUTOSPEC mass spectrometer in electron impact (EI) mode, a VG Quattro triple quadrupole instrument in positive electrospray (ES) mode, or a TofSpec 2E instrument (MALDI-TOF). Elemental analyses were performed in the Department of Chemistry, University of St. Andrews, or by MEDAC Ltd, Brunel Science Centre, Surrey UK. Optical rotations were measured at 20 °C in a 10 cm path length cell using a Perkin Elmer 343 polarimeter and are quoted in 10<sup>-1</sup> deg. cm<sup>2</sup> g<sup>-1</sup>. Flash chromatography was performed according to the method of Still et al.,<sup>19</sup> on columns of silica gel (Fluka Silica Gel 60; 35–70  $\mu$ m mesh, or Fluorochem; 40–60  $\mu$ m mesh). Etheral diazomethane was prepared from Diazald<sup>®</sup>. Petroleum ether bp 40–60 °C was distilled through a vigreux column prior to use. All other solvents were of Analar quality or were dried using standard procedures.

*Amino acid active esters.* Urethane and acetyl-protected amino acid *N*-hydroxysuccinimidyl ester derivatives were either commercially available (Calbiochem or SigmaAldrich), or were prepared by standard DCC-mediated esterifications.<sup>20,21</sup> Ac-L-Leu-OPfp was prepared by DCC-mediated esterification of Ac-L-Leu with pentafluorophenol.



## 4.2. Preparation of ALA ‘dipeptides’

**Urethane derivatives (typical procedure).** A suspension of the amino acid active ester (1.5 mmol) and 5-ALA·HCl (0.25 g, 1.5 mmol) in dry THF (20 mL) was cooled to  $-5^{\circ}\text{C}$  under argon. A solution of DIPEA (0.26 mL, 1.5 mmol) in dry THF (10 mL) was slowly added over 120 min, then the reaction mixture was stirred overnight under cooling. The solvent was evaporated and an excess of freshly prepared ethereal diazomethane (40 mL) was added with cooling in an ice bath. The reaction mixture was stirred at room temperature for 2 h, then the solvent was carefully evaporated. The crude product was redissolved in EtOAc (40 mL) and was washed with 5% aq citric acid, 5% aq  $\text{NaHCO}_3$ ,  $\text{H}_2\text{O}$ , and saturated aq  $\text{NaCl}$  (40 mL each). The organics were dried ( $\text{MgSO}_4$ ) and the solvent was evaporated to give the crude product which was purified by column chromatography (EtOAc/40–60 petrol or MeOH/ $\text{CH}_2\text{Cl}_2$  gradient) to give white solid or colourless oils. For **1f**, the product was purified by recrystallisation.

**Acetyl derivatives (Method A).** The coupling reaction and esterification were performed as for the urethane-protected derivatives, except that the base was added directly rather than in THF solution. The crude products were pre-absorbed onto silica using MeOH as solvent and purified by column chromatography using MeOH/ $\text{CH}_2\text{Cl}_2$  ( $\text{CH}_2\text{Cl}_2$  to 10% MeOH/ $\text{CH}_2\text{Cl}_2$ ) as eluent, followed by recrystallisation from EtOAc/40–60 petrol to give the dipeptides as white solids.

**Method B.** The coupling reaction and esterification were performed exactly as for the urethane-protected derivatives. The crude products were pre-absorbed onto silica using MeOH as solvent and purified by column chromatography using MeOH/ $\text{CH}_2\text{Cl}_2$  ( $\text{CH}_2\text{Cl}_2$  to 10% MeOH/ $\text{CH}_2\text{Cl}_2$ ) as eluent. If required, the dipeptides were further purified by recrystallisation from EtOAc/40–60 petrol as previously.

## 4.3. $^1\text{H}$ NMR chiral shift experiments with *N*-( $\alpha$ )-acetylated dipeptides

Optimum resolution was obtained when a molar ratio of  $\text{Eu}(\text{hfc})_3$  versus 5-ALA ‘dipeptide’ of approximately 1:4 was employed. In a typical experiment, a solution of the 5-ALA ‘dipeptide’ (10 mg, ca. 30  $\mu\text{mol}$ ) in dry  $\text{CDCl}_3$  (0.7 mL) was treated with  $\text{Eu}(\text{hfc})_3$  (10 mg, ca. 8  $\mu\text{mol}$ ). The method was verified by examining mixtures of Ac-D-Phe-ALA-OMe and Ac-L-Phe-ALA-OMe. Integral ratios for each enantiomer were found to be consistent with the ratio of each in solution.

**4.3.1. Boc-L-Ala-ALA-OMe (1a).** 1.10 mmol scale. Yield: 65% (colourless oil).  $[\alpha]_{\text{D}} -17.3$  ( $c=0.54$   $\text{CHCl}_3$ );  $\delta_{\text{H}}$  ( $\text{CDCl}_3$ ) 1.39 (3H, d,  $J=7.1$  Hz,  $\text{CH}_3$ -Ala), 1.47 (9H, s,  $\text{Bu}^t$ ), 2.66–2.69 (2H, m,  $\text{COCH}_2\text{CH}_2$ ), 2.75–2.79 (2H, m,  $\text{COCH}_2\text{CH}_2$ ), 3.70 (3H, s,  $\text{CO}_2\text{CH}_3$ ), 4.21–4.29 (3H, m,  $\text{NHCH}_2\text{CO}$ ,  $\text{CHCH}_3$ ), 5.01 (1H, br, urethane NH), 6.83 (1H, br, amide NH).  $\delta_{\text{C}}$  18.8 ( $\text{CHCH}_3$ ), 28.0 ( $\text{COCH}_2\text{CH}_2$ ), 28.7 ( $\text{C}(\text{CH}_3)_3$ ), 34.9 ( $\text{COCH}_2\text{CH}_2$ ), 49.5 ( $\text{NHCH}_2\text{CO}$ ), 50.5 ( $\text{CHCH}_3$ ), 52.3 ( $\text{CO}_2\text{CH}_3$ ), 80.7 ( $\text{C}(\text{CH}_3)_3$ ), 155.8 (urethane C=O), 173.2 (2 signals, amide and ester C=O), 203.9 (ketone C=O);  $m/z$  (ES) 317 (100%,  $[\text{M}+\text{H}]^+$ ), 339.2 (23,

$[\text{M}+\text{Na}]^+$ ); (Found: C, 53.07; H, 7.29; N, 8.75.  $\text{C}_{14}\text{H}_{24}\text{N}_2\text{O}_6$  requires: C, 53.15; H, 7.65; N, 8.85%).

**4.3.2. Boc-L-Leu-ALA-OMe (1b).** 2.98 mmol scale. Yield 87% (colourless oil).  $[\alpha]_{\text{D}} -17.0$  ( $c=1.62$   $\text{CHCl}_3$ );  $\delta_{\text{H}}$  ( $\text{CDCl}_3$ ) 0.95–0.98 (6H, m,  $\text{CH}_3$ -Leu), 1.47 (9H, s,  $\text{Bu}^t$ ), 1.55–1.73 (3H, m,  $\text{CHCH}_2(\text{CH}_3)_2$ ,  $\text{CHCH}_2(\text{CH}_3)_2$ ), 2.66–2.70 (2H, m,  $\text{COCH}_2\text{CH}_2$ ), 2.75–2.79 (2H, m,  $\text{COCH}_2\text{CH}_2$ ), 3.70 (3H, s,  $\text{CO}_2\text{CH}_3$ ), 4.21 (2H, d,  $J=4.7$  Hz,  $\text{NHCH}_2\text{CO}$ ), 4.13–4.29 (1H, m,  $\text{CHCH}_2\text{CH}(\text{CH}_3)_2$ ), 4.90 (1H, br, urethane NH), 6.80 (1H, br, amide NH);  $\delta_{\text{C}}$  22.1, 23.4 ( $\text{CH}_3$ -Leu), 25.1 ( $\text{CHCH}_2(\text{CH}_3)_2$ ), 27.9 ( $\text{COCH}_2\text{CH}_2$ ), 28.7 ( $\text{C}(\text{CH}_3)_3$ ), 34.9 ( $\text{COCH}_2\text{CH}_2$ ), 41.8 ( $\text{CHCH}_2\text{CH}(\text{CH}_3)_2$ ), 49.4 ( $\text{NHCH}_2\text{CO}$ ), 52.3 ( $\text{CO}_2\text{CH}_3$ ), 53.4 ( $\text{CHCH}_2\text{CH}(\text{CH}_3)_2$ ), 80.5 ( $\text{C}(\text{CH}_3)_3$ ), 156.1 (urethane C=O), 173.3 (amide C=O), 173.4 (ester C=O), 204.1 (ketone C=O);  $m/z$  (ES) 359 (100%,  $[\text{M}+\text{H}]^+$ ), 381 (16,  $[\text{M}+\text{Na}]^+$ ); (Found: C, 56.63; H, 8.13; N, 8.10.  $\text{C}_{17}\text{H}_{30}\text{N}_2\text{O}_6$  requires C, 56.97; H, 8.44; N, 7.82%).

**4.3.3. Boc-L-Lys(Z)-ALA-OMe (1c).** 1.50 mmol scale. Yield: 85% (white solid). Mp: 85–87  $^{\circ}\text{C}$  (from  $\text{CH}_2\text{Cl}_2$ /40–60 petrol);  $[\alpha]_{\text{D}} -9.6$  ( $c=0.87$   $\text{CHCl}_3$ );  $\delta_{\text{H}}$  ( $\text{CDCl}_3$ ) 1.32–1.70 (4H, m,  $\text{CHCH}_2\text{CH}_2\text{CH}_2\text{CH}_2\text{NH}$ ), 1.72–1.88 (2H, m,  $\text{CHCH}_2(\text{CH}_2)_3\text{NH}$ ), 1.45 (9H, s,  $\text{Bu}^t$ ), 2.64–2.68 (2H, m,  $\text{COCH}_2\text{CH}_2$ ), 2.72–2.76 (2H, m,  $\text{COCH}_2\text{CH}_2$ ), 3.18–3.24 (2H, m,  $\text{CH}_2\text{NH}$ ), 3.69 (3H, s,  $\text{CO}_2\text{CH}_3$ ), 4.14–4.25 (1H, m,  $\text{CH}(\text{CH}_2)_4\text{NH}$ ), 4.19 (2H, d,  $J=4.8$  Hz,  $\text{NHCH}_2\text{CO}$ ), 5.00 (1H, br,  $\text{CH}_2\text{NH}$ ), 5.11 (2H, s,  $\text{OCH}_2\text{Ph}$ ), 5.11–5.19 (1H, m,  $\text{Bu}^t\text{OCONH}$ ), 6.85 (1H, br, amide NH), 7.30–7.38 (5H, m, Ph);  $\delta_{\text{C}}$  22.8 ( $\text{CHCH}_2\text{CH}_2(\text{CH}_2)_2\text{NH}$ ), 27.9 ( $\text{COCH}_2\text{CH}_2$ ), 28.7 ( $\text{C}(\text{CH}_3)_3$ ), 29.8 ( $\text{CH}(\text{CH}_2)_2\text{CH}_2\text{CH}_2\text{NH}$ ), 32.4 ( $\text{CHCH}_2(\text{CH}_2)_3\text{NH}$ ), 34.9 ( $\text{COCH}_2\text{CH}_2$ ), 40.8 ( $\text{CH}(\text{CH}_2)_3\text{CH}_2\text{NH}$ ), 49.4 ( $\text{NHCH}_2\text{CO}$ ), 52.3 ( $\text{CO}_2\text{CH}_3$ ), 54.7 ( $\text{CH}(\text{CH}_2)_4\text{NH}$ ), 67.0 ( $\text{CH}_2\text{Ph}$ ), 128.5, 128.9, 137.0 (Ph), 156.1, 157.0 (urethane C=O), 172.7 (amide C=O), 173.3 (ester C=O), 204.1 (ketone C=O);  $m/z$  (ES) 508 (100%,  $[\text{M}+\text{H}]^+$ ), 530 (36,  $[\text{M}+\text{Na}]^+$ ), 546 (21,  $[\text{M}+\text{K}]^+$ ); (Found: C, 59.13; H, 7.49; N, 8.23.  $\text{C}_{25}\text{H}_{37}\text{N}_3\text{O}_8$  requires C, 59.16; H, 7.35; N, 8.27%).

**4.3.4. Boc-L-Phe-ALA-OMe (1d).** 1.10 mmol scale. Yield: 79% (colourless glass, Lit.,<sup>6a</sup> Mp: 83–85  $^{\circ}\text{C}$ );  $[\alpha]_{\text{D}} -1.4$  ( $c=0.89$   $\text{CHCl}_3$ );  $\delta_{\text{H}}$  ( $\text{CDCl}_3$ ) 1.33 (9H, s,  $\text{Bu}^t$ ), 2.57–2.65 (4H, m,  $\text{COCH}_2\text{CH}_2$ ), 3.01–3.12 (2H, m,  $\text{CH}_2\text{Ph}$ ), 3.60 (3H, s,  $\text{CO}_2\text{CH}_3$ ), 3.98–4.17 (2H, m,  $\text{NHCH}_2\text{CO}$ ), 4.35 (1H, br,  $\text{CHCH}_2\text{Ph}$ ), 4.85 (1H, br, urethane NH), 6.50 (1H, br, amide NH), 7.11–7.25 (5H, m, Ph);  $\delta_{\text{C}}$  28.0 ( $\text{COCH}_2\text{CH}_2$ ), 28.6 ( $\text{C}(\text{CH}_3)_3$ ), 34.9 ( $\text{COCH}_2\text{CH}_2$ ), 38.8 ( $\text{CHCH}_2\text{Ph}$ ), 49.5 ( $\text{NHCH}_2\text{CO}$ ), 52.3 ( $\text{CO}_2\text{CH}_3$ ), 56.1 ( $\text{CHCH}_2\text{Ph}$ ), 80.7 ( $\text{C}(\text{CH}_3)_3$ ), 127.4, 129.1, 129.7, 136.9 (Ph), 155.8 (urethane C=O), 171.8 (amide C=O), 173.2 (ester C=O), 203.6 (ketone C=O);  $m/z$  (ES) 393 (100%,  $[\text{M}+\text{H}]^+$ ), 415 (26,  $[\text{M}+\text{Na}]^+$ ), 431 (13,  $[\text{M}+\text{K}]^+$ ); (Found: C, 61.07; H, 7.26; N, 7.17.  $\text{C}_{20}\text{H}_{28}\text{N}_2\text{O}_6$  requires C, 61.21; H, 7.19; N, 7.14%).

**4.3.5. Boc-L-Val-ALA-OMe (1e).** 1.50 mmol scale. Yield: 32% (white solid). Mp: 73.5–77  $^{\circ}\text{C}$ ;  $[\alpha]_{\text{D}} -21.2$  ( $c=1.32$   $\text{CHCl}_3$ );  $\delta_{\text{H}}$  ( $\text{CDCl}_3$ ) 0.84 (3H, d,  $J=6.8$  Hz,  $\text{CH}_3$ -Val), 0.90 (3H, d,  $J=6.8$  Hz,  $\text{CH}_3$ -Val), 1.38 (9H, s,  $\text{Bu}^t$ ), 2.05–2.16 (1H, m,  $\text{CH}(\text{CH}_3)_2$ ), 2.56–2.61 (2H, m,  $\text{COCH}_2\text{CH}_2$ ), 2.66–2.70 (2H, m,  $\text{COCH}_2\text{CH}_2$ ), 3.61 (3H, s,  $\text{CO}_2\text{CH}_3$ ),

3.89–3.99 (1H, m,  $\text{CHCH}(\text{CH}_3)_3$ ), 4.14 (2H, d,  $J=4.8$  Hz,  $\text{NHCH}_2\text{CO}$ ), 4.95 (1H, br, urethane NH), 6.62 (1H, br, amide NH);  $\delta_c$  17.95, 19.6 ( $\text{CH}_3\text{-Val}$ ), 27.9 ( $\text{COCH}_2\text{CH}_2$ ), 28.7 ( $\text{C}(\text{CH}_3)_3$ ), 31.2 ( $\text{CH}(\text{CH}_3)_2$ ), 34.9 ( $\text{COCH}_2\text{CH}_2$ ), 49.4 ( $\text{NHCH}_2\text{CO}$ ), 52.3 ( $\text{CO}_2\text{CH}_3$ ), 60.2 ( $\text{CHCH}(\text{CH}_3)_2$ ), 80.3 ( $\text{C}(\text{CH}_3)_3$ ), 156.2 (urethane  $\text{C}=\text{O}$ ), 172.2 (amide  $\text{C}=\text{O}$ ), 173.2 (ester  $\text{C}=\text{O}$ ), 204.0 (ketone  $\text{C}=\text{O}$ );  $m/z$  (ES) 345 (100%,  $[\text{M}+\text{H}]^+$ ), 367 (100,  $[\text{M}+\text{Na}]^+$ ), 348 (48,  $[\text{M}+\text{K}]^+$ ); (Found: C, 55.45; H, 8.13; N, 8.10.  $\text{C}_{16}\text{H}_{26}\text{N}_2\text{O}_6$  requires: C, 55.80; H, 8.20; N, 8.13%).

**4.3.6. Z-Gly-ALA-OMe (1f).** 1.10 mmol scale. Yield 80% (white solid). Mp: 103–105 °C;  $\delta_H$  ( $\text{CDCl}_3$ ) 2.66–2.70 (2H, m,  $\text{COCH}_2\text{CH}_2$ ), 2.74–2.79 (2H, m,  $\text{COCH}_2\text{CH}_2$ ), 3.70 (3H, s,  $\text{CO}_2\text{CH}_3$ ), 3.94 (2H, d,  $J=5.6$  Hz,  $\text{NHCH}_2\text{CONH}$ ), 4.23 (2H, d,  $J=4.6$  Hz,  $\text{NHCH}_2\text{CO}$ ) 5.16 (2H, s,  $\text{OCH}_2\text{Ph}$ ), 5.51 (1H, br, urethane NH), 6.78 (1H, br, amide NH), 7.32–7.44 (5H, m, Ph);  $\delta_c$  27.9 ( $\text{COCH}_2\text{CH}_2$ ), 34.9 ( $\text{COCH}_2\text{CH}_2$ ), 44.7 ( $\text{NHCH}_2\text{CONH}$ ), 49.4 ( $\text{NHCH}_2\text{CO}$ ), 52.4 ( $\text{CO}_2\text{CH}_3$ ), 67.6 ( $\text{OCH}_2\text{Ph}$ ), 128.5, 128.6, 128.9, 136.6 (Ph), 157.1 (urethane  $\text{C}=\text{O}$ ), 169.8 (amide  $\text{C}=\text{O}$ ), 173.3 (ester  $\text{C}=\text{O}$ ), 204.2 (ketone  $\text{C}=\text{O}$ );  $m/z$  (ES) 337 (100%,  $[\text{M}+\text{H}]^+$ ), 359 (35,  $[\text{M}+\text{Na}]^+$ ), 375 (12,  $[\text{M}+\text{K}]^+$ ); (Found: C, 57.11; H, 6.00; N, 8.35.  $\text{C}_{16}\text{H}_{20}\text{N}_2\text{O}_6$  requires C, 57.14; H, 5.99; N, 8.32%).

**4.3.7. Ac-Gly-ALA-OMe (2a).** Method A. 2.30 mmol scale. Yield: 32%. Mp: 192–194 °C.  $\delta_H$  ( $\text{CDCl}_3$ ) 2.06 (3H, s,  $\text{COCH}_3$ ), 2.64–2.69 (2H, m,  $\text{COCH}_2\text{CH}_2$ ), 2.73–2.78 (2H, m,  $\text{COCH}_2\text{CH}_2$ ), 3.67 (3H, s,  $\text{CO}_2\text{CH}_3$ ), 3.99 (2H, d,  $J=5.0$  Hz,  $\text{NHCH}_2\text{CONH}$ ), 4.22 (2H, d,  $J=5.0$  Hz,  $\text{NHCH}_2\text{CO}$ ), 6.33 (1H, br,  $\text{CH}_3\text{CONHCH}_2$ ), 6.76 (1H, br,  $\text{NHCH}_2\text{COCH}_2\text{CH}_2$ );  $\delta_c$  23.4 ( $\text{COCH}_3$ ), 28.1 ( $\text{COCH}_2\text{CH}_2$ ), 35.0 ( $\text{COCH}_2\text{CH}_2$ ), 43.5 ( $\text{NHCH}_2\text{CONH}$ ), 49.6 ( $\text{NHCH}_2\text{CO}$ ), 52.5 ( $\text{CO}_2\text{CH}_3$ ), 169.7, 171.5 (amide  $\text{C}=\text{O}$ ), 173.4 (ester  $\text{C}=\text{O}$ ), 204.1 (ketone  $\text{C}=\text{O}$ );  $m/z$  (EI) 244 (11%,  $\text{M}^+$ ), 213 (7,  $[\text{M}-\text{OMe}]^+$ ), 171 (8) 130 (45), 115 (78), 100 (100,  $[\text{M}-\text{ALA}-\text{OCH}_3]^+$ ); (Found: C, 49.14; H, 6.60; N, 11.44.  $\text{C}_{10}\text{H}_{16}\text{N}_2\text{O}_5$  requires C, 49.18; H, 6.60; N, 11.47%).

**4.3.8. Ac-L-Ala-ALA-OMe (2b).** Method A. 1.50 mmol scale. Yield: 26%. Mp: 102–106 °C.  $\delta_H$  ( $\text{CDCl}_3$ ) 1.38 (3H, d,  $J=6.9$  Hz,  $\text{CH}_3\text{-Ala}$ ), 2.01 (3H, s,  $\text{COCH}_3$ ), 2.63–2.67 (2H, m,  $\text{COCH}_2\text{CH}_2$ ), 2.72–2.77 (2H, m,  $\text{COCH}_2\text{CH}_2$ ), 3.70 (3H, s,  $\text{CO}_2\text{CH}_3$ ), 4.18 (2H, d,  $J=4.8$  Hz,  $\text{NHCH}_2\text{CO}$ ), 4.50–4.60 (1H, m,  $\text{CHCH}_3$ ), 6.31 (1H, d,  $J=6.6$  Hz,  $\text{CH}_3\text{CONH}$ ), 6.94 (1H, br,  $\text{NHCHCH}_3\text{CO}$ );  $\delta_H$  ( $\text{CDCl}_3/\text{Eu}(\text{hfc})_3$ ) 3.709 (2.2H, s,  $\text{CO}_2\text{CH}_3\text{-L-Ala}$ ), 3.742 (0.8H, s,  $\text{CO}_2\text{CH}_3\text{-D-Ala}$ );  $\delta_c$  17.9 ( $\text{CHCH}_3$ ), 22.4 ( $\text{CH}_3\text{CO}$ ), 27.0 ( $\text{COCH}_2\text{CH}_2$ ), 33.9 ( $\text{COCH}_2\text{CH}_2$ ), 48.5 ( $\text{NHCH}_2\text{CO}$ ), 48.9 ( $\text{CHCH}_3$ ), 51.4 ( $\text{CO}_2\text{CH}_3$ ), 170.2, 172.6 (amide  $\text{C}=\text{O}$ ), 173.0 (ester  $\text{C}=\text{O}$ ), 204.0 (ketone  $\text{C}=\text{O}$ );  $m/z$  (MALDI-TOF) 281 (100%,  $[\text{M}+\text{Na}]^+$ ), 297 (23,  $[\text{M}+\text{K}]^+$ ); (Found: C, 51.30; H, 6.87; N, 11.08.  $\text{C}_{11}\text{H}_{18}\text{N}_2\text{O}_5$  requires C, 51.19; H, 7.03; N, 10.85%).

*Method B.* 1.50 mmol scale. Yield: 51%.  $\delta_H$  ( $\text{CDCl}_3/\text{Eu}(\text{hfc})_3$ ) single enantiomer.

**4.3.9. Ac-D-Ala-ALA-OMe (2c).** Method A. 1.50 mmol scale. Yield: 47%. Mp: 102–104 °C.  $\delta_H$  ( $\text{CDCl}_3/\text{Eu}(\text{hfc})_3$ ) 3.709 (0.9H, s,  $\text{CO}_2\text{CH}_3\text{-D-Ala}$ ), 3.742 (2.1H, s,  $\text{CO}_2\text{CH}_3\text{-L}$

Ala); (Found: C, 51.05; H, 7.06; N, 10.76.  $\text{C}_{11}\text{H}_{18}\text{N}_2\text{O}_5$  requires C, 51.19; H, 7.03; N, 10.85%).

*Method B.* 1.30 mmol scale. Yield 73%.  $\delta_H$  ( $\text{CDCl}_3/\text{Eu}(\text{hfc})_3$ ) single enantiomer.

**4.3.10. Ac-L-Leu-ALA-OMe (2d).** Method A (using the pentafluorophenyl ester). 1.50 mmol scale. Yield: 37%. Mp: 74–76 °C.  $\delta_H$  ( $\text{CDCl}_3$ ) 0.92–0.95 (6H, m,  $\text{CH}_3\text{-Leu}$ ), 1.50–1.70 (3H, m,  $\text{CHCH}_2(\text{CH}_3)_2$ ,  $\text{CHCH}_2(\text{CH}_3)_2$ ), 2.01 (3H, s,  $\text{COCH}_3$ ), 2.63–2.67 (2H, m,  $\text{COCH}_2\text{CH}_2$ ), 2.72–2.76 (2H, m,  $\text{COCH}_2\text{CH}_2$ ), 3.68 (3H, s,  $\text{CO}_2\text{CH}_3$ ), 4.08–4.24 (2H, m,  $\text{NHCH}_2\text{CO}$ ), 4.51–4.56 (1H, m,  $\text{CHCH}_2\text{CH}(\text{CH}_3)_2$ ), 6.25 (1H, d,  $J=5.2$  Hz,  $\text{CH}_3\text{CONH}$ ), 7.00 (1H, br,  $\text{NHCHCH}_2\text{-CH}(\text{CH}_3)_2\text{CO}$ );  $\delta_H$  ( $\text{CDCl}_3/\text{Eu}(\text{hfc})_3$ ) 3.767 (1.5H, s,  $\text{CO}_2\text{CH}_3\text{-L-Leu}$ ), 3.813 (1.5H, s,  $\text{CO}_2\text{CH}_3\text{-D-Leu}$ );  $\delta_c$  22.0, 22.8 ( $\text{CH}_3\text{-Leu}$ ), 23.0 ( $\text{COCH}_3$ ), 24.7 ( $\text{CHCH}_2(\text{CH}_3)_2$ ), 27.4 ( $\text{COCH}_2\text{CH}_2$ ), 34.4 ( $\text{COCH}_2\text{CH}_2$ ), 41.2 ( $\text{CHCH}_2\text{-CH}(\text{CH}_3)_2$ ), 49.0 ( $\text{NHCH}_2\text{CO}$ ), 51.5 ( $\text{CO}_2\text{CH}_3$ ), 51.8 ( $\text{CHCH}_2\text{CH}(\text{CH}_3)_2$ ), 170.4, 172.6 (amide  $\text{C}=\text{O}$ ), 173.0 (ester  $\text{C}=\text{O}$ ), 203.7 (ketone  $\text{C}=\text{O}$ );  $m/z$  (EI) 300 (3%,  $\text{M}^+$ ), 269 (7,  $[\text{M}-\text{OCH}_3]^+$ ), 156 (62,  $[\text{M}-\text{ALA}-\text{OCH}_3]^+$ ), 86 (100); (Found: C, 56.20; H, 7.97; N, 9.23.  $\text{C}_{14}\text{H}_{24}\text{N}_2\text{O}_5$  requires C, 55.99; H, 8.05; N, 9.33%).

*Method B (using the succinimidyl ester).* 1.50 mmol scale. Yield 47%.  $\delta_H$  ( $\text{CDCl}_3/\text{Eu}(\text{hfc})_3$ ) 3.611 (2.85H, s,  $\text{CO}_2\text{CH}_3\text{-L-Leu}$ ), 3.6689 (0.15H, s,  $\text{CO}_2\text{CH}_3\text{-D-Leu}$ ).

From *Boc-L-Leu-OCH<sub>3</sub>*. **1b** (0.796 g, 2.22 mmol) was treated with 4 M HCl in dioxane (14 mL) and the resulting solution was stirred at room temperature for 40 min. The solvent was evaporated and the crude hydrochloride salt was dried thoroughly in vacuo. A suspension of the hydrochloride salt in  $\text{CH}_2\text{Cl}_2$  (30 mL) was cooled in an ice bath and was treated with DIPEA (0.46 mL, 2.64 mmol), followed by acetic anhydride (0.42 mL, 4.45 mmol). The reaction mixture was allowed to attain room temperature overnight, then it was diluted with  $\text{CH}_2\text{Cl}_2$  (30 mL) and was washed with 5% aq  $\text{NaHCO}_3$ , 5% aq citric acid and saturated aq NaCl (30 mL each). The aqueous layers were back-extracted with  $\text{CH}_2\text{Cl}_2$  (4 × 30 mL) and the combined organics were dried ( $\text{MgSO}_4$ ) and the solvent evaporated to give a colourless oil which was purified by column chromatography using  $\text{MeOH}/\text{CH}_2\text{Cl}_2$  ( $\text{CH}_2\text{Cl}_2$  to 7%  $\text{MeOH}/\text{CH}_2\text{Cl}_2$ ) as eluant. This gave a white solid (0.508 g, 76%), indistinguishable ( $^1\text{H}$ ,  $^{13}\text{C}$  NMR) from the samples prepared by Methods A and B.

**4.3.11. Ac-L-Phe-ALA-OMe (2e).** Method A. 1.38 mmol scale. Yield: 43%. Mp: 129–130 °C.  $\delta_H$  ( $\text{CDCl}_3$ ) 1.95 (3H, s,  $\text{COCH}_3$ ), 2.60–2.70 (4H, m,  $\text{COCH}_2\text{CH}_2$ ), 3.00–3.15 (2H, m,  $\text{CH}_2\text{Ph}$ ), 3.68 (3H, s,  $\text{CO}_2\text{CH}_3$ ), 4.00–4.20 (2H, m,  $\text{NHCH}_2\text{CO}$ ), 4.70–4.80 (1H, br,  $\text{CHCH}_2\text{Ph}$ ), 6.20 (1H, br,  $\text{CH}_3\text{CONH}$ ), 6.70 (1H, br,  $\text{NHCHCH}_2\text{Ph}$ );  $\delta_H$  ( $\text{CDCl}_3/\text{Eu}(\text{hfc})_3$ ) single enantiomer;  $\delta_c$  23.1 ( $\text{COCH}_3$ ) 27.5 ( $\text{COCH}_2\text{CH}_2$ ), 35.0 ( $\text{COCH}_2\text{CH}_2$ ), 38.3 ( $\text{CH}_2\text{Ph}$ ), 49.0 ( $\text{NHCH}_2\text{CO}$ ), 52.0 ( $\text{CO}_2\text{CH}_3$ ), 56.1 ( $\text{CHCH}_2\text{Ph}$ ), 127.0, 128.6, 129.2, 136.3 (Ph), 170.1, 170.9 (amide  $\text{C}=\text{O}$ ), 172.8 (ester  $\text{C}=\text{O}$ ), 203.2 (ketone  $\text{C}=\text{O}$ );  $m/z$  (EI) 334 (11%,  $\text{M}^+$ ), 303 (3,  $[\text{M}-\text{OCH}_3]^+$ ), 275 (15,  $[\text{M}-\text{CO}_2\text{CH}_3]^+$ ), 219 (5), 190 (20), 171 (8), 120 (100); (Found: C, 60.75; H,

6.68; N, 8.15 C<sub>17</sub>H<sub>22</sub>N<sub>2</sub>O<sub>5</sub> requires C, 61.07; H, 6.61; N, 8.38%).

**4.3.12. Ac-D-Phe-ALA-OMe (2f).** Method A. 1.38 mmol scale. Yield: 41%. Mp: 126–128 °C.  $\delta_{\text{H}}$  (CDCl<sub>3</sub>/Eu(hfc)<sub>3</sub>) single enantiomer. (Found: C, 60.78; H, 6.63; N, 8.36. C<sub>17</sub>H<sub>22</sub>N<sub>2</sub>O<sub>5</sub> requires C, 61.07; H, 6.61; N, 8.38%).

**4.3.13. Ac-L-Val-ALA-OMe (2g).** Method A. 1.50 mmol scale. Yield: 33%. Mp: 147–148 °C.  $\delta_{\text{H}}$  (CDCl<sub>3</sub>) 0.94 (3H, d,  $J=4.6$  Hz, CH<sub>3</sub>-Val), 0.96 (3H, d,  $J=4.6$  Hz, CH<sub>3</sub>-Val), 2.00–2.12 (4H, m, COCH<sub>3</sub>, CH(CH<sub>3</sub>)<sub>2</sub>), 2.62–2.67 (2H, m, COCH<sub>2</sub>CH<sub>2</sub>), 2.72–2.77 (2H, m, COCH<sub>2</sub>CH<sub>2</sub>), 3.67 (3H, s, CO<sub>2</sub>CH<sub>3</sub>), 4.10–4.28 (2H, m, NHCH<sub>2</sub>CO) 4.34–4.39 (1H, m, CHCH(CH<sub>3</sub>)<sub>3</sub>), 6.35 (1H, br, CH<sub>3</sub>CONH), 6.70 (1H, br, NHCH(CH<sub>3</sub>)<sub>2</sub>CO);  $\delta_{\text{H}}$  (CDCl<sub>3</sub>/Eu(hfc)<sub>3</sub>) 3.723 (2.45H, s, CO<sub>2</sub>CH<sub>3</sub>-L-Val), 3.775 (0.55H, s, CO<sub>2</sub>CH<sub>3</sub>-D-Val);  $\delta_{\text{C}}$  18.0, 19.0 (CH<sub>3</sub>-Val), 23.1 (COCH<sub>3</sub>), 27.4 (COCH<sub>2</sub>CH<sub>2</sub>), 31.0 (CH(CH<sub>3</sub>)<sub>2</sub>), 34.4 (COCH<sub>2</sub>CH<sub>2</sub>), 49.0 (NHCH<sub>2</sub>CO), 52.0 (CO<sub>2</sub>CH<sub>3</sub>), 58.3 (CHCH(CH<sub>3</sub>)<sub>2</sub>), 170.3, 172.2 (amide C=O), 172.9 (ester C=O), 203.6 (ketone C=O);  $m/z$  (EI) 286 (3%, M<sup>+</sup>), (5, M-OCH<sub>3</sub>), 142 (40, [M-ALA-OCH<sub>3</sub>]<sup>+</sup>), 114 (100), 72 (95); (Found: C, 54.86; H, 7.92; N, 9.71. C<sub>13</sub>H<sub>22</sub>N<sub>2</sub>O<sub>5</sub> requires C, 54.53; H, 7.74; N, 9.78%).

Method B. 1.50 mmol scale. Yield: 38%.  $\delta_{\text{H}}$  (CDCl<sub>3</sub>/Eu(hfc)<sub>3</sub>) single enantiomer.

From Boc-L-Val-OCH<sub>3</sub>. **1e** (0.164 g, 0.476 mmol) was treated with 4 M HCl in dioxane (2 mL) and the resulting solution was stirred at room temperature for 1 h. The solvent was evaporated and the crude hydrochloride salt was dried thoroughly in vacuo. A suspension of the hydrochloride salt in CH<sub>2</sub>Cl<sub>2</sub> (4 mL) was cooled in an ice bath and was treated with DIPEA (0.11 mL, 0.63 mmol), followed by acetic anhydride (96  $\mu$ L, 1.02 mmol). The reaction mixture was allowed to attain room temperature overnight, then it was diluted with CH<sub>2</sub>Cl<sub>2</sub> (25 mL) and was washed with 5% aq NaHCO<sub>3</sub>, 5% aq citric acid and saturated aq NaCl (25 mL each). The aqueous layers were back-extracted with CH<sub>2</sub>Cl<sub>2</sub> (4  $\times$  25 mL) and the combined organics were dried (MgSO<sub>4</sub>) and the solvent evaporated to give an off-white solid which was recrystallised from CH<sub>2</sub>Cl<sub>2</sub>-hexane to give a white solid (90 mg, 66%), indistinguishable (<sup>1</sup>H, <sup>13</sup>C NMR) from the samples prepared by Methods A and B.

**4.3.14. N-(tert-Butoxycarbonyl)-L-phenylalanyl-N<sup>ε</sup>-(benzyloxycarbonyl)-L-lysiny-5-aminolaevulinic acid methyl ester (Boc-L-Phe-L-Lys(Z)-ALA-OMe) (3a).** **1c** (0.141 g, 0.278 mmol) was treated with 4 M HCl in dioxane (2.5 mL) and the resulting solution was stirred at room temperature for 30 min. The solvent was evaporated and the crude hydrochloride salt was dried thoroughly in vacuo. A stirred solution of Boc-L-Phe (74 mg, 0.279 mmol) and 1-hydroxybenzotriazole monohydrate (58 mg, 0.429 mmol) in CH<sub>2</sub>Cl<sub>2</sub> (1.5 mL) and DMF (1.5 mL) was cooled in an ice bath and EDC·HCl (53 mg, 0.276 mmol) was added. After 40 min, a solution of the preceding hydrochloride salt in DMF (2 mL) was added, followed by DIPEA (0.11 mL, 0.63 mmol) and the reaction mixture was allowed to attain room temperature overnight. After evaporation of the solvents, the residue was dissolved in EtOAc (20 mL) and was washed with 5% aq citric acid, 5% aq NaHCO<sub>3</sub>, H<sub>2</sub>O, and saturated aq NaCl

(20 mL each). The organic layer was dried (MgSO<sub>4</sub>) and the solvent was evaporated to give an off-white solid which was purified by column chromatography using MeOH/CH<sub>2</sub>Cl<sub>2</sub> (5–9% MeOH/CH<sub>2</sub>Cl<sub>2</sub>) as eluant. This gave a white solid (0.163 g, 89%). Mp: 103.5–107.5 °C;  $[\alpha]_{\text{D}}$  –17.0 ( $c=1.0$  CHCl<sub>3</sub>);  $\delta_{\text{H}}$  (CDCl<sub>3</sub>) 0.83–1.54 (4H, m, CHCH<sub>2</sub>CH<sub>2</sub>CH<sub>2</sub>CH<sub>2</sub>NH), 1.31 (9H, s, Bu<sup>t</sup>), 1.70–1.90 (2H, m, CHCH<sub>2</sub>(CH<sub>2</sub>)<sub>3</sub>), 2.55–2.57 (2H, m, COCH<sub>2</sub>CH<sub>2</sub>), 2.61–2.63 (2H, m, COCH<sub>2</sub>CH<sub>2</sub>), 2.93–3.10 (4H, m, CH(CH<sub>2</sub>)<sub>3</sub>CH<sub>2</sub>NH, CHCH<sub>2</sub>Ph), 3.59 (3H, s, CO<sub>2</sub>CH<sub>3</sub>), 4.01–4.10 (2H, m, NHCH<sub>2</sub>CO), 4.32–4.37 (2H, m, CH(CH<sub>2</sub>)<sub>4</sub>NH, CHCH<sub>2</sub>Ph), 4.95–5.10 (4H, m, OCH<sub>2</sub>Ph, 2  $\times$  urethane NH), 6.60–6.67 (2H, m, 2  $\times$  amide NH), 7.10–7.34 (10H, m, 2  $\times$  Ph);  $\delta_{\text{C}}$  22.6 (CHCH<sub>2</sub>CH<sub>2</sub>CH<sub>2</sub>CH<sub>2</sub>NH), 27.9 (CHCH<sub>2</sub>CH<sub>2</sub>CH<sub>2</sub>CH<sub>2</sub>NH), 28.6 (C(CH<sub>3</sub>)<sub>3</sub>), 29.7 (COCH<sub>2</sub>CH<sub>2</sub>), 31.8 (CHCH<sub>2</sub>(CH<sub>2</sub>)<sub>3</sub>-NH), 34.6 (COCH<sub>2</sub>CH<sub>2</sub>), 38.4 (CHCH<sub>2</sub>Ph), 40.8 (CH(CH<sub>2</sub>)<sub>3</sub>CH<sub>2</sub>NH), 49.4 (NHCH<sub>2</sub>CO), 52.3 (CO<sub>2</sub>CH<sub>3</sub>), 53.3 (CH(CH<sub>2</sub>)<sub>4</sub>NH), 56.4 (CHCH<sub>2</sub>Ph), 67.0 (OCH<sub>2</sub>Ph), 80.9 (C(CH<sub>3</sub>)<sub>3</sub>), 127.4, 128.5, 128.9, 129.1, 136.7, 137.0 (Ph), 156.1, 157.0 (urethane C=O), 171.7, 172.0 (amide C=O), 173.3 (ester C=O), 203.0 (ketone C=O);  $m/z$  (ES) 655 (57%, [M+H]<sup>+</sup>), 677.4 (16, [M+Na]<sup>+</sup>); (Found: C, 62.32; H, 7.26; N, 8.47. C<sub>34</sub>H<sub>46</sub>N<sub>4</sub>O<sub>8</sub> requires C, 62.37; H, 7.08; N, 8.55%).

**4.3.15. N-Acetyl-L-phenylalanyl-N<sup>ε</sup>-(benzyloxycarbonyl)-L-lysiny-5-aminolaevulinic acid methyl ester (Ac-L-Phe-L-Lys(Z)-ALA-OMe) (3b).** **3a** (0.122 g, 0.186 mmol) was treated with 4 M HCl in dioxane (2 mL) and the resulting solution was stirred at room temperature for 1 h. The solvent was evaporated and the crude hydrochloride salt was dried thoroughly in vacuo. A suspension of the hydrochloride salt in CH<sub>2</sub>Cl<sub>2</sub> (4 mL) was cooled in an ice bath and was treated with DIPEA (40  $\mu$ L, 0.23 mmol), followed by acetic anhydride (35  $\mu$ L, 0.37 mmol). The reaction mixture was allowed to attain room temperature overnight at which point a gelatinous white solid had separated out. The reaction mixture was diluted with CH<sub>2</sub>Cl<sub>2</sub> (25 mL) to dissolve the solid and was washed with 5% aq NaHCO<sub>3</sub>, 5% aq citric acid and saturated aq NaCl (25 mL each). Drying (MgSO<sub>4</sub>) and evaporation of the solvent gave an off-white solid which was precipitated from CH<sub>2</sub>Cl<sub>2</sub>/hexane to give a white powder (95 mg, 85%). Mp: 144–146 °C;  $[\alpha]_{\text{D}}$  –6.9 ( $c=1.0$  CH<sub>3</sub>OH);  $\delta_{\text{H}}$  (CDCl<sub>3</sub>) 1.20–1.91 (6H, m, CHCH<sub>2</sub>CH<sub>2</sub>CH<sub>2</sub>CH<sub>2</sub>NH), 1.87 (3H, s, COCH<sub>3</sub>), 2.55–2.58 (2H, m, COCH<sub>2</sub>CH<sub>2</sub>), 2.62–2.66 (2H, m, COCH<sub>2</sub>CH<sub>2</sub>), 2.92–3.10 (4H, m, CH(CH<sub>2</sub>)<sub>3</sub>CH<sub>2</sub>NH, CHCH<sub>2</sub>Ph), 3.60 (3H, s, CO<sub>2</sub>CH<sub>3</sub>), 4.01–4.08 (2H, m, NHCH<sub>2</sub>CO), 4.30–4.40 (1H, m, CH(CH<sub>2</sub>)<sub>4</sub>NH), 4.65 (1H, ABq, CHCH<sub>2</sub>Ph) 5.01–5.18 (4H, m, OCH<sub>2</sub>Ph, 2  $\times$  urethane NH), 6.25 (1H, d,  $J=7.2$  Hz, CH<sub>3</sub>CONH) 6.55–6.60 (1H, m, amide NH), 6.68 ((1H, d,  $J=7.7$  Hz, amide NH), 7.12–7.32 (10H, m, 2  $\times$  Ph);  $\delta_{\text{C}}$  22.6 (CHCH<sub>2</sub>CH<sub>2</sub>CH<sub>2</sub>CH<sub>2</sub>NH), 23.3 (COCH<sub>3</sub>) 27.9 (CHCH<sub>2</sub>CH<sub>2</sub>CH<sub>2</sub>CH<sub>2</sub>NH), 29.7 (COCH<sub>2</sub>CH<sub>2</sub>), 32.4 (CHCH<sub>2</sub>(CH<sub>2</sub>)<sub>3</sub>NH), 34.9 (COCH<sub>2</sub>CH<sub>2</sub>), 38.8 (CHCH<sub>2</sub>Ph), 40.9 (CH(CH<sub>2</sub>)<sub>3</sub>CH<sub>2</sub>NH), 49.5 (NHCH<sub>2</sub>CO), 52.3 (CO<sub>2</sub>CH<sub>3</sub>), 53.3 (CH(CH<sub>2</sub>)<sub>4</sub>NH), 54.8 (CHCH<sub>2</sub>Ph), 66.9 (OCH<sub>2</sub>Ph), 127.3, 128.4, 128.9, 129.7, 136.9, 137.1 (Ph), 157.1 (urethane C=O), 170.9, 171.9 (2 signals) (amide C=O), 173.3 (ester C=O), 204.3 (ketone C=O);  $m/z$  (ES) 597 (100%, [M+H]<sup>+</sup>), 619 (27, [M+Na]<sup>+</sup>); (Found: C,



62.02; H, 6.73; N, 9.31. C<sub>34</sub>H<sub>46</sub>N<sub>4</sub>O<sub>8</sub> requires C, 62.40; H, 6.76; N, 9.39%).

**4.3.16. N-Acetylglycyl-5-aminolaevulinic acid hexyl ester (Ac-Gly-ALA-OHex) (4).** A stirred solution of **2a** (0.152 g, 0.53 mmol) in CH<sub>3</sub>OH (1.2 mL) and H<sub>2</sub>O (1.8 mL) was treated with LiOH (16 mg, 0.66 mmol). The reaction mixture was stirred at room temperature for 40 min, then it was applied to a column of Amberlyst IR 120 resin (plus) cation exchange resin which was eluted with 60% aq CH<sub>3</sub>OH. Acidic fractions were collected and the solvent was evaporated to give the crude acid as a white solid (0.182 g). A solution of the acid (70 mg, 0.25 mmol) in CHCl<sub>3</sub> (10 mL) was treated with DCC (58 mg, 0.28 mmol), DMAP (5 mg, 40 μmol) and hexan-1-ol (40 μL, 0.32 mmol). The reaction mixture was stirred at room temperature for 21 h, then it was filtered to remove DCU and the solvent was evaporated. The crude product was purified by column chromatography using 5% MeOH/CH<sub>2</sub>Cl<sub>2</sub> as eluant, then recrystallised from CH<sub>3</sub>OH/diethyl ether to give a white solid (52 mg, 65%); Mp: 124–125 °C; δ<sub>H</sub> (CDCl<sub>3</sub>) 0.82 (3H, t, *J*=6.7 Hz, (CH<sub>2</sub>)<sub>5</sub>CH<sub>3</sub>), 1.10–1.35 (6H, m, (CH<sub>2</sub>)<sub>2</sub>-CH<sub>2</sub>CH<sub>2</sub>CH<sub>2</sub>CH<sub>3</sub>), 1.40–1.70 (2H, m, CH<sub>2</sub>CH<sub>2</sub>(CH<sub>2</sub>)<sub>3</sub>-CH<sub>3</sub>), 1.99 (3H, s, COCH<sub>3</sub>), 2.57–2.68 (4H, m, COCH<sub>2</sub>CH<sub>2</sub>), 3.91 (2H, d, *J*=5.2 Hz, NHCH<sub>2</sub>CONH), 4.16 (2H, d, *J*=4.7 Hz, NHCH<sub>2</sub>CO), 6.10 (1H, br, CH<sub>3</sub>-CONH), 6.50 (1H, br, NHCH<sub>2</sub>COCH<sub>2</sub>CH<sub>2</sub>); δ<sub>C</sub> 14.0 ((CH<sub>2</sub>)<sub>5</sub>CH<sub>3</sub>), 22.5, 25.5, 27.8, 28.5 (CH<sub>2</sub>)<sub>2</sub>CH<sub>2</sub>CH<sub>2</sub>CH<sub>2</sub>-CH<sub>3</sub>, COCH<sub>2</sub>CH<sub>2</sub>), 31.3 (CH<sub>2</sub>CH<sub>2</sub>(CH<sub>2</sub>)<sub>3</sub>CH<sub>3</sub>), 34.5 (COCH<sub>2</sub>CH<sub>2</sub>), 43.0 (NHCH<sub>2</sub>CONH), 49.1 (NHCH<sub>2</sub>CO), 65.1 (CH<sub>2</sub>(CH<sub>2</sub>)<sub>4</sub>CH<sub>3</sub>), 169.1, 170.1 (amide C=O), 172.5 (ester C=O), 203.6 (ketone C=O); [Found: (EI) 314.18417, C<sub>15</sub>H<sub>26</sub>N<sub>2</sub>O<sub>5</sub> requires 314.18351]; *m/z* (ES) 315 (70%, [M+H]<sup>+</sup>), 337 (100, [M+Na]<sup>+</sup>), 353 (10, [M+Na]<sup>+</sup>).

#### Acknowledgements

We thank the Association for International Cancer Research for financial support.

#### References and notes

1. (a) Bonnett, R. *Chem. Soc. Rev.* **1995**, *24*, 19–33. (b) Bonnett,

R. *Chemical Aspects of Photodynamic Therapy*; Gordon and Breach: Amsterdam, 2000.

- Milgrom, L.; MacRobert, A. J. *Chem. Brit.* **1998**, 45–50.
- Peng, Q.; Warloe, T.; Berg, K.; Moan, J.; Kongshaug, M.; Giercksky, K.-E.; Nesland, J. M. *Cancer* **1997**, *79*, 2282–2308.
- (a) Casas, A.; Battle, A. *Curr. Med. Chem.* **2002**, *2*, 465–475. (b) Lopez, R. F. V.; Lange, N.; Guy, R.; Bentley, M. V. L. B. *Adv. Drug. Deliv. Rev.* **2004**, *56*, 77–94.
- Casas, A.; Battle, A. M. C.; Butler, A. R.; Robertson, D.; Brown, E. H.; MacRobert, A.; Riley, P. A. *Br. J. Cancer* **1999**, *80*, 1525–1532.
- (a) Berger, Y.; Greppi, A.; Siri, O.; Neier, R.; Juillerat-Jeanneret, L. *J. Med. Chem.* **2000**, *43*, 4738–4746. (b) Berger, Y.; Ingrassia, L.; Neier, R.; Juillerat-Jeanneret, L. *Bioorg. Med. Chem.* **2003**, *11*, 1343–1351.
- Maurcaurrelle, L. A.; Bertozzi, C. R. *Tetrahedron Lett.* **1998**, *39*, 7279–7282.
- Gadmar, O. B.; Moan, J.; Scheie, E.; Ma, L. W.; Peng, Q. *J. Photochem. Photobiol.* **2002**, *67*, 187–193.
- Jaffe, E. K.; Rajagopalan, J. S. *Bioorg. Chem.* **1990**, *18*, 381–394.
- Butler, A. R.; George, S. *Tetrahedron* **1992**, *48*, 7879–7886.
- Rogers, L. M.-A. 'Synthesis and biological evaluation of 5-aminolaevulinic acid derivatives for improved photodynamic therapy', Ph.D., St. Andrews, 2001.
- Shute, R. E.; Rich, D. H. *J. Chem. Soc., Chem. Commun.* **1987**, 1155–1156.
- Thieriet, N.; Gomez-Martinez, P.; Guibé, F. *Tetrahedron Lett.* **1999**, *40*, 2505–2508.
- Nakanishi, H.; Rogers, L.-M.; Gerscher, S.; Butler, A. R.; Eggleston, I. M.; MacRobert, A. J. In preparation.
- Dubowchik, G. M.; Firestone, R. A. *Bioorg. Med. Chem. Lett.* **1998**, *8*, 3341–3346.
- Terada, T.; Inui, K. *Curr. Drug Metab.* **2004**, *5*, 85–94.
- Jones, J. H. *The Chemical Synthesis of Peptides*; Oxford University Press: Oxford, 1991.
- Hassner, A.; Alexanian, V. *Tetrahedron Lett.* **1978**, *19*, 4475–4478.
- Still, W. C.; Kahn, M.; Mitra, A. *J. Org. Chem.* **1978**, *43*, 2923–2925.
- Anderson, G. W.; Zimmerman, J. E.; Callahan, F. M. *J. Am. Chem. Soc.* **1963**, *85*, 3039.
- Blumberg, S.; Vallee, B. L. *Biochemistry* **1975**, *14*, 2411–2418.

# Highly enantioselective synthesis of multifunctionalized allylic building blocks via oxazaborolidine-catalyzed borane reduction

Byung Tae Cho\* and Sung Hye Shin

Department of Chemistry, Hallym University, Chunchon 200-702, South Korea

Received 25 April 2005; revised 10 May 2005; accepted 11 May 2005

Available online 4 June 2005

**Abstract**—A simple and convenient synthesis of optically active alkenyl  $\beta$ -hydroxy sulfides with high enantiomeric excess by CBS-oxazaborolidine-catalyzed borane reduction of the corresponding  $\beta$ -keto sulfides and its application to synthesis of chiral alkenic diols have been established.

© 2005 Elsevier Ltd. All rights reserved.

## 1. Introduction

Optically active allylic alcohols represent an important structural motif and have attracted synthetic chemists for their wide range of applications.<sup>1,2</sup> Most syntheses of chiral allylic alcohols are based on kinetic resolution of racemic allylic alcohols by chemical<sup>3</sup> or biological process,<sup>2c–e,4</sup> asymmetric hydrogenation,<sup>5</sup> or enantioselective reduction<sup>6</sup> of vinylic ketones and reductive elimination of 2,3-epoxy<sup>7</sup> or *O*-isopropylidene halides<sup>8</sup> and *O*-isopropylidene acetal tosylhydrazones.<sup>9</sup> On the other hand, non-racemic  $\beta$ -hydroxy sulfides are widely used as starting materials for the synthesis of a variety of chiral intermediates in the synthesis of chiral oxiranes,<sup>10a–c</sup> aziridines,<sup>10d</sup> thiiranes,<sup>10e</sup> tetrahydrofurans<sup>10f,g</sup> and  $\beta$ -hydroxy esters.<sup>10h,i</sup> Moreover, they are easily oxidized to  $\beta$ -hydroxy sulfoxides or sulfones, which serve as extremely useful chiral building blocks for the synthesis of a variety of chiral organic compounds,<sup>11a,b</sup> such as chiral oxiranes,<sup>11c,d</sup> allylic alcohols,<sup>11e,f,12a</sup> lactones,<sup>11g,p,12b–e</sup> macrolides,<sup>11h–l</sup> pheromones,<sup>11m–o</sup> diols<sup>11q</sup> and tetrahydrofurans<sup>12f</sup> because the  $\alpha$ -carbon atom of sulfinyl or sulfonyl groups of the compounds can be further functionalized by the formation of sulfur-stabilized carbanions.<sup>10b,13</sup> Very recently we reported highly efficient synthesis of  $\beta$ -hydroxy sulfides with high enantiomeric purity by CBS-oxazaborolidine-catalyzed borane reduction.<sup>14</sup> Using the same methodology, we therefore undertook to study the synthesis of optically active allylic alcohols bearing an adjacent sulfamyl group,

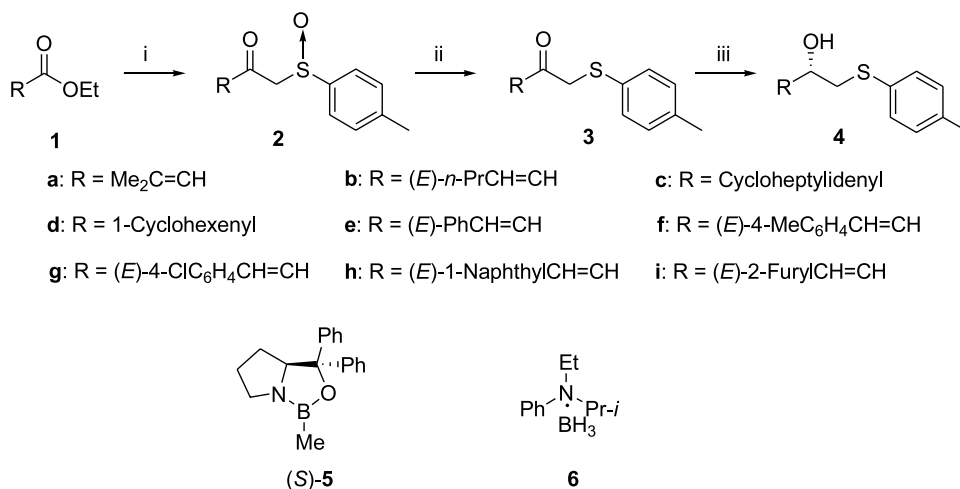
which could be used as versatile chiral intermediates for synthesis of biologically active substances.

## 2. Results and discussion

The overall synthetic route is outlined in Scheme 1. The starting alkenyl  $\beta$ -keto sulfides **3** were obtained from condensation of  $\alpha$ -alkenyl esters **1** with methyl *p*-tolyl sulfoxide in the presence of base, followed by deoxygenation of product alkenyl  $\beta$ -keto sulfoxides **2**. Thus, methyl *p*-tolyl sulfoxide was reacted with LDA in THF at  $-78^\circ\text{C}$  for 1 h and the resulting mixture was added to the alkenic esters **1** in THF at  $-78^\circ\text{C}$  using the literature procedure.<sup>15</sup> The reactions were maintained at  $-78^\circ\text{C}$  for 24 h with stirring to provide alkenyl  $\beta$ -keto sulfoxides **2** in 55–65% yield. When **2** was treated with sodium iodide in the presence of trifluoroacetic anhydride in acetone at  $0^\circ\text{C}$  according to the known procedure,<sup>16</sup> alkenyl  $\beta$ -keto sulfides **3** were obtained in 88–95% yield. Finally, (*S*)-CBS-oxazaborolidine (**5**)-catalyzed asymmetric borane reduction of **3** using *N*-ethyl-*N*-isopropylaniline–borane complex **6** as borane carrier was carried out.<sup>14</sup> To minimize the hydroboration of alkenyl group by borane, these reductions were performed by use of 0.5 equiv of **6** at  $0^\circ\text{C}$ . As shown Table 1, all the reduction examined afforded the corresponding  $\beta$ -hydroxy sulfides **4** within 10 min in high yields. Their optical purities were determined by HPLC analysis using a Chiralcel OD-H or Whelk-O1 chiral column. The reduction of keto sulfides **3** bearing acyclic (**3a** and **3b**), exocyclic (**3c**) and endocyclic (**3d**) alkenyl groups furnished the corresponding alkenyl  $\beta$ -hydroxy sulfides **4a–d** with 90–95% ee (runs 1–4). For aryl-substituted analogues (**3e–h**), the reduction provided very high enantioselection (runs

**Keywords:** Asymmetric reduction; Oxazaborolidine-catalyzed reduction; Chiral alkenyl  $\beta$ -hydroxy sulfides; Dianion alkylation; Chiral  $\alpha,\beta$ -unsaturated diol.

\* Corresponding author. Tel.: +82 33 248 2071; fax: +82 33 251 8491; e-mail: btcho@hallym.ac.kr



**Scheme 1.** (i) LDA (2.1 equiv), MeSOtoly-*p* (2.0 equiv),  $-78\text{ }^{\circ}\text{C}$ , THF, 24 h, 55–65% yield. (ii) NaI (2.0 equiv), (CF<sub>3</sub>CO)<sub>2</sub>O (3.0 equiv),  $0\text{ }^{\circ}\text{C}$ , acetone, 88–95% yield. (iii) (*S*)-**5** (0.1 equiv), **6** (0.5 equiv),  $0\text{ }^{\circ}\text{C}$ , 93–99% yield.

**Table 1.** Preparation of optically active allylic  $\beta$ -hydroxy sulfides<sup>a</sup>

Run no.	Product <b>4</b>	Yield (%) <sup>b</sup>	$[\alpha]_{\text{D}}^{20}$ in CHCl <sub>3</sub>	ee (%)	Abs. Config	
1		<b>4a</b>	93	$-10.05$ ( <i>c</i> 1.51)	90 <sup>c</sup>	<i>S</i> <sup>d</sup>
2		<b>4b</b>	95	$-1.71$ ( <i>c</i> 1.04)	97 <sup>c</sup>	<i>S</i> <sup>d</sup>
3		<b>4c</b>	97	$-0.61$ ( <i>c</i> 0.8)	90 <sup>c</sup>	<i>S</i> <sup>d</sup>
4		<b>4d</b>	95	$+6.92$ ( <i>c</i> 2.01)	95 <sup>c</sup>	<i>S</i> <sup>e</sup>
5		<b>4e</b>	97	$-92.33$ ( <i>c</i> 0.50)	98 <sup>f</sup>	<i>S</i> <sup>e</sup>
6		<b>4f</b>	98	$-114.12$ ( <i>c</i> 0.72)	98 <sup>c</sup>	<i>S</i> <sup>d</sup>
7		<b>4g</b>	99	$-110.51$ ( <i>c</i> 1.11)	98 <sup>c</sup>	<i>S</i> <sup>d</sup>
8		<b>4h</b>	99	$-64.93$ ( <i>c</i> 5.51)	96 <sup>c</sup>	<i>S</i> <sup>d</sup>
9		<b>4i</b>	95	$-97.32$ ( <i>c</i> 1.13)	97 <sup>c</sup>	<i>S</i> <sup>d</sup>

<sup>a</sup> By reduction of **3** with 0.5 equiv of **6** in the presence of 0.1 equiv of **5** in THF at  $0\text{ }^{\circ}\text{C}$ .

<sup>b</sup> Isolated yield.

<sup>c</sup> Determined by HPLC analysis using a 25 cm Chiralcel OD-H chiral column.

<sup>d</sup> Determined by HPLC analysis using a 25 cm Whelk O1 chiral column.

<sup>e</sup> Absolute configuration is unknown, but probably *S* based on comparison of the elution order of HPLC analysis of **4d** and **4e**.

<sup>f</sup> By comparison of their known configuration after conversion of **4d** and **4e** into **7** and **8**, respectively.

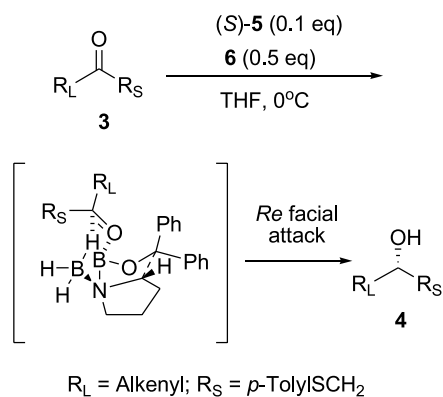


Figure 1.

5–8). Also, the reduction of a heterocyclic analogue **3i** having 2-furyl group gave 95% ee (run 9). In this reaction, we found that  $\beta$ -keto sulfides bearing alkenyl group provided much higher enantioselectivity than the corresponding unhindered aliphatic analogues. For example, the reduction of **4b** containing 1-pentenyl group provided 95% ee, whereas the case of  $\beta$ -keto sulfide having *n*-pentyl group afforded 74% ee.<sup>14</sup> These phenomena are attributable that the alkenyl group behaves as effectively larger than alkyl group in the oxazaborolidine-catalyzed borane reduction,<sup>6</sup> although the reason is unclear so far. All the product  $\beta$ -hydroxy sulfides **4** obtained are consistently enriched in the *S*-enantiomers. The stereochemical course can be explained by the generally accepted mechanism for **5**-catalyzed borane reduction,<sup>12f</sup> where the  $\beta$ -keto sulfides **3** are attacked by hydride on their *Re* faces to provide (*S*)-**4** (Fig. 1).<sup>17</sup> On the other hand, non-racemic alkenic diols, such as **9**<sup>18</sup> and **10**,<sup>19</sup> are frequently used as important starting materials for synthesis of biologically active substances. Since  $\beta$ -hydroxy sulfides are easily converted into diols by Pummerer reaction,<sup>11q</sup> we examined preparation of optically active alkenic diols **9** and **10** from **4d** and **4e**, respectively. When  $\beta$ -hydroxy sulfides **4d** and **4e** were treated with 1.1 equiv of *m*-chloroperbenzoic acid in dichloromethane at 0 °C, the corresponding sulfoxides **7** were obtained in 96–99% yields. It was subsequently

reacted with 2.5 equiv of sodium acetate in acetic anhydride at reflux condition to give 1,2-diacetoxy sulfides **8**. Without further purification, these were directly treated with 1.0 equiv of sodium borohydride in 6 N NaOH at room temperature to give chiral 1,2-diols **9** with >95% ee and **10** with 98% ee in 65 and 60% yields from **4d** and **4e**, respectively (Scheme 2).

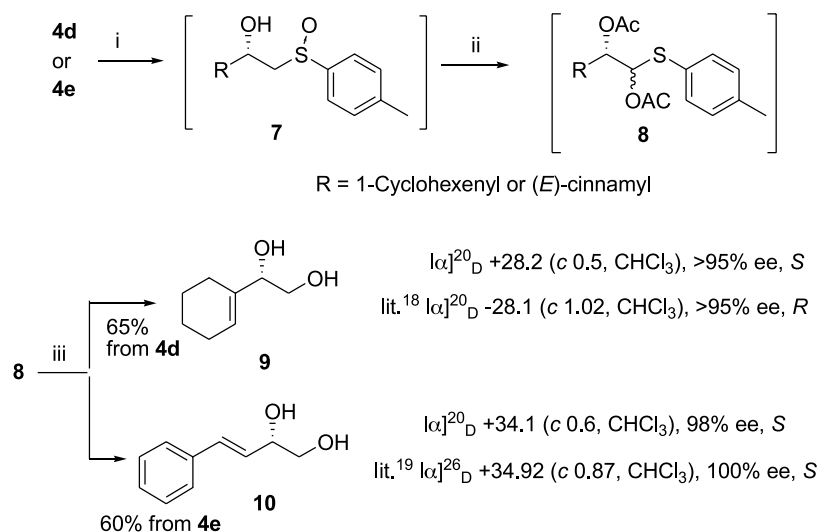
### 3. Conclusion

We have established a simple and convenient synthesis of optically active alkenic  $\beta$ -hydroxy sulfides, which can be used as versatile chiral intermediates for synthesis of a wide range of non-racemic compounds including biologically active substances by employing **5**-oxazaborolidine-catalyzed borane reduction of the corresponding  $\beta$ -keto sulfides. The reduction provided high enantioselectivity in all the case of acyclic, endocyclic and exocyclic analogues.  $\beta$ -Hydroxy sulfides **4d** and **4e** obtained were successfully converted into chiral alkenic diols **9** and **10** without racemization under Pummerer reaction conditions, respectively.

### 4. Experimental

#### 4.1. General

All operations with air-sensitive materials were carried out under a nitrogen atmosphere with oven-dried glassware. Liquid materials were transferred with a double-ended needle. The reactions were monitored by TLC using silica gel plates and the products were purified by flash column chromatography on silica gel (Merck; 230–400 mesh). NMR spectra were recorded at 300 MHz for <sup>1</sup>H and 75 MHz for <sup>13</sup>C using Me<sub>4</sub>Si as the internal standard in CDCl<sub>3</sub>. Optical rotations were measured with a high resolution digital polarimeter. Melting points were uncorrected. Enantiomeric excesses (ees) of the product  $\beta$ -hydroxy sulfides and diols were determined with a HPLC apparatus



Scheme 2. (i) *m*-CPBA (1.1 equiv), CH<sub>2</sub>Cl<sub>2</sub>, 0 °C. (ii) NaOAc (2.5 equiv), Ac<sub>2</sub>O, reflux. (iii) NaBH<sub>4</sub> (2.5 equiv), 6 N–NaOH–EtOH, rt.

fitted with a 25 cm Chiralcel OD-H (Daicel) or Whelk-O1 (Regis) chiral column.

## 4.2. Materials

Most of organic compounds utilized in this study were commercial products of the highest purity. They were further purified by distillation when necessary. THF was distilled over sodium benzophenone ketyl and stored in ampules under nitrogen atmosphere. (*S*)-CBS reagent **5** and *N*-ethyl-*N*-isopropylaniline–borane complex **6** were purchased from the Aldrich Chemical Company.

## 4.3. Preparation of alkenyl $\beta$ -keto sulfoxides **2**

**4.3.1. General procedure.**<sup>15</sup> To a solution of LDA (5.5 mmol) in THF (15 mL) was added a solution of methyl *p*-tolyl sulfoxide (5 mmol) in THF (7.5 mL) dropwise at  $-78^\circ\text{C}$ . After the mixture was stirred at  $-78^\circ\text{C}$  for 1 h and this was slowly added to a solution of  $\alpha$ -alkenic ester **1** (5 mmol) in THF (25 mL) at the same temperature via a syringe with stirring. After 24 h at  $-78^\circ\text{C}$ , the reaction mixture was decomposed with a saturated ammonium chloride solution (50 mL) and ether (50 mL). Organic layer was separated and the aqueous solution was extracted with ether ( $3 \times 15$  mL). The combined extracts were washed with brine, dried over anhydrous magnesium sulfate, filtered and evaporated. The crude alkenyl  $\beta$ -hydroxy sulfoxides **2** obtained were further purified by a flash column chromatography on silica gel (230–400 mesh) using ethyl acetate/hexane (1/1) as the eluent.

**4.3.2. 1-[(*RS*)-*p*-Tolylsulfinyl]-4-methyl-3-penten-2-one **2a**.**  $R_f$  0.48; oil; 65% yield; IR (neat,  $\text{cm}^{-1}$ ): 3479, 3461, 2976, 2912, 1674, 1615, 1445, 1381, 1227, 1044, 915, 811;  $^1\text{H}$  NMR (300 MHz,  $\text{CDCl}_3$ )  $\delta$  1.82 (d, 3H,  $J=1.1$  Hz), 2.05 (d, 3H,  $J=1.1$  Hz), 2.33 (s, 3H), 3.64 (d, 1H,  $J=13.20$  Hz), 3.83 (d, 1H,  $J=13.20$  Hz), 6.00 (s, 1H), 7.22 (d, 2H,  $J=8.22$  Hz), 7.45 (d, 2H,  $J=8.25$  Hz);  $^{13}\text{C}$  NMR (75 MHz,  $\text{CDCl}_3$ )  $\delta$  21.67, 21.79, 28.26, 70.34, 123.64, 124.36, 130.14, 140.37, 142.09, 160.14, 190.30; Anal. Calcd for  $\text{C}_{13}\text{H}_{16}\text{O}_2\text{S}$ : C, 66.07; H, 6.82; S, 13.57. Found: C, 66.12; H, 6.79; S, 13.54.

**4.3.3. (3*E*)-1-[(*RS*)-*p*-Tolylsulfinyl]-3-hepten-2-one **2b**.**  $R_f$  0.45; oil; 62% yield; IR (neat,  $\text{cm}^{-1}$ ): 3475, 2960, 2931, 2872, 1685, 1617, 1457, 1288, 1085, 1046, 1015, 978, 810;  $^1\text{H}$  NMR (300 MHz,  $\text{CDCl}_3$ )  $\delta$  0.92 (t, 3H,  $J=7.43$  Hz), 1.46 (sextuplet, 2H,  $J=7.43$  Hz), 2.18 (qd, 2H,  $J=7.01$ , 1.51 Hz), 2.40 (s, 3H), 3.87 (d, 1H,  $J=13.20$  Hz), 4.08 (d, 1H,  $J=13.20$  Hz), 6.09 (m, 1H), 6.81 (m, 1H), 7.23 (d, 2H,  $J=7.98$  Hz), 7.51–7.55 (m, 2H);  $^{13}\text{C}$  NMR (75 MHz,  $\text{CDCl}_3$ )  $\delta$  14.01, 21.51, 21.80, 35.01, 66.82, 124.41, 130.19, 130.62, 140.14, 142.27, 151.78, 190.83; Anal. Calcd for  $\text{C}_{14}\text{H}_{18}\text{O}_2\text{S}$ : C, 67.16; H, 7.25; S, 12.81. Found: C, 67.23; H, 7.28; S, 12.83.

**4.3.4. 1-[(*RS*)-*p*-Tolylsulfinyl]-3-cycloheptylidenyl-2-propanone **2c**.**  $R_f$  0.63; oil; 57% yield; IR (neat,  $\text{cm}^{-1}$ ): 3481, 2923, 2853, 1673, 1597, 1444, 1396, 1202, 1088, 1041, 1016, 810;  $^1\text{H}$  NMR (300 MHz,  $\text{CDCl}_3$ )  $\delta$  1.50–1.62 (m, 8H), 2.32–2.35 (m, 2H), 2.40 (s, 3H), 2.78–2.82 (m, 2H), 3.72 (d, 1H,  $J=13.20$  Hz), 3.92 (d, 1H,  $J=12.93$  Hz),

6.03 (s, 1H), 7.29 (d, 2H,  $J=7.98$  Hz), 7.51–7.54 (m, 2H);  $^{13}\text{C}$  NMR (75 MHz,  $\text{CDCl}_3$ )  $\delta$  21.80, 26.52, 28.29, 29.53, 30.13, 33.95, 39.71, 70.40, 123.01, 124.43, 130.11, 130.26, 142.05, 171.13, 189.95; Anal. Calcd for  $\text{C}_{17}\text{H}_{22}\text{O}_2\text{S}$ : C, 70.31; H, 7.64; S, 11.04. Found: C, 70.34; H, 7.67; S, 11.24.

**4.3.5. 1-[(*RS*)-*p*-Tolylsulfinyl]-2-(cyclohexen-1-yl)-2-ethanone **2d**.**  $R_f$  0.59; oil; 60% yield; IR (neat,  $\text{cm}^{-1}$ ): 3471, 2938, 2859, 1668, 1597, 1454, 1434, 1245, 1086, 1041, 1023, 809;  $^1\text{H}$  NMR (300 MHz,  $\text{CDCl}_3$ )  $\delta$  1.61–1.65 (m, 8H), 2.40 (s, 3H), 4.06 (d, 1H,  $J=13.20$  Hz), 4.25 (d, 1H,  $J=13.20$  Hz), 6.62 (m, 1H), 7.33–7.58 (m, 4H);  $^{13}\text{C}$  NMR (75 MHz,  $\text{CDCl}_3$ )  $\delta$  21.64, 21.72, 22.12, 24.17, 26.58, 70.35, 130.22, 131.29, 132.54, 137.35, 140.20, 145.76, 190.82; Anal. Calcd for  $\text{C}_{15}\text{H}_{18}\text{O}_2\text{S}$ : C, 68.67; H, 6.92; S, 12.22. Found: C, 68.56; H, 6.95; S, 12.25.

**4.3.6. (3*E*)-1-[(*RS*)-*p*-Tolylsulfinyl]-4-phenyl-3-buten-2-one **2e**.**  $R_f$  0.34; mp  $86\text{--}88^\circ\text{C}$ ; 60% yield; IR (KBr,  $\text{cm}^{-1}$ ): 3448, 3044, 3025, 2921, 1652, 1627, 1595, 1449, 1268, 1036, 984, 810, 688;  $^1\text{H}$  NMR (300 MHz,  $\text{CDCl}_3$ )  $\delta$  2.38 (s, 3H), 4.00 (d, 1H,  $J=13.20$  Hz), 4.16 (d, 1H,  $J=13.20$  Hz), 6.69 (d, 1H,  $J=16.23$  Hz), 7.24–7.41 (m, 5H), 7.46–7.5 (m, 5H);  $^{13}\text{C}$  NMR (75 MHz,  $\text{CDCl}_3$ )  $\delta$  21.80, 67.38, 124.44, 125.98, 128.87, 129.19, 130.25, 131.36, 134.08, 142.39, 145.89, 190.57; Anal. Calcd for  $\text{C}_{17}\text{H}_{16}\text{O}_2\text{S}$ : C, 71.80; H, 5.67; S, 11.28. Found: C, 71.89; H, 5.77; S, 11.42.

**4.3.7. (3*E*)-1-[(*RS*)-*p*-Tolylsulfinyl]-4-*p*-tolyl-3-buten-2-one **2f**.**  $R_f$  0.44; mp  $82\text{--}84^\circ\text{C}$ ; 55% yield; IR (KBr,  $\text{cm}^{-1}$ ): 3264, 3036, 3021, 2917, 1636, 1629, 1597, 1492, 1316, 1159, 1037, 992, 806, 700;  $^1\text{H}$  NMR (300 MHz,  $\text{CDCl}_3$ )  $\delta$  2.37 (s, 6H), 3.98 (d, 1H,  $J=13.20$  Hz), 4.16 (d, 1H,  $J=13.20$  Hz), 6.65 (d, 1H,  $J=15.95$  Hz), 7.16–7.57 (m, 9H);  $^{13}\text{C}$  NMR (75 MHz,  $\text{CDCl}_3$ )  $\delta$  21.80, 21.94, 67.41, 124.45, 125.02, 128.41, 128.92, 129.95, 130.22, 131.35, 142.08, 142.33, 146.01, 190.58; Anal. Calcd for  $\text{C}_{18}\text{H}_{18}\text{O}_2\text{S}$ : C, 72.45; H, 6.08; S, 10.75. Found: C, 72.50; H, 6.16; S, 10.85.

**4.3.8. (3*E*)-1-[(*RS*)-*p*-Tolylsulfinyl]-4-(*p*-chlorophenyl)-3-buten-2-one **2g**.**  $R_f$  0.30; mp  $116\text{--}118^\circ\text{C}$ ; 57% yield; IR (KBr,  $\text{cm}^{-1}$ ): 3421, 3044, 3026, 2921, 1652, 1627, 1595, 1450, 1310, 1296, 1268, 1074, 1037, 984, 810;  $^1\text{H}$  NMR (300 MHz,  $\text{CDCl}_3$ )  $\delta$  2.38 (s, 3H), 3.98 (d, 1H,  $J=13.20$  Hz), 4.11 (d, 1H,  $J=13.20$  Hz), 6.67 (d, 1H,  $J=15.95$  Hz), 7.28–7.55 (m, 9H);  $^{13}\text{C}$  NMR (75 MHz,  $\text{CDCl}_3$ )  $\delta$  21.79, 67.35, 124.39, 126.36, 128.60, 129.50, 129.97, 130.26, 132.62, 137.35, 142.41, 144.23, 190.36; Anal. Calcd for  $\text{C}_{17}\text{H}_{15}\text{ClO}_2\text{S}$ : C, 64.04; H, 4.74; S, 10.06. Found: C, 64.17; H, 4.86; S, 10.01.

**4.3.9. (3*E*)-1-[(*RS*)-*p*-Tolylsulfinyl]-4-(1'-naphthyl)-3-butene-2-one **2h**.**  $R_f$  0.35; mp  $75\text{--}77^\circ\text{C}$ ; 65% yield; IR (KBr,  $\text{cm}^{-1}$ ): 3421, 3335, 3052, 2913, 1644, 1629, 1594, 1493, 1277, 1084, 1041, 978, 813, 732;  $^1\text{H}$  NMR (300 MHz,  $\text{CDCl}_3$ )  $\delta$  2.27 (s, 3H), 4.01 (d, 1H,  $J=13.20$  Hz), 4.13 (d, 1H,  $J=13.20$  Hz), 6.69 (d, 1H,  $J=15.95$  Hz), 7.20–8.31 (m, 12H);  $^{13}\text{C}$  NMR (75 MHz,  $\text{CDCl}_3$ )  $\delta$  21.82, 67.35, 123.39, 124.39, 124.47, 125.60, 125.69, 126.60, 127.42, 128.35, 129.03, 130.29, 131.35, 131.70, 131.81, 133.86, 142.43, 142.95, 190.50; Anal. Calcd for  $\text{C}_{21}\text{H}_{18}\text{O}_2\text{S}$ : C, 75.42; H, 5.42; S, 9.59. Found: C, 75.53; H, 5.54; S, 9.55.



**4.3.10. (3E)-1-[(RS)-p-Tolylsulfinyl]-4-(2'-furyl)-3-buten-2-one 2i.**  $R_f$  0.30; mp 107–109 °C; 58% yield; IR (KBr,  $\text{cm}^{-1}$ ): 3115, 2923, 1614, 1642, 1595, 1445, 1370, 1265, 1012, 974, 841, 700;  $^1\text{H}$  NMR (300 MHz,  $\text{CDCl}_3$ )  $\delta$  2.38 (s, 3H), 3.93 (d, 1H,  $J=13.20$  Hz), 4.10 (d, 1H,  $J=13.20$  Hz), 6.48 (m, 1H), 6.60 (d, 1H,  $J=15.67$  Hz), 6.70 (d, 1H,  $J=3.58$  Hz), 7.25–7.31 (m, 3H), 7.49–7.56 (m, 3H);  $^{13}\text{C}$  NMR (75 MHz,  $\text{CDCl}_3$ )  $\delta$  21.78, 67.74, 113.08, 117.63, 123.11, 124.40, 130.21, 131.42, 141.10, 142.29, 145.90, 150.83, 190.07; Anal. Calcd for  $\text{C}_{15}\text{H}_{14}\text{O}_2\text{S}$ : C, 65.67; H, 5.14; S, 11.69. Found: C, 65.76; H, 5.32; S, 11.74.

#### 4.4. Preparation of $\beta$ -keto sulfides 3 from sulfoxides 2

**4.4.1. General procedure.**<sup>16</sup> To a suspension of the sulfoxides 2 (2 mmol) and sodium iodide (4 mmol) in acetone (20 mL) at 0 °C was added dropwise trifluoroacetic anhydride (4.8 mmol) at the same temperature with stirring. After 15 min, the solvent was evaporated under reduced pressure. To this, a 1:1 saturated solution of sodium sulfite and sodium bicarbonate was added, extracted with ether (3  $\times$  15 mL). The combined organic layer was dried over anhydrous magnesium sulfate, filtered and evaporated in vacuo to dryness. The crude alkenyl  $\beta$ -hydroxy sulfides 3 obtained were further purified by a flash column chromatography on silica gel (230–400 mesh) using ethyl acetate/hexane (1/4) as the eluent.

**4.4.2. 1-(p-Tolylsulfonyl)-4-methyl-3-penten-2-one 3a.**  $R_f$  0.56; oil; 93% yield; IR (neat,  $\text{cm}^{-1}$ ): 3425, 2975, 2919, 1679, 1666, 1494, 1445, 1391, 1091, 1041, 804;  $^1\text{H}$  NMR (300 MHz,  $\text{CDCl}_3$ )  $\delta$  1.90 (d, 3H,  $J=1.37$  Hz), 2.11 (d, 3H,  $J=1.10$  Hz), 2.30 (s, 3H), 3.59 (s, 2H), 6.26 (m, 1H), 7.06 (d, 2H,  $J=8.53$  Hz), 7.22–7.25 (m, 2H);  $^{13}\text{C}$  NMR (75 MHz,  $\text{CDCl}_3$ )  $\delta$  21.29, 21.40, 28.20, 45.99, 122.06, 129.94, 130.64, 131.42, 137.06, 158.05, 194.72; Anal. Calcd for  $\text{C}_{13}\text{H}_{16}\text{OS}$ : C, 70.87; H, 7.32; S, 14.55. Found: C, 70.85; H, 7.41; S, 14.57.

**4.4.3. (3E)-1-(p-Tolylsulfonyl)-3-hepten-2-one 3b.**  $R_f$  0.47; oil; 91% yield; IR (neat,  $\text{cm}^{-1}$ ): 3390, 3367, 2959, 2930, 2871, 1689, 1626, 1490, 1456, 1089, 1041, 806;  $^1\text{H}$  NMR (300 MHz,  $\text{CDCl}_3$ )  $\delta$  0.92 (t, 3H,  $J=7.43$  Hz), 1.47 (m, 2H), 2.18 (m, 2H), 2.30 (s, 3H), 3.70 (s, 2H), 6.28 (m, 1H), 6.84 (m, 1H), 7.07 (d, 2H,  $J=7.70$  Hz), 7.24–7.27 (m, 2H);  $^{13}\text{C}$  NMR (75 MHz,  $\text{CDCl}_3$ )  $\delta$  14.04, 21.41, 21.62, 34.85, 43.54, 128.15, 130.01, 131.19, 137.45, 149.22, 194.27; Anal. Calcd for  $\text{C}_{14}\text{H}_{18}\text{OS}$ : C, 71.75; H, 7.74; S, 13.68. Found: C, 71.79; H, 7.81; S, 13.71.

**4.4.4. 1-(p-Tolylsulfonyl)-3-cycloheptylidene-2-propa- none 3c.**  $R_f$  0.70; oil; 95% yield; IR (neat,  $\text{cm}^{-1}$ ): 3019, 2923, 2852, 1672, 1604, 1493, 443, 804;  $^1\text{H}$  NMR (300 MHz,  $\text{CDCl}_3$ )  $\delta$  1.45–1.50 (m, 4H), 1.58–1.63 (m, 4H), 2.30 (s, 3H), 2.34–2.38 (m, 2H), 2.78–2.72 (m, 2H), 3.60 (s, 2H), 6.24 (s, 1H), 7.06 (d, 2H,  $J=8.53$  Hz), 7.22–7.25 (m, 2H);  $^{13}\text{C}$  NMR (75 MHz,  $\text{CDCl}_3$ )  $\delta$  21.40, 26.67, 28.46, 29.55, 30.16, 33.44, 39.64, 46.07, 121.57, 129.91, 130.04, 130.72, 130.83, 137.03, 168.77, 194.61; Anal. Calcd for  $\text{C}_{17}\text{H}_{22}\text{OS}$ : C, 74.40; H, 8.08; S, 11.68. Found: C, 74.53; H, 8.29; S, 11.70.

**4.4.5. 1-(p-Tolylsulfonyl)-2-(cyclohexen-1-yl)-2-ethanone 3d.**  $R_f$  0.69; oil; 92% yield; IR (neat,  $\text{cm}^{-1}$ ): 3019, 2933, 2859,

1666, 1634, 1493, 1434, 1277, 1180, 806;  $^1\text{H}$  NMR (300 MHz,  $\text{CDCl}_3$ )  $\delta$  1.56–1.64 (m, 4H), 2.20–2.24 (m, 4H), 2.31 (s, 3H), 3.91 (s, 2H), 6.80 (m, 1H), 7.01–7.08 (m, 2H), 7.24–7.27 (m, 2H);  $^{13}\text{C}$  NMR (75 MHz,  $\text{CDCl}_3$ )  $\delta$  21.42, 21.78, 22.22, 23.67, 26.53, 40.97, 129.92, 131.49, 131.85, 137.35, 138.30, 141.71, 195.46; Anal. Calcd for  $\text{C}_{15}\text{H}_{18}\text{OS}$ : C, 73.13; H, 7.36; S, 13.02. Found: C, 73.26; H, 7.54; S, 13.06.

**4.4.6. (3E)-1-(p-Tolylsulfonyl)-4-phenyl-3-buten-2-one 3e.**  $R_f$  0.67; mp 39–41 °C; 92% yield; IR (KBr,  $\text{cm}^{-1}$ ): 3391, 3058, 3025, 2919, 1683, 1608, 1575, 1494, 1331, 1204, 1073, 979, 808;  $^1\text{H}$  NMR (300 MHz,  $\text{CDCl}_3$ )  $\delta$  2.30 (s, 3H), 3.79 (s, 2H), 6.95 (d, 1H,  $J=15.95$  Hz), 7.07 (d, 2H,  $J=7.98$  Hz), 7.27–7.58 (m, 8H);  $^{13}\text{C}$  NMR (75 MHz,  $\text{CDCl}_3$ )  $\delta$  21.44, 44.29, 123.89, 128.65, 129.10, 130.10, 130.83, 131.40, 134.55, 137.66, 144.05, 194.02; Anal. Calcd for  $\text{C}_{17}\text{H}_{16}\text{OS}$ : C, 76.08; H, 6.01; S, 11.95. Found: C, 76.25; H, 6.11; S, 11.90.

**4.4.7. (3E)-1-(p-Tolylsulfonyl)-4-p-tolyl-3-buten-2-one 3f.**  $R_f$  0.56; mp 72–74 °C; 88% yield; IR (KBr,  $\text{cm}^{-1}$ ): 3420, 3021, 2914, 2861, 1678, 1616, 1601, 1566, 1493, 1393, 1183, 1161, 1081, 983, 800;  $^1\text{H}$  NMR (300 MHz,  $\text{CDCl}_3$ )  $\delta$  2.30 (s, 3H), 2.37 (s, 3H), 3.78 (s, 2H), 6.90 (d, 1H,  $J=15.95$  Hz), 7.05–7.55 (m, 9H);  $^{13}\text{C}$  NMR (75 MHz,  $\text{CDCl}_3$ )  $\delta$  21.42, 21.88, 44.24, 122.95, 128.67, 129.84, 130.07, 131.35, 131.82, 133.95, 137.58, 141.38, 144.14, 194.13; Anal. Calcd for  $\text{C}_{18}\text{H}_{18}\text{OS}$ : C, 76.56; H, 6.42; S, 11.35. Found: C, 76.54; H, 6.46; S, 11.38.

**4.4.8. (3E)-1-(p-Tolylsulfonyl)-4-(p-chlorophenyl)-3-buten-2-one 3g.**  $R_f$  0.47; mp 86–88 °C; 93% yield; IR (KBr,  $\text{cm}^{-1}$ ): 3453, 2914, 2874, 1678, 1612, 1587, 1489, 1406, 1343, 1077, 1013, 981, 809;  $^1\text{H}$  NMR (300 MHz,  $\text{CDCl}_3$ )  $\delta$  2.30 (s, 3H), 3.77 (s, 2H), 6.91 (d, 1H,  $J=15.96$  Hz), 7.06–7.09 (m, 2H), 7.26–7.52 (m, 7H);  $^{13}\text{C}$  NMR (75 MHz,  $\text{CDCl}_3$ )  $\delta$  21.43, 44.33, 124.23, 129.39, 129.75, 130.12, 131.40, 133.06, 136.74, 137.74, 142.49, 193.72; Anal. Calcd for  $\text{C}_{17}\text{H}_{15}\text{ClOS}$ : C, 67.43; H, 4.99; S, 10.59. Found: C, 67.55; H, 5.05; S, 10.63.

**4.4.9. (3E)-1-(p-Tolylsulfonyl)-4-(1'-naphthyl)-3-buten-2-one 3h.**  $R_f$  0.52; mp 62–64 °C; 92% yield; IR (KBr,  $\text{cm}^{-1}$ ): 3025, 2919, 1683, 1656, 1652, 1576, 1494, 1131, 1073, 807, 689;  $^1\text{H}$  NMR (300 MHz,  $\text{CDCl}_3$ )  $\delta$  2.30 (s, 3H), 3.85 (s, 2H), 7.05–7.11 (m, 2H), 7.30–7.52 (m, 6H), 7.75–7.90 (m, 3H), 8.11–8.45 (m, 2H);  $^{13}\text{C}$  NMR (75 MHz,  $\text{CDCl}_3$ )  $\delta$  21.46, 44.40, 123.52, 125.40, 125.61, 126.29, 126.46, 127.15, 128.96, 129.09, 129.92, 130.15, 131.12, 131.43, 131.85, 133.89, 133.97, 140.84, 193.98; Anal. Calcd for  $\text{C}_{21}\text{H}_{18}\text{OS}$ : C, 79.21; H, 5.70; S, 10.07. Found: C, 79.32; H, 5.89; S, 10.13.

**4.4.10. (3E)-1-(p-Tolylsulfonyl)-4-(2'-furyl)-3-buten-2-one 3i.**  $R_f$  0.56; oil; 90% yield; IR (neat,  $\text{cm}^{-1}$ ): 3483, 3124, 3021, 2920, 1674, 1606, 1553, 1493, 1389, 1281, 1264, 1082, 1071, 807;  $^1\text{H}$  NMR (300 MHz,  $\text{CDCl}_3$ )  $\delta$  2.28 (s, 3H), 3.74 (s, 2H), 6.45 (m, 1H), 6.63 (d, 1H,  $J=3.58$  Hz), 6.86 (d, 1H,  $J=15.40$  Hz), 7.06 (d, 2H,  $J=8.53$  Hz), 7.25–7.47 (m, 4H);  $^{13}\text{C}$  NMR (75 MHz,  $\text{CDCl}_3$ )  $\delta$  21.43, 44.40, 112.84, 116.45, 121.24, 130.02, 130.06, 130.91, 131.14, 133.86, 137.48, 145.28, 151.25, 193.67; Anal. Calcd for

$C_{15}H_{14}O_2S$ : C, 69.74; H, 5.46; S, 12.41. Found: C, 69.77; H, 5.54; S, 12.48.

#### 4.5. Preparation of optically active alkenyl $\beta$ -hydroxy sulfides **4**

**4.5.1. General procedure.** To a solution of **5** (0.2 mmol; 0.2 M, 1.0 mL) in THF was added a solution of *N*-ethyl-*N*-isopropylaniline–borane complex **6** (1.0 mmol; 2.0 M, 0.5 mL) in THF. To this was added slowly 2.5 mL of THF solution of **3** (2 mmol) over a period of 1.5 h using a syringe pump at 0 °C. After the addition, the reaction mixture was stirred for 10 min, quenched cautiously with methanol (0.5 mL), and stirred for additional 30 min. The solvent was evaporated under reduced pressure. The crude alkenyl  $\beta$ -hydroxy sulfides **4** obtained were further purified by a flash column chromatography on silica gel (230–400 mesh) using ethyl acetate/hexane (1/4) as the eluent. The enantiomeric excesses of **4** were determined by HPLC analysis using a 25 cm Chiralcel OD-H or Whelk-O1 chiral column. Absolute configurations were assigned by comparison of the literature values reported or analogy based on the elution order of HPLC analysis and/or the sign of the optical rotation values compared to those of the *p*-tolyl- or phenylsulfamyl analogues published.<sup>14</sup>

**4.5.2. (2S)-1-(*p*-Tolylsulfamyl)-4-methyl-3-penten-2-ol **4a**.**  $R_f$  0.33; oil; 93% yield; IR (neat,  $cm^{-1}$ ): 3395, 3373, 2969, 2919, 2869, 1493, 1376, 1091, 1017, 982, 804;  $^1H$  NMR (300 MHz,  $CDCl_3$ )  $\delta$  1.53 (d, 3H,  $J=1.1$  Hz), 1.64 (d, 3H,  $J=1.1$  Hz), 2.24 (s, 3H), 2.27 (d, 1H,  $J=2.48$  Hz), 2.80 (dd, 1H,  $J=13.62$ , 8.66 Hz), 2.97 (dd, 1H,  $J=13.48$ , 4.13 Hz), 4.30 (m, 1H), 5.10 (m, 1H), 7.00–7.23 (m, 4H);  $^{13}C$  NMR (75 MHz,  $CDCl_3$ )  $\delta$  18.71, 21.39, 26.12, 42.91, 66.77, 125.68, 129.97, 130.81, 131.61, 136.89; Anal. Calcd for  $C_{13}H_{18}OS$ : C, 70.22; H, 8.16; S, 14.42. Found: C, 70.25; H, 8.27; S, 14.38;  $[\alpha]_D^{20} -10.05$  ( $c$  1.51,  $CHCl_3$ ), *S*; HPLC analysis using a 25 cm Chiralcel OD-H chiral column (*iso*-PrOH/hexane: 1/9; flow rate: 1.0 mL/min; detector: 254 nm) showed it to be 90% ee ( $t_R(S)$  5.62 min and  $t_R(R)$  6.47 min).

**4.5.3. (2S, 3E)-1-(*p*-Tolylsulfamyl)-3-hepten-2-ol **4b**.**  $R_f$  0.35; oil; 95% yield; IR (neat,  $cm^{-1}$ ): 3363, 3356, 2957, 2925, 2870, 1493, 1399, 1090, 1025, 1015, 969, 806;  $^1H$  NMR (300 MHz,  $CDCl_3$ )  $\delta$  0.89 (t, 3H,  $J=7.43$  Hz), 1.38 (m, 2H), 1.99 (m, 2H), 2.31 (s, 3H), 2.43 (d, 1H,  $J=3.03$  Hz), 2.88 (dd, 1H,  $J=13.48$ , 8.53 Hz), 3.08 (dd, 1H,  $J=13.62$ , 3.99 Hz), 4.10 (m, 1H), 5.44 (m, 1H), 5.68 (m, 1H), 7.08–7.10 (m, 2H), 7.23–7.30 (m, 2H);  $^{13}C$  NMR (75 MHz,  $CDCl_3$ )  $\delta$  14.01, 21.37, 22.49, 34.62, 43.31, 70.53, 129.99, 130.57, 131.14, 131.53, 133.51, 137.04; Anal. Calcd for  $C_{14}H_{20}OS$ : C, 71.14; H, 8.53; S, 13.57. Found: C, 71.17; H, 8.55; S, 13.60;  $[\alpha]_D^{20} -1.71$  ( $c$  1.04,  $CHCl_3$ ), *S*; HPLC analysis using a 25 cm Chiralcel OD-H chiral column (*iso*-PrOH/hexane: 1/9; flow rate: 0.3 mL/min; detector: 254 nm) showed it to be 90% ee ( $t_R(S)$  17.69 min and  $t_R(R)$  18.74 min).

**4.5.4. (2S)-1-(*p*-Tolylsulfamyl)-3-cycloheptylidenyl-2-propanol **4c**.**  $R_f$  0.49; oil; 97% yield; IR (neat,  $cm^{-1}$ ): 3394, 3355, 2921, 2851, 1493, 1435, 1091, 1042, 1017, 986, 803;  $^1H$  NMR (300 MHz,  $CDCl_3$ )  $\delta$  1.47–1.56 (m, 8H),

2.17–2.22 (m, 4H), 2.32 (s, 3H), 2.88 (dd, 1H,  $J=13.62$ , 8.67 Hz), 3.05 (dd, 1H,  $J=13.48$ , 4.13 Hz), 4.38 (m, 1H), 5.17 (m, 1H), 7.08 (d, 2H,  $J=7.01$  Hz), 7.24–7.23 (m, 2H);  $^{13}C$  NMR (75 MHz,  $CDCl_3$ )  $\delta$  21.38, 27.59, 29.09, 29.2, 29.95, 30.61, 38.11, 42.94, 66.37, 125.76, 129.95, 130.70, 131.73, 136.83, 146.35; Anal. Calcd for  $C_{17}H_{24}OS$ : C, 73.86; H, 8.75; S, 11.60. Found: C, 73.90; H, 8.89; S, 11.59;  $[\alpha]_D^{20} -0.61$  ( $c$  0.8,  $CHCl_3$ ), *S*; HPLC analysis using a 25 cm Chiralcel OD-H chiral column (*iso*-PrOH/hexane: 1/9; flow rate: 0.3 mL/min; detector: 254 nm) showed it to be 90% ee ( $t_R(S)$  18.86 min and  $t_R(R)$  20.17 min).

**4.5.5. (2S)-1-(*p*-Tolylsulfamyl)-2-(cyclohexen-1-yl)-2-ethanol **4d**.**  $R_f$  0.33; oil; 95% yield; IR (neat,  $cm^{-1}$ ): 3373, 3364, 2921, 2850, 1493, 1445, 1360, 1240, 1091, 1042, 1017, 974, 802;  $^1H$  NMR (300 MHz,  $CDCl_3$ )  $\delta$  1.07–1.28 (m, 4H), 1.71–1.91 (m, 4H), 2.31 (s, 3H), 2.98 (dd, 1H,  $J=13.34$ , 7.56 Hz), 3.05 (dd, 1H,  $J=13.48$ , 3.85 Hz), 3.83 (m, 1H), 4.63 (s, 1H), 7.07 (d, 2H,  $J=7.71$  Hz), 7.24–7.23 (m, 2H);  $^{13}C$  NMR (75 MHz,  $CDCl_3$ )  $\delta$  21.39, 22.80, 22.87, 24.27, 25.31, 41.64, 73.72, 124.42, 129.96, 131.02, 131.61, 136.94, 137.88; Anal. Calcd for  $C_{15}H_{20}OS$ : C, 72.53; H, 8.12; S, 12.91. Found: C, 72.66; H, 8.34; S, 11.45;  $[\alpha]_D^{20} -6.92$  ( $c$  2.01,  $CHCl_3$ ), *S*; HPLC analysis using a 25 cm Chiralcel OD-H chiral column (*iso*-PrOH/hexane: 1/9; flow rate: 0.3 mL/min; detector: 254 nm) showed it to be 95% ee ( $t_R(S)$  21.68 min and  $t_R(R)$  23.14 min).

**4.5.6. (2S,3E)-1-(*p*-Tolylsulfamyl)-4-phenyl-3-buten-2-ol **4e**.**  $R_f$  0.35; oil; 97% yield; IR (neat,  $cm^{-1}$ ): 3395, 3373, 3057, 3024, 2960, 2919, 1493, 1448, 1399, 1091, 1017, 966, 805, 750, 692;  $^1H$  NMR (300 MHz,  $CDCl_3$ )  $\delta$  2.32 (s, 3H), 2.64 (d, 1H,  $J=3.03$  Hz), 2.97 (dd, 1H,  $J=13.62$ , 8.40 Hz), 3.18 (dd, 1H,  $J=13.62$ , 3.99 Hz), 4.33 (m, 1H), 6.16 (dd, 1H,  $J=15.68$ , 6.33 Hz), 6.60 (d, 1H,  $J=15.95$  Hz), 7.09–7.34 (m, 9H);  $^{13}C$  NMR (75 MHz,  $CDCl_3$ )  $\delta$  21.43, 43.31, 70.50, 126.72, 127.99, 128.73, 129.84, 130.12, 131.17, 131.42, 131.53, 136.59, 137.34; Anal. Calcd for  $C_{17}H_{18}OS$ : C, 75.51; H, 6.71; S, 11.86. Found: C, 75.57; H, 6.97; S, 11.90;  $[\alpha]_D^{20} -92.33$  ( $c$  0.50,  $CHCl_3$ ), *S*; HPLC analysis using a 25 cm Whelk-O1 chiral column (*iso*-PrOH/hexane: 1/9; flow rate: 1.0 mL/min; detector: 254 nm) showed it to be 98% ee ( $t_R(S)$  7.21 min and  $t_R(R)$  8.78 min).

**4.5.7. (2S,3E)-1-(*p*-Tolylsulfamyl)-4-*p*-tolyl-3-buten-2-ol **4f**.**  $R_f$  0.37; oil; 98% yield; IR (neat,  $cm^{-1}$ ): 3405, 3381, 3020, 2919, 1493, 1446, 1410, 1091, 1017, 968, 802;  $^1H$  NMR (300 MHz,  $CDCl_3$ )  $\delta$  2.32 (s, 6H), 2.59 (d, 1H,  $J=3.03$  Hz), 2.97 (dd, 1H,  $J=13.75$ , 8.53 Hz), 3.18 (dd, 1H,  $J=13.75$ , 4.13 Hz), 4.31 (m, 1H), 6.10 (dd, 1H,  $J=15.95$ , 6.33 Hz), 6.56 (d, 1H,  $J=15.68$  Hz), 7.07–7.34 (m, 8H);  $^{13}C$  NMR (75 MHz,  $CDCl_3$ )  $\delta$  21.40, 21.56, 43.33, 70.63, 126.62, 128.81, 129.42, 130.08, 131.29, 131.36, 131.50, 133.82, 137.26, 137.84; Anal. Calcd for  $C_{18}H_{20}OS$ : C, 76.01; H, 7.09; S, 11.27. Found: C, 76.23; H, 7.26; S, 11.35;  $[\alpha]_D^{20} -114.12$  ( $c$  0.72,  $CHCl_3$ ), *S*; HPLC analysis using a 25 cm Chiralcel OD-H chiral column (*iso*-PrOH/hexane: 1/9; flow rate: 1.0 mL/min; detector: 254 nm) showed it to be 98% ee ( $t_R(S)$  10.10 min and  $t_R(R)$  14.80 min).

**4.5.8. (2S,3E)-1-(*p*-Tolylsulfamyl)-4-(*p*-chlorophenyl)-3-buten-2-ol **4g**.**  $R_f$  0.34; oil; 98% yield; IR (neat,  $cm^{-1}$ ): 3452, 3425, 2921, 1495, 1410, 1301, 1148, 1089, 1037,



1015, 959, 811, 760;  $^1\text{H}$  NMR (300 MHz,  $\text{CDCl}_3$ )  $\delta$  2.32 (s, 3H), 2.64 (d, 1H,  $J=3.03$  Hz), 2.97 (dd, 1H,  $J=13.62$ , 8.40 Hz), 3.17 (dd, 1H,  $J=13.75$ , 4.13 Hz), 4.31 (m, 1H), 6.12 (dd, 1H,  $J=15.68$ , 6.05 Hz), 6.55 (dd, 1H,  $J=15.95$ , 1.38 Hz), 7.08–7.33 (m, 8H);  $^{13}\text{C}$  NMR (75 MHz,  $\text{CDCl}_3$ )  $\delta$  21.40, 43.28, 70.36, 127.90, 128.88, 130.12, 130.20, 130.57, 131.46, 133.60, 135.14, 137.41; Anal. Calcd for  $\text{C}_{17}\text{H}_{17}\text{ClOS}$ : C, 66.98; H, 5.62; S, 11.63. Found: C, 67.15; H, 5.65; S, 11.73;  $[\alpha]_{\text{D}}^{20} -110.51$  ( $c$  1.11,  $\text{CHCl}_3$ ),  $S$ ; HPLC analysis using a 25 cm Whelk-O1 chiral column (*iso*-PrOH/hexane: 1/9; flow rate: 0.5 mL/min; detector: 254 nm) showed it to be 98% ee ( $t_{\text{R}}(S)$  11.91 min and  $t_{\text{R}}(R)$  13.57 min).

**4.5.9. (2*S*,3*E*)-1-(*p*-Tolylsulfamyl)-4-(1-naphthyl)-3-buten-2-ol 4h.**  $R_{\text{f}}$  0.36; oil; 99% yield; IR (neat,  $\text{cm}^{-1}$ ): 3394, 3374, 3055, 3043, 2918, 1493, 1396, 1091, 1016, 969, 797, 775;  $^1\text{H}$  NMR (300 MHz,  $\text{CDCl}_3$ )  $\delta$  2.33 (s, 3H), 2.73 (d, 1H,  $J=3.30$  Hz), 3.06 (dd, 1H,  $J=13.48$ , 8.25 Hz), 3.25 (dd, 1H,  $J=13.62$ , 4.26 Hz), 4.45 (m, 1H), 6.19 (dd, 1H,  $J=15.68$ , 6.05 Hz), 7.11 (d, 2H,  $J=7.70$  Hz), 7.34–8.07 (m, 10H);  $^{13}\text{C}$  NMR (75 MHz,  $\text{CDCl}_3$ )  $\delta$  21.43, 43.37, 70.70, 123.97, 124.14, 125.72, 125.97, 126.24, 128.30, 128.69, 130.15, 131.26, 131.32, 131.47, 133.14, 133.75, 134.41, 137.36; Anal. Calcd for  $\text{C}_{21}\text{H}_{20}\text{OS}$ : C, 78.71; H, 6.29; S, 10.01. Found: C, 78.78; H, 6.44; S, 9.90;  $[\alpha]_{\text{D}}^{20} -64.93$  ( $c$  5.51,  $\text{CHCl}_3$ ),  $S$ ; HPLC analysis using a 25 cm Chiralcel OD-H chiral column (*iso*-PrOH/hexane: 1/9; flow rate: 1.0 mL/min; detector: 254 nm) showed it to be 96% ee ( $t_{\text{R}}(S)$  19.01 min and  $t_{\text{R}}(R)$  29.81 min).

**4.5.10. (2*S*,3*E*)-1-(*p*-Tolylsulfamyl)-4-(2'-furyl)-3-buten-2-ol 4i.**  $R_{\text{f}}$  0.31; oil; 95% yield; IR (neat,  $\text{cm}^{-1}$ ): 3394, 3373, 2920, 1493, 1398, 1091, 1014, 962, 805, 737;  $^1\text{H}$  NMR (300 MHz,  $\text{CDCl}_3$ )  $\delta$  2.32 (s, 3H), 2.59 (d, 1H,  $J=3.30$  Hz), 2.93 (dd, 1H,  $J=13.75$ , 8.53 Hz), 3.16 (dd, 1H,  $J=13.62$ , 3.99 Hz), 4.28 (m, 1H), 6.10 (dd, 1H,  $J=15.82$ , 6.05 Hz), 6.21 (d, 1H,  $J=3.30$  Hz), 6.44 (dd, 1H,  $J=15.48$ , 1.38 Hz), 6.33 (dd, 1H,  $J=3.30$ , 1.65 Hz), 7.07–7.32 (m, 5H);  $^{13}\text{C}$  NMR (75 MHz,  $\text{CDCl}_3$ )  $\delta$  21.40, 43.30, 69.99, 108.61, 111.50, 119.65, 128.36, 130.08, 131.16, 131.38, 137.31, 142.26, 152.33; Anal. Calcd for  $\text{C}_{15}\text{H}_{16}\text{O}_2\text{S}$ : C, 69.20; H, 6.19; S, 12.32. Found: C, 69.34; H, 6.32; S, 12.08;  $[\alpha]_{\text{D}}^{20} -97.35$  ( $c$  1.13,  $\text{CHCl}_3$ ),  $S$ ; HPLC analysis using a 25 cm Chiralceli OD-H chiral column (*iso*-PrOH/hexane: 1/9; flow rate: 1.0 mL/min; detector: 254 nm) showed it to be 97% ee ( $t_{\text{R}}(S)$  10.01 min and  $t_{\text{R}}(R)$  11.37 min).

## 4.6. Preparation of alkenyl diols 9 and 10

**4.6.1. General procedure.** To a solution of **4d** or **4e** (2 mmol) in dichloromethane (10 mL) was added dropwise a solution of *m*-chloroperbenzoic acid (2.2 mmol) in dichloromethane (15 mL) for 10 min at 0 °C. After the mixture was stirred for 30 min at room temperature, organic layer was separated, washed with 2 N NaOH (2 × 10 mL) and brine (2 × 10 mL), dried over anhydrous  $\text{MgSO}_4$ , filtered and concentrated to give **7**, which could be used for the following reaction without further purification. A stirred mixture of **7** and NaOAc (5 mmol) in acetic anhydride (6 mL) was heated to reflux for 3 h. After excess of acetic anhydride and acetic acid were removed under reduced pressure, the residue was dissolved in ether (10 mL)

and passed through silica gel. Crude 1,2-diacetoxy sulfides **8** obtained from the evaporation of the solvent followed by drying under vacuum were dissolved in ethanol (10 mL). To this was added  $\text{NaBH}_4$  (3 mmol) in 6 N NaOH (1 mL) and stirred for 4 h at room temperature. After the reaction mixture was extracted with ether (3 × 10 mL), the combined extracts are concentrated to give **9** or **10**, which was further purified by a flash column chromatography on silica gel (230–400 mesh) using ethyl acetate/hexane (1/1) as the eluent.

**4.6.2. (S)-1-(Cyclohexen-1-yl)-1,2-ethanediol 9 from 4d.**  $R_{\text{f}}$  0.17; mp 68–70 °C (lit.<sup>18</sup> 72–73 °C; 65% yield; IR (KBr,  $\text{cm}^{-1}$ ): 3277, 3252, 2950, 2915, 2873, 1447, 1078, 1054;  $^1\text{H}$  NMR (300 MHz,  $\text{CDCl}_3$ )  $\delta$  1.55–1.68 (m, 4H), 1.87–2.17 (m, 4H), 3.52–3.63 (m, 2H), 4.08 (m, 1H), 5.75 (m, 1H);  $^{13}\text{C}$  NMR (75 MHz,  $\text{CDCl}_3$ )  $\delta$  22.82, 22.90, 25.20, 25.27, 65.67, 76.48, 124.21, 136.77; Anal. Calcd for  $\text{C}_8\text{H}_{14}\text{O}_2$ : C, 67.57; H, 9.92; S, 11.86. Found: C, 67.53; H, 9.95;  $[\alpha]_{\text{D}}^{20} +28.2$  ( $c$  0.50,  $\text{CHCl}_3$ ), >95% ee with (*S*)-configuration based on  $[\alpha]_{\text{D}}^{20} -28.1$  ( $c$  1.02,  $\text{CHCl}_3$ ), >95% ee for (*R*)-**9**.<sup>17</sup>

**4.6.3. (2*S*,3*E*)-4-Phenyl-1,2-butanediol 8 from 4e.**  $R_{\text{f}}$  0.14; mp 49–51 °C; 60% yield; IR (KBr,  $\text{cm}^{-1}$ ): 3424, 3387, 2948, 2910, 2876, 1447, 1079, 1042;  $^1\text{H}$  NMR (300 MHz,  $\text{CDCl}_3$ )  $\delta$  3.57–3.77 (m, 2H), 4.44 (m, 1H), 6.19 (dd, 1H,  $J=15.95$ , 6.23 Hz), 6.68 (dd, 1H,  $J=15.95$ , 0.83 Hz), 7.24–7.39 (m, 5H);  $^{13}\text{C}$  NMR (75 MHz,  $\text{CDCl}_3$ )  $\delta$  66.77, 73.51, 126.72, 127.83, 128.15, 128.82, 133.5, 136.43; Anal. Calcd for  $\text{C}_{10}\text{H}_{12}\text{OS}$ : C, 73.15; H, 7.37. Found: C, 73.09; H, 7.49;  $[\alpha]_{\text{D}}^{20} +34.1$  ( $c$  0.50,  $\text{CHCl}_3$ ),  $S$  [lit.<sup>19</sup>  $[\alpha]_{\text{D}}^{26} +34.92$  ( $c$  0.87,  $\text{CHCl}_3$ ) for (*S*)-**10**]; HPLC analysis using a 25 cm Chiralcel OD-H chiral column (*iso*-PrOH/hexane: 1/9; flow rate: 0.5 mL/min; detector: 254 nm) showed it to be 98% ee ( $t_{\text{R}}(S)$  16.63 min and  $t_{\text{R}}(R)$  19.07 min).

## Acknowledgements

This work was supported by the Research Grant from Hallym University, Korea

## References and notes

- For reviews, see: (a) Cha, J. K.; Kim, N.-S. *Chem. Rev.* **1995**, *95*, 1761–1795. (b) Hoveyda, A. H.; Evans, D. A.; Fu, G. C. *Chem. Rev.* **1993**, *93*, 1307–1370.
- (a) Yang, D.; Jiao, G.-S.; Yip, Y.-C.; Lai, T.-H.; Wong, M.-K. *J. Org. Chem.* **2001**, *66*, 4619–4624. (b) Bach, J.; Berenguer, R.; Garcia, J.; Vilarrasa, J. *Tetrahedron Lett.* **1995**, *36*, 3425–3428. (c) Fehr, C.; Galindo, J. *Angew. Chem., Int. Ed.* **2000**, *39*, 569–573. (d) Brenna, E.; Fuganti, C.; Grasselli, P.; Serra, S. *Eur. J. Org. Chem.* **2001**, 1349–1357. (e) Aleu, J.; Bergamo, B.; Brenna, E.; Fuganti, C.; Serra, S. *Eur. J. Org. Chem.* **2000**, 3031–3038. (f) Liu, Z.; Lan, J.; Li, Y. *Tetrahedron: Asymmetry* **1998**, *9*, 3755–3762.
- (a) Gao, Y.; Hanson, R. M.; Klunder, J. M.; Ko, S. Y.; Masamune, H.; Sharpless, K. B. *J. Am. Chem. Soc.* **1987**, *109*, 5765–5780. (b) Adam, W.; Humpf, H.-U.; Roshmann, K. J.;

- Saha-Möller, C. R. *J. Org. Chem.* **2001**, *66*, 5796–5800. (c) Vedejs, E.; MacKay, J. A. *Org. Lett.* **2001**, *3*, 535–536.
4. (a) Wong, C.-H.; Whitesides, G. M. *Enzymes in Synthetic Organic Chemistry*; Pergamon: Oxford, 1994. (b) Ghanem, A.; Schurig, V. *Tetrahedron: Asymmetry* **2003**, *14*, 57–62. (c) Lindner, E.; Ghanem, A.; Warad, I.; Eichele, K.; Mayer, H. A.; Schurig, V. *Tetrahedron: Asymmetry* **2003**, *14*, 1045–1053. (d) Kamal, A.; Sandbhor, M.; Shaik, A. A.; Sravanthi, V. *Tetrahedron: Asymmetry* **2003**, *14*, 2839–2844. (e) Itoh, T.; Akasaki, E.; Nishimura, Y. *Chem. Lett.* **2002**, 154–155. (f) Lee, D.; Huh, E. A.; Kim, M.-H.; Jung, H. M.; Koh, J. H.; Park, J. *Org. Lett.* **2000**, *2*, 2377–2379.
5. Noyori, R.; Ohkuma, T. *Angew. Chem., Int. Ed.* **2001**, *40*, 40–73.
6. For reviews, see: (a) Cho, B. T. *Aldrichim. Acta* **2002**, *35*, 3–16. (b) Corey, E. J.; Helal, C. J. *Angew. Chem., Int. Ed.* **1998**, *37*, 1986–2012.
7. Liu, Z.; Lan, J.; Li, Y. *Tetrahedron: Asymmetry* **1998**, *9*, 3755–3762.
8. Yadav, J. S.; Reddy, B. V. S.; Reddy, K. S. *Tetrahedron* **2003**, *59*, 5333–5336.
9. Chandrasekhar, S.; Takhi, M.; Yadav, J. S. *Tetrahedron Lett.* **1995**, *36*, 5071–5074.
10. (a) Sánchez-Obregón, R.; Ortiz, B.; Walls, F.; Yuste, F.; García Ruano, J. L. *Tetrahedron: Asymmetry* **1999**, *10*, 947–955. (b) Goergens, U.; Schneider, M. P. *J. Chem. Soc., Chem. Commun.* **1991**, 1064–1066. (c) Fujisawa, T.; Itoh, T.; Nakai, M.; Sato, T. *Tetrahedron Lett.* **1985**, *26*, 771–774. (d) Toshimitsu, A.; Abe, H.; Hirosawa, C.; Tamao, K. *J. Chem. Soc., Perkin Trans. 1* **1994**, 3465–3471. (e) Nunno, L. D.; Franchini, C.; Nacci, A.; Scilimati, A.; Sinicropi, M. S. *Tetrahedron: Asymmetry* **1999**, *10*, 1913–1926. (f) Gruttadauria, M.; Meo, P. L.; Noto, R. *Tetrahedron* **1999**, *55*, 4769–4782. (g) Eames, J.; Jones, R. V. H.; Warren, S. *Tetrahedron Lett.* **1996**, *37*, 4823–4826. (h) Itoh, T.; Yonekawa, Y.; Sato, T.; Fujisawa, T. *Tetrahedron Lett.* **1986**, *27*, 5405–5408. (i) Fujisawa, T.; Itoh, T.; Sato, T. *Tetrahedron Lett.* **1984**, *25*, 5083–5086.
11. For reviews, see: (a) Carreño, M. C. *Chem. Rev.* **1995**, *95*, 1717–1760. (b) Walker, A. J. *Tetrahedron: Asymmetry* **1992**, *3*, 961–998. (c) Solladié, G.; Demailly, G.; Greck, C. *Tetrahedron Lett.* **1985**, *26*, 435–438. (d) Kosugi, H.; Konta, H.; Uda, H. *J. Chem. Soc., Chem. Commun.* **1985**, 211–213. (e) Bueno, A. B.; Carreño, M. C.; García Ruano, J. L.; Hamdouchi, C. *Tetrahedron: Asymmetry* **1995**, *6*, 1237–1240. (f) Solladié, G.; Demailly, G.; Greck, C. *J. Org. Chem.* **1985**, *50*, 1552–1554. (g) Bravo, P.; Resnati, G.; Viani, F.; Arnone, A. *Tetrahedron* **1987**, *43*, 4635–4647. (h) Solladié, G.; Rubio, A.; Carreño, M. C.; García Ruano, J. L. *Tetrahedron: Asymmetry* **1990**, *1*, 187–198. (i) Solladié, G.; Fernandez, I.; Maestro, C. *Tetrahedron Lett.* **1991**, *32*, 509–512. (j) Solladié, G.; Fernandez, I.; Maestro, C. *Tetrahedron: Asymmetry* **1991**, *2*, 801–819. (k) Solladié, G.; Maestro, M. C.; Rubio, A.; Pedregal, C.; Carreño, M. C.; García Ruano, J. L. *J. Org. Chem.* **1991**, *56*, 2317–2322. (l) Solladié, G.; Gerber, C. *Synlett* **1992**, 449–450. (m) Solladié, G.; Almario, A.; Colobert, F. *Synlett* **1992**, 167–168. (n) Solladié, G.; Huser, N. *Tetrahedron: Asymmetry* **1994**, *5*, 255–260. (o) Sato, T.; Itoh, T.; Fujisawa, T. *Tetrahedron Lett.* **1987**, *28*, 5677–5680. (p) Raghavan, S.; Joseph, S. C. *Tetrahedron: Asymmetry* **2003**, *14*, 101–105. (q) Cho, B. T.; Choi, O. K.; Kim, D. J. *Bull. Kor. Chem. Soc.* **2003**, *24*, 1023–1025.
12. (a) Tanikaga, R.; Hosoya, K.; Kaji, A. *J. Chem. Soc., Perkin Trans. 1* **1987**, 1799–1803. (b) Solladié, G.; Frechou, C.; Demailly, G.; Greck, C. *J. Org. Chem.* **1986**, *51*, 1912–1914. (c) Robin, S.; Huet, F.; Fauve, A.; Veschambre, H. *Tetrahedron: Asymmetry* **1993**, *4*, 239–246. (d) Kozikowski, A. P.; Mugrage, B. B.; Li, C. S.; Felder, L. *Tetrahedron Lett.* **1986**, *27*, 4817–4820. (e) Sato, T.; Okumura, Y.; Itai, J.; Fujisawa, T. *Chem. Lett.* **1988**, 1537–1540. (f) Tanikaga, R.; Hosoya, K.; Kaji, A. *Chem. Lett.* **1987**, 829–832.
13. (a) Ogura, K. In *Comprehensive Organic Synthesis: Selectivity, Strategy and Efficiency in Modern Organic Chemistry*; Trost, B. M., Fleming, I., Eds.; Sulfa stabilization; Pergamon: Seoul, 1991; Vol. 1, pp 505–539. (b) Metzner, P.; Thuillier, A. *Sulfur Reagent in Organic Synthesis*; Academic: New York, 1994.
14. Cho, B. T.; Choi, O. K.; Kim, D. J. *Tetrahedron: Asymmetry* **2002**, *13*, 697–703. CBS is commonly used for reagent **5**. It represents the first initial of the researchers who discovered it.
15. Sánchez-Obregón, R.; Ortiz, B.; Walla, F.; Yuste, F.; Ruano, J. L. G. *Tetrahedron: Asymmetry* **1999**, *10*, 947–955.
16. Arnone, A.; Bravo, P.; Frigerio, M.; Viani, F.; Soloshonok, V. A. *Tetrahedron* **1998**, *54*, 11825–11840.
17. *Re face* is assigned by the sequence rule.
18. Sabol, J. S.; Cregge, R. J. *Tetrahedron Lett.* **1990**, *31*, 27–30.
19. Kang, S. H.; Kim, C. M.; Youn, J.-H. *Tetrahedron Lett.* **1999**, *40*, 3581–3582.

# Photoinduced electron transfer across linearly fused oligo-norbornyl structures

Tahsin J. Chow,<sup>a,\*</sup> Yan-Ting Pan,<sup>b</sup> Yu-Shan Yeh,<sup>b</sup> Yuh-Sheng Wen,<sup>a</sup> Kew-Yu Chen<sup>b</sup>  
and Pi-Tai Chou<sup>b</sup>

<sup>a</sup>*Institute of Chemistry, Academia Sinica, Taipei 115, Taiwan, ROC*

<sup>b</sup>*Department of Chemistry, National Taiwan University, Taipei 106, Taiwan, ROC*

Received 28 March 2005; revised 9 May 2005; accepted 11 May 2005

Available online 4 June 2005

**Abstract**—The rates of photoinduced electron transfer (ET) reactions across two oligo-norbornyl spacer groups (S), that is, structure **1** fused by two norbornadiene (NBD) units and structure **2** fused by three NBD units, are examined. Substituted naphthalene acted as an electron donor (D), whilst ethylene-1,2-dicarboxylate as an electron acceptor (A). ET rates were measured by fluorescence quenching experiments on these D–S–A dyads, and the results were correlated with reaction free energies according to the Marcus relationship. It was found that naphthalene with phenyl substituents showed relatively slower ET rates. The conformational flexibility of phenyl substituents may cause a hindrance on the electronic coupling between D and A. Another salient feature was the abnormally high quenching rates observed in nonpolar solvents such as cyclohexane, the results of which may be ascribed to a competing energy transfer process.

© 2005 Elsevier Ltd. All rights reserved.

## 1. Introduction

Electron transfer process occurs ubiquitously in many physical and biological pathways, and the fundamental and applications of which have received much attention. Recent advances in this field have extended to the design of molecular devices, in which donor (D) and acceptor (A) pairs are ingeniously linked by covalent spacers (S) to form D–S–A dyads. Electron transfers between D and A across S in a controlled manner may thus, display useful functionalities such as molecular rectifiers,<sup>1</sup> switches,<sup>2</sup> electrochemical sensors,<sup>3</sup> photovoltaic cells,<sup>4</sup> and nonlinear optical materials,<sup>5</sup> etc. Spacer groups that have been utilized are versatile, including small molecules, for example, cyclohexane,<sup>6</sup> adamantane,<sup>7</sup> bicyclo[2.2.2]octane,<sup>8</sup> steroids,<sup>9</sup> and oligomers of various sizes, for example, polynorbornanes,<sup>10</sup> and ladderanes,<sup>11</sup> etc. Among numerous types of spacers, rigid linear rod-shaped structures, however, are not commonly seen.<sup>12,13</sup> The highly symmetrical structures reduce the complexity due to the constraint of geometrical and conformational variations. In our previous studies on photoinduced electron transfer (ET) reactions, the rates of ET in two series of oligo-norbornyl (NB) derivatives (**1** and **2**) have been estimated.<sup>14</sup> The geometry of these compounds

has the virtue of high symmetry as well as structural rigidity, so that the D and A chromophores can be aligned linearly across a  $\sigma$ -skeleton. The distance between the centers of D and A in compounds **1** and **2** is then adjustable by the number of NB units. Their ET rates were found to correlate well with both D–A distance and solvent polarities. For example, varying the D–A distance from **1** ( $5.5 \times 10^9 \text{ s}^{-1}$  for **5a** in diethyl ether) to **2** ( $5.4 \times 10^7 \text{ s}^{-1}$  for **7a**) reduced the ET rates by approximately two orders of magnitude. A  $\beta$  value of 0.77 was estimated according to an exponential decay relationship expressed in Eq. 6 (vide infra). The value of electronic coupling element  $H_{el}$  can further be deduced, which was found to be a function of D–A orientation and the bonding nature of the spacer. Such information is valuable for the future design of molecular devices utilizing these spacer groups. In this report, a comprehensive work based on the design and synthesis of analogues of compound **1** and **2** was performed to shed light on their associated ET dynamics. Consequently, the mechanism of photoinduced ET process is rigorously examined.

## 2. Results and discussion

### 2.1. Compounds preparation and characterization

Compounds **1** and **2** were prepared through a coupling reaction of norbornadiene (NBD) catalyzed by

**Keywords:** Electron transfer; Donor and acceptor; Poly-norbornyl; Marcus relationship; Charge transfer.

\* Corresponding author. Tel.: +886 2 27898552; fax: +886 2 27884179; e-mail: tjchow@chem.sinica.edu.tw

$\text{Co}_2(\text{CO})_6(\text{PPh}_3)$ .<sup>15</sup> The naphthalene donor (D) groups of **4a–c** and **6a–c** were fused on by [4+2] cycloaddition of respective *o*-quinodimethane derivatives.<sup>16</sup> The two ortho-bromo substituents of **4b** and **6b** were transformed to the phenyl groups of **4d** and **6d** by Suzuki coupling reaction using  $\text{PhB}(\text{OH})_2$  and  $\text{Pd}(\text{PPh}_3)_4$ .<sup>17</sup> The dicarboxylate acceptor (A) groups of **5a–d** and **7a–d** were made by [2+2] cycloaddition reactions with dimethyl acetylenedicarboxylate (DMAD) upon the catalysis of  $\text{RuH}_2(\text{CO})(\text{PPh}_3)_3$ .<sup>18</sup> All compounds exhibited two-fold symmetry on NMR spectral signals.

X-ray diffraction analysis on a single crystal of **5c** was performed. An ORTEP drawing of the structure is shown in Figure 1. It appears that the central skeleton of  $(\text{NBD})_2$  is zig-zag in shape. The special orientation between D and A attached onto spacer **1** (i.e., **5a–c**) is slightly different from that attached onto spacer **2** (**7a–c**). For example, structure of **5c** consists of both D and A groups locked rigidly via the spacer (S), forming a dihedral angle of ca.  $110^\circ$ . The estimated center-to-center distance was 10.9 Å from the central bond of naphthalene to the middle of the line connecting the two carbonyl groups. In the homologous compound **7c**, the D–A

distance was estimated to be 14.7 Å. The  $\pi$ -faces of D and A were aligned parallel to each other, yet not on the same plane.

## 2.2. Spectroscopic property

Figure 2 depicts the absorption and emission spectra of two prototypical models **4c** and **4d**, in which **4c** consists of two major absorption bands on the long wavelength side of the UV spectra. The one at 300–320 nm, corresponding to the first ( $\pi, \pi^*$ ) transition of naphthalene moiety, is assigned to the  $^1\text{A} \rightarrow ^1\text{L}_b$  transition according to the Platt classification,<sup>19</sup> whereas the next higher level transition at 245–290 nm is assigned to the  $^1\text{A} \rightarrow ^1\text{L}_a$  transition (Fig. 2). Both bands exhibit distinctive vibronic progressions as a result of conformation rigidity. Excitation at 310 nm induced a fluorescence at 320–380 nm. The high-energy edge of the emission spectrum overlaps well with 0–0 band of absorption. The nearly negligible amount of Stokes' shift reflects a high structural similarity between the ground and excited states. Similar spectral features also appeared on **4a** and **4b**.

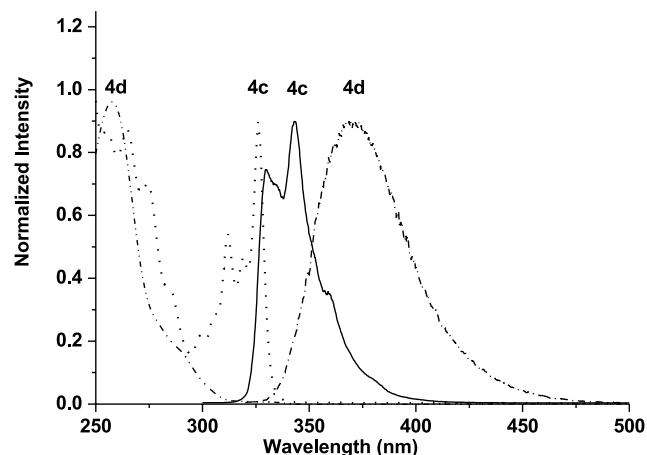
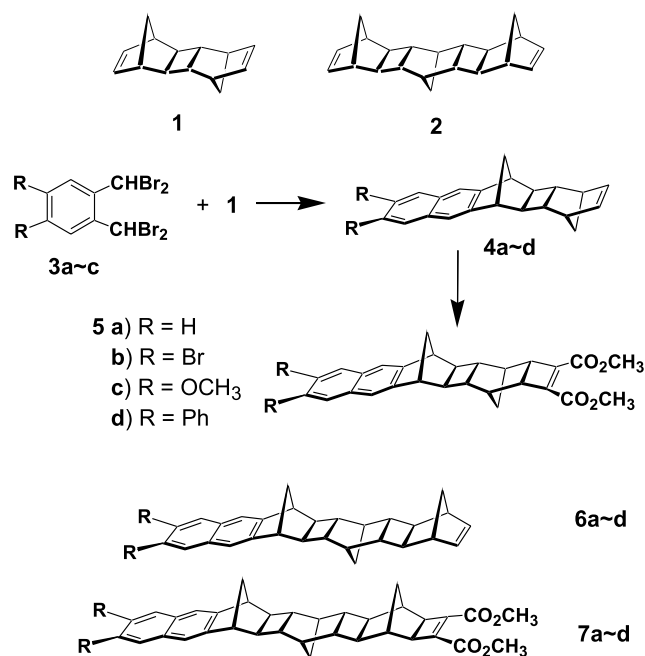


Figure 2. Absorption and emission spectra of compounds **4c** and **4d** in  $\text{CH}_3\text{CN}$ .

In a sharp contrast, the UV spectra of diphenyl substituted derivatives **4d–7d** exhibit a quite different pattern. The major absorption band of **4d** is broad with a peak wavelength at 258 nm ( $^1\text{B}_b$  band), accompanied by a

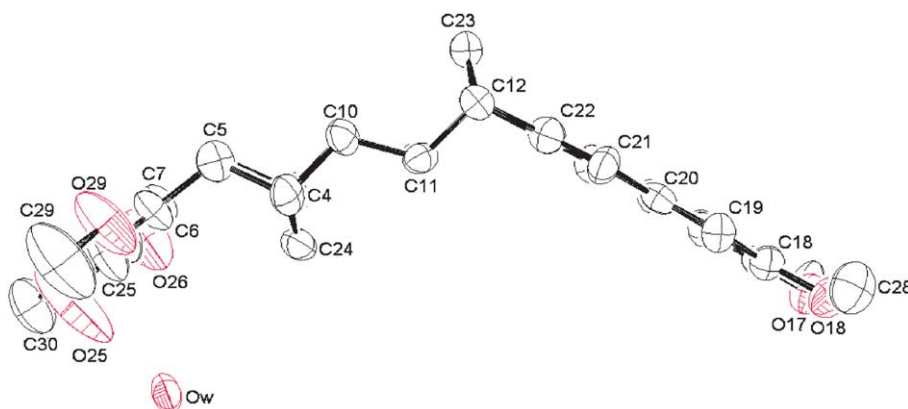


Figure 1. Molecular structure of compound **5c** in single crystal.

shoulder at  $\sim 280$  nm ( $^1L_a$  band). The  $S_1$  transition ( $^1L_b$  band) appears in low intensity at 310–335 nm (Fig. 2). It is well understood that phenyl substituents at C-2 position shift the  $^1L_b$  band bathochromically because of its longitudinal polarization.<sup>20</sup> The broad and featureless shape is apparently caused by the rotational flexibility of the phenyl groups. The fluorescence spectrum of **4d** ( $\lambda_{\max}$  at 370 nm) exhibited a substantial red-shift (37 nm) and wider full width at half maximum (fwhm  $\sim 56$  nm) comparing to that of **4c** ( $\lambda_{\max} \sim 343$  nm, fwhm  $\sim 26$  nm). The broadening of emission band in **4c** indicates either a significant mixing between phenyl  $\pi$ -orbitals and naphthalene chromophore or, in part, the diphenyl conformational flexibility.

### 2.3. Electron transfer kinetics

The oxidation potentials of naphthalene moieties were measured by cyclic voltammetry (see Table 1). The values obtained for **5a–c** agreed with the substituent effect, for example, 1.27 V for **5c** (di-MeO) and 1.78 V for **5b** (di-Br). The reduction potential of ethylene-1,2-dicarboxylate moiety was estimated to be  $-1.57$  V. These values were used for evaluating the free-energy ( $\Delta G$ ) of ET between an excited-state donor molecule ( $D^*$ ) and a ground-state acceptor at a defined distance ( $d$ ) according to Eq. 1:<sup>21</sup>

$$\Delta G(d) = E_{\text{ox}}(D) - E_{\text{red}}(A) - E_{00}(D) - (e^2/\epsilon d) - (e^2/2)(1/r_D^+ + 1/r_A^-)(1/37 - 1/\epsilon) \quad (1)$$

**Table 1.** The oxidation potentials and 0–0 band of absorptions

	<b>5a/7a</b>	<b>5b/7b</b>	<b>5c/7c</b>	<b>5d/7d</b>
$E_{\text{ox}}$ (eV)	1.74	1.78	1.27	1.50
$E_{00}$ (nm)	317	330	326	335

where  $E_{\text{ox}}(D)$  and  $E_{\text{red}}(A)$  are the oxidation and reduction potentials of D and A molecules, respectively, in acetonitrile.  $E_{00}(D)$  is the energy of 0–0 transition,  $r_D^+$  and  $r_A^-$  are effective ionic radii,  $\epsilon$  is the dielectric constant of solvent, and  $d$  is the center-to-center distance between D and A. An approximation was further, made on  $r = r_D^+ = r_A^- = 4.5$  Å.<sup>22</sup> With all of the values substituted into Eq. 1, the free energies were calculated and listed in Table 2. Figure 3 shows a linear plot of  $\Delta G$  versus  $1/\epsilon$ . Obviously, the ET processes are calculated to be exothermic in most solvents, except in a few nonpolar media such as *n*-hexane.

The rates of ET were estimated by Stern–Volmer relationship expressed as  $k_{\text{ET}} = [(\Phi_{\text{rel}} - 1)/\Phi_{\text{rel}}](1/\tau_D)$ ; where  $\Phi_{\text{rel}}$  is the relative fluorescence intensity of D–S–A dyads molecules **5** and **7** with respect to those of standards **4** and **6**, while  $\tau_D$  is the fluorescence lifetime of the latter. The measurements were performed in five different solvents in order to examine the effect of solvent and the results are listed in Table 2. Note that data relevant to compounds **5a/4a** and **7a/6a** were extracted from our previous report.<sup>14</sup> As supported by Table 2, it was apparent that the ET rates increase upon decreasing the values of  $\Delta G$ .

Theoretically, upon excitation electron migrates (or tunnels) from donor to acceptor site via the spacer, forming a charge-separated ion pair. Charge recombination to the ground state may result in a low energy emission as the charge-transfer band (CT band). Our previous analyses have shown that the decaying rate of fluorescence coincides with the rising dynamics of the CT band. In many cases, however, the CT band may not be readily detected due to its weak intensity, particularly in high polarity solvents such as acetonitrile, in which the lower energy emission is subject to dominant radiationless deactivation described by an energy gap law.<sup>23</sup> As shown in Figure 4, in contrast to a unique normal fluorescence for **4d** in THF, dual emission was observed in **5d**, in which a broad CT band centered at  $\sim 500$  nm was resolved. CT emissions in other solvents such as dichloromethane and ethyl acetate can also be detected, yet in very

**Table 2.** Free energies ( $\Delta G$ ), relative luminescence quantum yields ( $\Phi_{\text{rel}}$ ) and  $k_{\text{ET}}$  of electron transfer reactions for the dipolar compounds **4–7** in various solvents

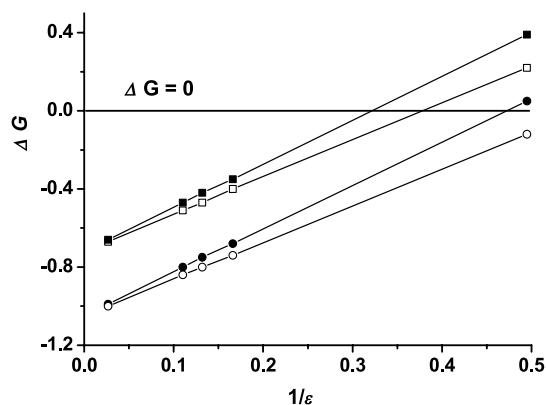
Solvent	$\tau$ (ns)	$\Delta G$ (eV)	$\Phi_{\text{rel}}$	$k_{\text{ET}}$ ( $\times 10^8$ s $^{-1}$ )	$H_{\text{el}}$ (cm $^{-1}$ )	$\tau$ (ns)	$\Delta G$ (eV)	$\Phi_{\text{rel}}$	$k_{\text{ET}}$ ( $\times 10^8$ s $^{-1}$ )	$H_{\text{el}}$ (cm $^{-1}$ )	$\beta'$	$\beta$
	<b>4a<sup>a</sup></b>	<b>5a</b>	<b>5a/4a<sup>b</sup></b>	<b>5a</b>	<b>5a</b>	<b>6a<sup>a</sup></b>	<b>7a</b>	<b>7a/6a<sup>b</sup></b>	<b>7a</b>	<b>7a</b>	<b>7a/5a</b>	<b>7a/5a</b>
Et <sub>2</sub> O	41	−0.25	0.044	55	1.2	57	−0.17	0.247	0.54	0.046	0.77	1.01
EtOAc	61	−0.37	0.020	83	1.8	51	−0.32	0.163	1.01	0.097	0.73	0.97
THF	58	−0.44	0.017	100	2.3	57	−0.39	0.012	1.3	0.125	0.72	0.97
CH <sub>2</sub> Cl <sub>2</sub>	37	−0.48	0.023	120	2.6	48	−0.44	0.047	4.2	0.25	0.56	0.78
	<b>4c<sup>a</sup></b>	<b>5c</b>	<b>5c/4c</b>	<b>5c</b>	<b>5c</b>	<b>6c</b>	<b>7c</b>	<b>7c/6c</b>	<b>7c</b>	<b>7c</b>	<b>7c/5c</b>	<b>7c/5c</b>
C <sub>6</sub> H <sub>12</sub>	6.84	−0.12	0.104	13	—	11	0.05	0.64	0.51	—	0.54	—
EtOAc	5.96	−0.74	0.0068	246	9.1	12	−0.68	0.35	1.55	0.58	0.84	0.92
THF	6.78	−0.80	0.0124	117	6.4	12	−0.75	0.22	2.95	0.82	0.61	0.68
CH <sub>2</sub> Cl <sub>2</sub>	7.45	−0.84	0.00104	1400	22	10	−0.80	0.17	4.88	1.08	0.94	1.00
CH <sub>3</sub> CN	6.76	−1.00	0.0021	700	17	11	−0.99	0.18	4.14	1.08	0.85	0.92
	<b>4d</b>	<b>5d</b>	<b>5d/4d</b>	<b>5d</b>	<b>5d</b>	<b>6d</b>	<b>7d</b>	<b>7d/6d</b>	<b>7d</b>	<b>7d</b>	<b>7d/5d</b>	<b>7d/5d</b>
C <sub>6</sub> H <sub>12</sub>	42	0.22	0.85	0.04	—	40	0.39	0.98	0.005	—	0.35	—
EtOAc	40	−0.40	0.24	0.75	0.20	39	−0.35	0.94	0.016	0.015	0.64	0.86
THF	39	−0.47	0.08	2.9	0.44	38	−0.42	0.93	0.02	0.018	0.83	1.07
CH <sub>2</sub> Cl <sub>2</sub>	31	−0.51	0.04	7.8	0.75	30	−0.47	0.92	0.03	0.025	0.92	1.13
CH <sub>3</sub> CN	25	−0.67	0.03	13	1.2	41	−0.66	0.92	0.02	0.026	1.08	1.28

The data of compounds **4a**, **5a**, **6a** and **7a** were abstracted from Ref. 14.

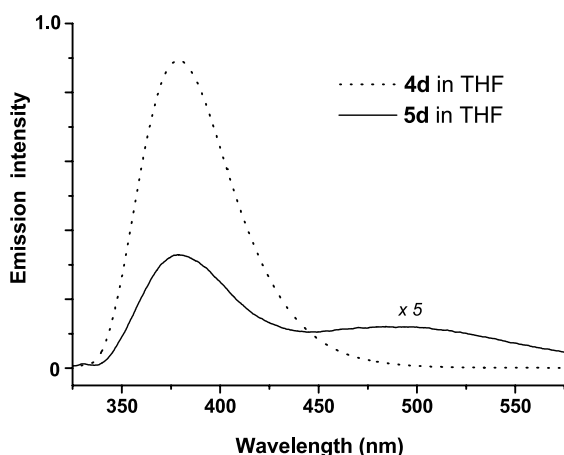
<sup>a</sup> Measured by a picosecond dynamic apparatus (Ref. 29); all others by a Hitachi U-3310 spectrophotometer.

<sup>b</sup> Estimated by the difference of lifetimes, otherwise calculated by relative luminescence quantum yields.





**Figure 3.** Linear plots of the free energy of ET ( $\Delta G$ ) versus the reciprocal of solvent dielectric constant ( $\epsilon$ ) for compounds **5c** (○), **7c** (●), **5d** (□) and **7d** (■), respectively. Points below the line of  $\Delta G=0$  indicate exothermic ET processes.



**Figure 4.** The fluorescence spectra of compounds **4d** (dotted line) and **5d** (solid line) in THF. The quenching of fluorescence (378 nm) on **5d** is apparent by the reduction of emission intensity. A broad band appeared on the right side (495 nm) originating from the emission of charges-separated species (CT band).

low quantum yields. According to Marcus formulation, the energy gap of CT emission is related to the barrier of nuclear reorganization ( $\lambda$ ) during the ET processes. In the case of **5d** in THF, the value of  $\lambda$  can be deduced by the following relationship

$$\lambda = \Delta G + E_{00} - h\nu_{CT} \quad (2)$$

Taking the data of  $\Delta G$  and  $E_{00}$  listed in Tables 1 and 2,  $\lambda$  was then deduced to be, for example,  $\sim 0.75$  eV in THF.

The rate constant for a nonadiabatic ET process can be expressed by Fermi's golden rule:

$$k_{et} = \frac{2\pi}{\hbar} |H_{el}|^2 FC \quad (3)$$

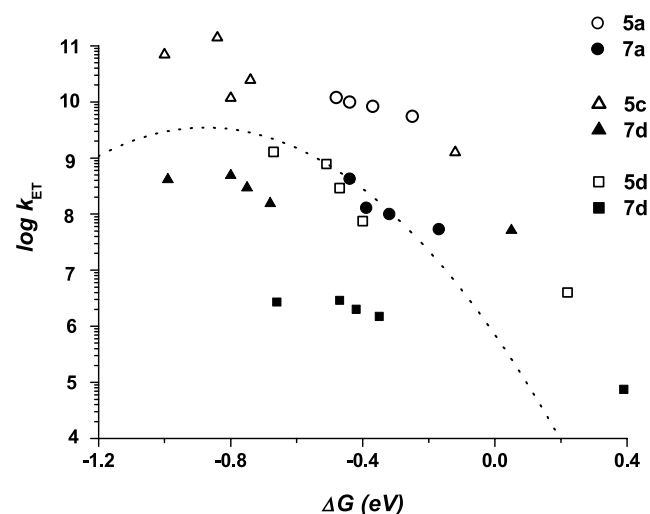
where FC is the Franck-Condon factor, that is, the sum of products of overlap integrals of the vibrational and solvent wave functions of the reactants with those of the products. These factors are weighted for the Boltzmann population of all vibrational energy levels. In the high-temperature limit, Marcus has provided the following expression, which

involves an electron-coupling matrix element  $|H_{el}|$ :

$$k_{et} = \frac{2\pi}{(4\pi\lambda k_B T)^{1/2} \hbar} |H_{el}|^2 \exp\left[\frac{-(\Delta G + \lambda)^2}{4\lambda k_B T}\right] \quad (4)$$

The value of  $H_{el}$  can be deduced from  $\Delta G$ ,  $\lambda$ , and  $k_{et}$ , and can further, be used as a criteria for judging the effectiveness of the  $\sigma$ -spacer group as a modulator for ET dynamics according to a superexchange mechanism.<sup>24</sup> Figure 5 reveals the plots of  $\log k_{et}$  versus  $\Delta G$  based on all experimentally available data points of compounds **5** and **7** bearing three kinds of substituents  $-\text{H}$  (**a**),  $-\text{OCH}_3$  (**c**), and  $-\text{Ph}$  (**d**). Note that the fluorescence intensity of bromo-substituted derivatives (**b**) was too weak to have a reliable value. For the purpose of comparison a simulated curve (Eq. 4) for **5d** in dichloromethane is plotted and shown in Figure 5. Two noteworthy features can be pointed out from the scattering pattern of data points depicted in Figure 5: (1) the ET rates of **5d** and **7d** are slower than the corresponding ones of **5a,c** and **7a,c** by approximately two orders of magnitude; and (2) the ET rates of all compounds in cyclohexane seem to be substantially faster than what were expected. As shown in the plots of Figure 3, the estimated free energy of ET in nonpolar solvents such as cyclohexane is either greater or close to zero. Accordingly, the rates of ET in such solvents (with  $\Delta G \sim 0$ ) are expected to be substantially slower than those in polar solvents (cf.  $\Delta G \sim -0.4$  eV as shown in Fig. 5). The unexpected high rate of fluorescence quenching in nonpolar solvents is intriguing and may be ascribed to the competing processes associated with electronic energy transfer. Although, the absorption wavelength of acceptor is apparently shorter than the emission wavelength of donor, processes of this kind proceeded in high electronically excited state have been known previously.<sup>25</sup> In polar solvents the comparatively slow rate of energy transfer is overshadowed by the faster rate of ET process and is likely to be ignored.

Another salient feature is regarding the slow ET rate for **5d** and **7d**, which may be rationalized by a mismatch of orbital symmetry between donor and acceptor. The magnitude of



**Figure 5.** Plots of  $\log k_{ET}$  versus  $\Delta G$  of compounds **5a** (○), **5d** (□), **7a** (●), **7c** (▲), and **7d** (■) in different solvents. The ET rates of **5a** and **7a** are faster ( $\sim 10^2$ ) than the corresponding rates of **5d** and **7d**. A simulated curve according to Eq. 4 for **5d** in THF (...) is drawn as a reference.

electronic coupling between donor and acceptor depends upon the degree of superexchange interactions, the strength of which relies not only on the relative orientation between the donor and acceptor, but also on the corresponding geometry of spacer group.<sup>24</sup> The all-trans  $\sigma$ -array is known to be suitable for modulating electronic interactions.<sup>26,27</sup> In the structure of **5c** (Fig. 1), it is clear that the  $\pi$ -face of naphthalene (D) is held rigidly and parallel to the  $\pi$ -face of ethylene dicarboxylate (A). Similar geometry is maintained in the bromo and methoxy substituted derivatives, that is, **5b,c** and **7b,c**, as evidenced by the high similarity among their absorption spectra. However, the situation for the diphenyl substituted derivatives such as **5d** and **7d** is rather different, in that the  $\pi$ -orbitals of naphthalene are perturbed by the free-rotating phenyl groups. Support of this viewpoint is rendered by the absorption spectral features of **5d** and **7d**, which are distinctively different from those of **5a–c** (not shown here). Likewise, a significant Stokes' shift is observed on their emissions. The spectral difference indicates the presence of conformational variations in both ground and excited states. We thus, tentatively propose that the non-planar conformation of naphthalene chromophores of **5d** and **7d** reduce the degree of electron coupling between D and A, and consequently retard the rate of ET processes.

The value of electronic coupling element  $H_{el}$  is a function of D–A distance and orientation, as well as the bonding nature ( $\sigma$  or  $\pi$ ) and geometry of the spacer. As a trend with similar structures, its value decreases exponentially with respect to the edge-to-edge distance ( $d-2r$ ) between D and A expressed as

$$H_{el} = H_{el}^0 \exp[-\beta^0(d-2r)] = H_{el}^0 \exp[-n\beta] \quad (5)$$

where  $H_{el}^0$  is a value at contact distance  $2r$  for D and A, and  $\beta^0$  is an attenuation coefficient. The value of  $H_{el}$  usually is rather difficult to measure accurately. Empirically, the distance-dependence of ET rate in a specific solvent may be alternatively expressed by the number of  $\sigma$ -bonds ( $n$ ) separating D and A:

$$k_{ET} = k_0 \exp(-2n\beta') \quad (6)$$

McConnell has calculated the distance dependence of electronic coupling in a series of  $\alpha,\omega$ -diphenylalkanes and found the value of  $\beta'$  to be ca. 2.5.<sup>28</sup> Paddon-Row et al. have measured the ET rates across a series of fused norbornadiene skeletons. They found out the value of  $\beta'$  to be in a range of 0.4–0.63 depending on the solvents.<sup>27</sup> These values complied well with that estimated by Hoffmann,<sup>26</sup> and were much smaller than what were predicted by McConnell. From the rate constants listed in Table 2, the value of  $\beta'$  can be deduced via comparisons between compounds **5** (6  $\sigma$ -bonds between D and A) and **7** (9  $\sigma$ -bonds). For example, the  $\beta$  value derived from **5a/7a** in THF was 0.72 in THF, whereas those derived from **5c/7c** and **5d/7d** were 0.61 and 0.83, respectively, (Table 2). It should be noted that these numbers were neither corrected for distance dependence of the Franck-Condon factor in Eq. 3, nor the conformational variations between the structures of **5** and **7**. As depicted by molecular modeling, a change of bending angles between the  $\pi$ -facial planes of D and A appears to be  $60^\circ$  in **5** (see Fig. 1) and  $0^\circ$  in **7**.

Precise estimation on the electronic coupling element  $H_{el}$  remains a difficult task. According to Eq. 2 the value of  $\lambda$  can be estimated from the CT emission. It can be divided into two parts, that is, an internal part  $\lambda_i$  and a solvent dependent part  $\lambda_s$ . The value of  $\lambda_s$  can be estimated by

$$\lambda_s = e^2(1/r_D^+ + 1/r_A^- - 1/d)(1/n^2 - 1/\epsilon) \quad (7)$$

where  $n$  is the refractive index of the solvent. The value  $\lambda_i$  can then be obtained from  $\lambda$  (Eq. 2) and  $\lambda_s$ , and is presumably solvent independent. A reasonable estimation on  $\lambda_i$  was in the range of 0.10–0.20 eV. This value was taken for the calculation of  $H_{el}$  by Eq. 4, and the results were listed in Table 2. Apparently,  $H_{el}$  of  $<10 \text{ cm}^{-1}$  clearly indicate a weak coupling and hence, a nonadiabatic ET process in all cases applied in this study. The averaged  $\beta$  value for these ladder-shaped spacers was thus, estimated to be about 1.0.

### 3. Conclusion

In conclusion, the rates of electron transfer were measured across two types of spacer groups, that is, **1** and **2**, where substituted naphthalene acted as the electron donor and ethylene-1,2-dicarboxylate as the acceptor. The methoxyl substituents resonate effectively with the aromatic  $\pi$ -system, therefore, enrich the electron density of the donor group. Their ET rates became faster in all solvents than the one without methoxy substituents. On the contrary, the presence of phenyl substituents retarded the rates of ET as judged from the same  $\Delta G$  values. The conformational flexibility of phenyl substituents seem to perturb the well-aligned symmetry relationship between D and A, resulting in a reduction of effective electronic coupling. Furthermore, the free-rotated phenyl substituents render a much wider Stokes shifts, as well as a substantial band broadening in the emission spectra.

The free energies of ET were deduced from redox potentials of both D and A and the 0–0 absorption of D. The reorganization energy  $\lambda$  was estimated according to the charge transfer emission of **5d** (Fig. 4) by Eq. 2. Accordingly, electronic coupling element  $H_{el}$  was deduced from  $\Delta G$  and  $\lambda$ . Comparing the  $H_{el}$  values of systems **1** and **2**, the exponential decaying parameter  $\beta$  were computed according to the relationship of Eq. 5. The values ranging from 0.6 to 0.9 were not much deviated from analogous cases published in the literatures. The values reveal the nature of these linear ladder-shaped oligonorbornyl spacer groups using as ET modulator, of which the choice is crucial for a proper design of molecular devices.

## 4. Experimental

### 4.1. General

Infrared spectra were recorded on a Perkin-Elmer 682 infrared spectrophotometer. Elemental analyses were obtained on a Perkin-Elmer 2400 CHN instrument. Melting points were measured with a Thomas-Hoover mp apparatus and are uncorrected.  $^1\text{H}$  and  $^{13}\text{C}$  spectra were obtained on a Bruker APX-400 spectrometer. Mass spectra were carried



out on a VG70-250S spectrometer. Cyclic voltammetry measurements were performed using a voltammetric analyzer and a glassy-carbon working electrode in acetonitrile containing 0.1 M tetra-*n*-butylammonium tetrafluoroborate as a supporting electrolyte. Solvents were all of spectrgrade quality. Samples were degassed by three freeze–pump–thaw cycles in vacuo.

Steady-state absorption and emission spectra were recorded by a Hitachi (U-3310) spectrophotometer and an Edinburgh (FS920) fluorimeter, respectively. Details of picosecond dynamical measurements have been elaborated in the previous report.<sup>29</sup>

**4.1.1. 15,16-Dibromoheptacyclo[10.8.1.1<sup>4,7</sup>.0<sup>3,8</sup>.0<sup>2,9</sup>.0<sup>11,20</sup>.0<sup>13,18</sup>]docosa-5,11,13,15,-17,19-hexene (4b).** A two-neck round bottom flask, fitted with a condenser and a nitrogen inlet–outlet, was filled with a solution of compound **1** (1.3 g, 7.0 mmol) in freshly distilled DMF (88 mL). To it was added  $\alpha,\alpha,\alpha',\alpha'$ -hexabromo-*o*-xylene (4.5 g, 7.7 mmol), followed by sodium iodide (7.0 g, 47 mmol) in a nitrogen atmosphere. The resulted solution was heated to 60–70 °C for 20 h, then was poured slowly into an aqueous solution (350 mL) of sodium bisulfide (5 g). The mixture was extracted three times with methylene chloride. The combined organic phase was dried over anhydrous magnesium sulfate, and concentrated in vacuo. The product was purified by passing through a silica gel chromatographic column eluted with hexane/methylene chloride (5:1) to yield white solids (1.9 g, 62%), mp 223.4–224.4 °C. IR (KBr): 3053, 2970, 2955, 1638, 1619, 1579, 1559, 1466, 1400, 1323, 1273, 1261, 1209, 1190, 1101, 947, 928, 898, 885, 703 cm<sup>-1</sup>; <sup>1</sup>H NMR (400 MHz, CDCl<sub>3</sub>):  $\delta$  7.99 (s, 2H), 7.38 (s, 2H), 6.01 (s, 2H), 3.26 (s, 2H), 2.68 (s, 2H), 2.44 (d, 1H, *J* = 10 Hz), 1.72 (d, 1H, *J* = 10 Hz), 1.57 (m, 3H), 1.55 (s, 2H), 1.18 (d, 1H, *J* = 9 Hz); <sup>13</sup>C NMR (100 MHz, CDCl<sub>3</sub>):  $\delta$  148.6, 136.4, 133.0, 132.4, 120.9, 118.0, 46.4, 44.8, 42.7, 42.4, 42.3, 40.3; MS (EI, 70 eV): *m/z* (%) 442 (M<sup>+</sup>, 100), 376 (54), 323 (15), 243 (15), 163 (15). Anal. Calcd for C<sub>22</sub>H<sub>18</sub>Br<sub>2</sub>: C, 59.76%; H, 4.10%. Found: C, 60.07%, H, 4.36%.

**4.1.2. 15,16-Dimethoxyheptacyclo[10.8.1.1<sup>4,7</sup>.0<sup>3,8</sup>.0<sup>2,9</sup>.0<sup>11,20</sup>.0<sup>13,18</sup>]docosa-5,11,13,-15,17,19-hexene (4c).** A two-neck round bottom flask, fitted with a condenser and a nitrogen inlet–outlet, was filled with a solution of compound **1** (1.3 g, 7.0 mmol) in freshly distilled DMF (65 mL). To it was added  $\alpha,\alpha,\alpha',\alpha'$ -hexabromo-4,5-di-methoxy-*o*-xylene (3.7 g, 7.7 mmol), followed by sodium iodide (7.0 g, 47 mmol) in a nitrogen atmosphere. The resulted solution was heated to 60–70 °C for 20 h, then was poured slowly into an aqueous solution (350 mL) of sodium bisulfide (5 g). The yellow precipitates were filtered and dried in vacuo. It was purified by passing through a silica gel chromatographic column eluted with hexane/ethyl acetate (6:1) to yield white solids (1.6 g, 68%), mp 198.6–199.8 °C. IR (KBr): 3011, 2957, 2926, 1620, 1507, 1460, 1427, 1248, 1144, 1006, 879, 832, 714 cm<sup>-1</sup>; <sup>1</sup>H NMR (400 MHz, CDCl<sub>3</sub>):  $\delta$  7.38 (s, 2H), 7.05 (s, 2H), 6.01 (s, 2H), 3.95 (s, 6H), 3.23 (s, 2H), 2.67 (s, 2H), 2.22 (d, 1H, *J* = 9 Hz), 1.71 (d, 1H, *J* = 9 Hz), 1.52–1.57 (m, 5H), 1.17 (d, 1H, *J* = 7 Hz); <sup>13</sup>C NMR (100 MHz, CDCl<sub>3</sub>):  $\delta$  148.8, 145.2, 136.1, 128.0, 117.6, 55.1, 46.1, 44.5, 42.7, 42.6, 42.1, 40.1; MS (EI,

70 eV): *m/z* (%) 344 (M<sup>+</sup>, 100), 278 (29), 226 (39), 195 (7), 165 (11). Anal. Calcd for C<sub>24</sub>H<sub>24</sub>O<sub>2</sub>: C, 83.69%; H, 7.02%. Found: C, 83.49%, H, 7.34%.

**4.1.3. 15,16-Diphenylheptacyclo[10.8.1.1<sup>4,7</sup>.0<sup>3,8</sup>.0<sup>2,9</sup>.0<sup>11,20</sup>.0<sup>13,18</sup>]docosa-5,11,13,15,-17,19-hexene (4d).** A three-neck round bottom flask, fitted with a condenser and a nitrogen inlet–outlet, was filled with a solution of compound **4b** (1.5 g, 3.4 mmol) in freshly distilled DMF (100 mL). To it under a nitrogen atmosphere was added tetrakis(triphenylphosphine)palladium(0) (0.2 g, 0.17 mmol), followed by phenylboronic acid (0.9 g, 7.5 mmol) and a potassium phosphate solution (2 N, 20 mL). The resulted mixture was heated to reflux for 72 h, then was allowed to cool. It was extracted three times with methylene chloride. The combined organic phase was dried over anhydrous magnesium sulfate, and concentrated in vacuo. The product was purified by passing through a silica gel chromatographic column eluted with hexane/methylene chloride (5:1) to form colorless solids (0.17 g, 11%), mp 238.6–239.8 °C. IR (KBr): 3021, 2965, 2921, 1653, 1637, 1474, 1458, 1324, 1209, 1187, 1071, 996, 946, 902, 770, 708, 702 cm<sup>-1</sup>; <sup>1</sup>H NMR (400 MHz, CDCl<sub>3</sub>):  $\delta$  7.77 (s, 2H), 7.55 (s, 2H), 7.16–7.24 (m, 10H), 6.02 (s, 2H), 3.30 (s, 2H), 2.69 (s, 2H), 2.27 (d, 1H, *J* = 10 Hz), 1.77 (d, 1H, *J* = 10 Hz), 1.61 (s, 2H), 1.60 (d, 1H, *J* = 9 Hz), 1.57 (s, 2H), 1.18 (d, 1H, *J* = 9 Hz); <sup>13</sup>C NMR (100 MHz, CDCl<sub>3</sub>):  $\delta$  147.2, 141.8, 138.0, 135.8, 132.0, 130.0, 129.3, 127.8, 126.3, 118.3, 46.0, 44.3, 42.2, 42.0, 40.0; MS (EI, 70 eV): *m/z* (%) 436 (M<sup>+</sup>, 100), 370 (45), 317 (47), 241 (15), 165 (3).

**4.1.4. 15,16-Dibromo-6,7-dicarbomethoxyoctacyclo[10.10.1.1<sup>4,9</sup>.0<sup>2,11</sup>.0<sup>3,10</sup>.0<sup>5,8</sup>.0<sup>13,22</sup>.-0<sup>15,20</sup>]tetracos-6,13,15,17,19,21-hexene (5b).** Compound **5b** was collected in 78% yield following a similar procedure to that of **5c**. Physical data of **5b**: mp 254–256 °C. IR (KBr): 3011, 2954, 2925, 1738, 1717, 1638, 1629, 1463, 1433, 1402, 1267, 1232, 1197, 1136, 1120, 1101, 1050, 929, 896 cm<sup>-1</sup>; <sup>1</sup>H NMR (400 MHz, CDCl<sub>3</sub>):  $\delta$  8.01 (s, 2H), 7.40 (s, 2H), 3.79 (s, 6H), 3.27 (s, 2H), 2.62 (s, 2H), 2.38 (d, 1H, *J* = 10 Hz), 2.20 (s, 2H), 1.74–1.77 (m, 4H), 1.62–1.65 (m, 2H), 1.29 (d, 1H, *J* = 10 Hz); <sup>13</sup>C NMR (100 MHz, CDCl<sub>3</sub>):  $\delta$  161.5, 147.3, 142.0, 132.5, 131.8, 120.5, 117.5, 51.8, 45.6, 45.6, 43.7, 42.9, 41.8, 36.8, 26.0; MS (EI, 70 eV): *m/z* (%) 584 (M<sup>+</sup>, 100), 553 (9), 350 (41), 323 (18), 243 (27), 163 (26). Anal. Calcd for C<sub>28</sub>H<sub>24</sub>Br<sub>2</sub>O<sub>4</sub>: C, 57.56%; H, 4.14%. Found: C, 57.55%, H, 4.11%.

**4.1.5. 6,7-Dicarbomethoxy-15,16-dimethoxyoctacyclo[10.10.1.1<sup>4,9</sup>.0<sup>2,11</sup>.0<sup>3,10</sup>.0<sup>5,8</sup>.0<sup>13,22</sup>.0<sup>15,20</sup>]tetracos-6,13,15,17,19,21-hexene (5c).** To a two-neck round bottom flask, fitted with a condenser and a nitrogen inlet–outlet, were added of compound **4c** (100 mg, 0.3 mmol), dimethyl acetylenedicarboxylate (0.04 mL, 0.3 mmol), and a catalytic amount of RuH<sub>2</sub>CO(PPh<sub>3</sub>)<sub>3</sub> in freshly distilled benzene (10 mL). The resulted solution was stirred with a magnetic bar for 15 min at ambient temperature, then was heated to reflux for 24 h. The solvent was evaporated in vacuo, and the product was purified by passing through a silica gel chromatographic column eluted with hexane/ethyl acetate (6:1) to yield white solids (121 mg, 83%), mp 214–215 °C. IR (KBr): 3007, 2952, 1722, 1627, 1508, 1464,

1433, 1318, 1251, 1195, 1147, 1050, 1011, 887, 743  $\text{cm}^{-1}$ ;  $^1\text{H}$  NMR (400 MHz,  $\text{CDCl}_3$ ):  $\delta$  7.40 (s, 2H), 7.07 (s, 2H), 3.97 (s, 6H), 3.78 (s, 6H), 3.24 (s, 2H), 2.62 (s, 2H), 2.36 (d, 1H,  $J=10$  Hz), 2.19 (s, 2H), 1.73–1.76 (m, 5H), 1.65 (d, 1H,  $J=11$  Hz), 1.27 (d, 1H,  $J=11$  Hz);  $^{13}\text{C}$  NMR (100 MHz,  $\text{CDCl}_3$ ):  $\delta$  161.8, 148.8, 144.5, 142.3, 128.1, 117.6, 107.0, 56.1, 52.0, 46.0, 45.9, 44.4, 43.3, 42.4, 37.0, 26.2; MS (EI, 70 eV):  $m/z$  (%) 486 ( $\text{M}^+$ , 100), 455 (5), 277 (4), 252 (16), 226 (26), 165.1 (4). Anal. Calcd for  $\text{C}_{30}\text{H}_{30}\text{O}_6$ : C, 74.06%; H, 6.21%. Found: C, 73.84%, H, 5.97%.

The crystal structure of **5c** was solved on a Nonius diffractometer using the  $\theta/\theta$  scan method. It was monoclinic in space group  $C2/c$  with  $a=30.929(7)$  Å,  $b=8.700(1)$  Å, and  $c=21.194(3)$  Å,  $\alpha=90^\circ$ ,  $\beta=113.466(14)^\circ$ ,  $\gamma=90^\circ$ . Crystallographic data has been deposited with the Cambridge Crystallographic Data Centre as supplementary publication numbers CCDC 266303. Copies of the data can be obtained, free of charge, on application to CCDC, 12 Union Road, Cambridge CB2 1EZ, UK [fax: 144 (0)1223 336033 or e-mail: [deposit@ccdc.cam.ac.uk](mailto:deposit@ccdc.cam.ac.uk)].

**4.1.6. 6,7-Dicarbomethoxy-15,16-diphenyloctacyclo[10.10.1.1<sup>4,9,0</sup>2,11,0<sup>3,10</sup>5,8,0<sup>13,22</sup>0<sup>15,20</sup>]tetracos-6,13,15,17,19,21-hexene (5d).** Compound **5d** was collected in 78% yield following a similar procedure to that of **5c**. Physical data of **5d**: mp 217.5–219 °C. IR (KBr): 3053, 2965, 2952, 1738, 1720, 1638, 1629, 1474, 1437, 1322, 1298, 1282, 1265, 1228, 1217, 1197, 1133, 1121, 1051, 947, 905, 770, 748, 700  $\text{cm}^{-1}$ ;  $^1\text{H}$  NMR (400 MHz,  $\text{CDCl}_3$ ):  $\delta$  7.77 (s, 2H), 7.55 (s, 2H), 7.15–7.22 (m, 10H), 3.76 (s, 6H), 3.28 (s, 2H), 2.60 (s, 2H), 2.37 (d, 1H,  $J=10$  Hz), 2.18 (s, 2H), 1.76–1.77 (d, 5H), 1.62 (d, 1H,  $J=11$  Hz), 1.26 (d, 1H,  $J=11$  Hz);  $^{13}\text{C}$  NMR (100 MHz,  $\text{CDCl}_3$ ):  $\delta$  161.5, 146.4, 142.0, 141.8, 138.1, 132.0, 130.0, 129.3, 127.8, 126.3, 118.4, 51.8, 45.7, 44.1, 43.3, 41.9, 36.8, 26.0; MS (EI, 70 eV):  $m/z$  (%) 578.1 ( $\text{M}^+$ , 100), 547.1 (4), 344.1 (31), 318.1 (30), 241.1 (5), 165.1 (1). Anal. Calcd for  $\text{C}_{40}\text{H}_{34}\text{O}_4$ : C, 83.02%; H, 5.92%. Found: C, 82.78%, H, 6.00%.

**4.1.7. 21,22-Dibromodecacyclo[14.10.1.1<sup>4,13</sup>1<sup>7,10</sup>0<sup>2,15</sup>0<sup>3,14</sup>0<sup>5,12</sup>0<sup>6,11</sup>0<sup>17,26</sup>0<sup>19,24</sup>]hexacos-8,17,19,21,23,25-hexene (6b).** A two-neck round bottom flask, fitted with a condenser and a nitrogen inlet–outlet, was filled with a solution of compound **2** (1.9 g, 7.0 mmol) in freshly distilled DMF (95 mL). To it was added  $\alpha,\alpha,\alpha',\alpha'$ -hexabromo-*o*-xylene (4.5 g, 7.7 mmol), followed by sodium iodide (7.0 g, 47 mmol) in a nitrogen atmosphere. The resulted solution was heated to 60–70 °C for 20 h, then was poured slowly into an aqueous solution (350 mL) of sodium bisulfide (5 g). The mixture was extracted three times with methylene chloride. The combined organic phase was dried over anhydrous magnesium sulfate, and concentrated in vacuo. The product was purified by passing through a silica gel chromatographic column eluted with hexane/methylene chloride (5:1) to yield white solids (2.2 g, 60%), mp 289–291 °C. IR (KBr): 3048, 2963, 2930, 1631, 1583, 1464, 1402, 1326, 1266, 1225, 1102, 949, 928, 896, 715  $\text{cm}^{-1}$ ;  $^1\text{H}$  NMR (400 MHz,  $\text{CDCl}_3$ ):  $\delta$  8.01 (s, 2H), 7.38 (s, 2H), 5.93 (s, 2H), 3.22 (s, 2H), 2.61 (s, 2H), 2.36 (d, 1H,  $J=10$  Hz), 1.93 (s, 2H), 1.77–1.65 (m, 4H), 1.68 (s, 2H), 1.62 (s, 2H), 1.38 (s, 2H), 1.35 (s, 2H), 1.16 (d, 1H,  $J=8.2$  Hz);  $^{13}\text{C}$

NMR (100 MHz,  $\text{CDCl}_3$ ):  $\delta$  157.9, 135.5, 132.7, 132.0, 129.0, 127.4, 117.6, 46.0, 44.4, 43.6, 42.6, 41.9, 41.6, 41.7, 40.9, 29.1; MS (EI, 70 eV):  $m/z$  (%) 534 ( $\text{M}^+$ , 100), 468 (46), 376 (14), 350 (45), 269 (11), 189 (15), 163 (11). Anal. Calcd for  $\text{C}_{29}\text{H}_{26}\text{Br}_2$ : C, 65.19%; H, 4.90%. Found: C, 65.46%, H, 5.49%.

**4.1.8. 21,22-Dimethoxydecacyclo[14.10.1.1<sup>4,13</sup>1<sup>7,10</sup>0<sup>2,15</sup>0<sup>3,14</sup>0<sup>5,12</sup>0<sup>6,11</sup>0<sup>17,26</sup>0<sup>19,24</sup>]hexacos-8,17,19,21,23,25-hexene (6c).** Compound **6c** was collected in 63% yield according to a similar procedure to the preparation of **6b**. Physical data of **6c**: mp 258.5–259.5 °C. IR (KBr): 2961, 2921, 1621, 1511, 1464, 1426, 1251, 1144, 1005, 884, 710  $\text{cm}^{-1}$ ;  $^1\text{H}$  NMR (400 MHz,  $\text{CDCl}_3$ ):  $\delta$  7.35 (s, 2H), 7.04 (s, 2H), 5.91 (s, 2H), 3.95 (s, 6H), 3.17 (s, 2H), 2.59 (s, 2H), 2.31 (d, 1H,  $J=10.0$  Hz), 1.90 (s, 2H), 1.75 (d, 1H,  $J=9$  Hz), 1.70–1.65 (m, 5H), 1.66 (s, 2H), 1.32 (s, 2H), 1.23 (s, 2H), 1.14 (d, 1H,  $J=9$  Hz);  $^{13}\text{C}$  NMR (100 MHz,  $\text{CDCl}_3$ ):  $\delta$  148.5, 144.7, 135.3, 127.8, 117.2, 106.8, 55.8, 45.8, 44.2, 44.0, 42.5, 42.1, 41.8, 41.5, 41.4, 40.7, 28.9; MS (EI, 70 eV):  $m/z$  (%) 436 ( $\text{M}^+$ , 100), 370 (15), 277 (4), 252 (15), 226 (15), 165 (4). Anal. Calcd for  $\text{C}_{31}\text{H}_{32}\text{O}_2$ : C, 85.28%; H, 7.39%. Found: C, 85.28%, H, 7.45%.

**4.1.9. 21,22-Diphenyldecacyclo[14.10.1.1<sup>4,13</sup>1<sup>7,10</sup>0<sup>2,15</sup>0<sup>3,14</sup>0<sup>5,12</sup>0<sup>6,11</sup>0<sup>17,26</sup>0<sup>19,24</sup>]hexacos-8,17,19,21,23,25-hexene (6d).** A three-neck round bottom flask, fitted with a condenser and a nitrogen inlet–outlet, was filled with a solution of compound **6b** (2.0 g, 3.7 mmol) in freshly distilled DMF (100 mL). To it under a nitrogen atmosphere was added tetrakis(triphenylphosphine)palladium(0) (0.22 g, 0.185 mmol), followed by phenylboronic acid (1.0 g, 8.1 mmol) and a potassium phosphate solution (2 N, 20 mL). The resulted mixture was heated to reflux for 72 h, then was allowed to cool. It was extracted three times with methylene chloride. The combined organic phase was dried over anhydrous magnesium sulfate, and concentrated in vacuo. The product was purified by passing through a silica gel chromatographic column eluted with hexane/methylene chloride (5:1) to form white solids (0.20 g, 10%), mp 289–291 °C. IR (KBr): 3052, 2960, 2924, 1600, 1476, 1463, 1443, 1420, 1325, 1261, 1071, 949, 903, 770, 760, 747, 700, 567  $\text{cm}^{-1}$ ;  $^1\text{H}$  NMR (400 MHz,  $\text{CDCl}_3$ ):  $\delta$  7.77 (s, 2H), 7.56 (s, 2H), 7.20–7.27 (m, 10H), 5.94 (s, 2H), 3.26 (s, 2H), 2.61 (s, 2H), 2.40 (d, 1H,  $J=10$  Hz), 1.95 (s, 2H), 1.79 (d, 1H,  $J=9$  Hz), 1.78–1.72 (m, 5H), 1.72 (s, 2H), 1.39 (s, 2H), 1.38 (s, 2H), 1.15 (d, 1H,  $J=8.0$  Hz);  $^{13}\text{C}$  NMR (100 MHz,  $\text{CDCl}_3$ ):  $\delta$  1147.1, 142.1, 138.2, 135.5, 132.2, 130.3, 129.5, 128.0, 126.5, 118.4, 46.1, 44.5, 44.1, 42.8, 42.1, 42.0, 41.8, 41.7, 40.9, 29.2; MS (EI, 70 eV):  $m/z$  (%) 528 ( $\text{M}^+$ , 100), 462 (11), 370 (5), 344 (30), 318 (15), 241 (5), 165 (1); MS (EI, 70 eV):  $m/z$  (%) 528 ( $\text{M}^+$ , 100), 462 (10), 344 (22), 331 (18), 318 (20).

**4.1.10. 9,10-Dibromo-23,24-dicarbomethoxyundecacyclo[16.10.1.1<sup>4,15</sup>1<sup>21,26</sup>0<sup>2,17</sup>0<sup>3,16</sup>0<sup>5,14</sup>0<sup>7,12</sup>0<sup>19,28</sup>0<sup>20,27</sup>0<sup>22,25</sup>]octacos-5,7,9,11,13,23-hexene (7b).** Compound **7b** was collected in 78% yield following a similar procedure to that of **5c**. Physical data of **7b**: mp 319.5–321.0 °C. IR (KBr): 2951, 2927, 1740, 2719, 1627, 1618, 1559, 1435, 1267, 1232, 1197, 1138, 1124, 1100, 1049, 929, 896, 670  $\text{cm}^{-1}$ ;  $^1\text{H}$  NMR (400 MHz,  $\text{CDCl}_3$ ):  $\delta$  8.0 (s, 2H), 7.38 (s, 1H), 3.78 (s, 6H), 3.22 (s, 2H), 2.51 (s, 2H), 2.35 (d, 1H,

$J=10$  Hz), 2.10 (s, 2H), 1.58–1.92 (m, 14H), 1.30 (d, 1H,  $J=11$  Hz);  $^{13}\text{C}$  NMR (100 MHz,  $\text{CDCl}_3$ ):  $\delta$  161.8, 147.8, 142.2, 132.7, 132.0, 120.6, 117.6, 52.0, 46.0, 45.8, 44.81, 44.2, 43.7, 42.2, 42.0, 41.7, 37.0, 29.2, 26.2; MS (EI, 70 eV):  $m/z$  (%) 676 ( $\text{M}^+$ , 100), 645 (8), 442 (8), 376 (9), 350 (34), 323 (11), 243 (16), 163 (8). Anal. Calcd for  $\text{C}_{35}\text{H}_{32}\text{Br}_2\text{O}_4$ : C, 62.15%; H, 4.77%. Found: C, 62.29%, H, 4.89%.

**4.1.11. 23,24-Dicarbomethoxy-9,10-dimethoxyundecacyclo[16.10.1.1<sup>4,15</sup>.1<sup>21,26</sup>.0<sup>2,17</sup>.0<sup>3,16</sup>.0<sup>5,14</sup>.0<sup>7,12</sup>.0<sup>19,28</sup>.0<sup>20,27</sup>.0<sup>22,25</sup>]octacos-5,7,9,11,13,23-hexene (7c).** Compound **7c** was collected in 78% yield following a similar procedure to that of **5c**. Physical data of **7c**: mp 306.5–308.5 °C. IR (KBr): 2953, 2921, 1727, 1625, 1506, 1466, 1430, 1321, 1249, 1196, 1143, 1046, 1008, 880  $\text{cm}^{-1}$ ;  $^1\text{H}$  NMR (400 MHz,  $\text{CDCl}_3$ ):  $\delta$  7.35 (s, 2H), 7.04 (s, 2H), 3.94 (s, 6H), 3.75 (s, 6H), 3.15 (s, 2H), 2.48 (s, 2H), 2.29 (d, 1H,  $J=10$  Hz), 2.07 (s, 2H), 1.87 (s, 2H), 1.87–1.80 (m, 2H), 1.71 (d,  $J=10$  Hz, 1H), 1.70 (s, 2H), 1.70–1.69 (m, 1H), 1.58 (s, 2H), 1.55 (s, 2H), 1.53 (s, 2H), 1.27 (d, 1H,  $J=11$  Hz);  $^{13}\text{C}$  NMR (100 MHz,  $\text{CDCl}_3$ ):  $\delta$  161.2, 148.7, 144.6, 142.1, 127.9, 117.4, 106.9, 55.9, 51.9, 45.9, 45.7, 44.7, 44.1, 44.1, 42.2, 42.2, 41.6, 36.9, 29.0, 26.1; MS (EI, 70 eV):  $m/z$  (%) 578 ( $\text{M}^+$ , 100), 547 (4), 344 (2), 252 (15), 226 (18), 165 (16). Anal. Calcd for  $\text{C}_{37}\text{H}_{38}\text{O}_6$ : C, 76.79%; H, 6.62%. Found: C, 76.71%, H, 6.70%.

**4.1.12. 23,24-Dicarbomethoxy-9,10-diphenylundecacyclo[16.10.1.1<sup>4,15</sup>.1<sup>21,26</sup>.0<sup>2,17</sup>.0<sup>3,16</sup>.0<sup>5,14</sup>.0<sup>7,12</sup>.0<sup>19,28</sup>.0<sup>20,27</sup>.0<sup>22,25</sup>]octacos-5,7,9,11,13,23-hexene (7d).** Compound **7d** was collected in 78% yield following a similar procedure to that of **5c**. Physical data of **7d**: mp 294.5–296 °C. IR (KBr): 3060, 2950, 2922, 1736, 1719, 1632, 1598, 1474, 1436, 1322, 1267, 1232, 1208, 1198, 1049, 966, 949, 904, 770, 742, 697  $\text{cm}^{-1}$ ;  $^1\text{H}$  NMR (400 MHz,  $\text{CDCl}_3$ ):  $\delta$  7.76 (s, 2H), 7.52 (s, 2H), 7.17–7.19 (m, 10H), 3.76 (s, 6H), 3.22 (s, 2H), 2.49 (s, 2H), 2.34 (d, 1H,  $J=10$  Hz), 2.08 (s, 2H), 1.89 (s, 2H), 1.89–1.80 (m, 2H), 1.73–1.70 (m, 2H), 1.70 (s, 2H), 1.59 (s, 2H), 1.56 (s, 4H), 1.27 (d, 1H,  $J=11$  Hz);  $^{13}\text{C}$  NMR (100 MHz,  $\text{CDCl}_3$ ):  $\delta$  161.6, 146.7, 142.0, 141.8, 138.0, 132.0, 130.0, 129.3, 127.8, 126.3, 118.2, 51.8, 45.9, 45.6, 44.6, 44.0, 43.9, 42.1, 41.9, 41.5, 36.8, 28.9, 26.0; MS (EI, 70 eV):  $m/z$  (%) 670 ( $\text{M}^+$ , 100), 639 (3), 436 (1), 370 (5), 344 (14), 318 (11), 241 (3).

### Acknowledgements

Supports from Academia Sinica and the National Science Council of Taiwan are gratefully acknowledged.

### References and notes

- (a) Metzger, R. M. *J. Mater. Chem.* **2000**, *10*, 55–62. (b) Scheib, S.; Cava, M. P.; Baldwin, J. W.; Metzger, R. M. *J. Org. Chem.* **1998**, *63*, 1198–1204. (c) Aviram, A.; Ratner, M. A. *Chem. Phys. Lett.* **1974**, *29*, 277–283.
- (a) Chen, J.; Reed, M. A.; Rawlett, A. M.; Tour, J. M. *Science* **1999**, *286*, 1550–1552. (b) de Silva, A. P.; Gunaratne, H. Q. N.; Gunnlaugsson, T.; Huxley, A. J. M.; McCoy, C. P.; Rademacher, J. T.; Rice, T. E. *Chem. Rev.* **1997**, *97*, 1515–1566.
- (a) Yu, C. J.; Chong, Y.; Kayyem, J. F.; Gozin, M. *J. Org. Chem.* **1999**, *64*, 2070–2079. (b) Lewis, F. D.; Wu, T.; Zhang, Y.; Letsinger, R. L.; Greenfield, S. R.; Wasielewski, M. R. *Science* **1997**, *277*, 673–676.
- (a) Gust, D.; Moore, T. A.; Moore, A. L. *Acc. Chem. Res.* **1993**, *26*, 198–205. (b) Roest, M. R.; Verhoeven, J. W.; Schuddeboom, W.; Warman, J. M.; Lawson, J. M.; Paddon-Row, M. N. *J. Am. Chem. Soc.* **1996**, *118*, 1762–1768.
- Boyd, R. W. *Nonlinear Optics*; Academic: New York, 1992. Prasad, P. N.; Williams, D. J. *Introduction to Nonlinear Optical Effects in Molecular and Polymers*; Wiley: New York, 1991.
- (a) Chattoraj, M.; Paulson, B.; Shi, Y.; Closs, G. L.; Levy, D. H. *J. Phys. Chem.* **1994**, *98*, 3361–3368. (b) Chattoraj, M.; Bal, B.; Closs, G. L.; Levy, D. H. *J. Phys. Chem.* **1992**, *95*, 9666–9673.
- Balzani, V.; Juris, A.; Venturi, M. *Chem. Rev.* **1996**, *96*, 759–834.
- Zimmerman, H. E.; Goldman, T. D.; Hirzel, T. K.; Schmidt, S. P. *J. Org. Chem.* **1980**, *45*, 3933–3951.
- (a) Tung, C. H.; Zhang, L. P.; Li, Y.; Cao, H.; Tanimoto, Y. *J. Am. Chem. Soc.* **1997**, *119*, 5348–5254. (b) Agyin, J. K.; Timberlake, L. D.; Morrison, H. *J. Am. Chem. Soc.* **1997**, *119*, 7945–7953.
- Warrener, R. N. *Eur. J. Org. Chem.* **2000**, 3363–3380.
- Warrener, R. N.; Pitt, I. G.; Butler, D. N. *J. Chem. Soc., Chem. Commun.* **1983**, 1340–1341.
- Warrener, R. N.; Abbenante, G.; Kennard, C. H. L. *J. Am. Chem. Soc.* **1994**, *116*, 3645–3636.
- (a) Chiou, N. R.; Chow, T. J.; Chen, C. Y.; Hsu, M. A.; Chen, H. C. *Tetrahedron Lett.* **2001**, *42*, 29–31. (b) Chow, T. J.; Hon, Y. S.; Chen, C. Y.; Huang, M. S. *Tetrahedron Lett.* **1999**, *40*, 7799–7801.
- Chen, K.-Y.; Chow, T. J.; Chou, P.-T.; Cheng, Y.-M.; Tsaia, S.-H. *Tetrahedron Lett.* **2002**, *43*, 8115–8119.
- (a) Hieber, W.; Sedlmeier, J. *Chem. Ber.* **1954**, *87*, 789. (b) Arnold, D. R.; Trecker, D. J.; Whipple, E. B. *J. Am. Chem. Soc.* **1965**, *87*, 2596–2602.
- (a) Paddon-Row, M. N.; Patney, H. K. *Synthesis* **1986**, 328–330. (b) Cava, M. P.; Deana, A. A.; Muth, K. *J. Am. Chem. Soc.* **1959**, *81*, 6458–6460. (c) Mcomie, J. F. W.; Perry, D. H. *Synthesis* **1973**, 416–417.
- (a) Miyaura, N.; Yanagi, T.; Suzuki, A. *Synth. Commun.* **1981**, *11*, 513–519. (b) Miyaura, N.; Suzuki, A. *Chem. Rev.* **1995**, *95*, 2457–2483.
- (a) Ahmad, N.; Levison, J. J.; Robinson, S. D.; Uttley, M. G. *Inorg. Synth.* **1974**, *15*, 45–64. (b) Kumar, K.; Tepper, R. J.; Zeng, Y.; Zimmt, M. B. *J. Org. Chem.* **1995**, *60*, 4051–4066.
- Platt, J. R. *J. Chem. Phys.* **1949**, *17*, 484–495.
- Jaffé, H. H.; Orchin, M. *Theory and Applications of Ultraviolet Spectroscopy*; Wiley: New York, 1962.
- (a) Marcus, R. A. *J. Chem. Phys.* **1965**, *43*, 679–701. (b) Marcus, R. A. *Annu. Rev. Phys. Chem.* **1964**, *15*, 155–196. (c) Marcus, R. A. *J. Chem. Phys.* **1956**, *24*, 966–978. (d) Marcus, R. A. *Discuss. Faraday Soc.* **1960**, *29*, 21. (e) Marcus, R. A.; Sutin, N. *Biochim. Biophys. Acta* **1985**, *811*, 265–322.
- Oevering, H.; Paddon-Row, M. N.; Heppener, M.; Oliver, A. M.; Cotsaris, E.; Verhoeven, J. A.; Hush, N. S. *J. Am. Chem. Soc.* **1987**, *109*, 3258–3269.
- Chow, T. J.; Chen, H.-C.; Chiu, N.-R.; Chen, C.-Y.; Yu,

- W.-S.; Cheng, Y.-M.; Cheng, C.-C.; Chang, C.-P.; Chou, P.-T. *Tetrahedron* **2003**, *59*, 5719–5730.
24. Siders, P.; Cave, R. J.; Marcus, R. A. *J. Chem. Phys.* **1984**, *81*, 5613–5624.
25. Lokan, N.; Paddon-Row, M. N.; Smith, T. A.; Rosa, M. L.; Ghiggino, K. P.; Speiser, S. *J. Am. Chem. Soc.* **1999**, *121*, 2917–2919.
26. (a) Hoffmann, R.; Imamura, A.; Hehre, W. *J. Am. Chem. Soc.* **1968**, *90*, 1499–1509. (b) Hoffmann, R. *Acc. Chem. Res.* **1971**, *4*, 1–9.
27. (a) Paddon-Row, M. N. *Acc. Chem. Res.* **1994**, *27*, 18–25. (b) Jordan, K. D.; Paddon-Row, M. N. *J. Phys. Chem.* **1992**, *96*, 1188–1196.
28. McConnell, H. M. *J. Chem. Phys.* **1961**, *35*, 508–515.
29. Chou, P. T.; Chen, Y. C.; Yu, W. S.; Chou, Y. H.; Wei, C. Y.; Cheng, Y. M. *J. Phys. Chem. A* **2001**, *105*, 1731–1740.

# Understanding the enantioselectivity of a heterogeneous catalyst: the influence of ligand loading and of silica passivation

Dalit Rechavi,<sup>a,†</sup> Belén Albela,<sup>b</sup> Laurent Bonneviot<sup>b</sup> and Marc Lemaire<sup>a,\*</sup>

<sup>a</sup>Laboratoire CASO, UMR 5622, Université Claude Bernard Lyon1, 3 rue Victor Grignard, 69616 Villeurbanne Cedex, France

<sup>b</sup>Laboratoire de Chimie, UMR-CNRS 5182, Ecole Normale Supérieure de Lyon, 46 Allée d'Italie, 69364 Lyon Cedex 07, France

Received 21 March 2005; revised 4 May 2005; accepted 11 May 2005

Available online 4 June 2005

**Abstract**—One of the major drawbacks of heterogeneous catalysts is an inferior catalytic performance relative to their homogeneous counterparts. This is often attributed to high local concentration of the catalyst, and in certain cases to various active groups of the heterogeneous support and to its steric effects. We tested the influence of these factors in the case of a silica-grafted bis(oxazoline) catalyst used in the Diels–Alder reaction, by varying the ligand loading and the degrees of passivation of the silica. We show that, in the present case, the enantioselectivity of the catalyst is linearly correlated with the passivation of the silica, and high ligand loadings can be used without damaging the performance of the catalyst. This is, to the best of our knowledge, the first example of a correlation between silica passivation and the enantioselectivity of a heterogeneous catalyst.

© 2005 Elsevier Ltd. All rights reserved.

## 1. Introduction

Supported heterogeneous catalysis is a fast-developing field.<sup>1</sup> Catalysts have been heterogenized by non-covalent immobilization on surfaces such as clays and zeolites,<sup>2–4</sup> by covalent grafting onto organic polymers or inorganic surfaces,<sup>5–7</sup> and by polymerization of adequately functionalized catalysts.<sup>8</sup> The raison d'être of this field is the increased ease of isolation of the catalyst, which facilitates both purification of the products from the reaction mixture and reuse of the catalyst. Chiral bis(oxazoline) ligands have been used in a variety of enantioselective reactions, giving good yields and enantioselectivities.<sup>9–15</sup> However, most transformations require the use of large amounts of the catalyst to obtain good enantioselectivities. This is probably what incited an increasing number of reports concerning their heterogenization.<sup>16–25</sup>

One of the main drawbacks of heterogeneous catalysts is their often reduced activity relative to their homogeneous counterparts. In the case of chiral catalysts, the enantioselectivity of the heterogeneous systems is usually lower as

well,<sup>6,7,16,26–29</sup> although some contrary cases have been reported.<sup>30–34</sup> These phenomena have been related to the local density of the catalysts on the heterogeneous material,<sup>35</sup> to accessibility of the catalysts on the materials, and to various interactions with functional groups of the material.<sup>26</sup> However, to the best of our knowledge, so far no experiments have shown a linear correlation between the enantioselectivity and the presence of other functional groups on the material. We have recently reported the heterogenization of a bis(oxazoline) ligand, indaBOX **1**, by grafting onto silica (Scheme 1), and its successful use in the Diels–Alder reaction.<sup>36,37</sup> We report here a systematic study of the manner in which the concentration of the ligands on the silica and the protection of the silanol groups of the silica influence the enantioselectivity of the system.

## 2. Results and discussion

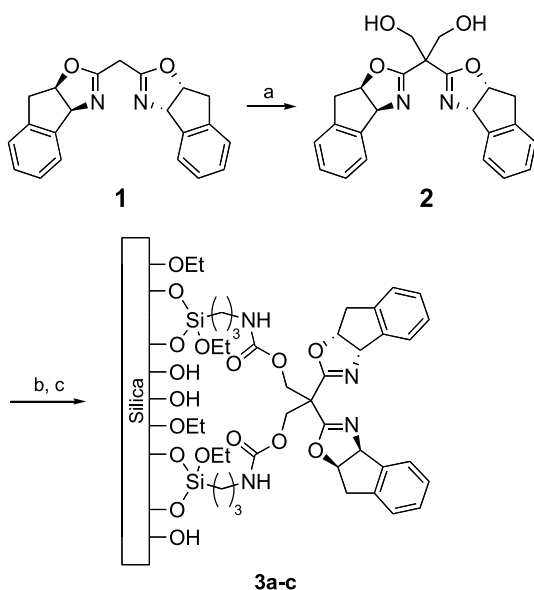
IndaBOX **1** was grafted onto commercially available Matrex<sup>®</sup> Si-60 silica (particle size 70–200 μm).<sup>36,37</sup> Different ratios of **2**/silica were used in order to obtain materials with different ligand loadings (**3a–c**, Scheme 1). The ligand loading as well as the overall yield of the reaction (starting from **2**) were calculated according to microanalysis (Table 1). Logically, the ligand loading rises when a higher **2**/silica ratio is used: from 0.15 mmol ligand per gram material in **3a** to 0.34 in **3c**. The overall yield of the grafting rises when a lower **2**/silica ratio is used: from 55% for material **3c** to 85% for **3a**. This can be rationalized

**Keywords:** Enantioselective heterogeneous catalysis; Chirality; Silica; Grafted catalyst; Catalyst loading; Silica passivation.

\* Corresponding author. Tel.: +33 0472448209; fax: +33 0472431408; e-mail: marc.lemaire@univ-lyon1.fr

† Present address: The Skaggs Institute for Chemical Biology, The Scripps Research Institute, 10550 North Torrey Pines Road (MB26), La Jolla, CA 92037, USA.





**Scheme 1.** Grafting of indaBOX onto silica. Reaction conditions: (a) CH<sub>2</sub>O (2.5 equiv), NEt<sub>3</sub>, CH<sub>2</sub>Cl<sub>2</sub>, dioxane, THF H<sub>2</sub>O. (b) 3-(Isocyanatopropyl)-triethoxysilane, Et<sub>3</sub>N, DMF, 48 h, then addition of polystyrene–NH<sub>2</sub> resin and mixing for 1 h, followed by filtering of the polystyrene–NH<sub>2</sub> resin and evaporation of the solvents. (c) Silica (previously treated with HCl), toluene, reflux overnight.

**Table 1.** Silicas 3a–c: ligand loading and overall yield from 2

No.	Silica	mmol of 2 per g of silica <sup>a</sup>	Ligand loading (±2%) <sup>b</sup>	Yield <sup>c</sup>
1	3a	0.1875	0.15	85
2	3b	0.375	0.25	75
3	3c	0.750	0.34	55

<sup>a</sup> The ratio used in the reaction described in Scheme 1.

<sup>b</sup> mmol of ligand per g of material (material=silica+grafted ligand)

<sup>c</sup> Overall yield starting from 2.

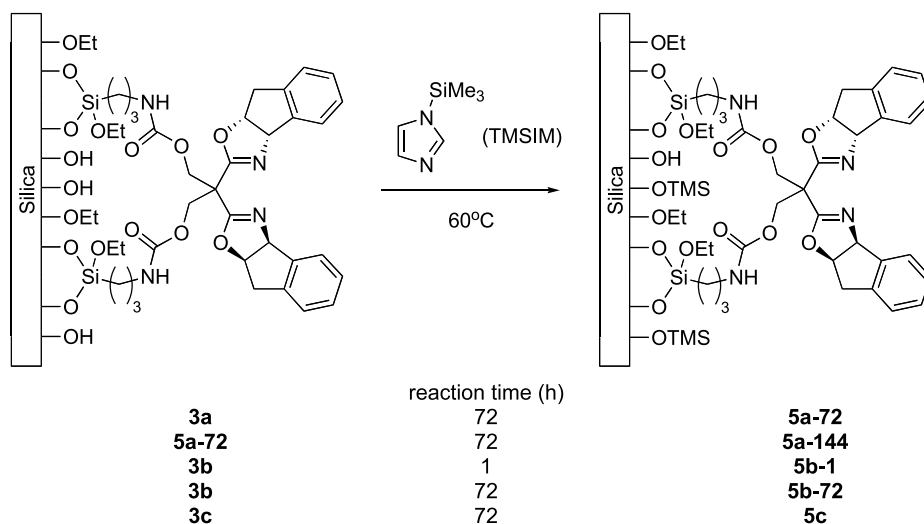
by a certain saturation in the number of silanol groups available for ligand grafting at higher 2/silica ratios.

The presence of the ligand on the silica was also verified using IR spectroscopy, and CPMAS NMR (cross polarization with magic angle spinning). The <sup>13</sup>C-CPMAS NMR spectra were particularly informative, and all the peaks of the ligand were clearly observed (see Section 3).

The silanol groups of 3a–c were end-capped with TMS groups using the mild reagent *N*-trimethylsilylimidazole (TMSIM). Reactions of variable duration gave five modified materials 5a–72, 5a–144, 5b–1, 5b–72, and 5c (Scheme 2).

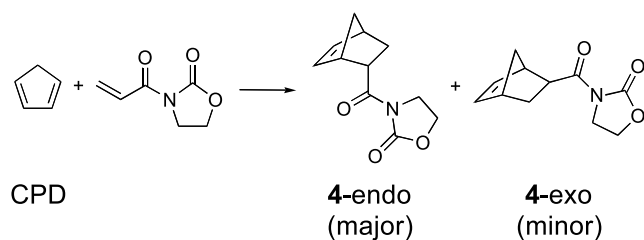
The eight catalytic materials were used in the catalysis of the benchmark Diels–Alder reaction between cyclopentadiene (CPD) and *N*-acryloyl oxazolidinone<sup>38,39</sup> to give 4-endo (major product) and 4-exo<sup>40,41</sup> (Scheme 3). In all cases the catalytic materials were mixed with Cu(ClO<sub>4</sub>)<sub>2</sub>·6H<sub>2</sub>O prior to the reaction and the reagents were then added to the reaction tube. The reaction was performed under air-humidity conditions (inert atmosphere is not required with this system).<sup>36,37,42</sup> This is especially beneficial in the case of a heterogeneous catalyst, since recycling involves only simple filtration and washing of the catalyst—drying of the catalyst is not required. We have previously demonstrated that the enantioselectivities do not show a tendency to decline upon recycling.<sup>36,37</sup>

Table 2 presents the enantioselectivities obtained by the materials in the catalysis of the benchmark Diels–Alder reaction described in Scheme 3. The best enantioselectivity obtained (81% at rt) equals that of the homogeneous catalyst under the same conditions.<sup>36,37</sup> It has been previously shown, that in some cases the enantioselectivity of a heterogeneous compound has a tendency to diminish when the ligand loading is higher.<sup>43</sup> Visibly, this is not the case in our system. On the contrary, the enantioselectivity of the different catalysts has a tendency to rise with higher ligand loading (Table 2). However, no significant correlation is



**Scheme 2.** Passivation of the indaBOX-grafted silicas 3a–c.





Scheme 3. The benchmark Diels–Alder reaction.

A graph of the enantioselectivity as a function of the passivation of the silica is shown in Figure 1. A good correlation is obtained between these parameters ( $r=0.88$ ,  $p\text{-value}^{\ddagger}=0.44\%$ ). To the best of our knowledge, this is the first case where such a correlation is reported. It indicates that most of the variation in the enantioselectivity can be attributed to the protection of the silanol groups on the silica.<sup>46–48, §</sup> The ligand loading does not have a major effect on the enantioselectivity of the reaction. This has the practical advantage of allowing high ligand loadings, thus

Table 2. Diels–Alder results at room temperature, the ligand loading and number of silanol groups protected per gram of material

No.	Silica	Ligand loading (mmol of ligand per g of material)	Number of ethyl groups eliminated <sup>a</sup>	Number of TMS groups (mmol/g)	Overall protected silanol groups (mmol/g material) <sup>b</sup>	%ee (endo)
1	<b>3a</b>	0.15	3.5	—	0.5	58
2	<b>5a–72</b>	0.14	—	1.2	1.7	61.5
3	<b>5a–144</b>	0.14	—	1.3	1.8	75
4	<b>3b</b>	0.25	5.5	—	1.4	65
5	<b>5b–1</b>	0.25	—	0.75	2.1	71
6	<b>5b–72</b>	0.22	—	1.2	2.4	81
7	<b>3c</b>	0.34	5.5	—	1.9	69
8	<b>5c</b>	0.33	—	0.87	2.7	80

<sup>a</sup> Number of ethyl groups eliminated on average per ligand during the grafting reaction, calculated according to the N/C ratio of the microanalysis.

<sup>b</sup> Calculated according to: (ligand loading) × (number of ethyl groups eliminated in the non-passivated silica) + (number of TMS groups).

observed. The reason for this rise could be the different degrees of passivation of the silicas.

In order to quantify the passivation of the silica, the number of silanol groups which are protected on each material was calculated. In the non-passivated materials **3a–c**, the silanol groups are protected only by the ligand itself. The number of silanol groups covered by the ligand can be estimated from the number of EtOH groups eliminated from the ligand in the process of grafting onto the silica surface, which in turn can be calculated from the N/C ratio of the microanalysis. In the passivated silicas **5a–c**, the TMS groups should also be taken into account. Their number can also be calculated from elemental analysis, since they are the only new source of carbon added to the silica during the passivation reaction described in Scheme 2. The degrees of passivation (number of silanol groups protected per gram of material) of the various materials are shown in Table 2. The overall passivation of the silicas varies over a wide range, from 0.5 mmol/g for **3a**, to 2.7 for **5c**.

The calculations above as well as <sup>29</sup>Si NMR spectra (see below) show that, after a similar passivation reaction period (72 h), materials with higher ligand loading have lower TMS functionalization. This saturation phenomenon can be attributed to the reduced number of residual silanol groups available on the corresponding non-passivated silicas. The non-functionalized Matrex silica has between 4 and 5 silanol groups per square nanometer,<sup>44,45</sup> which corresponds to 3.3–4.1 mmol SiOH/g (the BET surface of the Matrex silica was measured to be 492 m<sup>2</sup>/g). The silica/material ratio in the functionalized silicas can be calculated according to microanalysis, and the initial number of silanol groups in the materials can then be estimated. For silica **5c**, for example, this calculation gives 2.5–3.3 mmol SiOH/g material, indicating that its passivation approaches the maximum.

employing relatively small amounts of the heterogeneous catalyst.

It has been previously shown that, in some cases, the activity<sup>26,49</sup> or enantioselectivity<sup>43</sup> of a heterogeneous catalyst are harmed at higher ligand loading. In the case of the catalytic system presented here, an increase in the ligand loading seems to be mostly beneficial, probably because it increases the passivation of the silica. Previous reports about the influence of silica passivation on enantioselectivity of heterogeneous silica-grafted catalysts exist as well.<sup>5,16,35,37</sup> In most cases, passivation of the silica

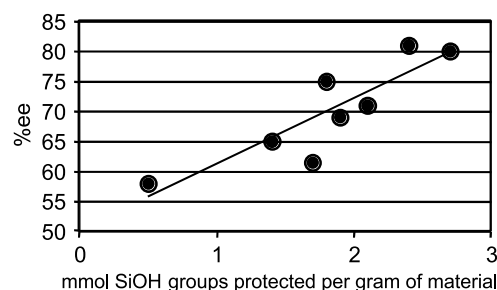


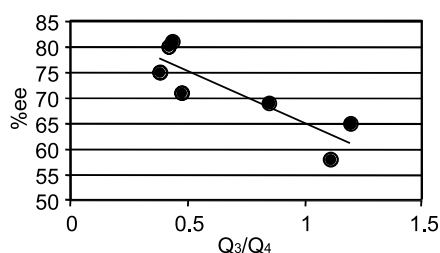
Figure 1. The enantioselectivity of the endo isomer in the benchmark Diels–Alder reaction as a function of the number of protected silanol groups per gram of material.

<sup>‡</sup> The  $p$ -value is the probability that the observed correlation is due to chance. A  $p$ -value under 5% indicates a significant correlation, and the smaller the  $p$ -value the more significant the correlation. See also: <http://www.graphpad.com/quickcalcs/PValue1.cfm>.

<sup>§</sup> Shortly after our first publication, a similar system has been reported.<sup>46</sup> In this system, in one example, the passivation of the mesoporous silica slightly decreased the enantioselectivity of the catalytic material. The authors do not propose an explanation to this phenomenon. However, in our opinion this can be explained by the high temperatures the authors use during the passivation process, which can damage the ligand as well as the structure and porosity of the silica.<sup>47,48</sup> See also Ref. 16.

results in improved enantioselectivities.<sup>46, §</sup> This is probably due to the non-enantioselective metal complexes formed between the metal and the silanol groups of the silica, which act as competing non-enantioselective catalysts of the reaction. However, this is the first report of a good correlation between silica passivation and enantioselectivity.

To reinforce our results, we calculated the passivation of the materials using a different method. The number of residual silanol groups was estimated using the <sup>29</sup>Si NMR of the solid material. Using the CPMAS NMR technique, the resulting spectra were deconvolved to give the relative ratios of the Q<sub>4</sub> (internal Si atoms), Q<sub>3</sub> (silanol groups on the silica), and Q<sub>2</sub> (gem-silanol groups on the silica) peaks (for a representative spectrum and fit see Supplementary data). The CPMAS technique allows the acquisition of a spectrum over only one night. However, for Q<sub>2</sub>, Q<sub>3</sub> and Q<sub>4</sub> species there is a different spin magnetization transfer from proton to silicon nuclei that prevents an absolute quantification. The consequent difference in relaxation times causes the Q<sub>2</sub> and Q<sub>3</sub> peaks to appear larger than their true value relative to the Q<sub>4</sub> peak; however, this bias is identical for all the materials. Thus, the integrals of the peaks cannot be added, but the Q<sub>3</sub>/Q<sub>4</sub> ratios calculated for the different silicas are representative of the number of residual silanol groups relative to the number of internal Si atoms of the silicas (the amount of Q<sub>2</sub> groups is always negligible). A good correlation was observed between the Q<sub>3</sub>/Q<sub>4</sub> ratios and the enantioselectivities of the various silicas (Fig. 2;  $r = -0.87$ ,  $p$ -value = 1.08%).



**Figure 2.** Enantioselectivities as a function of the Q<sub>3</sub>/Q<sub>4</sub> ratios of the various silicas.

The two quantification methods of the passivation of the silicas—via solid NMR and via microanalysis—are in full agreement, indicating that a better passivation leads to higher enantioselectivities.

In conclusion, we grafted indaBOX **1** onto silica, and tested the efficiency of the resulting materials in the catalysis of the Diels–Alder reaction. The best catalytic results obtained equal the performances of the homogeneous catalyst. We showed that in this system the enantioselectivities obtained in the Diels–Alder reaction depend mainly on the protection of the silanol groups of the silica, and are not diminished by a higher ligand loading. The enantioselectivities exhibited a strong correlation with the passivation of the silica as calculated from two different sources—microanalysis of the materials and solid NMR. It has already been documented that in some silica-grafted catalysts there is a qualitative rise in enantioselectivity upon passivation of the silica, which can be attributed to competing catalytic species formed by

complexation of the metal with silanol groups of the silica surface. However, this is the first time a linear correlation has been demonstrated. The quantification of this phenomenon, doubly proved by the two different ways of characterizing the passivation of the silica surface, shows the importance of this aspect of heterogeneous catalysts design. In the case of silica-supported materials, this is especially important for reactions, which are catalyzed through Lewis acid mechanisms, where the silanol groups of the silica can compete with the chiral catalyst. It has also been claimed that high ligand loading can reduce the enantioselectivity of a system. This is a limiting aspect in the practicality of heterogeneous catalysts, since low catalyst loading implies the use of large volumes of the catalyst. Importantly, in the system described here the ligand loading can be increased without causing a decrease in the enantioselectivity of the catalyst, permitting the use of relatively small volumes of catalytic material.

### 3. Experimental

#### 3.1. General

NMR spectra were recorded on 200 or 300 MHz apparatuses. Peaks are given in ppm, coupling constants ( $J$ s) in Hz. <sup>29</sup>Si CP-MAS solid NMR measurements were collected on a Bruker DSXv400 spectrometer. For <sup>29</sup>Si (79.49 MHz), a 4 μs (corresponding to  $\theta = \pi/3$ ) pulse was used with a repetition time of 4 s. The spinning rate of the rotor was about 5 kHz and the number of scans, between 2000 and 15,000, depends on the rate of grafting. IR spectra were taken with an FT spectrometer. The solids were pressed with KBr. The absorption is expressed in cm<sup>-1</sup>. Cu analysis was performed by plasma emission spectrometry. Chiral HPLC analyses were performed on a Chiralcel-OD column. Cyclopentadiene was freshly cracked from bicyclopentadiene before each use, using a distillation system with a Vigreux column heated to 50 °C. The cyclopentadiene was used directly in the reaction, or kept at -20 °C for a maximum of 1 day. Compounds **1**<sup>36,37,50</sup> and **2**,<sup>36,37</sup> as well as *N*-acryloyl-2-oxazolidinone,<sup>38,39</sup> were prepared according to literature procedures.

**3.1.1. Treatment of silica with HCl.** Silica (Matrex Si-60 from Millipore, particle size 70–200 μm, ca. 13 g) was refluxed with HCl (33%, 50 ml) for ca. 2 h. It was filtered and washed with water. After drying (vacuum, 70–80 °C, 24 h), about 10–11 g of activated silica were obtained.

**3.1.2. Preparation of catalyst **3b**<sup>36,37</sup>—grafting of **2** onto silica.** In a typical experiment, the functionalized ligand **2** (1.5 mmol, 0.5857 g) was dissolved in dry DMF (approx. 7 ml) and dry Et<sub>3</sub>N (0.75 ml, 5 mmol), under Ar. 3-(Isocyanatopropyl)triethoxysilane (3.3 mmol, 0.8175 g, 0.82 ml) was added over a period of 10–20 min, at rt. The solution was stirred for ca. 48 h. A polystyrene-NH<sub>2</sub> resin (0.8715 g of 1.1 mmol NH<sub>2</sub>/g resin) was added in order to capture the excess isocyanate. The mixture was stirred for another hour, following which the amine resin was filtered off and washed with CH<sub>2</sub>Cl<sub>2</sub>. The solvents were evaporated, and the resulting oil was added to a suspension of activated silica (4.00 g) in toluene (30 ml). The suspension was

refluxed overnight, then filtered through a sinter and washed with toluene followed by ethyl acetate and  $\text{CH}_2\text{Cl}_2$ . After drying overnight in vacuum, 4.6720 g of the resulting catalyst were obtained. IR 3429, 2981 (very small), 1648 (oxazolines), 1095 (very br), 800, 476  $\text{cm}^{-1}$ ; IR taken after use for catalysis of the Diels–Alder reaction—essentially the same (sometimes small peaks at 1780, 1700 indicated the presence of some product or substrate which were not entirely washed away). Microanalysis: found: C, 9.65%; H, 1.72%; N, 1.41%; Si, 38.85% (O: the rest = 48.37%). Since there are four nitrogen atoms per ligand, the ratio mmol ligand per gram of **3b** was calculated as follows:  $0.0141[\text{g N to g } \mathbf{3b}]/\{14.007[\text{g N to mol N}]\times 4[\text{mol N to mol ligand}]\} \times 1000[\text{mmol/mol}] = 0.252[\text{mmol ligand/g of } \mathbf{3b}]$ . Overall weight of the functionalized catalytic material, 4.5016 g; overall mmol of ligand, 1.13 mmol; yield from **2**,  $(1.13/1.5) \times 100 = 75.5\%$ . Solid NMR by cross polarization magic-angle spinning (CPMAS):  $^{13}\text{C}$  NMR  $\delta$  165, 158 (NC=O, OC=N), 141, 126 (Ar), 84, 76 (CHN+CHO of BOX), 58 ( $\text{CH}_2\text{O}$  on BOX bridge +  $\text{CH}_2\text{OSi}$ ), 48 (C of BOX bridge), 43 ( $\text{CH}_2\text{NH}$  near carbamate), 39 ( $\text{CH}_2$  near CHO of BOX), 16 ( $\text{CH}_3\text{CH}_2\text{OSi} + \text{CH}_2\text{CH}_2\text{Si}$ ), 9 ( $\text{CH}_2\text{Si}$ );  $^1\text{H}$  NMR  $\delta$  5.0, 4.0 (br), 1.8 (small), 1.1,  $-0.2$  (small shoulder);  $^{29}\text{Si}$  NMR  $\delta$   $-57.7$  (br m, small hill, ligand Si),  $-101.9$  ( $\text{Si}(\text{OSi})_3(\text{OH})$ , br),  $-110.9$  ( $\text{Si}(\text{OSi})_4$ , br).

**3.1.3. Catalysts 3a, 3c.** The title compound were prepared in a similar manner, according to the ratios given in Table 1, and had similar  $^{29}\text{Si}$  NMR and IR spectra. The size of peaks corresponding to the ligand and to the silanol groups changed according to ligand loading.

**Compound 3a.** Microanalysis: C, 6.48%; H, 1.28%; N, 0.84%; Si, 38.44%, that is, 0.150 mmol ligand/g.

**Compound 3c:** Microanalysis: C, 13.03%; H, 1.96%; N, 1.89%; Si, 38.44%, that is, 0.337 mmol ligand/g.

**3.1.4. Catalyst 5b–1<sup>36,37</sup>—protecting the silanol groups of catalyst 3b.** Catalyst **3b** (1 g) was mixed in TMSIM (4.7 ml, 0.032 mol) for 1 h. It was filtered and washed with MeOH ( $5 \times 20$  ml). After drying in vacuum overnight the catalyst weighed 1.0125 g. Microanalysis: found: C, 12.36%; H, 2.06%; N, 1.41%; Si, 37.40%, that is, 0.252 mmol ligand/g **5b–1**; IR 3434 (smaller than the same peak for **3a**, indicating less OH groups), 2964 ( $\text{CH}_3$ ), 1655 (oxazolines), 1091 (very br), 845, 802, 758, 474  $\text{cm}^{-1}$ .

**3.1.5. Catalyst 5b–72.<sup>36,37</sup>** The title compound was prepared like **5b–1**, but mixing for 72 h. Microanalysis: C, 12.69%; H, 2.22%; N, 1.22%; Si, 35.33%, that is, 0.217 mmol ligand/g **5b–72**; IR: similar to that of **5b–1**, but the peak of  $\text{CH}_3$  was relatively bigger; % Cu before use of the silica (calculated from amounts of catalyst **5b–72** and  $\text{Cu}(\text{ClO}_4)_2 \cdot 6\text{H}_2\text{O}$  put at 1/1 molar ratios): 1.46%; % Cu according to elemental analysis after use: 1.21%; that is ratio of Cu to ligand after use:  $1.46/1.21 = 1.21$  (this is the molar ratio usually used for homogeneous catalysis);  $^{29}\text{Si}$  NMR  $\delta$  13.3 (br,  $\text{Si}(\text{OSi})_3\text{OMe}$ ),  $-57.7$  (br m, small hill, ligand Si),  $-101.9$  ( $\text{Si}(\text{OSi})_3(\text{OH})$ ),  $-110.9$  ( $\text{Si}(\text{OSi})_4$ ).

**3.1.6. Catalysts 5a–72, 5a–144 and 5c.** The title compounds were prepared like **5b–72**, and had similar

$^{29}\text{Si}$  NMR and IR spectra, with the size of the peaks corresponding to the ligand and to the number of silanol groups changing according to ligand loading and to the passivation of the material.

**Compound 5a–72.** Microanalysis: C, 10.39%; H, 2.18%; N, 0.79%; Si, 38.40%, that is, 0.141 mmol ligand/g.

**Compound 5a–144.** Microanalysis: C, 10.77%; H, 2.18%; N, 0.79%; Si, 37.77%, that is, 0.141 mmol ligand/g.

**Compound 5c.** Microanalysis: C, 16.04%; H, 2.55%; N, 1.87%; Si, 34.70%, that is, 0.334 mmol ligand/g.

**3.1.7. Determination of Q<sub>3</sub> and Q<sub>4</sub>.** CPMAS  $^{29}\text{Si}$  NMR spectra of the materials were taken. The Q<sub>2</sub>, Q<sub>3</sub>, and Q<sub>4</sub> peaks were not well separated, and the determination of their ratios was performed by deconvolution, using MestReC<sup>51</sup> and Dmfit<sup>52</sup> programs. The shifts ( $\delta$ ), line widths ( $\Delta\omega$ ), and line shape (100% Gaussian) of the Q<sub>2</sub> ( $\delta = -91$  ppm,  $\Delta\omega = 6.3$  ppm), Q<sub>3</sub> ( $\delta = -100.2$  ppm,  $\Delta\omega = 7.9$  ppm), and Q<sub>4</sub> ( $\delta = -109.7$  ppm,  $\Delta\omega = 9.2$  ppm) peaks were obtained using a trial and error approach on all the spectra to obtain the best set of parameters such as the fit was reasonably good in each case. At the end of the processes, the intensity was the only parameter varying from one spectrum to another. The peak position, line width and line shape found for each species were typical of data reported in the literature. This procedure allowed us to increase the level of confidence even in difficult cases when one signal was appearing as a shoulder rather than as a separate peak (this was always the case for Q<sub>2</sub> signal).

## Supplementary data

Supplementary data associated with this article can be found, in the online version, at [doi:10.1016/j.tet.2005.05.028](https://doi.org/10.1016/j.tet.2005.05.028). A representative  $^{29}\text{Si}$  NMR and its fit are provided as supplementary material.

## References and notes

1. *Chem. Rev.*, **2002**, *102*, 3215–3892. This issue was dedicated to *Recoverable Catalysts and Reagents*; Gladysz J. A., Ed.
2. Fraile, J. M.; Garcia, J. I.; Herrerias, C. I.; Mayoral, J. A.; Harmer, M. A. *J. Catal.* **2004**, *221*, 532–540.
3. Fraile, J. M.; Garcia, J. I.; Harmer, M. A.; Herrerias, C. I.; Mayoral, J. A.; Reiser, O.; Werner, H. *J. Mater. Chem.* **2002**, *12*, 3290–3295.
4. Alcòn, M. J.; Corma, A.; Iglesias, M.; Sánchez, F. *J. Organomet. Chem.* **2002**, *655*, 134–145.
5. Bae, S. J.; Kim, S. W.; Hyeon, T.; Kim, B. M. *Chem. Commun.* **2000**, 31–32.
6. De Vos, D. E.; Dams, M.; Sels, B. F.; Jacobs, P. A. *Chem. Rev.* **2002**, *102*, 3615–3640.
7. Song, C. E.; Lee, S.-g. *Chem. Rev.* **2002**, *102*, 3495–3524.

8. Clapham, B.; Reger, T. S.; Janda, K. D. *Tetrahedron* **2001**, *57*, 4637–4662.
9. Ghosh, A. K.; Mathivanan, P.; Cappiello, J. *Tetrahedron: Asymmetry* **1998**, *9*, 1–45.
10. McManus, H. A.; Guiry, P. J. *Chem. Rev.* **2004**, *104*, 4151–4202.
11. Johnson, J. S.; Evans, D. A. *Acc. Chem. Res.* **2000**, *33*, 325–335.
12. Evans, D. A.; Johnson, J. S.; Olhava, E. J. *J. Am. Chem. Soc.* **2000**, *122*, 1635–1649.
13. Thorhaug, J.; Roberson, M.; Hazell, R. G.; Jørgensen, K. A. *Chem. Eur. J.* **2002**, *8*, 1888–1898.
14. Pericas, M. A.; Puigjaner, C.; Riera, A.; Vidal-Ferran, A.; Gomez, M.; Jimenez, F.; Muller, G.; Rocamora, M. *Chem. Eur. J.* **2002**, *8*, 4164–4178.
15. Desimoni, G.; Faita, G.; Quadrelli, P. *Chem. Rev.* **2003**, *103*, 3119–3154.
16. Rechavi, D.; Lemaire, M. *Chem. Rev.* **2002**, *102*, 3467–3494.
17. Weissberg, A.; Portnoy, M. *Chem. Commun.* **2003**, 1538–1539.
18. Wan, Y.; McMorn, P.; Hancock, F. E.; Hutchings, G. J. *Catal. Lett.* **2003**, *91*, 145–148.
19. Cornejo, A.; Fraile, J. M.; Garcia, J. I.; Gil, M. J.; Herrerias, C. I.; Legarreta, G.; Martinez-Merino, V.; Mayoral, J. A. *J. Mol. Catal. A: Chem.* **2003**, *196*, 101–108.
20. Annunziata, R.; Benaglia, M.; Cinquini, M.; Cozzi, F.; Pozzi, G. *Eur. J. Org. Chem.*, **2003**, 1191–1197.
21. Davies, D. L.; Kandola, S. K.; Patel, R. K. *Tetrahedron: Asymmetry* **2004**, *15*, 77–80.
22. Yang, B.-Y.; Chen, X.-M.; Deng, G.-J.; Zhang, Y.-L.; Fan, Q.-H. *Tetrahedron Lett.* **2003**, *44*, 3535–3538.
23. Mandoli, A.; Orlandi, S.; Pini, D.; Salvadori, P. *Chem. Commun.* **2003**, 2466–2467.
24. Mandoli, A.; Orlandi, S.; Pini, D.; Salvadori, P. *Tetrahedron: Asymmetry* **2004**, *15*, 3233–3244.
25. Lundgren, S.; Lutsenko, S.; Joensson, C.; Moberg, C. *Org. Lett.* **2003**, *5*, 3663–3665.
26. Pugin, B. *J. Mol. Catal. A: Chem.* **1996**, *107*, 273–279.
27. Fache, F.; Schulz, Z.; Tommasino, M. L.; Lemaire, M. *Chem. Rev.* **2000**, *100*, 2159–2231.
28. Leadbeater, N. E.; Marco, M. *Chem. Rev.* **2002**, *102*, 3217–3273.
29. Fan, Q.-H.; Li, Y.-M.; Chan, A. S. C. *Chem. Rev.* **2002**, *102*, 3385–3465.
30. Taylor, S.; Gullick, J.; McMorn, P.; Bethell, D.; Page, P. C. B.; Hancock, F. E.; King, F.; Hutchings, G. J. *J. Chem. Soc., Perkin Trans. 2* **2001**, 1714–1723.
31. Taylor, S.; Gullick, J.; McMorn, P.; Bethell, D.; Page, P. C. B.; Hancock, F. E.; King, F.; Hutchings, G. J. *J. Chem. Soc. Perkin Trans. 2* **2001**, 1724–1728.
32. Johnson, B. F. G.; Raynor, S. A.; Shephard, D. S.; Mashmeyer, T.; Thomas, J. M.; Sankar, G.; Bromley, S.; Oldroyd, R.; Gladden, L.; Mantle, M. D. *Chem. Commun.* **1999**, 1167–1168.
33. Corma, A.; García, H.; Moussaif, A.; Sabater, M. J.; Zniber, R.; Redouane, A. *Chem. Commun.* **2002**, 1058–1059.
34. Simonsen, K. B.; Jørgensen, K. A.; Hu, Q. S.; Pu, L. *Chem. Commun.* **1999**, 811–812.
35. Belloccq, N.; Abramson, S.; Lasperas, M.; Brunel, D.; Moreau, P. *Tetrahedron: Asymmetry* **1999**, *10*, 3229–3241.
36. Rechavi, D.; Lemaire, M. *Org. Lett.* **2001**, *3*, 2493–2496.
37. Rechavi, D.; Lemaire, M. *J. Mol. Catal. A: Chem.* **2002**, *182–183*, 239–247.
38. Evans, D. A.; Chapman, K. T.; Bisaha, J. *J. Am. Chem. Soc.* **1988**, *110*, 1238–1256.
39. Ho, G.-J.; Mathre, D. J. *J. Org. Chem.* **1995**, *60*, 2271–2273.
40. Evans, D. A.; Miller, S. J.; Lectka, T.; von Matt, P. *J. Am. Chem. Soc.* **1999**, *121*, 7559–7573.
41. Davies, I. W.; Gerena, L.; Castonguay, L.; Senanayake, C. H.; Larsen, R. D.; Verhoeven, T. R.; Reider, P. J. *J. Chem. Soc., Chem. Commun.* **1996**, 1753–1754.
42. Ghosh, A. K.; Cho, H.; Cappiello, J. *Tetrahedron: Asymmetry* **1998**, *9*, 3687–3691.
43. Vidal-Ferran, A.; Bampos, N.; Moyano, A.; Pericàs, M. A.; Riera, A.; Sanders, J. K. M. *J. Org. Chem.* **1998**, *63*, 6309–6318.
44. Iler, R. K. *The Chemistry of Silica: Solubility, Polymerization, Colloid and Surface Properties, and Biochemistry*; Wiley: New York, 1979.
45. Batteas, J. D.; Weldon, M. K.; Raghavachari, K. In *Nanotribology Critical Assessment and Research Needs*; Hsu, S. M., Ying, Z. C., Eds.; Kluwer Academic: Boston, 2002.
46. Park, J. K.; Kim, S.-W.; Hyeon, T.; Kim, B. M. *Tetrahedron: Asymmetry* **2001**, *12*, 2931–2935.
47. Maschmeyer, T. *Curr. Opin. Solid State Mater. Sci.* **1998**, *3*, 71–78.
48. Clark, J. H.; Kybett, A. P.; Macquarrie, D. J. *Supported Reagents Preparation, Analysis, and Applications*; VCH: NY/Weinheim/Cambridge, 1992.
49. Grubbs, R.; Lau, C. P.; Cukier, R.; Brubaker, C., Jr. *J. Am. Chem. Soc.* **1977**, *99*, 4517–4518.
50. Hall, J.; Lehn, J.-M.; DeCian, A.; Fischer, J. *Helv. Chim. Acta* **1991**, *74*, 1–6.
51. MestRe-C 2.3a (1995–2000), Departamento de Química Orgánica, Universidad de Santiago de Compostela, Spain (mestrec@usc.es).
52. Dmfit 98, dm2000NT, D. Massiot, CRMHT-CNRS Orléans, France (massiot@cnrs-orleans.fr).



# Diastereoselectivity-switchable and regiospecific hetero Diels–Alder reaction of *N*-sulfinylper(poly)fluoroalkanesulfinamides with dienes

Xiao-Jin Wang and Jin-Tao Liu\*

Key Laboratory of Organofluorine Chemistry, Shanghai Institute of Organic Chemistry, Chinese Academy of Sciences, 354 Fenglin Road, Shanghai 20032, China

Received 29 December 2004; revised 11 May 2005; accepted 11 May 2005

Available online 4 June 2005

**Abstract**—*N*-Sulfinylper(poly)fluoroalkanesulfinamides reacted readily with dienes in methylene chloride at  $-78\text{ }^{\circ}\text{C}$  to give the corresponding cycloadducts with complete regioselectivities and good diastereoselectivities. The diastereoselectivity of the reaction was switchable to the opposite under the catalysis of Lewis acids such as  $\text{TiCl}_4$  and  $\text{SnCl}_4$ .

© 2005 Elsevier Ltd. All rights reserved.

## 1. Introduction

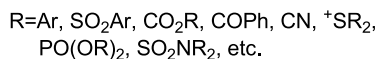
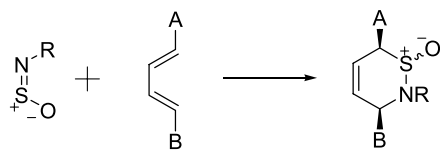
Fluorine-containing heterocycles are fascinating targets for their unique bioactivities.<sup>1</sup> Accordingly, considerable effort has been devoted to the development of their synthetic strategies in recent years. Among various reactions available, hetero Diels–Alder reaction is an extremely useful method for the synthesis of heterocycles.<sup>2</sup> Hetero Diels–Alder reactions of *N*-sulfinylaniline and conjugated dienes were first described by Wichterle and Roček in 1953. Since then a number of Diels–Alder reactions for various *N*-sulfinyl compounds have been reported (Scheme 1).<sup>3</sup> The cycloaddition usually takes place under mild conditions to afford dihydro-1,2-thiazine-1-oxides, which are precursors for unsaturated vicinal amino-alcohols and homoallylic amines, as well as a useful intermediate in

the total synthesis of natural products and biologically active compounds.<sup>4</sup> Although the reactions of *N*-sulfinyl compounds are well studied, their fluorine-containing analogs are less reported.<sup>5</sup> To the best of our knowledge, *N*-sulfinyltrifluoromethanesulfinamide,  $\text{CF}_3\text{SONSO}$ , was first prepared in 1976.<sup>6</sup> However, its chemistry has not been studied yet, neither did the reaction of both *N*-sulfinylsulfinamides and their fluorinated analogs. In order to investigate the reaction of fluorine-containing *N*-sulfinyl compounds and synthesize fluorinated sulfur-containing heterocycles, *N*-sulfinylper(poly)fluoroalkanesulfinamides were prepared and their reaction with dienes was studied. The results are reported in this paper.

## 2. Results and discussion

*N*-Sulfinylper(poly)fluoroalkanesulfinamides (**5**) were prepared from per(poly)fluoroalkyl iodides (**1**) as shown in Scheme 2. Under mild conditions **1** readily reacted with sodium dithionite to give the corresponding sodium per(poly)fluoroalkanesulfonates.<sup>7</sup> Distillation of the sodium salts and concentrated sulfuric acid mixture gave free sulfinic acids **2**. Sulfinyl chlorides **3** were obtained from **2** by the treatment with thionylchloride, which were further treated with hexamethyldisilazane to afford compound **4**. The reaction of **4** with thionylchloride gave **5** in moderate yields.

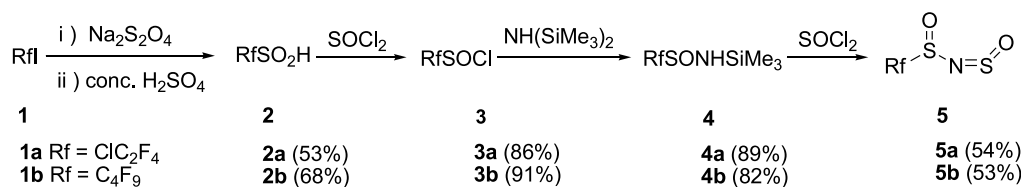
The reaction of **5** with dienes was first carried out at room temperature. In methylene chloride, compound **5** reacted



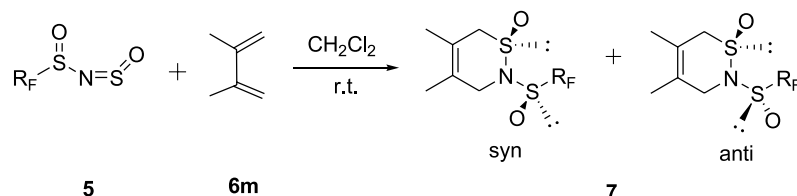
Scheme 1.

**Keywords:** *N*-Sulfinylper(poly)fluoroalkanesulfinamide; Hetero Diels–Alder reaction; Diene.

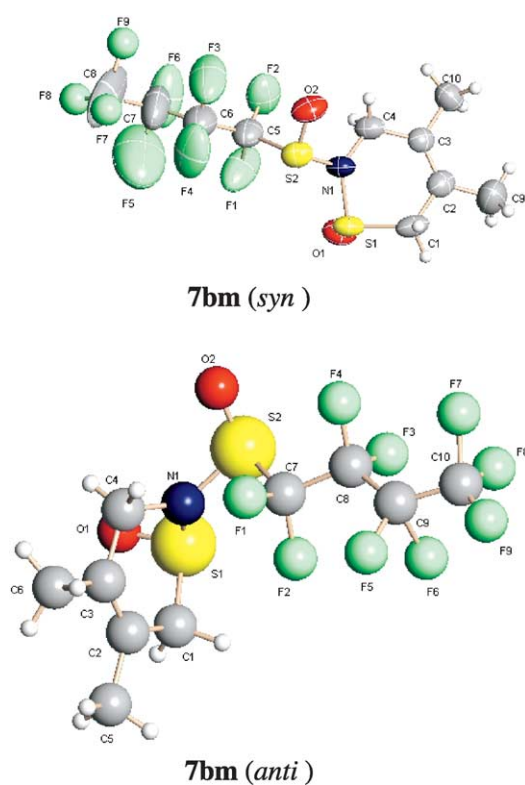
\* Corresponding author. Tel.: +86 21 54925188; fax: +86 21 64166128; e-mail: jtliu@mail.sioc.ac.cn



Scheme 2.



Scheme 3.

Figure 1. Molecular structure of **7bm**.

readily with 2,3-dimethyl-but-1,3-diene (**6m**) to give the corresponding cycloadduct **7** as a mixture of *syn*- and *anti*-isomers (Scheme 3). The two isomers could be separated by column chromatography. Their structures were determined on the basis of their NMR spectral and X-ray crystallographic study (Fig. 1).

To improve the stereoselectivity of the above reaction, various conditions were examined. As shown in Table 1, the ratio of two isomers changed distinctly when Lewis acids were added to the reaction mixture as a catalyst. Surprisingly it was found that opposite stereoselectivity was obtained with the addition of Lewis acids such as  $\text{TiCl}_4$  and  $\text{SnCl}_4$ , and  $\text{TiCl}_4$  gave the best result among the Lewis acids examined. Temperature also had effect on the stereoselectivity of the reaction. Much better stereoselectivities were obtained when the reaction was carried out at  $-78^\circ\text{C}$  (entries 7 and 9, Table 1). In all reactions, per(poly)fluoroalkanesulfonamides,  $\text{RfSONH}_2$ , were formed as a by-product from the hydrolysis of **5** although the reaction was carried out under inert and anhydrous conditions.

The effect of  $\text{TiCl}_4$  on the reaction diastereoselectivity might be explained as follows. The cycloaddition of *N*-sulfinyl compounds with dienes has been proved to be pericyclic.<sup>8</sup> The weight of evidence is that *N*-sulfinyl compounds exists in ground states in the *Z* configuration about the  $\text{N}=\text{S}$  double bond.<sup>9</sup> In the absence of  $\text{TiCl}_4$ , the dienophile prefers conformation **A** to minimize the electrostatic interaction between the two sulfanyl oxygens,<sup>10</sup>

Table 1. The reaction of **5** and **6m** under different conditions

Entry	Rf	Temperature	Catalyst	Product	Yield (%) <sup>a</sup>	<i>syn/anti</i>
1	$\text{ClC}_2\text{F}_4$	rt	—	<b>7am</b>	66	15:85
2	$\text{ClC}_2\text{F}_4$	rt	$\text{BF}_3 \cdot \text{Et}_2\text{O}$	<b>7am</b>	71	18:82
3	$\text{ClC}_2\text{F}_4$	rt	$\text{ZnCl}_2$	<b>7am</b>	54	15:85
4	$\text{ClC}_2\text{F}_4$	rt	$\text{AlCl}_3$	<b>7am</b>	68	37:63
5	$\text{ClC}_2\text{F}_4$	rt	$\text{SnCl}_4$	<b>7am</b>	72	73:27
6	$\text{ClC}_2\text{F}_4$	rt	$\text{TiCl}_4$	<b>7am</b>	66	85:15
7	$\text{ClC}_2\text{F}_4$	$-78^\circ\text{C}$	—	<b>7am</b>	79	7:93
8	$\text{ClC}_2\text{F}_4$	$-78^\circ\text{C}$	$\text{TiCl}_4$	<b>7am</b>	59	98:2
9	$\text{C}_4\text{F}_9$	$-78^\circ\text{C}$	—	<b>7bm</b>	74	5:95
10	$\text{C}_4\text{F}_9$	$-78^\circ\text{C}$	$\text{TiCl}_4$	<b>7bm</b>	70	94:6

<sup>a</sup> Isolated yields based on **5**.



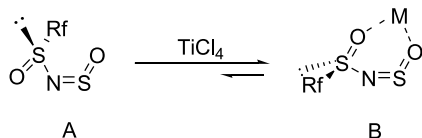


Figure 2.

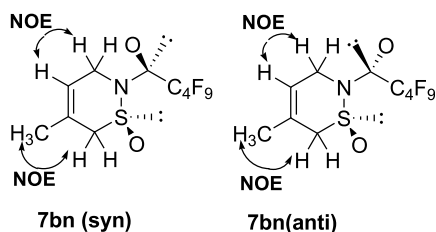
electrophilic *N*-sulfinyl compounds had better regioselectivity in the hetero Diels–Alder reactions with dienes on the basis of the Hückel frontier orbital approach and experimental evidence.<sup>8</sup> So it is clear that the regioselectivity of this reaction is attributed to the strong electron-withdrawing ability of perfluoroalkylsulfinyl group.

Table 2. The cycloaddition reaction of **5** and asymmetrical dienes<sup>a</sup>

Entry	Rf	Diene	Catalyst	Product	Yield (%) <sup>b</sup>	<i>syn/anti</i>
1	ClC <sub>2</sub> F <sub>4</sub>	<b>6n</b>	—	<b>7an</b>	55	26:74
2	ClC <sub>2</sub> F <sub>4</sub>	<b>6n</b>	TiCl <sub>4</sub>	<b>7an</b>	64	87:13
3	C <sub>4</sub> F <sub>9</sub>	<b>6n</b>	—	<b>7bn</b>	66	28:72
4	C <sub>4</sub> F <sub>9</sub>	<b>6n</b>	TiCl <sub>4</sub>	<b>7bn</b>	62	90:10
5	ClC <sub>2</sub> F <sub>4</sub>	<b>6l</b>	—	<b>7al</b>	76	24:76
6	C <sub>4</sub> F <sub>9</sub>	<b>6l</b>	—	<b>7bl</b>	72	16:84

<sup>a</sup> All reactions were carried out at  $-78$  °C.

<sup>b</sup> Isolated yields based on **5**.

Figure 3. NOE correlations from NOESY spectra of **7bn**.

resulting in the predominant formation of *anti* cycloadducts when reacted with dienes (Fig. 2). While in the presence of TiCl<sub>4</sub> the reaction takes place through the chelating complex B, formed by the bonding of metal cation and two sulfinyl oxygens. Thus, the other side is the most accessible for the approach of the diene and opposite stereoselectivity is obtained.

To demonstrate the regioselectivity of this reaction, reactions of **5** and some asymmetrical dienes were investigated using the optimized conditions (Scheme 4). The results are summarized in Table 2. The cycloaddition of **5b** and **6n** gave only two isomers as indicated by <sup>19</sup>F NMR spectra of the crude products. Their structures were determined on the basis of NOESY spectra of purified products (Fig. 3). This indicated that the reaction proceeded in a completely regioselective manner with good diastereoselectivities. Similar results were reported in the literatures.<sup>8,11</sup> Hanson and Stockburn reported that less

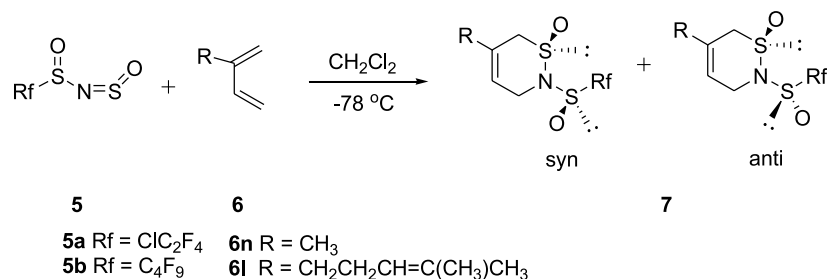
In summary, the cycloaddition reaction of *N*-sulfinyl-per(poly)fluoroalkanesulfinamides with dienes has been demonstrated, providing a facile method for the preparation of per(poly)fluoroalkanesulfinyl substituted dihydro-1,2-thiazine-1-oxides with complete regioselectivity and good diastereoselectivity.

### 3. Experimental

Melting points were uncorrected. <sup>1</sup>H NMR spectra were recorded in CDCl<sub>3</sub> on a Bruker AM-300 spectrometer (300 MHz) with TMS as internal standard. <sup>19</sup>F NMR spectra were taken on a Bruker AM-300 (282 MHz) spectrometer using CFCl<sub>3</sub> as external standard. IR spectra were obtained with a Nicolet AV-360 spectrophotometer. Mass spectra and high resolution mass spectra (HRMS) were obtained on a Finnigan GC-MS 4021 and a Finnigan MAT-8430 spectrometer, respectively. Dichloromethane was distilled from CaH<sub>2</sub> and reagents were purified before use. Compound **5** was easy to hydrolyse and stored in CH<sub>2</sub>Cl<sub>2</sub> solution.

#### 3.1. General procedure for the synthesis of per(poly)-fluoroalkanesulfinic acids **2**

With magnetic stirring, a mixture of Na<sub>2</sub>S<sub>2</sub>O<sub>4</sub> (34.8 g, 0.2 mol) and NaHCO<sub>3</sub> (16.8 g, 0.2 mol) was added to the mixture of per(poly)fluoroalkyl iodides **1** (0.15 mol), 180 mL H<sub>2</sub>O and 120 mL CH<sub>3</sub>CN at room temperature.



Scheme 4.

After addition, the mixture was stirred for a few hours at room temperature to the completion of reaction (monitored by  $^{19}\text{F}$  NMR). The resulting mixture was extracted with ethyl acetate (100 mL  $\times$  4). The combined organic layer was washed with saturated aqueous NaCl solution (100 mL  $\times$  3) and dried over anhydrous  $\text{Na}_2\text{SO}_4$ . After the removal of solvent, the residue was dissolved in 120 mL of concentrated  $\text{H}_2\text{SO}_4$  and distilled under reduced pressure to give 2 as a colorless oil.

**3.1.1. 2-Chlorotetrafluoroethanesulfonic acid (2a).** Colorless oil. Bp 62–63 °C/1 Torr. FT-IR (film): 2910, 1273, 1167  $\text{cm}^{-1}$ .  $^1\text{H}$  NMR (300 MHz,  $\text{CDCl}_3$ ):  $\delta$  10.28 (s, 1H).  $^{19}\text{F}$  NMR (282 MHz,  $\text{CDCl}_3$ ):  $\delta$  -68.30 (m, 2F), -122.34 (m, 2F). EIMS ( $m/z$ , %): 201 ( $\text{M}^+ + 1$ , 0.74), 135 (17.37), 116 (15.21), 100 (34.39), 85 (46.53), 65 (100.00), 50 (17.45), 48 (22.70), 45 (15.82). Anal. Calcd for  $\text{C}_2\text{HClF}_4\text{O}_2\text{S}$ : C, 11.98; H, 0.50. Found: C, 12.07; H, 0.66.

**3.1.2. Nonafluorobutanesulfonic acid (2b).**<sup>12</sup> Colorless oil. Bp 65–66 °C/1 Torr. FT-IR (film): 3397, 1299, 1254, 1291, 1141  $\text{cm}^{-1}$ .  $^1\text{H}$  NMR (300 MHz,  $\text{CDCl}_3$ ):  $\delta$  9.60 (s, 1H).  $^{19}\text{F}$  NMR (282 MHz,  $\text{CDCl}_3$ ):  $\delta$  -81.21 (t,  $J=7.6$  Hz, 3F), -122.77 (m, 2F), -123.24 (m, 2F), -126.59 (m, 2F). EIMS ( $m/z$ , %): 285 ( $\text{M}^+ + 1$ , 0.67), 169 (16.24), 150 (19.38), 131 (30.83), 119 (28.92), 100 (29.85), 69 (100.00), 65 (78.37), 45 (44.44).

### 3.2. General procedure for the synthesis of perfluoroalkanesulfinyl chlorides 3

Perfluoroalkanesulfonic acid **2** (0.1 mol) was added dropwise to thionylchloride (7.4 mL, 0.1 mol) with stirring at 0 °C. After the addition, stirring was continued for 2 h at room temperature. The product was purified by distillation under reduced pressure.

**3.2.1. 2-Chlorotetrafluoroethanesulfinyl chloride (3a).** Colorless oil. Bp 58 °C/160 Torr. FT-IR (film): 1262, 1202, 1176, 1121, 1010, 792  $\text{cm}^{-1}$ .  $^{19}\text{F}$  NMR (282 MHz,  $\text{CDCl}_3$ ):  $\delta$  -66.98 (m, 2F), -110.55, -117.60 (AB,  $J_{\text{AB}}=223.1$  Hz, 2F). EIMS ( $m/z$ , %): 218 ( $\text{M}^+$ , 0.26), 151 (17.33), 137 (34.02), 135 (100.00), 100 (28.19), 87 (20.08), 85 (81.31), 83 (69.59), 48 (22.11). Anal. Calcd for  $\text{C}_2\text{Cl}_2\text{F}_4\text{OS}$ : C, 10.97. Found: C, 10.94.

**3.2.2. Nonafluorobutanesulfinyl chloride (3b).**<sup>12</sup> Colorless oil. Bp 33–34 °C/40 Torr. FT-IR (film): 1719, 1351, 1239, 1140, 111, 747, 723  $\text{cm}^{-1}$ .  $^{19}\text{F}$  NMR (282 MHz,  $\text{CDCl}_3$ ):  $\delta$  -81.4 (m, 3F), -111.2, -117.3 (AB,  $J_{\text{AB}}=233.57$  Hz, 2F), -120.8 (m, 2F), -126.5 (m, 2F). EIMS ( $m/z$ , %): 169 (14.44), 131 (41.30), 119 (20.89), 100 (26.67), 69 (100.00), 65 (74.98), 48 (13.85), 47 (20.63).

### 3.3. General procedure for the synthesis of *N*-(trimethylsilyl)perfluoroalkanesulfinamides 4

To  $\text{NH}(\text{SiMe}_3)_2$  (16 mL, 0.075 mol) was added dropwise perfluoroalkanesulfinyl chlorides (0.075 mol) at 0 °C. After addition, stirring was continued for 2 h at room temperature. The product was purified by distillation under reduced pressure.

**3.3.1. *N*-Trimethylsilyl-2-chlorotetrafluoroethanesulfinamide (4a).** Oil. Bp 62–63 °C/0.1 Torr. FT-IR (film): 1260, 1172, 1127, 1016, 911  $\text{cm}^{-1}$ .  $^1\text{H}$  NMR (300 MHz,  $\text{CDCl}_3$ ):  $\delta$  0.28 (s, 9H), 5.01 (s, 1H).  $^{19}\text{F}$  NMR (282 MHz,  $\text{CDCl}_3$ ):  $\delta$  -67.1 (m, 2F), -110.1, -126.21 (AB,  $J_{\text{AB}}=232.2$  Hz, 2F). EIMS ( $m/z$ , %): 272 ( $\text{M}^+ + 1$ , 0.02), 100 (7.30), 85 (12.22), 73 (17.31), 66 (7.13), 64 (100.00), 48 (11.80), 47 (6.59), 46 (13.23). HRMS: calcd for  $\text{C}_5\text{H}_{10}\text{ClF}_4\text{NNaOSSi}$ : 293.9769. Found: 293.9767.

**3.3.2. *N*-Trimethylsilyl-nonafluorobutanesulfinamide (4b).**<sup>12</sup> Oil. Bp 52–53 °C/0.01 Torr. FT-IR (film): 3221, 1353, 1237, 1142, 852  $\text{cm}^{-1}$ .  $^1\text{H}$  NMR (300 MHz,  $\text{CDCl}_3$ ):  $\delta$  0.31 (s, 9H), 4.82 (s, 1H).  $^{19}\text{F}$  NMR (282 MHz,  $\text{CDCl}_3$ ):  $\delta$  -81.2 (m, 3F), -120.1, -128.2 (AB,  $J_{\text{AB}}=234.9$  Hz, 2F), -122.3 (m, 2F), -126.6 (m, 2F). EIMS ( $m/z$ , %): 131 (13.37), 100 (10.37), 69 (40.57), 66 (7.80), 64 (100.00), 48 (21.41), 47 (7.99), 46 (19.98).

### 3.4. General procedure for the synthesis of *N*-sulfinylper(poly)fluoroalkanesulfinamides 5

To thionyl chloride (3.7 mL, 0.05 mol) was added slowly *N*-(trimethylsilyl)-perfluoroalkanesulfinamide (0.05 mol) by a syringe pump at room temperature. After addition, the mixture was stirred at room temperature for a few hours to the completion of reaction (monitored by  $^{19}\text{F}$  NMR). The resulting mixture was distilled under reduced pressure to give 5.

**3.4.1. *N*-Sulfinyl-2-chlorotetrafluoroethanesulfinamide (5a).** Oil. Bp 60 °C/15 Torr. FT-IR (film): 1236, 1168, 1122, 1075, 1015, 801  $\text{cm}^{-1}$ .  $^{19}\text{F}$  NMR (282 MHz,  $\text{CDCl}_3$ ):  $\delta$  -66.8 (m, 2F), -112.6, -116.5 (AB,  $J_{\text{AB}}=223.1$  Hz, 2F). EIMS ( $m/z$ , %): 245 ( $\text{M}^+$ , 2.04), 202 (37.62), 201 (8.47), 200 (100.00), 85 (11.30), 64 (93.32), 48 (23.14), 47 (12.46), 46 (33.93). Anal. Calcd for  $\text{C}_2\text{ClF}_4\text{NO}_2\text{S}_2$ : C, 9.78; N, 5.70. Found: C, 9.95; N, 5.90.

**3.4.2. *N*-Sulfinylnonafluorobutanesulfinamide (5b).** Oil. Bp 66–67 °C/15 Torr. FT-IR (film): 1353, 1236, 1212, 1141, 1109, 726, 696  $\text{cm}^{-1}$ .  $^{19}\text{F}$  NMR (282 MHz,  $\text{CDCl}_3$ ):  $\delta$  -81.2 (m, 3F), -114.1, -117.1 (AB,  $J_{\text{AB}}=291.5$  Hz, 2F), -121.4 (m, 2F), -126.6 (m, 2F). EIMS ( $m/z$ , %): 329 ( $\text{M}^+$ , 4.49), 284 (100.00), 282 (13.08), 131 (10.04), 69 (31.29), 64 (91.92), 48 (39.24), 47 (13.61), 46 (44.27). HRMS: calcd for  $\text{C}_4\text{F}_9\text{NO}_2\text{S}_2$ : 328.9227. Found: 328.9261.

### 3.5. General procedure for the reaction of *N*-sulfinylper(poly)fluoroalkanesulfinamides 5 and dienes

To a flame-dried flask were added *N*-sulfinylper(poly)fluoroalkanesulfinamide **5** (1 mmol), Lewis acid (1.2 mmol) and dry  $\text{CH}_2\text{Cl}_2$  (5 mL) at -78 °C under  $\text{N}_2$  atmosphere. After stirring for 30 min, diene (2 mmol) was added to the solution via a syringe and the mixture was stirred for 8 h. The reaction mixture was diluted with dichloromethane and washed with saturated aqueous  $\text{NaHCO}_3$  solution and saturated aqueous NaCl solution, dried over anhydrous  $\text{Na}_2\text{SO}_4$ . After the removal of solvent, the residue was purified by chromatography on silica gel using ethyl acetate/hexane (v/v: 1:8) as elute to give compound 7.

### 3.5.1. 4,5-Dimethyl-2-(2-chlorotetrafluoroethanesulfinyl)-3,6-dihydro-2H-[1,2]thiazine-1-oxide (7am).

*syn Isomer*. White solid, mp 72–73 °C. FT-IR (KBr): 1185, 1161, 1119, 1095, 1056, 883, 796 cm<sup>-1</sup>. <sup>1</sup>H NMR (300 MHz, CDCl<sub>3</sub>): δ 1.82 (s, 6H), 3.30, 3.75 (AB,  $J_{AB}$  = 15.9 Hz, 2H), 3.96, 4.09 (AB,  $J_{AB}$  = 15.6 Hz, 2H). <sup>19</sup>F NMR (282 MHz, CDCl<sub>3</sub>): δ -68.0 (m, 2F), -110.1, -117.9 (AB,  $J_{AB}$  = 228.0 Hz, 2F). EIMS ( $m/z$ , %): 328 (M<sup>+</sup> + 1, 0.16), 144 (91.12), 129 (52.85), 95 (61.46), 94 (58.44), 81 (72.41), 67 (100.00), 41 (92.50), 39 (56.36). Anal. Calcd for C<sub>8</sub>H<sub>10</sub>ClF<sub>4</sub>O<sub>2</sub>S<sub>2</sub>: C, 29.32; H, 3.08; N, 4.27. Found: C, 29.17; H, 3.35; N, 4.31.

*anti Isomer*. White solid, mp 61–62 °C. FT-IR (KBr): 2932, 1174, 1154, 1013, 796 cm<sup>-1</sup>. <sup>1</sup>H NMR (300 MHz, CDCl<sub>3</sub>): δ 1.83 (s, 6H), 3.27, 3.56 (AB,  $J_{AB}$  = 16.2 Hz, 2H), 3.76, 4.05 (AB,  $J_{AB}$  = 17.1 Hz, 2H). <sup>19</sup>F NMR (282 MHz, CDCl<sub>3</sub>): δ -67.8 (m, 2F), -111.7, -116.9 (AB,  $J_{AB}$  = 229.0 Hz, 2F). EIMS ( $m/z$ , %): 328 (M<sup>+</sup> + 1, 42.60), 192 (80.64), 144 (100.00), 129 (72.26), 95 (67.83), 94 (53.71), 81 (64.48), 67 (63.46), 41 (68.69). Anal. Calcd for C<sub>8</sub>H<sub>10</sub>ClF<sub>4</sub>O<sub>2</sub>S<sub>2</sub>: C, 29.32; H, 3.08; N, 4.27. Found: C, 29.46; H, 3.26; N, 4.25.

### 3.5.2. 4,5-Dimethyl-2-(nonafluorobutanesulfinyl)-3,6-dihydro-2H-[1,2]thiazine-1-oxide (7bm).

*syn Isomer*. White solid, mp 74–75 °C. IR (KBr): 1249, 1221, 1196, 1108, 997, 884 cm<sup>-1</sup>. <sup>1</sup>H NMR (300 MHz, CDCl<sub>3</sub>): δ 1.82 (s, 6H), 3.31, 3.78 (AB,  $J_{AB}$  = 16.2 Hz, 2H), 3.95, 4.11 (AB,  $J_{AB}$  = 14.9 Hz, 2H). <sup>19</sup>F NMR (282 MHz, CDCl<sub>3</sub>): δ -81.0 (m, 3F), -110.8, -119.2 (AB,  $J_{AB}$  = 238.8 Hz, 2F), -122.1 (m, 2F), -126.3 (m, 2F). EIMS ( $m/z$ , %): 412 (M<sup>+</sup> + 1, 0.20), 192 (55.40), 144 (100.00), 129 (47.89), 95 (53.78), 81 (59.71), 69 (58.95), 67 (73.08), 41 (63.63). Anal. Calcd for C<sub>10</sub>H<sub>10</sub>F<sub>9</sub>NO<sub>2</sub>S<sub>2</sub>: C, 29.20; H, 2.45; N, 3.41. Found: C, 29.34; H, 2.48; N, 3.34.

*anti Isomer*. White solid, mp 69–70 °C. IR (KBr): 1239, 1197, 1177, 1148 cm<sup>-1</sup>. <sup>1</sup>H NMR (300 MHz, CDCl<sub>3</sub>): δ 1.82–1.85 (m, 6H), 3.30, 3.57 (AB,  $J_{AB}$  = 16.2 Hz, 2H), 3.78, 4.06 (AB,  $J_{AB}$  = 17.4 Hz, 2H). <sup>19</sup>F NMR (282 MHz, CDCl<sub>3</sub>): δ -80.9 (t,  $J$  = 12.1 Hz, 3F), -112.1, -119.2 (AB,  $J_{AB}$  = 242.5 Hz, 2F), -122.4 (m, 2F), -126.3 (m, 2F). EIMS ( $m/z$ , %): 412 (M<sup>+</sup> + 1, 6.55), 129 (37.62), 95 (43.84), 94 (50.25), 81 (50.25), 69 (69.61), 53 (39.71), 41 (63.63). Anal. Calcd for C<sub>10</sub>H<sub>10</sub>F<sub>9</sub>NO<sub>2</sub>S<sub>2</sub>: C, 29.20; H, 2.45; N, 3.41. Found: C, 29.20; H, 2.50; N, 3.37. Crystallographic data (excluding structure factors) for the structures in this paper have been deposited with the Cambridge Crystallographic Data Centre as supplementary publication numbers CCDC 248677 and 248678. Copies of the data can be obtained, free of charge, on application to CCDC, 12 Union Road, Cambridge CB2 1EZ, UK [fax: +44(0) 1223 336033 or e-mail: deposit@ccdc.cam.ac.uk].

### 3.5.3. 5-Methyl-2-(2-chlorotetrafluoroethanesulfinyl)-3,6-dihydro-2H-[1,2]thiazine-1-oxide (7an).

FT-IR (KBr): 2979, 2316, 1169, 1142, 1112 cm<sup>-1</sup>. <sup>1</sup>H NMR (300 MHz, CDCl<sub>3</sub>): δ 1.88 (s, 3H), 3.25, 3.53 (AB,  $J_{AB}$  = 15.9 Hz, 2H), 3.96, 4.12 (AB,  $J_{AB}$  = 17.1 Hz, 2H), 5.79–5.81 (m, 1H) (*anti*); 1.86 (s, 3H), 3.28, 3.68 (AB,  $J_{AB}$  = 16.2 Hz, 2H), 4.03, 4.27 (AB,  $J_{AB}$  = 16.5 Hz, 2H), 5.76–5.77 (m, 1H) (*syn*). <sup>19</sup>F NMR (282 MHz, CDCl<sub>3</sub>): δ -67.9

(m, 2F), -111.8, -117.0 (AB,  $J_{AB}$  = 228.4 Hz, 2F) (*anti*); -67.8 (m, 2F), -109.8, -117.5 (AB,  $J_{AB}$  = 222.8 Hz, 2F) (*syn*). EIMS ( $m/z$ , %): 361 (47.58), 360 (14.22), 359 (100.00), 289 (7.76), 237 (15.70), 209 (9.09), 176 (6.46), 135 (9.73). Anal. Calcd for C<sub>7</sub>H<sub>8</sub>ClF<sub>4</sub>NO<sub>2</sub>S<sub>2</sub>: C, 26.80; H, 2.57; N, 4.46. Found: C, 26.52; H, 2.49; N, 4.57.

### 3.5.4. 5-Methyl-2-nonafluorobutanesulfinyl-3,6-dihydro-2H-[1,2]thiazine-1-oxide (7bn).

*syn Isomer*. White solid, mp 70–71 °C. IR (KBr): 1352, 1237, 1202, 1181 cm<sup>-1</sup>. <sup>1</sup>H NMR (300 MHz, CDCl<sub>3</sub>): δ 1.88 (s, 3H), 3.32, 3.72 (AB,  $J_{AB}$  = 16.5 Hz, 2H), 4.06, 4.31 (AB,  $J_{AB}$  = 16.5 Hz, 2H), 5.78–5.79 (m, 1H). <sup>19</sup>F NMR (282 MHz, CDCl<sub>3</sub>): δ -81.0 (t,  $J$  = 12.4 Hz, 3F), -110.8, -119.1 (AB,  $J_{AB}$  = 238.3 Hz, 2F), -122.1 (m, 2F), -126.3 (m, 2F). EIMS ( $m/z$ , %): 398 (M<sup>+</sup> + 1, 0.70), 178 (100.00), 130 (36.47), 115 (36.47), 82 (38.20), 81 (56.63), 80 (39.97), 67 (45.27), 53 (40.51). Anal. Calcd for C<sub>9</sub>H<sub>8</sub>F<sub>9</sub>NO<sub>2</sub>S<sub>2</sub>: C, 27.21; H, 2.03; N, 3.53. Found: C, 27.16; H, 2.19; N, 3.47.

*anti Isomer*. White solid, mp 63–64 °C. IR (KBr): 2980, 1358, 1263, 1241 cm<sup>-1</sup>. <sup>1</sup>H NMR (300 MHz, CDCl<sub>3</sub>): δ 1.90 (s, 3H), 3.28, 3.54 (AB,  $J_{AB}$  = 16.5 Hz, 2H), 3.98, 4.14 (AB,  $J_{AB}$  = 18.3 Hz, 2H), 5.81–5.82 (m, 1H). <sup>19</sup>F NMR (282 MHz, CDCl<sub>3</sub>): δ -81.0 (t,  $J$  = 9.3 Hz, 3F), -112.3, -119.3 (AB,  $J_{AB}$  = 239.7 Hz, 2F), -122.4 (m, 2F), -126.4 (m, 2F). EIMS ( $m/z$ , %): 398 (M<sup>+</sup> + 1, 0.32), 178 (100.00), 115 (42.25), 81 (14.52), 69 (56.52), 68 (68.58), 67 (86.68), 53 (49.56), 41 (55.38). Anal. Calcd for C<sub>9</sub>H<sub>8</sub>F<sub>9</sub>NO<sub>2</sub>S<sub>2</sub>: C, 27.21; H, 2.03; N, 3.53. Found: C, 27.16; H, 2.26; N, 3.47.

### 3.5.5. 5-(4-Methylpent-3-enyl)-2-(2-chlorotetrafluoroethanesulfinyl)-3,6-dihydro-2H-[1,2]thiazine-1-oxide (7al).

FT-IR (KBr): 1162, 1120, 1014, 793 cm<sup>-1</sup>. <sup>1</sup>H NMR (300 MHz, CDCl<sub>3</sub>): δ 1.62 (s, 3H), 1.70 (s, 3H), 2.12–2.16 (m, 4H), 3.27–3.73 (m, 2H), 3.96–4.36 (m, 2H), 5.07–5.08 (m, 1H), 5.77–5.81 (m, 1H). <sup>19</sup>F NMR (282 MHz, CDCl<sub>3</sub>): δ -67.9 (m, 2F), -111.8, -116.6 (AB,  $J_{AB}$  = 229.3 Hz, 2F) (*anti*); -67.8 (m, 2F), -111.0, -117.6 (AB,  $J_{AB}$  = 222.8 Hz, 2F) (*syn*). EIMS ( $m/z$ , %): 183 (32.40), 169 (27.93), 134 (30.80), 133 (31.11), 107 (33.41), 105 (26.35), 80 (28.02), 67 (26.17). Anal. Calcd for C<sub>12</sub>H<sub>16</sub>ClF<sub>4</sub>NO<sub>2</sub>S<sub>2</sub>: C, 37.75; H, 4.22; N, 3.67. Found: C, 37.73; H, 4.13; N, 3.71.

### 3.5.6. 5-(4-Methylpent-3-enyl)-2-nonafluorobutanesulfinyl-3,6-dihydro-2H-[1,2]thiazine-1-oxide (7bl).

FT-IR (KBr): 1352, 1236, 1214, 1179, 1139, 1109, 1092 cm<sup>-1</sup>. <sup>1</sup>H NMR (300 MHz, CDCl<sub>3</sub>): δ 1.61 (s, 3H), 1.70 (s, 3H), 2.00–2.17 (m, 4H), 3.29–3.56 (m, 2H), 3.97–4.19 (m, 2H), 5.07–5.12 (m, 1H), 5.80–5.81 (m, 1H). <sup>19</sup>F NMR (282 MHz, CDCl<sub>3</sub>): δ -80.9 (m, 3F), -111.2, -119.0 (AB,  $J_{AB}$  = 252.1 Hz, 1.7F, *anti isomer*), -110.8, -119.0 (AB,  $J_{AB}$  = 237.7 Hz, 0.3F, *syn isomer*), -122.1 (m, 2F), -126.3 (m, 2F). EIMS ( $m/z$ , %): 246 (53.79), 183 (26.28), 135 (28.17), 121 (37.53), 93 (50.94), 91 (27.37), 69 (100.00), 41 (97.84). Anal. Calcd for C<sub>14</sub>H<sub>16</sub>F<sub>9</sub>NO<sub>2</sub>S<sub>2</sub>: C, 36.13; H, 3.47; N, 3.01. Found: C, 36.27; H, 3.47; N, 2.98.

## Acknowledgements

We thank the National Natural Science Foundation of China for financial support (No. 20172065).

**References and notes**

1. (a) Sloop, J. C.; Bumgardner, C. L.; Leohle, W. D. *J. Fluorine Chem.* **2002**, *118*, 135–147. (b) Zhu, S. Z.; Wang, Y. L.; Peng, W. M.; Song, L. P. *Curr. Org. Chem.* **2002**, *6*, 1057–1096.
2. (a) Amii, H.; Kobayashi, T.; Terasawa, H.; Uneyama, K. *Org. Lett.* **2001**, *3*, 3103–3105. (b) Zimmer, R.; Reissig, H. U. *J. Org. Chem.* **1992**, *57*, 339–347.
3. Garipipati, R. S.; Freyer, A. J.; Whittle, R. R.; Weinreb, S. M. *J. Am. Chem. Soc.* **1984**, *106*, 7861–7867.
4. Bayer, A.; Hansen, L. K.; Gautun, O. R. *Tetrahedron: Asymmetry* **2002**, *13*, 2407–2415.
5. Zhu, S. Z.; Liu, X. Y.; Wang, S. W. *Tetrahedron* **2003**, *59*, 9669–9676.
6. Roesky, H. W.; Holtschneider, G. *J. Fluorine Chem.* **1976**, *7*, 77–84.
7. Hu, L. Q.; Huang, W. Y. *Youji Huaxue (Chin. J. Org. Chem.)* **1991**, *11*, 126–132.
8. Hanson, P.; Stockburn, W. A. *J. Chem. Soc., Perkin Trans. 2* **1985**, 589–595.
9. (a) Caminati, W.; Mirri, A.; Maccagnani, G. *J. Mol. Struct.* **1977**, *36*, 368–374. (b) Meij, R.; Oskam, A.; Stufkens, D. *J. Mol. Struct.* **1979**, *51*, 37–49.
10. García Ruano, J. L.; Alemparte, C.; Martín Castro, A. M.; Adams, H.; Rodríguez Ramos, J. H. *J. Org. Chem.* **2000**, *65*, 7938–7943.
11. Serramedan, D.; Delmond, B.; Deleris, G. *Tetrahedron Lett.* **1990**, *31*, 7007–7010.
12. Roesky, H. W.; Tutkunkardes, S. *Chem. Ber.* **1974**, *107*, 508–517.

# Effective reductive amination of carbonyl compounds with hydrogen catalyzed by iridium complex in organic solvent and in ionic liquid

Daisuke Imao, Shoichiro Fujihara, Takeshi Yamamoto, Tetsuo Ohta\* and Yoshihiko Ito

Department of Molecular Science and Technology, Faculty of Engineering, Doshisha University, Kyotanabe, Kyoto 610-0394, Japan

Received 30 November 2004; revised 11 May 2005; accepted 11 May 2005

Available online 6 June 2005

**Abstract**—The direct reductive amination (DRA) of carbonyl compounds with amines has been achieved using homogenous iridium catalyst and gaseous hydrogen. It appeared that the cationic iridium catalyst,  $[\text{Ir}(\text{cod})_2]\text{BF}_4$ , without any other ligands was sufficient for the reaction. For the DRA of the ketone substrates, an ionic liquid,  $[\text{Bmim}]\text{BF}_4$ , was found to be superior to the other organic solvent used. Especially, the counter anion of the ionic liquid has a significant influence on the selectivity, and at the same time, a high reaction temperature was found to be crucial for the excellent selectivity.

© 2005 Elsevier Ltd. All rights reserved.

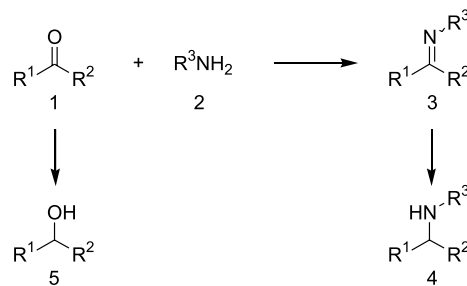
## 1. Introduction

The reductive amination of carbonyl compounds is attractive in organic synthesis because ketones and aldehydes can be transformed, in one vessel, directly to the corresponding secondary or primary alkylamines without isolation of the intermediary imines or hydroxy amines.<sup>1</sup> Sodium cyanoborohydride has been used to carry out this reaction, but the reagent needs to be stoichiometrically used.<sup>2</sup> To utilize gaseous hydrogen as a reducing reagent, palladium carbon (Pd/C) is usually used, but a heterogeneous catalyst is difficult to modify in order to control its reactivity.<sup>3</sup> Many enantioselective reductions of an isolated imine with a homogeneous catalyst have been reported. Those catalysts are effective though the imine is very sensitive to hydrolysis that sometimes the difficulty of completing the condensation to obtain the imine has been considered as a big problem for reduction.<sup>4</sup> To overcome this problem, some groups have recently proposed some ideas to realize the direct reductive amination with a homogeneous iridium catalyst and gaseous hydrogen.<sup>5</sup> Zhang et al. achieved the reaction by means of adding  $\text{Ti}(\text{O}^i\text{Pr})_4$  and  $\text{I}_2$  to the reaction system to promote the condensation reaction and almost quantitatively produced a secondary amine.<sup>6</sup> Chaloner et al. have also proclaimed that the cationic iridium–phosphine system is effective for

reductive amination.<sup>7</sup> However, this system requires the addition of a catalytic amount of acid and phosphine ligand, and complete deoxygenation of the reaction solution in order to prevent oxidation of the phosphine ligand. In this paper, we introduced another possibility for the highly selective direct reductive amination of carbonyl compounds with gaseous hydrogen catalyzed by an iridium complex without any additives or any acid and even without any effort to complete the deoxygenation.

## 2. Results and discussion

First of all, we examined several hydrogenation catalysts for the direct reductive amination (DRA). To achieve an efficient catalytic DRA method, we paid close attention not only to its reactivity but also to its selectivity, because, under the DRA reaction condition, ketone **1** can also be

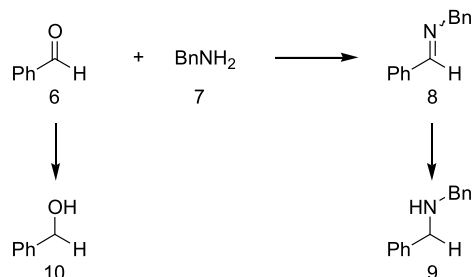


Scheme 1.

**Keywords:** Direct reductive amination; Iridium; Ionic liquid; Secondary amine.

\* Corresponding author. Tel.: +81 774 65 6548; fax: +81 774 65 6789; e-mail: tota@mail.doshisha.ac.jp



**Table 1.** DRA of benzaldehyde (**6**) with benzylamine (**7**)<sup>a</sup>

Entry	Cat. <sup>b</sup>	Time (h)	Yield of <b>8</b> (%) <sup>c</sup>	Yield of <b>9</b> (%) <sup>c</sup>	Yield of <b>10</b> (%) <sup>c</sup>
1	A	0.5	51	45	4
2	A	3	0	93	7
3	B	0.5	68	31	1
4	B	3	0	94	6

<sup>a</sup> H<sub>2</sub> pressure (50 kg/m<sup>2</sup>) and EtOH as solvent were used at room temperature.

<sup>b</sup> A, [IrCl(cod)]<sub>2</sub>; B, [Ir(cod)<sub>2</sub>]BF<sub>4</sub>.

<sup>c</sup> Yields were determined by <sup>1</sup>H NMR.

reduced to an alcohol **5**, which is recognized as a by-product (Scheme 1). Using ruthenium and rhodium complexes, the alcohol **5** was produced as the main product, while the iridium complexes showed reverse and desirable selectivities. Representative results obtained from the reaction of benzaldehyde (**6**) with benzylamine (**7**) using [IrCl(cod)]<sub>2</sub> (A) and [Ir(cod)<sub>2</sub>]BF<sub>4</sub> (B) are listed in Table 1. The DRA was performed using 2 mol% of a catalyst (based on iridium atom) in EtOH at rt under a H<sub>2</sub> atmosphere (50 kg/cm<sup>3</sup>) without any purging procedure. Both catalysts did work with no problem, but [Ir(cod)<sub>2</sub>]BF<sub>4</sub> showed a slightly lower catalytic activity, but seemed more effective in terms of the DRA selectivity.

The solvent effect is summarized in Table 2. To observe their differences in detail, the reactions were quenched in 0.5 h. These results indicated no crucial difference except the one with CH<sub>2</sub>Cl<sub>2</sub>. As CH<sub>2</sub>Cl<sub>2</sub> seems not to have significant effect for the deteriorating formation of an imine, CH<sub>2</sub>Cl<sub>2</sub> may have some influence on the catalytic cycle, but the mechanism is still unclear.

Now that the optimized condition has been determined, other aldehydes were employed for this reaction to create a variety of secondary amines (Table 3). All these results showed good to excellent yields and selectivities in 3 h. Aniline was also a good amine substrate instead of benzylamine (entry 2 and 4), and there seemed to be no difference in reactivity. When propanal was used with benzylamine or aniline (entries 3 and 4), the reaction was

complete even within 0.5 h with excellent selectivity. In contrast, the reaction with the 1- and 2-naphthaldehydes produced considerable amounts of alcohols. On the other hand, no difference was observed in terms of the position of the substituent attached to the phenyl ring of the substrate.

Now that an effective DRA with aldehydes was achieved, the reaction with ketones should be next investigated. Acetophenone (**14**) was chosen as the ketone, and the reaction became sluggish. In order to obtain a high conversion and/or yield, heating and prolonging the reaction time were necessary. Again, the solvent effect was studied (Table 4). As shown in the Table, a higher temperature gave a better conversion, but the selectivity was not different. [IrCl(cod)]<sub>2</sub> was tested instead of [Ir(cod)<sub>2</sub>]BF<sub>4</sub> in toluene (entry 5), and the result showed a clearer difference in selectivity.

Various ketones were subjected to this RDA reaction (Table 5). The results appeared to be good to excellent yields and selectivities with some exceptions. First, in contrast to the reductive amination of aldehydes, the reaction with aniline gave low alcohol yields and no secondary amines (entries 2 and 5), in which considerable amount of unidentifiable by-products were formed. This may be caused by the lower nucleophilicity of aniline compared to benzylamine. No distinguishable effect was observed with the difference in the substituent position attached to the aromatic ring of the substrate ketone. Interestingly, 2-acetonaphthone gave the worst selectivity,

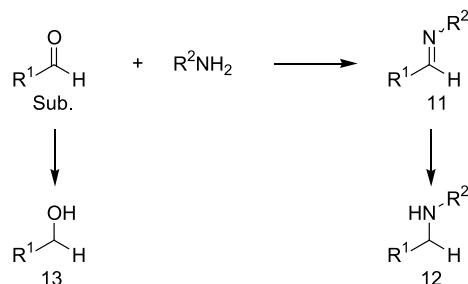
**Table 2.** Solvent effect on DRA of **6** with **7**<sup>a</sup>

Entry	Solvent	Conv. of <b>6</b> (%) <sup>b</sup>	Yield of <b>8</b> (%) <sup>b</sup>	Yield of <b>9</b> (%) <sup>b</sup>	Yield of <b>10</b> (%) <sup>b</sup>
1	MeOH	100	58	40	2
2	EtOH	100	51	45	4
3	Benzene	100	46	50	4
4	Toluene	100	47	48	5
5	CH <sub>2</sub> Cl <sub>2</sub>	93	79	13	1
6	CH <sub>3</sub> CN	100	46	40	4

<sup>a</sup> H<sub>2</sub> pressure (50 kg/m<sup>2</sup>) and [Ir(cod)<sub>2</sub>]BF<sub>4</sub> as catalyst were used at room temperature, 0.5 h.

<sup>b</sup> Yields were determined by <sup>1</sup>H NMR using internal standard (bibenzyl) method.



**Table 3.** DRA for a range of aldehydes with amines<sup>a</sup>

Entry	Sub.		Conv. (%)	Yield of product (%) <sup>b</sup>		
	R <sup>1</sup>	R <sup>2</sup>		<b>11</b>	<b>12</b>	<b>13</b>
1	Ph	Bn	100	0	94	6
2	Ph	Ph	100	0	91	9
3	Et <sup>c</sup>	Bn	100	0	>99	0
4	Et <sup>c</sup>	Ph	100	0	>99	0
5	1-Naph	Bn	100	0	83	17
6	2-Naph	Bn	100	0	85	15
7	<i>o</i> -MeOPh	Bn	100	0	94	6
8	<i>m</i> -MeOPh	Bn	100	2	90	8
9	<i>p</i> -MeOPh	Bn	100	0	92	8
10	<i>p</i> -ClPh	Bn	94	11	79	4

<sup>a</sup> H<sub>2</sub> pressure (50 kg/m<sup>2</sup>) and [Ir(cod)<sub>2</sub>]BF<sub>4</sub> as catalyst and benzene as solvent were used at room temperature, 3 h.

<sup>b</sup> Yields were determined by <sup>1</sup>H NMR using internal standard (bibenzyl) method.

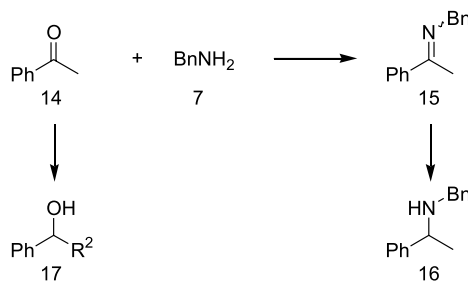
<sup>c</sup> Reaction was completed in 0.5 h.

while 1-acetonaphthone was converted to the secondary amine with a similar selectivity for the reaction of the acetophenone derivatives.

The DRA of an aldehyde with an amine proceeded with a good selectivity better than 10 in the ratio of secondary amine **12**/by-product alcohol **13**, except for 1- and 2-naphthalenecarbaldehyde, while that of ketone with the amine was less than 10 in the ratio of **19/20**. For achieving better selectivity, an ionic liquid was investigated for this DRA of ketones with amine. The ionic liquid has recently been used as a solvent for many catalyses and has shed light on not only due to its environmentally friendly

characteristics<sup>8</sup> but for its unique effect on catalytic cycles.<sup>9,10</sup> The reaction of acetophenone with benzylamine was carried out in commonly used several kind of ILs (Fig. 1, Table 6).

In the ionic liquid, [Bmim]Cl or [Emim]Cl, in which the chloride is a counter anion (entry 1 and 2), the reaction selectivity was significantly affected and was worse than the one in toluene. In contrast to these results, the selectivity in IL, [Bmim]BF<sub>4</sub>, in which BF<sub>4</sub><sup>-</sup> is the counter anion, was the best of all results obtained from the DRA of ketones in this study. The reaction with [IrCl(cod)]<sub>2</sub> instead of [Ir(cod)<sub>2</sub>]BF<sub>4</sub> in [Bmim]BF<sub>4</sub> was carried out and gave a

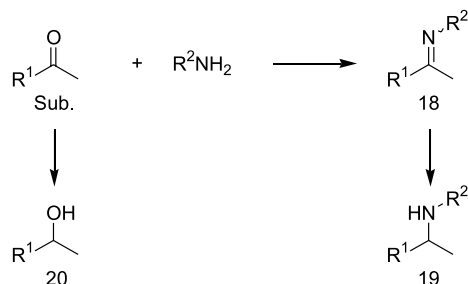
**Table 4.** Solvent effect on DRA of acetophenone (**14**) with benzylamine (**7**)<sup>a</sup>

Entry	Solvent	Temp. (°C)	Conv. of <b>14</b> (%) <sup>b</sup>	Yield of <b>15</b> (%) <sup>b</sup>	Yield of <b>16</b> (%) <sup>b</sup>	Yield of <b>17</b> (%) <sup>b</sup>
1	MeOH	60	97	3	84	10
2	EtOH	70	100	0	88	12
3	Benzene	70	100	0	87	13
4	Toluene	100	100	0	89	11
5 <sup>c</sup>	Toluene	100	100	0	78	22
6	CH <sub>2</sub> Cl <sub>2</sub>	rt	60	48	8	4
7	CH <sub>3</sub> CN	70	100	0	88	12

<sup>a</sup> H<sub>2</sub> pressure (50 kg/m<sup>2</sup>) and [Ir(cod)<sub>2</sub>]BF<sub>4</sub> as catalyst were used for 24 h.

<sup>b</sup> Yields were determined by <sup>1</sup>H NMR using internal standard (bibenzyl) method.

<sup>c</sup> [IrCl(cod)]<sub>2</sub> was used instead of [Ir(cod)<sub>2</sub>]BF<sub>4</sub>.

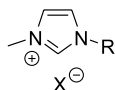
**Table 5.** DRA of a range of ketones with amines<sup>a</sup>

Entry	Sub.		Conv. (%)	Yield of product (%) <sup>b</sup>		
	R <sup>1</sup>	R <sup>2</sup>		18	19	20
1	Ph	Bn	100	0	89	11
2	Ph	Ph	100	29	0	15
3	Ph <sup>c</sup>	Bn	100	0	86	14
4	Et	Bn	100	0	91	2
5	Et	Ph	100	0	0	12
6	1-Naph	Bn	100	0	87	13
7	2-Naph	Bn	100	0	59	41
8	<i>o</i> -MeOPh	Bn	100	0	89	11
9	<i>m</i> -MeOPh	Bn	100	2	91	9
10	<i>p</i> -MeOPh	Bn	100	0	92	8
11	<i>p</i> -ClPh	Bn	100	0	89	11

<sup>a</sup> H<sub>2</sub> pressure (50 kg/m<sup>2</sup>) and [Ir(cod)<sub>2</sub>]BF<sub>4</sub> as catalyst and toluene as solvent were adopted at 100 °C, 24 h.

<sup>b</sup> Yields were determined by <sup>1</sup>H NMR using internal standard (bibenzyl) method.

<sup>c</sup> Propiophenone was used.



[Bmim]BF<sub>4</sub> : R = *n*-Bu, X = BF<sub>4</sub><sup>-</sup>

[Bmim]Cl : R = *n*-Bu, X = Cl<sup>-</sup>

[Emim]Cl : R = Et, X = Cl<sup>-</sup>

**Figure 1.** Ionic liquid used in this study.

selectivity comparable to that of [Ir(cod)<sub>2</sub>]BF<sub>4</sub>. In toluene, [IrCl(cod)]<sub>2</sub> was less effective than [Ir(cod)<sub>2</sub>]BF<sub>4</sub> (Table 4, entry 5) in selectivity. This would be attributed to the effect of the anion exchange on the rhodium catalyst with Cl<sup>-</sup> and BF<sub>4</sub><sup>-</sup>, and the cationic iridium catalyst was assumed to be generated in situ.

The combination of [Bmim]BF<sub>4</sub> as the solvent and [Ir(cod)<sub>2</sub>]BF<sub>4</sub> as the catalyst gave the best selectivity for the DRA of ketone. The effect of temperature and hydrogen pressure on the DRA were investigated for determining milder reaction conditions (Table 7).

Surprisingly, the higher temperature gave not only a better yield, but also a better selectivity. The ratio (product 16/

alcohol 17) increased 54 times from 20 to 100 °C. The reaction selectivity also became better as the H<sub>2</sub> pressure increased (16/17: 7 times increased from 1 to 40 kg/cm<sup>2</sup>). These phenomena have not yet been explained, but a high temperature (100 °C) and a high H<sub>2</sub> pressure (40 kg/cm<sup>2</sup>) were the choices for obtaining an excellent selectivity.

### 3. Conclusion

In summary, we have found that [Ir(cod)<sub>2</sub>]BF<sub>4</sub> is sufficiently effective for the direct reductive amination of carbonyl compounds with amines without any deoxygenation procedure. Yields up to 99% with an aldehyde, and up to 92% with a ketone were obtained in benzene and toluene, respectively. In [Bmim]BF<sub>4</sub>, acetophenone was effectively converted to the corresponding secondary amine in up to 97% yield with excellent selectivity. To the best of our knowledge, this would be the first example of the direct reductive amination with a homogeneous catalyst was carried out in an ionic liquid. It appeared that the reaction conditions, especially temperature, played a critical role in exclusively obtaining secondary amines.

**Table 6.** Ionic liquid effect on DRA<sup>a</sup>

Entry	Solvent	Cat. <sup>b</sup>	Conv. of 14 (%) <sup>c</sup>	Yield of 15 (%) <sup>c</sup>	Yield of 16 (%) <sup>c</sup>	Yield of 17 (%) <sup>c</sup>
1	[Bmim]Cl	B	93	8	57	28
2	[Emim]Cl	B	92	0	69	17
3	[Bmim]BF <sub>4</sub>	B	98	0	97	1
4	[Bmim]BF <sub>4</sub>	A	98	2	95	1

<sup>a</sup> H<sub>2</sub> pressure (40 kg/m<sup>2</sup>) was adopted at 100 °C, 24 h.

<sup>b</sup> A, [IrCl(cod)]<sub>2</sub>; B, [Ir(cod)<sub>2</sub>]BF<sub>4</sub>.

<sup>c</sup> Yields were determined by <sup>1</sup>H NMR using internal standard (bibenzyl) method.

**Table 7.** Temperature and pressure effect on DRA in [Bmim]BF<sub>4</sub><sup>a</sup>

Entry	Temp.	p(H <sub>2</sub> ) (kg/cm <sup>2</sup> )	Conv. of <b>14</b> (%) <sup>b</sup>	Yield of <b>15</b> (%) <sup>b</sup>	Yield of <b>16</b> (%) <sup>b</sup>	Yield of <b>17</b> (%) <sup>b</sup>	Ratio of <b>16/17</b>
1	20	40	56	39	11	6	1.8
2	50	40	77	11	54	11	4.9
3	80	40	99	0	86	13	6.6
4	100	40	98	0	97	1	97
5	100	1	65	22	40	3	13
6	100	5	88	8	75	5	15
7	100	10	91	6	82	3	27
8	100	20	93	1	88	4	22
9	100	30	97	—	95	2	48

<sup>a</sup> [Ir(cod)<sub>2</sub>]BF<sub>4</sub> as catalyst was adopted for 24 h.

<sup>b</sup> Yields were determined by <sup>1</sup>H NMR using internal standard (bibenzyl) method.

#### 4. Experimental

The <sup>1</sup>H NMR spectra were measured using a Varian MERCURYplus300-4N (300 MHz) spectrometer with tetramethylsilane as the internal standard. The solvents were purified by conventional methods and stored under an argon atmosphere. [IrCl(cod)]<sub>2</sub><sup>11</sup> and [Ir(cod)]BF<sub>4</sub><sup>12</sup> were prepared according to the literature. All other materials were purchased and used without further purification. The reaction products were identified by <sup>1</sup>H NMR analysis and compared to authentic commercial products.

##### 4.1. General procedure for direct reductive amination

The catalyst (2.0 × 10<sup>-2</sup> mmol), carbonyl compound (1.0 mmol), amine (1.0 mmol), solvent (0.2 mL) and a magnetic stir bar were added to a stainless steel autoclave under hydrogen atmosphere at the pressure and temperature cited in each table. After the reaction, bibenzyl as an internal standard was added, and the mixture was directly analyzed by <sup>1</sup>H NMR. For isolation of the secondary amine, the reaction mixture was poured into a mixture of ether and 2 N HCl aq. The water layer was washed with ether several times, and became basic with 2 N NaOH aq. Addition. The ether extract of the water layer was concentrated and then isolated by column chromatography (Alumina). When an ionic liquid was used as the solvent, the reaction mixture was extracted with hexane until no organic materials were detected in hexane layer. The hexane layer was concentrated, and then the similar procedure described above was performed.

#### Acknowledgements

This work was partially supported by a grant to RCAST at Doshisha University from the Ministry of Education, Japan.

#### References and notes

- (a) Trost, B. M.; Verhoeven, T. R. In Wilkinson, G., Stone, F. G. A., Abel, E. W., Eds.; *Comprehensive Organometallic Chemistry*; Pergamon: Oxford, 1982; Vol. 8, p 84. (b) March, J.; *Advanced Organic Chemistry*; Wiley: New York, 1992; pp 889–890. (c) Hutchins, R. O.; Hutchins, M. K. In Trost, B. M., Fleming, I., Eds.; *Comprehensive Organic Synthesis*; Pergamon: Oxford, 1991; Vol. 8; p 25.
- (a) Lane, C. F. *Synthesis* **1975**, 135. (b) Borch, R. F.; Bernstein, M. D.; Durst, H. D. *J. Am. Chem. Soc.* **1971**, *93*, 2897.
- Heinen, A. W.; Peters, J. A.; van Bekkum, H. *Eur. J. Org. Chem.* **2000**, 2501.
- Blaser, H.-U.; Spindler, F. In Jacobsen, E. N., Pfaltz, A., Yamamoto, H., Eds.; *Comprehensive Asymmetric Catalysis*; Springer: Berlin, 1999; Vol. 1, pp 247–265.
- (a) Tararov, V. I.; Kadyrov, R.; Riermeier, T. H.; Dingerdisen, U.; Börner, A. *Org. Prep. Proc. Int.* **2004**, *36*, 99. (b) Tararov, V. I.; Kadyrov, R.; Riermeier, T. H.; Börner, A. *Adv. Synth. Catal.* **2002**, *344*, 200. (c) Gross, T.; Seayad, A. M.; Ahmad, M.; Beller, M. *Org. Lett.* **2002**, *4*, 2055.
- Chi, Y. W.; Zhou, Y.-G.; Zhang, X. *J. Org. Chem.* **2003**, *68*, 4120.
- Chaloner, P. A.; Collard, S.; Ellis, R. D.; Keep, A. K. EP 1078915 A1, 2001.
- Wasserscheid, P.; Keim, W. *Angew. Chem., Int. Ed.* **2000**, *39*, 3772.
- Dupont, J.; de Souza, R. F.; Suarez, P. A. Z. *Chem. Rev.* **2002**, *102*, 3667.
- Welton, T. *Chem. Rev.* **1999**, *99*, 2071.
- Herde, J. L.; Lambert, J. C.; Senoff, C. V. *Inorg. Synth.* **1974**, *15*, 18.
- Shenck, T. G.; Downs, J. M.; Milne, C. R. C.; Mackenzie, P. B.; Boucher, H.; Whealan, J.; Bosnich, B. *Inorg. Synth.* **1985**, *24*, 2334.

# Studies on the stereochemistry of 1,2,6-trimethyl-4-piperidone

Florian Diwischek,<sup>a</sup> Mario Arnone,<sup>b</sup> Bernd Engels<sup>b,\*</sup> and Ulrike Holzgrabe<sup>a,\*</sup>

<sup>a</sup>Institut für Pharmazie und Lebensmittelchemie, Universität Würzburg, Am Hubland, 97074 Würzburg, Germany

<sup>b</sup>Institut für Organische Chemie, Universität Würzburg, Am Hubland, 97074 Würzburg, Germany

Received 7 February 2005; revised 10 May 2005; accepted 10 May 2005

Available online 4 June 2005

**Abstract**—In the effort to create new derivatives of analgesically active spiro-piperidines intermediate 1,2,6-trimethyl-4-piperidone was synthesized. The substitution of the skeleton gives rise to configurational as well as conformational isomerism. Despite the symmetry of 1,2,6-trimethyl-4-piperidone two different sets of signals were present in the <sup>1</sup>H and <sup>13</sup>C NMR spectra. They were supposed to arise from a *cis/trans* mixture of 1,2,6-trimethyl-4-piperidone. In contrast to this explanation only two signals of the methyl groups and hydrogens at carbon atoms 2 and 6 were observed in the <sup>1</sup>H and <sup>13</sup>C NMR spectra, normally expecting one for the *cis*- and two for the *trans*-isomer. To solve this discrepancy, the kind of isomeric mixture of 1,2,6-trimethyl-4-piperidone leading to the <sup>1</sup>H and <sup>13</sup>C NMR spectra was examined. Energy differences between chair conformations of both the *cis*- and the *trans*-isomer of 1,2,6-trimethyl-4-piperidone and the potential energy surface of the equilibration process of the *trans*-isomer of 1,2,6-trimethyl-4-piperidone between its chair conformers were determined by quantum chemical calculations. The barrier height of the equilibration process was measured by high and low temperature NMR measurements to confirm the theoretical outcome. The results of all investigations agree nicely and proved a *cis/trans*-mixture of 1,2,6-trimethyl-4-piperidone being present at room temperature.

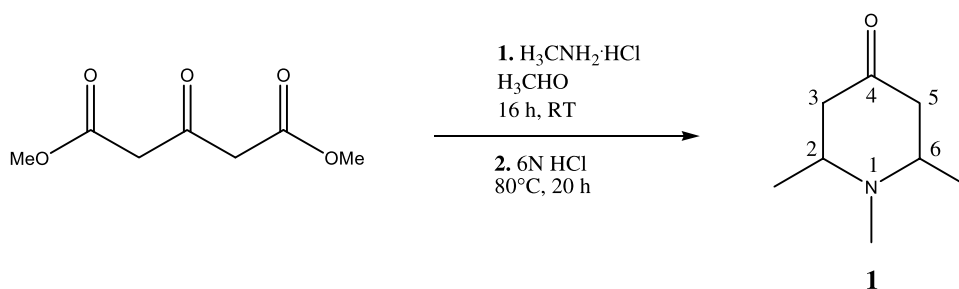
© 2005 Elsevier Ltd. All rights reserved.

## 1. Introduction

The high pharmacological concern about 4-piperidones is due to their important role as intermediates in the synthesis of many drugs, especially opioid analgesics. Not only preparation of reversed esters of pethidine is done via piperidones<sup>1</sup> but also of drugs possessing high affinity for the ORL1-receptor,<sup>2</sup> discovered in 1994.<sup>3</sup> The pharmacological effect of potential drugs depends sensitively on the stereochemistry and ring conformation especially in the case of 2,6-disubstituted 4-piperidones.<sup>4</sup> Therefore, elucidation of the stereochemistry of these piperidones is of great

interest. In the effort to create new derivatives of new analgetically active spiro-piperidines<sup>5</sup> the synthetic pathway via 1,2,6-trimethyl-4-piperidone (**1**) was chosen. This piperidone was achieved by a Mannich procedure starting from dimethyl oxoglutarate, acetaldehyde and methylamine followed by a decarboxylation to give **1** (Fig. 1).<sup>6</sup>

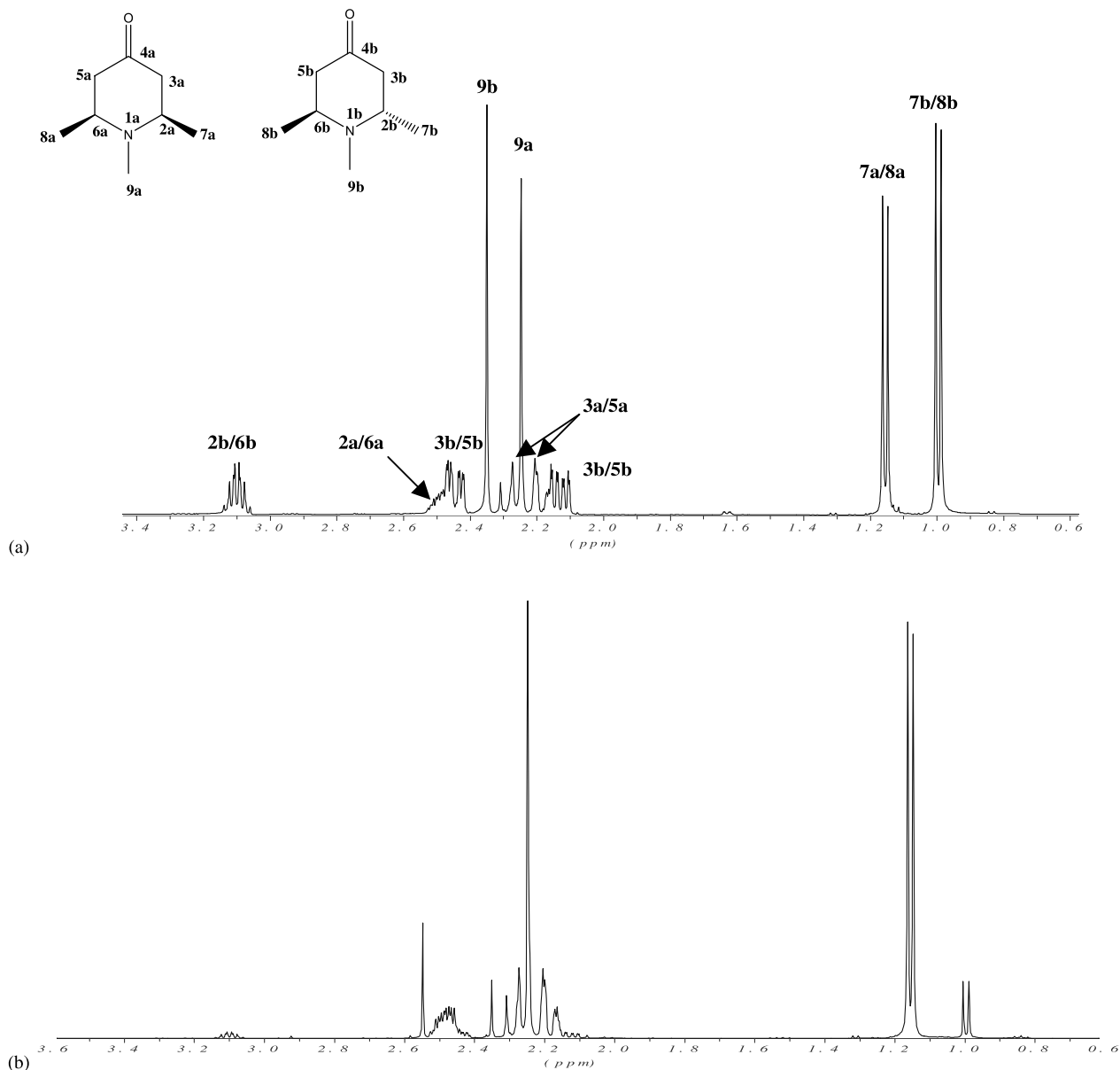
Due to the symmetry of **1** half a set of signals should be expected in <sup>1</sup>H and <sup>13</sup>C NMR spectra. Despite of this symmetry two different sets of signals, which may occur in a slightly different ratio from sample to sample, are present. This was explored previously and supposed to result from a



**Figure 1.** Synthesis of 1,2,6-trimethyl-4-piperidone.

**Keywords:** Piperidones; Stereochemistry of piperidones; Energy pathway.

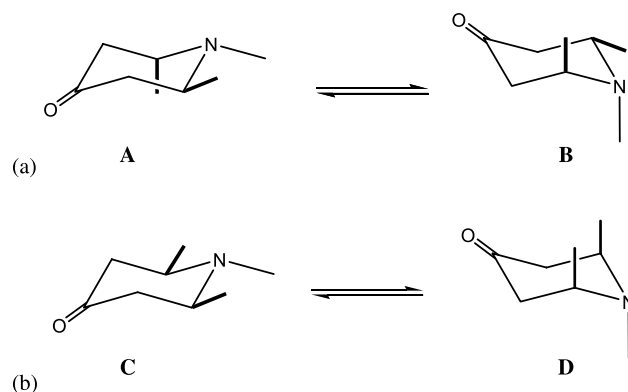
\* Corresponding authors. Tel.: +49 931 8885394; fax: +49 931 8884606 (B.E.); tel.: +49 931 8885460; fax: +49 931 8885494 (U.H.); e-mail addresses: bernd@chemie.uni-wuerzburg.de; u.holzgrabe@pharmazie.uni-wuerzburg.de



**Figure 2.** (a) <sup>1</sup>H NMR spectrum of 1,2,6-trimethyl-4-piperidone (**1**) synthesized as in Figure 1 (index a for the *cis*- and index b for the *trans*-isomer). (b) <sup>1</sup>H NMR spectrum of 1,2,6-trimethyl-4-piperidone (**1**) with the predominating *cis* isomer synthesized by hydrogenation.

*cis/trans* mixture of 1,2,6-trimethyl-4-piperidone (**1**).<sup>4,6</sup> In the case of the *cis/trans* mixture, each set of signals would consist of a signal for the methylene hydrogens on carbon atoms 3/5 (Fig. 2a; index a for the *cis*- and index b for the *trans*-isomer) and one for the methyl group at the nitrogen (position 9). In addition, for the methyl groups and hydrogens on carbon atoms 2/6 one signal each in the case of the *cis*-isomer and two signals each in case of the *trans*-isomer are expected.

The observed (Fig. 2a) and the expected spectra were only identical concerning methylene hydrogens at carbon atoms 3 and 5 and the methyl group at the nitrogen (in position 9). For methyl groups and hydrogens on carbon atoms 2 and 6 only two signals were observed in both <sup>1</sup>H and <sup>13</sup>C NMR spectra (Fig. 2a), thus missing one signal for the methyl groups and one for the hydrogens in position 2/6.



**Figure 3.** (a) Representation of the proposed<sup>6</sup> conformational equilibrium of the *trans*-isomer<sup>7</sup>. (b) Representation of the possible conformational equilibrium of the *cis*-isomer<sup>7</sup>.



An explanation for these findings can be the presence of two configurational isomers with a fast conformational equilibrium for one of the diastereomers at room temperature (Fig. 3), because due to the fast equilibration the methyl groups and the hydrogens on position 2 and 6 would appear to be equal.

Different stable conformational isomers of only one configurational isomer can also explain the signals found in the NMR spectrum (Fig. 2a). Thus, the purpose of this study was to gain more insight into the kind of isomeric mixture of **1** being present in the  $^1\text{H}$  and  $^{13}\text{C}$  NMR spectra by quantum chemical calculations as well as high and low temperature NMR measurements.

## 2. Results and discussion

In the case of the presence of only one configurational isomer (*cis* or *trans*) with different conformers, the measured NMR spectra could only be explained if an unexpected large energy difference between the conformers is assumed. High temperature NMR measurements could prove this situation since it should lead to a calescence of the signals (and therefore to a single set in the NMR spectra) due to a fast equilibrium between both conformers. In the opposite case of the presence of a *cis/trans*-mixture with different conformers of at least one of the *cis/trans*-isomers, a small energy difference between the conformers has to be assumed to explain the spectra. Due to this small energy difference a fast equilibrium between the conformers of one of these configurational isomers at room temperature occurred. This situation could be confirmed by low temperature NMR measurements since a separation of the signals of these conformers in the NMR spectrum would be obtained.

### 2.1. High temperature NMR

To find out whether only one configurational isomer (*cis* or *trans*) with different conformers or two configurational isomers (*cis* and *trans*) with the equilibrium of one of the diastereomers (Fig. 3) are present at room temperature, high temperature NMR experiments were carried out at first. Measurement of high temperature  $^1\text{H}$  NMR ( $\text{C}_2\text{D}_2\text{Cl}_4$ , 400 MHz) spectra from 300 to 360 K (in steps of 10 K, spectra being recorded 15 min after setting the temperature) revealed no alteration concerning the position of any signal indicating a *cis/trans*-mixture rather than conformational isomerism of one configurational isomer. The missing

signals for a *cis/trans* isomerism in  $^1\text{H}$  and  $^{13}\text{C}$  NMR spectra of **1** due to a different position for the methyl groups and hydrogens on carbon atoms 2 and 6 (Fig. 2a) of the *trans*-isomer, was also observed by Langlois et al.<sup>6</sup> A fast equilibrium of the piperidone ring of the *trans*-isomer (Fig. 3a) was assumed providing an equivalence of the substituents and therefore having no possibility to differentiate between the positions of methyl groups and hydrogens on carbon atoms 2 and 6 of the *trans*-isomer. Overlapping of the second signal of the *trans*- with the *cis*-isomer signal could also be excluded due to the integrals being observed.

1,2,6-Trimethyl-4-piperidone (**1**) could be obtained also by a different synthetic route starting from dehydroacetic acid to the corresponding pyrone followed by catalytic hydrogenation and a Swern oxidation<sup>8</sup> to yield 1,2,6-trimethyl-4-piperidone (Fig. 4) mostly as the *cis*-isomer (Fig. 2b). These findings suggest that the two sets of NMR signals obtained after the Mannich reaction are caused by two configurational rather than only one configurational isomer with different conformers also being in accord with earlier quantum chemical calculations of a series of differently substituted piperidones, where *cis* and *trans*-isomers show only slight energy differences<sup>9</sup> and therefore being able to be present at room temperature.

The next step was to find out whether the spectrum (Fig. 2a) can be assigned to a *cis/trans*-isomeric mixture. In this case, a fusion of the NMR signals of the methyl groups and hydrogens at carbon atoms 2 and 6 in a single signal each concerning the *trans*-isomer is expected. If the NMR spectrum is assigned to a mixture of *cis*- and *trans*-1,2,6-trimethyl-4-piperidone, the missing signals of the *trans*-isomer for the methyl groups and hydrogens on C2/6 then are probably due to the fast equilibrium (Fig. 3a) of the piperidone ring of the *trans*-isomer.

### 2.2. Quantum chemical calculations

The fast conformational equilibrium of *trans*-1,2,6-trimethyl-4-piperidone (Fig. 3a), proposed by Langlois et al.,<sup>6</sup> provides an equivalence of the methyl substituents and hydrogens at carbon atoms 2 and 6 (Fig. 2a) of the *trans*-isomer of **1**. In order to prove whether this equilibrium of *trans*-1,2,6-trimethyl-4-piperidone is indeed present, quantum chemical calculations were performed. The two chair conformations (Fig. 3a) as the lowest lying points on the potential surface were optimized and the energy differences were calculated by different theoretical methods (Table 1). The computations were performed as single point

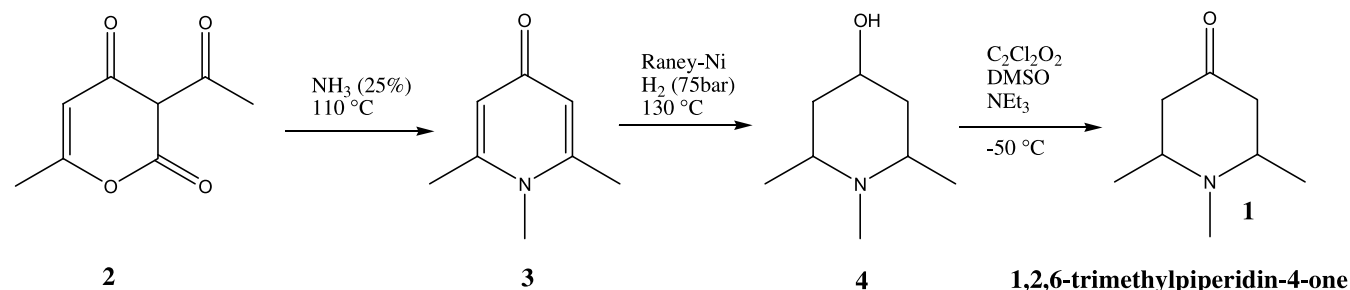
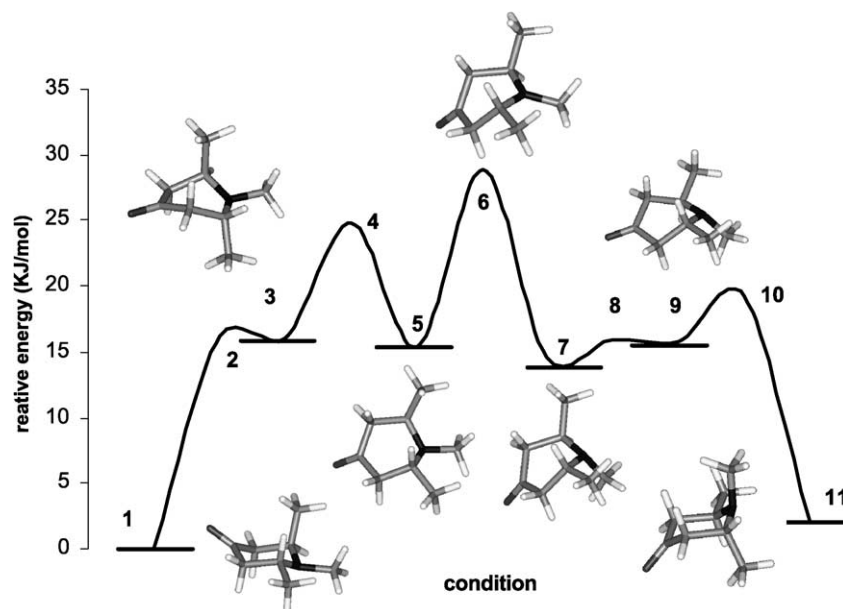


Figure 4. Synthesis of 1,2,6-trimethyl-4-piperidone via hydrogenation.

**Table 1.** Energy differences between both conformers of the *trans* and both conformers of the *cis* isomers in  $\text{kJ mol}^{-1}$  (the position after the point is only presented for better differentiation between given values)

Type of calculation	$\Delta E$ <i>trans</i> -isomers ( $\text{kJ mol}^{-1}$ )	$\Delta E$ <i>cis</i> -isomers ( $\text{kJ mol}^{-1}$ )
RI-BLYP/SVP <sup>10,11,12,15</sup>	1.8	12.0
RI-BLYP/TZVP <sup>10,11,15,16</sup>	2.1	15.7
B3LYP/TZVP <sup>11,16,17</sup>	3.4	17.4
AM1 <sup>13</sup>	2.9	2.0
RI-MP2/TZVP <sup>18</sup>	3.3	17.2

**Figure 5.** Energy pathway of the equilibration process of *trans*-1,2,6-trimethyl-4-piperidone with structures of the obtained minima and the highest maximum. Values of the single point calculations with the B3LYP-functional<sup>11,17</sup> and TZVP<sup>16</sup> basis set are shown in the diagram (further details are discussed in Section 4).

calculations employing geometries obtained with a BLYP/SVP<sup>10–12</sup> approach (for further details see Section 4). Semiempirical AM1<sup>13</sup> optimizations were used to test its reliability to describe such systems. In addition, for the sake of comparison energy differences between the two possible *cis*-conformers (Fig. 3b) were calculated. AM1 optimizations were found to be appropriate for the *trans*-, but not for the *cis*-isomers.

All applied types of calculation except AM1<sup>13</sup> show similar tendencies of energy values. The difference between both *trans*-conformers is comparably low with respect to those obtained for the *cis*-conformers. Due to the fact of one conformer of the *cis*-1,2,6-trimethyl-4-piperidone possessing an 1,3-diaxial interaction of the methyl groups in 2 and 6 position and the other conformer having both methyl groups in the equatorial position as the more favourable one,<sup>14</sup> a larger difference between the *cis*-conformers was expected in comparison to the conformers of *trans*-1,2,6-trimethyl-4-piperidone. The differences between the *trans*- and the *cis*-isomers indicate the proposed equilibrium between the conformers of *trans*-1,2,6-trimethyl-4-piperidone at room temperature and therefore also the explanation for the missing signals in the <sup>1</sup>H NMR spectrum. Since these values represent only energy differences between the chair conformers, further

computational investigations were executed to evaluate the energy barriers of the equilibration of the chair conformers of *trans*-1,2,6-trimethyl-4-piperidone and its energy pathway (for further details Section 4). For each conformer (one with an equatorial (NEQ) and the other with axial (NAX) positioned methyl group on the nitrogen atom (Fig. 3a)) of *trans*-1,2,6-trimethyl-4-piperidone one chair (conformer 1 (NEQ) and 11 (NAX) in Fig. 5/Table 2), one boat (conformer 3 (NEQ) and 9 (NAX)) and one twisted conformation (conformer 5 (NEQ) and 7 (NAX)) were

**Table 2.** Energy values of Figure 5 given in  $\text{kJ mol}^{-1}$  (the position after the point is only presented for better differentiation between given values)

Conformer	$\Delta E$ to 1 B3LYP/TZVP <sup>11,16,17</sup>	$\Delta E$ to 1 RI-BLYP/TZVP <sup>10,11,15,16</sup>
1	0	0
2	17.6	16.1
3	17.2	16.2
4	25.5	24.8
5	16.0	15.4
6	29.9	28.9
7	15.5	14.6
8	16.6	16.0
9	16.1	15.7
10	20.8	19.2
11	3.4	2.1

obtained as minima. Furthermore, transition states between the calculated minima were determined (chair-boat (**2**), boat-twisted (**4**); NEQ-twisted-NAX-twisted (**6**); NAX-twisted-NAX-boat (**8**), NAX-boat-NAX-chair (**10**)) and the whole energy pathway of the equilibration process of *trans*-1,2,6-trimethyl-4-piperidone with the required activation energy barrier was obtained.

In Figure 5, the optimized minima and transition states are given. In addition, structures of the minima and the highest maximum are shown. The corresponding relative energy values for all points (minima and maxima) are displayed in Table 2. It contains the computations employing the RI-BLYP<sup>10,11,15</sup> and the B3LYP<sup>11,17</sup> functional in combination with the TZVP<sup>16</sup> basis. The energy pathway shows that both chair conformations of *trans*-1,2,6-trimethyl-4-piperidone are the most stable geometries (no. 1 for the conformer with an equatorial position of the methyl group on the nitrogen (NEQ), and no. 11 for the conformer with an axial-positioned methyl group attached to the nitrogen (NAX)). The boat conformations (no. 3 (NEQ) and no. 9 (NAX)) show the highest energy values of all minima. The twist conformations (no. 5 (NEQ) and no. 7 (NAX)) are only slightly lower. Concerning twist and boat structures, the conformers with an axial methyl group at the nitrogen are more favourable. This is in contrast to the chair conformations, where an equatorial position of the methyl group on the nitrogen shows a lower energy condition.

To obtain the free activation enthalpy  $\Delta G^\ddagger$  for the equilibration process of the piperidone-ring of *trans*-1,2,6-trimethyl-4-piperidone the energies for the lowest minimum (no. 1 in Fig. 5) and the highest maximum (no. 6) were zero point energy and entropy corrected. Thus,  $\Delta G^\ddagger$  was received as 27 kJ mol<sup>-1</sup> with the B3LYP<sup>11,17</sup> functional showing the expected small influence of the entropy on the process. Due to the unpolar solvent used in the NMR-experiments, insensitivity to the solvent environment should also be given.

### 2.3. Low temperature NMR experiments

Low temperature NMR experiments were performed to verify the theoretically calculated activation barrier of the ring inversion and the proposed fast equilibration between the piperidone conformers of *trans*-1,2,6-trimethyl-4-piperidone (Fig. 3a). Due to freezing of the equilibrium between the two different chair conformers of *trans*-1,2,6-trimethyl-4-piperidone (**1**), splitting of the single signal for both methyl groups on carbon atoms 2 and 6 (Fig. 2a) into two signals is expected as well as splitting of the hydrogens attached to the same carbon atoms as the methyl groups. NMR spectra of **1** were recorded every 10 K downwards, starting from 296 K, later on in steps of 5 K and close to the coalescence of the signals a spectrum was measured in one degree K steps. NMR spectra were recorded 15 min after setting the corresponding temperature. Due to the fact of measuring below the normal freezing point of CD<sub>2</sub>Cl<sub>2</sub> as the solvent, low temperature experiments were executed twice and in every case measuring was possible that low, indicating a subcooled solution of the samples. Figure 6 shows a selection of <sup>1</sup>H NMR spectrum expansions of the region of interest at the

given temperature from the first NMR measurement (*T*<sub>1</sub>) (see below).

As presented in Figure 6, the splitting of the single signal of the methyl groups in position 7 and 8 (Fig. 2a) of the *trans*-isomer and therefore freezing of the ring inversion process of *trans*-1,2,6-trimethyl-4-piperidone (Fig. 3a) can be seen at the coalescence temperature (*T*<sub>C</sub>) of 162 K of both methyl groups for the first low temperature NMR experiment (*T*<sub>1</sub>). The second low temperature NMR measurement (*T*<sub>2</sub>, 300 MHz) revealed a coalescence temperature (*T*<sub>C</sub>) of 155 K for the methyl groups. At 145 K a good separation of the methyl groups of *trans*-1,2,6-trimethyl-4-piperidone is achieved (Fig. 6), the signal representing the methyl groups of the *cis*-isomer is still present as a single signal. In the case of the equilibrium of the chair conformers of *trans*-1,2,6-trimethyl-4-piperidone (Fig. 3a), the activation barrier was calculated using the Eyring equation 1, where  $\Delta G^\ddagger$  is the free activation enthalpy, *R* the universal gas constant (8.31 J/K), *T* the absolute temperature (K), *N*<sub>A</sub> Avagadro's number (6.022 × 10<sup>23</sup> mol<sup>-1</sup>) and *h* is the Planck's constant (6.6256 × 10<sup>-34</sup> J/s).

$$k = \frac{RT}{N_A h} e^{-\Delta G^\ddagger/RT} \quad (1)$$

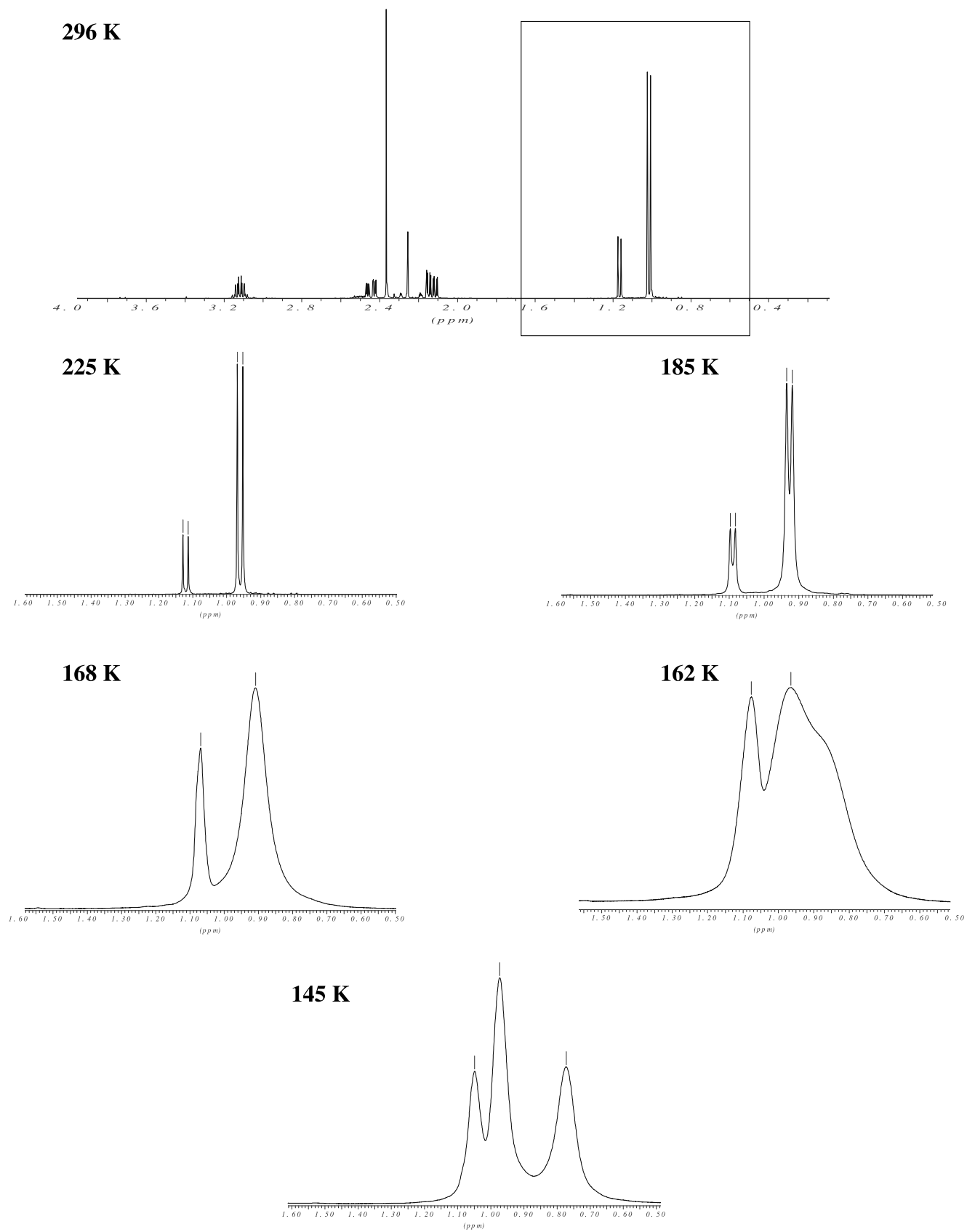
At the point of coalescence, the following (Eq. 2) is available:<sup>19</sup>

$$\Delta G^\ddagger = 19.1 \times 10^{-3} T_C (9.97 + \log T_C - \log |\nu_A - \nu_B|) \quad (2)$$

Thus, the free activation enthalpy for the ring inversion process of *trans*-1,2,6-trimethyl-4-piperidone (Fig. 3a) was calculated to be 32 kJ mol<sup>-1</sup> (*T*<sub>1</sub>) and 31 kJ mol<sup>-1</sup> (*T*<sub>2</sub>) for the methyl groups in position 7 and 8 (Fig. 2a), being quite in accordance with the result obtained by the earlier discussed quantum chemical calculations. In addition to that, the hydrogens on carbon atoms 2 and 6 (Fig. 2a) of the piperidone ring of *trans*-1,2,6-trimethyl-4-piperidone showed splitting into two signals (data not shown). Since, these signals show different splitting  $\Delta\delta$ , they also possess slightly different *T*<sub>C</sub> values (168 K for *T*<sub>1</sub> and 163 K for *T*<sub>2</sub>). Using this data the activation barrier for the equilibrium of the chair conformations of *trans*-1,2,6-trimethyl-4-piperidone (Fig. 3a) was also found to be 32 kJ mol<sup>-1</sup> (*T*<sub>1</sub>) and 31 kJ mol<sup>-1</sup> (*T*<sub>2</sub>) for the corresponding hydrogens attached to carbon atoms 2 and 6 (Fig. 2a). Because all obtained values are within a close range of energy values and differ less than 2 kJ mol<sup>-1</sup> even though obtained by two different low temperature NMR experiments, they confirm the corresponding values obtained by quantum chemical calculations (see above) for the activation barrier of the ring inversion process of *trans*-1,2,6-trimethyl-4-piperidone (Fig. 3a).

### 3. Conclusions

Due to the investigations executed the earlier stated *cis/trans* isomerism<sup>4,6</sup> could not only be verified, but also the activation barrier values for the conformational



**Figure 6.** Low temperature  $^1\text{H}$  NMR peaks ( $\text{CD}_2\text{Cl}_2$ , 400 MHz) of the 2,6 methyl groups at given temperatures from the first low temperature experiment T1.

equilibrium of *trans*-1,2,6-trimethyl-4-piperidone could be obtained (Fig. 3a). Quantum chemical calculations were carried out to obtain energy differences between both chair conformers of *cis*- and *trans*-isomers and to obtain information about the activation barrier and the energy pathway of the ring inversion process of *trans*-1,2,6-trimethyl-4-piperidone. The activation barrier of this equilibrium of *trans*-1,2,6-trimethyl-4-piperidone was verified by low temperature NMR experiments.

The quantum chemically calculated values show good agreement to those determined by low temperature NMR spectroscopy and confirm the equilibrium (Fig. 3a) of the conformers of *trans*-1,2,6-trimethyl-4-piperidone at room temperature. Therefore, both theory and experiment prove that a *cis/trans* isomeric mixture is present at room temperature in the spectrum of 1,2,6-trimethyl-4-piperidone (Fig. 2a) when synthesised as in Figure 1. Considering the pharmacological aspects, the affinity to a corresponding receptor should not be influenced by the different conformers (Fig. 3a) of *trans*-1,2,6-trimethyl-4-piperidone, because they can be easily converted into each other due to their low energy difference. However, a *cis/trans*-mixture should be avoided for pharmacological evaluation, because a conversion is impossible due to a bond cleavage being necessary to transform one into another. Isolation of a mixture with the *cis*-isomer predominating can only be achieved by a different synthetic pathway (Fig. 4).

## 4. Experimental

### 4.1. NMR investigations

All synthesised compounds were characterized by  $^1\text{H}$  and  $^{13}\text{C}$  NMR spectroscopy.  $^1\text{H}$  NMR spectra were performed on a Bruker DRX 300 (300.13 MHz) and Bruker Avance 400 (400.13 MHz), respectively. The temperatures of the probe were calibrated by a low temperature calibration with 4% methanol in  $[\text{D}_4]$  methanol.<sup>20</sup>  $^{13}\text{C}$  NMR spectra were performed on a Bruker Avance 400 (100.62 MHz). For  $^1\text{H}$  NMR spectra with the Bruker Avance 400 ( $T_1$ , 400.13 MHz) [DRX 300 ( $T_2$ , 300.13 MHz)], 32 [16] scans were collected into 64 K [72 K] data points giving a digital resolution of 0.25 Hz [0.16 Hz] per point. The spectral width was 8278 Hz [6188 Hz], the transmitter offset 6.18 ppm [6.18 ppm]. Using an acquisition time of 3.96 s [5.99 s] and an additional delay of 1 s [1 s], a pulse repetition period of 4.96 s [6.99 s] results. An appropriate window function was applied before Fourier transformation in order to enhance the spectral resolution. For  $^{13}\text{C}$  NMR spectra 512 scans were collected into 64 K data points, giving a digital resolution of 0.73 Hz per point. The spectral width was 23981 Hz and the transmitter offset 100 ppm. Using an acquisition time of 1.37 s and an additional delay of 2 s, a pulse repetition period of 3.37 s results. An appropriate window function was applied before Fourier transformation in order to enhance the spectral resolution.

### 4.2. Quantum chemical calculations

For the geometry optimizations of the two chair conformations density functional theory (DFT) calculations were

employed with the BLYP<sup>10,11</sup> functional, the SVP<sup>12</sup> basis set and the RI<sup>15</sup> approximation performed with the TURBOMOLE<sup>21</sup> program package. Furthermore, a semi-empirical AM1<sup>13</sup> optimization was used for comparison. Single point calculations for the energy difference were carried out with the TZVP<sup>16</sup> basis set and the RI-BLYP,<sup>10,11,15</sup> B3LYP<sup>11,17</sup> and RIMP2<sup>18</sup> method on the BLYP/SVP<sup>10,11,12</sup> geometry.

To obtain the energy pathway of *trans*-1,2,6-trimethyl-4-piperidone a conformational search<sup>22</sup> applying the MMFF94s<sup>23</sup> force field in the MacroModel 8.0<sup>24</sup> program was executed to locate the minima on the energy surface of *trans*-1,2,6-trimethyl-4-piperidone. The obtained structures were reoptimized by DFT calculations employing the RI-BLYP<sup>10,11,15</sup> functional in combination with the SVP<sup>12</sup> basis set. Single point calculations were done with the BLYP<sup>10,11</sup> and B3LYP<sup>11,17</sup> functional and the TZVP<sup>16</sup> basis set. These stationary points were verified as local minima by the absence of imaginary frequencies (AOFORCE<sup>21</sup>). Transition states were obtained by Gaussian 03<sup>25</sup> QST2 calculations applying the BLYP/SVP<sup>10,11,12</sup> level of theory and were also confirmed by AOFORCE<sup>21</sup> calculations as transition states (imag. freq.=1). Reoptimizations of the calculated transition states were executed with TURBOMOLE<sup>21</sup> and the RI-BLYP/SVP<sup>10,11,12,15</sup> method (STATPT), single point calculations with the BLYP<sup>10,11</sup> and B3LYP<sup>11,17</sup> functional and the TZVP<sup>16</sup> basis set. To connect the so far obtained minima and transition states, further quantum chemical calculations were performed between boat-boat and twist-twist conditions, that were calculated as transition states as above. Thus, the whole energy pathway of the equilibration process of *trans*-1,2,6-trimethyl-4-piperidone with the required activation energy barrier (Fig. 6) was obtained.

**4.2.1. 1,2,6-Trimethylpiperidin-4-one (1) via 1,2,6-trimethyl-4-piperidone-3,5-dimethyldicarboxylate.** Synthesis was executed by a modified instruction of Langlois et al.<sup>6</sup> 5.22 g (30.0 mmol) of 1,3-acetone dicarboxylate (97%) was added to an ice-cold mixture of 2.02 g (30.0 mmol) methylamine hydrochloride in 10 ml of water and 2.73 g (62.0 mmol) acetaldehyde. After warming to room temperature, the solution was stirred for additional 16 h, the solvent was completely removed in vacuo and a small amount of acetone was added to precipitate 6.25 g (21.3 mmol) of 1,2,6-trimethyl-4-piperidone-3,5-dimethyldicarboxylate after cooling. 1,2,6-Trimethyl-4-piperidone-3,5-dimethyldicarboxylate (2.00 g (6.81 mmol)) were dissolved in 20 ml 6 M HCl and stirred for 20 h at 80 °C. After neutralisation with a saturated KOH solution, the reaction mixture was extracted three times with 20 ml  $\text{CH}_2\text{Cl}_2$ , organic phases were dried with  $\text{Na}_2\text{SO}_4$  and the solvent was removed in vacuo. The oily, orange residue was distilled by vacuum distillation and 0.69 g (4.89 mmol) of **1** was obtained as a colourless oil (bp 30 °C ( $0.1 \times 10^{-2}$  mbar)).

$^1\text{H}$  NMR (400 MHz,  $\text{CDCl}_3$ ,  $\delta$ =ppm,  $J$ =Hz): Isomer A: 3.03–3.12 (m, 2H, H2,6), 2.42 (dd, 2H, overlapping with H2,6 Isomer B,  $J$ =13.9, 4.54 Hz, H3,5<sup>eq</sup>), 2.33 (s, 3H, H9), 2.11 (dd, 2H,  $J$ =13.9, 6.68 Hz, H3,5<sup>ax</sup>), 0.97 (d, 6H,  $J$ =6.56 Hz, H7,8); Isomer B: 2.39–2.45 (m, overlapping with H3,5 Isomer A, H2,6), 2.18–2.29 (m, overlapping with H3,5



Isomer A, H3,5), 2.22 (s, 3H, H9), 1.13 (d, 6H,  $J=6.32$  Hz, H2,6);  $^{13}\text{C}$  NMR (100 MHz,  $\text{CDCl}_3$ ,  $\delta$ =ppm): Isomer A: 209.28 (C4), 54.10 (C2,6), 47.63 (C3,5), 38.07 (C9), 16.45 (C7,8); Isomer B: 208.37 (C4), 58.60 (C2,6), 48.15 (C3,5), 34.57 (C9), 21.15 (C2,6).

**4.2.2. 3-Acetyl-6-methyl-pyran-2,4-dione (dehydracetic acid) (2).** Synthesis of **2** followed the preparation of Arndt et al.<sup>26</sup> Freshly distilled ethyl acetoacetate (100 g (0.77 mol)) and 50 mg sodium carbonate were heated to 200–210 °C. The formed ethanol was removed by distillation by a modified dry-ice condenser connected with an additional condenser set for distillation. The modified condenser was filled with toluene, and a reflux condenser was attached to the top to keep the rest of the solution in the reaction mixture. The reaction was maintained for 7–8 h at that temperature followed by vacuum distillation of the remaining brown solution while still being hot to yield 53.06 g (0.32 mol) of **2** (mp 110 °C (lit.:<sup>26</sup> 104–110 °C)).

**4.2.3. 1,2,6-Trimethyl-1H-pyridin-4-one (N-methyl-lutidone) (3).** The title compound **3** was synthesised as executed by Iguchi et al.<sup>27</sup> A sealed tube was charged with 3.67 g (0.02 mol) dehydracetic acid **2** and 20 ml aqueous methylamine solution (25%) was added and heated to 110 °C for 6 h. After cooling, the raw product precipitated as white needles. After filtration and recrystallisation from hot water, **3** was dried at 115 °C in vacuo. The title compound **3** (2.17 g (15.8 mmol)) was obtained (mp 248 °C (lit.<sup>27</sup>: 245 °C)).

**4.2.4. 1,2,6-Trimethylpiperidin-4-ol (4).** The instruction of Langlois et al.<sup>6</sup> was used for the synthesis of **4**. 1,2,6-Trimethyl-1H-pyridin-4-one (**3**) (5.00 g (36.5 mmol)) was dissolved in 100 ml ethanol and treated with 10 ml of a suspension of Raney<sup>®</sup>-Nickel 2800 (Aldrich). The reaction mixture was stirred for 16 h at 130 °C under  $\text{H}_2$  atmosphere (75 bar), the solvent was removed and the residue was distilled to give 2.98 g (20.8 mmol) of **4** (bp 35 °C (0.1  $\times$  10<sup>-2</sup> mbar)).

**4.2.5. 1,2,6-Trimethylpiperidin-4-one (1) from 1,2,6-trimethylpiperidin-4-ol (4).** A common Swern oxidation was applied to synthesize **1**.<sup>8</sup> Oxalyl chloride (1.47 ml (16.24 mmol)) in 50 ml dry dichloromethane was cooled to -50 °C under argon. DMSO (2.52 (32.48 mmol)), dried with  $\text{P}_2\text{O}_5$ , was added and stirred for 10 min at -50 °C. Afterwards, 2.1 g (14.67 mmol) of 1,2,6-trimethylpiperidin-4-ol (**4**) in 10 ml of dry dichloromethane were added within 5 min and stirred for additional 15 min at -50 °C. Triethylamine (20 ml (70 mmol)) was added dropwise and the solution was slowly warmed up to room temperature. After addition of 100 ml of water the solution was three times extracted with 100 ml of dichloromethane. Organic phases were extracted with saturated KOH-solution, dried with  $\text{Na}_2\text{SO}_4$  and the solvent was removed. The oily residue was distilled under vacuum (10<sup>-3</sup> bar) to yield 1.30 g (9.2 mmol) of **1**.

#### Acknowledgements

This work was supported by the Sonderforschungsbereich

630. The authors wish to thank Dr. Rüdiger Bertermann for measuring low temperature NMR experiments and Dr. Ralph Deubner for measuring high temperature NMR experiments.

#### Supplementary data

Supplementary data associated with this article can be found, in the online version, at doi:10.1016/j.tet.2005.05.030

The supporting information material contains Cartesian Coordinates, computed total energies and the imaginary frequencies (where applicable) of the obtained structures in Table 1 (conformers A–D) and in Table 2 (conformers 1–11).

#### References and notes

1. Casy, A.; McErlane, K. *J. Chem. Soc., Perkin. Trans. 1* **1972**, 5, 726–731.
2. Wichmann, J.; Adam, G.; Röver, S.; Cesura, A.; Dautzenberg, F.; Jenck, F. *Bioorg. Med. Chem. Lett.* **1999**, 9, 2343–2348.
3. Meunier, J.; Mollereau, C.; Toll, L.; Suaudeau, C.; Misand, C.; Suaudeau, C.; Moisan, C.; Alvinerie, P.; Butour, J.; Guillemot, J.; Ferrara, P.; Monsarrat, B.; Mzarguil, H.; Vassart, G.; Parmentier, M.; Costentin, J. *Nature* **1995**, 377, 532–535.
4. Casy, A.; Coates, J.; Rostron, C. *J. Pharm. Pharmacol.* **1976**, 28, 106–110.
5. Röver, S.; Adam, G.; Cesura, A.; Galley, G.; Jenck, F.; Monsma, F.; Wichman, J.; Dautzenberg, F. *J. Med. Chem.* **2000**, 43, 1329–1338.
6. Langlois, M.; Donglai, Y.; Soulier, J.; Florac, C. *Synth. Commun.* **1992**, 22, 3115–3127.
7. Due to the fact that the methyl group on the nitrogen is able to oscillate at room temperature with the lone electron pair at the nitrogen, only one possible position of this methyl group is represented in Figure 3a as well as in Figure 3b.
8. Omura, K.; Swern, D. *Tetrahedron* **1978**, 34, 1651–1660.
9. Holzgrabe, U.; Friedrichsen, W.; Hesse, K. *Z. Naturforsch B* **1990**, 46, 1237–1250.
10. Becke, A. *Phys. Rev. A* **1988**, 38, 3098–3100.
11. Lee, C.; Yang, W.; Parr, R. *Phys. Rev. B* **1988**, 37, 785–789.
12. Ahlrichs, R.; Schäfer, A.; Horn, H. *J. Chem. Phys.* **1992**, 97, 2571–2577.
13. Dewarand, M.; Zoebisch, E.; Healy, E. *J. Am. Chem. Soc.* **1985**, 107, 3902–3909.
14. Arnason, I.; Kvaran, A.; Jonsdottir, S.; Gudnason, P.; Oberhammer, H. *J. Org. Chem.* **2002**, 67, 3827–3831.
15. Eichkorn, K.; Treutler, O.; Öhm, H.; Häslers, M.; Ahlrichs, R. *Chem. Phys. Lett.* **1995**, 240, 283–290. Eichkorn, K.; Treutler, O.; Öhm, H.; Häslers, M.; Ahlrichs, R. *Chem. Phys. Lett.* **1995**, 242, 652–660.
16. Ahlrichs, R.; Schäfer, A.; Horn, H. *J. Chem. Phys.* **1994**, 100, 5829–5835.
17. Becke, A. *J. Chem. Phys.* **1993**, 98, 5648–5652.

18. Weigend, F.; Häser, M. *Theor. Chem. Acc.* **1997**, *97*, 331–340.
19. Hesse, M.; Meier, H.; Zeeh, B. In *Spektroskopische Methoden in der Organischen Chemie, 6 Aufl.*; Thieme: Stuttgart, 2002.
20. Braun, S.; Kalinowski, H.; Berger, S. *150 and more basic NMR experiments*, 2nd ed.; Wiley-VCH: Weinheim, 1999.
21. Ahlrichs, R.; Bär, M.; Baron, H.; Bauernschmitt, R.; Böcker, S.; Ehrig, M.; Eichkorn, K.; Elliott, S.; Haase, F.; Häser, M.; Horn, H.; Huber, C.; Huniar, U.; Kattaneck, M.; Kölmel, C.; Kollwitz, M.; Ochsenfeld, C.; Öhm, H.; Schäfer, A.; Schneider, U.; Treutler, O.; von Arnim, M.; Weigend, F.; Weis, F.; Weiss H. *TURBOMOLE since 1988*; Quant. Chem. Group, University of Karlsruhe: Germany.
22. Kolossvaryan, I.; Guida, W. *J. Am. Chem. Soc.* **1996**, *118*, 5011–5019.
23. Halgen, T. *J. Comput. Chem.* **1999**, *20*, 720–729. Halgen, T. *J. Comput. Chem.* **1999**, *20*, 730–748.
24. *Macromodel 8.0*, Schrödinger, 1500 SW First Ave.; Suite 1180, Portland, OR, 97201.
25. Frisch, M. J.; Trucks, G. W.; Schlegel, H. B.; Scuseria, G. E.; Robb, M. A.; Cheeseman, J. R.; Montgomery, J. A., Jr.; Vreven, T.; Kudin, K. N.; Burant, J. C.; Millam, J. M.; Iyengar, S. S.; Tomasi, J.; Barone, V.; Mennucci, B.; Cossi, M.; Scalmani, G.; Rega, N.; Petersson, G. A.; Nakatsuji, H.; Hada, M.; Ehara, M.; Toyota, K.; Fukuda, R.; Hasegawa, J.; Ishida, M.; Nakajima, T.; Honda, Y.; Kitao, O.; Nakai, H.; Klene, M.; Li, X.; Knox, J. E.; Hratchian, H. P.; Cross, J. B.; Adamo, C.; Jaramillo, J.; Gomperts, R.; Stratmann, R. E.; Yazyev, O.; Austin, A. J.; Cammi, R.; Pomelli, C.; Ochterski, J. W.; Ayala, P. Y.; Morokuma, K.; Voth, G. A.; Salvador, P.; Dannenberg, J. J.; Zakrzewski, V. G.; Dapprich, S.; Daniels, A. D.; Strain, M. C.; Farkas, O.; Malick, D. K.; Rabuck, A. D.; Raghavachari, K.; Foresman, J. B.; Ortiz, J. V.; Cui, Q.; Baboul, A. G.; Clifford, S.; Cioslowski, J.; Stefanov, B. B.; Liu, G.; Liashenko, A.; Piskorz, P.; Komaromi, I.; Martin, R. L.; Fox, D. J.; Keith, T.; Al-Laham, M. A.; Peng, C. Y.; Nanayakkara, A.; Challacombe, M.; Gill, P.M. W.; Johnson, B.; Chen, W.; Wong, M. W.; Gonzalez, C.; Pople, J. A. *Gaussian 03, Revision A.1*; GAUSSIAN, Inc.: Pittsburgh PA, 2003.
26. Arndt, F.; Hartman, W.; Weissberger, A. *Org. Synth.* **1940**, *3*, 231–233.
27. Iguchi, S.; Inoue, A.; Kurahashi, C. *Chem. Pharm. Bull.* **1963**, *11*, 385–390.

# Reactions of bis(tetrazole)phenylenes. Surprising formation of vinyl compounds from alkyl halides

Adrienne Fleming,<sup>a</sup> Fintan Kelleher,<sup>a</sup> Mary F. Mahon,<sup>b</sup> John McGinley<sup>a,c,\*</sup> and Vipa Prajapati<sup>a</sup>

<sup>a</sup>Department of Applied Science and Advanced Smart Materials Research Center, Institute of Technology, Tallaght, Dublin 24, Ireland

<sup>b</sup>Department of Chemistry, University of Bath, Claverton Down, Bath BA2 7AY, England

<sup>c</sup>Department of Chemistry, National University of Ireland Maynooth, Maynooth, Co. Kildare, Ireland

Received 4 February 2005; revised 25 April 2005; accepted 5 May 2005

Available online 6 June 2005

**Abstract**—The reactions of 1,2-bis(tetrazol-5-yl)benzene (**1**), 1,3-bis(tetrazol-5-yl)benzene (**2**), 1,4-bis(tetrazol-5-yl)benzene (**3**), 1,2-(Bu<sub>3</sub>SnN<sub>4</sub>C)<sub>2</sub>C<sub>6</sub>H<sub>4</sub> (**4**), 1,3-(Bu<sub>3</sub>SnN<sub>4</sub>C)<sub>2</sub>C<sub>6</sub>H<sub>4</sub> (**5**) and 1,4-(Bu<sub>3</sub>SnN<sub>4</sub>C)<sub>2</sub>C<sub>6</sub>H<sub>4</sub> (**6**) with 1,2-dibromoethane were carried out by two different methods in order to synthesise pendant alkyl halide derivatives of the parent bis-tetrazoles. This led to the formation of several alkyl halide derivatives, substituted at either N1 or N2 on the tetrazole ring, as well as the surprising formation of several vinyl derivatives. The crystal structures of both 1,2-[(2-vinyl)tetrazol-5-yl]benzene (1-*N*,2-*N'*) (**1b**) and 1,3-bis[(2-bromoethyl)tetrazol-5-yl]benzene (2-*N*,2-*N'*) (**5d**) are discussed.

© 2005 Elsevier Ltd. All rights reserved.

## 1. Introduction

Tetrazoles have roles in coordination chemistry as ligands, in medicinal chemistry as metabolically stable surrogates for carboxylic acids and in materials science applications, including photography and explosives.<sup>1,2</sup> The synthesis of tetrazoles from the cycloaddition reaction between a nitrile and an azide is well documented.<sup>1–6</sup> The three main synthetic approaches towards this type of transformation involve the use of tin azides,<sup>4,5</sup> strong Lewis acids,<sup>7</sup> and employment of acidic media.<sup>8</sup> Our interest in tetrazoles surrounds their potential as precursors in the formation of new functionalised poly-tetrazoles which can be used in other areas of chemistry, for example—sensors or molecular recognition. In this paper, we report our initial findings regarding the addition of pendant alkyl halide arms of some bis-tetrazoles. Earlier investigations by Molloy et al. revealed the formation of bis-tetrazole derivatives either with pendant alkyl halide arms or with a cyclophane structure.<sup>5</sup> In our hands, syntheses have yielded not only bis-tetrazole derivatives with pendant alkyl halide arms but also, and rather surprisingly, bis-tetrazole derivatives with pendant vinyl arms. The crystal structure of one such derivative is presented herein and discussed.

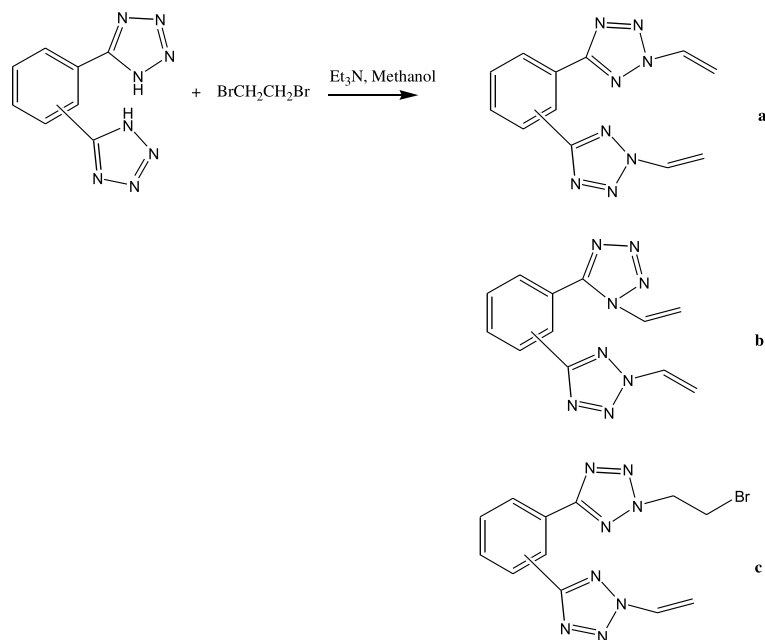
## 2. Results and discussion

The reaction of 1,2-(Bu<sub>3</sub>SnN<sub>4</sub>C)<sub>2</sub>C<sub>6</sub>H<sub>4</sub> (**4**) with 1,2-dibromoethane has been shown to form either a cyclophane or bis(bromoalkyltetrazolyl)benzenes, depending on the ratio of the dibromoethane employed in the reaction.<sup>5</sup> When using a 10-fold excess, the cyclophane was obtained; a larger excess (25:1) resulted in the formation of the bis(bromoalkyltetrazolyl)benzenes, either the 2-*N*, 2-*N'*- or the 1-*N*,2-*N'*- isomer, with the 2-*N*, 2-*N'*-isomer predominating in a ratio of 3:1. Butler and Fleming have also synthesised bis(bromoalkyltetrazolyl)benzenes from *N*-unsubstituted tetrazoles and dihaloalkanes in the presence of Et<sub>3</sub>N with the 2-*N*, 2-*N'*-isomer again predominating.<sup>9</sup> Our strategy was to use both of these approaches to obtain sufficient quantities of the 2-*N*,2-*N'*-isomer of various bis(bromoalkyltetrazolyl)benzenes with a view to subsequently generating derivatised tetra-tetrazole macrocycles.

The reaction of either 1,2-bis[tetrazol-5-yl]benzene (**1**), 1,3-bis[tetrazol-5-yl]benzene (**2**) or 1,4-bis[tetrazol-5-yl]benzene (**3**) with Et<sub>3</sub>N and 1,2-dibromoethane in methanol at reflux temperature for 24 h (see Scheme 1) yielded four spots by TLC; the largest spot, in all cases, being the starting bis-tetrazole. In all reactions undertaken, on average, 50% of the starting bis-tetrazole was uniformly recovered. Our initial belief was that both the 2-*N*, 2-*N'*- and the 1-*N*, 2-*N'*- isomers of the bis(bromoethyltetrazolyl)benzene and the cyclophane had formed in the reaction, based solely on

**Keywords:** Tetrazole; Organotin; X-ray; Vinyl; NMR.

\* Corresponding author. Tel.: +353 1 708 4615; fax: +353 1 708 3815; e-mail: [john.mcginley@nuim.ie](mailto:john.mcginley@nuim.ie)



Isomer	a	b	c
<b>1,2-</b>	1a (13.8 %)	1b (10.5 %)	1c (8.1 %)
<b>1,3-</b>	2a (15.6 %)	2b (10.2 %)	2c (8.3 %)
<b>1,4-</b>	3a (12.8 %)	3b (11.6 %)	3c (9.8 %)

\* % Yield in parentheses

Scheme 1.

published results in the literature,<sup>5,9</sup> and that longer reaction time would increase the yields of the three products. Unfortunately, increasing the reaction time, in some cases up to 120 h, did not improve the yield in any instance. Column chromatography, using a hexane/ethyl acetate mixture as eluent, separated the products. <sup>1</sup>H and <sup>13</sup>C NMR spectra were obtained for all samples. The isomeric 2-*N*, 2-*N'*- and the 1-*N*, 2-*N'*-derivatives should be readily distinguishable from their respective <sup>1</sup>H and <sup>13</sup>C NMR spectra, as described by Molloy et al.<sup>5</sup>

Surprisingly, all three products showed the distinct signal pattern for the presence of vinyl groups, while in the cases of **1c**, **2c** and **3c**, the presence of a bromoalkyl group was also observed. The formation of the vinyl group must be due to the presence of unreacted triethylamine abstracting HBr from the initially formed alkylbromo compound in all cases, although no sign of this initial bis-alkylbromotetrazole derivative was observed by TLC. Thus, the three products formed were the symmetrical 2-*N*,2-*N'*-bis(vinyl)-derivative, the unsymmetrical 1-*N*,2-*N'*-bis(vinyl)-derivative and the 2-*N*,2-*N'*-vinyl-bromoethyl-derivative. No obvious reason was apparent for the difference between these results and those published previously by Butler and Fleming.<sup>9</sup> Crystals of compound **1b**, suitable for an X-ray diffraction study, were obtained from chloroform and the X-ray structure obtained confirmed the presence of the pendant vinyl groups (see Fig. 1). It is notable that in the molecule the two tetrazole rings are not co-planar with each other, the angle between the least-squares planes of these two rings being 87.9°.

The reaction of 1,2-(Bu<sub>3</sub>SnN<sub>4</sub>C)<sub>2</sub>C<sub>6</sub>H<sub>4</sub> (**4**), 1,3-(Bu<sub>3</sub>SnN<sub>4</sub>C)<sub>2</sub>C<sub>6</sub>H<sub>4</sub> (**5**) or 1,4-(Bu<sub>3</sub>SnN<sub>4</sub>C)<sub>2</sub>C<sub>6</sub>H<sub>4</sub> (**6**) with 1,2-dibromoethane forms either a cyclophane or bis(bromoalkyltetrazolyl)benzenes, depending on the ratio of the dibromoethane employed in the reaction.<sup>5</sup> In all the reactions that we tried, no evidence for a cyclophane was detected. Generally, four products were obtained from each reaction, with compounds **a**, **b** and **c** always being present (see Scheme 2) and either **d** or **e** being the remaining product. In these reactions also, not all the starting bis-tetrazole was consumed in the reaction, with the largest spot by TLC being the starting tin tetrazole. What is intriguing is the presence of vinyl groups in these products as well as

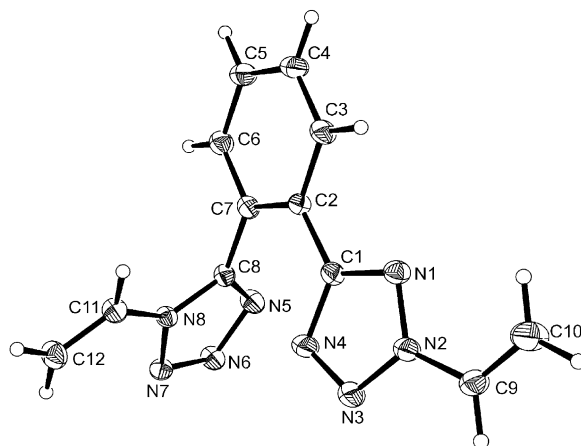
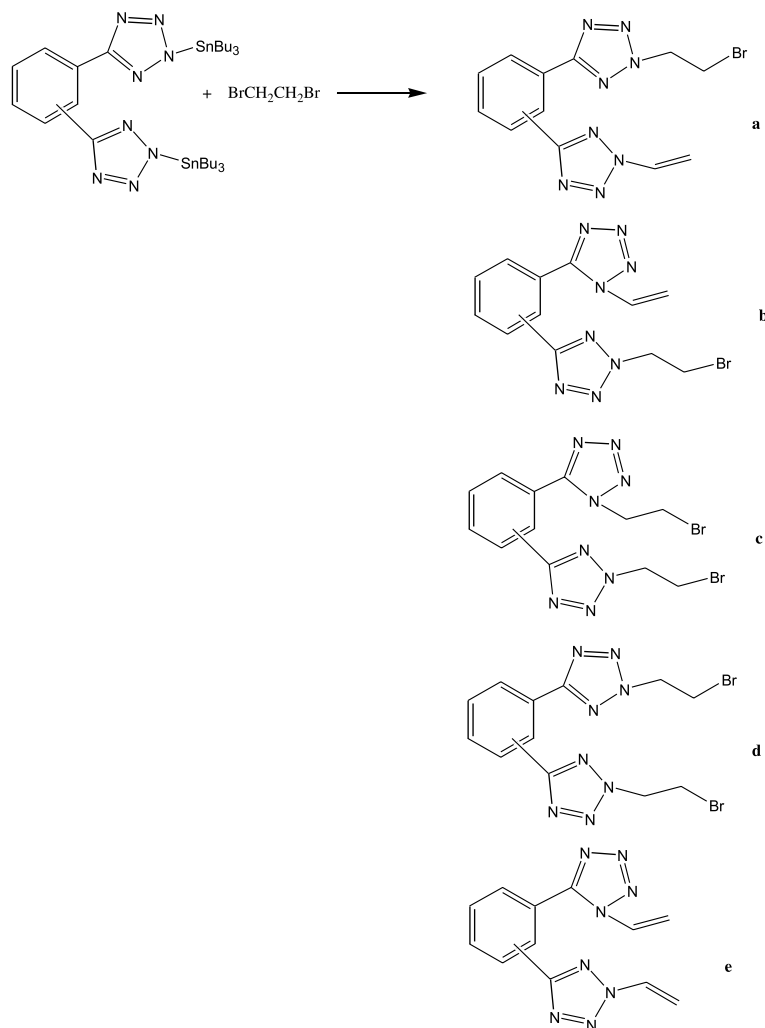


Figure 1. Molecular structure of **1b**, showing the labelling scheme used. Ellipsoids are represented at 30% probability.



Isomer	a	b	c	d	e
<b>1,2-</b>	4a (10.6 %)	4b (10.2 %)	4c (8.3 %)	-	4e (6.4 %)
<b>1,3-</b>	5a (11.8 %)	5b (9.8 %)	5c (7.6 %)	5d (6.3 %)	-
<b>1,4-</b>	6a (10.9 %)	6b (10.1 %)	6c (8.1 %)	-	6e (7.3 %)

\* % Yield in parentheses

**Scheme 2.**

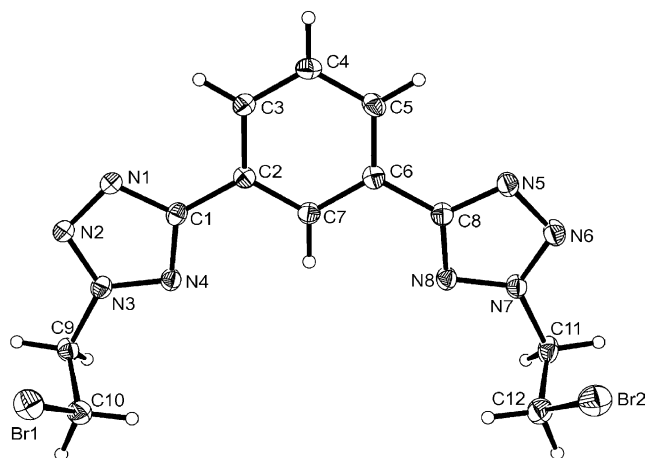
those products already discussed above. In the previous set of reactions, described above, it was easier to rationalise the presence of the vinyl group as a result of excess base being present, resulting from not all the starting bis-tetrazole being consumed in the reaction.

There are three 'plausible' explanations for the formation of the N-vinyl compound in the absence of triethylamine. First, it is a thermal elimination (pyrolysis) of the hydrogen halide. This is unlikely as the reaction temperature is only 120 °C, and the fact that not all the bromoethyl arms are converted to vinyl groups would rule this out as a possibility. Secondly, the tributyltin bromide by-product under the reaction conditions produces the tributyltin radical, which then abstracts a bromide radical with subsequent loss of a proton to give the vinyl. While this appears plausible, the reaction conditions are very mild (120 °C reflux) compared to those published in the literature (for example, in the presence of a catalytic amount of

azobisisobutyronitrile (AIBN) or UV irradiation in toluene).<sup>10,11</sup> On that basis, we believe that this pathway, though plausible, is not a possibility. The final plausible explanation is that the bromide ion formed in the first displacement acts as a base in 1,2-dibromoethane, as there is no solvent present to solvate the ion. It immediately abstracts a hydrogen from the product containing the bromoethyl arm resulting in a negative charge residing on the carbon atom. Loss of bromide ion removes the negative charge and also results in the formation of the vinyl group. Of the three possible routes, this final route appears the most plausible.

Despite our best endeavours, we were unable to grow suitable crystals of any of the **a** or **b** compounds but we did manage to grow suitable crystals of **5d**. The X-ray structure for this compound has been previously published<sup>5</sup> but this compound **5d** is a different polymorph. The major difference between the two sets of structural data is that the structure already published showed that the crystal was





**Figure 2.** Molecular structure of **5d**, showing the labelling scheme used. Ellipsoids are represented at 30% probability.

monoclinic in the  $C2/c$  space group whereas in this case the structure is triclinic in the  $P-1$  space group. This difference manifests itself in the orientation of the pendant bromoethyl arms. In the previously reported structure,<sup>5</sup> the pendant bromoethyl arms are pointing in opposite directions relative to the central phenyl ring, whereas in **5d**, the pendant bromoethyl arms are directed in the same direction (see Fig. 2).

The tetrazole rings and the phenyl ring are almost co-planar, with both bromoethyl arms on the same face of the phenyl ring. The packing diagram (see Fig. 3) illustrates this feature to greater effect. Here, distinct channels of bis-tetrazole units are evident with intermolecular interactions between adjacent units. Analysis of the supramolecular array reveals the presence of slipped  $\pi$ -stacking between the phenyl ring and the tetrazole based on C8, the distance between most

proximate pairs of such rings in the supramolecular array being 3.36 Å. The tetrazoles based on C1 are also involved in  $\pi$ -stacking with each other. In this case an interplane distance of 3.36 Å is observed between said rings in closest lattice neighbours. The closest Br $\cdots$ Br distance of 3.854 Å mitigates against the presence of any significant bromine–bromine interactions.

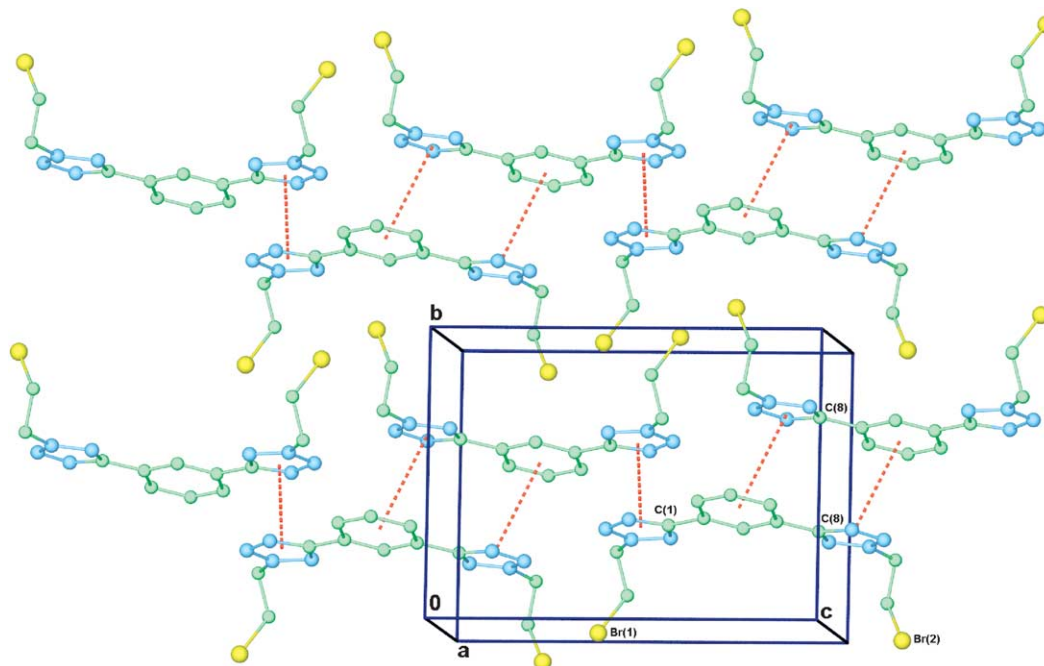
Crystallographic data for the structural analysis on **1b** and **5d** have been deposited with the Cambridge Crystallographic Data Centre, CCDC No. 261954 and 261955, respectively. Copies of this information may be obtained free of charge from [deposit@ccdc.cam.ac.uk](mailto:deposit@ccdc.cam.ac.uk) or [www: http://www.ccdc.cam.ac.uk](http://www.ccdc.cam.ac.uk)

### 3. Conclusions

The reactions of either  $1,n\text{-(HN}_4\text{C)}_2\text{C}_6\text{H}_4$  or  $1,n\text{-(Bu}_3\text{SnN}_4\text{C)}_2\text{C}_6\text{H}_4$  ( $n=2, 3, 4$ ) with 1,2-dibromoethane yields compounds containing pendant bromoethyl or vinyl groups with substitution occurring at either  $1\text{-}N,2\text{-}N'$  or  $2\text{-}N,2\text{-}N'$ , respectively. This is not in agreement with previously published work in this area. The next objective is to improve the reaction yields with a view to attaining our goal of synthesising tetra-tetrazole macrocycles.

### 4. Experimental

$^1\text{H}$  and  $^{13}\text{C}$  NMR ( $\delta$  ppm;  $J$  Hz) spectra were recorded on a JOEL JNM-LA300 FT-NMR spectrometer using saturated  $\text{CDCl}_3$  solutions with  $\text{Me}_4\text{Si}$  reference, unless indicated otherwise, with resolutions of 0.18 Hz and 0.01 ppm, respectively. Infrared spectra ( $\text{cm}^{-1}$ ) were recorded as KBr discs or liquid films between KBr plates using a Nicolet



**Figure 3.** Partial packing diagram for structure **5d**, to illustrate the relative orientation of the pendant groups on the tetrazole rings and the  $\pi$ -stacking interactions.

Impact 410 FT-IR. All uv/vis spectra were recorded on a Shimadzu UV-160A spectrometer. Melting points were measured with a Stuart Scientific melting point apparatus (SMP1) without correction. Microanalysis was carried out at the Microanalytical Laboratory of University College, Dublin. Standard Schlenk techniques were used throughout.

#### 4.1. Syntheses

1,2-(Bu<sub>3</sub>SnN<sub>4</sub>C)<sub>2</sub>C<sub>6</sub>H<sub>4</sub> (**4**), 1,3-(Bu<sub>3</sub>SnN<sub>4</sub>C)<sub>2</sub>C<sub>6</sub>H<sub>4</sub> (**5**) and 1,4-(Bu<sub>3</sub>SnN<sub>4</sub>C)<sub>2</sub>C<sub>6</sub>H<sub>4</sub> (**6**) were prepared as described previously.<sup>4</sup> 1,2-Bis(tetrazol-5-yl)benzene (**1**), 1,3-bis(tetrazol-5-yl)benzene (**2**) and 1,4-bis(tetrazol-5-yl)benzene (**3**) were prepared by a different method to that of Molloy et al.<sup>5</sup> but the analytical data in all cases were the same. All other reagents were commercially obtained and used without further purification. **CAUTION.** Owing to their potentially explosive nature, all preparations of and subsequent reactions with organotin azides were conducted under an inert atmosphere behind a rigid safety screen.

The numbering scheme for the 1,2-, 1,3- and 1,4-bis-tetrazoles are shown in the figures below and all NMR assignments are based on these diagrams (Figs. 4–6).

**4.1.1. 1,2-Bis(tetrazol-5-yl)benzene (**1**)**<sup>5</sup> A suspension of 1,2-dicyanobenzene (12.8 g, 0.10 mol), sodium azide (14.3 g, 0.22 mol), ammonium chloride (11.76 g, 0.22 mol) and lithium chloride (3.0 g, 0.07 mol) in anhydrous dimethylformamide (100 ml) was stirred at 110 °C for 10 h. After this time, the solution was cooled and the insoluble salts were removed by filtration. The solvent was then evaporated under reduced pressure and the residue was dissolved in deionised water (200 ml) and acidified with concentrated HCl (3 ml), to initiate precipitation. The product was filtered, washed with water (3 × 40 ml) and

dried to give a white solid. Recrystallisation from ethanol gave white needle-like crystals (14.55 g, 68% yield), mp 234–236 °C. Analysis: δ<sub>H</sub> (300 MHz, d<sub>6</sub>-DMSO): 7.85 (2H, dd, aromatic-H), 7.91 (2H, d, aromatic-H); δ<sub>C</sub> (300 MHz, d<sub>6</sub>-DMSO): 124.5 (2 i-C<sub>6</sub>H<sub>4</sub>), 130.8 (2 C<sup>2</sup>-C<sub>6</sub>H<sub>4</sub>), 131.3 (2 C<sup>1</sup>-C<sub>6</sub>H<sub>4</sub>), 155.5 (2 CN<sub>4</sub>).

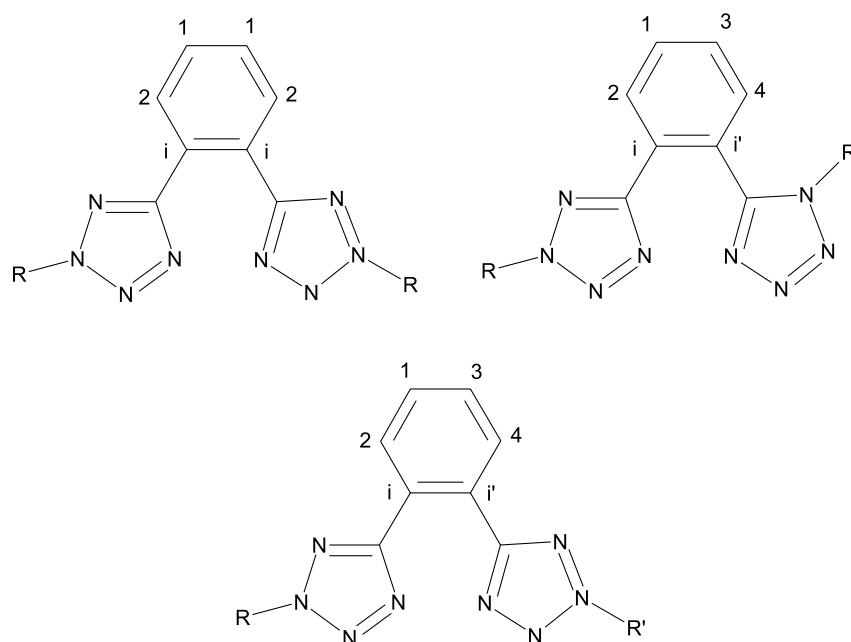
Compounds **2** and **3** were also prepared by the same methodology.

**4.1.2. 1,3-Bis(tetrazol-5-yl)benzene (**2**)**<sup>5</sup> Recrystallisation from ethanol gave white needle-like solid (67.5% yield), mp 268–270 °C. Analysis: δ<sub>H</sub> (300 MHz, d<sub>6</sub>-DMSO): 7.86 (1H, t, H<sup>1</sup>), 8.24 (2H, dd, H<sup>2</sup>), 8.78 (1H, s, H<sup>3</sup>); δ<sub>C</sub> (300 MHz, d<sub>6</sub>-DMSO): 125.3 (C<sup>1</sup>-C<sub>6</sub>H<sub>4</sub>), 125.7 (2*i*-C<sub>6</sub>H<sub>4</sub>), 129.3 (2C<sup>2</sup>-C<sub>6</sub>H<sub>4</sub>), 130.8 (C<sup>3</sup>-C<sub>6</sub>H<sub>4</sub>), 155.5 (2 CN<sub>4</sub>).

**4.1.3. 1,4-Bis(tetrazol-5-yl)benzene (**3**)**<sup>5</sup> Recrystallisation from ethanol gave white needle-like solid (69.7% yield), mp 291–294 °C. Analysis: δ<sub>H</sub> (300 MHz, d<sub>6</sub>-DMSO): 8.27 (4H, 6, H<sup>1</sup>); δ<sub>C</sub> (300 MHz, d<sub>6</sub>-DMSO): 126.7 (2*i*-C<sub>6</sub>H<sub>4</sub>), 127.9 (2C<sup>1</sup>-C<sub>6</sub>H<sub>4</sub>), 155.5 (2CN<sub>4</sub>).

#### 4.2. Synthesis of compounds **1a**, **1b** and **1c**

1,2-Bis[tetrazol-5-yl]benzene (**1**), (1.0 g, 4.7 mmol) was dissolved in methanol (30 ml), and to the stirred solution was added triethylamine (3.0 ml, 2.8 mmol). The resulting solution was heated to reflux for half an hour, and to the hot solution was added 1,2-dibromoethane (2.6 g, 1.4 mmol). The reaction mixture was then heated to reflux for a further 24 h. After cooling, the solvent was removed under reduced pressure to afford the mixture of isomers **1a**, **1b** and **1c**. These isomers were separated by column chromatography on silica gel (initially at the ratio of hexane–ethyl acetate 80:20, followed by the ratio 60:40).



**Figure 4.** Labelling scheme used for central core in the 1,2-bis(tetrazole) derivatives.

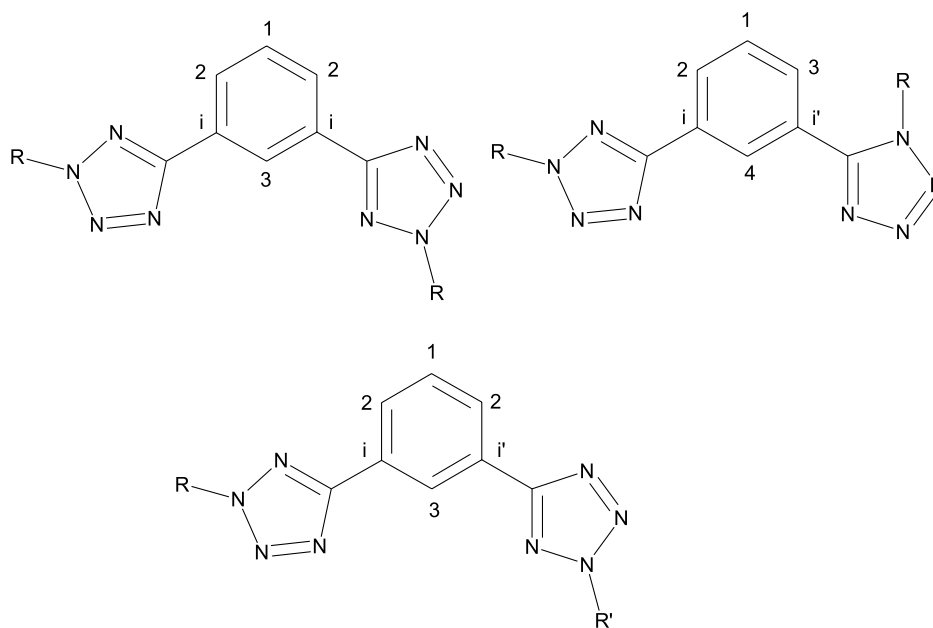


Figure 5. Labelling scheme used for central core in the 1,3-bis(tetrazole) derivatives.

**4.2.1. 1,2-Bis[(2-vinyl)tetrazol-5-yl]benzene (2-*N*,2-*N'*) (1a).** White solid. Analysis: Found: C, 54.52; H, 3.96; N, 42.35. Calcd for C<sub>12</sub>H<sub>10</sub>N<sub>8</sub>: C, 54.13; H, 3.76; N, 42.10. Yield: 13.8%. Mp 95–98 °C;  $\nu_{\max}$  (KBr) 3150, 3090, 2910, 1610, 1648, 1490, 1102, 986, 910, 800 cm<sup>-1</sup>;  $\delta_{\text{H}}$ : 5.25 [dd, 2H<sub>cis</sub>,  $J_{\text{trans}}=8.8$  Hz,  $J_{\text{gem}}=1.8$  Hz, N<sup>2</sup>CH=CH<sub>2</sub>, N<sup>2</sup>CH=CH<sub>2</sub>], 6.35 [dd, 2H<sub>trans</sub>,  $J_{\text{cis}}=15.5$  Hz,  $J_{\text{gem}}=1.6$  Hz, N<sup>2</sup>CH=CH<sub>2</sub>, N<sup>2</sup>CH=CH<sub>2</sub>], 7.59 [dd, 2H<sub>gem</sub>,  $J_{\text{trans}}=15.5$  Hz,  $J_{\text{cis}}=8.8$  Hz, N<sup>2</sup>CH=CH<sub>2</sub>, N<sup>2</sup>CH=CH<sub>2</sub>], 7.65 [d, 2H,  $J=6.6$  Hz, H<sup>1</sup>-C<sub>6</sub>H<sub>4</sub>], 7.85 [d, 2H,  $J=6.5$  Hz, H<sup>2</sup>-C<sub>6</sub>H<sub>4</sub>];  $\delta_{\text{C}}$ : 29.6 [CH<sub>2</sub>], 109.9 [*i*-C<sub>6</sub>H<sub>4</sub>], 130.6 [C<sup>1</sup>-C<sub>6</sub>H<sub>4</sub>], 134.8 [C<sup>2</sup>-C<sub>6</sub>H<sub>4</sub>], 164.2 [CN<sub>4</sub>].

**4.2.2. 1,2-Bis[(2-vinyl)tetrazol-5-yl]benzene (1-*N*,2-*N'*) (1b).** White solid. Analysis: Found: C, 54.45; H, 4.01; N, 42.29. Calcd for C<sub>12</sub>H<sub>10</sub>N<sub>8</sub>: C, 54.13; H, 3.76; N, 42.10. Yield: 10.5%. Mp 110–112 °C;  $\nu_{\max}$  (KBr) 3169, 3109, 2910, 2896, 1615, 1589, 1475, 1090, 956, 910, 779 cm<sup>-1</sup>;  $\delta_{\text{H}}$ : 5.04 [dd, 1H, H<sub>cis</sub>,  $J_{\text{trans}}=8.8$  Hz,  $J_{\text{gem}}=1.5$  Hz, N<sup>1</sup>CH=CH<sub>2</sub>], 5.25 [dd, 1H, H<sub>cis</sub>,  $J_{\text{trans}}=8.6$  Hz,  $J_{\text{gem}}=1.6$  Hz, N<sup>2</sup>CH=CH<sub>2</sub>], 5.78 [dd, 1H, H<sub>trans</sub>,  $J_{\text{cis}}=15.5$  Hz,

$J_{\text{gem}}=1.8$  Hz, N<sup>1</sup>CH=CH<sub>2</sub>], 5.88 [dd, 1H, H<sub>trans</sub>,  $J_{\text{cis}}=13.9$  Hz,  $J_{\text{gem}}=1.3$  Hz, N<sup>2</sup>CH=CH<sub>2</sub>], 6.59 [dd, 1H, H<sub>gem</sub>,  $J_{\text{trans}}=15.5$  Hz,  $J_{\text{cis}}=8.8$  Hz, N<sup>1</sup>CH=CH<sub>2</sub>], 7.30 [dd, 1H, H<sub>gem</sub>,  $J_{\text{trans}}=15.5$  Hz,  $J_{\text{cis}}=8.8$  Hz, N<sup>2</sup>CH=CH<sub>2</sub>], 7.53 [d, 1H,  $J=6.5$  Hz, H<sup>1</sup>-C<sub>6</sub>H<sub>4</sub>], 7.62 [t, 1H,  $J=6.5$  Hz, H<sup>2</sup>-C<sub>6</sub>H<sub>4</sub>], 7.78 [t, 1H,  $J=6.5$  Hz, H<sup>3</sup>-C<sub>6</sub>H<sub>4</sub>], 8.41 [d, 1H,  $J=6.5$  Hz, H<sup>4</sup>-C<sub>6</sub>H<sub>4</sub>];  $\delta_{\text{C}}$ : 109.3 [CH<sub>2</sub>], 109.5 [CH<sub>2</sub>], 122.5 [*i*-C<sub>6</sub>H<sub>4</sub>], 125.6 [CHN<sup>2</sup>], 127.0 [*i'*-C<sub>6</sub>H<sub>4</sub>], 128.8 [CHN<sup>1</sup>], 129.6 [C<sup>1</sup>-C<sub>6</sub>H<sub>4</sub>], 130.9 [C<sup>2</sup>-C<sub>6</sub>H<sub>4</sub>], 131.6 [C<sup>3</sup>-C<sub>6</sub>H<sub>4</sub>], 132.0 [C<sup>4</sup>-C<sub>6</sub>H<sub>4</sub>], 152.6 [N<sup>1</sup>CN<sub>4</sub>], 162.4 [N<sup>2</sup>CN<sub>4</sub>].

**4.2.3. 1,2-Bis[(2-bromoethyl)tetrazol-5-yl]((2-vinyl)tetrazol-5'-yl)benzene (2-*N*,2-*N'*) (1c).** White solid. Analysis: Found: C, 41.76; H, 3.45; N, 32.35. Calcd for C<sub>12</sub>H<sub>11</sub>N<sub>8</sub>Br: C, 41.50; H, 3.17; N, 32.28. Yield: 8.1%. Mp 102–104 °C;  $\nu_{\max}$  (KBr) 3150, 3100, 2890, 1755, 1650, 1648, 1459, 1210, 1175, 1005, 996, 907, 746, 650 cm<sup>-1</sup>;  $\delta_{\text{H}}$ : 3.66 [t, 2H,  $J=6.6$  Hz, CH<sub>2</sub>Br], 4.38 [t, 2H,  $J=6.6$  Hz, NCH<sub>2</sub>], 5.27 [dd, 1H, H<sub>cis</sub>,  $J_{\text{trans}}=8.8$  Hz,  $J_{\text{gem}}=1.5$  Hz, NCH=CH<sub>2</sub>], 5.88 [dd, 1H, H<sub>trans</sub>,  $J_{\text{cis}}=15.4$  Hz,  $J_{\text{gem}}=1.6$  Hz, NCH=CH<sub>2</sub>], 7.35 [dd, 1H, H<sub>gem</sub>,  $J_{\text{trans}}=15.5$  Hz,

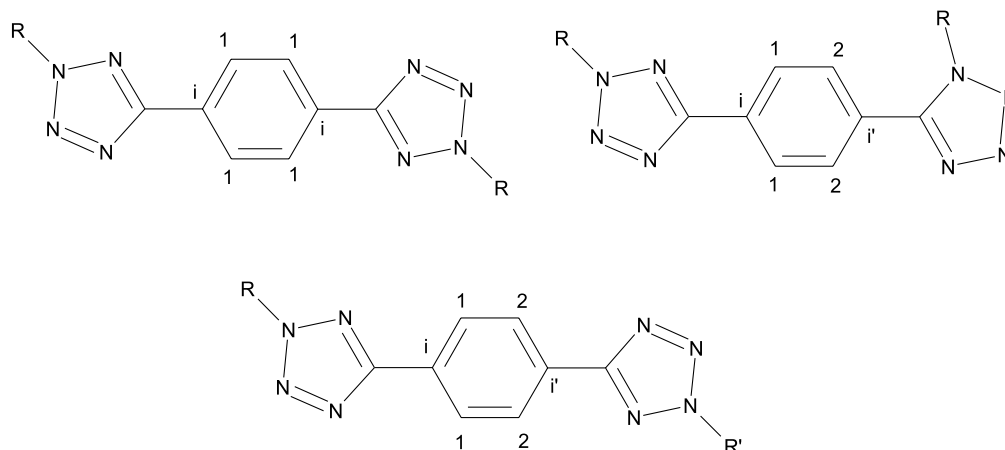


Figure 6. Labelling scheme used for central core in the 1,4-bis(tetrazole) derivatives.

$J_{cis}$  = 8.6 Hz, NCH=CH<sub>2</sub>], 7.54 [d, 1H,  $J$  = 7.0 Hz, H<sup>1</sup>-C<sub>6</sub>H<sub>4</sub>], 7.62 [t, 1H,  $J$  = 7.0 Hz, H<sup>2</sup>-C<sub>6</sub>H<sub>4</sub>], 7.71 [d, 1H,  $J$  = 6.5 Hz, H<sup>3</sup>-C<sub>6</sub>H<sub>4</sub>], 8.37 [t, 1H,  $J$  = 6.5 Hz, H<sup>4</sup>-C<sub>6</sub>H<sub>4</sub>];  $\delta_C$ : 27.0 [CH<sub>2</sub>Br], 48.6 [CH<sub>2</sub>N], 109.4 [CH<sub>2</sub>], 122.5 [*i*-C<sub>6</sub>H<sub>4</sub>], 126.9 [*i'*-C<sub>6</sub>H<sub>4</sub>], 128.7 [C<sup>1</sup>-C<sub>6</sub>H<sub>4</sub>], 129.2 [CHN], 129.6 [C<sup>2</sup>-C<sub>6</sub>H<sub>4</sub>], 130.8 [C<sup>3</sup>-C<sub>6</sub>H<sub>4</sub>], 131.9 [C<sup>4</sup>-C<sub>6</sub>H<sub>4</sub>], 162.6 [CN<sub>4</sub>].

### 4.3. Synthesis of compounds 2a, 2b and 2c

These compounds were prepared by the same general method from 1,3-bis[tetrazol-5-yl]benzene (2), triethylamine and 1,2-dibromoethane, resulting in a mixture of 2a, 2b and 2c which were isolated from each other by column chromatography on silica gel as described previously.

**4.3.1. 1,3-Bis[(2-vinyl)tetrazol-5-yl]benzene (2-N,2-N') (2a).** White solid. Analysis: Found: C, 54.23; H, 3.69; N, 42.45. Calcd for C<sub>12</sub>H<sub>10</sub>N<sub>8</sub>: C, 54.13; H, 3.76; N, 42.10. Yield: 15.6%. Mp 112–116 °C;  $\nu_{max}$  (KBr) 3124, 3100, 2921, 2848, 1699, 1649, 1458, 1213, 1182, 1003, 905, 910, 738 cm<sup>-1</sup>;  $\delta_H$ : 5.43 [dd, 2H, H<sub>cis</sub>,  $J_{trans}$  = 8.8 Hz,  $J_{gem}$  = 1.6 Hz, NCH=CH<sub>2</sub>], 6.33 [dd, 2H, H<sub>trans</sub>,  $J_{cis}$  = 15.5 Hz,  $J_{gem}$  = 1.6 Hz, NCH=CH<sub>2</sub>], 7.62 [dd, 2H, H<sub>gem</sub>,  $J_{trans}$  = 15.5 Hz,  $J_{cis}$  = 8.8 Hz, NCH=CH<sub>2</sub>], 7.66 [t, 1H,  $J$  = 7.0 Hz, H<sup>1</sup>-C<sub>6</sub>H<sub>4</sub>], 8.34 [d, 2H,  $J$  = 7.0 Hz, H<sup>2</sup>-C<sub>6</sub>H<sub>4</sub>], 9.03 [s, 1H, H<sup>3</sup>-C<sub>6</sub>H<sub>4</sub>];  $\delta_C$ : 108.8 [CH<sub>2</sub>], 125.6 [C<sup>1</sup>-C<sub>6</sub>H<sub>4</sub>], 127.8 [*i*-C<sub>6</sub>H<sub>4</sub>], 129.1 [C<sup>2</sup>-C<sub>6</sub>H<sub>4</sub>], 129.6 [CHN], 129.8 [C<sup>3</sup>-C<sub>6</sub>H<sub>4</sub>], 164.2 [CN<sub>4</sub>].

**4.3.2. 1,3-Bis[(2-vinyl)tetrazol-5-yl]benzene (1-N,2-N') (2b).** White solid. Analysis: Found: C, 54.26; H, 3.85; N, 42.32. Calcd for C<sub>12</sub>H<sub>10</sub>N<sub>8</sub>: C, 54.13; H, 3.76; N, 42.10. Yield: 10.2%. Mp 120–122 °C;  $\nu_{max}$  (KBr) 3179, 3067, 2897, 1605, 1596, 1470, 1105, 998, 905, 805 cm<sup>-1</sup>;  $\delta_H$ : 5.46 [dd, 1H, H<sub>cis</sub>,  $J_{trans}$  = 8.8 Hz,  $J_{gem}$  = 1.6 Hz, N<sup>1</sup>CH=CH<sub>2</sub>], 5.52 [dd, 1H, H<sub>cis</sub>,  $J_{trans}$  = 8.8 Hz,  $J_{gem}$  = 1.6 Hz, N<sup>2</sup>CH=CH<sub>2</sub>], 6.27 [dd, 1H, H<sub>trans</sub>,  $J_{cis}$  = 13.2 Hz,  $J_{gem}$  = 1.6 Hz, N<sup>1</sup>CH=CH<sub>2</sub>], 6.32 [dd, 1H, H<sub>trans</sub>,  $J_{cis}$  = 13.6 Hz,  $J_{gem}$  = 1.6 Hz, N<sup>2</sup>CH=CH<sub>2</sub>], 7.15 [dd, 1H, H<sub>gem</sub>,  $J_{trans}$  = 15.4 Hz,  $J_{cis}$  = 8.8 Hz, N<sup>1</sup>CH=CH<sub>2</sub>], 7.59 [dd, 1H, H<sub>gem</sub>,  $J_{trans}$  = 15.7 Hz,  $J_{cis}$  = 8.8 Hz, N<sup>2</sup>CH=CH<sub>2</sub>], 7.75 [t, 1H,  $J$  = 7.7 Hz, H<sup>2</sup>-C<sub>6</sub>H<sub>4</sub>], 7.87 [d, 1H,  $J$  = 7.4 Hz, H<sup>1</sup>-C<sub>6</sub>H<sub>4</sub>], 8.45 [d, 1H,  $J$  = 7.2 Hz, H<sup>3</sup>-C<sub>6</sub>H<sub>4</sub>], 8.55 [s, 1H, H<sup>4</sup>-C<sub>6</sub>H<sub>4</sub>];  $\delta_C$ : 109.3 [CH<sub>2</sub>], 111.8 [CH<sub>2</sub>], 124.4 [*i*-C<sub>6</sub>H<sub>4</sub>], 125.0 [*i'*-C<sub>6</sub>H<sub>4</sub>], 126.0 [C<sup>3</sup>-C<sub>6</sub>H<sub>4</sub>], 127.6 [C<sup>2</sup>-C<sub>6</sub>H<sub>4</sub>], 128.4 [C<sup>1</sup>-C<sub>6</sub>H<sub>4</sub>], 130.0 [CHN<sup>2</sup>], 131.2 [CHN<sup>1</sup>], 135.2 [C<sup>4</sup>-C<sub>6</sub>H<sub>4</sub>], 152.4 [CN<sub>4</sub>], 163.6 [CN<sub>4</sub>].

**4.3.3. 1,3-Bis[[(2-bromoethyl)tetrazol-5-yl][(2-vinyl)tetrazol-5'-yl]]benzene (2-N,2-N') (2c).** White solid. Analysis: Found: C, 41.68; H, 3.33; N, 32.46. Calcd for C<sub>12</sub>H<sub>11</sub>N<sub>8</sub>Br: C, 41.50; H, 3.17; N, 32.28. Yield: 8.3%. Mp 104–106 °C;  $\nu_{max}$  (KBr) 3150, 3100, 2890, 1755, 1650, 1459, 1210, 1175, 1005, 907, 746, 650 cm<sup>-1</sup>;  $\delta_H$ : 3.80 [t, 2H,  $J$  = 6.6 Hz, CH<sub>2</sub>Br], 4.95 [t, 2H,  $J$  = 6.6 Hz, CH<sub>2</sub>N<sup>2</sup>], 5.29 [dd, 1H, H<sub>cis</sub>,  $J_{trans}$  = 9.0 Hz,  $J_{gem}$  = 1.6 Hz, N<sup>2</sup>CH=CH<sub>2</sub>], 6.18 [dd, 1H, H<sub>trans</sub>,  $J_{cis}$  = 15.9 Hz,  $J_{gem}$  = 1.6 Hz, N<sup>2</sup>CH=CH<sub>2</sub>], 7.45 [dd, 1H, H<sub>gem</sub>,  $J_{trans}$  = 15.9 Hz,  $J_{cis}$  = 9.1 Hz, N<sup>2</sup>CH=CH<sub>2</sub>], 7.53 [d, 2H,  $J$  = 8.4 Hz, H<sup>2</sup>-C<sub>6</sub>H<sub>4</sub>], 8.18 [t, 1H,  $J$  = 7.9 Hz, H<sup>1</sup>-C<sub>6</sub>H<sub>4</sub>], 8.85 [s, 1H, H<sup>3</sup>-C<sub>6</sub>H<sub>4</sub>];  $\delta_C$ : 27.0 [CH<sub>2</sub>Br], 54.1 [CH<sub>2</sub>N<sup>2</sup>], 109.1 [CH<sub>2</sub>], 125.6

[C<sup>1</sup>-C<sub>6</sub>H<sub>4</sub>], 127.8 [*i*-C<sub>6</sub>H<sub>4</sub>], 129.1 [C<sup>2</sup>-C<sub>6</sub>H<sub>4</sub>], 129.5 [CHN], 129.8 [C<sup>3</sup>-C<sub>6</sub>H<sub>4</sub>], 164.2 [CN<sub>4</sub>].

### 4.4. Synthesis of compounds 3a, 3b and 3c

These compounds were prepared by the same general method from 1,4-bis[tetrazol-5-yl]benzene (3), triethylamine and 1,2-dibromoethane resulting in a mixture of 3a, 3b and 3c which were individually isolated by column chromatography on silica gel as previously described.

**4.4.1. 1,4-Bis[(2-vinyl)tetrazol-5-yl]benzene (2-N,2-N') (3a).** White solid. Analysis: Found: C, 54.36; H, 4.18; N, 42.08. Calcd for C<sub>12</sub>H<sub>10</sub>N<sub>8</sub>: C, 54.13; H, 3.76; N, 42.10. Yield: 12.8%. Mp 124–126 °C;  $\nu_{max}$  (KBr) 3148, 3108, 2910, 2894, 1690, 1650, 1429, 1150, 1005, 990, 913, 810 cm<sup>-1</sup>;  $\delta_H$ : 5.44 [dd, 2H, H<sub>cis</sub>,  $J_{trans}$  = 9.7 Hz,  $J_{gem}$  = 1.6 Hz, NCH=CH<sub>2</sub>], 6.32 [dd, 2H, H<sub>trans</sub>,  $J_{cis}$  = 15.5 Hz,  $J_{gem}$  = 1.2 Hz, NCH=CH<sub>2</sub>], 7.56 [dd, 2H, H<sub>gem</sub>,  $J_{trans}$  = 12.2 Hz,  $J_{cis}$  = 8.8 Hz, NCH=CH<sub>2</sub>], 7.81 [s, 4H, C<sub>6</sub>H<sub>4</sub>];  $\delta_C$ : 108.9 [CH<sub>2</sub>], 127.5 [C<sup>1</sup>-C<sub>6</sub>H<sub>4</sub>], 129.0 [*i*-C<sub>6</sub>H<sub>4</sub>], 129.8 [CHN], 164.3 [CN<sub>4</sub>].

**4.4.2. 1,4-Bis[(2-vinyl)tetrazol-5-yl]benzene (1-N,2-N') (3b).** White solid. Analysis: Found: C, 54.26; H, 3.56; N, 42.33. Calcd for C<sub>12</sub>H<sub>10</sub>N<sub>8</sub>: C, 54.13; H, 3.76; N, 42.10. Yield: 11.6%. Mp 116–120 °C;  $\nu_{max}$  (KBr) 3105, 3089, 2928, 2890, 1603, 1567, 1470, 1096, 980, 905, 803 cm<sup>-1</sup>;  $\delta_H$ : 5.47 [dd, 1H, H<sub>cis</sub>,  $J_{trans}$  = 8.8 Hz,  $J_{gem}$  = 1.5 Hz, N<sup>1</sup>CH=CH<sub>2</sub>], 5.51 [dd, 1H, H<sub>cis</sub>,  $J_{trans}$  = 8.6 Hz,  $J_{gem}$  = 1.5 Hz, N<sup>2</sup>CH=CH<sub>2</sub>], 6.27 [dd, 1H, H<sub>trans</sub>,  $J_{cis}$  = 15.5 Hz,  $J_{gem}$  = 1.6 Hz, N<sup>1</sup>CH=CH<sub>2</sub>], 6.33 [dd, 1H, H<sub>trans</sub>,  $J_{cis}$  = 15.4 Hz,  $J_{gem}$  = 1.3 Hz, N<sup>2</sup>CH=CH<sub>2</sub>], 7.12 [dd, 1H, H<sub>gem</sub>,  $J_{trans}$  = 15.5 Hz,  $J_{cis}$  = 8.7 Hz, N<sup>1</sup>CH=CH<sub>2</sub>], 7.59 [dd, 1H, H<sub>gem</sub>,  $J_{trans}$  = 15.4 Hz,  $J_{cis}$  = 8.8 Hz, N<sup>2</sup>CH=CH<sub>2</sub>], 7.89 [d, 2H,  $J$  = 8.2 Hz, H<sup>2</sup>-C<sub>6</sub>H<sub>4</sub>], 8.42 [d, 2H,  $J$  = 8.2 Hz, H<sup>1</sup>-C<sub>6</sub>H<sub>4</sub>];  $\delta_C$ : 109.2 [CH<sub>2</sub>], 111.8 [CH<sub>2</sub>], 125.4 [*i*-C<sub>6</sub>H<sub>4</sub>], 126.0 [*i'*-C<sub>6</sub>H<sub>4</sub>], 127.9 [C<sup>1</sup>-C<sub>6</sub>H<sub>4</sub>], 128.2 [C<sup>2</sup>-C<sub>6</sub>H<sub>4</sub>], 129.9 [CHN<sup>2</sup>], 133.1 [CHN<sup>1</sup>], 152.4 [CN<sub>4</sub>], 163.6 [CN<sub>4</sub>].

**4.4.3. 1,4-Bis[[(2-bromoethyl)tetrazol-5-yl][(2-vinyl)tetrazol-5'-yl]]benzene (2-N,2-N') (3c).** White solid. Analysis: Found: C, 41.44; H, 3.36; N, 32.45. Calcd for C<sub>12</sub>H<sub>11</sub>N<sub>8</sub>Br: C, 41.50; H, 3.17; N, 32.28. Yield: 9.8%. Mp 128–130 °C;  $\nu_{max}$  (KBr) 3128, 3094, 2905, 1610, 1548, 1460, 1238, 1100, 1003, 960, 838, 610 cm<sup>-1</sup>;  $\delta_H$ : 3.94 [t, 2H,  $J$  = 6.6 Hz, CH<sub>2</sub>Br], 5.08 [t, 2H,  $J$  = 6.6 Hz, CH<sub>2</sub>N<sup>2</sup>], 5.45 [dd, 1H, H<sub>cis</sub>,  $J_{trans}$  = 8.8 Hz,  $J_{gem}$  = 1.6 Hz, N<sup>2</sup>CH=CH<sub>2</sub>], 6.31 [dd, 1H, H<sub>trans</sub>,  $J_{cis}$  = 15.6 Hz,  $J_{gem}$  = 1.5 Hz, N<sup>2</sup>CH=CH<sub>2</sub>], 7.58 [dd, 1H, H<sub>gem</sub>,  $J_{trans}$  = 15.5 Hz,  $J_{cis}$  = 8.8 Hz, N<sup>2</sup>CH=CH<sub>2</sub>], 8.30 [d, 2H,  $J$  = 8.8 Hz, C<sup>1</sup>-C<sub>6</sub>H<sub>4</sub>], 8.34 [d, 2H,  $J$  = 8.8 Hz, C<sup>2</sup>-C<sub>6</sub>H<sub>4</sub>];  $\delta_C$ : 27.0 [CH<sub>2</sub>Br], 54.1 [CH<sub>2</sub>N], 108.8 [CH<sub>2</sub>], 127.5 [C<sup>1</sup>-C<sub>6</sub>H<sub>4</sub>], 127.7 [C<sup>2</sup>-C<sub>6</sub>H<sub>4</sub>], 128.8 [*i*-C<sub>6</sub>H<sub>4</sub>], 129.1 [*i'*-C<sub>6</sub>H<sub>4</sub>], 129.8 [CHN], 164.8 [CN<sub>4</sub>].

### 4.5. Synthesis of compounds 4a, 4b, 4c and 4e

1,2-Bis[2-(tributylstannyl)tetrazol-5-yl]benzene (4) (1.0 g, 1.25 mmol) was heated to 120 °C in 1,2-dibromoethane (5.5 ml) for 24 h. A viscous solution resulted which, on cooling, yielded a mixture of 4a, 4b, 4c and 4e. These were individually isolated by column chromatography on silica gel as previously described.

**4.5.1. 1,2-Bis[[(2-bromoethyl)tetrazol-5-yl]((2-vinyl)tetrazol-5'-yl)]benzene (2-*N*,2-*N'*) (4a).** White solid.

Analysis: Found: C, 41.69; H, 3.42; N, 32.08. Calcd for  $C_{12}H_{11}N_8Br$ : C, 41.50; H, 3.17; N, 32.28. Yield: 10.6%. Mp 102–104 °C;  $\nu_{max}$  (KBr) 3100, 3098, 2954, 2879, 1605, 1545, 1460, 1256, 1100, 1010, 990, 905, 850, 602  $cm^{-1}$ ;  $\delta_H$ : 3.66 [t, 2H,  $J=6.6$  Hz,  $CH_2Br$ ], 4.38 [t, 2H,  $J=6.6$  Hz,  $N^2CH=CH_2$ ], 5.27 [dd, 1H,  $H_{cis}$ ,  $J_{trans}=8.8$  Hz,  $J_{gem}=1.5$  Hz,  $N^2CH=CH_2$ ], 5.88 [dd, 1H,  $H_{trans}$ ,  $J_{cis}=15.4$  Hz,  $J_{gem}=1.6$  Hz,  $N^2CH=CH_2$ ], 7.35 [dd, 1H,  $H_{gem}$ ,  $J_{trans}=15.5$  Hz,  $J_{cis}=8.6$  Hz,  $N^2CH=CH_2$ ], 7.54 [d, 1H,  $J=7.0$  Hz,  $H^1-C_6H_4$ ], 7.62 [t, 1H,  $J=7.0$  Hz,  $H^2-C_6H_4$ ], 7.71 [t, 1H,  $J=6.5$  Hz,  $H^3-C_6H_4$ ], 8.37 [d, 1H,  $J=6.5$  Hz,  $H^4-C_6H_4$ ];  $\delta_C$ : 27.0 [ $CH_2Br$ ], 48.6 [ $CH_2N$ ], 109.4 [ $CH_2$ ], 122.5 [ $i-C_6H_4$ ], 126.9 [ $i'-C_6H_4$ ], 128.7 [ $C^1-C_6H_4$ ], 129.2 [ $CHN$ ], 129.6 [ $C^2-C_6H_4$ ], 130.8 [ $C^3-C_6H_4$ ], 131.9 [ $C^4-C_6H_4$ ], 162.6 [ $CN_4$ ].

**4.5.2. 1,2-Bis[[(2-bromoethyl)tetrazol-5-yl]((2-vinyl)tetrazol-5'-yl)]benzene (1-*N*,2-*N'*) (4b).** White solid.

Analysis: Found: C, 41.89; H, 3.36; N, 32.42. Calcd for  $C_{12}H_{11}N_8Br$ : C, 41.50; H, 3.17; N, 32.28. Yield: 10.2%. Mp 108–112 °C;  $\nu_{max}$  (KBr) 3100, 3098, 2954, 2879, 1605, 1545, 1460, 1256, 1100, 1010, 990, 905, 850, 602  $cm^{-1}$ ;  $\delta_H$ : 3.92 [t, 2H,  $J=6.6$  Hz,  $CH_2Br$ ], 4.92 [t, 2H,  $J=6.6$  Hz,  $CH_2N^1$ ], 5.50 [dd, 1H,  $H_{cis}$ ,  $J_{trans}=8.6$  Hz,  $J_{gem}=1.5$  Hz,  $N^2CH=CH_2$ ], 6.28 [dd, 1H,  $H_{trans}$ ,  $J_{cis}=15.4$  Hz,  $J_{gem}=1.3$  Hz,  $N^2CH=CH_2$ ], 7.15 [dd, 1H,  $H_{gem}$ ,  $J_{trans}=15.3$  Hz,  $J_{cis}=8.6$  Hz,  $N^2CH=CH_2$ ], 7.61 [d, 1H,  $J=7.0$  Hz,  $H^1-C_6H_4$ ], 7.69 [t, 1H,  $J=7.0$  Hz,  $H^2-C_6H_4$ ], 7.78 [t, 1H,  $J=7.0$  Hz,  $H^3-C_6H_4$ ], 8.38 [d, 1H,  $J=7.0$  Hz,  $H^4-C_6H_4$ ];  $\delta_C$ : 27.0 [ $CH_2Br$ ], 54.0 [ $CH_2N^1$ ], 112.0 [ $CH_2$ ], 123.4 [ $i-C_6H_4$ ], 126.1 [ $i'-C_6H_4$ ], 127.5 [ $C^1-C_6H_4$ ], 129.8 [ $C^2-C_6H_4$ ], 130.2 [ $CHN^2$ ], 132.2 [ $C^3-C_6H_4$ ], 132.3 [ $C^4-C_6H_4$ ], 152.6 [ $CN_4$ ], 162.4 [ $CN_4$ ].

**4.5.3. 1,2-Bis[(2-bromoethyl)tetrazol-5-yl]benzene (1-*N*,2-*N'*) (4c).** White solid. Analysis: Found: C, 33.50; H, 2.96; N, 26.25. Calcd for  $C_{12}H_{12}N_8Br_2$ : C, 33.70; H, 2.81; N, 26.10. Yield: 8.3%. Mp 124–126 °C;  $\nu_{max}$  (KBr) 3099, 3087, 2850, 1543, 1460, 1276, 1090, 1005, 830, 605  $cm^{-1}$ ;  $\delta_H$ : 3.70 [t, 2H,  $J=6.6$  Hz,  $CH_2Br$ ], 3.74 [t, 2H,  $J=6.6$  Hz,  $CH_2Br$ ], 4.42 [t, 2H,  $J=6.6$  Hz,  $CH_2N^1$ ], 4.89 [t, 2H,  $J=6.6$  Hz,  $CH_2N^2$ ], 7.61 [d, 1H,  $J=7.0$  Hz,  $H^1-C_6H_4$ ], 7.69 [t, 1H,  $J=7.0$  Hz,  $H^2-C_6H_4$ ], 7.78 [t, 1H,  $J=7.0$  Hz,  $H^3-C_6H_4$ ], 8.38 [d, 1H,  $J=7.0$  Hz,  $H^4-C_6H_4$ ];  $\delta_C$ : 27.2 [ $CH_2Br$ ], 48.9 [ $CH_2N$ ], 54.4 [ $CH_2N^2$ ], 122.7 [ $i-C_6H_4$ ], 127.5 [ $i'-C_6H_4$ ], 129.8 [ $C^1-C_6H_4$ ], 131.0 [ $C^2-C_6H_4$ ], 132.2 [ $C^3-C_6H_4$ ], 132.3 [ $C^4-C_6H_4$ ], 154.8 [ $CN_4$ ], 163.6 [ $CN_4$ ].
**4.5.4. 1,2-Bis[(2-vinyl)tetrazol-5-yl]benzene (1-*N*,2-*N'*) (4e).** White solid. Analysis: Found: C, 54.33; H, 3.99; N, 42.35. Calcd for  $C_{12}H_{10}N_8$ : C, 54.13; H, 3.76; N, 42.10. Yield: 6.4%. Mp 92–94 °C.  $\nu_{max}$  (KBr) 3169, 3109, 2910, 2896, 1615, 1589, 1475, 1090, 956, 910, 779  $cm^{-1}$ ;  $\delta_H$ : 5.04 [dd, 1H,  $H_{cis}$ ,  $J_{trans}=8.8$  Hz,  $J_{gem}=1.5$  Hz,  $N^1CH=CH_2$ ], 5.25 [dd, 1H,  $H_{cis}$ ,  $J_{trans}=8.6$  Hz,  $J_{gem}=1.6$  Hz,  $N^2CH=CH_2$ ], 5.78 [dd, 1H,  $H_{trans}$ ,  $J_{cis}=15.5$  Hz,  $J_{gem}=1.8$  Hz,  $N^1CH=CH_2$ ], 5.88 [dd, 1H,  $H_{trans}$ ,  $J_{cis}=13.9$  Hz,  $J_{gem}=1.3$  Hz,  $N^2CH=CH_2$ ], 6.59 [dd, 1H,  $H_{gem}$ ,  $J_{trans}=15.5$  Hz,  $J_{cis}=8.8$  Hz,  $N^1CH=CH_2$ ], 7.30 [dd, 1H,  $H_{gem}$ ,  $J_{trans}=15.5$  Hz,  $J_{cis}=8.8$  Hz,  $N^2CH=CH_2$ ], 7.53 [d, 1H,  $J=6.5$  Hz,  $H^1-C_6H_4$ ], 7.62 [t, 1H,  $J=6.5$  Hz,  $H^2-C_6H_4$ ], 7.78 [t, 1H,  $J=6.5$  Hz,  $H^3-C_6H_4$ ], 8.41 [d, 1H,  $J=$ 

6.5 Hz,  $H^4-C_6H_4$ ];  $\delta_C$ : 109.3 [ $CH_2$ ], 109.5 [ $CH_2$ ], 122.5 [ $i-C_6H_4$ ], 125.6 [ $CHN^2$ ], 127.0 [ $i'-C_6H_4$ ], 128.8 [ $CHN^1$ ], 129.6 [ $C^1-C_6H_4$ ], 130.9 [ $C^2-C_6H_4$ ], 131.6 [ $C^3-C_6H_4$ ], 132.0 [ $C^4-C_6H_4$ ], 152.6 [ $CN_4$ ], 162.4 [ $CN_4$ ].

**4.6. Synthesis of compounds 5a, 5b, 5c and 5d**

These compounds were prepared by the same method as above but using 1,3-bis[2-(tributylstannyl)tetrazol-5-yl]benzene (**5**) instead. A viscous solution resulted again which, on cooling, yielded a mixture of **5a**, **5b**, **5c** and **5d**. These were isolated by column chromatography on silica gel as previously described.

**4.6.1. 1,3-Bis[[(2-bromoethyl)tetrazol-5-yl]((2-vinyl)tetrazol-5'-yl)]benzene (2-*N*,2-*N'*) (5a).** White solid.

Analysis: Found: C, 41.45; H, 3.55; N, 32.25. Calcd for  $C_{12}H_{11}N_8Br$ : C, 41.50; H, 3.17; N, 32.28. Yield: 11.8%. Mp 104–106 °C;  $\nu_{max}$  (KBr) 3150, 3100, 2890, 1755, 1650, 1459, 1210, 1175, 1005, 907, 746, 650  $cm^{-1}$ ;  $\delta_H$ : 3.93 [t, 2H,  $J=6.6$  Hz,  $CH_2Br$ ], 5.08 [t, 2H,  $J=6.6$  Hz,  $CH_2N^2$ ], 5.44 [dd, 1H,  $H_{cis}$ ,  $J_{trans}=9.0$  Hz,  $J_{gem}=1.7$  Hz,  $N^2CH=CH_2$ ], 6.33 [dd, 1H,  $H_{trans}$ ,  $J_{cis}=15.7$  Hz,  $J_{gem}=1.6$  Hz,  $N^2CH=CH_2$ ], 7.58 [dd, 1H,  $H_{gem}$ ,  $J_{trans}=17.9$  Hz,  $J_{cis}=7.7$  Hz,  $N^2CH=CH_2$ ], 7.63 [d, 2H,  $J=8.4$  Hz,  $H^2-C_6H_4$ ], 8.39 [t, 1H,  $J=7.9$  Hz,  $H^1-C_6H_4$ ], 8.99 [s, 1H,  $H^3-C_6H_4$ ];  $\delta_C$ : 27.0 [ $CH_2Br$ ], 54.2 [ $CH_2N^2$ ], 109.1 [ $CH_2$ ], 125.6 [ $C^1-C_6H_4$ ], 127.5 [ $i-C_6H_4$ ], 129.0 [ $C^2-C_6H_4$ ], 129.5 [ $CHN$ ], 130.0 [ $C^3-C_6H_4$ ], 164.2 [ $CN_4$ ].

**4.6.2. 1,3-Bis[[(2-bromoethyl)tetrazol-5-yl]((2-vinyl)tetrazol-5'-yl)]benzene (1-*N*,2-*N'*) (5b).** White solid.

Analysis: Found: C, 41.54; H, 3.34; N, 32.48. Calcd for  $C_{12}H_{11}N_8Br$ : C, 41.50; H, 3.17; N, 32.28. Yield: 9.8%. Mp 99–100 °C;  $\nu_{max}$  (KBr) 3104, 3098, 2950, 1605, 1540, 1463, 1250, 1110, 1005, 998, 905, 856  $cm^{-1}$ ;  $\delta_H$ : 3.90 [t, 2H,  $J=6.6$  Hz,  $CH_2Br$ ], 4.86 [t, 2H,  $J=6.6$  Hz,  $CH_2N^1$ ], 5.49 [dd, 1H,  $H_{cis}$ ,  $J_{trans}=8.8$  Hz,  $J_{gem}=1.7$  Hz,  $N^2CH=CH_2$ ], 6.28 [dd, 1H,  $H_{trans}$ ,  $J_{cis}=15.3$  Hz,  $J_{gem}=1.8$  Hz,  $N^2CH=CH_2$ ], 7.15 [dd, 1H,  $H_{gem}$ ,  $J_{trans}=15.4$  Hz,  $J_{cis}=8.8$  Hz,  $N^2CH=CH_2$ ], 7.71 [t, 1H,  $J=7.9$  Hz,  $H^1-C_6H_4$ ], 7.84 [d, 1H,  $J=8.4$  Hz,  $H^2-C_6H_4$ ], 8.42 [d, 1H,  $J=8.4$  Hz,  $H^3-C_6H_4$ ], 8.53 [s, 1H,  $H^4-C_6H_4$ ];  $\delta_C$ : 27.1 [ $CH_2Br$ ], 54.3 [ $CH_2N^1$ ], 111.9 [ $CH_2$ ], 125.2 [ $i-C_6H_4$ ], 126.0 [ $i'-C_6H_4$ ], 127.4 [ $C^3-C_6H_4$ ], 127.6 [ $C^2-C_6H_4$ ], 129.9 [ $C^1-C_6H_4$ ], 130.2 [ $CHN^2$ ], 133.8 [ $C^4-C_6H_4$ ], 156.4 [ $CN_4$ ], 162.6 [ $CN_4$ ].

**4.6.3. 1,3-Bis[(2-bromoethyl)tetrazol-5-yl]benzene (1-*N*,2-*N'*) (5c).** White solid. Analysis: Found: C, 33.86; H, 3.01; N, 26.35. Calcd for  $C_{12}H_{12}N_8Br_2$ : C, 33.70; H, 2.81; N, 26.10. Yield: 7.6%. Mp 130–132 °C;  $\nu_{max}$  (Nujol) (KBr) 3109, 3086, 2910, 2850, 1545, 1456, 1270, 1105, 1003, 850, 715, 615  $cm^{-1}$ ;  $\delta_H$ : 3.87 [t, 2H,  $J=6.6$  Hz,  $CH_2Br$ ], 3.95 [t, 2H,  $J=6.6$  Hz,  $CH_2Br$ ], 4.87 [t, 2H,  $J=6.6$  Hz,  $CH_2N^1$ ], 5.10 [t, 2H,  $J=6.6$  Hz,  $CH_2N^2$ ], 7.83 [t, 1H,  $J=7.9$  Hz,  $H^1-C_6H_4$ ], 7.88 [d, 1H,  $J=8.4$  Hz,  $H^2-C_6H_4$ ], 8.42 [d, 1H,  $J=8.4$  Hz,  $H^3-C_6H_4$ ], 8.51 [s, 1H,  $H^4-C_6H_4$ ];  $\delta_C$ : 27.6 [ $CH_2Br$ ], 27.9 [ $CH_2Br$ ], 49.0 [ $CH_2N^1$ ], 54.2 [ $CH_2N^2$ ], 124.6 [ $i-C_6H_4$ ], 125.0 [ $i'-C_6H_4$ ], 127.4 [ $C^1-C_6H_4$ ], 128.6 [ $C^2-C_6H_4$ ], 129.9 [ $C^2-C_6H_4$ ], 130.2 [ $C^3-C_6H_4$ ], 154.5 [ $CN_4$ ], 164.4 [ $CN_4$ ].



**4.6.4. 1,3-Bis[(2-bromoethyl)tetrazol-5-yl]benzene (2-*N*,2-*N'*) (5d).** White solid. Analysis: Found: C, 33.58; H, 2.98; N, 26.25. Calcd for C<sub>12</sub>H<sub>12</sub>N<sub>8</sub>Br<sub>2</sub>: C, 33.70; H, 2.81; N, 26.10. Yield: 6.3%. Mp 118–122 °C;  $\nu_{\max}$  (KBr) 3109, 3086, 2910, 2850, 1545, 1456, 1270, 1105, 1003, 850, 715, 615 cm<sup>-1</sup>;  $\delta_{\text{H}}$ : 3.94 [t, 4H,  $J=6.6$  Hz, CH<sub>2</sub>Br], 5.09 [t, 4H,  $J=6.6$  Hz, CH<sub>2</sub>N], 7.64 [t, 1H,  $J=7.9$  Hz, H<sup>1</sup>-C<sub>6</sub>H<sub>4</sub>], 8.29 [d, 2H,  $J=8.4$  Hz, H<sup>2</sup>-C<sub>6</sub>H<sub>4</sub>], 8.94 [s, 1H, H<sup>3</sup>-C<sub>6</sub>H<sub>4</sub>];  $\delta_{\text{C}}$ : 27.7 [CH<sub>2</sub>Br], 54.1 [CH<sub>2</sub>N], 125.4 [*i*-C<sub>6</sub>H<sub>4</sub>], 128.0 [C<sup>1</sup>-C<sub>6</sub>H<sub>4</sub>], 128.8 [C<sup>2</sup>-C<sub>6</sub>H<sub>4</sub>], 129.6 [C<sup>3</sup>-C<sub>6</sub>H<sub>4</sub>], 164.9 [CN<sub>4</sub>].

#### 4.7. Synthesis of compounds 6a, 6b, 6c and 6e

These compounds were prepared by the same method from 1,4-bis[2-(tributylstannyl)tetrazol-5-yl]benzene (6) and 1,2-dibromoethane. A viscous solution resulted again which, on cooling, yielded a mixture of 6a, 6b, 6c and 6e. These were isolated by column chromatography on silica gel as previously described.

**4.7.1. 1,4-Bis[((2-bromoethyl)tetrazol-5-yl)((2-vinyl)tetrazol-5'-yl)]benzene (2-*N*,2-*N'*) (6a).** White solid. Analysis: Found: C, 41.69; H, 3.39; N, 32.05. Calcd for C<sub>12</sub>H<sub>11</sub>N<sub>8</sub>Br: C, 41.50; H, 3.17; N, 32.28. Yield: 10.9%. Mp 128–130 °C;  $\nu_{\max}$  (KBr) 3128, 3094, 2905, 1610, 1548, 1460, 1238, 1100, 1003, 960, 838, 610 cm<sup>-1</sup>;  $\delta_{\text{H}}$ : 3.94 [t, 2H,  $J=6.6$  Hz, CH<sub>2</sub>Br], 5.08 [t, 2H,  $J=6.6$  Hz, CH<sub>2</sub>N<sup>2</sup>], 5.45 [dd, 1H, H<sub>cis</sub>,  $J_{\text{trans}}=8.6$  Hz,  $J_{\text{gem}}=1.5$  Hz, N<sup>2</sup>CH=CH<sub>2</sub>], 6.33 [dd, 1H, H<sub>trans</sub>,  $J_{\text{cis}}=15.7$  Hz,  $J_{\text{gem}}=1.6$  Hz, N<sup>2</sup>CH=CH<sub>2</sub>], 7.58 [dd, 1H, H<sub>gem</sub>,  $J_{\text{trans}}=15.5$  Hz,  $J_{\text{cis}}=8.8$  Hz, N<sup>2</sup>CH=CH<sub>2</sub>], 8.30 [d, 2H,  $J=8.8$  Hz, C<sup>1</sup>-C<sub>6</sub>H<sub>4</sub>], 8.33 [d, 2H,  $J=8.8$  Hz, C<sup>1</sup>-C<sub>6</sub>H<sub>4</sub>];  $\delta_{\text{C}}$ : 26.9 [CH<sub>2</sub>Br], 54.3 [CH<sub>2</sub>N<sup>2</sup>], 108.8 [CH<sub>2</sub>], 127.6 [C<sup>1</sup>-C<sub>6</sub>H<sub>4</sub>], 127.9 [C<sup>2</sup>-C<sub>6</sub>H<sub>4</sub>], 128.8 [*i*-C<sub>6</sub>H<sub>4</sub>], 129.1 [*i'*-C<sub>6</sub>H<sub>4</sub>], 129.8 [CHN<sup>2</sup>], 164.8 [CN<sub>4</sub>].

**4.7.2. 1,4-Bis[((2-bromoethyl)tetrazol-5-yl)((2-vinyl)tetrazol-5'-yl)]benzene (1-*N*,2-*N'*) (6b).** White solid. Analysis: Found: C, 41.69; H, 3.28; N, 32.11. Calcd for C<sub>12</sub>H<sub>11</sub>N<sub>8</sub>Br: C, 41.50; H, 3.17; N, 32.28. Yield: 10.1%. Mp 122–126 °C;  $\nu_{\max}$  (Nujol) (KBr) 3128, 3094, 2905, 1610, 1548, 1460, 1238, 1100, 1003, 960, 838, 610 cm<sup>-1</sup>;  $\delta_{\text{H}}$ : 3.94 [t, 2H,  $J=6.6$  Hz, CH<sub>2</sub>Br], 5.10 [t, 2H,  $J=6.6$  Hz, CH<sub>2</sub>N<sup>1</sup>], 5.52 [dd, 1H, H<sub>cis</sub>,  $J_{\text{trans}}=8.6$  Hz,  $J_{\text{gem}}=1.5$  Hz, N<sup>2</sup>CH=CH<sub>2</sub>], 6.27 [dd, 1H, H<sub>trans</sub>,  $J_{\text{cis}}=15.4$  Hz,  $J_{\text{gem}}=1.3$  Hz, N<sup>2</sup>CH=CH<sub>2</sub>], 7.14 [dd, 1H, H<sub>gem</sub>,  $J_{\text{trans}}=15.3$  Hz,  $J_{\text{cis}}=8.6$  Hz, N<sup>2</sup>CH=CH<sub>2</sub>], 7.88 [d, 2H,  $J=8.8$  Hz, C<sup>1</sup>-C<sub>6</sub>H<sub>4</sub>], 8.38 [d, 2H,  $J=8.8$  Hz, C<sup>2</sup>-C<sub>6</sub>H<sub>4</sub>];  $\delta_{\text{C}}$ : 26.9 [CH<sub>2</sub>Br], 54.2 [CH<sub>2</sub>N<sup>1</sup>], 111.8 [CH<sub>2</sub>], 125.1 [*i*-C<sub>6</sub>H<sub>4</sub>], 126.1 [*i'*-C<sub>6</sub>H<sub>4</sub>], 127.6 [C<sup>1</sup>-C<sub>6</sub>H<sub>4</sub>], 129.8 [C<sup>2</sup>-C<sub>6</sub>H<sub>4</sub>], 130.2 [CHN<sup>2</sup>], 152.4 [CN<sub>4</sub>], 164.2 [CN<sub>4</sub>].

**4.7.3. 1,4-Bis[(2-bromoethyl)tetrazol-5-yl]benzene (1-*N*,2-*N'*) (6c).** White solid. Analysis: Found: C, 33.33; H, 2.74; N, 26.08. Calcd for C<sub>12</sub>H<sub>12</sub>N<sub>8</sub>Br<sub>2</sub>: C, 33.70; H, 2.81; N, 26.10. Yield: 8.1%. Mp 156–160 °C;  $\nu_{\max}$  (KBr) 3105, 3090, 2897, 1543, 1459, 1225, 1108, 1010, 897, 776, 609 cm<sup>-1</sup>;  $\delta_{\text{H}}$ : 3.92 [t, 2H,  $J=6.6$  Hz, CH<sub>2</sub>Br], 3.94 [t, 2H,  $J=6.6$  Hz, CH<sub>2</sub>Br], 4.38 [t, 2H,  $J=6.6$  Hz, CH<sub>2</sub>N<sup>1</sup>], 5.07 [t, 2H,  $J=6.6$  Hz, CH<sub>2</sub>N<sup>2</sup>], 8.15 [d, 2H,  $J=8.8$  Hz, H<sup>1</sup>-C<sub>6</sub>H<sub>4</sub>], 8.22 [d, 2H,  $J=8.8$  Hz, H<sup>2</sup>-C<sub>6</sub>H<sub>4</sub>].  $\delta_{\text{C}}$ : 27.7 [CH<sub>2</sub>Br], 54.2 [CH<sub>2</sub>N<sup>1</sup>], 54.4 [CH<sub>2</sub>N<sup>2</sup>], 116.8 [*i*-C<sub>6</sub>H<sub>4</sub>], 117.0 [*i'*-C<sub>6</sub>H<sub>4</sub>],

130.2 [C<sup>1</sup>-C<sub>6</sub>H<sub>4</sub>], 132.8 [C<sup>2</sup>-C<sub>6</sub>H<sub>4</sub>], 156.3 [CN<sub>4</sub>], 164.1 [CN<sub>4</sub>].

**4.7.4. 1,4-Bis[(2-vinyl)tetrazol-5-yl]benzene (1-*N*,2-*N'*) (6e).** White solid. Analysis: Found: C, 54.08; H, 3.49; N, 42.28. Calcd for C<sub>12</sub>H<sub>10</sub>N<sub>8</sub>: C, 54.13; H, 3.76; N, 42.10. Yield: 7.3%. Mp 116–120 °C;  $\nu_{\max}$  (KBr) 3099, 3089, 2928, 2894, 1610, 1568, 1475, 1106, 1008, 980, 905, 810 cm<sup>-1</sup>;  $\delta_{\text{H}}$ : 5.49 [dd, 1H, H<sub>cis</sub>,  $J_{\text{trans}}=8.8$  Hz,  $J_{\text{gem}}=1.5$  Hz, N<sup>1</sup>CH=CH<sub>2</sub>], 5.52 [dd, 1H, H<sub>cis</sub>,  $J_{\text{trans}}=8.8$  Hz,  $J_{\text{gem}}=1.5$  Hz, N<sup>2</sup>CH=CH<sub>2</sub>], 6.29 [dd, 1H, H<sub>trans</sub>,  $J_{\text{cis}}=15.5$  Hz,  $J_{\text{gem}}=1.6$  Hz, N<sup>1</sup>CH=CH<sub>2</sub>], 6.36 [dd, 1H, H<sub>trans</sub>,  $J_{\text{cis}}=15.5$  Hz,  $J_{\text{gem}}=1.5$  Hz, N<sup>2</sup>CH=CH<sub>2</sub>], 7.11 [dd, 1H, H<sub>gem</sub>,  $J_{\text{trans}}=15.5$  Hz,  $J_{\text{cis}}=8.6$  Hz, N<sup>1</sup>CH=CH<sub>2</sub>], 7.35 [dd, 1H, H<sub>gem</sub>,  $J_{\text{trans}}=15.5$  Hz,  $J_{\text{cis}}=8.8$  Hz, N<sup>2</sup>CH=CH<sub>2</sub>], 7.90 [d, 2H,  $J=8.2$  Hz, H<sup>2</sup>-C<sub>6</sub>H<sub>4</sub>], 8.43 [d, 2H,  $J=8.2$  Hz, H<sup>1</sup>-C<sub>6</sub>H<sub>4</sub>];  $\delta_{\text{C}}$ : 109.3 [CH<sub>2</sub>], 111.9 [CH<sub>2</sub>], 125.4 [*i*-C<sub>6</sub>H<sub>4</sub>], 126.1 [*i'*-C<sub>6</sub>H<sub>4</sub>], 127.9 [C<sup>1</sup>-C<sub>6</sub>H<sub>4</sub>], 128.2 [C<sup>2</sup>-C<sub>6</sub>H<sub>4</sub>], 129.9 [CHN<sup>2</sup>], 133.1 [CHN<sup>1</sup>], 152.0 [CN<sub>4</sub>], 165.0 [CN<sub>4</sub>].

#### 4.8. X-ray crystallography

Suitable crystals of 1b and 5d for X-ray study were obtained by recrystallisation from chloroform and acetonitrile solutions, respectively. Crystallographic details are given below. In each case, refinement was full-matrix least-squares on  $F^2$ . Data for compounds 1b and 5d were collected at room temperature on an Enraf–Nonius CAD4 diffractometer. In both cases, data were corrected for Lp and absorption. Hydrogen atoms were added at calculated positions. Software used was SHELXS86,<sup>12</sup> SHELXL97<sup>13</sup> and ORTEX.<sup>14</sup>

**4.8.1. Compound 1b.** *Crystal data:* C<sub>12</sub>H<sub>10</sub>N<sub>8</sub>,  $M=266.28$ , orthorhombic,  $a=12.9010(3)$  Å,  $b=12.9580(3)$  Å,  $c=7.5620(2)$  Å,  $U=4264.15(5)$  Å<sup>3</sup>, space group  $P2_12_12_1$ ,  $Z=4$ ,  $\mu(\text{Mo K}\alpha)=0.095$  mm<sup>-1</sup>. Crystallographic measurements were made at 150(2) K on a Nonius kappaCCD diffractometer in the range  $4.14 < \theta < 27.42^\circ$ . The solution of the structure (SHELXS86) and refinement (SHELXL97) converged to a conventional [i.e., based on 2775 $F$  data with  $F_o > 4\sigma(F_o)$ ]  $R_1=0.0393$  and  $wR_2=0.0836$ . Goodness of fit=1.019. CCDC No. 261954.

**4.8.2. Compound 5d.** *Crystal data:* C<sub>12</sub>H<sub>12</sub>Br<sub>2</sub>N<sub>8</sub>,  $M=428.12$ , triclinic,  $a=6.5230(4)$  Å,  $b=9.7510(6)$  Å,  $c=12.7850(9)$  Å,  $\alpha=88.149(3)^\circ$ ,  $\beta=75.839(3)^\circ$ ,  $\gamma=84.759(2)^\circ$ ,  $U=785.15(9)$  Å<sup>3</sup>, space group  $P-1$  (No. 2),  $Z=2$ ,  $\mu(\text{Mo K}\alpha)=5.172$  mm<sup>-1</sup>. Crystallographic measurements were made at 150(2) K on a Nonius kappaCCD diffractometer in the range  $3.70 < \theta < 27.57^\circ$ . The solution of the structure (SHELXS86) and refinement (SHELXL97) converged to a conventional [i.e., based on 2441 $F$  data with  $F_o > 4\sigma(F_o)$ ]  $R_1=0.0498$  and  $wR_2=0.1044$ . Goodness of fit=1.029. CCDC No. 261955.

#### Acknowledgements

We would like to thank Prof. D. Cunningham and Dr. B. A. Murray for useful discussions. VP would like to thank the Postgraduate R&D Skills programme (Technological Sector Research, Strand III) for financial assistance.

**References and notes**

1. Butler, R. N. In Rees, C. W., Scriven, E. F. V., Eds.; *Comprehensive heterocyclic chemistry*; Pergamon: Oxford, UK, 1996; Vol. 4.
2. Herr, R. J. *Bioorg. Med. Chem.* **2002**, *10*, 3379.
3. Sisido, K.; Nabika, K.; Isida, T.; Kozima, S. *J. Organomet. Chem.* **1971**, *33*, 337.
4. Hill, M.; Mahon, M. F.; McGinley, J.; Molloy, K. C. *J. Chem. Soc., Dalton Trans.* **1996**, 835.
5. Bethel, P. A.; Hill, M. S.; Mahon, M. F.; Molloy, K. C. *J. Chem. Soc., Perkin Trans. 1* **1999**, 3507.
6. Demko, Z. P.; Sharpless, K. B. *J. Org. Chem.* **2001**, *66*, 7945.
7. Kumar, A.; Narayanan, R.; Shechter, H. *J. Org. Chem.* **1996**, *61*, 4462.
8. Koguro, K.; Oga, T.; Mitsui, S.; Orita, R. *Synthesis* **1998**, 910.
9. Butler, R. N.; Fleming, A. F. M. *J. Heterocycl. Chem.* **1997**, *34*, 691.
10. Majumdar, K. C.; Chattopadhyay, S. K. *Tetrahedron Lett.* **2004**, *45*, 6871.
11. Doderio, V. I.; Koll, L. C.; Mandolesi, S. D.; Podestá, J. C. *J. Organomet. Chem.* **2002**, *650*, 173.
12. Sheldrick, G. M. *SHELXS86, A Computer Program for Crystal Structure Determination*; University of Göttingen: Göttingen, 1986.
13. Sheldrick, G. M. *SHELXL97, A Computer Program for Crystal Structure Refinement*; University of Göttingen: Göttingen, 1997.
14. McArdle, P. *J. Appl. Crystallogr.* **1995**, *28*, 65.

# Synthesis of new iminocoumarins and their transformations into *N*-chloro and hydrazono compounds

Julija Volmajer,<sup>a</sup> Renata Toplak,<sup>a,†</sup> Ivan Leban<sup>b</sup> and Alenka Majcen Le Marechal<sup>a,\*</sup>

<sup>a</sup>Faculty of Mechanical Engineering, University of Maribor, Smetanova 17, 2000 Maribor, Slovenia

<sup>b</sup>Faculty of Chemistry and Chemical Technology, University of Ljubljana, Aškerčeva 5, 1000 Ljubljana, Slovenia

Received 20 January 2005; revised 18 April 2005; accepted 5 May 2005

**Abstract**—The Knoevenagel reaction between 2-hydroxybenzaldehydes and active methylene compounds (malononitrile and ethyl cyanoacetate) produces iminocoumarins and/or coumarins. In order to study the reactivity of the prepared iminocoumarins, chlorination and reaction with *N*-nucleophiles were studied.

© 2005 Elsevier Ltd. All rights reserved.

## 1. Introduction

Natural and synthetic coumarin derivatives represent, nowadays, an important group of organic compounds that are used as antibiotics,<sup>1,2</sup> fungicides,<sup>3</sup> anti-inflammatory,<sup>4</sup> anticoagulant<sup>5</sup> and antitumor agents.<sup>6,7</sup> Regarding their high fluorescence ability, they are widely used as optical whitening agents, brighteners, laser dyes and also as fluorescent probes<sup>8</sup> in biology and medicine.<sup>9</sup> Their 2-imino analogues, iminocoumarins, are less known and comprise a very important class of protein tyrosine kinase (PTK) inhibitors with low molecular weight.<sup>10,11</sup> A great number of PTK inhibitors have been introduced recently as potential anti cancer agents. Some of them which derive from different 2-hydroxybenzaldehydes and cyanoacetamides, display moderate antitumour activity against P.388 lymphocytic leukaemia.<sup>12</sup> In order to obtain a larger spectrum of biologically active iminocoumarin substances, a novel series has been developed which contain the 2-iminocoumarin unit. In this paper we are expanding our preliminary results<sup>13</sup> to new differently substituted iminocoumarins, and to their possible chemical and biological activities.

## 2. Results and discussion

Iminocoumarins **4a–g** (2-imino-2*H*-chromene-3-carbo-

nitriles) were prepared using Knoevenagel condensation procedures, in one-pot reactions from 2-hydroxybenzaldehyde derivatives **1a–g** and malononitrile **2** in the presence of catalytic amounts of piperidine. The spontaneous cyclisation between the *ortho* hydroxy group and the side-chain cyano group of intermediate **3** led to iminocoumarin derivatives in moderate to good yields (47–98%), (Scheme 1).

In contrast, reactions of the 2-hydroxybenzaldehydes **1b–g** with ethyl cyanoacetate **5** do not lead just to iminocoumarins **8**, but also to coumarins **9**, **10**. The formation of iminocoumarins **8** and/or coumarins **9**, resulting from Knoevenagel condensation between the 2-hydroxybenzaldehydes **1** and ethyl cyanoacetate **5** was followed by an attack of the hydroxyl group of the intermediate (**6** or **7**) on the side-chain nitrile or ester group. The ratio between the products depends on the nature of the aromatic ring substituents (Scheme 2).

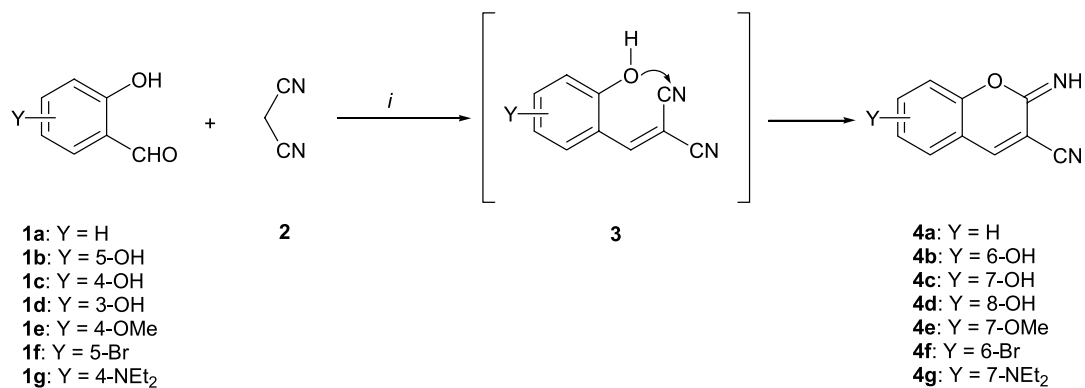
The Knoevenagel reaction between ethyl cyanoacetate **5** and 2-hydroxybenzaldehyde containing another hydroxyl group (**1b**, **1c**, **1d**) on the aromatic ring, forms iminocoumarins with only minor quantities of coumarins **9**. This suggests that the condensation in these cases is stereoselective yielding *E*-styryl derivatives **6** as the main intermediates in which the aromatic ring and the cyano group are in the *cis* configuration.

The coumarins **9** were formed as the main products, when the Knoevenagel reactions were performed between 2-hydroxy-4-methoxybenzaldehyde **1e**, or 4-diethylamino-2-hydroxybenzaldehyde **1g** and ethyl cyanoacetate **5**.

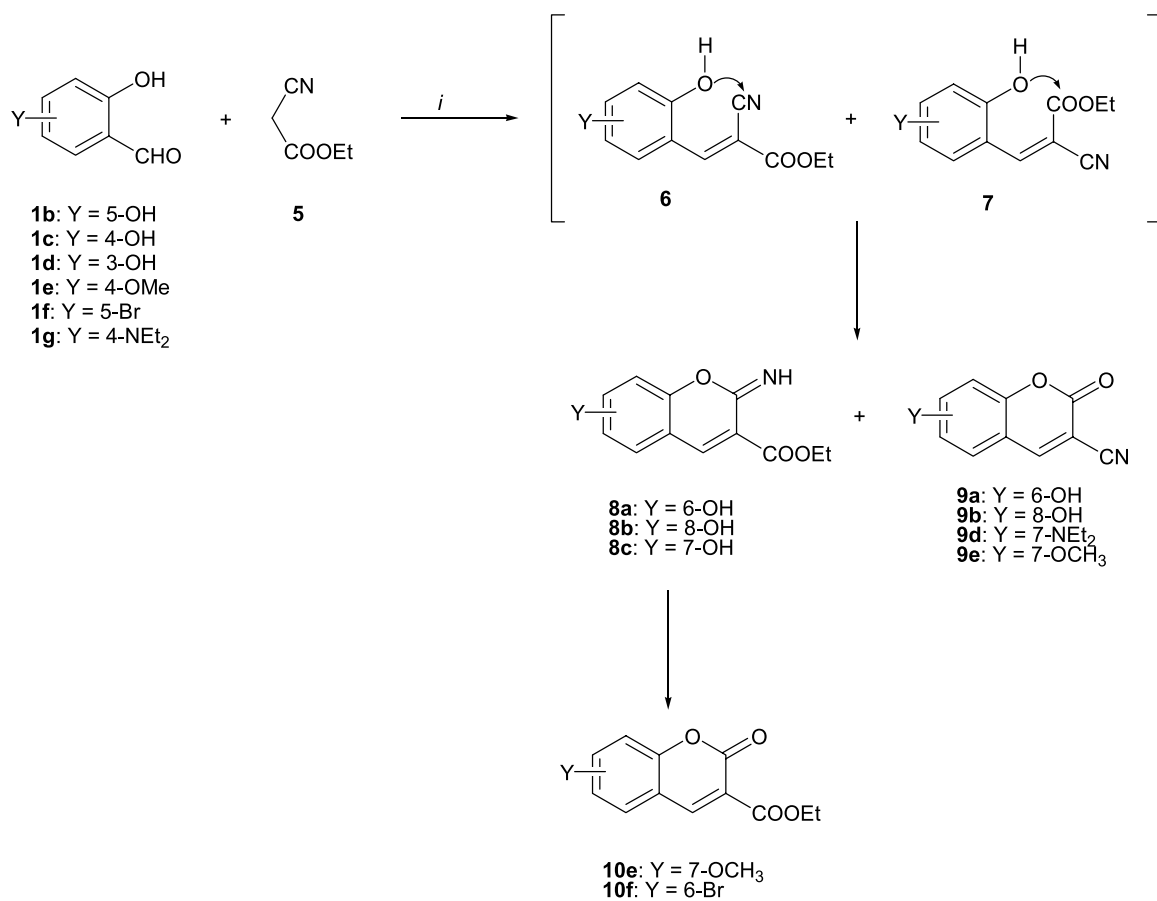
**Keywords:** Knoevenagel condensation; Iminocoumarins; Coumarins; *N*-Chlorination; *N*-Chloro iminocoumarins; *N*-Hydrazonocoumarins.

\* Corresponding author. Tel.: +386 2 220 7910; fax: +386 2 220 7990; e-mail: [alenka.majcen@uni-mb.si](mailto:alenka.majcen@uni-mb.si)

† Present address: Lek d.d., Verovškova 57, 1526 Ljubljana, Slovenia.



**Scheme 1.** Reaction conditions: (i) piperidine, EtOH, rt.



Y	8	9	10
6-OH	70 %	15 %	-
8-OH	84 %	1 %	-
7-OH	91 %	-	-
7-NEt <sub>2</sub>	-	89 %	-
7-OCH <sub>3</sub>	-	85 %	3 %
6-Br	-	-	44 %

**Scheme 2.** Reaction conditions: (i) piperidine, EtOH, rt.

**Table 1.** Iminocoumarins and coumarins

Compound	Y	Yield (%)	Mp (°C)
<b>8a</b> <sup>13</sup>	6-OH	70	240–242
<b>8b</b> <sup>13</sup>	8-OH	84	225–226
<b>8c</b>	7-OH	91	220–221
<b>9a</b> <sup>13</sup>	6-OH	17	237–238
<b>9b</b> <sup>13</sup>	8-OH	1	228–230
<b>9d</b>	7-NEt <sub>2</sub>	89	211–212
<b>9e</b>	7-OCH <sub>3</sub>	85	225–226
<b>10e</b>	7-OCH <sub>3</sub>	3	132–133
<b>10f</b>	6-Br	44	180–181

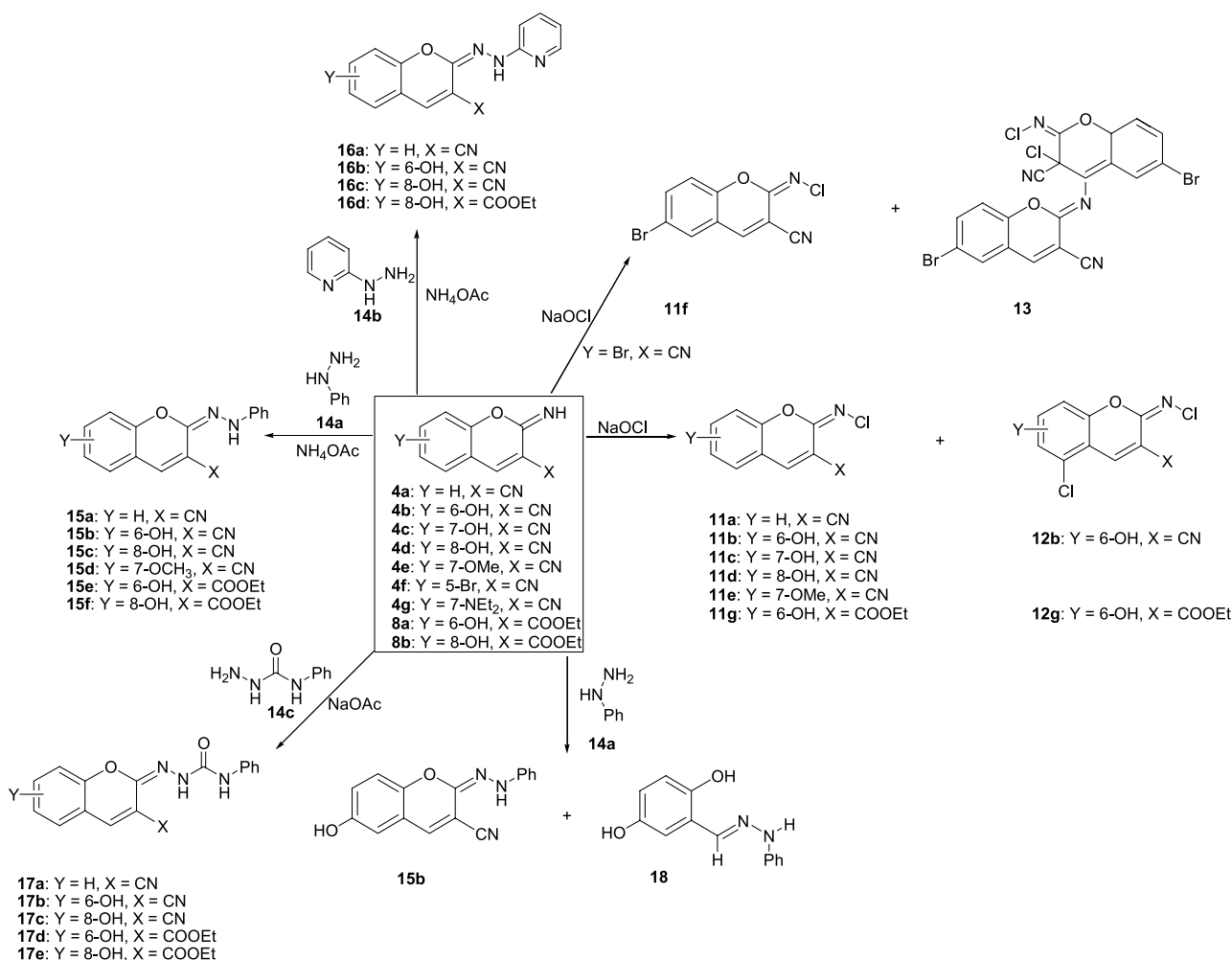
Iminocoumarins were also formed in minor quantities but we succeeded in isolating only the product of their hydrolysis, coumarins **10**. For example, in the reaction between the 5-bromo-2-hydroxybenzaldehyde **1f** and ethyl cyanoacetate **5** only the hydrolysed iminocoumarin **10f** was isolated (Scheme 2, Table 1).

The structure of the iminocoumarin and coumarin derivatives was determined by IR, <sup>1</sup>H NMR, mass spectra and elemental analysis. We can distinguish between coumarin and iminocoumarin formations on the basis of the IR spectra. Namely, the NH absorption band of the imino group observed between 3278 and 3312 cm<sup>-1</sup> (KBr) indicates the formation of iminocoumarins.

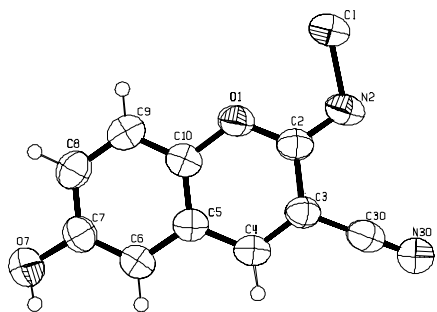
The formation of iminocoumarins and/or coumarins arises from the *E/Z* isomerisations of the styryl intermediate. We did not study which factors control the different selectivity to styryl intermediate **6** and/or **7** (Scheme 2), but it is evident that the effect of the substituents on the aromatic ring plays an important role. For example, salicylaldehyde derivatives containing groups with more negative inductive effect (Br, OH) yield in the Knoevenagel reaction, the *E*-styryl intermediate as the main intermediate. Furthermore, the results also indicate the involvement of an additional OH group on the phenyl ring in the stabilization of the *E*-styryl intermediate, supposedly through the formation of intermolecular hydrogen bonds.

The formation of coumarin and chromene derivatives during the Knoevenagel reaction is known,<sup>14</sup> as well as the transformations<sup>15</sup> of iminocoumarins into coumarins in basic aprotic solvents. The isomerisation of the 2-imino-2*H*-chromene-3-carboxamide was studied by <sup>1</sup>H NMR.<sup>16</sup> In a DMSO-*d*<sub>6</sub> solution of 2-imino-2*H*-chromene-3-carboxamide, a mixture of 2-imino-2*H*-chromene-3-carboxamide and its isomer 2-cyano-3-(2-hydroxyphenyl)-prop-2-enamide was observed. The authors explain the result as a consequence of the pyran ring opening.

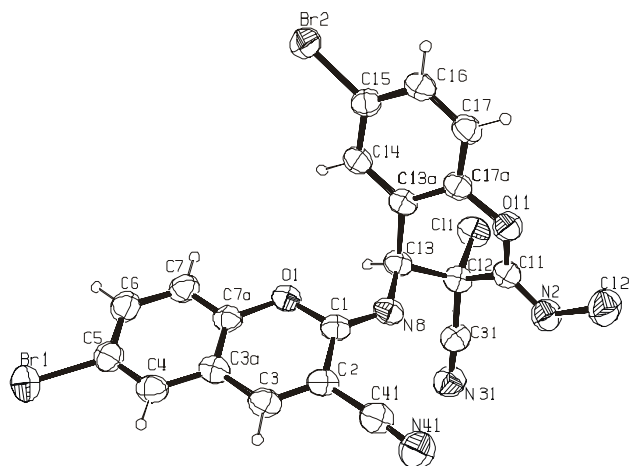
We focused our attention firstly on an investigation of the

**Scheme 3.**





**Figure 1.** ORTEP view of the compound **11b**. Crystallographic data for the structure **11b** have been deposited within the Cambridge Crystallographic Data Centre as supplementary publication number CCDC 200890.



**Figure 2.** ORTEP view of the compound **13**. Crystallographic data for the structure **13** have been deposited within the Cambridge Crystallographic Data Centre as supplementary publication number CCDC 260165.

iminocoumarins chlorination with sodium hypochlorite. The chlorination of the imino group of iminocoumarins with sodium hypochlorite yields chloroimino chromenes **11a–g**. The reactions were performed under acidic reaction conditions at 0 °C (Scheme 3). Within a few minutes the reaction was complete and the products precipitated from the reaction mixture on the addition of cold water.<sup>13</sup>

The *N*-chlorination of 6-hydroxy-2-imino-2*H*-chromene-3-carbonitrile **4b** and 6-hydroxy-2-imino-2*H*-chromene-3-carboxylate **8a** were accompanied by an electrophilic aromatic chlorination yielding compound **12b** and **12g**. In the reaction between 6-bromo-2-imino-2*H*-chromene-3-carbonitrile **4f** and sodium hypochlorite, dimeric product **13** was isolated beside the expected chloroimino chromene

**Table 2.** *N*-Chloroiminochromenes

Compound	Y	X	Yield (%)	Mp (°C)
<b>11a</b> <sup>13</sup>	H	CN	40	191–192
<b>11b</b> <sup>13</sup>	6-OH	CN	41	209–210
<b>11c</b>	7-OH	CN	48	210–211
<b>11d</b>	8-OH	CN	52	210–211
<b>11e</b>	7-OCH <sub>3</sub>	CN	41	224–225
<b>11f</b>	6-Br	CN	30	200–201
<b>11g</b> <sup>13</sup>	6-OH	COOEt	26	176–177
<b>12b</b> <sup>13</sup>	6-OH	CN	11	204–205
<b>12g</b> <sup>13</sup>	6-OH	COOEt	13	152–153

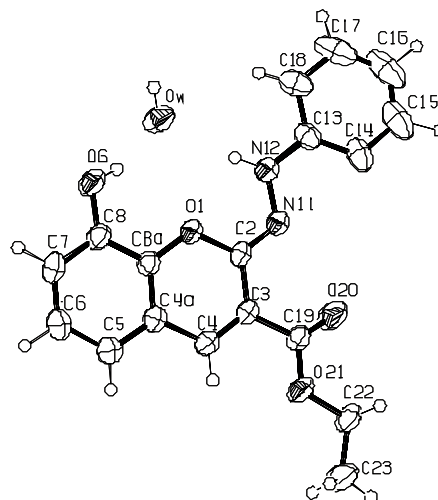
**11f** (Scheme 3). The average to low yields of *N*-chlorination indicates a polymerisation ability for the prepared *N*-chloro derivatives. The structures of the chloro iminochromenes were determined by IR, <sup>1</sup>H NMR, <sup>13</sup>C NMR, mass spectra and elemental analysis. The structures of the chloro iminochromene **11b**<sup>13</sup> and dimeric compound **13** were additionally confirmed by X-ray diffraction (Figs. 1 and 2) (Table 2).

The reactions of 2-iminochromene-3-carboxamides with *N*-phenylhydrazine<sup>17</sup> or primary amines<sup>18</sup> in acetic acid at rt are known and lead to 2-*N*-substituted iminocoumarins only.

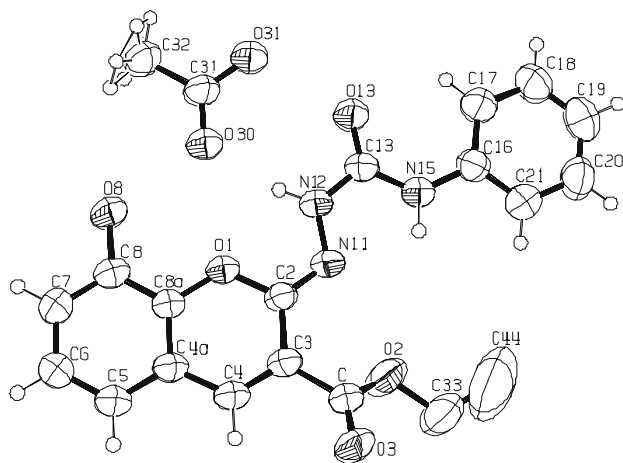
When we carried out a reaction between the 6-hydroxy-2-imino-2*H*-chromene-3-carbonitrile **4b** and *N*-phenylhydrazine **14a** in an acetic acid medium according to the above mentioned method, the reaction led to two products 6-hydroxy-2-(phenylhydrazono)-2*H*-chromene-3-carbonitrile **15b** and 2,5-dihydroxybenzaldehyde phenylhydrazone **18** (Scheme 3). Phenylhydrazine as *N*-nucleophile in this case attacked the C<sub>2</sub> and C<sub>4</sub> electrophilic centres. The selective formation of *N*-hydrazonochromenes proceeded in the reactions of 2-iminocoumarin-3-carbonitriles with hydrazine derivatives (phenylhydrazine **14a**, 2-hydrazinopyridine **14b**, *N*-phenylhydrazinecarboxamide **14c**) (Scheme 3) in glacial acetic acid at rt in the presence of NH<sub>4</sub>OAc or NaOAc. In this case the reactions took place without iminolactone ring opening.

The structures of compounds *N*-hydrazonochromenes were assigned by IR, <sup>1</sup>H NMR, <sup>13</sup>C NMR, mass spectra and elemental analysis. The structure of the products **15f** and **17e** were confirmed by X-ray diffraction (Figs. 3 and 4) (Table 3).

The antibacterial activity of the iminocoumarins and their derivatives was evaluated against common Gram-positive bacteria and Gram-negative bacteria. The chloroiminochromenes exhibit excellent antibacterial activity. Iminochromenes showed moderate activity whereas *N*-hydrazonochromenes did not exhibit antibacterial activity



**Figure 3.** ORTEP view of the compound **15f**. Crystallographic data for the structure **15f** have been deposited within the Cambridge Crystallographic Data Centre as supplementary publication number CCDC 260163.



**Figure 4.** ORTEP view of the compound **17e**. Crystallographic data for the structure **17e** have been deposited within the Cambridge Crystallographic Data Centre as supplementary publication number CCDC 260164.

**Table 3.** *N*-Hydrazonochromenes

Compound	Y	X	Yield (%)	Mp (°C)
<b>15a</b>	H	CN	37	205–206
<b>15b</b>	6-OH	CN	41	258–259
<b>15c</b>	8-OH	CN	38	>260
<b>15d</b>	7-OCH <sub>3</sub>	CN	47	247–248
<b>15e</b>	6-OH	COOEt	31	178–179
<b>15f</b>	8-OH	COOEt	64	208–209
<b>16a</b>	H	CN	48	164–165
<b>16b</b>	6-OH	CN	40	246–247
<b>16c</b>	8-OH	CN	38	255–256
<b>16d</b>	8-OH	COOEt	49	146–147
<b>17a</b>	H	CN	51	>260
<b>17b</b>	6-OH	CN	68	>260
<b>17c</b>	8-OH	CN	53	>260
<b>17d</b>	6-OH	COOEt	87	231–232
<b>17e</b>	8-OH	COOEt	91	226–227

at all. The preliminary studies of antiproliferative activity for compound **11b** on MCF-7 cells in vitro are promising. The survival of MCF-7 tumor cells cultured in a medium with compound **11b** drops beyond 40% at a concentration of **11b** above 112.5  $\mu\text{M}$ .

The synthesised iminocoumarins with electron donor groups at 6-position (**4b**, **8a**) and at 7-position (**4c**, **4e**, **4g**) revealed a high fluorescence efficiency while other iminocoumarins were photophysically inert.

It is interesting to note that some iminocoumarins undergo a dramatic change of colour with any change of pH in the medium. For example, iminocoumarins **4b**, **4d**, **8a**, **8b** exhibit a green colour in the acidic medium but they change to a red colour in the basic medium.

### 3. Conclusion

According to our results, we can conclude that iminocoumarins **4a–g**, **8a–c** were formed in condensation between salicylaldehyde derivatives and malononitrile, and in the reaction of ethyl cyanoacetate and hydroxy substituted salicylaldehydes. In other cases, coumarins **9d**,

**9e**, **10e**, **10f** were isolated. We noticed that the ratio between the possible products depends on the nature of the aromatic ring substituents. A series of new *N*-chloro iminocoumarin **11a–g** was prepared in moderate yields, by reacting sodium hypochlorite in an acidic medium with iminocoumarins. The reaction of the iminocoumarins with hydrazines led to *N*-hydrazonochromenes **15a–f**, **16a–d**, **17a–e**.

## 4. Experimental

Melting points were determined with Kofler hot stage apparatus. <sup>1</sup>H NMR spectra were recorded on a Bruker Avance DPX 300 (300 MHz) spectrometer with DMSO-*d*<sub>6</sub> as solvents and TMS as internal standard. <sup>13</sup>C NMR spectra were obtained on a Bruker AM 300 spectrometer at 75 MHz with DMSO-*d*<sub>6</sub> as solvents and TMS as internal standard. Mass spectra were performed on an Autospec Q spectrometer. The microanalyses for C, H and N were obtained on a Perkin-Elmer Analyser 2400. IR spectra were determined with a Perkin-Elmer 225 or a 1420 spectrometer. Column chromatography (CC) was performed on silica gel (Fluka, silica gel 60, 0.035–0.070 mm). All starting materials were commercially available (in most cases from Fluka).

### 4.1. General procedure for Knoevenagel reactions between 2-hydroxybenzaldehyde derivatives and malononitrile

A mixture of substituted 2-hydroxybenzaldehyde **1** (5 mmol) and malononitrile **2** (5 mmol) was dissolved in 5 mL of ethanol and one drop of piperidine was added. The reaction mixture was stirred at rt for 30 min. The product was precipitated from the reaction mixture and collected by filtration. It was recrystallized from an appropriate solvent.

The following compounds were prepared in this manner.

**4.1.1. 2-Imino-2*H*-chromene-3-carbonitrile 4a.** Prepared from salicylaldehyde **1a** (610 mg, 5 mmol) and malononitrile **2** (330 mg, 5 mmol) in 61% (518 mg) yield as a white solid; mp 140–141 °C; (mp<sup>19</sup> 183–185 °C) (EtOH). EI-MS:  $m/z = 170$  ( $\text{M}^+$ ). <sup>1</sup>H NMR (DMSO-*d*<sub>6</sub>): 7.18–7.21 (1H, m, *H*<sub>8</sub>); 7.24–7.29 (1H, m, *H*<sub>6</sub>); 7.55–7.61 (2H, m, *H*<sub>5</sub>, *H*<sub>7</sub>); 8.37 (1H, d, *J* = 0.9 Hz, *H*<sub>4</sub>); 8.83 (1H, s, *NH*). (Found: C, 70.31; H, 3.60, N, 16.37. C<sub>10</sub>H<sub>6</sub>N<sub>2</sub>O requires: C, 70.58; H, 3.55; N, 16.46);  $\nu_{\text{max}}$  (KBr) 3293, 2231, 1653 cm<sup>-1</sup>.

**4.1.2. 6-Hydroxy-2-imino-2*H*-chromene-3-carbonitrile 4b.** Prepared from 2,5-dihydroxybenzaldehyde **1b** (690 mg, 5 mmol) and malononitrile **2** (330 mg, 5 mmol) in 98% (912 mg) yield as a yellow-green solid; mp > 260 °C (EtOH). EI-MS:  $m/z = 186$  ( $\text{M}^+$ ). <sup>1</sup>H NMR (DMSO-*d*<sub>6</sub>): 6.39–7.04 (3H, m, *H*<sub>5</sub>, *H*<sub>7</sub>, *H*<sub>8</sub>); 8.31 (1H, s, *H*<sub>4</sub>); 8.61 (1H, s, *NH*); 9.75 (1H, br s, OH). <sup>13</sup>C NMR (DMSO-*d*<sub>6</sub>):  $\delta$  104.1, 113.7, 115.2, 116.3, 117.5, 121.4, 146.8, 146.9, 152.0, 153.4. (Found: C, 64.38; H, 3.19; N, 15.39. C<sub>10</sub>H<sub>6</sub>N<sub>2</sub>O<sub>2</sub> requires: C, 64.52; H, 3.25; N, 15.05);  $\nu_{\text{max}}$  (KBr) 3242, 2236, 1652 cm<sup>-1</sup>.

**4.1.3. 7-Hydroxy-2-imino-2*H*-chromene-3-carbonitrile 4c.** Prepared from 2,4-dihydroxybenzaldehyde **1c**

(690 mg, 5 mmol) and malononitrile **2** (330 mg, 5 mmol) in 90% (837 mg) yield as a yellow solid; mp > 260 °C (EtOH). EI-MS:  $m/z = 186$  ( $M^+$ ).  $^1\text{H NMR}$  (DMSO- $d_6$ ): 6.51 (1H, d,  $J = 2.0$  Hz,  $H_8$ ); 6.65–6.68 (1H, m,  $H_6$ ); 7.40 (1H, d,  $J = 8.7$  Hz,  $H_5$ ); 8.20 (1H, s,  $H_4$ ); 8.65 (s, 1H, NH). EI-HRMS:  $m/z = 186.0435$  ( $M^+$ );  $\text{C}_{10}\text{H}_6\text{N}_2\text{O}_2$  requires: 186.0429 ( $M^+$ );  $\nu_{\text{max}}$  (KBr) 3259, 2222, 1658  $\text{cm}^{-1}$ .

**4.1.4. 8-Hydroxy-2-imino-2H-chromene-3-carbonitrile 4d.** Prepared from 2,3-dihydroxybenzaldehyde **1d** (690 mg, 5 mmol) and malononitrile **2** (330 mg, 5 mmol) in 47% (438 mg) yield as a yellow-green solid; mp > 260 °C (EtOH). EI-MS:  $m/z = 186$  ( $M^+$ ).  $^1\text{H NMR}$  (DMSO- $d_6$ ): 7.98–7.01 (1H, m,  $H_7$ ); 7.03–7.06 (1H, m,  $H_6$ ); 7.8–7.10 (1H, m,  $H_5$ ); 8.31 (1H, s,  $H_4$ ), 8.65 (1H, s, NH). (Found: C, 64.73; H, 3.38; N, 14.85.  $\text{C}_{10}\text{H}_6\text{N}_2\text{O}_2$  requires: C, 64.52; H, 3.25; N, 15.05);  $\nu_{\text{max}}$  (KBr) 3344, 2225, 1646  $\text{cm}^{-1}$ .

**4.1.5. 7-Methoxy-2-imino-2H-chromene-3-carbonitrile 4e.** Prepared from 2-hydroxy-4-methoxybenzaldehyde **1e** (760 mg, 5 mmol) and malononitrile **2** (330 mg, 5 mmol) in 58% (580 mg) yield of a white solid; mp 176–177 °C (EtOH). EI-MS:  $m/z = 200$  ( $M^+$ ).  $^1\text{H NMR}$  (DMSO- $d_6$ ): 3.85 (3H, s,  $\text{OCH}_3$ ); 6.75 (1H, d,  $J = 2.4$  Hz,  $H_8$ ); 6.86 (1H, dd,  $J = 8.7, 2.4$  Hz,  $H_6$ ); 7.51 (1H, d,  $J = 8.7$  Hz,  $H_5$ ); 8.41 (1H, s,  $H_4$ ); 8.65 (1H, s, NH). (Found: C, 65.77; H, 4.33; N, 14.23.  $\text{C}_{11}\text{H}_8\text{N}_2\text{O}_2$  requires: C, 65.99; H, 4.03; N, 13.99);  $\nu_{\text{max}}$  (KBr) 3293, 2221, 1654  $\text{cm}^{-1}$ .

**4.1.6. 6-Bromo-2-imino-2H-chromene-3-carbonitrile 4f.** Prepared from 5-bromo-2-hydroxybenzaldehyde **1f** (1005 mg, 5 mmol) and malononitrile **2** (330 mg, 5 mmol) in 71% (884 mg) yield as a white solid; mp 198–199 °C (EtOH). EI-MS:  $m/z = 248$  ( $M^+$ ).  $^1\text{H NMR}$  (DMSO- $d_6$ ): 7.16 (1H, d,  $J = 9.0$  Hz,  $H_8$ ); 7.70–7.73 (1H, m,  $H_7$ ); 7.81–7.82 (1H, m,  $H_5$ ); 8.29 (1H, d,  $J = 1.5$  Hz,  $H_4$ ); 8.98 (1H, s, NH). (Found: C, 48.10; H, 2.30; N, 11.33.  $\text{C}_{10}\text{H}_5\text{N}_2\text{OBr}$  requires: C, 48.22; H, 2.02; N, 11.24);  $\nu_{\text{max}}$  (KBr) 3310, 2231, 1648  $\text{cm}^{-1}$ .

**4.1.7. 7-Diethylamino-2-imino-2H-chromene-3-carbonitrile 4g.** Prepared from 4-diethylamino-2-hydroxybenzaldehyde **1g** (965 mg, 5 mmol) and malononitrile **2** (330 mg, 5 mmol) in 51% (615 mg) yield as a yellow solid; mp 192–193 °C (EtOH). EI-MS:  $m/z = 241$  ( $M^+$ ).  $^1\text{H NMR}$  (DMSO- $d_6$ ): 1.11 (6H, t,  $J = 7.2$  Hz,  $2 \times \text{CH}_2\text{CH}_3$ ); 3.43 (4H, q,  $J = 7.2$  Hz,  $2 \times \text{CH}_2\text{CH}_3$ ); 6.30–6.31 (1H, m,  $H_8$ ); 6.59–6.61 (1H, m,  $H_6$ ); 7.31 (1H, d,  $J = 9.0$  Hz,  $H_5$ ); 8.06 (1H, s,  $H_4$ ); 8.19 (1H, s, NH). EI-HRMS:  $m/z = 241.1215$  ( $M^+$ );  $\text{C}_{14}\text{H}_{15}\text{N}_3\text{O}$  requires: 241.1212 ( $M^+$ );  $\nu_{\text{max}}$  (KBr) 3342, 2218, 1630  $\text{cm}^{-1}$ .

## 4.2. General procedure for the Knoevenagel reaction between 2-hydroxybenzaldehyde derivatives and ethyl cyanoacetate

A mixture of substituted 2-hydroxybenzaldehyde **1** (5 mmol) and ethyl cyanoacetate **5** (5 mmol) was dissolved in 5 mL of ethanol, one drop of piperidine was added. The reaction mixture was stirred at rt for 30 min. The product precipitated from the reaction mixture and was collected by filtration. The residue filtrate was evaporated in vacuo and purified by column chromatography.

**4.2.1. Ethyl 6-hydroxy-2-imino-2H-chromene-3-carboxylate 8a and 6-hydroxy-2-oxo-2H-chromene-3-carbonitrile 9a.** Prepared from 2,5-dihydroxybenzaldehyde **1b** (690 mg, 5 mmol) and ethyl cyanoacetate **5** (0.55 mL, 5 mmol). Compound **8a** was precipitated from the reaction mixture in 70% (815 mg) yield as a yellow-green solid; mp 240–242 °C (EtOH). EI-MS:  $m/z = 233$  ( $M^+$ ).  $^1\text{H NMR}$  (DMSO- $d_6$ ): 1.32 (3H, t,  $J = 7.2$  Hz,  $\text{CH}_2\text{CH}_3$ ); 4.34 (2H, q,  $J = 7.2$  Hz,  $\text{CH}_2\text{CH}_3$ ); 7.01 (3H, m,  $H_5, H_7, H_8$ ); 8.25 (1H, s,  $H_4$ ); 9.25 (1H, s, NH); 9.63 (1H, br s, OH). (Found: C, 61.88; H, 4.49; N, 5.83.  $\text{C}_{12}\text{H}_{11}\text{NO}_4$  requires: C, 61.80; H, 4.75; N, 6.01);  $\nu_{\text{max}}$  (KBr) 3282, 1726, 1633  $\text{cm}^{-1}$ . Compound **9a** was isolated using column chromatography (ethyl acetate) on the residue from the evaporated residue. It was isolated in 15% (140 mg) yield as a yellow solid; mp 237–238 °C (EtOH); (mp<sup>20</sup> 273–238.5 °C). EI-MS:  $m/z = 187$  ( $M^+$ ).  $^1\text{H NMR}$  (DMSO- $d_6$ ): 7.11 (1H, d,  $J_{\text{H}_6\text{H}_4} = 3.0$  Hz,  $H_5$ ); 7.21 (1H, dd,  $J_{\text{H}_4\text{H}_3} = 9.0$  Hz,  $J_{\text{H}_4\text{H}_6} = 3.0$  Hz,  $H_7$ ); 7.36 (1H, d,  $J_{\text{H}_3\text{H}_4} = 9.0$  Hz,  $H_8$ ); 8.87 (1H, s,  $H_4$ ); 10.03 (1H, s, OH);  $\nu_{\text{max}}$  (KBr) 2253, 1705  $\text{cm}^{-1}$ .

**4.2.2. Ethyl 8-hydroxy-2-imino-2H-chromene-3-carboxylate 8b and 8-hydroxy-2-oxo-2H-chromene-3-carbonitrile 9b.** Prepared from 2,3-dihydroxybenzaldehyde **1d** (690 mg, 5 mmol) and ethyl cyanoacetate **5** (0.55 mL, 5 mmol). Compound **8b** was precipitated from the reaction mixture in 84% (979 mg) yield as a yellow solid; mp 225–226 °C (EtOH). EI-MS:  $m/z = 233$  ( $M^+$ ).  $^1\text{H NMR}$  (DMSO- $d_6$ ): 1.32 (3H, t,  $J = 7.1$  Hz,  $\text{CH}_2\text{CH}_3$ ); 4.29 (2H, q,  $J = 7.1$  Hz,  $\text{CH}_2\text{CH}_3$ ); 7.06 (3H, m,  $H_5, H_6, H_7$ ); 8.67 (1H, s,  $H_4$ ); 8.90 (1H, s, NH). (Found: C, 61.96; H, 4.45; N, 5.90.  $\text{C}_{12}\text{H}_{11}\text{NO}_4$  requires: C, 61.80; H, 4.75; N, 6.01);  $\nu_{\text{max}}$  (KBr) 3297, 1703, 1600  $\text{cm}^{-1}$ . Compound **9b** was isolated using column chromatography ( $\text{CH}_2\text{Cl}_2/\text{MeOH}$ , 100:1) on the residue from the evaporated residue. It was isolated in 1% (9 mg) yield as a yellow solid; mp 228–230 °C (EtOH); (mp<sup>21</sup> 238–240 °C). EI-MS:  $m/z = 187$  ( $M^+$ ).  $^1\text{H NMR}$  (DMSO- $d_6$ ): 7.24–7.44 (3H, m,  $H_5, H_6, H_7$ ); 8.87 (s, 1H,  $H_4$ );  $\nu_{\text{max}}$  (KBr) 2253, 1746  $\text{cm}^{-1}$ .

**4.2.3. Ethyl 7-hydroxy-2-imino-2H-chromene-3-carboxylate 8c.** Prepared from 2,4-dihydroxybenzaldehyde **1c** (690 mg, 5 mmol) and ethyl cyanoacetate **5** (0.55 mL, 5 mmol). Compound **8c** was precipitated from the reaction mixture in 91% (1060 mg) yield as a yellow solid; mp 220–221 °C (EtOH). EI-MS:  $m/z = 233$  ( $M^+$ ).  $^1\text{H NMR}$  (DMSO- $d_6$ ): 1.31 (3H, t,  $J = 7.1$  Hz,  $\text{CH}_2\text{CH}_3$ ); 4.28 (2H, q,  $J = 7.1$  Hz,  $\text{CH}_2\text{CH}_3$ ); 6.43 (1H, m,  $H_8$ ); 6.57 (1H, dd,  $J = 8.7, 2.4$  Hz,  $H_6$ ); 7.51 (1H, d,  $J = 8.7$  Hz,  $H_5$ ); 8.21 (1H, s,  $H_4$ ); 9.23 (1H, s, NH). EI-HRMS:  $m/z = 233.0695$  ( $M^+$ );  $\text{C}_{12}\text{H}_{11}\text{NO}_4$  requires: 233.0688 ( $M^+$ );  $\nu_{\text{max}}$  (KBr) 3312, 1693, 1630  $\text{cm}^{-1}$ .

**4.2.4. 7-Diethylamino-2-oxo-2H-chromene-3-carbonitrile 9d.** Prepared from 4-diethylamino-2-hydroxybenzaldehyde **1g** (965 mg, 5 mmol) and ethyl cyanoacetate **5** (0.55 mL, 5 mmol). Compound **9d** was precipitated from the reaction mixture in 78% (944 mg) yield as a yellow solid; mp 211–212 °C (EtOH). EI-MS:  $m/z = 242$  ( $M^+$ ).  $^1\text{H NMR}$  (DMSO- $d_6$ ): 1.25 (6H, t,  $J = 6.9$  Hz,  $2 \times \text{CH}_2\text{CH}_3$ ); 3.46 (4H, q,  $J = 7.2$  Hz,  $2 \times \text{CH}_2\text{CH}_3$ ); 6.46 (1H, d,  $J = 2.1$  Hz,  $H_8$ ); 6.63 (1H, dd,  $J = 9.0, 2.4$  Hz,  $H_6$ ); 7.30 (1H, d,  $J = 9.0$  Hz,  $H_5$ ); 7.96 (1H, s,

$H_4$ ). (Found: C, 69.22; H, 5.84; N, 11.67.  $C_{14}H_{14}N_2O_2$  requires: C, 69.40; H, 5.82; N, 11.56);  $\nu_{\max}$  (KBr) 2218, 1717  $cm^{-1}$ .

**4.2.5. 7-Methoxy-2-oxo-2H-chromene-3-carbonitrile 9e and ethyl 7-methoxy-2-oxo-2H-chromene-3-carboxylate 10e.** Prepared from 2-hydroxy-4-methoxybenzaldehyde **1e** (760 mg, 5 mmol) and ethyl cyanoacetate **5** (0.55 mL, 5 mmol). Compound **9e** was precipitated from the reaction mixture in 85% (855 mg) yield as a white solid; mp 225–226 °C (EtOH). EI-MS:  $m/z=201$  ( $M^+$ ).  $^1H$  NMR (DMSO- $d_6$ ): 3.92 (3H, s,  $OCH_3$ ); 7.07 (1H, dd,  $J=2.4, 8.7$  Hz,  $H_6$ ); 7.12 (1H, d,  $J=2.4$  Hz,  $H_8$ ); 7.73 (1H, d,  $J=8.7$  Hz,  $H_5$ ); 8.84 (1H, s,  $H_4$ ). (Found: C, 65.84; H, 3.54; N, 6.61.  $C_{11}H_7NO_3$  requires: C, 65.67; H, 3.51; N, 6.96);  $\nu_{\max}$  (KBr) 2228, 1724  $cm^{-1}$ . Compound **10e** was isolated using column chromatography ( $CH_2Cl_2/MeOH$ , 200:1) on the residue from the evaporate residue. It was isolated in 3% (38 mg) yield as a white solid; mp 132–133 °C (EtOH). EI-MS:  $m/z=248$  ( $M^+$ ).  $^1H$  NMR (DMSO- $d_6$ ): 1.30 (3H, t,  $J=7.2$  Hz,  $CH_3CH_2$ ); 3.89 (3H, s,  $OCH_3$ ); 4.28 (2H, q,  $J=7.2$  Hz,  $CH_2CH_3$ ); 6.99–7.04 (2H, m,  $H_6, H_8$ ); 7.85 (1H, d,  $J=8.4$  Hz,  $H_5$ ); 8.72 (s, 1H,  $H_4$ ). (Found: C, 62.79; H, 4.77.  $C_{13}H_{12}O_5$  requires: C, 62.90; H, 4.87);  $\nu_{\max}$  (KBr) 1750, 1619  $cm^{-1}$ .

**4.2.6. Ethyl 6-bromo-2-oxo-2H-chromene-3-carboxylate 10f.** Prepared from 5-bromo-2-hydroxybenzaldehyde **1f** (1005 mg, 5 mmol) and ethyl cyanoacetate **5** (0.55 mL, 5 mmol) in 44% (651 mg) yield as a white solid; mp 180–181 °C (EtOH). EI-MS:  $m/z=296$  ( $M^+$ ).  $^1H$  NMR (DMSO- $d_6$ ): 1.31 (3H, t,  $J=7.2$  Hz,  $CH_3CH_2$ ); 4.30 (2H, q,  $J=7.2$  Hz,  $CH_2CH_3$ ); 7.42 (1H, d,  $J=8.7$  Hz,  $H_8$ ); 7.88 (1H, dd,  $J=8.7, 2.4$  Hz,  $H_7$ ); 8.17 (1H, d,  $J=2.4$  Hz,  $H_5$ ); 8.71 (1H, s,  $H_4$ ). (Found: C, 48.78; H, 3.10.  $C_{12}H_9O_4Br$  requires: C, 48.51; H, 3.05);  $\nu_{\max}$  (KBr) 1729, 1662  $cm^{-1}$ .

### 4.3. General procedure for the preparation of *N*-chloro-benzopyran-2-imine

A solution of the benzopyran-2-imine derivative (5 mmol) in 8 mL of acetonitrile was cooled in an ice bath to 0 °C. A 13% solution of sodium chlorate was added dropwise during a period of 10 min. Whilst the pH of the reaction mixture was simultaneously adjusted to 5–6 using a 2.5 M solution of  $H_2SO_4$ . The reaction mixture was stirred for an additional 10 min at 0 °C. Ice cold water (50 mL) was added to the reaction mixture on which the product precipitated. It was collected by filtration and chromatographed on a silica gel column with an appropriate eluent. The following compounds were prepared in this manner:

**4.3.1. 2-(Chloroimino)-2H-chromene-3-carbonitrile 11a.** This was prepared from 2-imino-2H-chromene-3-carbonitrile **4a** (850 mg, 5 mmol) and 13% NaOCl (9 mL) in 40% (408 mg) yield as a white solid. It was purified by column chromatography (ethyl acetate/heptane, 1:1) and had mp 191–192 °C (ethyl acetate). EI-MS:  $m/z=204$  ( $M^+$ ).  $^1H$  NMR (DMSO- $d_6$ ): 7.39–7.74 (4H, m,  $H_5, H_6, H_7, H_8$ ); 8.51 (1H, s,  $H_4$ ). (Found: C, 58.89; H, 2.67; N, 13.73.  $C_{10}H_5N_2OCl$  requires: C, 58.70; H, 2.46; N, 13.69);  $\nu_{\max}$  (KBr) 2235, 1626  $cm^{-1}$ .

**4.3.2. 2-(Chloroimino)-6-hydroxy-2H-chromene-3-carbonitrile 11b and 5-chloro-2-(chloroimino)-6-hydroxy-2H-chromene-3-carbonitrile 12b.** 6-Hydroxy-2-imino-2H-chromene-3-carbonitrile **4b** (935 mg, 5 mmol) and 13% NaOCl (15 mL) were reacted together in the standard conditions. The yellow solid precipitated was purified by column chromatography ( $CH_2Cl_2/MeOH$ , 1:1) to give products **11b** (451 mg, 41%) and **12b** (141 mg, 11%). Compound **11b** had mp 209–210 °C (ethyl acetate). EI-MS:  $m/z=220$  ( $M^+$ ).  $^1H$  NMR (DMSO- $d_6$ ): 7.04 (1H, d,  $J=3.0$  Hz,  $H_5$ ); 7.10 (1H, dd,  $J=9.0, 3.0$  Hz,  $H_7$ ); 7.31 (d, 1H,  $J=9.0$  Hz,  $H_8$ ); 8.44 (1H, s,  $H_4$ ); 10.06 (1H, s,  $OH$ ).  $^{13}C$  NMR (DMSO- $d_6$ ):  $\delta$  101.7, 113.8, 113.9, 116.8, 118.1, 122.1, 145.23, 145.8, 154.8, 157.9. (Found: C, 54.82; H, 2.30; N, 12.57.  $C_{10}H_5N_2O_2Cl$  requires: C, 54.44; H, 2.28; N, 12.70);  $\nu_{\max}$  (KBr) 3340, 2249, 1654  $cm^{-1}$ . Compound **12b** had mp 204–205 °C ( $CH_2Cl_2$ ). EI-MS:  $m/z=254$  ( $M^+$ ).  $^1H$  NMR (DMSO- $d_6$ ): 7.28 (1H, d,  $J=9.0$  Hz,  $H_7$ ); 7.33 (1H, d,  $J=9.0$  Hz,  $H_8$ ); 8.49 (1H, s,  $H_4$ ); 10.06 (1H, s,  $OH$ ). (Found: C, 47.01; H, 1.51; N, 10.60.  $C_{10}H_4N_2O_2Cl_2$  requires: C, 47.09; H, 1.58; N, 10.98);  $\nu_{\max}$  (KBr) 3058, 2237, 1619  $cm^{-1}$ .

**4.3.3. 2-(Chloroimino)-7-hydroxy-2H-chromene-3-carbonitrile 11c.** This was prepared from 7-hydroxy-2-imino-2H-chromene-3-carbonitrile **4c** (935 mg, 5 mmol) and 13% NaOCl (15 mL) in 48% (528 mg) yield as a yellow solid. It was purified by column chromatography ( $CHCl_3$ ) and had mp 210–211 °C ( $CH_2Cl_2$ ). EI-MS:  $m/z=220$  ( $M^+$ ).  $^1H$  NMR (DMSO- $d_6$ ): 7.04 (1H, d,  $J=2.4$  Hz,  $H_8$ ); 6.81 (1H, dd,  $J=8.4, 2.4$  Hz,  $H_6$ ); 7.53 (d, 1H,  $J=8.4$  Hz,  $H_5$ ); 8.36 (1H, s,  $H_4$ ); 11.17 (1H, s,  $OH$ ). (Found: C, 54.34; H, 2.29; N, 12.35.  $C_{10}H_5N_2O_2Cl$  requires: C, 54.44; H, 2.28; N, 12.70);  $\nu_{\max}$  (KBr) 3294, 2243, 1633  $cm^{-1}$ .

**4.3.4. 2-(Chloroimino)-8-hydroxy-2H-chromene-3-carbonitrile 11d.** This was prepared from 8-hydroxy-2-imino-2H-chromene-3-carbonitrile **4d** (935 mg, 5 mmol) and 13% NaOCl (10 mL) in 52% (572 mg) yield as a yellow solid. It was purified by column chromatography ( $CH_2Cl_2$ /heptane, 1:4) and had mp 210–211 °C ( $CH_2Cl_2$ ). EI-MS:  $m/z=220$  ( $M^+$ ).  $^1H$  NMR (DMSO- $d_6$ ): 7.09–7.12 (1H, m,  $H_7$ ); 7.18–7.22 (2H, m,  $H_6, H_5$ ); 8.44 (1H, s,  $H_4$ ); 10.58 (1H, s,  $OH$ ). (Found: C, 54.17; H, 2.27; N, 12.50.  $C_{10}H_5N_2O_2Cl$  requires: C, 54.44; H, 2.28; N, 12.70);  $\nu_{\max}$  (KBr) 3312, 2250, 1609  $cm^{-1}$ .

**4.3.5. 2-(Chloroimino)-7-methoxy-2H-chromene-3-carbonitrile 11e.** This was prepared from 7-methoxy-2-imino-2H-chromene-3-carbonitrile **4e** (1000 mg, 5 mmol) and 13% NaOCl (10 mL) in 41% (480 mg) yield as a white solid. It was purified by column chromatography ( $CHCl_3$ ) and had mp 224–225 °C ( $CHCl_3$ ). EI-MS:  $m/z=234$  ( $M^+$ ).  $^1H$  NMR (DMSO- $d_6$ ): 3.91 (3H, s,  $OCH_3$ ); 7.00 (1H, dd,  $J=8.7, 2.4$  Hz,  $H_6$ ); 7.06 (1H, d,  $J=2.4$  Hz,  $H_8$ ); 7.62 (1H, d,  $J=8.7$  Hz,  $H_5$ ); 8.41 (1H, s,  $H_4$ ). (Found: C, 56.26; H, 3.19; N, 12.17.  $C_{11}H_7N_2O_2Cl$  requires: C, 56.31; H, 3.01; N, 11.94);  $\nu_{\max}$  (KBr) 2227, 1630  $cm^{-1}$ .

**4.3.6. 2-(Chloroimino)-6-bromo-2H-chromene-3-carbonitrile 11f and 6-bromo-2-[[6-bromo-2-(chloroimino)-3,3-dimethyl-3,4-dihydro-2H-chromene-4-yl]imino]-2H-chromene-3-carbonitrile 13.** 6-Bromo-2-imino-2H-chromene-3-carbonitrile **4f** (1005 mg, 5 mmol) and 13% NaOCl

(7 mL) were reacted together in the standard conditions. A white solid precipitated which was purified by column chromatography ( $\text{CHCl}_3$ ) to give product **11f** (480 mg, 30%) and **13** (312 mg, 11%). Compound **11f** had mp 200–201 °C ( $\text{CHCl}_3$ ). EI-MS:  $m/z=282$  ( $\text{M}^+$ ).  $^1\text{H}$  NMR ( $\text{DMSO}-d_6$ ): 7.44 (1H, d,  $J=9.0$  Hz,  $H_8$ ); 7.85 (1H, dd,  $J=9.0, 2.7$  Hz,  $H_7$ ); 7.93 (1H, d,  $J=2.7$  Hz,  $H_5$ ); 8.40 (1H, s,  $H_4$ ). (Found: C, 42.45; H, 1.18; N, 9.49.  $\text{C}_{10}\text{H}_4\text{N}_2\text{OClBr}$  requires: C, 42.36; H, 1.42; N, 9.88);  $\nu_{\text{max}}$  (KBr) 2238, 1662  $\text{cm}^{-1}$ . Compound **13** had mp > 260 °C (ethyl acetate/toluene, 1:1). EI-MS:  $m/z=564$  ( $\text{M}^+$ ).  $^1\text{H}$  NMR ( $\text{DMSO}-d_6$ ): 5.99 (1H, s,  $H'_4$ ); 7.40 (1H, d,  $J=3.0$  Hz,  $H'_5$ ); 7.68 (1H, d,  $J=8.7$  Hz,  $H'_8$ ); 7.70–7.74 (1H, m,  $H'_7$ ); 7.91 (1H, d,  $J=2.7$  Hz,  $H_5$ ); 7.96 (1H, dd,  $J=9.0, 2.7$  Hz,  $H_7$ ); 8.07–8.08 (1H, m,  $H_8$ ); 8.34 (1H, s,  $H_4$ );  $\nu_{\text{max}}$  (KBr) 2232, 1650  $\text{cm}^{-1}$ .

**4.3.7. Ethyl 2-(Chloroimino)-6-hydroxy-2H-chromene-3-carboxylate 11g and ethyl 5-chloro-2-(chloroimino)-6-hydroxy-2H-chromene-3-carboxylate 12g.** Ethyl 6-hydroxy-2-imino-2H-chromene-3-carboxylate **8a** (1165 mg, 5 mmol) and 13% NaOCl (16 mL) were reacted together in the standard conditions. A yellow solid precipitated which was purified by column chromatography ( $\text{CH}_2\text{Cl}_2/\text{MeOH}$ , 100:1) to give **11g** (346 mg, 26%) and **12g** (196 mg, 13%). Compound **11g** had mp 176–177 °C ( $\text{CH}_2\text{Cl}_2$ ). EI-MS:  $m/z=267$  ( $\text{M}^+$ ).  $^1\text{H}$  NMR ( $\text{DMSO}-d_6$ ): 1.29 (3H, t,  $J=7.2$  Hz,  $\text{CH}_3\text{CH}_2$ ); 4.28 (2H, q,  $J=7.2$  Hz,  $\text{CH}_3\text{CH}_2$ ); 7.03 (1H, dd,  $J=8.7, 3.0$  Hz,  $H_7$ ); 7.08 (1H, d,  $J=2.7$  Hz,  $H_5$ ); 7.27 (1H, d,  $J=8.7$  Hz,  $H_8$ ); 8.05 (1H, s,  $H_4$ ); 9.86 (1H, s, OH).  $^{13}\text{C}$  NMR ( $\text{DMSO}-d_6$ ):  $\delta$  14.9, 62.4, 115.0, 117.3, 119.5, 121.2, 121.7, 139.4, 146.3, 155.3, 158.7, 163.6. (Found: C, 50.84; H, 3.95; N, 4.77.  $\text{C}_{12}\text{H}_{10}\text{NO}_4\text{Cl} \times \text{H}_2\text{O}$  requires: C, 50.45; H, 4.23; N, 4.90);  $\nu_{\text{max}}$  (KBr) 3321, 1713, 1747  $\text{cm}^{-1}$ . Compound **12g** had mp 152–153 °C ( $\text{CH}_2\text{Cl}_2$ ). EI-MS:  $m/z=301$  ( $\text{M}^+$ ).  $^1\text{H}$  NMR ( $\text{DMSO}-d_6$ ): 1.30 (3H, t,  $J=7.2$  Hz,  $\text{CH}_3\text{CH}_2$ ); 4.30 (2H, q,  $J=7.2$  Hz,  $\text{CH}_3\text{CH}_2$ ); 7.24 (1H, d,  $J=9.0$  Hz,  $H_7$ ); 7.29 (1H, dd,  $J=9.0, 0.9$  Hz,  $H_8$ ); 8.06 (1H, d,  $J=0.9$  Hz,  $H_4$ ); 10.65 (1H, s, OH). (Found: C, 46.37; H, 3.11; N, 4.21.  $\text{C}_{12}\text{H}_9\text{NO}_4\text{Cl}_2 \times \frac{1}{2}\text{H}_2\text{O}$  requires: C, 46.33; H, 3.24; N, 4.50);  $\nu_{\text{max}}$  (KBr) 3319, 1725, 1760  $\text{cm}^{-1}$ .

#### 4.4. General procedure for the preparation of N-hydrazono-benzopyran-2-imine

A mixture of benzopyran-2-imine derivatives (3 mmol), hydrazine derivatives (3 mmol) and  $\text{NH}_4\text{OAc}$  (3.5 mmol) or NaOAc (3 mmol) was dissolved in 15 mL of acetic acid and stirred at rt for 1 h. The product precipitated from the reaction mixture and was collected by filtration. It was recrystallized from an appropriate solvent. The following compounds were prepared in this manner.

**4.4.1. 2-(Phenylhydrazono)-2H-chromene-3-carbonitrile 15a.** This was prepared from 2-imino-2H-chromene-3-carbonitrile **4a** (510 mg, 3 mmol), phenylhydrazine **14a** (0.294 mL, 3 mmol) and  $\text{NH}_4\text{OAc}$  (270 mg, 3.5 mmol) in acetic acid (15 mL) as a red solid (483 mg, 37%). It had mp 205–206 °C (e.g., acetic acid). EI-MS:  $m/z=261$  ( $\text{M}^+$ ).  $^1\text{H}$  NMR ( $\text{DMSO}-d_6$ ): 6.74–6.80 (1H, m,  $H'_4$ ); 7.14–7.18 (2H, m,  $H'_2, H'_6$ ); 7.20–7.26 (4H, m,  $H_5, H_6, H'_3, H'_5$ ); 7.43–7.46 (1H, m,  $H_8$ ); 7.49–7.55 (1H, m,  $H_7$ ); 7.80 (1H, s,  $H_4$ ); 9.61

(1H, s, NH). (Found: C, 73.39; H, 4.58; N, 15.99.  $\text{C}_{16}\text{H}_{11}\text{N}_3\text{O}$  requires: C, 73.55; H, 4.24; N, 16.08);  $\nu_{\text{max}}$  (KBr) 3292, 2238  $\text{cm}^{-1}$ .

**4.4.2. 6-Hydroxy-2-(phenylhydrazono)-2H-chromene-3-carbonitrile 15b.** This was prepared from 6-hydroxy-2-imino-2H-chromene-3-carbonitrile **4b** (558 mg, 3 mmol), phenylhydrazine **14a** (0.294 mL, 3 mmol) and  $\text{NH}_4\text{OAc}$  (270 mg, 3.5 mmol) in acetic acid (15 mL) as a red solid (900 mg, 65%). It had mp 258–259 °C (e.g., acetic acid). EI-MS:  $m/z=277$  ( $\text{M}^+$ ).  $^1\text{H}$  NMR ( $\text{DMSO}-d_6$ ): 6.72–6.77 (1H, m,  $H'_4$ ); 6.82 (1H, d,  $J=3.0$  Hz,  $H_5$ ); 6.91 (1H, dd,  $J=8.7, 3.0$  Hz,  $H_7$ ); 7.09 (1H, d,  $J=8.7$  Hz,  $H_8$ ); 7.13–7.16 (2H, m,  $H'_2, H'_6$ ); 7.20–7.25 (2H, m,  $H'_3, H'_5$ ); 7.75 (1H, s,  $H_4$ ); 9.51 (1H, s, NH); 9.75 (1H, s, OH). (Found: C, 69.07; H, 4.10; N, 15.12.  $\text{C}_{16}\text{H}_{11}\text{N}_3\text{O}_2$  requires: C, 69.31; H, 3.99; N, 15.15);  $\nu_{\text{max}}$  (KBr) 3313, 2250  $\text{cm}^{-1}$ .

**4.4.3. 8-Hydroxy-2-(phenylhydrazono)-2H-chromene-3-carbonitrile 15c.** This was prepared from 8-hydroxy-2-imino-2H-chromene-3-carbonitrile **4d** (558 mg, 3 mmol), phenylhydrazine **14a** (0.294 mL, 3 mmol) and  $\text{NH}_4\text{OAc}$  (270 mg, 3.5 mmol) in acetic acid (15 mL) as a red solid (316 mg, 38%). It had mp > 260 °C (e.g., acetic acid). EI-MS:  $m/z=277$  ( $\text{M}^+$ ).  $^1\text{H}$  NMR ( $\text{DMSO}-d_6$ ): 6.77–6.82 (1H, m,  $H'_4$ ); 6.88–6.91 (1H, m,  $H_7$ ); 7.01–7.05 (2H, m,  $H_5, H_6$ ); 7.08–7.11 (2H, m,  $H'_2, H'_6$ ); 7.24–2.29 (2H, m,  $H'_3, H'_5$ ); 7.77 (1H, s,  $H_4$ ); 9.73 (s, 2H, NH, OH). (Found: C, 69.38; H, 4.14; N, 14.81.  $\text{C}_{16}\text{H}_{11}\text{N}_3\text{O}_2$  requires: C, 69.31; H, 3.99; N, 15.15);  $\nu_{\text{max}}$  (KBr) 3326, 2241  $\text{cm}^{-1}$ .

**4.4.4. 7-Methoxy-2-(phenylhydrazono)-2H-chromene-3-carbonitrile 15d.** This was prepared from 7-methoxy-2-imino-2H-chromene-3-carbonitrile **4e** (600 mg, 3 mmol), phenylhydrazine **14a** (0.294 mL, 3 mmol) and  $\text{NH}_4\text{OAc}$  (270 mg, 3.5 mmol) in acetic acid (15 mL) as a red solid (411 mg, 47%). It had mp 247–248 °C (e.g., acetic acid). EI-MS:  $m/z=291$  ( $\text{M}^+$ ).  $^1\text{H}$  NMR ( $\text{DMSO}-d_6$ ): 3.86 (3H, s,  $\text{OCH}_3$ ); 6.73–6.83 (3H, m,  $H'_4, H_6, H_8$ ); 7.12–7.15 (2H, m,  $H'_2, H'_6$ ); 7.20–7.25 (2H, m,  $H'_3, H'_5$ ); 7.39 (1H, dd,  $J=9.0$  Hz,  $H_5$ ); 7.76 (1H, s,  $H_4$ ); 9.50 (1H, s, NH). (Found: C, 69.88; H, 4.31; N, 14.35.  $\text{C}_{17}\text{H}_{13}\text{N}_3\text{O}_2$  requires: C, 70.09; H, 4.50; N, 14.42);  $\nu_{\text{max}}$  (KBr) 3305, 2230  $\text{cm}^{-1}$ .

**4.4.5. Ethyl 6-hydroxy-2-(phenylhydrazono)-2H-chromene-3-carboxylate 15e.** This was prepared from 6-hydroxy-2-imino-2H-chromene-3-carboxylate **8a** (699 mg, 3 mmol), phenylhydrazine **14a** (0.294 mL, 3 mmol) and  $\text{NH}_4\text{OAc}$  (270 mg, 3.5 mmol) in acetic acid (15 mL) as a red solid (302 mg, 31%). It had mp 178–179 °C (e.g., acetic acid). EI-MS:  $m/z=324$  ( $\text{M}^+$ ).  $^1\text{H}$  NMR ( $\text{DMSO}-d_6$ ): 1.34 (3H, t,  $J=7.2$  Hz,  $\text{CH}_2\text{CH}_3$ ); 4.30 (2H, q,  $J=7.2$  Hz,  $\text{CH}_2\text{CH}_3$ ); 6.68–6.73 (1H, m,  $H'_4$ ); 6.82–7.08 (3H, m,  $H_5, H_7, H_8$ ); 7.10–7.13 (2H, m,  $H'_2, H'_6$ ); 7.16–7.18 (2H, m,  $H'_3, H'_5$ ); 7.36 (1H, s,  $H_4$ ); 9.38 (1H, s, NH); 9.58 (rs, 1H, OH). (Found: C, 67.02; H, 5.30; N, 9.02.  $\text{C}_{18}\text{H}_{16}\text{N}_2\text{O}_4$  requires: C, 66.66; H, 4.97; N, 8.64);  $\nu_{\text{max}}$  (KBr) 3378, 1678  $\text{cm}^{-1}$ .

**4.4.6. Ethyl 8-hydroxy-2-(phenylhydrazono)-2H-chromene-3-carboxylate 15f.** This was prepared from 8-hydroxy-2-imino-2H-chromene-3-carboxylate **8b** (699 mg, 3 mmol), phenylhydrazine **14a** (0.294 mL,



3 mmol) and  $\text{NH}_4\text{OAc}$  (270 mg, 3.5 mmol) in acetic acid (15 mL) as red solid (622 mg, 64%). It had mp 208–209 °C (e.g., acetic acid). EI-MS:  $m/z=324$  ( $\text{M}^+$ ).  $^1\text{H}$  NMR (DMSO- $d_6$ ): 1.34 (3H, t,  $J=7.2$  Hz,  $\text{CH}_2\text{CH}_3$ ); 4.31 (2H, q,  $J=7.2$  Hz,  $\text{CH}_2\text{CH}_3$ ); 6.72–6.78 (1H, m,  $H'_4$ ); 6.95–6.98 (3H, m,  $H_5$ ,  $H_6$ ,  $H_7$ ); 7.06–7.09 (2H, m,  $H'_2$ ,  $H'_6$ ); 7.20–7.25 (2H, m,  $H'_3$ ,  $H'_5$ ); 7.40 (1H, s,  $H_4$ ); 9.68 (2H, s, OH, NH).  $^{13}\text{C}$  NMR (DMSO- $d_6$ ):  $\delta$  14.4, 61.4, 112.5, 119.1, 119.5, 119.8, 120.2, 122.7, 124.5, 129.41, 131.47, 135.9, 140.9, 144.1, 145.5, 164.0. (Found: C, 63.19; H, 5.13; N, 7.99.  $\text{C}_{18}\text{H}_{16}\text{N}_2\text{O}_4 \times \text{H}_2\text{O}$  requires: C, 63.15; H, 5.30; N, 8.18);  $\nu_{\text{max}}$  (KBr) 3395, 1717  $\text{cm}^{-1}$ .

**4.4.7. 2-(Pyridin-2-ylhydrazono)-2H-chromene-3-carbonitrile 16a.** This was prepared from 2-imino-2H-chromene-3-carbonitrile **4a** (170 mg, 1 mmol), 2-hydrazinopyridine **14b** (109 mg, 1 mmol) and  $\text{NH}_4\text{OAc}$  (115 mg, 1.5 mmol) in acetic acid (5 mL) as a red solid (127 mg, 48%). It had mp 164–165 °C (e.g., acetic acid). EI-MS:  $m/z=262$  ( $\text{M}^+$ ).  $^1\text{H}$  NMR (DMSO- $d_6$ ): 6.78–6.82 (1H, m,  $H'_5$ ); 7.12–7.15 (1H, m,  $H_8$ ); 7.19–7.25 (1H, m,  $H_6$ ); 7.34–7.37 (1H, m,  $H'_3$ ); 7.47 (1H, dd,  $J=7.5$ , 1.5 Hz,  $H_5$ ); 7.50–7.56 (1H, m,  $H'_4$ ); 7.65–7.71 (1H, m,  $H_7$ ); 7.93 (1H, s,  $H_4$ ); 8.13–8.15 (1H, m,  $H'_6$ ); 9.97 (1H, s, NH). (Found: C, 68.56; H, 3.92; N, 20.96.  $\text{C}_{15}\text{H}_{10}\text{N}_4\text{O}$  requires: C, 68.69; H, 3.84; N, 21.36);  $\nu_{\text{max}}$  (KBr) 2299, 1598  $\text{cm}^{-1}$ .

**4.4.8. 6-Hydroxy-2-(pyridin-2-ylhydrazono)-2H-chromene-3-carbonitrile 16b.** This was prepared from 6-hydroxy-2-imino-2H-chromene-3-carbonitrile **4b** (186 mg, 1 mmol), 2-hydrazinopyridine **14b** (109 mg, 1 mmol) and  $\text{NH}_4\text{OAc}$  (115 mg, 1.5 mmol) in acetic acid (5 mL) as a red solid (113 mg, 40%). It had mp 246–247 °C (e.g., acetic acid). EI-MS:  $m/z=278$  ( $\text{M}^+$ ).  $^1\text{H}$  NMR (DMSO- $d_6$ ): 6.76–6.79 (1H, m,  $H'_5$ ); 6.84 (1H, d,  $J=3.0$  Hz,  $H_5$ ); 6.92 (1H, dd,  $J=9.0$ , 3.0 Hz,  $H_7$ ); 7.10–7.13 (1H, m,  $H'_3$ ); 7.20 (1H, d,  $J=9.0$  Hz,  $H_8$ ); 7.64–7.70 (1H, m,  $H'_4$ ); 7.87 (1H, s,  $H_4$ ); 8.11–8.14 (1H, m,  $H'_6$ ); 8.29 (1H, br s, OH); 9.82 (1H, br s, NH). HRMS:  $m/z$  278.0811 ( $\text{M}^+$ , Calcd 278.0803 for  $\text{C}_{15}\text{H}_{10}\text{N}_4\text{O}_2$ );  $\nu_{\text{max}}$  (KBr) 2232, 1654  $\text{cm}^{-1}$ .

**4.4.9. 8-Hydroxy-2-(pyridin-2-ylhydrazono)-2H-chromene-3-carbonitrile 16c.** This was prepared from 8-hydroxy-2-imino-2H-chromene-3-carbonitrile **4d** (186 mg, 1 mmol), 2-hydrazinopyridine **14b** (109 mg, 1 mmol) and  $\text{NH}_4\text{OAc}$  (115 mg, 1.5 mmol) in acetic acid (5 mL) as a red solid (106 mg, 38%). It had mp 255–256 °C (e.g., acetic acid). EI-MS:  $m/z=278$  ( $\text{M}^+$ ).  $^1\text{H}$  NMR (DMSO- $d_6$ ): 6.78–6.82 (1H, m,  $H'_5$ ); 6.91 (1H, d,  $J=6.9$ , 2.4 Hz,  $H_5$ ); 6.99–7.04 (2H, m,  $H_6$ ,  $H_7$ ); 7.13–7.16 (1H, m,  $H'_3$ ); 7.69–7.72 (1H, m,  $H'_4$ ); 7.87 (1H, s,  $H_4$ ); 8.15 (1H, m,  $H'_6$ ); 10.64 (1H, s, NH). (Found: C, 60.32; H, 4.27; N, 16.27.  $\text{C}_{15}\text{H}_{10}\text{N}_4\text{O}_2 \times \text{AcOH}$  requires: C, 60.35; H, 4.17; N, 16.56);  $\nu_{\text{max}}$  (KBr) 2299, 1598  $\text{cm}^{-1}$ .

**4.4.10. Ethyl 8-hydroxy-2-(pyridin-2-ylhydrazono)-2H-chromene-3-carboxylate 16d.** This was prepared from 8-hydroxy-2-imino-2H-chromene-3-carboxylate **8b** (233 mg, 1 mmol), 2-hydrazinopyridine **14b** (109 mg, 1 mmol) and  $\text{NH}_4\text{OAc}$  (115 mg, 1.5 mmol) in acetic acid (5 mL) as a red solid (160 mg, 49%). It had mp 146–147 °C (e.g., acetic acid). EI-MS:  $m/z=325$  ( $\text{M}^+$ ).  $^1\text{H}$  NMR

(DMSO- $d_6$ ): 1.34 (3H, t,  $J=7.2$  Hz,  $\text{CH}_2\text{CH}_3$ ); 4.31 (2H, q,  $J=7.2$  Hz,  $\text{CH}_2\text{CH}_3$ ); 6.74–6.78 (1H, m,  $H'_5$ ); 6.93–7.04 (3H, m,  $H_5$ ,  $H_6$ ,  $H_7$ ); 7.10–7.13 (1H, m,  $H'_3$ ); 7.51 (1H, s,  $H_4$ ); 7.61–7.67 (1H, m,  $H'_4$ ); 8.11–8.13 (1H, m,  $H'_6$ ); 10.60 (1H, s, NH). (Found: C, 63.00; H, 4.72; N, 12.66.  $\text{C}_{17}\text{H}_{15}\text{N}_3\text{O}_4$  requires: C, 62.76; H, 4.65; N, 12.92);  $\nu_{\text{max}}$  (KBr) 1697, 1673  $\text{cm}^{-1}$ .

**4.4.11. 2-[(Anilincarboxyl)hydrazono]-2H-chromene-3-carbonitrile 17a.** This was prepared from 2-imino-2H-chromene-3-carbonitrile **4a** (170 mg, 1 mmol), *N*-phenylhydrazinocarboxamide **14c** (151 mg, 1 mmol) and NaOAc (82 mg, 1 mmol) in acetic acid (5 mL) as a yellow solid (95 mg, 31%). It had mp > 260 °C (e.g., acetic acid). EI-MS:  $m/z=304$  ( $\text{M}^+$ ).  $^1\text{H}$  NMR (DMSO- $d_6$ ): 6.98–7.04 (1H, m,  $H'_4$ ); 7.27–7.33 (4H, m,  $H_5$ ,  $H_6$ ,  $H_7$ ,  $H_8$ ); 7.48–7.52 (2H, m,  $H'_2$ ,  $H'_6$ ); 7.54–7.61 (2H, m,  $H'_3$ ,  $H'_5$ ); 8.09 (1H, s,  $H_4$ ); 8.74 (1H, s, NH); 10.07 (1H, s, NH). (Found: C, 67.43; H, 3.81; N, 18.13.  $\text{C}_{17}\text{H}_{12}\text{N}_4\text{O}_2$  requires: C, 67.10; H, 3.97; N, 18.41);  $\nu_{\text{max}}$  (KBr) 3379, 2236, 1704  $\text{cm}^{-1}$ .

**4.4.12. 2-[(Anilincarboxyl)hydrazono]-6-hydroxy-2H-chromene-3-carbonitrile 17b.** This was prepared from 6-hydroxy-2-imino-2H-chromene-3-carbonitrile **4b** (186 mg, 1 mmol), *N*-phenylhydrazinocarboxamide **14c** (151 mg, 1 mmol) and NaOAc (82 mg, 1 mmol) in acetic acid (5 mL) as a yellow solid (218 mg, 68%). It had mp > 260 °C (e.g., acetic acid). EI-MS:  $m/z=320$  ( $\text{M}^+$ ).  $^1\text{H}$  NMR (DMSO- $d_6$ ): 6.89 (1H, d,  $J=3.0$  Hz,  $H_5$ ); 7.96–7.03 (2H, m,  $H_7$ ,  $H'_4$ ); 7.15 (1H, d,  $J=8.7$  Hz,  $H_8$ ); 7.27–7.32 (2H, m,  $H'_3$ ,  $H'_5$ ); 7.48–7.51 (2H, m,  $H'_2$ ,  $H'_6$ ); 8.03 (1H, s,  $H_4$ ); 8.72 (1H, br s, NH); 9.97 (1H, br s, NH). HRMS:  $m/z$  320.0909 ( $\text{M}^+$ , Calcd 320.0910 for  $\text{C}_{17}\text{H}_{12}\text{N}_4\text{O}_3$ );  $\nu_{\text{max}}$  (KBr) 3377, 2237, 1728  $\text{cm}^{-1}$ .

**4.4.13. 2-[(Anilincarboxyl)hydrazono]-8-hydroxy-2H-chromene-3-carbonitrile 17c.** This was prepared from 8-hydroxy-2-imino-2H-chromene-3-carbonitrile **4d** (186 mg, 1 mmol), *N*-phenylhydrazinocarboxamide **14c** (151 mg, 1 mmol) and NaOAc (82 mg, 1 mmol) in acetic acid (5 mL) as a yellow solid (170 mg, 53%). It had mp > 260 °C (e.g., acetic acid). EI-MS:  $m/z=320$  ( $\text{M}^+$ ).  $^1\text{H}$  NMR (DMSO- $d_6$ ): 7.95–7.10 (4H, m,  $H_5$ ,  $H_6$ ,  $H_7$ ,  $H'_4$ ); 7.27–7.33 (2H, m,  $H'_3$ ,  $H'_5$ ); 7.53–7.56 (2H, m,  $H'_2$ ,  $H'_6$ ); 8.05 (1H, s,  $H_4$ ); 8.82 (1H, br s, NH); 10.72 (1H, br s, NH). (Found: C, 61.64; H, 4.22; N, 16.40.  $\text{C}_{17}\text{H}_{12}\text{N}_4\text{O}_3 \times \frac{1}{2}\text{AcOH}$  requires: C, 61.71; H, 4.03; N, 15.99);  $\nu_{\text{max}}$  (KBr) 3366, 2231, 1687  $\text{cm}^{-1}$ .

**4.4.14. Ethyl 2-[(anilincarboxyl)hydrazono]-6-hydroxy-2H-chromene-3-carboxylate 17d.** This was prepared from 6-hydroxy-2-imino-2H-chromene-3-carboxylate **8a** (233 mg, 1 mmol), *N*-phenylhydrazinocarboxamide **14c** (151 mg, 1 mmol) and NaOAc (82 mg, 1 mmol) in acetic acid (5 mL) as a yellow solid (250 mg, 68%). It had mp 231–232 °C (e.g., acetic acid). EI-MS:  $m/z=367$  ( $\text{M}^+$ ).  $^1\text{H}$  NMR (DMSO- $d_6$ ): 1.33 (3H, t,  $J=7.2$  Hz,  $\text{CH}_2\text{CH}_3$ ); 4.33 (2H, q,  $J=7.2$  Hz,  $\text{CH}_2\text{CH}_3$ ); 6.90–6.95 (m, 2H,  $H_5$ ,  $H_7$ ); 6.98–7.03 (1H, m,  $H'_4$ ); 7.18 (1H, d,  $J=8.4$  Hz,  $H_8$ ); 7.28–7.33 (2H, m,  $H'_3$ ,  $H'_5$ ); 7.48–7.52 (2H, m,  $H'_2$ ,  $H'_6$ ); 7.74 (1H, s,  $H_4$ ); 8.58 (1H, s, NH); 10.04 (1H, s, NH).  $^{13}\text{C}$  NMR (DMSO- $d_6$ ):  $\delta$  14.4, 21.5, 61.6, 114.5, 116.5, 119.0, 119.2, 119.9, 120.9, 122.7, 129.2, 136.2, 138.9, 139.2, 146.1,



153.1, 154.0, 163.4, 172.5. (Found: C, 62.33; H, 4.52; N, 11.52. C<sub>19</sub>H<sub>17</sub>N<sub>3</sub>O<sub>5</sub> requires: C, 62.12; H, 4.66; N, 11.44);  $\nu_{\max}$  (KBr) 3391, 1712, 1682 cm<sup>-1</sup>.

**4.4.15. Ethyl 2-[(anilincarbonyl)hydrazono]-8-hydroxy-2H-chromene-3-carboxylate 17e.** This was prepared from 8-hydroxy-2-imino-2H-chromene-3-carboxylate **8b** (233 mg, 1 mmol), *N*-phenylhydrazinecarboxamide **14c** (151 mg, 1 mmol) and NaOAc (82 mg, 1 mmol) in acetic acid (5 mL) as a yellow solid (334 mg, 91%). It had mp 226–227 °C (e.g., acetic acid). EI-MS:  $m/z$  = 367 (M<sup>+</sup>). <sup>1</sup>H NMR (DMSO-*d*<sub>6</sub>): 1.33 (3H, t,  $J$  = 6.9 Hz, CH<sub>2</sub>CH<sub>3</sub>); 4.34 (2H, q,  $J$  = 6.9 Hz, CH<sub>2</sub>CH<sub>3</sub>); 7.00–7.07 (m, 4H, H<sub>5</sub>, H<sub>6</sub>, H<sub>7</sub>, H'<sub>4</sub>); 7.29–7.34 (2H, m, H'<sub>3</sub>, H'<sub>5</sub>); 7.52–7.55 (2H, m, H'<sub>2</sub>, H'<sub>6</sub>); 7.78 (1H, s, H<sub>4</sub>); 8.62 (1H, br s, NH); 10.65 (1H, br s, NH); 12.00 (1H, br s, OH). (Found: C, 62.32; H, 4.52; N, 11.17. C<sub>19</sub>H<sub>17</sub>N<sub>3</sub>O<sub>5</sub> requires: C, 62.12; H, 4.66; N, 11.44);  $\nu_{\max}$  (KBr) 3363, 1713, 1687 cm<sup>-1</sup>.

**4.4.16. 6-Hydroxy-2-(phenylhydrazono)-2H-chromene-3-carbonitrile 15b and 2,5-dihydroxybenzaldehyde phenylhydrazine 18.** 6-Hydroxy-2-imino-2H-chromene-3-carbonitrile **4b** (558 mg, 3 mmol) and phenylhydrazine **14a** (0.294 mL, 3 mmol) in acetic acid (15 mL) were reacted together as usual. The red solid precipitated which was purified by column chromatography (diethyl ether/CH<sub>2</sub>Cl<sub>2</sub>, 1:20) to give product **15b** (341 mg, 41%) and **18** (145 mg, 21%). Compound **15b** had mp 258–259 °C (e.g., acetic acid). EI-MS:  $m/z$  = 277 (M<sup>+</sup>). <sup>1</sup>H NMR (DMSO-*d*<sub>6</sub>): 6.72–6.77 (1H, m, H'<sub>4</sub>); 6.82 (1H, d,  $J$  = 3.0 Hz, H<sub>5</sub>); 6.91 (1H, dd,  $J$  = 8.7, 3.0 Hz, H<sub>7</sub>); 7.09 (1H, d,  $J$  = 8.7 Hz, H<sub>8</sub>); 7.13–7.16 (2H, m, H'<sub>2</sub>, H'<sub>6</sub>); 7.20–7.25 (2H, m, H'<sub>3</sub>, H'<sub>5</sub>); 7.75 (1H, s, H<sub>4</sub>); 9.51 (1H, s, NH); 9.75 (1H, s, OH). Compound **18** had mp 206–207 °C (EtOH). EI-MS:  $m/z$  = 228 (M<sup>+</sup>). <sup>1</sup>H NMR (DMSO-*d*<sub>6</sub>): 6.58 (1H, dd,  $J$  = 8.7, 3.0 Hz, H<sub>4</sub>); 6.69 (1H, d,  $J$  = 8.7 Hz, H<sub>5</sub>); 6.73 (1H, t,  $J$  = 7.2 Hz, H'<sub>4</sub>); 6.97 (3H, m, H<sub>2</sub>, H'<sub>2</sub>, H'<sub>6</sub>); 7.23 (2H, m, H'<sub>3</sub>, H'<sub>5</sub>); 8.06 (1H, s, CH); 8.79 (1H, s, NH); 9.71 (1H, s, OH); 10.31 (s, 1H, OH). HRMS:  $m/z$  228.0899 (M<sup>+</sup>, Calcd 228.0901 for C<sub>13</sub>H<sub>12</sub>N<sub>2</sub>O<sub>2</sub>);  $\nu_{\max}$  (KBr) 3309, 1601 cm<sup>-1</sup>.

#### Acknowledgements

This research was supported by the Ministry of Education, Science and Sport of Slovenia (L1-6018-04/795). We thank Prof. Dr. Branko Stanovnik, Faculty of Chemistry and Chemical Technology, Ljubljana, for elemental analysis, Prof. Dr. Andrej Petrič, Faculty of Chemistry and Chemical Technology, Ljubljana, for <sup>1</sup>H NMR spectra, Dr. Bogdan Kralj, Institut Jožef Stefan, Ljubljana, for mass spectrometry and Prof. Dr. Dominique Lorcy, Université de Rennes 1, France, for <sup>13</sup>C NMR spectra.

#### References and notes

- Maxwell, A. *Mol. Microbiol.* **1993**, *9*, 681–686.
- Abd-Allah, O. A. *Farmaco* **2000**, *55*, 641–649.
- El-Agrody, A. M.; El-Latif, M. S. A.; El-Hady, N. A.; Fakary, A. H.; Bedair, A. H. *Molecules* **2001**, *6*, 519–527.
- Emmanuel-Giota, A. A.; Fylaktakidou, K. C.; Hadjipavlou-Litina, D. J.; Litinas, K. E.; Nicolaidis, D. N. *J. Heterocycl. Chem.* **2001**, *38*, 717–722.
- Manolov, I.; Danchev, N. D. *Eur. J. Med. Chem.* **1995**, *30*, 531–536.
- Dexeus, F. H.; Logothetis, C. J.; Sella, A.; Fitz, K.; Amato, R.; Reuben, J. M.; Dozier, N. *J. Clin. Oncol.* **1990**, *8*, 325–329.
- Nofal, Z. M.; El-Zahar, M. I.; El-Karim, S. S. A. *Molecules* **2000**, *5*, 99–113.
- Haugland, R. P. *Handbook of Fluorescent Probes and Research Products*, 9th ed.; Molecular probes: Eugene, 2002.
- Green, G. R.; Evans, J. M.; Vong, A. K. In *Comprehensive Heterocyclic Chemistry II*; Katritzky, A., Rees, C. W., Scriven, E. F. V., Eds.; Pyrans and their benzo derivatives: applications; Pergamon: Oxford, 1996; Vol. 5, Chapter 5.09, pp 469–500.
- Burke, T. R.; Lim, B.; Marquez, V. E.; Li, Z.-H.; Bolen, J. B.; Stefanova, I.; Horak, I. D. *J. Med. Chem.* **1993**, *36*, 425–432.
- Huang, C. K.; Wu, F. Y.; Ai, Y. X. *Bioorg. Med. Chem. Lett.* **1995**, *5*, 2423–2428.
- O'Callaghan, C. N.; Conalty, M. L. *P. Roy. Irish Acad.* **1979**, *6*, 87–98.
- Volmajer, J.; Toplak, R.; Bittner, S.; Leban, I.; Majcen Le Marechal, A. *Tetrahedron Lett.* **2003**, *44*, 2363–2366.
- Padmanabhan, S.; Peri, R.; Triggler, D. J. *Synth. Commun.* **1996**, *26*, 827–831.
- Silin, A. V.; Gorobetis, N. Y.; Sytnik, K. M.; Nikitchenko, V. M. *Visn. Khark. Univ.* **1997**, *395*, 274–277. *Chem. Abstr.* **1998**, *129*, 290037.
- O'Callaghan, C. N.; McMurphy, T. B. H.; O'Brien, J. E. *J. Chem. Soc., Perkin Trans. 2* **1998**, 425–429.
- Kovalenko, S. N.; Sytnik, K. M.; Nikitchenko, V. M.; Rusanova, S. V.; Chernykh, V. P.; Porokhnyak, A. O. *Chem. Heterocycl. Compd.* **1999**, *35*, 167–170.
- Zubkov, V. A.; Kovalenko, S. N.; Chernykh, V. P.; Ivkov, S. M. *Chem. Heterocycl. Compd.* **1994**, *30*, 665–670.
- Mhiri, C.; El Gharbi, R.; Le Bigot, Y. *Synth. Commun.* **1999**, *29*, 3385–3399.
- Bruce, J. M.; Creed, D.; Dawes, K. *J. Chem. Soc. (C)* **1971**, 3749.
- Brufola, G.; Fringuelli, F.; Piematti, O.; Pizzo, F. *Heterocycles* **1996**, *43*, 1257–1266.

# Cinchona alkaloid phase-transfer catalysts revisited: influence of substituted aryl groups on the enantioselectivity of glycine ester enolate alkylation

Sanjeev Kumar and Uma Ramachandran\*

Department of Pharmaceutical Technology, National Institute of Pharmaceutical Education & Research (NIPER), Sector-67, Mohali, Punjab 160 062, India

Received 17 December 2004; revised 15 April 2005; accepted 5 May 2005

**Abstract**—We report herein, the influence of substituted aryl groups in quaternary ammonium salts derived from cinchona alkaloids on enantioselectivity of the alkylation of glycine ester enolates.

© 2005 Elsevier Ltd. All rights reserved.

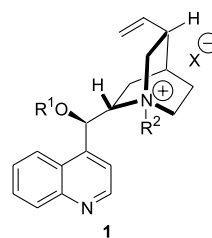
## 1. Introduction

Asymmetric synthesis using phase-transfer catalysts (PTCs) represent one of the important methodologies in organic chemistry. Since, the pioneering work by Dolling et al.<sup>1</sup> chiral PTCs derived from cinchona alkaloids have been applied to various organic reactions.<sup>2</sup>

In 1989, O'Donnell's group reported the enantioselective PTC alkylations of *N*-(diphenylmethylene)glycine *tert*-butyl ester (**8**) for the synthesis of  $\alpha$ -amino acids in enantiomerically pure form using catalyst **1a** derived from cinchonidine.<sup>3</sup> The enantioselective catalytic activity was improved by Lygo and Corey using third generation versions of these catalysts containing an *N*-9-anthracenylmethyl group either with a free OH (**1b**) or with an *O*-allyl group (**1c**), respectively.<sup>4</sup>

When the nitrogen on the bicyclic ring of the cinchona alkaloids are quaternized by the addition of the bulky and rigid anthracenylmethyl group, it seems to give the highest rigidity and steric effect to the catalyst's framework and leads to highly enantioselective alkylations as compared to a benzyl group. Jew et al. found that an *ortho* fluoro substituent on the benzyl group in the quaternary ammonium salt dramatically increased the enantioselectivity in the alkylation of a glycine anion equivalent which was attributed to the electronic effect.<sup>5</sup> They also

explored the combination of electronic and steric factor by way of *ortho*-fluoro-dimeric cinchona-derived PTCs.<sup>6</sup> Dimers and trimers of cinchona alkaloids have also been reported by other workers.<sup>7</sup>



- a) R<sup>1</sup> = H, R<sup>2</sup> = benzyl, X = Cl. b) R<sup>1</sup> = H, R<sup>2</sup> = anthracenylmethyl, X = Cl.  
c) R<sup>1</sup> = allyl, R<sup>2</sup> = anthracenylmethyl, X = Br. d) R<sup>1</sup> = R<sup>2</sup> = 2-methylnaphthyl, X = Br.

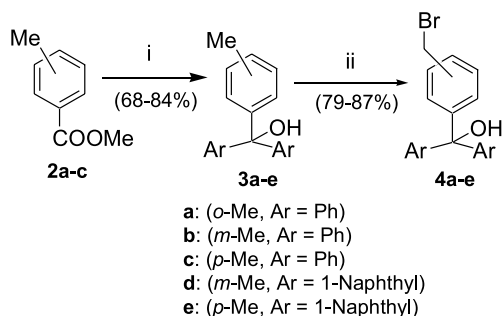
## 2. Results and discussion

We designed new catalysts having diaryl substitution at the 3- and 4-positions of the *N*-benzyl group in cinchonidinium salts to check how substituted aryl groups affect the asymmetric induction in the benzylation reaction as compared to those having flat linear aryl systems like naphthylmethyl and anthracenylmethyl groups.

For the preparation of new cinchona-derived quaternary ammonium salts, the corresponding 2-, 3- and 4-(bromo-methyl)phenyl(diaryl)methanols were prepared, starting from *o*-, *m*- and *p*-toluic acid methyl esters (Scheme 1).

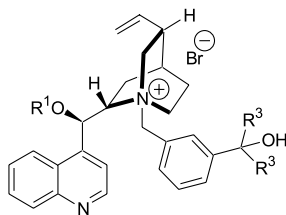
**Keywords:** Cinchona alkaloids; Phase-transfer catalysts; Asymmetric alkylations.

\* Corresponding author. Tel.: +91 172 2214682/87; fax: +91 172 2214692; e-mail: umaram54@yahoo.com



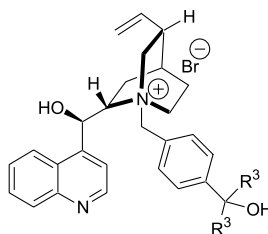
**Scheme 1.** Reagents: (i) ArBr, Mg, THF; (ii) NBS, CCl<sub>4</sub>.

2-, 3- and 4-(Bromomethyl)phenyl(diaryl)methanols thus, prepared were used for quaternization of cinchona alkaloids. This reaction was done in a mixture of acetonitrile and toluene (80:20) at 80 °C. While *meta*- and *para*-(bromomethyl)phenyl(diaryl)methanols formed the quaternary salts in 80–92% yields, the *ortho*-(bromomethyl)phenyl-(diaryl)methanol failed to quaternize cinchonidine.



(5): a) R<sup>1</sup> = H, R<sup>3</sup> = Ph. b) R<sup>1</sup> = H, R<sup>3</sup> = 1-Naphthyl.

(6) R<sup>1</sup> = Allyl, R<sup>3</sup> = 1-Naphthyl.



(7): a) R<sup>3</sup> = Ph.

b) R<sup>3</sup> = 1-Naphthyl.

The catalysts **5–7** were evaluated in the enantioselective phase-transfer benzylation of *N*-(diphenylmethylene)glycine *tert*-butyl ester. The reaction was carried out in toluene/dichloromethane (7:3) at 0 °C and at –20 °C using 50% aqueous KOH as a base under argon (Table 1).

**Table 1.** Benzylation of imine **8** using catalysts **1a** and **5–7**

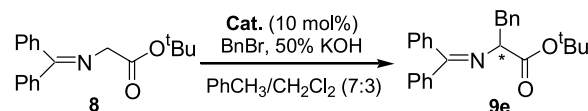
Entry	Catalyst	Time (h)	Temp (°C)	Yield <sup>a</sup> (%)	%ee <sup>b</sup> [config] <sup>c</sup>
1	<b>1a</b>	10	0	89	66 ( <i>S</i> )
2	<b>5a</b>	12	0	83	73 ( <i>S</i> )
3	<b>7a</b>	18	0	74	72 ( <i>S</i> )
4	<b>7b</b>	18	0	80	80 ( <i>S</i> )
5	<b>5b</b>	16	0	86	84 ( <i>S</i> )
6	<b>6</b>	5	0	90	90 ( <i>S</i> )
7	<b>6</b>	7	–20	92	92 ( <i>S</i> )

<sup>a</sup> Yields of isolated product.

<sup>b</sup> Based on HPLC analysis using Chiralcel OD-H column with hexanes/2-propanol (99.5:0.5) as eluent.

<sup>c</sup> The absolute configuration was determined by comparison of the HPLC retention time with that of an authentic sample, which was independently synthesized by the reported procedure.<sup>4</sup>

As shown in Table 1, substitution at the *meta*- and *para*-position with diphenyl moieties gave slight increases in the enantioselectivity as compared to the unsubstituted *N*-benzyl group (entries 1–3). The use of bulkier substituents, that is, di(1-naphthyl) moieties in place of di(phenyl) showed an increase in enantiomeric excess (entries 4–5). The *meta*-di(1-naphthyl) substituted catalyst **5b** gave higher enantiomeric excess as compared to the *para*-substituted counterpart **7b** (Scheme 2).



**Scheme 2.** Benzylation of imine **8** using various catalysts.

The catalyst **5b** was *O*(9)-allylated with allyl bromide in the presence of K<sub>2</sub>CO<sub>3</sub> to give the catalyst **6** in 88% yield. The use of catalyst **6** gave high enantiomeric excess (92%) favouring the (*S*)-isomer when the reaction was carried at –20 °C.

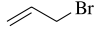

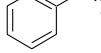
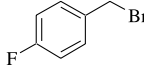
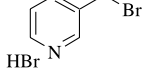
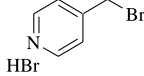
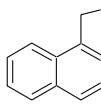
Our results show that the quaternary ammonium salts **5–7** containing the triaryl carbinol units provide better steric screens as compared to the naphthylmethyl group (**1d**, 49%)<sup>8</sup> in the asymmetric benzylation of **8**. Among them, *O*(9)-allyl-*N*-[3-(hydroxy-di-naphthalen-1-yl-methyl)-benzyl]cinchonidinium bromide (**6**) seems to give the best steric screen as well as cation rigidity for the formation of close ion-pairs between the bridgehead nitrogen and the enolate of **8**. However, it is less effective than **1c** which has an anthracenylmethyl group in the quaternary ammonium salt.

Taking catalyst **6**, phase-transfer alkylation of **8** with various alkyl halides was carried out. The results obtained for the asymmetric alkylation of **8** with various alkyl halides, using the similar conditions, and at –20 °C are given in Table 2. High enantiomeric excesses up to 94% were obtained with a wide variety of alkylating agents (entries 1–10) for the asymmetric synthesis of  $\alpha$ -amino acids (Scheme 3).

### 3. Conclusion

In conclusion, we studied various cinchona alkaloids quaternized by triarylcarbinol units in asymmetric PTC

**Table 2.** Alkylation of imine **8** using catalyst **6**

Entry	RX <sup>a</sup>	Time (h)	Product	Yield <sup>b</sup> (%)	%ee <sup>c</sup> [config] <sup>d</sup>
1	CH <sub>3</sub> CH <sub>2</sub> I <sup>c</sup>	8	<b>9a</b> <sup>7a</sup>	68	92 (S)
2	CH <sub>3</sub> (CH <sub>2</sub> ) <sub>4</sub> CH <sub>2</sub> I <sup>c</sup>	8	<b>9b</b> <sup>7a</sup>	78	94 (S)
3		3	<b>9c</b> <sup>7a</sup>	92	93 (S)
4		7	<b>9d</b> <sup>7a</sup>	90	93 (S)
5		6	<b>9e</b> <sup>4b</sup>	93	92 (S)
6		6	<b>9f</b> <sup>7a</sup>	93	91 (S)
7		10	<b>9g</b>	87	92 <sup>f</sup>
8		10	<b>9h</b>	85	91 <sup>f</sup>
9		8	<b>9i</b> <sup>4</sup>	89	89 (S)

<sup>a</sup> The reaction was carried out with RX (2.0 equiv) and aqueous KOH (50%, 12 equiv) in the presence of **6** (10 mol%) in toluene/CH<sub>2</sub>Cl<sub>2</sub> (7:3) at –20 °C.

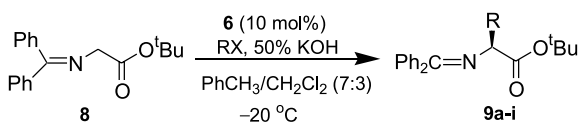
<sup>b</sup> Yields of isolated products.

<sup>c</sup> Based on chiral HPLC using a Chiralcel OD-H column.

<sup>d</sup> The absolute configuration was determined by comparison of the HPLC retention time with that of an authentic sample, which was independently synthesized by the reported procedure.<sup>4–7</sup>

<sup>e</sup> RX (5.0 equiv) was used.

<sup>f</sup> Absolute configuration not determined.

**Scheme 3.** Alkylation of imine **8** using catalyst **6**.

reactions. *O*(9)-Allyl-*N*-[3-(hydroxy-di-naphthalen-1-yl)-methyl]-benzyl]cinchonidinium bromide (**6**) proved to be the best as it gave very high ees in the alkylated products of **8**. The applications to other types of phase-transfer catalytic reactions using **6** are currently being investigated. Further, it would be interesting to synthesize and study the catalysts where R<sup>3</sup> aryl carbinol units can be heteroaromatic or further substituted aromatic systems.

## 4. Experimental

### 4.1. General

Melting points are uncorrected. <sup>1</sup>H and <sup>13</sup>C spectra were recorded at 300 and 75 MHz using a Bruker Advance spectrometer, respectively, with chemical shifts in ppm and tetramethylsilane as the internal standard. Infra-red absorption spectra were recorded on a Nicolet Impact 410 spectrometer; the frequencies in the IR spectra are indicated in cm<sup>-1</sup>. Mass spectral data were recorded on a Finnigan-MAT LCMS spectrometer. Elemental analyses were recorded on an Elementa Vario EL. HPLC was performed on a Shimadzu SPD-10A using a chiral phase column (DAICEL Chiralcel OD and Chiralcel OD-H, 254 nm). TLC

was performed on plates pre-coated (0.25 mm) with silica gel 60, Merck F-254. The plates were visualized by the use of a combination of UV (254 nm) and iodine. Column chromatography was carried out with silica gel Merck 60 (80–230 mesh).

### 4.2. General procedure for the synthesis of 2- or -3 or 4-methylphenyl(diphenyl)methanol

Under argon, to a suspension of magnesium turnings (5.9 g, 246 mmol) in dry tetrahydrofuran (100 mL) was added bromobenzene (26.3 mL, 249 mmol) dropwise at such a rate so as to maintain a gentle reflux over a period of 0.5 h. After stirring the reaction mixture for 1 h at rt, a solution of 2-, 3- or 4-toluic acid methyl esters (15 g, 99.8 mmol) in tetrahydrofuran (25 mL) was added dropwise and the stirring continued for 5 h at 50 °C. The reaction mixture was cooled to rt, poured onto ice and acidified with 2 N HCl. The aqueous layer was extracted with chloroform (3 × 60 mL) and the combined organic layers dried over Na<sub>2</sub>SO<sub>4</sub> and concentrated. Purification of the residue oil by column chromatography on silica gel (hexane/EtOAc, 95:5) gave 2- or -3 or 4-methylphenyl(diphenyl)methanols as white solids (70–84%).

**4.2.1. 2-Methylphenyl(diphenyl)methanol (3a).** 19.2 g, yield 70%; mp 100–101 °C; IR (KBr)  $\nu$  3468, 3058, 3027, 2929, 2863, 1598, 1509, 1445, 1328, 1153, 1007 cm<sup>-1</sup>; <sup>1</sup>H NMR (CDCl<sub>3</sub>)  $\delta$  2.33 (s, 3H), 2.77 (s, 1H), 7.09–7.33 (m, 14H); MS (APCI): *m/z* 257 (M<sup>+</sup> – OH, 100). Anal. Calcd for C, 87.56; H, 6.61. Found C, 87.14; H, 6.78.

**4.2.2. 3-Methylphenyl(diphenyl)methanol (3b).** 22.5 g, yield 82%; mp 62–63 °C; IR (KBr)  $\nu$  3462, 3049, 2928, 1594, 1490, 1440, 1321, 1154, 1010  $\text{cm}^{-1}$ ;  $^1\text{H}$  NMR ( $\text{CDCl}_3$ )  $\delta$  2.31 (s, 3H), 2.79 (s, 1H), 7.09–7.33 (m, 14H); MS (APCI):  $m/z$  274 ( $\text{M}^+$ ), 257. Anal. Calcd for C, 87.56; H, 6.61. Found C, 87.18; H, 6.71.

**4.2.3. 4-Methylphenyl(diphenyl)methanol (3c).** 23.1 g, yield 84%; mp 72–73 °C; IR (KBr)  $\nu$  3466, 3058, 1597, 1489, 1444, 1325, 1156, 1009  $\text{cm}^{-1}$ ;  $^1\text{H}$  NMR ( $\text{CDCl}_3$ )  $\delta$  2.13 (s, 3H), 2.96 (s, 1H), 7.17–7.32 (m, 14H); MS (APCI)  $m/z$  274 ( $\text{M}^+$ ), 257, 197, 105. Anal. Calcd for C, 87.56; H, 6.61. Found C, 87.23; H, 6.67.

#### 4.3. General procedure for the synthesis of 2-, 3- or 4-(bromomethyl)phenyl(diphenyl)methanol

To a solution of 3- or 4-methylphenyl(diphenyl)methanol (5.0 g, 18.2 mmol) in  $\text{CCl}_4$  (50 mL) at 70 °C was added *N*-bromosuccinimide (3.24 g, 18.2 mmol) and benzoyl peroxide (88 mg, 0.36 mmol) in two portions. The solution was stirred under reflux for 5 h and cooled to rt, washed successively with 10%  $\text{NaHCO}_3$ , water and brine, dried over anhydrous  $\text{Na}_2\text{SO}_4$  and the solvent evaporated in vacuo to afford the product as oils in 79–85% yield, which was used without purification for the next step.

**4.3.1. [2-(Bromomethyl)phenyl](diphenyl)methanol (4a).** 5.5 g, yield 85%; IR (neat)  $\nu$  3452, 3046, 1593, 1478, 1444, 1325, 1156, 1006  $\text{cm}^{-1}$ ;  $^1\text{H}$  NMR ( $\text{CDCl}_3$ )  $\delta$  4.52 (s, 2H), 5.18 (s, 1H), 7.10–7.33 (m, 14H); MS (APCI):  $m/z$  337 ( $\text{M}^+ - \text{OH}$ ), 335, 257, 255.

**4.3.2. [3-(Bromomethyl)phenyl](diphenyl)methanol (4b).** 5.2 g, yield 80%; IR (neat)  $\nu$  3442, 3029, 2923, 1598, 1442, 1356, 1148, 1012  $\text{cm}^{-1}$ ;  $^1\text{H}$  NMR ( $\text{CDCl}_3$ )  $\delta$  2.82 (s, 1H), 4.48 (s, 2H), 7.22–7.48 (m, 14H); MS (APCI):  $m/z$  (%) 354 ( $\text{M}^+$ ), 352 ( $\text{M}^+$ ), 337, 274.

**4.3.3. [4-(Bromomethyl)phenyl](diphenyl)methanol (4c).** 5.1 g, yield 79%; IR (neat)  $\nu$  3432, 3059, 2923, 1598, 1445, 1409, 1386, 1228, 11545, 1018  $\text{cm}^{-1}$ ;  $^1\text{H}$  NMR ( $\text{CDCl}_3$ )  $\delta$  2.81 (br s, 1H), 4.52 (s, 2H), 7.24–7.48 (m, 14H); MS (APCI):  $m/z$  354 ( $\text{M}^+$ ), 352 ( $\text{M}^+$ ), 273, 105.

#### 4.4. General procedure for the synthesis of 3- or 4-methylphenyl-di(1-naphthyl)methanol

Under argon, to a suspension of magnesium turnings (5.9 g, 246 mmol) in dry tetrahydrofuran (100 mL) was added a solution of 1-bromonaphthalene (51.2 g, 247 mmol) in tetrahydrofuran (40 mL) slowly at such a rate so as to maintain a gentle reflux over a period of 0.5 h. After stirring the reaction mixture for 2 h at 50 °C, a solution of 3- or 4-toluic acid methyl ester (15 g, 99.8 mmol) in tetrahydrofuran (25 mL) was added drop wise and the stirring continued for 8 h at 60 °C. The reaction mixture was cooled to rt, poured onto ice and acidified with 2 N HCl. The aqueous layer was extracted with chloroform (2  $\times$  100 mL) the combined organic layers dried over  $\text{Na}_2\text{SO}_4$  and concentrated in vacuo. Purification of the residue by crystallization from toluene/hexane gave the product as white solid (68–72%).

**4.4.1. 3-Methylphenyl-di(1-naphthyl)methanol (3d).** 27 g, yield 72%; mp 180–183 °C decomp.; IR (KBr)  $\nu$  3550, 3043, 2922, 1599, 1505, 1395, 1341, 1222, 1148, 1050, 1011  $\text{cm}^{-1}$ ;  $^1\text{H}$  NMR ( $\text{CDCl}_3$ )  $\delta$  2.29 (s, 3H), 3.60 (s, 1H), 6.84 (d,  $J=7.1$  Hz, 2H), 7.09–7.24 (m, 8H), 7.38 (t,  $J=7.3$  Hz, 2H), 7.77 (d,  $J=8.1$  Hz, 2H), 7.84 (d,  $J=8.1$  Hz, 2H), 8.25 (d,  $J=8.5$  Hz, 2H);  $^{13}\text{C}$  NMR ( $\text{CDCl}_3$ )  $\delta$  21.7, 85.2, 124.3, 125.1, 125.3, 125.5, 127.8, 127.9, 128.3, 128.6, 128.8, 129.1, 131.4, 135.1, 137.6, 142.2, 146.8; MS (APCI):  $m/z$  (%) 357 ( $\text{M}^+ - \text{OH}$ , 100). Anal. Calcd for C, 89.81; H, 5.92. Found C, 89.67; H, 5.98.

**4.4.2. 4-Methylphenyl-di(1-naphthyl)methanol (3e).** 25.4 g, yield 68%; mp 188–190 °C decomp.; IR (KBr)  $\nu$  3546, 3041, 2916, 1599, 1506, 1395, 1342, 1311, 1183, 1154, 998  $\text{cm}^{-1}$ ;  $^1\text{H}$  NMR ( $\text{CDCl}_3$ )  $\delta$  2.33 (s, 3H), 3.57 (s, 1H), 6.85 (d,  $J=7.1$  Hz, 2H), 7.11–7.26 (m, 8H), 7.37 (t,  $J=7.1$  Hz, 2H), 7.77 (d,  $J=8.0$  Hz, 2H), 7.83 (d,  $J=8.0$  Hz, 2H), 8.26 (d,  $J=8.5$  Hz, 2H);  $^{13}\text{C}$  NMR ( $\text{CDCl}_3$ )  $\delta$  20.4, 84.5, 123.6, 124.6, 124.8, 125.7, 126.8, 127.1, 127.6, 128.0, 128.1, 128.5, 129.6, 130.7, 134.4, 136.0, 141.6, 143.3; MS (APCI):  $m/z$  (%) 357 ( $\text{M}^+ - \text{OH}$ , 100). Anal. Calcd for C, 89.81; H, 5.92. Found C, 89.59; H, 6.01.

#### 4.5. General procedure for the synthesis of 3- and 4-bromomethylphenyl-di(1-naphthyl)methanol

The procedure discussed in Section 4.3 was followed.

**4.5.1. [3-(Bromomethyl)phenyl][di(1-naphthyl)]methanol (4d).** 4.9 g, yield 82%; mp 159–163 °C decomp.; IR (KBr)  $\nu$  3541, 3046, 1598, 1507, 1359, 1342, 1216, 1149, 1008  $\text{cm}^{-1}$ ;  $^1\text{H}$  NMR ( $\text{CDCl}_3$ )  $\delta$  3.6 (s, 1H), 4.4 (s, 2H), 6.83 (d,  $J=7.1$  Hz, 2H), 7.19–7.41 (m, 10H), 7.79 (d,  $J=7.9$  Hz, 2H), 7.84 (d,  $J=8.0$  Hz, 2H), 8.2 (br s, 2H);  $^{13}\text{C}$  NMR ( $\text{CDCl}_3$ )  $\delta$  34.2, 85.6, 122.4, 125.8, 125.9, 126.0, 126.1, 128.4, 128.5, 128.7, 128.8, 128.9, 129.1, 129.2 (2C), 129.3, 129.8, 131.6, 135.5, 138.1, 142.2, 148.0; MS (APCI):  $m/z$  (%) 437 ( $\text{M}^+ - \text{OH}$ , 74), 435 (74), 390 (40), 357 (100).

**4.5.2. 4-Bromomethylphenyl-di(1-naphthyl)methanol (4e).** 5.3 g, yield 87%; mp 168 °C decomp.; IR (neat)  $\nu$  3542, 3040, 2922, 2863, 1504, 1498, 1340, 1229, 1155  $\text{cm}^{-1}$ ;  $^1\text{H}$  NMR ( $\text{CDCl}_3$ )  $\delta$  3.62 (s, 1H), 4.41 (s, 2H), 6.82 (d,  $J=7.1$  Hz, 2H), 7.15–7.26 (m, 8H), 7.39 (t,  $J=7.1$  Hz, 2H), 7.76 (d,  $J=8.0$  Hz, 2H), 7.83 (d,  $J=8.0$  Hz, 2H), 8.23 (d,  $J=8.2$  Hz, 2H);  $^{13}\text{C}$  NMR ( $\text{CDCl}_3$ )  $\delta$  32.5, 85.6, 124.1, 124.7, 125.7, 125., 125.9, 126.0 (2C), 128.6, 128.7, 128.7, 128.8, 128.9, 129.2, 129.3, 129.5, 129.7, 131.6, 135.5, 137.0, 142.1, 147.6; MS (APCI):  $m/z$  (%) 437 ( $\text{M}^+ - \text{OH}$ , 74), 435 (100), 391 (35), 357 (25).

#### 4.6. General procedure for the synthesis of quaternary ammonium salts from cinchona alkaloids

A suspension of cinchonidine (1.0 g, 3.39 mmol) and 3- or 4-(bromomethyl)phenyl[di(aryl)]methanol (3.73 mmol) in acetonitrile/toluene (50:50, 20 mL) was stirred at 80 °C under argon for 6 h. The reaction mixture was cooled to rt, the solvent was removed in vacuo and the residue was purified by column chromatography ( $\text{SiO}_2$ ,  $\text{MeOH}/\text{CHCl}_3$  5:95) to afford the products [7a–b, 9a–b] as crystalline solids (80–92%).



**4.6.1. *N*-[3-(Hydroxy-diphenyl-methyl)-benzyl]cinchonidinium bromide (5a).** Yield 88%; mp 209–210 °C decomp.;  $[\alpha]_D^{30} - 71.24$  (*c* 0.52, MeOH); IR (KBr)  $\nu$  3424, 3173, 3061, 2955, 1614, 1454, 1294, 1158, 1146, 1034, 1016, 928  $\text{cm}^{-1}$ ;  $^1\text{H NMR}$  ( $\text{CDCl}_3 + \text{CD}_3\text{OD}$ )  $\delta$  1.28–1.31 (m, 1H), 1.73 (m, 1H), 2.00–2.22 (m, 3H), 2.56 (br s, 1H), 3.14–3.25 (m, 1H), 3.47–3.51 (m, 1H), 3.86 (t,  $J=8.5$  Hz, 1H), 4.52 (m, 1H), 4.98 (d,  $J=10.4$  Hz, 1H), 5.05 (d,  $J=4.4$  Hz, 1H), 5.09 (d,  $J=9.9$  Hz, 1H), 5.45–5.56 (m, 2H), 6.59 (s, 1H), 7.18–7.33 (m, 14H), 7.56–7.65 (m, 2H), 7.69 (d,  $J=7.4$  Hz, 1H), 7.75 (s, 1H), 7.82 (d,  $J=4.5$  Hz, 1H), 8.02 (d,  $J=7.6$  Hz, 1H), 8.08 (d,  $J=7.3$  Hz, 1H), 8.82 (d,  $J=4.5$  Hz, 1H);  $^{13}\text{C NMR}$  ( $\text{CDCl}_3 + \text{CD}_3\text{OD}$ )  $\delta$  21.3, 24.5, 26.2, 37.5, 50.9, 60.4, 63.6, 64.3, 67.9, 81.0, 117.2, 119.7, 122.6, 124.2, 126.3, 126.9, 127.6, 127.6, 128.2, 129.0, 129.5, 130.1, 132.0, 132.8, 136.2, 145.4, 146.4, 146.9, 148.4, 149.2; MS (APCI):  $m/z$  (%) 568 ( $\text{M}^+ - \text{Br}$ , 32), 567 (100), 549 (29). Anal. Calcd for  $\text{C}_{30}\text{H}_{39}\text{BrN}_2\text{O}_2$ : C, 72.33; H, 6.07; N, 4.33. Found: C, 71.57; H, 6.14; N, 4.26.

**4.6.2. *N*-[4-(Hydroxy-diphenyl-methyl)-benzyl]cinchonidinium bromide (7a).** Yield 92%; mp 205–206 °C decomp.;  $[\alpha]_D^{30} - 75.5$  (*c* 0.56, MeOH); IR (KBr)  $\nu$  3194, 1592, 1508, 1446, 1422, 1381, 1321, 1281, 1183, 1159, 1110, 1018, 938  $\text{cm}^{-1}$ ;  $^1\text{H NMR}$  ( $\text{CDCl}_3 + \text{CD}_3\text{OD}$ )  $\delta$  1.40 (t,  $J=11.3$  Hz, 1H), 1.88 (m, 1H), 2.06 (s, 1H), 2.14–2.29 (m, 2H), 2.27 (br s, 1H), 3.30 (s, 1H), 3.62–3.70 (m, 1H), 3.98 (t,  $J=8.9$  Hz, 1H), 4.43 (m, 1H), 4.97 (d,  $J=10.4$  Hz, 1H), 4.99 (d,  $J=12.2$  Hz, 1H), 5.12 (d,  $J=12.4$  Hz, 1H), 5.17 (d,  $J=7.5$  Hz, 1H), 5.48 (s, 1H), 5.61–5.72 (m, 1H), 6.65 (s, 1H), 7.25–7.34 (m, 12H), 7.50 (d,  $J=8.2$  Hz, 2H), 7.67 (d,  $J=8.2$  Hz, 2H), 7.80 (t,  $J=7.7$  Hz, 1H), 7.88 (t,  $J=7.8$  Hz, 1H), 7.99 (d,  $J=4.5$  Hz, 1H), 8.13 (d,  $J=8.2$  Hz, 1H), 8.28 (d,  $J=8.3$  Hz, 1H), 8.96 (d,  $J=4.5$  Hz, 1H);  $^{13}\text{C NMR}$  ( $\text{CDCl}_3 + \text{CD}_3\text{OD}$ )  $\delta$  22.5, 25.9, 28.0, 39.1, 52.8, 54.8, 62.1, 64.8, 66.4, 69.4, 82.6, 117.5, 121.4, 124.2, 126.2, 127.2, 128.3, 128.9, 129.3, 129.4, 129.8, 130.0, 131.7, 134.2, 138.7, 148.1, 148.4, 148.5, 150.5, 151.1; MS (APCI):  $m/z$  (%) 568 ( $\text{M}^+ - \text{Br}$ , 20), 567 (48), 549 (100). Anal. Calcd for  $\text{C}_{30}\text{H}_{39}\text{BrN}_2\text{O}_2$ : C, 72.33; H, 6.07; N, 4.33. Found: C, 71.80; H, 6.23; N, 4.09.

**4.6.3. *N*-[3-(Hydroxy-di-naphthalen-1-yl-methyl)-benzyl]cinchonidinium bromide (5b).** Yield 80%; mp 188–190 °C decomp.;  $[\alpha]_D^{30} - 59.43$  (*c* 0.85, MeOH); IR (KBr)  $\nu$  3215, 3047, 2944, 1597, 1508, 1454, 1391, 1336, 1314, 1232, 1164, 1038, 928  $\text{cm}^{-1}$ ;  $^1\text{H NMR}$  ( $\text{CDCl}_3$ )  $\delta$  0.82–0.87 (m, 1H), 1.37 (m, 1H), 1.64 (br s, 1H), 1.89–2.02 (m, 3H), 2.92 (br s, 1H), 3.85 (m, 1H), 4.22 (m, 1H), 5.11–5.24 (m, 3H), 5.79 (m, 1H), 6.52 (m, 2H), 6.49 (m, 2H), 7.20–7.35 (m, 15H), 7.70–7.81 (m, 8H), 8.04 (m, 1H), 8.27 (m, 1H), 8.61 (d,  $J=4.6$  Hz, 1H);  $^{13}\text{C NMR}$  ( $\text{CDCl}_3$ )  $\delta$  21.5, 24.7, 26.3, 29.6, 50.6, 60.5, 63.6, 68.8, 84.9, 117.5, 120.1, 124.2, 124.5 (2C), 125.4, 126.4, 127.5, 128.1, 128.3, 128.6, 129.0, 129.3, 129.5, 130.1, 131.3, 132.8, 134.9, 135.0, 136.1, 141.4, 141.6, 147.5, 148.4, 149.8; MS (APCI):  $m/z$  (%) 667 ( $\text{M}^+ - \text{Br}$ , 20), 650 (42), 649 (100). Anal. Calcd for  $\text{C}_{47}\text{H}_{43}\text{BrN}_2\text{O}_2$ : C, 75.49; H, 5.80; N, 3.75. Found: C, 74.89; H, 5.92; N, 3.62.

**4.6.4. *O*(9)-Allyl-*N*-[3-(hydroxy-di-naphthalen-1-yl-methyl)-benzyl]cinchonidinium bromide (6).** To a suspension of **5b** (0.500 g, 0.668 mmol) and allyl bromide

(0.160 g, 1.33 mmol) in  $\text{CH}_2\text{Cl}_2$  (10 mL) was added  $\text{K}_2\text{CO}_3$  (0.184 g, 1.33 mmol). The resulting mixture was stirred vigorously at rt for 12 h. The mixture was diluted with water (10 mL) and extracted with  $\text{CH}_2\text{Cl}_2$  ( $3 \times 20$  mL), the combined organic extracts were dried over anhydrous  $\text{Na}_2\text{SO}_4$  and concentrated in vacuo. The residue was purified by column chromatography ( $\text{SiO}_2$ ,  $\text{CH}_2\text{Cl}_2/\text{MeOH}$ , 90:10) to afford **6** as yellow solid (0.463 g, 88%); mp 195–196 °C (decomp.);  $[\alpha]_D^{30} - 44.26$  (*c* 0.30, MeOH); IR (KBr)  $\nu$  3393, 3040, 2929, 1608, 1450, 1340, 1287, 1166, 1063, 1040, 928  $\text{cm}^{-1}$ ;  $^1\text{H NMR}$  ( $\text{CDCl}_3$ )  $\delta$  1.87–2.03 (m, 3H), 2.8 (m, 1H), 3.24 (br s, 1H), 3.72 (br s, 1H), 4.06–4.49 (m, 3H), 4.72 (m, 2H), 4.98 (m, 1H), 4.99 (d,  $J=9.8$  Hz, 1H), 5.16 (d,  $J=9.7$  Hz, 2H), 5.30 (d,  $J=17.3$  Hz, 1H), 5.53–5.59 (m, 2H), 5.97 (m, 1H), 6.63 (m, 1H), 6.80 (m, 1H), 6.93 (d,  $J=7.05$  Hz, 2H), 7.26–7.61 (m, 11H), 7.72–7.90 (m, 7H), 8.09 (d,  $J=8.4$  Hz, 1H), 8.33 (m, 2H), 8.70 (m, 2H), 8.86 (d,  $J=4.2$  Hz, 1H);  $^{13}\text{C NMR}$  ( $\text{CDCl}_3$ )  $\delta$  22.4, 25.1, 26.6, 37.6, 50.2, 59.4, 62.2, 65.6, 70.1, 85.0, 118.3, 119.0, 119.6, 124.5, 124.6, 125.2, 125.3, 126.3, 128.3, 128.4, 128.7, 129.1, 129.7, 129.9, 130.2, 130.8, 131.2, 132.2, 133.4, 135.0, 135.9, 139.8, 141.6, 148.3, 149.2; MS (APCI):  $m/z$  (%) 707 ( $\text{M}^+ - \text{Br}$ , 100). Anal. Calcd for  $\text{C}_{50}\text{H}_{47}\text{BrN}_2\text{O}_2$ : C, 76.23; H, 6.01; N, 3.56. Found: C, 75.79; H, 6.24; N, 3.49.

**4.6.5. Synthesis of *N*-[4-(hydroxy-di-naphthalen-1-yl-methyl)-benzyl]cinchonidinium bromide (7b).** Yield 83%; mp 196–197 °C decomp.;  $[\alpha]_D^{30} - 72.92$  (*c* 0.80, MeOH); IR (KBr)  $\nu$  3400, 2944, 1634, 1502, 1388, 1159, 1115, 1018, 920  $\text{cm}^{-1}$ ;  $^1\text{H NMR}$  ( $\text{CDCl}_3$ )  $\delta$  1.49 (m, 1H), 1.54 (m, 1H), 1.99–2.07 (m, 2H), 2.63 (br s, 1H), 3.08–3.34 (m, 2H), 3.63 (br s, 1H), 3.87 (m, 1H), 4.62 (m, 1H), 4.78 (d,  $J=6.8$  Hz, 1H), 4.99 (d,  $J=11.8$  Hz, 1H), 5.41–5.47 (m, 2H), 5.77 (d,  $J=12.2$  Hz, 1H), 6.77 (s, 1H), 6.80 (t,  $J=7.9$  Hz, 1H), 7.12–7.16 (m, 3H), 7.26–7.47 (m, 6H), 7.67–7.89 (m, 10H), 8.00–8.30 (m, 5H), 8.65 (s, 1H), 8.73 (d,  $J=4.6$  Hz, 1H);  $^{13}\text{C NMR}$  ( $\text{CDCl}_3$ )  $\delta$  23.9, 24.7, 26.5, 37.6, 51.1, 54.7, 62.5, 66.3, 68.3, 84.9, 117.6, 118.7, 120.1, 122.7, 123.0, 124.3, 125.3, 125.9, 127.1, 127.7, 127.8, 128.6, 128.7, 129.1, 129.2, 129.6, 131.2, 132.1, 133.6, 135.0, 136.2, 136.9, 141.6, 144.9, 147.3, 149.6; MS (APCI):  $m/z$  (%) 667 ( $\text{M}^+ - \text{Br}$ , 25), 650 (50), 649 (100). Anal. Calcd for  $\text{C}_{47}\text{H}_{43}\text{BrN}_2\text{O}_2$ : C, 75.49; H, 5.80; N, 3.75. Found: C, 74.98; H, 6.04; N, 3.58.

#### 4.7. General procedure for enantioselective catalytic alkylation of **8** under phase-transfer conditions

To a mixture of *N*-(diphenylmethylene)glycine *tert*-butyl ester<sup>9</sup> (0.050 g, 0.17 mmol) and **6** (0.013 g, 0.017 mmol) in toluene/dichloromethane (7:3, 2 mL) was added alkyl halide (0.34 mmol). The reaction mixture was cooled to  $-20$  °C, 50% aqueous KOH (0.25 mL) was added and the resulting mixture stirred vigorously until the starting material had been consumed (3–10 h). The suspension was diluted with diethyl ether (30 mL), washed with water ( $2 \times 10$  mL), dried over  $\text{Na}_2\text{SO}_4$ , filtered and concentrated under reduced pressure to give crude product. Purification of the residue by flash chromatography ( $\text{SiO}_2$ , Hexane/EtOAc, 98:2) afforded the desired products in 68–93% yield.

**4.7.1. *tert*-Butyl (2*S*)-2-[(diphenylmethylene)amino]butanoate (9a).**<sup>7a</sup> Oil, yield 68%; IR (film)  $\nu$  3060, 2926,

2854, 1732, 1662, 1625, 1446, 1367, 1284, 1154  $\text{cm}^{-1}$ ;  $^1\text{H}$  NMR ( $\text{CDCl}_3$ ) 0.87 (t,  $J=7.6$  Hz, 3H), 1.44 (s, 9H), 1.87–1.91 (m, 2H), 4.01 (dd,  $J=8.0, 5.2$  Hz, 1H), 7.17 (dd,  $J=4.4, 1.6$  Hz, 2H), 7.30–7.44 (m, 6H),  $\delta$  7.65 (m, 2H); MS (MALDI):  $m/z$  324 ( $\text{M}^+ + 1$ );  $R_t$  HPLC (Chiralcel OD, 254 nm, 1 mL/min, 95.5:0.5, hexane/2-propanol,  $t_S = 11.6$  min,  $t_R = 13.3$  min).

**4.7.2. tert-Butyl (2S)-2-[(diphenylmethylene)amino]octanoate (9b).**<sup>4b</sup> Oil, yield 78%; IR (film)  $\nu$  2954, 2856, 1735, 1627, 1456, 1448, 1391, 1365, 1249, 1153  $\text{cm}^{-1}$ ;  $^1\text{H}$  NMR ( $\text{CDCl}_3$ )  $\delta$  0.87 (t,  $J=6.8$  Hz, 3H), 1.26–1.23 (m, 8H), 1.44 (s, 9H), 1.86 (m, 2H), 3.98 (t,  $J=6.7$  Hz, 1H), 7.18 (dd,  $J=5.1, 2.0$  Hz, 2H), 7.32–7.43 (m, 5H), 7.64–7.79 (m, 3H); MS (MALDI):  $m/z$  380 ( $\text{M}^+ + 1$ );  $R_t$  HPLC (Chiralcel OD, 254 nm, 1 mL/min, 95.5:0.5, hexane/2-propanol,  $t_S = 10.5$  min,  $t_R = 12.2$  min).

**4.7.3. tert-Butyl (2S)-2-[(diphenylmethylene)amino]pent-4-enoate (9c).**<sup>7a</sup> Oil, yield 92%; IR (film)  $\nu$  3061, 2928, 2930, 1734, 1624, 1598, 1576, 1446, 1367, 1277, 1152  $\text{cm}^{-1}$ ;  $^1\text{H}$  NMR ( $\text{CDCl}_3$ )  $\delta$  1.44 (s, 9H), 2.65 (m, 2H), 4.0 (dd,  $J=7.6, 5.5$  Hz, 1H), 4.99–5.09 (m, 2H), 5.72 (m, 1H), 7.17 (m, 2H), 7.30–7.47 (m, 6H), 7.64 (m, 2H); MS (MALDI): 336 [ $\text{M}^+ + 1$ ];  $R_t$  HPLC (Chiralcel OD-H, 254 nm, 0.5 mL/min, 99.5:0.5, hexane/isopropanol,  $t_S = 10.5$  min,  $t_R = 12.0$  min).

**4.7.4. tert-Butyl (2S)-2-[(diphenylmethylene)amino]pent-4-ynoate (9d).**<sup>7a</sup> Oil, yield 90%; IR (film)  $\nu$  3642, 3290, 2968, 1728, 1622, 1447, 1369, 1328, 1156  $\text{cm}^{-1}$ ;  $^1\text{H}$  NMR ( $\text{CDCl}_3$ )  $\delta$  1.44 (s, 9H), 1.96 (t,  $J=2.4$  Hz, 1H), 2.77 (m, 2H), 4.15 (dd,  $J=5.4, 7.6$  Hz, 1H), 7.23–7.48 (m, 8H), 7.63–7.67 (m, 2H); MS (MALDI):  $m/z$  332 ( $\text{M}^+ - 1$ );  $R_t$  HPLC (Chiralcel OD, 254 nm, 1 mL/min, 99.8:0.2, hexane/isopropanol,  $t_S = 18.4$  min,  $t_R = 21.2$  min).

**4.7.5. tert-Butyl-N-(diphenylmethylene)-L-phenylalaninate (9e).**<sup>7a</sup> Yield 93%;  $^1\text{H}$  NMR  $\delta$  ( $\text{CDCl}_3$ ) 1.41 (s, 9H), 3.22–3.09 (m, 2H), 4.08 (dd,  $J=5.0, 9.1$  Hz, 1H), 6.53–7.62 (m, 15H);  $R_t$  HPLC (Chiralcel OD-H, 254 nm, 0.5 mL/min, 99.5:0.5, hexane/isopropanol,  $t_S = 25.4$  min,  $t_R = 17.5$  min).

**4.7.6. tert-Butyl (2S)-3-(4-fluorophenyl)-2-[(diphenylmethylene)amino]propanoate (9f).**<sup>7a</sup> Yield 93%; IR (neat)  $\nu$  2977, 2928, 1726, 1626, 1508, 1446, 1369, 1285, 1148  $\text{cm}^{-1}$ ;  $^1\text{H}$  NMR ( $\text{CDCl}_3$ )  $\delta$  1.45 (s, 9H), 3.15 (dd,  $J=13.4, 8.6$  Hz, 1H), 3.22 (dd,  $J=13.4, 4.8$  Hz, 1H), 4.06 (dd,  $J=8.6, 4.8$  Hz, 1H), 6.69 (d,  $J=7.1$  Hz, 2H), 6.85–7.02 (m, 4H), 7.30–7.41 (m, 6H), 7.56–7.58 (m, 2H);  $R_t$  HPLC (Chiralcel OD, 254 nm, 1 mL/min, 99.5:0.5, hexane/isopropanol,  $t_S = 8.1$  min,  $t_R = 13.5$  min).

**4.7.7. tert-Butyl 2-[(diphenylmethylene)amino]-3-pyridin-3-ylpropanoate (9g).** Yield: 87%;  $[\alpha]_D^{25} - 184.32$  (c 1,  $\text{CH}_2\text{Cl}_2$ ); IR (neat)  $\nu$  2958, 2869, 1739, 1450, 1425, 1286, 1173  $\text{cm}^{-1}$ ;  $^1\text{H}$  NMR ( $\text{CDCl}_3$ )  $\delta$  1.44 (s, 9H), 3.25 (dd,  $J=5.3, 3.3$  Hz, 2H), 4.95 (dd,  $J=5.9, 3.3$  Hz, 1H), 6.87 (d,  $J=6.2$  Hz, 2H), 7.23 (dd,  $J=4.9, 2.8$  Hz, 1H), 7.39–7.58 (m, 7H), 7.76 (d,  $J=7.0$  Hz, 2H), 8.44 (s, 1H), 8.48 (d,  $J=4.7$  Hz, 1H);  $^{13}\text{C}$  NMR ( $\text{CDCl}_3$ )  $\delta$  27.9, 36.6, 67.1, 81.4, 122.9, 127.4, 128.2, 128.4, 128.6, 129.9, 130.3, 132.3, 133.8, 136.1, 137.3, 139.1, 147.6, 170.8; MS (MALDI):  $m/z$

386 ( $\text{M}^+$ );  $R_t$  HPLC (Chiralcel OD-H, 254 nm, 0.5 mL/min, 98:2, hexane/isopropanol,  $t_S = 20.4$  min,  $t_R = 22.8$  min). Anal. Calcd for  $\text{C}_{25}\text{H}_{26}\text{N}_2\text{O}_2$ : C, 77.69; H, 6.78; N, 7.25. Found: C, 77.58; H, 6.84; N, 7.18.

**4.7.8. tert-Butyl (2S)-2-[(diphenylmethylene)amino]-3-pyridin-4-ylpropanoate (9h).** Yield 85%;  $[\alpha]_D^{25} - 180.03$  (c 1,  $\text{CH}_2\text{Cl}_2$ ); IR (neat)  $\nu$  2941, 2856, 1736, 1456, 1253, 1168  $\text{cm}^{-1}$ ;  $^1\text{H}$  NMR ( $\text{CDCl}_3$ )  $\delta$  1.44 (s, 9H), 3.24 (t,  $J=6.7$  Hz, 2H), 4.97 (dd,  $J=6.4, 5.9$  Hz, 1H), 6.82 (d,  $J=6.8$  Hz, 1H), 7.15 (d,  $J=5.7$  Hz, 2H), 7.40–7.54 (m, 7H), 7.74 (d,  $J=7.2$  Hz, 2H), 8.50 (d,  $J=5.5$  Hz, 2H);  $^{13}\text{C}$  NMR ( $\text{CDCl}_3$ )  $\delta$  27.9, 36.5, 65.2, 81.2, 122.3, 127.2, 128.2, 128.2, 129.9, 130.8, 132.2, 133.8, 135.9, 137.2, 139.1, 148.6, 170.7; MS (MALDI):  $m/z$  386 ( $\text{M}^+$ );  $R_t$  HPLC (Chiralcel OD-H, 254 nm, 0.5 mL/min, 98:2, hexane/isopropanol,  $t_R = 44.6$  min,  $t_S = 48.8$  min). Anal. Calcd for  $\text{C}_{25}\text{H}_{26}\text{N}_2\text{O}_2$ : C, 77.69; H, 6.78; N, 7.25. Found: C, 77.54; H, 6.86; N, 7.16.

**4.7.9. tert-Butyl (2S)-2-[(diphenylmethylene)amino]-3-(1-naphthyl)propanoate (9i).**<sup>4</sup> Yield 89%; IR (film)  $\nu$  3054, 2975, 1730, 1622, 1576, 1446, 1367, 1287, 1150  $\text{cm}^{-1}$ ;  $^1\text{H}$  NMR ( $\text{CDCl}_3$ )  $\delta$  1.46 (s, 9H), 3.56 (dd,  $J=12.9, 8.2$  Hz, 1H), 3.86 (dd,  $J=12.9, 3.8$  Hz, 1H), 4.30 (dd,  $J=8.2, 3.8$  Hz, 1H), 6.68 (br s, 2H), 6.96 (t,  $J=7.5$  Hz, 2H), 7.12–7.34 (m, 8H), 7.39 (ddd,  $J=8.7, 6.9, 1.2$  Hz, 1H), 7.50–7.72 (m, 4H);  $R_t$  HPLC (Chiralcel OD, 254 nm, 1 mL/min, 95.5:0.5, hexane/2-propanol,  $t_S = 24.3$  min,  $t_R = 21.6$  min).

## Acknowledgements

This work was supported by grant from National Institute of Pharmaceutical Education & Research (NIPER), Mohali, India.

## References and notes

- Dolling, U.-H.; Davis, P.; Grabowski, E. J. J. *J. Am. Chem. Soc.* **1984**, *106*, 446–447.
- (a) Imperiali, B.; Roy, R. S. *J. Org. Chem.* **1995**, *60*, 1891–1894. (b) Arai, S.; Tsuge, H.; Oku, M.; Miura, M.; Shioiri, T. *Tetrahedron* **2002**, *58*, 1623–1630. (c) Kim, D. Y.; Huh, S. C. *Tetrahedron* **2001**, *57*, 8933–8938. (d) Kumar, S.; Ramachandran, U. *Tetrahedron: Asymmetry* **2003**, *14*, 2539–2545. (e) Kumar, S.; Ramachandran, U. *Tetrahedron Lett.* **2005**, *46*, 19–21. (f) Kumar, S.; Ramachandran, U. *Tetrahedron: Asymmetry* **2005**, *16*, 647–649. (g) Kumar, S.; Ramachandran, U. *Tetrahedron* **2005**, *61*, 4141–4148.
- O'Donnell, M. J.; Bennett, W. D.; Wu, S. *J. Am. Chem. Soc.* **1989**, *111*, 2353–2355.
- (a) Lygo, B.; Wainwright, P. G. *Tetrahedron Lett.* **1997**, *38*, 8595–8598. (b) Corey, E. J.; Xu, F.; Noe, M. C. *J. Am. Chem. Soc.* **1997**, *119*, 12414–12415.
- Jew, S.-s.; Yoo, M.-S.; Jeong, B.-S.; Park, Y.; Park, H.-g. *Org. Lett.* **2002**, *4*, 4245–4248.
- Park, H.-g.; Jeong, B.-S.; Yoo, M.-S.; Lee, H.-g.; Park, B.-s.; Kim, M. G.; Jew, S.-s. *Tetrahedron Lett.* **2003**, *44*, 3497–3500.
- (a) Park, H.-g.; Jeong, B.-S.; Yoo, M.-S.; Lee, H.-g.; Park, M.-K.; Lee, Y.; Kim, J.-M.; Jew, S.-s. *Angew. Chem., Int. Ed.*

- 2002**, 41, 3036–3038. (b) Park, H.-g.; Jeong, B.-s.; Yoo, M.-s.; Park, M.-K.; Huh, H.; Jew, S.-s. *Tetrahedron Lett.* **2001**, 42, 4645–4648. (c) Chinchilla, R.; Mazon, P.; Nájera, C. *Tetrahedron: Asymmetry* **2002**, 13, 927–931.
8. O'Donnell, M. J.; Wu, S.; Esikova, I.; Mi, A. U.S. Patent 5,554,753, 1996.
9. O'Donnell, M. J.; Polt, R. L. *J. Org. Chem.* **1982**, 47, 2663–2666.

# Pallado-catalysed *P*-arylations and *P*-vinylation of 2-hydrogeno-2-oxo-1,4,2-oxazaphosphinanes

Jean-Luc Pirat,\* Jérôme Monbrun, David Virieux and Henri-Jean Cristau\*

Laboratoire de Chimie Organique, UMR 5076, ENSCM, 8 rue de l'École Normale, 34296 Montpellier Cedex 5, France

Received 18 March 2005; revised 29 April 2005; accepted 2 May 2005

**Abstract**—A simple and effective preparation of 2-aryl- (or 2-vinyl)-1,4,2-oxazaphosphinanes, phosphorus analogues of aryl-morpholinols has been developed, involving palladium catalysed coupling of aryl (or vinyl)-halides with 2-*H*-1,4,2-oxazaphosphinane in presence of triethylamine. A deprotection step was also proposed to afford the corresponding *P*-aryl- $\alpha$ -aminobenzylphosphinic acid.

© 2005 Elsevier Ltd. All rights reserved.

## 1. Introduction

Among various organophosphorus compounds synthesized during the last decades,  $\alpha$ -aminophosphinic derivatives have shown interesting biological properties especially as enzyme inhibitors: leucine aminopeptidase<sup>1a</sup> or isoaspartyl/ $\beta$ -aspartyl zinc peptidase (**A**),<sup>1b</sup> HIV-1 protease (**B**).<sup>1c–g</sup> On the other hand, arylphosphinic acid derivatives are also known as agents of treating hypercholesterolemia or atherosclerosis (**C**)<sup>1h</sup> or as microsomal aminopeptidase<sup>1i</sup> and thrombin inhibitors (**D**) (Fig. 1).<sup>1j</sup>

As a part of our ongoing efforts in discovery and synthesis of new potent organophosphorus inhibitors (virucide,

plant regulators...), the challenge in synthesis of phosphorus containing heterocycle was particularly stimulating. Indeed, it is well known that heterocyclic compounds received much attention of chemists due to their pharmaceutical importance and extensive application in organic synthesis.<sup>2</sup>

In previous works, we described the synthesis of a new class of 1,4,2-oxazaphosphinanes **1** bearing a reactive P–H bond, and the diastereoselective additions of **1** to aldehydes and imines.<sup>3a,b</sup> Arylation of such structure would lead to compounds **2**, phosphorus heterocycles analogues of morpholinols derivatives **3**, widely described for their antidepressing activities (Fig. 2).<sup>4</sup>

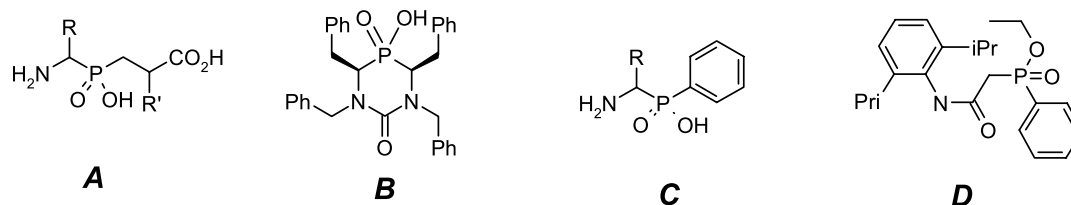


Figure 1. Various biologically active phosphinic derivatives.

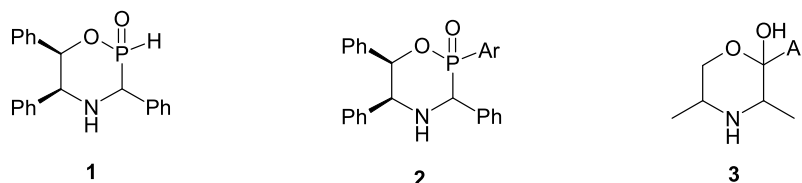


Figure 2. Analogy between *P*-aryl-1,4,2-oxazaphosphinanes and aryl-morpholinols.

**Keywords:** Arylphosphinate; Aminoalkylarylphosphinic acid; Vinylation; Arylation; Pallado-catalyse.

\* Corresponding authors. Tel.: +33 4 67 14 72 43; fax: +33 4 67 14 43 19 (J.-L.P.); e-mail addresses: [pirat@cit.enscm.fr](mailto:pirat@cit.enscm.fr); [cristau@cit.enscm.fr](mailto:cristau@cit.enscm.fr)

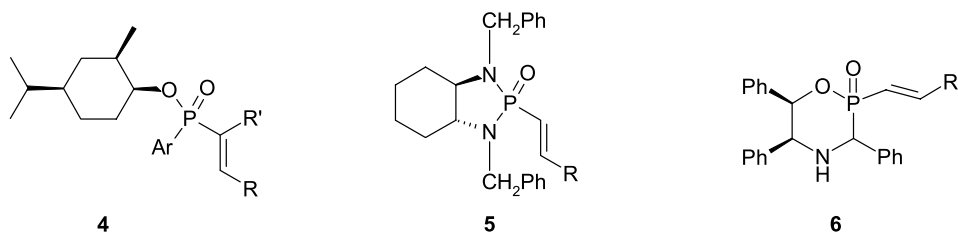


Figure 3. Chiral phosphonic and phosphinic Michael-type olefins.

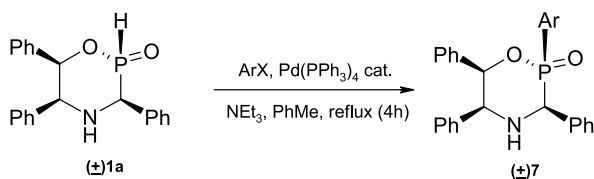
In addition, vinylphosphoryl derivatives<sup>5</sup> **4** and **5** (Fig. 3) were developed to induce diastereoselective additions on the C=C double bond, as the intracyclic phosphorus atoms of these activated olefins is substituted by a chiral group. Vinylation of structure **1** could also give efficient derivatives **6** for diastereoselective reactions.<sup>6</sup>

To the best of our knowledge, only few papers deal with 1,4,2-oxazaphosphinane structures. One of them describes the synthesis of a 2-phenyl-1,4,2-oxazaphosphinane ring starting with chlorophosphines, aminophenol and various substituted aldehydes.<sup>7</sup> We propose herein a different approach via a direct pallado-catalysed arylation or vinylation of 2-hydrogeno-2-oxo-1,4,2-oxazaphosphinane **1** affording *P*-aryl- or *P*-vinyl-oxazaphosphinanes.

## 2. Results and discussion

### 2.1. Arylation of 2-hydrogeno-2-oxo-1,4,2-oxazaphosphinane **1a**

Diastereoisomer **1a** was chosen as substrate for arylation and vinylation reactions as its relative stereochemistry was already fully determined by X-ray analysis.<sup>3a</sup> Arylation takes place in the conditions usually described in the literature:<sup>8</sup> oxazaphosphinane **1a** is arylated using catalytic amounts of tetrakis(triphenylphosphine) palladium (10 mol%), Ar-X (1 equiv), NEt<sub>3</sub> (3 equiv) under refluxing toluene to give as expected, only one diastereoisomer in good yields (69 to 75%) (Scheme 1, Table 1); indeed, these results are in accordance with the well established phosphorus retention of configuration during pallado-catalysed arylation.<sup>9</sup>



Scheme 1. Arylation of 2-hydrogeno-2-oxo-1,4,2-oxazaphosphinanes **1a**.

Table 1. Arylation of 2-*H*-2-oxo-1,4,2-oxazaphosphinane **1a**

Compound	Ar-X	Yield (%) <sup>a</sup>
<b>7a</b>	Ph-I	69
<b>7b</b>	<i>p</i> -Br-C <sub>6</sub> H <sub>4</sub> -I	73
<b>7c</b>	<i>p</i> -MeO-C <sub>6</sub> H <sub>4</sub> -Br	71
<b>7d</b>	2-Br-thiophene	70
<b>7e</b>	2-Br-pyridine	75

<sup>a</sup> Yield after purification by column chromatography.

Suitable crystals for X-ray analysis (Fig. 5) were obtained for the 2-pyridyl substituted compound **7e** after crystallization from chloroform. As noted above, retention of configuration at phosphorus atom is then confirmed (arylation occurs at the same side of the initial P-H bond). Moreover, we can point out the intramolecular H-bond between pyridyl nitrogen and proton of exocyclic amine. Using racemic oxazaphosphinane **1a**, both enantiomers appear on the crystal cell (Fig. 4). It is interesting to observe the  $\pi$ -stacking phenomenon between pyridyl and phenyl substituents of each enantiomer.

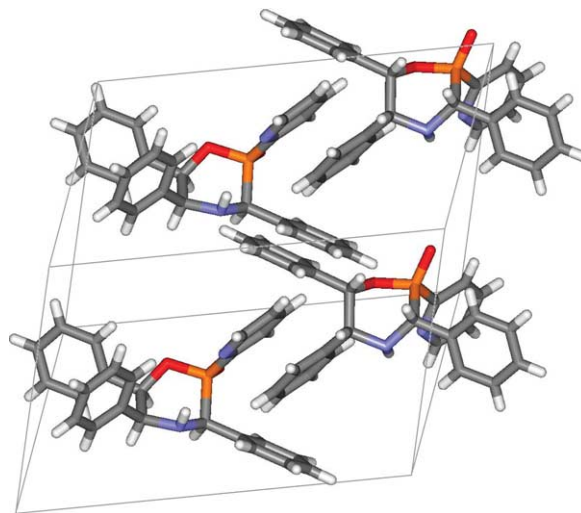


Figure 4. X-ray-cell of (+)-2-pyridyl-1,4,2-oxazaphosphinane **7e**.

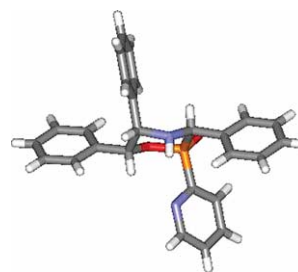
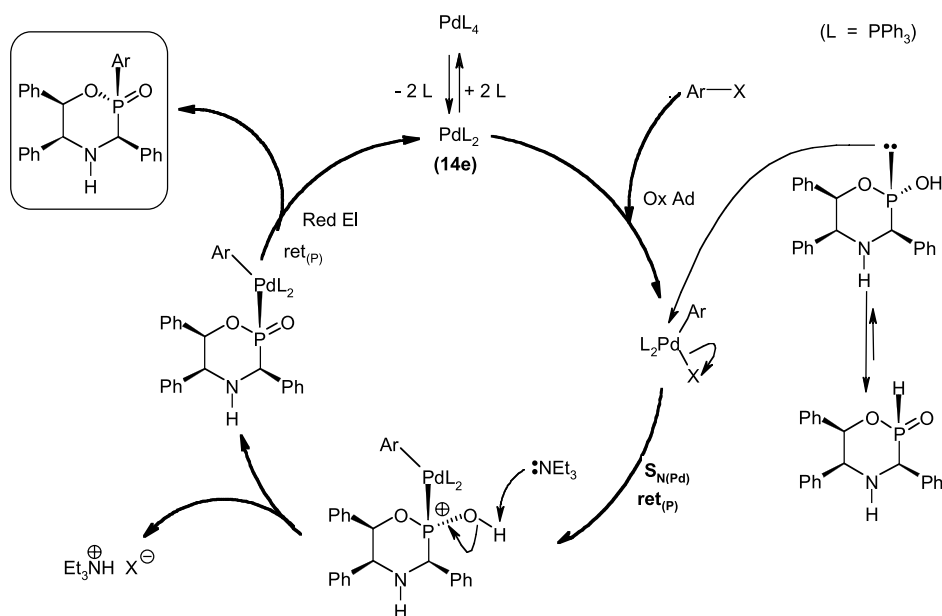


Figure 5. X-ray structure of 2-pyridyl-1,4,2-oxazaphosphinane **7f** derived from **1b**.

The mechanism of the catalysis also fully justifies the retention process (Scheme 2): The active catalyst PdL<sub>2</sub>, a 14 electrons complex, gives a classical oxidative addition of the aryl halide and affords a 16 electrons intermediate. Further, the tetracoordinated oxazaphosphinane is stereoselectively in equilibrium, with the tricoordinated phosphinite form, which can give a nucleophilic substitution of





**Scheme 2.** Mechanism of the catalytic arylation.

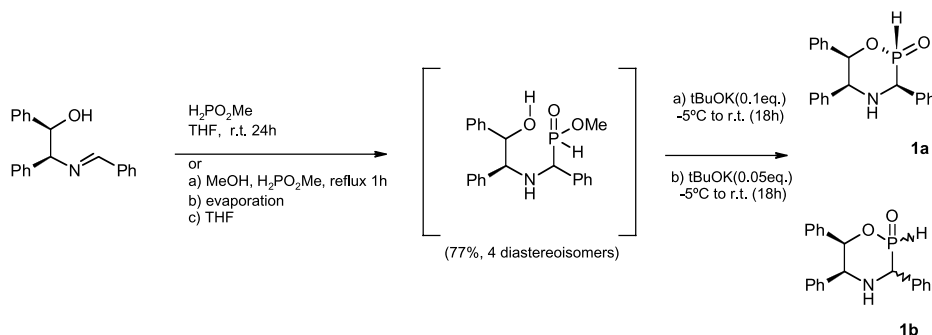
halogen (iodide or bromide) on palladium, and affords after deprotonation by the tertiary amine the metallated oxazaphosphinane with retention of configuration at phosphorus. The last step of catalytic cycle occurs also by a front reductive elimination with retention of configuration at phosphorus.

## 2.2. Determination of stereochemistry of 2-hydrogeno-2-oxo-1,4,2-oxazaphosphinane **1b**

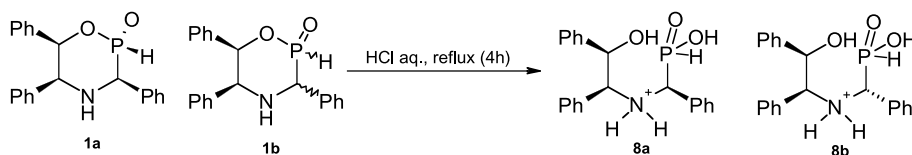
In our previous work dealing with synthesis of 2-*H*-2-oxo-1,4,2-oxazaphosphinane compounds,<sup>3</sup> two diastereoisomers **1a** and **1b** were obtained (Scheme 3). However, although we easily obtained suitable crystals of the diastereoisomer **1a** for X-ray analysis, we were unable to crystallize the second one **1b**.

Configurational relationship between **1a** and **1b** at C<sub>3</sub> position was easily demonstrated by ring opening of each compound with aqueous hydrochloric acid (Scheme 4): indeed, acidic treatment removes chirality at phosphorus center, then the C<sub>3</sub> chiral position only remains; treatment of a mixture of both diastereoisomers **1a** and **1b** leads to two opened structures **8a** and **8b**, they are consequently epimers at C<sub>3</sub> position. However, it was impossible to assign the stereochemistry of the phosphorus atom.

The full determination of relative stereochemistry of the second diastereoisomer **1b** not only at the C<sub>3</sub> position but also at the phosphorus center could be made by arylation of the second diastereoisomer with bromopyridine following the same procedure as described for arylations of **1a**. As expected, arylation of **1b** proceeds in a similar way (65% yield after column chromatography, one diastereoisomer **7f**)



**Scheme 3.** 2-Hydrogeno-1,4,2-oxazaphosphinane synthesis via an intramolecular transesterification.

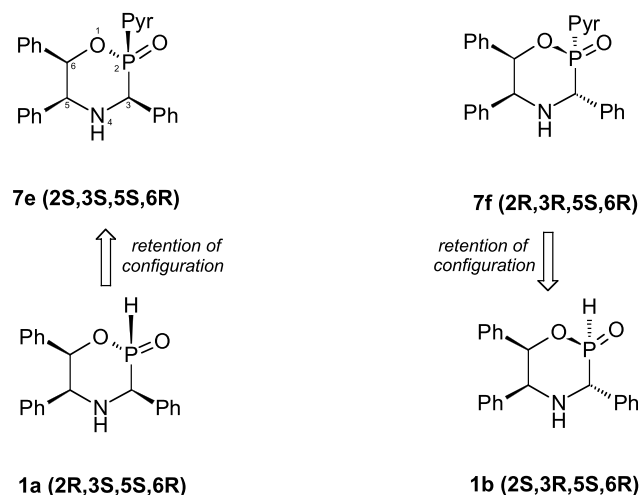


**Scheme 4.** Acidic ring opening to settle up the relative configurations at C<sub>3</sub> position.



and we were pleased to obtain suitable crystals by crystallization from chloroform for X-ray analysis, after chromatographic purification (Fig. 5).

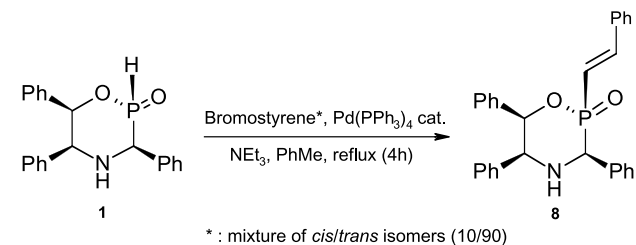
As compound **7f** has the pyridyl-group (P<sub>2</sub> position) and the phenyl-group (C<sub>3</sub> position) anti to the phenyl-groups at C<sub>5</sub> and C<sub>6</sub> positions, the relative stereochemistry of **1b** should be as follows (Scheme 5).



Scheme 5. Structure elucidation of diastereoisomer **1b**.

### 2.3. Vinylation of 2-hydrogeno-2-oxo-1,4,2-oxazaphosphinane

Vinylation of oxazaphosphinane heterocycle was performed (Scheme 6) with  $\beta$ -bromo-styrene (a mixture of *cis/trans*



Scheme 6. Pallado-catalysed vinylation of 2-*H*-oxazaphosphinane **1a**.

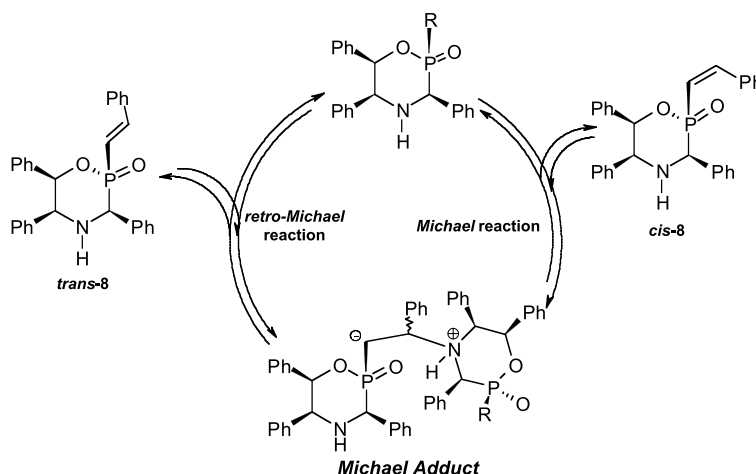
isomers: 10/90). The first experiment using the same conditions as described above for arylation (110 °C, 4 h) afforded only one stereoisomer (*trans* compound as determined by <sup>1</sup>H NMR coupling constants) and no *cis* isomer coming from the starting  $\beta$ -bromostyrene is detected. At first glance, this result seems to be in contradiction with the well established stereospecificity of the reaction.

A first explanation for the high *trans* stereoselectivity could consist with a preliminary in situ isomerisation of  $\beta$ -bromostyrene. Indeed, it is known that prolonged heating can isomerize the double bond to the thermodynamically more stable *trans*-derivative.<sup>10</sup> As a consequence, we tried to use softer conditions (55 °C, 1 h) but no presence of *cis*-derivative was detected leading us to make a NMR study of  $\beta$ -bromo-styrene isomerization under these reaction conditions. The reaction mixture (bromostyrene and triethylamine in deuterated benzene) checked by <sup>1</sup>H NMR analysis, after 1 h heating at 55 °C, shown that no isomerization occurred, even after addition of 10% Pd(PPh<sub>3</sub>)<sub>4</sub> followed by 1 h heating.

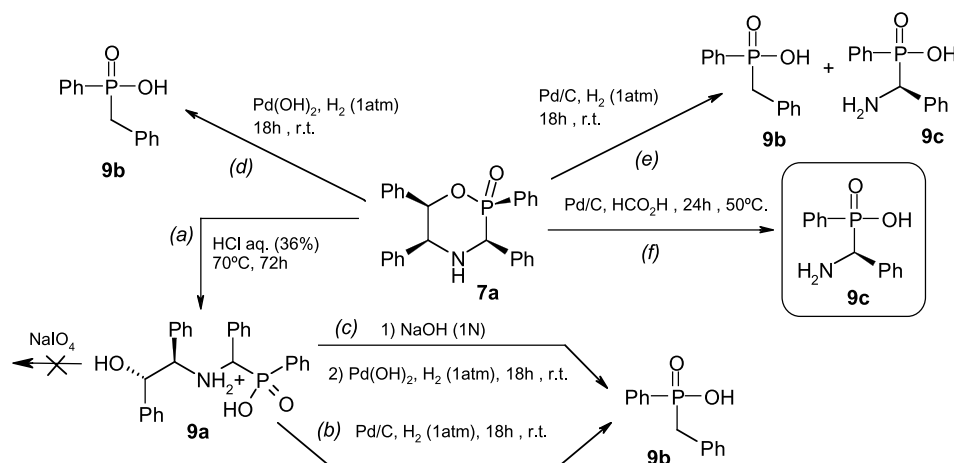
Another explanation could consist with in situ isomerization of vinyloxazaphosphinane due to its Michael olefin nature and presence of an intracyclic secondary amine function (Scheme 7). Indeed, it is well known that secondary amine catalyze isomerization of activated double bond from *cis* stereoisomer to *trans* one, as demonstrated for *cis*-chalcone<sup>11</sup> via Michael/*retro*-Michael reactions.

### 2.4. Deprotection of arylated 2-hydrogeno-2-oxo-1,4,2-oxazaphosphinane structure

Removal of the chiral inductor was carried out on the phenyl substituted compound **7a** (Scheme 8). Several ways could be considered: hydrogenolysis catalysed by palladium derivatives as well as oxidative cleavage by sodium periodate (as the inductor initially used is an aminoalcohol). The latter needs one more step for ring opening before oxidative cleavage, but the difficulty of hydrogenolysis consists on the regioselectivity of the cleavage due to the presence of two benzylic C–N bonds.



Scheme 7. Possible isomerization of *cis*-**8** catalysed by oxazaphosphinane secondary amine.



Scheme 8. 2-Phenyl-oxazaphosphinane deprotection to free phenyl-aminobenzylphosphinic acids.

Ring-opening of compound **9a** was easily obtained from cyclic starting material **7a** after acidic treatment (way a). However, sodium periodate gave no reaction even after several days.

Catalytic hydrogenolysis of **9a** over palladium on charcoal (way b) or palladium hydroxide (way c) (after neutralisation by aqueous NaOH 1 N solution) under 1 atm of hydrogen was tried but gave unfortunately the wrongly deprotected benzyl-phenylphosphinic acid **9b**, leading us to try hydrogenolysis directly to the arylated heterocycle **7a**. As above, palladium hydroxide leads to the wrong deprotected derivative **9b** (way d). Surprisingly, palladium on charcoal gave the expected  $\alpha$ -aminobenzyl-phenylphosphinic acid **9c**, with small amount of **9b** (way e). These results incited us to choose mild hydrogen donor as formic acid under Pd/C catalysis: in such conditions (way f), very clean reaction occurred affording only the correctly deprotected compound **9c** with high isolated yield (75%). Petnehazy et al. recently described<sup>12</sup> the deprotection of *N*-methylbenzyl- $\alpha$ -amino benzylphosphinic acid to compound **9c** using Pd/C hydrogenolysis under 10 atm of hydrogen. However, according to the chemical shifts (<sup>31</sup>P and <sup>1</sup>H NMR) and melting point given, it is likely that they actually isolated compound **9b**.

### 3. Conclusion

In conclusion, we synthesized several aryl or heteroaryl oxazaphosphinanes via a palladium(0) catalysed arylation of 2-hydrogeno-1,4,2-oxazaphosphinane with aromatic or heteroaromatic bromides or iodides affording heterocyclic phosphorus analogues of arylated morpholinols. Furthermore, vinylation of these structures was also tried to afford activated olefin containing chiral functionalized phosphinate moiety, usable for several diastereoselective reactions (Michael addition, Diels–Alder reactions...). Cleavage of the chiral inductor using catalytic hydrogenolysis was finally described opening new perspectives in the synthesis of  $\alpha$ -aminophosphinic derivatives.

### 4. Experimental

All reactions involving air or moisture sensitive reagents or intermediates were carried out under dry nitrogen in flame-dried glassware. Reagents and solvents were distilled before use and stored under nitrogen over sodium wires (THF) or molecular sieves (dichloromethane). All reactions were monitored by <sup>31</sup>P NMR. Merck silica gel (35–70  $\mu$ m) was used for column chromatography. NMR spectra were recorded on BRUKER AC 200, 250 or 400 (<sup>1</sup>H frequency: 200.13, 250.13 or 400.13 MHz; <sup>13</sup>C frequency: 50.32, 62.89 or 100.62 MHz, <sup>31</sup>P frequency: 81.02, 101.25, 162.04 MHz, respectively). Chemical shifts are given in  $\delta$  units with respect to TMS (<sup>1</sup>H, <sup>13</sup>C NMR) or H<sub>3</sub>PO<sub>4</sub> 85% (<sup>31</sup>P), coupling constants are expressed in Hz. Infrared spectra were recorded on PERKIN-ELMER 377 or FT-NICOLET 210 spectrometer. Mass spectra were measured on JEOL JMS DX-300 spectrometer (positive FAB ionisation and High Resolution using *p*-nitrobenzyl alcohol NBA).

#### 4.1. General procedure for arylation of 2-hydrogeno-2-oxo-1,4,2-oxazaphosphinane (**7a–7f**, **8**)

In a 10 ml flask containing 675 mg of **1a** (1.94 mmol) and 224 mg of palladium-tetrakis(triphenylphosphine) (0.194 mmol, 0.1 equiv) under N<sub>2</sub> are added under stirring 3.7 ml of dry toluene followed by 810  $\mu$ l of triethylamine (5.82 mmol) and aryl-halide or vinyl-halide (1.94 mmol) at room temperature. The reaction mixture is heated at 110 °C and precipitation of triethylammonium halide occurs. After 4 h stirring at 110 °C, compound **1a** was completely consumed and heating was stopped. After cooling, the reaction mixture is dissolved in chloroform and saturated aqueous NaCl solution is added. After extraction with chloroform, the organic layers are dried over Na<sub>2</sub>SO<sub>4</sub>. The crude solution is evaporated affording a solid purified by column chromatography (dichloromethane/ethyl acetate gradient: 100/0 to 50/50).

**4.1.1. (2*R*\*,3*R*\*,5*R*\*,6*S*\*)-(+/-)-2-Oxo-2,3,5,6-tetra-phenyl-1,4,2-oxazaphosphinane **7a**.** White solid (570 mg, 1.34 mmol, 1 diastereoisomer), mp = 223.9 °C; yield 69%;

<sup>31</sup>P NMR (81.02 MHz, CDCl<sub>3</sub>): 42.77; <sup>1</sup>H NMR (250.13 MHz, CDCl<sub>3</sub>): 2.20 (d, 1H, <sup>3</sup>J<sub>PH</sub>=28.9 Hz, NH), 4.93 (dd, 1H, <sup>3</sup>J<sub>HH</sub>=4.6, 4.6 Hz, NCHPh), 5.13 (d, 1H, <sup>2</sup>J<sub>PH</sub>=13.4 Hz, PCHPh), 6.20 (dd, 1H, <sup>3</sup>J<sub>PH</sub>=7.1 Hz, <sup>3</sup>J<sub>HH</sub>=5.8 Hz, OCHPh), 7.18–7.80 (m, 20H, CHar): <sup>13</sup>C NMR (MHz, DMSO-*d*<sub>6</sub>): 59.60 (d, <sup>1</sup>J<sub>PC</sub>=106.5 Hz, HNCHP), 63.36 (s, NCHPh), 76.47 (d, <sup>2</sup>J<sub>PC</sub>=4.8 Hz, OCHPh), 127.09–129.56 (m, CHar), 136.17 (d, <sup>2</sup>J<sub>PC</sub>=5.8 Hz, Car), 137.95 (d, <sup>3</sup>J<sub>PC</sub>=8.2 Hz, Car), 141.04 (s, Car), 139.19 (d, <sup>2</sup>J<sub>PC</sub>=9.1 Hz, PCarChar): IR (KBr): 3440, 3280, 3080, 3020, 2840, 1590, 1480, 1450, 1230, 1200, 1180, 1125, 1060, 1030, 990, 690; HRMS (FAB<sup>+</sup>): calcd for C<sub>27</sub>H<sub>24</sub>NO<sub>2</sub>P 425.1623. Found 425.1605; 426 [M+H]<sup>+</sup> (32%), 284 (95%), 180 (100%), 106 (21%), 91 (38%).

**4.1.2. (2R\*,3R\*,5R\*,6S\*)-(+/-)-2-Oxo-3,5,6-triphenyl-2-*p*-bromophenyl-1,4,2-oxazaphosphinane 7b.** White solid (714 mg, 1.42 mmol, 1 diastereoisomer), mp=228.8 °C; 73% yield; <sup>31</sup>P NMR (81.02 MHz, CDCl<sub>3</sub>): 42.05; <sup>1</sup>H NMR (250.13 MHz, CDCl<sub>3</sub>): 2.23 (d, 1H, <sup>3</sup>J<sub>PH</sub>=30.3 Hz, NH), 4.91 (dd, 1H, <sup>3</sup>J<sub>HH</sub>=4.3 Hz, <sup>3</sup>J<sub>HH</sub>=4.3 Hz, N CHPh), 5.13 (d, 1H, <sup>2</sup>J<sub>PH</sub>=13.0 Hz, PCHPh), 6.18 (dd, 1H, <sup>3</sup>J<sub>PH</sub>=7.3 Hz, <sup>3</sup>J<sub>HH</sub>=5.7 Hz, OCHPh), 7.17–7.57 (m, 19H, CHar): <sup>13</sup>C NMR (52.32 MHz, DMSO-*d*<sub>6</sub>): 59.18 (d, <sup>1</sup>J<sub>PC</sub>=100.9 Hz, HNCHP), 62.18 (s, NCHPh), 75.68 (d, <sup>2</sup>J<sub>PC</sub>=4.5 Hz, OCHPh), 126.19–128.58 (m, CHar), 131.04 (d, <sup>2</sup>J<sub>PC</sub>=13.0 Hz, Car), 134.37 (d, <sup>2</sup>J<sub>PC</sub>=9.7 Hz, Car), 135.21 (d, <sup>2</sup>J<sub>PC</sub>=5.6 Hz, CarCH[(P),(NH)]), 137.07 (d, <sup>3</sup>J<sub>PC</sub>=8.9 Hz, CarCH[(O),(CH)]), 140.0 (s, CarCHN), 137.07 (d, <sup>2</sup>J<sub>PC</sub>=8.9 Hz, PCarChar): IR (KBr): 3360, 3290, 3080, 3020, 2860, 1600, 1490, 1450, 1240, 1190, 1120, 1070, 1030, 990, 960, 690; HRMS (FAB<sup>+</sup>): calcd for C<sub>27</sub>H<sub>23</sub>BrNO<sub>2</sub>P: 503.0728. Found: 503.0673; 504 [M+H]<sup>+</sup> (24%), 284 (100%), 180 (67%), 106 (20%), 91 (27%).

**4.1.3. (2R\*,3R\*,5R\*,6S\*)-(+/-)-2-Oxo-3,5,6-triphenyl-2-*p*-methoxyphenyl-1,4,2-oxazaphosphinane 7c.** White solid (627 mg, 1.38 mmol, 1 diastereoisomer), mp=233.1 °C; 71% yield; <sup>31</sup>P NMR (81.02 MHz, CDCl<sub>3</sub>): 42.95; <sup>1</sup>H NMR (250.13 MHz, CDCl<sub>3</sub>): 2.15 (d, 1H, <sup>3</sup>J<sub>PH</sub>=28.4 Hz, NH), 3.80 (s, 3H, CH<sub>3</sub>), 4.86 (dd, 1H, <sup>3</sup>J<sub>HH</sub>=4.5 Hz, <sup>3</sup>J<sub>HH</sub>=5.1 Hz, NCHPh), 5.07 (d, 1H, <sup>2</sup>J<sub>PH</sub>=12.5 Hz, PCHPh), 6.16 (dd, 1H, <sup>3</sup>J<sub>PH</sub>=7.2 Hz, <sup>3</sup>J<sub>HH</sub>=5.9 Hz, OCHPh), 7.14–7.59 (m, 19H, CHar): <sup>13</sup>C NMR (62.90 MHz, DMSO-*d*<sub>6</sub>): 56.17 (s, CH<sub>3</sub>), 60.30 (d, <sup>1</sup>J<sub>PC</sub>=99.8 Hz, HNCHP), 63.27 (s, NCHPh), 76.09 (d, <sup>2</sup>J<sub>PC</sub>=4.8 Hz, OCHPh), 114.41 (d, <sup>2</sup>J<sub>PC</sub>=13.9 Hz, PCarCH), 119.27 (d, <sup>1</sup>J<sub>PC</sub>=140.1 Hz, PCar), 127.09–129.56 (m, CHar), 135.42 (d, <sup>3</sup>J<sub>PC</sub>=10.6 Hz, MeOCarChar), 136.71 (d, <sup>2</sup>J<sub>PC</sub>=5.3 Hz, CarCH[(P),(NH)]), 138.32 (d, <sup>3</sup>J<sub>PC</sub>=8.2 Hz, CarCH[(O),(CH)]), 141.21 (s, CarCHN), 163.34 (d, <sup>4</sup>J<sub>PC</sub>=2.9 Hz, MeOCar): IR (KBr): 3270, 3080, 3020, 2960, 2820, 1600, 1490, 1450, 1260, 1230, 1180, 1130, 1060, 1030, 990, 950, 700; HRMS (FAB<sup>+</sup>): calcd for C<sub>28</sub>H<sub>26</sub>NO<sub>3</sub>P: 455.1729. Found: 455.1729; 456 [M+H]<sup>+</sup> (29%), 284 (100%), 180 (80%), 106 (10%), 91 (15%).

**4.1.4. (2R\*,3R\*,5R\*,6S\*)-(+/-)-2-Oxo-3,5,6-triphenyl-2-(2-thienyl)-1,4,2-oxazaphosphinane 7d.** White solid (653 mg, 1.51 mmol, 1 diastereoisomer), mp=224.8 °C; 78% yield; <sup>31</sup>P NMR (81.02 MHz, CDCl<sub>3</sub>): 38.39; <sup>1</sup>H NMR (250.13 MHz, CDCl<sub>3</sub>): 2.25 (d, 1H, <sup>3</sup>J<sub>PH</sub>=28.9 Hz, NH),

4.84 (dd, 1H, <sup>3</sup>J<sub>HH</sub>=4.4 Hz, <sup>3</sup>J<sub>HH</sub>=4.4 Hz, NCHPh), 5.14 (d, 1H, <sup>2</sup>J<sub>PH</sub>=11.5 Hz, PCHPh), 6.18 (dd, 1H, <sup>3</sup>J<sub>PH</sub>=8.4 Hz, <sup>3</sup>J<sub>HH</sub>=5.8 Hz, OCHPh), 7.04–7.41 (m, 17H, CHar), 7.68 (dd, 1H, <sup>3</sup>J<sub>HH</sub>=3.8 Hz, <sup>4</sup>J<sub>HH</sub>=3.8 Hz, SCH); <sup>13</sup>C NMR (62.90 MHz, DMSO-*d*<sub>6</sub>): 59.61 (d, <sup>1</sup>J<sub>PC</sub>=107.0 Hz, HNCHP), 63.37 (s, NCHPh), 76.48 (d, <sup>2</sup>J<sub>PC</sub>=4.8 Hz, OCHPh), 127.0–129.73 (m, CHar), 136.51 (d, <sup>4</sup>J<sub>PC</sub>=4.3 Hz, SCHar), 136.17 (d, <sup>2</sup>J<sub>PC</sub>=6.2 Hz, CarCH[(P),(NH)]), 137.95 (d, <sup>3</sup>J<sub>PC</sub>=8.6 Hz, CarCH[(O),(CH)]), 141.04 (s, CarCHN), 139.20 (d, <sup>4</sup>J<sub>PC</sub>=11.0 Hz, [(P),(S)]CarCH): IR (KBr): 3420, 3270, 3080, 3030, 2990, 2840, 1600, 1490, 1450, 1230, 1200, 1130, 1060, 1030, 990, 955, 700, 695; HRMS (FAB<sup>+</sup>): calcd for C<sub>25</sub>H<sub>22</sub>NO<sub>2</sub>PS: 431.1187. Found: 431.1196; 432 [M+H]<sup>+</sup> (43%), 284 (100%), 180 (73%), 106 (11%), 91 (19%).

**4.1.5. (2S\*,3S\*,5R\*,6S\*)-(+/-)-2-Oxo-3,5,6-triphenyl-2-(2-pyridyl)-1,4,2-oxazaphosphinane 7e.** White solid (620 mg, 1.46 mmol, 1 diastereoisomer), mp=221.2 °C; 75% yield; <sup>31</sup>P NMR (81.02 MHz, CDCl<sub>3</sub>): 34.52; <sup>1</sup>H NMR (250.13 MHz, CDCl<sub>3</sub>): 3.47 (ddd, 1H, <sup>3</sup>J<sub>PH</sub>=20.7 Hz, <sup>3</sup>J<sub>HH</sub>=9.2, 11.9 Hz, NH), 4.78 (dd, 1H, <sup>3</sup>J<sub>HH</sub>=6.5, 7.7 Hz, NCHPh), 5.10 (dd, 1H, <sup>2</sup>J<sub>PH</sub>=16.1 Hz, <sup>3</sup>J<sub>HH</sub>=11.7 Hz, PCHPh), 6.21 (dd, 1H, <sup>3</sup>J<sub>PH</sub>=7.9 Hz, <sup>3</sup>J<sub>HH</sub>=5.7 Hz, OCHPh), 7.08–7.48 (m, 16H, CHar), 7.68 (m, 1H, [N,P]CarCHChar), 7.93 (dd, 1H, <sup>2</sup>J<sub>PH</sub>=7.3 Hz, <sup>3</sup>J<sub>HH</sub>=7.3 Hz, [P,N]CarChar), 7.93 (d, 1H, <sup>3</sup>J<sub>HH</sub>=4.4 Hz, NCHar); <sup>13</sup>C NMR (50.32 MHz, CDCl<sub>3</sub>): 58.60 (d, <sup>1</sup>J<sub>PC</sub>=83.0 Hz, HNCHP), 65.05 (d, <sup>4</sup>J<sub>PC</sub>=1.5 Hz, NCHPh), 76.92 (d, <sup>2</sup>J<sub>PC</sub>=6.3 Hz, OCHPh), 127.09–129.56 (m, CHar), 134.30 (d, <sup>3</sup>J<sub>PC</sub>=1.1 Hz, [P,N]CarCharChar), 136.52 (d, <sup>2</sup>J<sub>PC</sub>=6.3 Hz, CarCH[(P),(NH)]), 135.96 (d, <sup>3</sup>J<sub>PC</sub>=10.4 Hz, CarCH[(O),(CH)]), 138.89 (s, CarCHN), 149.59 (d, <sup>3</sup>J<sub>PC</sub>=19.3 Hz, NCHar), 151.86 (d, <sup>1</sup>J<sub>PC</sub>=163.0 Hz, PCar): IR (KBr): 3420, 3270, 3080, 3020, 2920, 1590, 1490, 1450, 1250, 1230, 1185, 1155, 1090, 1060, 1010, 990, 950, 710, 690; HRMS (FAB<sup>+</sup>): calcd for C<sub>26</sub>H<sub>23</sub>N<sub>2</sub>O<sub>2</sub>P: 426.1575. Found: 426.1558; 427 [M+H]<sup>+</sup> (45%), 284 (100%), 180 (54%), 106 (8%), 91 (16%).

**4.1.6. (2R\*,3R\*,5S\*,6R\*)-(+/-)-2-Oxo-3,5,6-triphenyl-2-(2-pyridyl)-1,4,2-oxazaphosphinane 7f.** White solid (618 mg, 1.45 mmol, 1 diastereoisomer), mp=221.2 °C; 75% yield; <sup>31</sup>P NMR (81.02 MHz, CDCl<sub>3</sub>): 24.55; <sup>1</sup>H NMR (250.13 MHz, CDCl<sub>3</sub>): 3.36 (bs, 1H, NH), 4.17 (d, 1H, <sup>3</sup>J<sub>HH</sub>=3.2 Hz, N CHPh), 4.12 (d, 1H, <sup>2</sup>J<sub>PH</sub>=19.4 Hz, PCHPh), 7.15 (m, 1H, OCHPh), 7.13–7.65 (m, 18H, CHar), 8.75 (m, 1H, NCHar): <sup>13</sup>C NMR (62.90 MHz, CDCl<sub>3</sub>): 56.31 (d, <sup>1</sup>J<sub>PC</sub>=99.6 Hz, HNCHP), 61.93 (d, <sup>4</sup>J<sub>PC</sub>=3.1 Hz, NCHPh), 86.46 (d, <sup>2</sup>J<sub>PC</sub>=10.0 Hz, OCHPh), 125.44–130.59 (all CHar), 134.87 (d, <sup>3</sup>J<sub>PC</sub>=1.9 Hz, Car), 138.34 (d, <sup>2</sup>J<sub>PC</sub>=6.2 Hz, Car), 136.33 (d, <sup>3</sup>J<sub>PC</sub>=10.8 Hz, Car), 136.50 (s, Car), 149.61 (d, <sup>3</sup>J<sub>PC</sub>=21.5 Hz, NCHar), 154.52 (d, <sup>1</sup>J<sub>PC</sub>=166.9 Hz, PCar): IR (KBr): 3430, 3300, 3080, 3020, 2920, 2860, 1595, 1490, 1445, 1270, 1230, 1170, 1110, 1070, 1040, 1025, 970, 690; HRMS (FAB<sup>+</sup>): calcd for C<sub>26</sub>H<sub>23</sub>N<sub>2</sub>O<sub>2</sub>P 426.1575. Found: 426.1586; 427 [M+H]<sup>+</sup> (44%), 284 (80%), 180 (49%), 106 (24%), 91 (29%).

**4.1.7. Vinylolation of 2-hydrogeno-2-oxo-1,4,2-oxazaphosphinane 1a; (2R\*,3R\*,5R\*,6S\*)-(+/-)-2-oxo-3,5,6-triphenyl-2-styryl-1,4,2-oxazaphosphinane 8.** White solid

(604 mg, 1.34 mmol, 1 diastereoisomer), mp = 196.4 °C; 69% yield;  $^{31}\text{P}$  NMR (81.02 MHz,  $\text{CDCl}_3$ ): 39.12;  $^1\text{H}$  NMR (250.13 MHz,  $\text{CDCl}_3$ ): 2.26 (bm, 1H,  $^3J_{\text{PH}} = 29.2$  Hz, NH), 4.87 (dd, 1H,  $^3J_{\text{HH}} = 4.1$ , 4.1 Hz, NCHPh), 5.01 (d, 1H,  $^2J_{\text{PH}} = 13.9$  Hz, PCHPh), 5.98 (dd, 1H,  $^3J_{\text{PH}} = 8.2$  Hz,  $^3J_{\text{HH}} = 4.1$  Hz, OCHPh), 6.20 (dd, 1H,  $^2J_{\text{PH}} = 21.5$  Hz,  $^3J_{\text{HH}} = 17.4$  Hz, vinyl), 7.14–7.62 (m, 20H, CHar);  $^{13}\text{C}$  NMR (50.32 MHz,  $\text{DMSO}-d_6$ ): 62.53 (d,  $^1J_{\text{PC}} = 99.3$  Hz, HNCHP), 63.91 (d,  $^3J_{\text{PC}} = 1.6$  Hz, NCHPh), 79.57 (d,  $^2J_{\text{PC}} = 7.5$  Hz, OCHPh), 114.19 (d,  $^1J_{\text{PC}} = 156.2$  Hz, PCHCH), 127.54–130.56 (m, CHar), 135.99 (d,  $^2J_{\text{PC}} = 5.9$  Hz, CarCH[(P),(NH)]), 136.75 (d,  $^3J_{\text{PC}} = 7.5$  Hz, CarCH[(O),(CH)]), 139.24 (s, CarCHN), 135.46 (d,  $^2J_{\text{PC}} = 22.4$  Hz, PCHCH), 150.56 (d,  $^1J_{\text{PC}} = 156.2$  Hz, CHCHCar); IR (KBr): 3420, 3290, 3080, 3020, 2840, 1590, 1485, 1440, 1230, 1210, 1190, 1180, 1090, 1060, 1025, 990, 955, 700; HRMS (FAB $^+$ ): calcd for  $\text{C}_{20}\text{H}_{26}\text{NO}_2\text{P}$  451.1779. Found: 451.1768; 452 [M+H] $^+$  (35%), 284 (100%), 180 (58%), 106 (8%), 91 (18%).

## 4.2. General procedure for deprotection of arylated 2-hydrogeno-2-oxo-1,4,2-oxazaphosphinane compounds

**4.2.1.  $\alpha$ -[(2-Hydroxy-1,2-diphenyl-ethylamino)-benzyl]-phenyl-phosphinic acid 9a.** In a 250 ml flask containing 800 mg of **7a** (1.75 mmol) is added 50 ml of concentrated aqueous HCl solution (35%). Under stirring, the reaction mixture is heating 3 days at 80 °C. Then, after cooling, the reaction mixture is dissolved in chloroform and saturated with aqueous NaCl solution. After extraction with chloroform, the organic layers are dried over  $\text{Na}_2\text{SO}_4$ . The crude solution is evaporated affording a yellow-brown solid purified by column chromatography (dichloromethane/Ethyl acetate gradient: 100/0 to 70/30).

White solid (780 mg, 1.76 mmol, 1 diastereoisomer), mp = 209.6 °C; 92% yield;  $^{31}\text{P}$  NMR (81.02 MHz,  $\text{DMSO}-d_6$ ): 28.93;  $^1\text{H}$  NMR (250.13 MHz,  $\text{DMSO}-d_6$ ): 4.45 (d, 1H,  $^2J_{\text{PH}} = 12.0$  Hz, PCHPh), 4.49 (d, 1H,  $^3J_{\text{HH}} = 2.4$  Hz, NCHPh), 5.53 (d, 1H,  $^3J_{\text{HH}} = 2.4$  Hz, OCHPh), 6.88–7.53 (m, 20H, CHar);  $^{13}\text{C}$  NMR (100.62 MHz,  $\text{DMSO}-d_6$ ): 60.38 (d,  $^1J_{\text{PC}} = 95.8$  Hz, HNCHP), 67.14 (s, NCHPh), 71.15 (s, OCHPh), 125.97–132.18 (all CHar), 130.97 (d,  $^1J_{\text{PC}} = 133.9$  Hz, Car), 135.92 (s, Car), 141.03 (s, Car); IR (KBr): 3260, 3130, 3040, 2920, 1585, 1490, 1440, 1425, 1450, 1220, 1190, 1070, 950, 700; HRMS (FAB $^+$ ): calcd for  $\text{C}_{27}\text{H}_{26}\text{NO}_3\text{P}$  443.1729. Found: 443.1716; 444 [M+H] $^+$  (21%), 887 [2M+H] $^+$  (10%), 302 (100%), 284 (51%), 180 (11%), 106 (100%).

**4.2.2. Benzyl-phenyl-phosphinic acid 9b.** A 10 ml flask, containing 300 mg (0.71 mmol) of **7a**, 300 mg of palladium catalyst  $[\text{Pd}(\text{OH})_2]$  and 5 ml of methanol is placed under hydrogen atmosphere (1 atm). After 18 h stirring at ambient temperature, reaction mixture is filtrated over celite, and the filtrate evaporated. 2 ml of aqueous solution of NaOH (1 N) are added. After 3 h stirring, the milky suspension is filtered and rinsed with 1 ml water. Filtrate is precipitated by acidification to pH = 5 with aqueous HCl solution (1 N). Final filtration afforded pure **9b**.

White solid (127 mg, 0.55 mmol), mp = 187.2 °C; 92% yield;  $^{31}\text{P}$  NMR (101.25 MHz,  $\text{CD}_3\text{OD}$ ): 38.87;  $^1\text{H}$  NMR

(250.13 MHz,  $\text{CD}_3\text{OD}$ ): 3.32 (d, 2H,  $^2J_{\text{PH}} = 17.9$  Hz, PCHPh), 7.07–7.68 (m, 10H, CHar);  $^{13}\text{C}$  NMR (50.32 MHz,  $\text{CD}_3\text{OD}$ ): 37.70 (d,  $^1J_{\text{PC}} = 94.2$  Hz, HNCHP), 126.04–132.70 (all CHar), 131.40 (d,  $^1J_{\text{PC}} = 130.6$  Hz, PCar); IR (KBr): 3040, 3020, 2990, 2860, 1650, 1455, 1440, 1240, 1200, 1170, 1140, 960, 700; HRMS (FAB $^+$ ): calcd for  $\text{C}_{13}\text{H}_{13}\text{O}_2\text{P}$  233.0731. Found: 233.0735; 233 [M+H] $^+$  (100%), 91 (45%); 77 (30%).

**4.2.3.  $\alpha$ -Aminobenzyl-phenylphosphinic acid 9c.** In a 10 ml flask containing 300 mg (0.71 mmol) of **7a** and 300 mg of palladium catalyst (Pd/C 10% on activated charcoal, 0.28 mmol) is added 10.6 ml of methanolic solution of formic acid (10% vol/vol). After 3 h stirring at 55 °C, the reaction mixture is filtrated over celite, and the filtrate evaporated. 2 ml of aqueous solute of NaOH (1 N) are added. The suspension is then filtered and the filtrate is evaporated. The white solid is recrystallized in methanol to afford **9c** as white crystals.

White solid, (132 mg, 0.53 mmol, 1 diastereoisomer), mp = 205.8 °C; 75% yield;  $^{31}\text{P}$  NMR (101.25 MHz,  $\text{CD}_3\text{OD}$ ): 32.16;  $^1\text{H}$  NMR (250.13 MHz,  $\text{CD}_3\text{OD}$ ): 4.27 (d, 1H,  $^2J_{\text{PH}} = 12.0$  Hz, PCHPh), 7.23–7.47 (m, 20H, CHar);  $^{13}\text{C}$  NMR (62.90 MHz,  $\text{CD}_3\text{OD}$ ): 57.29 (d,  $^1J_{\text{PC}} = 96.5$  Hz, HNCHP), 127.24–132.28 (all CHar), 134.00 (d,  $^1J_{\text{PC}} = 122.4$  Hz, PCar), 139.01 (d,  $^2J_{\text{PC}} = 1.9$  Hz, CarCHP); IR (KBr): 3240, 3000, 1600, 1490, 1430, 1200, 1170, 1130, 1045, 1000, 690, 570, 545, 490; HRMS (FAB $^+$ ): calcd for  $\text{C}_{13}\text{H}_{14}\text{NO}_2\text{P}$  248.0840. Found 248.0848; 248 [M+H] $^+$  (12%), 106 (33%), 77 (24%). (N $^\circ$  CAS: 25891-89-8).

## Acknowledgements

Jérôme Monbrun is grateful to MRT for a scholarship and Monique Tillard is warmly acknowledged for X-ray analyses.

## References and notes

- (a) Grembecka, J.; Mucha, A.; Cierpicki, T.; Kafarski, P. *J. Med. Chem.* **2003**, *46*, 2641–2655. (b) Maskos, K.; Jozic, D.; Kaiser, J. T.; Huber, R.; Bode, W. *J. Mol. Biol.* **2003**, *332*, 243–256. (c) Stowasser, B.; Budt, K.-H.; Jian-Qi, L.; Peyman, A.; Ruppert, D. *Tetrahedron Lett.* **1992**, *33*, 6625–6628. (d) Stowasser, B.; Li, J. Q.; Peyman, A.; Budt, K. H. US Patent 5663139, 1997. *Chem. Abstr.* **121**, 280877. (e) Dreyer, G. B.; Abdel-Meguid, S. S.; Zhao, B.; Murthy, K.; Winborne, E.; Choi, J. W.; DesJarlais, R. L.; Minnich, M. D.; Culp, J. S.; Debouck, C.; Tomaszek, T. A., Jr.; Meek, T. D. *Biochemistry* **1993**, *32*, 7972–7980. (f) Dreyer, G. B. World Patent 9200954, 1992; *Chem. Abstr.* **116**, 236170. (g) Peyman, A.; Stahl, W.; Budt, K.-H.; Ruppert, D.; Schuessler, H.; Wagner, K. US patent 5707979, 1998; *Chem. Abstr.* **124**, 261356. (h) Bolton, G. L.; Padia, J. K.; Trivedi, B. K. US Patent 5208224, 1993; *Chem. Abstr.* **119**, 95833. (i) Lejczak, B.; Kafarski, P.; Zygmunt, J. *Biochemistry* **1989**, *28*, 3549–3555. (j) Li, M.; Lin, Z.; Johnson, M. E. *Bioorg. Med. Chem. Lett.* **1999**, *9*, 1957–1962.

2. (a) Nishizuka, Y. *Nature* **1984**, *308*, 693–698. (b) Boyd, V. L.; Summers, M. F.; Ludeman, S. M.; Ega, W.; Zon, G.; Regan, J. B. *J. Med. Chem.* **1987**, *30*, 366–374. (c) Bergman, J.; Van der Plas, H. C.; Simonyi, M. *Heterocycles in Bioorganic Chemistry*; RSC: Cambridge, 1991. (d) Wu, S. Y.; Casida, J. E. *Phosphorus, Sulfur, Silicon* **1995**, *102*, 177. (e) Reddy, C. D.; Reddy, M. S.; Berlin, K. D. *Phosphorus, Sulfur, Silicon* **1995**, *102*, 103. (f) Lipshutz, B. H. *Chem. Rev.* **1986**, *86*, 795–819.
3. (a) Cristau, H.-J.; Monbrun, J.; Tillard, M.; Pirat, J.-L. *Tetrahedron Lett.* **2003**, *44*, 3183–3186. (b) Pirat, J.-L.; Monbrun, J.; Virieux, D.; Volle, J.-N.; Tillard, T.; Cristau, H.-J. *J. Org. Chem.* Submitted for publication.
4. (a) Chrysselis, M. C.; Rekkas, E. A.; Kourounakis, P. N. *J. Med. Chem.* **2000**, *43*, 609–612. (b) Kelley, J. L.; Musso, D. L.; Boswell, G. E.; Soroko, F. E.; Cooper, B. R. *J. Med. Chem.* **1996**, *39*, 347–349. (c) Musso, D. L.; Kelley, J. L. *Tetrahedron: Asymmetry* **1995**, *8*, 1841–1844. (d) Kelley, J. L.; Musso, D. L.; Boswell, G. E.; Cooper, B. R. Eur. Pat. 426416, 1991; *Chem. Abstr.* *115*, 92281. (e) Morgan, P. F.; Musso, D. L.; Partridge, J. J. World Patent 9937305, 1999; *Chem. Abstr.* *131*, 111445.
5. Wyatt, P. B.; Villalonga-Barber, C.; Motevalli, M. *Tetrahedron Lett.* **1999**, *40*, 149–152.
6. (a) Katagiri, N.; Yamamoto, M.; Iwaoka, T.; Kaneko, C. *Chem. Commun.* **1991**, *20*, 1429–1430. (b) Afarinkia, K.; Binch, H. M.; Forristal, I. *Synlett* **2000**, *12*, 1771–1772. (c) Hamilton, R.; Shute, R. E.; Travers, J.; Walker, B.; Walker, B. J. *Tetrahedron Lett.* **1994**, *21*, 3597–3600. (d) Afarinkia, K.; De Pascale, E.; Amara, S. *Arkivoc* **2002**, *vi*, 205–211. (e) Ragulin, V. V. *Russ. J. Gen. Chem.* **2001**, *71*, 1823–1824.
7. Zhou, J.; Qiu, Y.; Feng, K.; Chen, R. *Synthesis* **1999**, *1*, 40–42.
8. (a) Xu, Y.; Zhang, J.; Huang, G.; Guo, H. *Tetrahedron Lett.* **1988**, *29*, 1955–1958. (b) Xu, Y.; Li, Z. *Tetrahedron Lett.* **1986**, *27*, 3017–3020. (c) Xu, Y.; Wei, H.; Zhang, J.; Huang, G. *Tetrahedron Lett.* **1989**, *30*, 949–952. (d) Cristau, H.-J.; Hervé, A.; Virieux, D. *Synthesis* **2003**, *14*, 2216–2220. (e) Lei, H.; Stoakes, M. S.; Schwabacher, A. L. *Synthesis* **1992**, 1255–1260.
9. Xu, Y.; Zhang, J. *Chem. Commun.* **1986**, 1606.
10. Ogawa, T.; Usuki, N.; Ono, N. *J. Chem. Soc., Perkin Trans. 1* **1998**, 2953–2958.
11. Menger, F. M.; Smith, J. H. *J. Am. Chem. Soc.* **1969**, 4211–4216.
12. Szabo, A.; Jaszay, Z. M.; Hegedus, L.; Toke, L.; Penehazy, I. *Tetrahedron Lett.* **2003**, *44*, 4603–4606.

# Five novel flavonoids from *Wasabia japonica*

Takahiro Hosoya, Young Sook Yun and Akira Kunugi\*

Graduate School of Life Science, Tokyo University of Pharmacy and Life Science, 1432-1 Horinouchi, Hachioji, Tokyo 192-0392, Japan

Received 3 February 2005; accepted 18 April 2005

**Abstract**—From the fresh leaves of *Wasabia japonica* Matsum., five novel flavonoids **1–5**, isovitexin derivatives having a *trans*-sinapoyl group at C-7, were isolated together with five known flavonoids, and their structures were elucidated on the basis of their spectroscopic data (NMR, MS, UV, and IR) and chemical evidence.

© 2005 Elsevier Ltd. All rights reserved.

## 1. Introduction

*Wasabia japonica* Matsumura (Sawa-wasabi in Japanese) is an edible plant that belongs to Cruciferae. The paste of its root, liberating allyl isothiocyanate by hydrolysis with myrosinase,<sup>1</sup> has been used for a long time in Japanese meals as a pungent spice. Interests of this plant have been focused on volatile components, especially isothiocyanates, and the other components have not been studied. We conducted the chemical studies on Wasabi leaves, and isolated five new flavone glycosides (**1–5**) along with five known flavonoids (**6–10**) (Scheme 1). Compounds **1–5** were new flavone glycosides characterized by an isovitexin (**6**) unit acylated by a *trans*-sinapic acid at the C-7 hydroxyl group, and their structures were determined on the basis of the spectroscopic data including 2D NMR spectra and chemical evidence.

## 2. Results and discussion

By repeated column chromatography and preparative reversed-phase HPLC as described in the experimental section, the MeOH extract of the fresh leaves of *W. japonica* gave eight flavone glycosides **1–7**, **10** and flavones **8** and **9**.

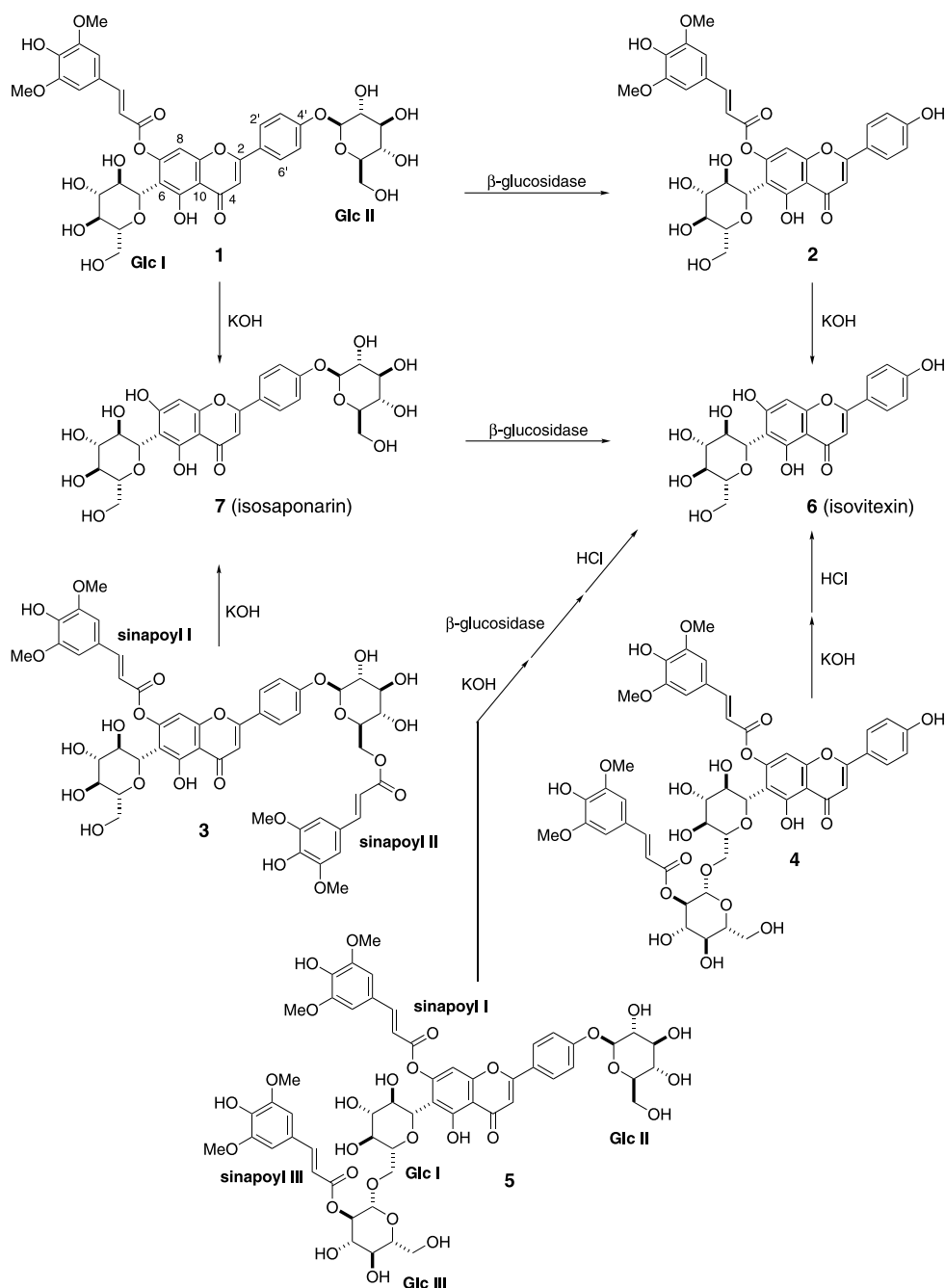
Compounds **6–10** were identified as isovitexin (apigenin 6-*C*- $\beta$ -D-glucopyranoside),<sup>2,3</sup> isosaponarin (isovitexin 4'-*O*- $\beta$ -D-glucopyranoside),<sup>4</sup> apigenin,<sup>2,5</sup> luteolin,<sup>2,5</sup> and isorientin (luteolin 6-*C*- $\beta$ -D-glucopyranoside),<sup>2,6</sup> respectively, by comparison of their spectroscopic data with those in the literature.

Compound **1** was obtained as a yellow amorphous solid, and its molecular formula was determined to be C<sub>38</sub>H<sub>40</sub>O<sub>19</sub> by HRESIMS. The IR spectral absorptions showed the presence of hydroxyl (3421 cm<sup>-1</sup>) and conjugated carbonyl (1691 cm<sup>-1</sup>) groups and aromatic rings (1643 and 1512 cm<sup>-1</sup>) in the molecule. The UV absorption band at 325 nm implied the presence of a highly conjugated double bond system in the molecule. The <sup>1</sup>H NMR spectrum in DMSO-*d*<sub>6</sub> showed the signals for eight aromatic protons ( $\delta$  6.48, 6.85, 6.89 $\times$ 2, 7.16 $\times$ 2, and 8.00 $\times$ 2), two olefinic protons ( $\delta$  6.30 and 7.32, each 1H, d, *J*=15.8 Hz), two methoxyl groups ( $\delta$  3.76 $\times$ 2), two anomeric protons ( $\delta$  4.86 and 5.01, each 1H, d, *J*=10.0 and 7.3 Hz, respectively), sugar-derived protons ( $\delta$  3.18–3.75), and a hydrogen-bonded hydroxyl proton ( $\delta$  13.56). The <sup>13</sup>C NMR spectrum showed signals caused by a conjugated ketonic carbon ( $\delta$  181.9), an ester carbonyl carbon ( $\delta$  165.3), nineteen aromatic or olefinic carbons ( $\delta$  103.1–162.9), two methoxyl groups ( $\delta$  56.0 $\times$ 2), and twelve sugar-derived carbons ( $\delta$  60.6, 61.4, 69.6, 70.6 $\times$ 2, 71.8, 73.1, 76.4, 76.5, 77.1, 81.8, and 99.8). Analysis of its 2D NMR spectra revealed the presence of a C-6-substituted apigenin-type flavone structure, one sinapoyl group, and two glucoses. An HMBC correlation between H-1 ( $\delta$  4.86) of one of the glucose and C-6 ( $\delta$  107.1) of the flavone unit and the characteristic chemical shift of the anomeric carbon ( $\delta$  70.6) suggested a C-glucoside linkage at C-6. Another was determined to be link to the hydroxyl group at C-4' by observation of an HMBC correlation between H-1 ( $\delta$  5.01) of another glucose and C-4' ( $\delta$  160.3). The  $\beta$ -anomeric configurations for both glucoses were determined from their <sup>3</sup>*J*<sub>H1,H2</sub> coupling constants (10.0 and 7.3 Hz, respectively). HMBC correlations between the phenolic hydroxyl proton and C-6 and C-10 indicated the presence of a hydroxyl group at C-5. Thus, the location of the sinapoyl group was determined to be at the C-7 oxygen. The structure of **1** was confirmed by

**Keywords:** Isovitexin; Flavone; *Wasabia japonica*.

\* Corresponding author. Tel.: +81 426 76 7256; fax: 81 426 76 9412; e-mail: kunugi@ls.toyaku.ac.jp





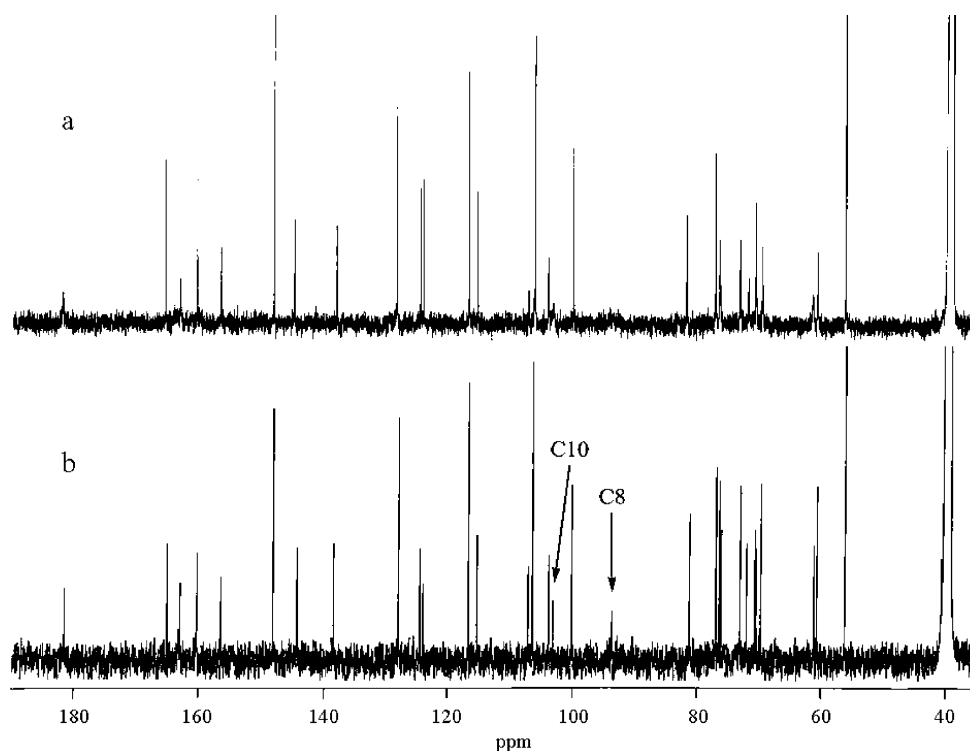
Scheme 1. Correlations of 1–7.

the chemical correlations with isovitexin (**6**) and isosaponarin (**7**). Treatment of **1** with methanolic KOH gave isosaponarin (**7**), and subsequent enzymatic hydrolysis of **7** using  $\beta$ -glucosidase afforded isovitexin (**6**). Accordingly, compound **1** was determined to be 7-*O*-*trans*-sinapoyl-isovitexin 4'-*O*- $\beta$ -D-glucopyranoside.

In the NMR spectra of **1** at 300 K, broadening or complication of the signals of the glucosyl and ring-A moieties was observed, which was ameliorated by measuring spectra at 343 K (Fig. 1). This phenomenon was attributed to the sinapoyl group at C-7, inhibiting free rotation of the C-6 glucosyl group, since sharp signals were

observed for the corresponding protons or carbons of the deacylated compounds **6** and **7**.

Compound **2** was obtained as a yellow amorphous solid. Its molecular formula was determined to be  $C_{32}H_{30}O_{14}$  by HRESIMS. The UV, IR, and  $^1H$  and  $^{13}C$  NMR spectral features of **2** were generally similar to those of **1**. The signal of a hydrogen-bonded phenolic hydroxyl proton was observed at  $\delta$  13.62 in the  $^1H$  NMR spectrum and long range coupled with C-6 and C-10 in the HMBC spectrum, indicating presence of a hydroxyl group at C-5. A long range coupling was observed between the anomeric proton ( $\delta$  4.86) and C-6 ( $\delta$  107.0) in the HMBC spectrum to show



**Figure 1.**  $^{13}\text{C}$  NMR spectra of compound **1** in  $\text{DMSO-}d_6$ . (a) At 300 K, (b) at 343 K.

that the sugar moiety was located at the C-6 carbon atom. Although the HMBC spectrum was not able to give information about the location of the sinapoyl group, broadening or complication of the NMR signals observed as in **1** suggested acylation at the C-7 oxygen. Enzymatic hydrolysis of **1** by  $\beta$ -glucosidase afforded **2**, while treatment of **2** with methanolic KOH gave isovitexin (**6**), which was identified by  $^1\text{H}$  and  $^{13}\text{C}$  NMR analysis. Thus, compound **2** was determined to be 7-*O-trans*-sinapoylisovitexin.

Compound **3**, obtained as a yellow amorphous solid, was determined to have the molecular formula of  $\text{C}_{49}\text{H}_{50}\text{O}_{23}$  by HRESIMS. As shown in the experimental section, the UV and IR spectral features of **3** were generally similar to those of **1** and **2**. Its  $^1\text{H}$  and  $^{13}\text{C}$  NMR spectral data implied that it had a flavone unit, two sinapoyl groups and two glucoses. The long range correlations between an anomeric proton ( $\delta$  5.03, d,  $J=7.2$  Hz) and C-4' ( $\delta$  161.6) and between another anomeric proton ( $\delta$  5.13, d,  $J=10.0$  Hz) and C-6 ( $\delta$  108.1) showed that glucoses were linked to the C-4' oxygen atom and the C-6 carbon atom, respectively. One of the sinapoyl groups was determined to be linked to the C-6 hydroxyl oxygen of the sugar linked to C-4' by observation of correlations between the methylene protons ( $\delta$  4.41 and 4.53) and the carbonyl carbon ( $\delta$  168.8) of the sinapoyl group in the HMBC experiment and the low-field shifted C-6 signal at  $\delta$  64.5. The close similarity between the  $^1\text{H}$  and  $^{13}\text{C}$  NMR data in  $\text{CD}_3\text{OD}$  for the A ring portion in this molecule and the corresponding resonances observed in **1** and line broadening of the NMR signals for this portion suggested the presence of another sinapoyl group at the C-7 oxygen. Treatment of **3** with methanolic KOH afforded isosaponarin (**7**). Thus, compound **3** was determined to be 7-*O-trans*-sinapoylisovitexin 4'-*O*-(6-*O-trans*-sinapoyl- $\beta$ -D-glucopyranoside).

Compound **4** was obtained as a yellow amorphous solid. The molecular formula was determined to be  $\text{C}_{49}\text{H}_{50}\text{O}_{23}$  by HRESIMS. The  $^1\text{H}$  and  $^{13}\text{C}$  NMR spectral data suggested that it had a flavone unit, two sinapoyl groups and two glucoses. HMBC correlations between the anomeric proton ( $\delta$  4.84, d,  $J=10.0$  Hz) of the internal glucose and the C-6 carbon atom ( $\delta$  106.7) of the flavone unit and between the anomeric proton ( $\delta$  4.54, d,  $J=8.1$  Hz) of the terminal glucose and C-6 ( $\delta$  68.8) of the internal glucose revealed that one glucose was bonded to C-6 of the flavone unit and the other glucose was linked to the oxygen atom at C-6 of the internal glucose with both  $\beta$ -anomeric configurations. The HMBC correlation between H-2 ( $\delta$  4.64) of the terminal glucose and the carbonyl carbon ( $\delta$  165.6) of a sinapoyl group showed that a sinapoyl group bonded to the C-2 oxygen atom of the terminal glucose. Line broadening of the NMR signals of the A ring moiety suggested the presence of another sinapoyl group at the C-7 oxygen as in **1–3**. When compound **4** was hydrolyzed with methanolic KOH followed by treatment with HCl, the resultant product was identified as isovitexin (**6**) and the sugar was identified as D-glucose by the HPLC analysis with an optical rotation detector. Accordingly, compound **4** was determined to be 6''-*O*-(2-*O-trans*-sinapoyl- $\beta$ -D-glucopyranosyl)-7-*O-trans*-sinapoylisovitexin.

Compound **5** was obtained as a yellow amorphous solid. The molecular formula was determined to be  $\text{C}_{55}\text{H}_{60}\text{O}_{28}$  by HRESIMS, which corresponded to that of **4** with one extra hexose unit. The hexose was assigned as glucose by its chemical shifts in the  $^1\text{H}$  and  $^{13}\text{C}$  NMR spectra. The HMBC correlation between the anomeric proton ( $\delta$  5.02, d,  $J=7.1$  Hz) and C-4' ( $\delta$  160.2) showed that the extra glucose unit was linked to the C-4' oxygen atom with  $\beta$ -anomeric configuration. Sequential treatment of **5** with methanolic

KOH,  $\beta$ -glucosidase, and boiling HCl afforded isovitexin (**6**). Thus, compound **5** was determined to be 6''-O-(2-O-trans-sinapoyl- $\beta$ -D-glucopyranosyl)-7-O-trans-sinapoylisovitexin 4'-O- $\beta$ -D-glucopyranoside (**5**).

Although many flavonoids have been isolated from natural sources, their phenylpropanoid esters are rare, and only one sinapoyl ester has been reported.<sup>7</sup> Therefore, compounds **1–5** having a C-glucoside structure acylated by sinapoyl groups are unique.

Compounds **1**, **2**, **4**, and **5** showed super oxide anion radical ( $O_2^-$ ) scavenging activity with inhibition rates of DMPO- $O_2^-$  adduct production of 30.0, 44.0, 64.5, and 22.1% at 1 mg/mL, respectively.

### 3. Experimental

#### 3.1. General experimental procedures

Optical rotations were measured on a JASCO DIP-360 automatic digital polarimeter. UV spectra were obtained on a Hitachi U-2001 spectrophotometer, and IR spectra were recorded on a JASCO FT/IR-620 spectrophotometer.  $^1H$  and  $^{13}C$  NMR spectra were recorded on a Bruker DRX-500 spectrometer. Standard pulse sequences and parameters were used for the experiments. The chemical shift values are reported in ppm ( $\delta$ ) units and the coupling constants ( $J$ ) are in Hz.  $^1H$  chemical shifts in  $CD_3OD$  and  $DMSO-d_6$  were referenced to residual  $CD_2HOD$  (3.31 ppm) and  $CD_3SOCHD_2$  (2.50 ppm), respectively;  $^{13}C$  chemical shifts were referenced to the solvent ( $CD_3OD$ , 49.0 ppm and  $CD_3SOCD_3$ , 39.5 ppm). High-resolution ESI-MS was obtained on a Micromass LCT spectrometer. HPLC was carried out on a Shimadzu LC-10AT pump equipped with a SPE-10vp detector ( $\lambda$  254 nm) and a Mightysil RP-18 column (for analytical HPLC,  $250 \times 4.6$  mm i.d., 5  $\mu$ m particle size and for preparative HPLC,  $250 \times 20$  mm i.d., 5  $\mu$ m particle size, Kanto Kagaku, Tokyo, Japan), by using a  $CH_3CN/H_2O$  solvent system. The HPLC analysis of the sugar component was carried out using an optical rotation detector, SHODEX OR-2 (Showadenko, Tokyo, Japan), a Capcell Pak  $NH_2$  UG80 column ( $250 \times 4.6$  mm i.d., 5  $\mu$ m particle size, Shiseido, Tokyo, Japan), and  $CH_3CN/H_2O$  (85:15) solvent system (0.9 mL/min).  $\beta$ -Glucosidase (from almonds, EC 3.2.1.21) was purchased from Sigma-Aldrich (St. Louis, MO, USA).

#### 3.2. Plant material and separation of individual flavonoids

The leaves of *W. japonica* Matsumura, cultivated in Okutama, Tokyo, Japan were harvested in October, 2002.

The fresh leaves (7.0 kg) were extracted with MeOH ( $3 \times 36$  L, a week each) at room temperature. After filtration and removal of the solvent by evaporation in vacuo, a residue (362.8 g) was obtained, which was suspended in water and extracted successively with hexane and EtOAc to give hexane-, EtOAc-, and water-soluble portions.

The EtOAc-soluble portion gave, on removal of the solvent,

30.0 g of a residue, which was placed on a Diaion HP-20 column and eluted sequentially with MeOH/ $H_2O$  mixtures (40:60, 60:40, 80:20, and 100:0), and EtOAc to give five fractions. The MeOH/ $H_2O$  (80:20) eluate was concentrated, and the residue (4.6 g) was subjected to silica gel column chromatography using a gradient solvent system ( $CHCl_3/MeOH$  100:0  $\rightarrow$  50:50) to give five fractions (frs. 1–5). Fr. 2 (895.0 mg) was placed on a Sephadex LH-20 column and eluted with MeOH to afford four fractions. The fourth fraction (22.0 mg) was separated by preparative HPLC with  $CH_3CN/H_2O$  (40:60) to give **8** (3.5 mg) and **9** (7.4 mg). Fr. 3 (828.0 mg) was subjected to preparative HPLC using  $CH_3CN/H_2O$  (27:73) to give **2** (63.0 mg). Similarly, fr. 4 (556.0 mg) gave **4** (29.3 mg) using  $CH_3CN/H_2O$  (20:80). Sephadex LH-20 column chromatography of fr. 5 (1.1 g) using MeOH gave five fractions. The fourth fraction (143.0 mg) was subjected to preparative HPLC using  $CH_3CN/H_2O$  (20:80) to give **3** (5.8 mg).

The water-soluble portion (146.3 g) was placed on a Diaion HP-20 column and eluted sequentially with 4 L each of MeOH/ $H_2O$  mixtures (0:100, 20:80, 40:60, 50:50, 60:40, 80:20, and 100:0) and acetone. The MeOH/ $H_2O$  (60:40) fraction (13.4 g) was subjected to ODS column chromatography using MeOH/ $H_2O$  mixtures (30:70, 50:50, 80:20, and 100:0) to give 11 fractions. The second fraction (1.2 g) eluted with MeOH/ $H_2O$  (30:70) was subjected to preparative HPLC using  $CH_3CN/H_2O$  (15:85) to give **6** (10.0 mg) and the fourth (447.4 mg) and sixth (536.5 mg) fractions using  $CH_3CN/H_2O$  (17:83) to give **1** (16.1 mg) and **6** (12.1 mg), respectively. The MeOH/ $H_2O$  (80:20) fraction (4.0 g) was separated by Sephadex LH-20 column chromatography to give five fractions (frs. A–E). Fr. B (1.9 g) was placed on an ODS column and eluted sequentially with MeOH/ $H_2O$  mixtures (20:80, 40:60, 50:50, 80:20 and 100:0). The second fraction (262.0 mg) was subjected to preparative HPLC using  $CH_3CN/H_2O$  (17:83) to give **5** (26.3 mg), and the fourth fraction (221.0 mg) gave **10** (41.7 mg) and **7** (7.5 mg). Frs. C (518.1 mg) and D (131.5 mg) were each subjected to preparative HPLC using  $CH_3CN/H_2O$  (20:80 and 17:83, respectively) to give **1** (60.7 mg) and **6** (36.5 mg), respectively.

#### 3.3. Characteristics of each compound

**3.3.1. 7-O-trans-Sinapoylisovitexin 4'-O- $\beta$ -D-glucopyranoside (1).** Yellow amorphous solid;  $[\alpha]_D^{25} -155$  (c 0.21, pyridine); IR (neat)  $\nu_{max}$  3421, 2924, 1691, 1643, 1512  $cm^{-1}$ ; UV (MeOH)  $\lambda_{max}$  ( $\log \epsilon$ ) 215 nm (4.49), 274 (4.23), 325 (4.39) nm;  $^1H$  and  $^{13}C$  NMR spectral data in  $DMSO-d_6$  given in Tables 1 and 2, respectively;  $^1H$  NMR ( $CD_3OD$ , 500 MHz, 300 K)  $\delta$  7.79 (2H, d,  $J=8.3$  Hz, H-2', 6'), 7.39 (1H, d,  $J=15.8$  Hz, sinapoyl H- $\beta$ ), 7.17 (2H, d,  $J=8.3$  Hz, H-3', 5'), 6.72 (2H, s, sinapoyl H-2, 6), 6.49 (1H, s, H-3), 6.41 (1H, s, H-8), 6.17 (1H, d,  $J=15.8$  Hz, sinapoyl H- $\alpha$ ), 5.68 (1H, brm, H-2 of Glc at C-6), 5.13 (1H, d,  $J=9.9$  Hz, H-1 of Glc at C-6), 5.01 (1H, d,  $J=6.3$  Hz, H-1 of Glc at C-4'), 3.94 (1H, d,  $J=11.9$  Hz, H-6 of Glc at C-6), 3.92 (1H, d,  $J=12.1$  Hz, H-6 of Glc at C-4'), 3.81 (1H, overlapped, H-6 of Glc at C-6), 3.78 (6H, s, sinapoyl OMe), 3.77 (1H, overlapped, H-3 of Glc at C-6), 3.71 (1H, dd,  $J=5.7, 12.1$  Hz, H-6 of Glc at C-4'), 3.62 (1H, overlapped, H-4 of Glc at C-6), 3.51 (1H, overlapped, H-5 of Glc at C-6), 3.50 (3H, overlapped, H-2, 3, 5 of Glc at

**Table 1.**  $^1\text{H}$  NMR (500 MHz) spectral data for **1–5** at 300 K<sup>a</sup>

	<b>1</b> <sup>b</sup>	<b>2</b> <sup>b</sup>	<b>3</b> <sup>c</sup>	<b>4</b> <sup>b</sup>	<b>5</b> <sup>b</sup>
3	6.85 (1H, s)	6.73 (1H, s)	6.32 (1H, s)	6.65 (1H, s)	6.76 (1H, s)
8	6.48 (1H, s)	6.45 (1H, s)	6.26 (1H, s)	6.37 (1H, s)	6.41 (1H, s)
2', 6'	8.00 (2H, d, 9.0)	7.89 (2H, d, 8.8)	7.68 (2H, d, 8.8)	7.85 (2H, d, 8.7)	7.96 (2H, d, 8.8)
3', 5'	7.16 (2H, d, 9.0)	6.90 (2H, d, 8.8)	7.12 (2H, d, 8.8)	6.89 (2H, d, 8.7)	7.16 (2H, d, 8.8)
5-OH	13.56 (1H, brs)	13.62 (1H, brs)		13.60 (1H, brs)	13.60 (1H, brs)
Glc I at C-6					
1	4.86 (1H, d, 10.0)	4.86 (1H, d, 10.0)	5.13 (1H, d, 10.0)	4.84 (1H, d, 10.0)	4.84 (1H, d, 10.0)
2	5.68 (1H, brm)	5.68 (1H, brm)	5.69 (1H, brm)	5.62 (1H, brm)	5.62 (1H, brm)
3	3.49 (1H, <sup>d</sup> )	3.48 (1H, <sup>d</sup> )	3.76 (1H, <sup>d</sup> )	3.43 (1H, <sup>d</sup> )	3.44 (1H, <sup>d</sup> )
4	3.28 (1H, <sup>d</sup> )	3.27 (1H, <sup>d</sup> )	3.62 (1H, dd, 9.3, 9.3)	3.22 (1H, <sup>d</sup> )	3.22 (1H, <sup>d</sup> )
5	3.28 (1H, <sup>d</sup> )	3.27 (1H, <sup>d</sup> )	3.51 (1H, m)	3.40 (1H, <sup>d</sup> )	3.39 (1H, <sup>d</sup> )
6	3.46 (1H, <sup>d</sup> )	3.46 (1H, <sup>d</sup> )	3.81 (1H, <sup>d</sup> )	3.60 (1H, m)	3.60 (1H, m)
	3.75 (1H, <sup>d</sup> )	3.75 (1H, <sup>d</sup> )	3.94 (1H, dd, 1.7, 12.0)	4.02 (1H, d, 10.9)	4.04 (1H, d, 10.8)
Sinapoyl I at C-7					
2, 6	6.89 (2H, s)	6.89 (2H, s)	6.73 (2H, s)	6.87 (2H, s)	6.87 (2H, s)
$\alpha$	6.30 (1H, d, 15.8)	6.30 (1H, d, 15.8)	6.21 (1H, d, 15.8)	6.24 (1H, d, 15.8)	6.25 (1H, d, 15.8)
$\beta$	7.32 (1H, d, 15.8)	7.32 (1H, d, 15.8)	7.41 (1H, d, 15.8)	7.28 (1H, d, 15.8)	7.28 (1H, d, 15.8)
OMe	3.76 (6H, s)	3.76 (6H, s)	3.77 (6H, s)	3.75 (6H, s)	3.75 (6H, s)
Glc II at C-4'					
1	5.01 (1H, d, 7.3)		5.03 (1H, d, 7.2)		5.02 (1H, d, 7.1)
2	3.27 (1H, <sup>d</sup> )		3.53 (1H, <sup>d</sup> )		3.28 (1H, <sup>d</sup> )
3	3.31 (1H, <sup>d</sup> )		3.53 (1H, <sup>d</sup> )		3.30 (1H, <sup>d</sup> )
4	3.18 (1H, <sup>d</sup> )		3.44 (1H, m)		3.18 (1H, <sup>d</sup> )
5	3.39 (1H, <sup>d</sup> )		3.78 (1H, <sup>d</sup> )		3.39 (1H, <sup>d</sup> )
6	3.46 (1H, <sup>d</sup> )		4.41 (1H, dd, 7.2, 11.8)		3.47 (1H, <sup>d</sup> )
	3.69 (1H, d, 11.5)		4.53 (1H, dd, 1.8, 11.8)		3.70 (1H, <sup>d</sup> )
Sinapoyl II at C-6 of Glc II					
2, 6			6.77 (2H, s)		
$\alpha$			6.33 (1H, d, 15.8)		
$\beta$			7.49 (1H, d, 15.8)		
OMe			3.74 (6H, s)		
Glc III at C-6 of Glc I					
1				4.54 (1H, d, 8.1)	4.54 (1H, d, 8.1)
2				4.64 (1H, dd, 8.1, 9.5)	4.65 (1H, dd, 8.1, 9.5)
3				3.33 (1H, <sup>d</sup> )	3.32 (1H, <sup>d</sup> )
4				3.18 (1H, <sup>d</sup> )	3.16 (1H, <sup>d</sup> )
5				3.13 (1H, m)	3.14 (1H, <sup>d</sup> )
6				3.49 (1H, dd, 5.7, 11.3)	3.47 (1H, <sup>d</sup> )
				3.69 (1H, d, 11.3)	3.70 (1H, <sup>d</sup> )
Sinapoyl III at C-2 of Glc III					
2, 6				6.99 (2H, s)	6.98 (2H, s)
$\alpha$				6.49 (1H, d, 15.8)	6.48 (1H, d, 15.8)
$\beta$				7.53 (1H, d, 15.8)	7.52 (1H, d, 15.8)
OMe				3.77 (6H, s)	3.77 (6H, s)

<sup>a</sup> *J*-values are given in Hz in parentheses.<sup>b</sup> In DMSO-*d*<sub>6</sub>.<sup>c</sup> In CD<sub>3</sub>OD.<sup>d</sup> Multiplicity was not determined due to overlapping and/or broadening of the signals.

C-4'), 3.41 (1H, m, H-4 of Glc at C-4'); <sup>13</sup>C NMR (CD<sub>3</sub>OD, 125 MHz, 300 K)  $\delta$  183.8 (C-4), 168.2 (sinapoyl C=O), 165.4 (C-2), 165.2 (C-5), 162.0 (C-4'), 158.8 (C-9), 149.3 (sinapoyl C-3, 5), 147.0 (sinapoyl C- $\beta$ ), 139.4 (sinapoyl C-4), 129.2 (C-2', 6'), 126.5 (sinapoyl C-1), 125.9 (C-1'), 118.0 (C-3', 5'), 115.7 (sinapoyl C- $\alpha$ ), 108.1 (C-6), 106.7 (sinapoyl C-2, 6), 105.0 (C-10), 104.9 (C-3), 101.7 (C-1 of Glc at C-4'), 82.9 (C-5 of Glc at C-6), 78.3 (C-5 of Glc at C-4'), 78.0 (C-3 of Glc at C-6), 77.9 (C-3 of Glc at C-4'), 74.8 (C-2 of Glc at C-4'), 74.0 (C-2 of Glc at C-6), 73.2 (C-1 of Glc at C-6), 71.8 (C-4 of Glc at C-6), 71.3 (C-4 of Glc at C-4'), 62.8 (C-6 of Glc at C-6), 62.5 (C-6 of Glc at C-4'), 56.7 (sinapoyl OMe); HRESIMS *m/z* 801.2248 [M+H]<sup>+</sup> (calcd for C<sub>38</sub>H<sub>41</sub>O<sub>19</sub>, 801.2242).

**3.3.2. 7-O-trans-Sinapoylisovitexin (2).** Yellow amorphous solid; [ $\alpha$ ]<sub>D</sub><sup>25</sup> –190 (*c* 0.18, pyridine); IR (neat)  $\nu_{\text{max}}$  3415, 2924, 1699, 1630, 1514 cm<sup>-1</sup>; UV (MeOH)  $\lambda_{\text{max}}$  (log  $\epsilon$ ) 214 (4.45), 272 (4.11), 328 (4.35) nm; <sup>1</sup>H and <sup>13</sup>C NMR spectral

data given in Tables 1 and 2, respectively; HRESIMS *m/z* 639.1708 [M+H]<sup>+</sup> (calcd for C<sub>32</sub>H<sub>31</sub>O<sub>14</sub>, 639.1714).

**3.3.3. 7-O-trans-Sinapoylisovitexin 4'-O-(6-O-trans-sinapoyl- $\beta$ -D-glucopyranoside) (3).** Yellow amorphous solid; [ $\alpha$ ]<sub>D</sub><sup>25</sup> –107 (*c* 0.49, pyridine); IR (neat)  $\nu_{\text{max}}$  3367, 2922, 1693, 1606, 1510 cm<sup>-1</sup>; UV (MeOH)  $\lambda_{\text{max}}$  (log  $\epsilon$ ) 204 (4.70), 273 (4.28), 328 (4.62) nm; <sup>1</sup>H and <sup>13</sup>C NMR spectral data given in Tables 1 and 2, respectively; HRESIMS *m/z* 1007.2899 [M+H]<sup>+</sup> (calcd for C<sub>49</sub>H<sub>51</sub>O<sub>23</sub>, 1007.2821).

**3.3.4. 6''-O-(2-O-trans-Sinapoyl- $\beta$ -D-glucopyranosyl)-7-O-trans-sinapoylisovitexin (4).** Yellow amorphous solid; [ $\alpha$ ]<sub>D</sub><sup>25</sup> –183 (*c* 0.27, pyridine); IR (neat)  $\nu_{\text{max}}$  3417, 2925, 1695, 1630, 1512 cm<sup>-1</sup>; UV (MeOH)  $\lambda_{\text{max}}$  (log  $\epsilon$ ) 205 (4.66), 276 (4.31), 325 (4.56) nm; <sup>1</sup>H and <sup>13</sup>C NMR spectral data given in Tables 1 and 2, respectively; HRESIMS *m/z* 1007.2899 [M+H]<sup>+</sup> (calcd for C<sub>49</sub>H<sub>51</sub>O<sub>23</sub>, 1007.2821).

**Table 2.**  $^{13}\text{C}$  NMR (125 MHz) spectral data for **1–5** at 300 K

	<b>1</b> <sup>a</sup>	<b>2</b> <sup>a</sup>	<b>3</b> <sup>b</sup>	<b>4</b> <sup>a</sup>	<b>5</b> <sup>a</sup>
2	162.9	163.6	165.1	163.5	162.9
3	103.8	102.8	104.9	102.8	103.8
4	181.9	181.8	183.6	181.7	181.8
5	c	c	c	c	c
6	107.1	107.0	108.1	106.7	106.8
7	c	c	c	c	c
8	c	c	c	c	c
9	156.4	156.3	158.7	156.3	156.3
10	103.1	103.1	105.0	103.0	103.1
1'	123.8	121.1	126.1	121.1	123.9
2', 6'	128.2	128.5	129.1	128.4	128.2
3', 5'	116.5	116.0	118.1	115.9	116.5
4'	160.3	161.2	161.6	161.1	160.2
Glc I at C-6					
1	70.6	70.6	73.3	70.7	70.7
2	71.8	71.9	74.0	71.8	71.7
3	76.4	76.4	78.1	76.3	76.3
4	70.6	70.6	71.8	70.4	70.4
5	81.8	81.8	82.9	80.6	80.6
6	61.4	61.4	62.9	68.8	68.9
Sinapoyl I at C-7					
1	124.3	124.4	126.5	124.3	124.3
2, 6	106.0	106.0	106.8	105.9	105.9
3, 5	147.9	148.0	149.3	147.9	147.9
4	138.1	138.1	139.5	138.0	138.1
$\alpha$	115.2	115.2	115.8	115.1	115.1
$\beta$	144.7	144.7	147.1	144.7	144.7
CO	165.3	165.3	168.3	165.2	165.2
3, 5-OMe	56.0	56.0	56.8	56.0	56.0
Glc II at C-4'					
1	99.8		101.4		99.9
2	73.1		74.8		73.2
3	76.5		77.9		76.5
4	69.6		72.0		69.6
5	77.1		75.6		77.1
6	60.6		64.5		60.6
Sinapoyl II at C-6 of Glc II					
1			126.6		
2, 6			106.8		
3, 5			149.4		
4			139.7		
$\alpha$			115.6		
$\beta$			147.4		
CO			168.8		
3, 5-OMe			56.8		
Glc III at C-6 of Glc I					
1				100.8	100.9
2				73.4	73.4
3				74.4	74.4
4				70.1	70.1
5				77.1	77.1
6				60.8	60.8
Sinapoyl III at C-2 of Glc III					
1				124.5	124.6
2, 6				106.0	105.9
3, 5				147.9	147.9
4				138.1	138.1
$\alpha$				115.2	115.2
$\beta$				145.2	145.2
CO				165.6	165.6
3, 5-OMe				56.0	56.0

<sup>a</sup> In DMSO-*d*<sub>6</sub>.<sup>b</sup> In CD<sub>3</sub>OD.<sup>c</sup> The signal was not detected.

**3.3.5. 6''-O-(2-O-trans-Sinapoyl- $\beta$ -D-glucopyranosyl)-7-O-trans-sinapoylisovitexin 4'-O- $\beta$ -D-glucopyranoside (5).** Yellow amorphous solid;  $[\alpha]_{\text{D}}^{25} - 103$  (*c* 0.35, pyridine); IR (neat)  $\nu_{\text{max}}$  3421, 2924, 1695, 1641, 1510  $\text{cm}^{-1}$ ; UV (MeOH)  $\lambda_{\text{max}}$  (log  $\epsilon$ ) 205 (4.69), 275 (4.32), 325 (4.56) nm;

$^1\text{H}$  and  $^{13}\text{C}$  NMR spectral data given in Tables 1 and 2, respectively; HRESIMS  $m/z$  1169.3582  $[\text{M} + \text{H}]^+$  (calcd for C<sub>55</sub>H<sub>61</sub>O<sub>28</sub>, 1169.3349).

**3.3.6. Isovitexin (6).** Yellow amorphous solid;  $[\alpha]_{\text{D}}^{25} + 4.8$

(*c* 0.45, pyridine);  $^1\text{H}$  NMR (DMSO- $d_6$ , 500 MHz, 300 K)  $\delta$  13.55 (1H, brs, OH-5), 7.93 (2H, d,  $J=8.8$  Hz, H-2', 6'), 6.93 (2H, d,  $J=8.8$  Hz, H-3', 5'), 6.78 (1H, s, H-3), 6.51 (1H, s, H-8), 4.59 (1H, d,  $J=9.8$  Hz, H-1 of Glc), 4.04 (1H, dd,  $J=8.5, 9.8$  Hz, H-2 of Glc), 3.68 (1H, d,  $J=11.7$  Hz, H-6 of Glc), 3.41 (1H, dd,  $J=5.9, 11.7$  Hz, H-6 of Glc), 3.20 (1H, overlapped, H-3 of Glc), 3.17 (1H, overlapped, H-5 of Glc), 3.13 (1H, overlapped, H-4 of Glc);  $^{13}\text{C}$  NMR (DMSO- $d_6$ , 125 MHz, 300 K)  $\delta$  181.9 (C-4), 163.4 (C-2), 163.4 (C-7), 161.2 (C-4'), 160.6 (C-5), 156.2 (C-9), 128.4 (C-2', 6'), 121.1 (C-1'), 115.9 (C-3', 5'), 108.9 (C-6), 103.3 (C-10), 102.7 (C-3), 93.6 (C-8), 81.5 (C-5 of Glc), 78.9 (C-3 of Glc), 73.0 (C-1 of Glc), 70.6 (C-4 of Glc), 70.2 (C-2 of Glc), 61.4 (C-6 of Glc); HRESIMS  $m/z$  433.1136  $[\text{M} + \text{H}]^+$  (calcd for  $\text{C}_{21}\text{H}_{21}\text{O}_{10}$ , 433.1135).

**3.3.7. Isosaponarin (7).** Yellow amorphous solid;  $[\alpha]_{\text{D}}^{25} -29$  (*c* 0.43, pyridine);  $^1\text{H}$  NMR (DMSO- $d_6$ , 500 MHz, 300 K)  $\delta$  13.49 (1H, brs, OH-5), 8.04 (2H, d,  $J=8.9$  Hz, H-2', 6'), 7.19 (2H, d,  $J=8.9$  Hz, H-3', 5'), 6.89 (1H, s, H-3), 6.55 (1H, s, H-8), 5.03 (1H, d,  $J=7.3$  Hz, H-1 of Glc at C-4'), 4.60 (1H, d,  $J=9.8$  Hz, H-1 of Glc at C-6), 4.04 (1H, dd,  $J=7.7, 9.8$  Hz, H-2 of Glc at C-6), 3.71 (1H, overlapped, H-6 of Glc at C-4'), 3.69 (1H, overlapped, H-6 of Glc at C-6), 3.48 (1H, m, H-6 of Glc at C-4'), 3.41 (1H, overlapped, H-6 of Glc at C-6), 3.40 (1H, overlapped, H-5 of Glc at C-4'), 3.32 (1H, overlapped, H-3 of Glc at C-4'), 3.30 (1H, overlapped, H-2 of Glc at C-4'), 3.20 (1H, overlapped, H-3 of Glc at C-6), 3.19 (1H, overlapped, H-4 of Glc at C-4'), 3.18 (1H, overlapped, H-5 of Glc at C-6), 3.14 (1H, overlapped, H-4 of Glc at C-6);  $^{13}\text{C}$  NMR (DMSO- $d_6$ , 125 MHz, 300 K)  $\delta$  182.0 (C-4), 163.4 (C-7), 162.9 (C-2), 160.7 (C-5), 160.3 (C-4'), 156.3 (C-9), 128.2 (C-2', 6'), 123.9 (C-1'), 116.6 (C-3', 5'), 109.0 (C-6), 103.8 (C-3), 103.5 (C-10), 99.9 (C-1 of Glc at C-4'), 93.8 (C-8), 81.6 (C-5 of Glc at C-6), 78.9 (C-3 of Glc at C-6), 77.2 (C-5 of Glc at C-4'), 76.6 (C-3 of Glc at C-4'), 73.2 (C-2 of Glc at C-4'), 73.1 (C-1 of Glc at C-6), 70.6 (C-4 of Glc at C-6), 70.2 (C-2 of Glc at C-6), 69.7 (C-4 of Glc at C-4'), 61.5 (C-6 of Glc at C-6), 60.7 (C-6 of Glc at C-4'); HRESIMS  $m/z$  595.1660  $[\text{M} + \text{H}]^+$  (calcd for  $\text{C}_{27}\text{H}_{31}\text{O}_{15}$ , 595.1663).

### 3.4. Hydrolysis of compounds 1–5

**3.4.1. Enzymatic hydrolysis of compound 1.** Compound 1 (10.0 mg) was treated with  $\beta$ -glucosidase (7.4 mg) in HOAc/NaOAc buffer (pH 5.0, 3.0 mL) at 37 °C for 24 h. The crude hydrolysate was chromatographed on Diaion HP-20 eluting sequentially with  $\text{H}_2\text{O}$  and MeOH. The MeOH eluate was purified by HPLC with  $\text{CH}_3\text{CN}/\text{H}_2\text{O}$  (25:75) to give a product (7.0 mg), which was identified as **2** by comparison of their  $^1\text{H}$  NMR and mass spectra.

**3.4.2. Alkaline hydrolysis of compound 1.** Compound 1 (8.4 mg) was treated with 2 M KOH (0.15 mL) in MeOH (0.5 mL) at room temperature for 30 min. After neutralization with 2 M HCl, the solution was extracted three times with THF. The combined extracts were washed with brine, dried over  $\text{Na}_2\text{SO}_4$ , and evaporated. The residue was purified by HPLC with  $\text{CH}_3\text{CN}/\text{H}_2\text{O}$  (25:75) to give a product (3.5 mg), which was identified as isosaponarin (**7**) by comparison of their  $^1\text{H}$ ,  $^{13}\text{C}$  NMR and mass spectra.

**3.4.3. Alkaline hydrolysis of compound 2.** Compound 2 (10.0 mg) was treated with 2 M KOH in the same manner described above and purified by HPLC with  $\text{MeOH}/\text{H}_2\text{O}$  (30:70) to give a product (6.5 mg), which was shown to be identical to isovitexin (**6**) by comparison of their  $^1\text{H}$ ,  $^{13}\text{C}$  NMR and mass spectra.

**3.4.4. Alkaline hydrolysis of compound 3.** Compound 3 (1.7 mg) was treated with 2 M KOH in the same manner as described above and purified by HPLC with  $\text{MeOH}/\text{H}_2\text{O}$  (20:80) to give a product (0.5 mg), which was shown to be identical to isosaponarin (**7**) by comparison of their  $^1\text{H}$  NMR and mass spectra.

**3.4.5. Hydrolysis of compound 4 and identification of the sugar component and degradation product.** Compound 4 (5.1 mg) was treated with 2 M KOH in the same manner as described above, and the product was dissolved in 2 M HCl (2 mL) and heated at 100 °C for 3 h. After cooling, the mixture was passed through a short Amberlite IRA-400 column and then a short Diaion HP-20 column eluting sequentially with  $\text{H}_2\text{O}$  and MeOH. Each eluate was evaporated to dryness. The  $\text{H}_2\text{O}$  fraction was dissolved in  $\text{MeOH}/\text{H}_2\text{O}$  (20:80), passed through a Sep-Pak C18 cartridge, and analyzed by HPLC using  $\text{CH}_3\text{CN}/\text{H}_2\text{O}$  (15:85). The sugar component was identified as *D*-glucose by the retention time,  $t_{\text{R}}$  14.8 min, and the sign (positive) of the optical rotation. The MeOH fraction was analyzed by HPLC (with a solvent system of 20–80% MeOH gradient) to identify **6** ( $t_{\text{R}}$  7.28 min).

**3.4.6. Hydrolysis of compound 5 and identification of the sugar component and degradation product.** Compound 5 (5.4 mg) was treated with 2 M KOH and then neutralized with 2 M HCl in the same manner as described above. The mixture was chromatographed on Diaion HP-20 eluting sequentially with  $\text{H}_2\text{O}$  and MeOH. The MeOH elute was treated with  $\beta$ -glucosidase (5.0 mg) in HOAc/NaOAc buffer (pH 5.0, 3.0 mL) at 37 °C for 24 h. The crude hydrolysate was chromatographed on Diaion HP-20 eluting sequentially with  $\text{H}_2\text{O}$  and MeOH. The MeOH elute was purified by HPLC with  $\text{CH}_3\text{CN}/\text{H}_2\text{O}$  (17:83) to give a product (5.1 mg), which was dissolved in 2 M HCl and heated at 100 °C for 3 h. The hydrolysate was passed through a short Amberlite IRA-400 column, and the eluted fraction was chromatographed on Diaion HP-20 eluting sequentially with  $\text{H}_2\text{O}$  and MeOH. The MeOH fraction was identified as isovitexin (**6**) by HPLC analysis and the  $\text{H}_2\text{O}$  extract as *D*-glucose by HPLC retention time,  $t_{\text{R}}$  14.8, and the sign (positive) of the optical rotation.

### 3.5. Superoxide radical anion scavenging activity

**3.5.1. Chemicals.** Diethylenetriaminepentaacetic acid (DETAPAC) and phosphate buffer powder were purchased from Wako Pure Chemical Industries (Osaka, Japan). The trapping agent, 5,5-dimethyl-1-pyrroline *N*-oxide (DMPO) was purchased from Dojin Chemical (Kumamoto, Japan), and hypoxanthine (HPX) was purchased from Sigma-Aldrich. Xanthine oxidase (XOD) from Roche (IN, U.S.A.) was used for active oxygen generation.

**3.5.2. General procedure.** ESR spectra were recorded on



a JEOL JES-FR30 spectrometer. The conditions of the ESR measurements were as follows: magnetic field:  $335.5 \pm 5$  mT; power: 4 mW, 9.4 GHz; sweep time: 1 min; modulation: 100 kHz; Mod. Wid.: 0.1 mT; amplitude: 160; time constant: 0.1 s; temperature: 293 K.

**3.5.3. ESR spin-trapping for measuring  $O_2^-$  scavenging activity.** The HPX-XOD reaction system was used for the evaluation of the superoxide anion radical scavenging activity. First, 35  $\mu$ L of 5.5 mmol/L DETAPAC, 15  $\mu$ L of 9.2 mmol/L DMPO, 50  $\mu$ L of 2 mmol/L HPX, and 50  $\mu$ L of the each compound were mixed in a test tube. The mixture was transferred to the ESR spectrometry cell and the DMPO- $O_2^-$  spin-adduct was quantified for 45 s after the addition of 50  $\mu$ L of 0.4 unit/mL XOD from cow's milk. The signal intensities were evaluated in terms of the peak height of the first signal of the DMPO- $O_2^-$  spin-adduct.

#### Acknowledgements

The authors are grateful to Drs. Kinzo Watanabe and Yukio

Hitotsuyanagi (Tokyo University of Pharmacy and Life Science) for their helpful suggestions.

#### References and notes

1. Kojima, M.; Uchida, M.; Akahori, Y. *Yakugaku Zasshi* **1973**, *93*, 453–459.
2. (a) Agrawal, P. K. Carbon 13 NMR of flavonoids; Elsevier: Amsterdam, 1989. (b) Harborne, J. B. The flavonoids In *Advances in research since 1986*; Chapman & Hall: New York, 1994.
3. Ramarathnam, N.; Osawa, T.; Namiki, M.; Kawakishi, S. *J. Agric. Food Chem.* **1999**, *37*, 316–319.
4. Sherwood, R. T.; Kroschewsky, J. R. *Phytochemistry* **1973**, *12*, 2275–22788.
5. Nawwar, M. A. M.; El-Mousallamy, A. M. D.; Barakat, H. H.; Buddrus, J.; Linscheid, M. *Phytochemistry* **1989**, *28*, 3201–3206.
6. Mun'im, A.; Negishi, O.; Ozawa, T. *Biosci. Biotechnol. Biochem.* **2003**, *67*, 410–414.
7. Bikbulatova, T. N.; Korul'kina, L. M. *Chem. Nat. Compd.* **2001**, *37*, 216–218.

# Structural analyses of 4-benzoylpyridine thiosemicarbazone using NMR techniques and theoretical calculations

Ana Mena Barreto Bastos, Antônio F. de Carvalho Alcântara\* and Heloisa Beraldo\*

Departamento de Química, ICEx, Universidade Federal de Minas Gerais, Av. Pres. Antônio Carlos, 6627, 31270-901 Belo Horizonte, MG, Brazil

Received 16 November 2004; revised 12 April 2005; accepted 14 April 2005

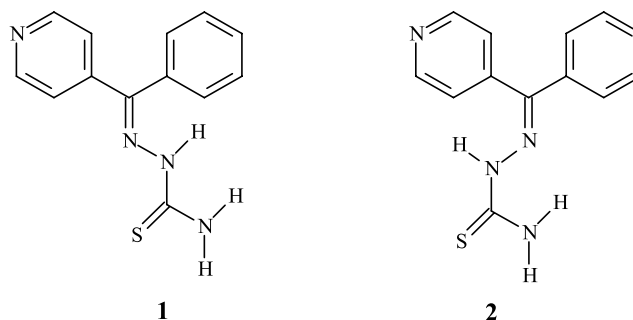
**Abstract**—The reaction of 4-benzoylpyridine and thiosemicarbazide gave at least two products, characterized by  $^1\text{H}$ ,  $^{13}\text{C}$  and 2D NMR experiments as *E*- and *Z*-4-benzoylpyridine thiosemicarbazone. Conformational distribution of *E*-4-benzoylpyridine thiosemicarbazone was carried out by means of the PM3 method, and geometry optimization using the Density Functional Theory (DFT), with consideration of solvent effects by PCM. The results indicated that the conformation of lowest energy is the same as that obtained in the solid, as confirmed by X-ray crystal structure determinations. A similar procedure used to determine the conformational distribution of *Z*-4-benzoylpyridine thiosemicarbazone suggested the existence of a dimer formed by intermolecular hydrogen bonds in the gas phase as well as in solution, which is in accordance with NOESY correlations.

© 2005 Elsevier Ltd. All rights reserved.

## 1. Introduction

Thiosemicarbazones are a class of interesting compounds presenting a wide range of pharmacological applications as antitumoral, antimicrobial and antiviral agents.<sup>1</sup>  $\alpha(\text{N})$ -Heterocyclic thiosemicarbazones have been extensively investigated by other authors<sup>2</sup> and by our group.<sup>3</sup> Much less attention has been given to the  $\beta$  and  $\gamma(\text{N})$ -heterocyclic analogues. In previous works, we investigated 3- and 4-formylpyridine thiosemicarbazone and 3- and 4-acetylpyridine thiosemicarbazone as well as their platinum(II) complexes.<sup>4</sup>

More recently, we started a study of 4-benzoylpyridine-derived thiosemicarbazones. The structural and spectral characteristics of 4-benzoylpyridine thiosemicarbazone (H4BzDH) and its N(4)-phenyl derivative (H4Bz4Ph) were determined.<sup>5</sup> In that study, reaction between 4-benzoylpyridine and thiosemicarbazide using concentrated hydrochloric acid as catalyst gave *E*-4-benzoylpyridine thiosemicarbazone **1** (Fig. 1), as shown by X-ray diffraction studies,<sup>5</sup> indicating stereo selectivity. Spectral analyses of the product did not reveal the presence of the *Z*-isomer (**2**, Fig. 1).

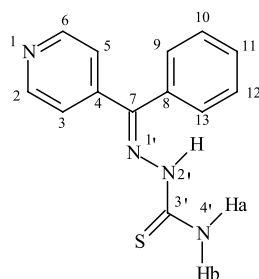


**Figure 1.** *E* (**1**) and *Z* (**2**) conformers of 4-benzoylpyridine thiosemicarbazone.

Due to the low yield obtained (23%),<sup>5</sup> a second procedure was tried in the present work, to prepare H4Bz4DH starting with the same reagents but using boron trifluoride etherate ( $\text{BF}_3/\text{OEt}_2$ ) as catalyst instead of concentrated HCl. Microanalyses of the product (mp 218.7–220.9 °C) gave C: 60.50%; H: 4.52%; N: 22.50%, close to the calculated values for (**1**): C: 60.94%; H: 4.69%; N: 21.88%. However, the  $^1\text{H}$  and  $^{13}\text{C}$  NMR spectra of the product revealed the presence of at least two species. In order to explain these results, theoretical studies of the structures evidenced by  $^1\text{H}$  and  $^{13}\text{C}$  as well as the HMQC, HMBC, COSY and NOESY NMR correlation techniques were carried out. Geometry optimization was performed using the PM3 semi-empirical and the Density Functional Theory (DFT) methods, as

**Keywords:** 4-Benzoylpyridine thiosemicarbazones; Structural analyses by NMR; Density functional theory.

\* Corresponding authors. Tel.: +55 31 3499 5728; fax: +55 31 3499 5700 (A.F.d.C.A.); tel.: +55 31 3499 5740; fax: +55 31 3499 5700 (H.B.); e-mail addresses: aalcantara@zeus.qui.ufmg.br; hberaldo@ufmg.br

**Table 1.**  $^1\text{H}$  (400 MHz) and  $^{13}\text{C}$  (100 MHz) NMR data (including HMQC, HMBC, COSY and NOESY correlations) of *E*-benzoylpyridine thiosemicarbazone in  $\text{DMSO-}d_6$  using TMS as internal standard

Atom	HMQC		HMBC		COSY		NOESY
	$\delta_{\text{C}}$	$\delta_{\text{H}}$ (multiplicity)	$^2J_{\text{C,H}}$	$^3J_{\text{C,H}}$	$^3J_{\text{H,H}}$	$^4J_{\text{H,H}}$	
2/6	145.59	8.71 (d, $J=5.6$ Hz)	7.92		7.92		7.92
3/5	122.64	7.92 (d, $J=5.6$ Hz)	8.71		8.71		7.41; 8.71
4	148.13			8.71			
7	144.71			7.92; 7.41			
8	129.29		7.41	7.67			
9/13	128.48	7.41 (m)	7.67	7.62	7.67	7.62	7.67; 7.92; 8.94
10/12	130.05	7.67 (m)	7.62		7.41; 7.62		7.41; 7.62
11	127.40	7.62 (m)	7.67	7.41	7.67	7.41	7.67
2'		8.69					8.90
3'	178.61		8.94				
4'		Ha 8.90 (l) Hb 8.94 (l)					8.69; 8.94 7.41; 8.90

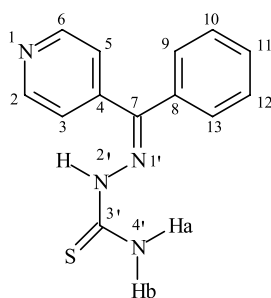
reported in previous works, by some of us on pyridine-derived compounds.<sup>6</sup>

## 2. Methodology

H4Bz4DH was prepared by refluxing a solution containing 0.02 mmol of 4-benzoylpyridine in dichloromethane and 1.34 mL of  $\text{BF}_3/\text{OEt}_2$ . Thiosemicarbazide (0.02 mmol) was

added to the reaction mixture. After 8 h under reflux the mixture was washed with a  $\text{NaHCO}_3$  solution. The organic phase was concentrated and the yellow solid was washed with ethanol and ether (yield 80.5%). Infrared and electronic spectral data of the product were previously described.<sup>5</sup> The NMR data are listed in Tables 1 and 2.

$^1\text{H}$  and  $^{13}\text{C}$  NMR spectra, and HMQC, HMBC, COSY and NOESY contour maps were recorded on a Bruker DRX 400

**Table 2.**  $^1\text{H}$  NMR (400 MHz) and  $^{13}\text{C}$  NMR data (including HMQC, HMBC, COSY and NOESY correlations) of *Z*-benzoylpyridine thiosemicarbazone in  $\text{DMSO-}d_6$  and TMS as internal standard

Atom	HMQC		HMBC		COSY		NOESY
	$\delta_{\text{C}}$	$\delta_{\text{H}}$ (multiplicity)	$^2J_{\text{C,H}}$	$^3J_{\text{C,H}}$	$^3J_{\text{H,H}}$	$^4J_{\text{HS,H}}$	
2/6	148.38	8.92 (d, $J=6.2$ Hz)	7.60		7.60		7.60; 9.54
3/5	124.90	7.60 (d, $J=6.2$ Hz)	8.92		8.92		8.92; 9.54
4	143.05		7.60	8.92			
7	145.20						
8	135.36	7.41					
9/13	128.43	7.41 (m)	7.69	7.64	7.69	7.64	7.69
10/12	130.52	7.69	7.41; 7.64		7.41; 7.64		7.41; 7.64
11	129.90	7.64 (m)	7.69		7.69	7.41	7.69
2'		9.54					7.60; 8.92
3'	178.86		9.54				
4'		Ha 8.30 Hb 8.54					8.54 8.30

AVANCE, in DMSO- $d_6$ , without sample degasification. The chemical shifts were recorded in ppm ( $\delta$  units) in relation to TMS as internal standard. Pulse conditions were as follows: for  $^1\text{H}$  NMR, dwell time (DW) 149.600  $\mu\text{s}$ , acquisition time (AQ) 3.985 s, number of transients (NS) 16, recycle delay (RD) 1.000 s; for  $^{13}\text{C}$  NMR spectra, DW 31.400  $\mu\text{s}$ , AQ 2.058 s, NS 1024, RD 2.000 s, decoupling multiple resonance method Waltz-16; for the NOESY contour maps, DW 178.800  $\mu\text{s}$ , AQ 0.366 s, NS 16, RD 2.000 s, missing time 200 ms, time evolution 3  $\mu\text{s}$ , TD 2048 ( $F_2$ ) and 1024 ( $F_1$ ); for HMBC contour maps, DW 357.600  $\mu\text{s}$ , AQ 0.366 s, NS 16, RD 2.000 s, missing time 500 ms, TD 1024 ( $F_2$ ) and 512 ( $F_1$ ); for HMQC contour maps, DW 121.600  $\mu\text{s}$ , AQ 0.125 s, NS 8, RD 2.000 s, missing time 500 ms, TD 1024 ( $F_2$ ) and 512 ( $F_1$ ); and for COSY, DW 357.600  $\mu\text{s}$ , AQ 0.732 s, NS 1, RD 2.000 s, TD 1024 ( $F_2$ ) and 512 ( $F_1$ ).

Theoretical studies were carried out using the software packages TITAN<sup>7</sup> and GAUSSIAN03.<sup>8</sup> Spatial arrangements determined through NOESY experiments were used as initial models for geometry optimization calculations using the semi-empirical PM3 method<sup>9</sup> in the gaseous state. The same calculation conditions were used for conformational search of dimer structures. Geometry optimizations of the dimer structures were performed starting with the optimized structures of the monomers, with freezing of appropriate intermolecular distances (50 possible intermolecular distances were tried). Geometries obtained by the PM3 method were again optimized using the Density Functional Theory (DFT)<sup>10</sup> method with BLYP functionals<sup>11</sup> using a 6-31G\*<sup>12</sup> basis set (DFT/BLYP/6-31G\*). All structures obtained by theoretical calculations were characterized as true energy minima in PES through frequency calculations (when the frequencies are real, it corresponds to a minimum).

Solvent effects were included by re-optimizing HF/3-21G\* structures using HF/6-31G\*\* level within the Polarizable Continuum Model (PCM).<sup>13</sup> In these cases, electronic-nuclear,  $E_{\text{ele-nuc}}$  (hartree) and solvation energies,  $E_{\text{solv}}$  (kcal/mol) were obtained.

### 3. Results and discussion

Figure 2 presents the  $^1\text{H}$  and  $^{13}\text{C}$  NMR spectra of the product obtained in the reaction of 4-benzoylpyridine and thiosemicarbazide with  $\text{BF}_3/\text{OEt}_2$  as catalyst. The number of signals suggests the presence of at least two different structures. The NMR spectra remain unchanged for several months at 20 °C in different solvents. Table 1 lists the  $^1\text{H}$ ,  $^{13}\text{C}$ , HMQC, HMBC, COSY and NOESY data of the main species. The NOESY data show correlation of H-4' $b$  ( $\delta_{\text{H}}$  8.94) and H-9/13 ( $\delta_{\text{H}}$  7.41), indicating the proximity the phenyl hydrogens and the hydrogens from the thiosemicarbazone moiety, characteristic of 4-benzoylpyridine thiosemicarbazone in the *E*-configuration (**1**).

Conformational distribution of **1** in the gaseous state using semi-empirical calculations (PM3) was carried out with geometry optimization of the conformers. Figure 3 shows the five conformers of **1** of lowest energies: **1-I**, **1-II**, **1-III**,

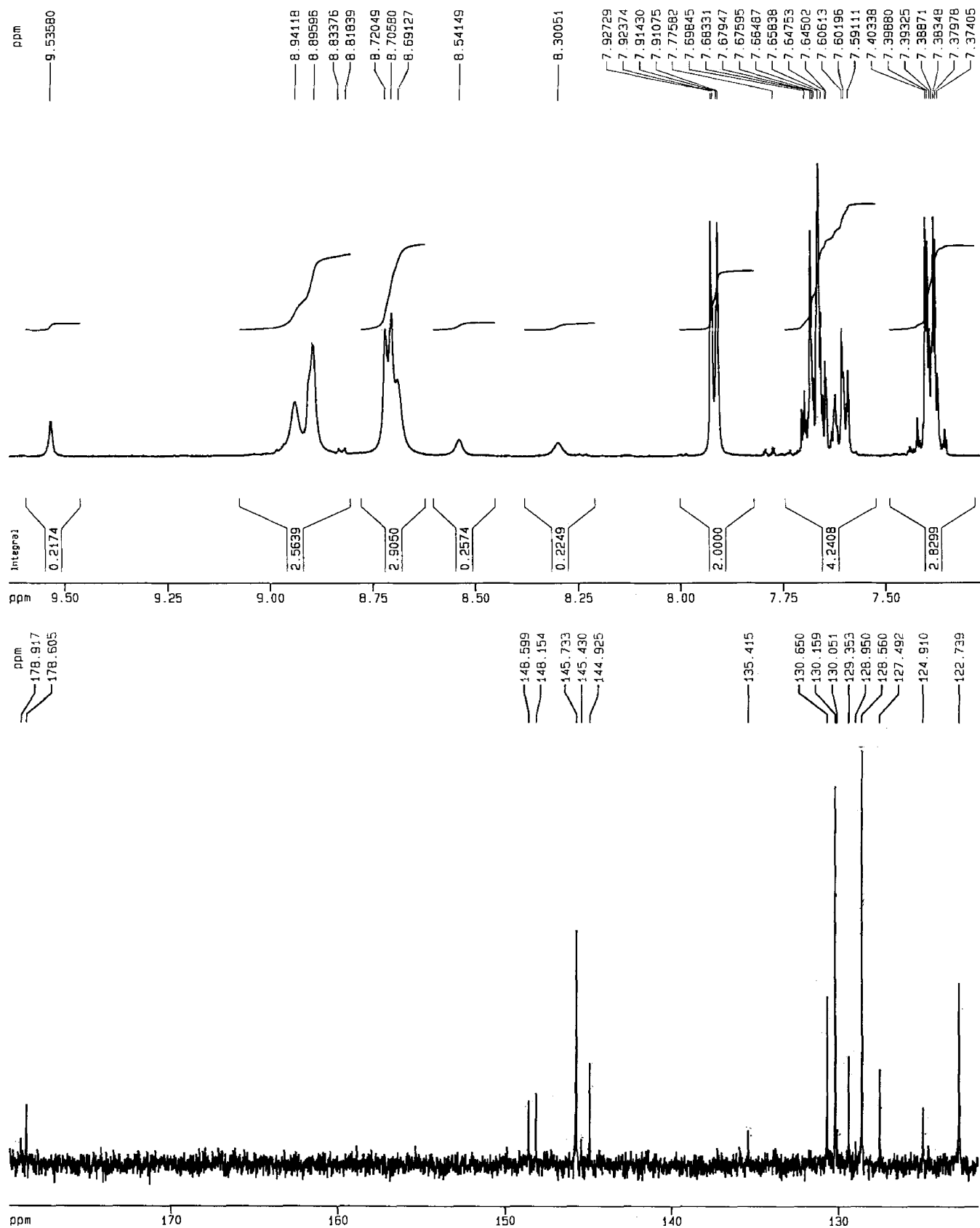
**1-IV** and **1-V** ( $\Delta H_{\text{f}}$ =118.04, 122.14, 122.14, 122.59 and 127.55 kcal/mol, respectively). Re-optimizations of these structures by means of the HF/3-21G\*, HF/6-31G\*, DFT/BLYP/6-31G\* and DFT/B3LYP/6-31G\* methods were in perfect agreement with the results obtained by PM3. In all conformations the angle between the planes of the thiosemicarbazone and the pyridine ring is smaller (and hence, electronic delocalization is facilitated) than that between the thiosemicarbazone plane and the benzene ring, as shown by the crystal structure of *E*-4-benzoylpyridine thiosemicarbazone.<sup>5</sup>

Since, the geometry optimization was performed for the gaseous state, the effect of DMSO- $d_6$  used as solvent for the NMR experiments was considered for the conformational analyses of **1**. DFT/BLYP/6-31G\* calculations with the PCM method were employed for the geometry optimization of conformers **1-I** to **1-V**. The results indicate a lowering of the energy of **1-I** to **1-V** upon solvation, with solvation enthalpy  $\Delta H_{\text{SE}}$ =−8.19, −9.53, −9.57, −9.57 and −10.13 kcal/mol, respectively. These results suggest that in DMSO the populations of **1-I** to **1-IV** in the conformational distribution of **1** are significant. Although, X-ray diffraction data of **1** confirm the presence of only **1-I** in the solid,<sup>5</sup> the NOESY correlations in DMSO- $d_6$  are compatible with the existence of **1-II**, **1-III** and **1-IV**, indicating the presence of these conformers along with the lowest energy conformer **1-I**.

According to the literature reactions of aldehydes with amines lead to the formation of *E*-isomers,<sup>14</sup> but the formation of the corresponding *Z*-isomers has been observed under certain experimental conditions.<sup>15</sup> Therefore, formation of *Z*-4-benzoylpyridine thiosemicarbazone (**2**), with less intense hydrogen and carbon signals in the NMR spectra as the secondary product of the syntheses was considered. Table 2 lists the  $^1\text{H}$ ,  $^{13}\text{C}$ , HMQC, HMBC, COSY and NOESY data for **2**. NOESY correlations were observed for H-2' ( $\delta_{\text{H}}$  9.54) and H-3/5 ( $\delta_{\text{H}}$  7.60), indicating the proximity of the pyridine and thiosemicarbazone hydrogens, characteristic of the *Z*-isomer.

Semi-empirical calculations (PM3) of conformational distribution of **2** in the gaseous state were carried out with geometry optimization of the conformers. Figure 4 presents the five conformers of **2**, **2-I** to **2-V** with the smallest calculated enthalpies,  $\Delta H_{\text{f}}$ =118.48, 122.70, 127.91, 128.07 and 128.17 kcal/mol, respectively. Re-optimizations of these structures by means of the HF/3-21G\*, HF/6-31G\*, DFT/BLYP/6-31G\* and DFT/B3LYP/6-31G\* methods were in perfect agreement with the results obtained by PM3, confirming **2-I** as the lowest energy isomer.

Although, the literature reports higher stability for *E*-isomers than for the corresponding *Z*-forms,<sup>16</sup> the calculated enthalpy values of **2** are not very different from those of **1**. In the case of 4-benzoylpyridine thiosemicarbazones, which presents a cetimine structure, the pyridine and phenyl substituents exhibit similar van der Waals repulsion effects on the imine group. Therefore, steric effects of the aromatic rings have no influence on the relative stabilities of **1** and **2**, and the differences in energies are probably due to electronic effects. In all conformations



**Figure 2.** <sup>1</sup>H and <sup>13</sup>C NMR spectra (DMSO-*d*<sub>6</sub>) of the product of reaction between 4-benzoylpyridine and thiosemicarbazide using BF<sub>3</sub>/OEt<sub>2</sub> as catalyst.

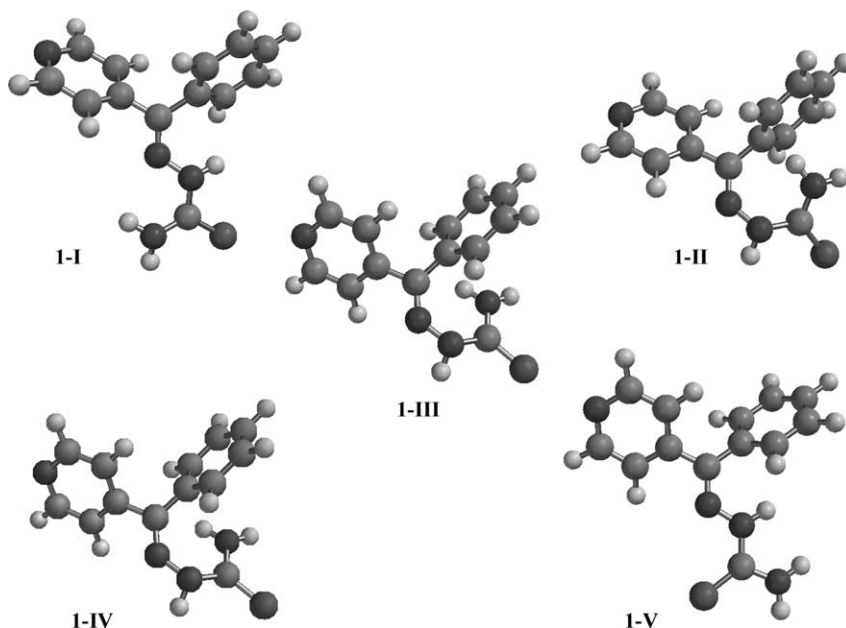


Figure 3. Conformers of **1** obtained by geometry optimization (DFT/BLYP/6-31G\*).

of **2** the angle between the planes of the thiosemicarbazone and the benzene ring is smaller (and hence, electronic delocalization is facilitated) than that between the thiosemicarbazone plane and the pyridine ring.

As in the previous case, the effect of DMSO- $d_6$  used as solvent for the NMR experiments was considered for the conformational analyses of **2**. DFT/BLYP/6-31G\* calculations were employed for the geometry optimization of conformers **2-I** to **2-V** and the obtained geometries were optimized considering the solvent (DMSO) effects by the PCM method. The lowering of the formation enthalpies of **2-I** to **2-V** upon solvation were  $\Delta H_{SE} = -8.22$ ,  $-9.44$ ,  $-10.11$ ,  $-11.74$ , and  $-11.70$  kcal/mol. Therefore, theoretical calculations suggest that *Z*-4-benzoylpyridine

thiosemicarbazone adopts conformation **2-I**. These results are in agreement with the observed NOESY correlations for **2** (Table 2).

Comparison of the data of Tables 1 and 2, shows that the chemical shifts of the atoms in positions 2/6 of **2** ( $\delta_{C-2/6}$  148.38 and  $\delta_{H-2/6}$  8.92) are appreciably different from those of the corresponding atoms of **1** ( $\delta_{C-2/6}$  145.59 and  $\delta_{H-2/6}$  8.71). The same effect is observable for the chemical shifts of the atoms at positions 3/5 of **2** ( $\delta_{C-3/5}$  124.90 and  $\delta_{H-3/5}$  7.60) relative to those of the corresponding atoms of **1** ( $\delta_{C-3/5}$  122.64 and  $\delta_{H-3/5}$  7.92), and the chemical shift of the carbon at position 4 of **2** ( $\delta_{C-4}$  143.05) relative to the same carbon of **1** ( $\delta_{C-4}$  148.13). However, the chemical shifts of the phenyl group are not very different in **1** and **2**, indicating that the

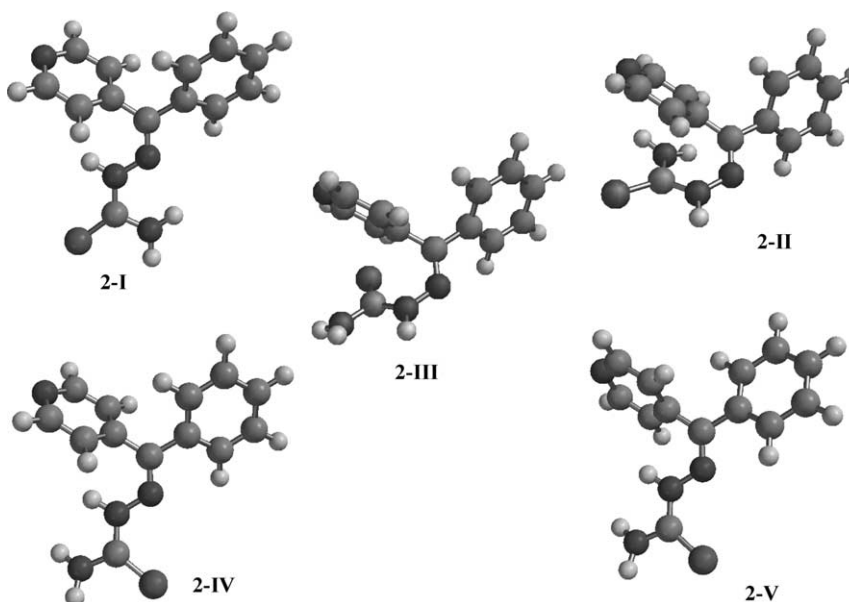
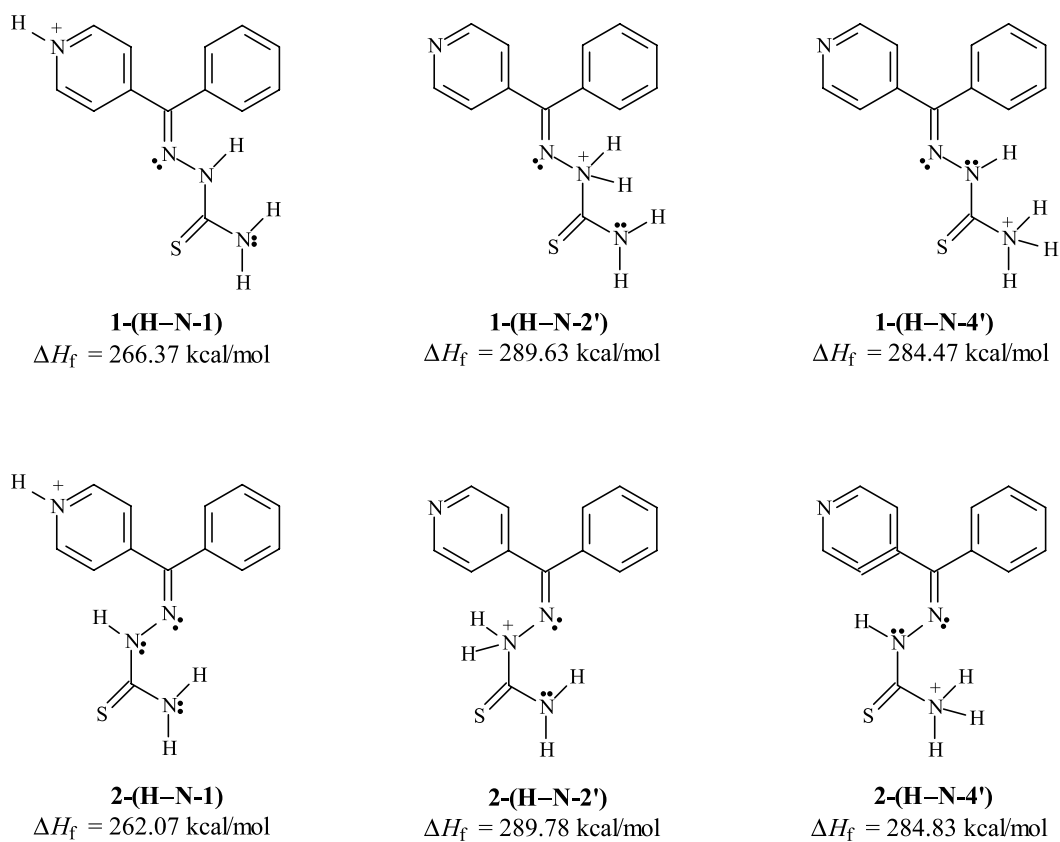
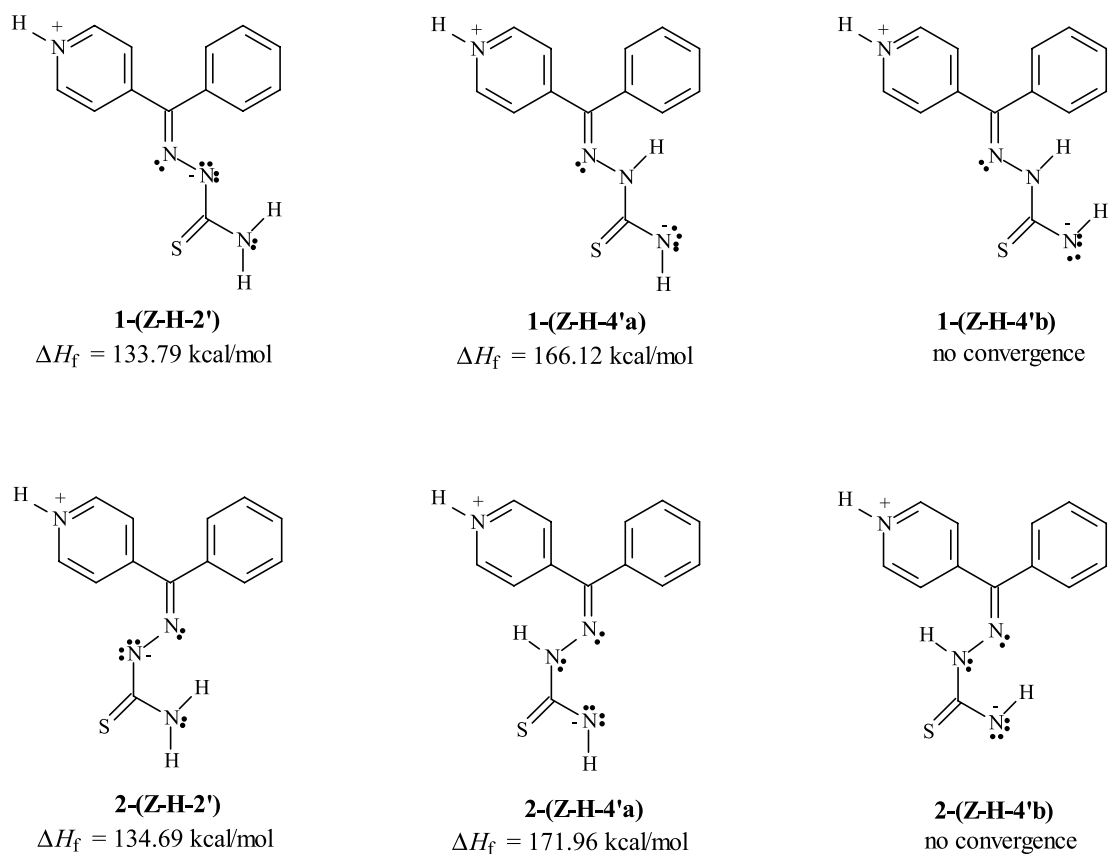


Figure 4. Conformers of **2** obtained by geometry optimization (DFT/BLYP/6-31G\*).





**Figure 5.** Calculated (PM3) formation enthalpies ( $\Delta H_f$ ) of cationic structures obtained upon protonation of **1** and **2**.



**Figure 6.** Calculated (PM3) formation enthalpies ( $\Delta H_f$ ) of zwitterions of **1** and **2**.

most significant structural differences between these conformers occur in the pyridine ring and in the thiosemicarbazone group.

The chemical shift of H-2' in **2** ( $\delta_{\text{H-2}'}$  9.54) is significantly higher than that of the corresponding signal of **1** ( $\delta_{\text{H-2}'}$  8.69), see Tables 1 and 2, and could be attributed to a hydrogen attached to a positively charged nitrogen. Therefore, PM3 calculations of geometry optimization were performed for cationic structures of **1** and **2** considering protonation of N-1, N-2' or N-4', **1-(H-N-1)**, **1-(H-N-2')**, **1-(H-N-4')** and **2-(H-N-1)**, **2-(H-N-2')** and **2-(H-N-4')**, respectively. Figure 5 shows the calculated formation enthalpies  $\Delta H_f$  for the cationic structures. In both isomers the structure protonated at N-1, **1-(H-N-1)** and **2-(H-N-1)**, presents the lowest enthalpy of formation, in accordance with X-ray crystal diffraction data.<sup>5</sup> The lower energy of **2-(H-N-1)**,  $\Delta H_f = 262.07$  kcal/mol, relative to **1-(H-N-1)**,  $\Delta H_f = 266.37$  kcal/mol, suggests higher basicity of N-1 in **2**.

Taking into consideration that the integration curves of the <sup>1</sup>H NMR spectra indicate only three acidic hydrogens (H-2', H-4'a and H-4'b) and that the structures of Figure 5 present five acidic hydrogens we suggest that the spectra of Figure 2 are not attributable to these protonated species. PM3 calculations of geometry optimization were carried out for zwitterionic structures of **1** and **2**, by transferring to N-1 the hydrogens H-2', H-4'a or H-4'b, **1-(Z-H-2')**, **1-(Z-H4'a)** and **1-(Z-H-4'b)**, respectively and **2-(Z-H-2')**, **2-(Z-H4'a)** and **2-(Z-H-4'b)**, respectively. Figure 6 presents the calculated formation enthalpies  $\Delta H_f$  for the optimized zwitterion structures of **1** and **2**. The geometry optimization for **1-(Z-H-4'b)** and **2-(Z-H-4'b)** did not lead to convergence to a minimum of energy, indicating low probability of existence of these zwitterionic structures. The other zwitterionic structures **1-(Z-H-2')** and **2-(Z-H-2')** could exist, presenting significantly lower enthalpies of formation than **1-(Z-H-4'a)** and **2-(Z-H-4'b)**. The foregoing results indicate an amphoteric character for **1** and **2** with a basic site at N-1 and an acidic site at H-2'–N-2'. NOESY correlations were only observed between H-2/6 and H-2' of **2** at  $\delta_{\text{H-2}'}$  8.92 and 9.54, respectively (see Table 2). However, the theoretical calculations discard intra-molecular interaction between H-2/6 and H-2' as well as N-1 and

H-2'. Therefore, these interactions probably occur between two different molecules of **2**.

Although, no NOESY correlations were observed between H-2/6 and H-2' of **1** the X-ray diffraction structure revealed two molecules of (**1**) connected by one HCl and one water molecule.<sup>4</sup> Therefore, PM3 calculations were performed for geometry optimization of dimer structures containing two units (A and B) of **1**, in the **1-I** conformation, taking into consideration intermolecular interactions involving N-1(A)···H-2'(B) and N-1(B)···H-2'(A), in the so called **1-(N-1-H-2')** dimer. The calculated enthalpy for **1-(N-1-H-2')** was  $\Delta H_f = 254.51$  kcal/mol, which is more than twice the value of enthalpy for the corresponding monomer ( $\Delta H_f = 118.04$  kcal/mol). These results indicate that **1** exists in the unassociated form.

Similarly, PM3 calculations were performed for geometry optimization of dimer structures containing two units (A and B) of **2**, with N-1(A)···H-2'(B) and N-1(B)···H-2'(A) interactions, in the so called **2-(N-1-H-2', H-4'b)** dimer.

Figure 7 presents the structures of the two dimers of **2**, after geometry optimization. The calculated enthalpy of **2-(N-1-H-2')**,  $\Delta H_f = 232.21$  kcal/mol is significantly lower than the enthalpy for **2-(N-1-H-2', H-4'b)**,  $\Delta H_f = 251.15$  kcal/mol. In addition, only the enthalpy of **2-(N-1-H-2')** is less than twice the value of the enthalpy of **2-I** ( $\Delta H_f = 118.48$  kcal/mol), suggesting that **2** exists predominantly as structure **2-(N-1-H-2')**, with  $C_{2v}$  symmetry. This symmetry of **2-(N-1-H-2')** leads to chemical identity of the corresponding atoms of each unit of **2** and therefore, identical <sup>1</sup>H and <sup>13</sup>C NMR spectra. Moreover, Figure 7 reveals that H-2' in **2-(N-1-H-2')** is in a more deshielded region of the pyridine ring than H-2' in conformer **1-I**. The deshielding effect leads to a higher frequency chemical shift for this hydrogen in **2** ( $\delta_{\text{H-2}'}$  9.54) than in **1** ( $\delta_{\text{H-2}'}$  8.69).

According to the literature structures containing  $\alpha$ -hydrogens to C-substituents of imino groups can allow inter-conversion of *E/Z* configuration<sup>17</sup> through formation of enamine intermediates.<sup>18</sup> Therefore, *E/Z* inter-conversion involving **1** and **2**, through this mechanism would not be expected since, both structures do not present C-imino-substituents containing

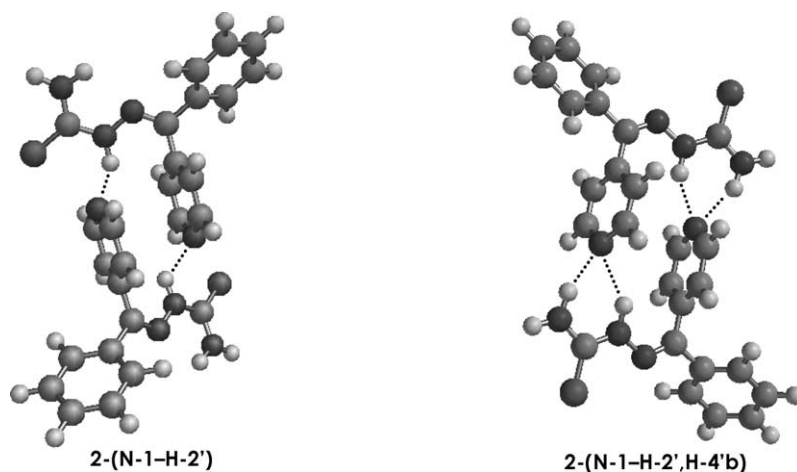


Figure 7. Calculated (PM3) dimeric structures of **2**: (a) **2-(N-1-H-2')**; (b) **2-(N-1-H-2', H-4'b)**.

$\alpha$ -hydrogens. For the product of the reaction between 4-benzoylpyridine and thiosemicarbazide (Fig. 2), the ratio between the integration curves of the  $^1\text{H}$  NMR signals (DMSO- $d_6$ , at 300 K) at  $\delta_{\text{H}}$  9.54 (attributed to H-2' of **2**) and  $\delta_{\text{H}}$  7.92 (attributed to H-3/5 of **1**) gives 18% of **2** and 82% of **1** (0.22:1.00). The signal attributed to H-2' of **2** decreases with increasing the temperature. At 351.0 K, the signal of H-2' is found at  $\delta_{\text{H}}$  9.00. Above 351 K, the spectra are too complicated to be interpreted. This effect of the temperature on the chemical shift of H-2' of **2** could be due to the conversion of the dimer to the monomer (**2-I**). However, since the literature reports *E/Z* isomerization for compounds with structures similar to that of 4-benzoylpyridine thiosemicarbazone,<sup>19</sup> *E/Z* inter-conversion cannot be discarded to explain the observed decrease in the signal of H-2' of **2**.

#### 4. Conclusions

The foregoing results showed that the reaction between 4-benzoylpyridine and thiosemicarbazide, using  $\text{BF}_3/\text{OEt}_2$  as catalyst gave *E*- and *Z*-4-benzoylpyridine thiosemicarbazone as indicated by NMR data. Theoretical studies based on NOESY correlations suggested that protonation is favored at the pyridine nitrogen (N-1) over protonation at the other two nitrogen sites. Moreover, N-1 protonation of the *Z*-isomer is thermodynamically favored in relation to N-1 protonation of the *E* analogue. NOESY experiments indicated correlations of H-2/6 of one molecule with H-2' of a second molecule exclusively for (*Z*)-4-benzoylpyridine thiosemicarbazone forming a dimeric structure. Theoretical calculations showed that only a dimer formed by hydrogen bonding between N-1 of one molecule and H-2' of a second molecule and vice-versa would be thermodynamically favored.

#### 5. Supplementary material

Tables with all optimized geometrical parameters and other results for all structures considered in the present work, are available from the authors upon request.

#### Acknowledgements

The authors thank the Conselho Nacional de Desenvolvimento Científico e Tecnológico (CNPq) and the Fundação Coordenação de Aperfeiçoamento de Pessoal de Nível Superior (CAPES) for financial support, and I. S. Lula and R. A. Machado for recording NMR spectra.

#### References and notes

- Beraldo, H.; Gambino, D. *Mini-Rev. Med. Chem.* **2004**, *4*, 31.
- (a) West, D. X.; Liberta, A. E.; Padhye, S. B.; Rajeev, R. C.; Sonawane, P. B.; Kumbhar, A. S.; Yerande, R. G. *Coord. Chem. Rev.* **1993**, *123*, 49. (b) Altun, A.; Kumru, M.; Dimoglo, A. *J. Mol. Struct. (Theochem)* **2001**, *535*, 235. (c) Cory, J. G.; Cory, A. H.; Rappa, G.; Lorico, A.; Liu, M.; Lin, T.; Sartorelli, A. C. *Biochem. Pharmacol.* **1994**, *48*, 335. (d) Liu, M. C.; Lin, T.; Cory, J. G.; Cory, A. H.; Sartorelli, A. C. *J. Med. Chem.* **1996**, *39*, 2586. (e) Finch, R. A.; Liu, M.; Grill, S. P.; Rose, W. C.; Loomis, R.; Vasquez, K. M.; Cheng, Y.; Sartorelli, A. C. *Biochem. Pharmacol.* **2000**, *59*, 983.
- (a) Beraldo, H.; Tosi, L. *Inorg. Chim. Acta* **1983**, *75*, 249. (b) Beraldo, H.; Tosi, L. *Inorg. Chim. Acta* **1986**, *125*, 173. (c) Abras, A.; Beraldo, H.; Fantini, E.; Borges, R. H.; Rocha, M. A.; Tosi, L. *Inorg. Chim. Acta* **1990**, *172*, 113. (d) Borges, R. H.; Paniago, E.; Beraldo, H. *J. Inorg. Biochem.* **1997**, *65*, 267. (e) Borges, R. H.; Abras, A.; Beraldo, H. *J. Braz. Chem. Soc.* **1997**, *8*, 33. (f) Perez-Rebolledo, A.; Lima, G. M.; Gambi, L. N.; Speziali, N. L.; Maia, D. F.; Pinheiro, C. B.; Ardisson, J. D.; Cortés, M. E.; Beraldo, H. *Appl. Organomet. Chem.* **2003**, *17*, 945.
- Mendes, I. M. C.; Teixeira, L. R.; Lima, R. L.; Carneiro, T. M.; Beraldo, H. *Transition Met. Chem.* **1999**, *24*, 665.
- Beraldo, H.; Barreto, A. M.; Vieira, R. P.; Rebolledo, A. P.; Speziali, N. L.; Pinheiro, C. B.; Chapuis, G. *J. Mol. Struct. (Theochem)* **2003**, *645*, 213.
- (a) Alcântara, A. F. C.; Veloso, D. P.; Stumpf, H. O.; Almeida, W. B. *Tetrahedron* **1997**, *53*, 16911. (b) Alcântara, A. F. C.; Santos, H. F.; Almeida, W. B.; Vaz, M. G. F.; Stumpf, H. O. *Struct. Chem.* **1999**, *10*, 367. (c) Alcântara, A. F. C.; Stumpf, H. O.; Vaz, M. G. F.; Pinheiro, L. M. M.; Golhen, S.; Ouahab, L.; Cador, O.; Mathonière, C.; Kan, O. *Chem. Eur. J.* **1999**, *5*, 1486. (d) Vaz, M. G. F.; Pedrosa, E. F.; Speziali, N. L.; Novak, M. A.; Alcântara, A. F. C.; Stumpf, H. O. *Inorg. Chim. Acta* **2001**, *326*, 65. (e) Vaz, M. G. F.; Knobel, M.; Speziali, N. L.; Moreira, A. M.; Alcântara, A. F. C.; Stumpf, H. O. *J. Braz. Chem. Soc.* **2002**, *13*, 183. (f) Alcântara, A. F. C.; Veloso, D. P.; Stumpf, H. O.; Vaz, M. G. F.; Almeida, W. B. *Helv. Chim. Acta* **2004**, *87*, 425.
- TITAN 1999: Wavefunction, Inc., Irvine CA & Schrödinger, Inc., Portland, 1999.
- Frisch, M. J.; Trucks, G. W.; Schlegel, H. B.; Scuseria, G. E.; Robb, M. A.; Cheeseman, J. R.; Montgomery, J. A., Jr.; Vreven, T.; Kudin, K. N.; Burant, J. C.; Millam, J. M.; Iyengar, S. S.; Tomasi, J.; Barone, V.; Mennucci, B.; Cossi, M.; Scalmani, G.; Rega, N.; Petersson, G. A.; Nakatsuji, H.; Hada, M.; Ehara, M.; Toyota, K.; Fukuda, R.; Hasegawa, J.; Ishida, M.; Nakajima, T.; Honda, Y.; Kitao, O.; Nakai, H.; Klene, M.; Li, X.; Knox, J. E.; Hratchian, H. P.; Cross, J. B.; Adamo, C.; Jaramillo, J.; Gomperts, R.; Stratmann, R. E.; Yazyev, O.; Austin, A. J.; Cammi, R.; Pomelli, C.; Ochterski, J. W.; Ayala, P. Y.; Morokuma, K.; Voth, G. A.; Salvador, P.; Dannenberg, J. J.; Zakrzewski, V. G.; Dapprich, S.; Daniels, A. D.; Strain, M. C.; Farkas, O.; Malick, D. K.; Rabuck, A. D.; Raghavachari, K.; Foresman, J. B.; Ortiz, J. V.; Cui, Q.; Baboul, A. G.; Clifford, S.; Cioslowski, J.; Stefanov, B. B.; Liu, G.; Liashenko, A.; Piskorz, P.; Komaromi, I.; Martin, R. L.; Fox, D. J.; Keith, T.; Al-Laham, M. A.; Peng, C. Y.; Nanayakkara, A.; Challacombe, M.; Gill, P. M. W.; Johnson, B.; Chen, W.; Wong, M. W.; Gonzalez, C.; Pople, J. A. Gaussian 03, Revision B.04, Gaussian Inc.: Pittsburgh PA, 2003.
- Dewar, M. J. S.; Zoebish, E. G.; Healy, E. F.; Stewart, J. J. P. *J. Am. Chem. Soc.* **1985**, *107*, 902.
- Parr, R. G.; Yang, W. *Density Functional Theory of Atoms and Molecules*; Oxford: New York, 1989.
- (a) Becke, A. D. *Phys. Rev. A* **1988**, *38*, 3098. (b) Lee, C.; Yang, W.; Parr, R. G. *Phys. Rev. B* **1993**, *37*, 785.

12. (a) Ditchfield, R.; Hehre, W. J.; Pople, J. A. *J. Chem. Phys.* **1971**, *54*, 724. (b) Hehre, W. J.; Ditchfield, R.; Pople, J. A. *J. Chem. Phys.* **1972**, *56*, 2257. (c) Hariharan, P. C.; Pople, J. A. *Mol. Phys.* **1974**, *27*, 209. (d) Gordon, M. S. *Chem. Phys. Lett.* **1980**, *76*, 163. (e) Hariharan, P. C.; Pople, J. A. *Theor. Chim. Acta* **1973**, *28*, 213.
13. (a) Ditchfield, R.; Hehre, W. J.; Pople, J. A. *J. Chem. Phys.* **1971**, *54*, 724. (b) Hehre, W. J.; Ditchfield, R.; Pople, J. A. *J. Chem. Phys.* **1972**, *56*, 2257. (c) Cossi, M.; Barone, V.; Camimi, R.; Tomasi, J. *Chem. Phys. Lett.* **1996**, *255*, 327. (d) Barone, V.; Cossi, M.; Tomasi, J. *J. Chem. Phys.* **1997**, *107*, 3210.
14. Alcântara, A. F. C.; Pilo-Veloso, D.; Nelson, D. L. *J. Braz. Chem. Soc.* **1996**, *7*, 225.
15. (a) Buchanan, G. W.; Dawson, B. A. *Can. J. Chem.* **1977**, *55*, 1437. (b) Bjørge, J.; Boyd, D. R.; Watson, C. G.; Jennings, W. B. *J. Chem. Soc., Perkin Trans. 2* **1974**, 757.
16. Felluga, F.; Nitti, P.; Pitacco, G.; Valentin, E. *J. Chem. Res. (S)* **1977**, 1437.
17. (a) Nielsen, A. T.; Atkins, R. L.; Moore, D. W.; Scott, R.; Mallory, D.; Laberger, J. M. *J. Org. Chem.* **1973**, *38*, 3288. (b) Rossi, M. H.; Atachissini, A. S.; Amaral, L. *J. Org. Chem.* **1990**, *55*, 1300. (c) Forlani, L.; Marianucci, E.; Todesco, P. E. *J. Chem. Res. (S)* **1984**, 126. (d) Middleton, W. J.; Carlson, H. D. *Org. Synth.* **1970**, *50*, 81.
18. (a) Grigg, R.; Montgomery, J.; Somasunderam, A. *Tetrahedron* **1992**, *48*, 10431. (b) De Kimpe, N.; Verhe, R.; Buyck, L.; Schamp, N. *J. Royal Netherlands Chem. Soc.* **1977**, *96*, 242. (c) Poirier, R. A.; Yu, D.; Surjan, P. R. *Can. J. Chem.* **1991**, *69*, 1589. (d) Body, D. R.; Jennings, W. B.; Waring, V. *J. Org. Chem.* **1986**, *51*, 992. (e) Dureau, R.; Joucla, M. *Tetrahedron Lett.* **1999**, *31*, 6017. (f) Arjona, D.; Perez-Ozorio, R.; Perez-Rubalcaba, A.; Plumet, J.; Santesmases, M. J. *J. Org. Chem.* **1984**, *49*, 2624. (g) Ahlbrecht, H.; Hanisch, H.; Funk, W.; Kalas, R. D. *Tetrahedron* **1972**, *28*, 5481. (h) Fustero, S.; Dias, M. D.; Carlon, R. P. *Tetrahedron Lett.* **1993**, *34*, 725. (i) Nagata, W.; Wakabayashi, T.; Hayase, Y. *Org. Synth.* **1972**, *53*, 44. (j) Gilson, H. S. R.; Honig, B. H.; Croteau, A.; Zarrilli, G.; Nakanishi, K. *Biophys. J.* **1988**, *53*, 261. (k) Hine, J.; Cholod, M. S.; King, R. A. *J. Am. Chem. Soc.* **1974**, *96*, 835. (l) Bruice, P. Y. *J. Am. Chem. Soc.* **1989**, *111*, 962. (m) Clark, A. A.; Parker, D. C. *J. Am. Chem. Soc.* **1971**, *93*, 7257. (n) Teysseyre, J.; Arriau, J.; Dargelos, A.; Elguero, J.; Katritzky, A. R. *Bull. Soc. Chim. Belges* **1976**, *85*, 39.
19. (a) Ota, A. T.; Temperini, M. L. A.; Áreas, E. P. G.; Loos, M. *J. Mol. Struct. (Theochem)* **1998**, *451*, 269. (b) Temperini, M. L. A.; Santos, M. R.; Monteiro, V. R. P. *Spectrochim. Acta, Part A* **1995**, *51*, 1517. (c) Pessoa, M. M. B.; Andrade, G. F. S.; Monteiro, V. R. P.; Temperini, M. L. A. *Polyhedron* **2001**, *10*, 3133.

# Facile access to methoxylated 2-phenylnaphthalenes and epoxydibenzocyclooctenes

Cédric Maurin, Fabrice Bailly and Philippe Cotelle\*

Laboratoire de Chimie Organique et Macromoléculaire, UMR CNRS 8009, Université de Lille 1, 59655 Villeneuve d'Ascq, France

Received 10 January 2005; revised 8 February 2005; accepted 17 February 2005

Available online 3 June 2005

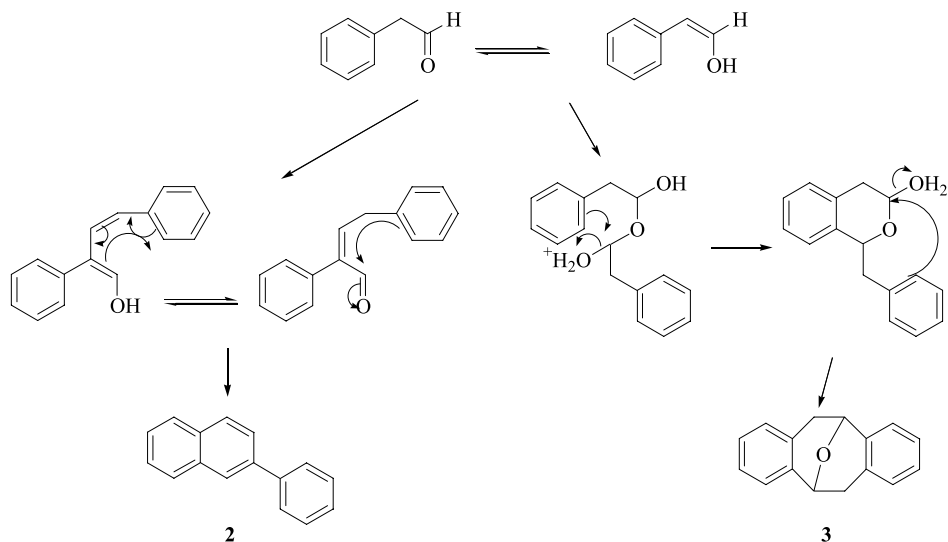
**Abstract**—Methoxylated phenylethanals were treated with concentrated hydrochloric acid in 1,4-dioxane to give methoxylated 2-phenylnaphthalenes or 1,2,9,10-tetrahydro-1,9-epoxydibenzo[*a,e*]cyclooctenes. Yields in 2-phenylnaphthalenes were quite good and 1,2,9,10-tetrahydro-1,9-epoxydibenzo[*a,e*]cyclooctenes could be easily isolated. 2-Phenylnaphthalenes were obtained by a tandem aldol condensation-intramolecular Friedel–Crafts cyclisation and 1,2,9,10-tetrahydro-1,9-epoxydibenzo[*a,e*]cyclooctenes by a O-condensation followed by a double intramolecular Friedel–Crafts alkylation.

© 2005 Elsevier Ltd. All rights reserved.

## 1. Introduction

Acid treatment of aryloethanals **1** may lead to 2-phenylnaphthalenes **2** or 1,2,9,10-tetrahydro-1,9-epoxydibenzo[*a,e*]cyclooctenes **3** (Kagan's ethers). **2** are obtained by a C-condensation of the enol form on the keto form. The resulting aldol condensation product undergoes an intramolecular reaction to give, after rearomatisation, the 2-phenylnaphthalenes (Scheme 1).

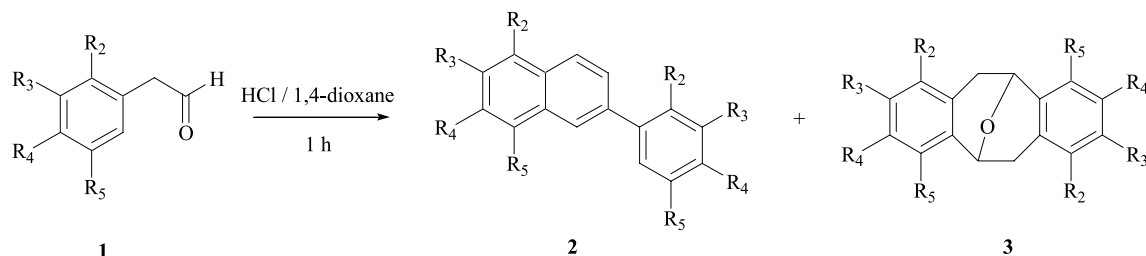
Kagan's ethers **3** are the results of an O-condensation of the ketal derivatives on the keto forms. The resulting hemiacetals cyclize to give benzisopyrans, which cyclize by an intramolecular Friedel–Crafts reaction to give Kagan's ethers (Scheme 1). The balance between the condensations at O- or C-position depends on the nature of the acid and the substitution on the aryl ring. The Kagan's pioneer work<sup>1,2</sup> used strong Brønsted acid, that is, fluorosulfonic acid, and other protic acids (HCl or H<sub>2</sub>SO<sub>4</sub>)<sup>3,4</sup> in order to promote the



Scheme 1.

**Keywords:** 2-Phenylnaphthalenes; Epoxydibenzo[*a,e*]cyclooctenes; Aldol condensation; Friedel–Crafts reaction.

\* Corresponding author. Tel.: +33 320337231; fax: +33 320336309; e-mail: philippe.cotelle@univ-lille1.fr



Scheme 2.

aldol condensation of arylethanal. The yields in isolated products were generally poor and could be increased using trimethylsilyliodide<sup>5</sup> or boron tribromide.<sup>4</sup> Using these reagents, high yields in Kagan's ether may be obtained and the cyclisations are regioselective. 2-Phenylnaphthalene can be isolated in modest yield from the reaction of phenylethanal with boron tribromide indicating that BBr<sub>3</sub> reaction conditions are not favorable for the double Friedel–Crafts cyclisation, which does not occur when the aromatic ring is not electronically-rich enough. The acid-catalysed aldol condensation of phenylacetone has previously been reported by Cort et al.<sup>7</sup> They showed the formation of 1-benzyl-3-methylnaphthalene from phenylacetone and 70% sulfuric acid under reflux. Kagan et al.<sup>2</sup> have also submitted phenylacetone to fluorosulfonic acid treatment and found only an electrophilic substitution of the aromatic ring *ortho* and *para* by a fluorosulfonyl group. They did not explain the contrast between phenylethanal and phenylacetone and simply evoked a steric effect due to the additional substituent at the carbonyl function. In our hand, we found<sup>8</sup> that arylacetones treated with boron tribromide give the 1,3-dimethyl-2-phenylnaphthalenes in good yields with a concomitant demethylation when the aromatic ring is substituted by methoxy group(s). The mechanism is a tandem aldol condensation–intramolecular cyclisation with a high regioselectivity. The scope and the limitations of the reaction of arylacetones with boron tribromide<sup>9</sup> were clearly defined. The cross-condensation, that is, reaction of two different arylacetones, was carried out using 3,4-dimethoxyphenylacetone and another variable arylacetone.<sup>10</sup> The objective was to obtain from only one experiment and after repeated chromatographies at least four different molecules tested as HIV-1 integrase inhibitors.

In continuation of our programme dealing with the discovery of new polyphenolic HIV-1 integrase inhibitors,<sup>10–13</sup> we needed to develop a facile and efficient synthesis of polymethoxylated 2-phenylnaphthalenes and

1,2,9,10-tetrahydro-1,9-epoxydibenzo[*a,e*]cyclooctenes. The reaction of 2-(3,4-dimethoxyphenyl)ethanal with concentrated HCl in dioxane was reported to give 6,7-dimethoxy-2-(3,4-dimethoxyphenyl)naphthalene in unsatisfactory low yields (12%,<sup>14</sup> 20%).<sup>4</sup> We, therefore, decided to revisit this reaction with the triple goal to obtain easily (the simpler purification process), efficiently (the two condensation products from each reactant if possible) and rapidly (short reaction time) the products of O- and C-condensation. With this goal in mind, we rapidly pointed out that the key parameters were the quality of 1,4-dioxane and the reagent concentrations. Freshly distilled dioxane on sodium and benzophenone (in order to avoid free radicals) was used and the concentration of arylethanal was adjusted to 0.2 M. Under these conditions, the yields were singularly improved (Scheme 2).

## 2. Results and discussion

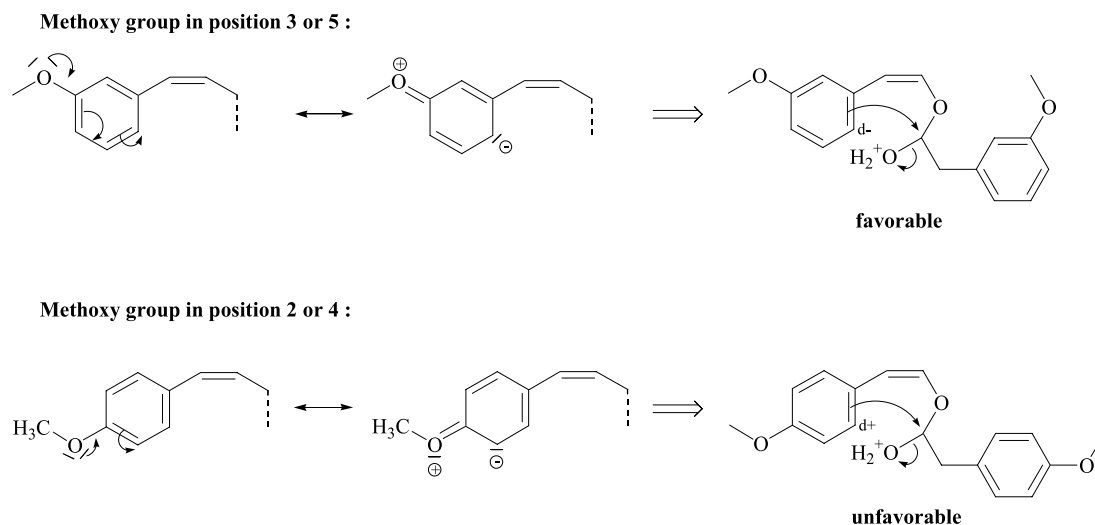
Arylethanal **1a–f** were prepared according to a known procedure<sup>15</sup> and submitted to acidic treatment in aqueous dioxane during 1 h at room temperature. In all cases, high yields in crude products were obtained and after purification 2-arylnaphthalenes **2a–f** were isolated in satisfactory yields (32–87%) (Table 1). Four of the six 1,2,9,10-tetrahydro-1,9-epoxydibenzo[*a,e*]cyclooctenes **3** were isolated in good yields (comparatively to their relative proportions in the crude product) (Table 1). The presence of at least one methoxy group on position 3 or 5 is absolutely required for the conversion of **1** into **2** or **3**. Under the same reaction conditions, phenylethanal, 2-methoxyphenylethanal and 4-methoxyphenylethanal gave polymers (data not shown) indicating that the intramolecular cyclisation required the presence of a methoxy group *ortho* or *para* to the newly formed C–C bond (Scheme 3). It must be noted that in the case of **1a**, the intramolecular cyclisations after C and O-condensation are regioselective.

Table 1. Yields and relative proportions of **2** and **3**

	R <sub>2</sub>	R <sub>3</sub>	R <sub>4</sub>	R <sub>5</sub>	<b>2</b>		<b>3</b>	
					Relative proportion (%) <sup>a</sup>	Yield (%)	Relative proportion (%) <sup>a</sup>	Yield (%)
<b>a</b>	H	OMe	H	H	75	32	25	10
<b>b</b>	OMe	OMe	H	H	80	62	20	12
<b>c</b>	H	OMe	OMe	H	90	87	10	3
<b>d</b>	OMe	H	H	OMe	100	54	Not detected	X
<b>e</b>	OMe	OMe	OMe	H	95	65	5	0
<b>f</b>	H	OMe	OMe	OMe	67	53	33	15

<sup>a</sup> The relative proportions in **2** and **3** were measured from the <sup>1</sup>H NMR spectra of the crude products obtained by extraction of the reaction mixture even when a precipitate was observed.





Scheme 3.

2,4-Dimethoxyphenylethanal also gave a dark material from which no organic compound could be isolated confirming the requirement of a methoxy group in position 3 or 5. Good yields in isolated products were obtained from the reaction

of **1b–1f** possibly due to the presence of two or three methoxy groups. In the case of **1d**, **3d** was not observed, whereas in the case of **1e**, the product of O-condensation **3e** could not be isolated.

Table 2. Spectroscopic data of compounds **2** and **3**

Product	<sup>1</sup> H NMR (300 MHz, CDCl <sub>3</sub> ) δ, ppm ( <i>J</i> , Hz)	<sup>13</sup> C NMR (75 MHz, CDCl <sub>3</sub> ) δ, ppm
<b>2a</b>	3.90 (s, 3H), 3.94 (s, 3H), 6.92 (ddd, 1H, <sup>3</sup> <i>J</i> =8.0 Hz, <sup>4</sup> <i>J</i> =2.7, 1.0 Hz), 7.17 (br s, 1H), 7.18 (dd, 1H, <sup>3</sup> <i>J</i> =8.8 Hz, <sup>4</sup> <i>J</i> =2.4 Hz), 7.25 (m, 1H), 7.30 (dm, 1H, <sup>3</sup> <i>J</i> =8.0 Hz), 7.40 (t, 1H, <sup>3</sup> <i>J</i> =8.0 Hz), 7.71 (dd, 1H, <sup>3</sup> <i>J</i> =8.3 Hz, <sup>4</sup> <i>J</i> =1.7 Hz), 7.80 (d, 1H, <sup>3</sup> <i>J</i> =8.8 Hz), 7.81 (d, 1H, <sup>3</sup> <i>J</i> =8.3 Hz), 7.98 (d, 1H, <sup>4</sup> <i>J</i> =1.7 Hz)	55.3 (2CH <sub>3</sub> ), 105.6 (CH), 112.5 (CH), 113.0 (CH), 119.2 (CH), 119.8 (CH), 125.7 (CH), 126.0 (CH), 127.2 (CH), 129.1 (C), 129.7 (CH), 129.8 (CH), 133.9 (C), 136.3 (C), 142.8 (C), 157.8 (C), 160.0 (C)
<b>3a</b>	2.69 (d, 2H, <sup>2</sup> <i>J</i> =16.1 Hz), 3.50 (dd, 2H, <sup>2</sup> <i>J</i> =16.1 Hz, <sup>3</sup> <i>J</i> =5.7 Hz), 3.70 (s, 6H), 5.23 (d, 2H, <sup>3</sup> <i>J</i> =5.7 Hz), 6.50 (d, 2H, <sup>4</sup> <i>J</i> =2.2 Hz), 6.69 (dd, 2H, <sup>3</sup> <i>J</i> =8.55 Hz, <sup>4</sup> <i>J</i> =2.2 Hz), 6.99 (d, 2H, <sup>3</sup> <i>J</i> =8.55 Hz)	36.6 (2CH <sub>2</sub> ), 55.1 (2CH <sub>3</sub> ), 69.0 (2CH), 112.5 (2CH), 113.5 (2CH), 126.1 (2CH), 129.9 (2C), 132.9 (2C), 158.3 (2C)
<b>2b</b>	3.60 (s, 3H), 3.94 (s, 3H), 4.02 (s, 3H), 4.05 (s, 3H), 6.96 (dd, 1H, <sup>3</sup> <i>J</i> =7.6 Hz, <sup>4</sup> <i>J</i> =1.9 Hz), 7.07 (dd, 1H, <sup>3</sup> <i>J</i> =7.6 Hz, <sup>4</sup> <i>J</i> =1.9 Hz), 7.14 (t, 1H, <sup>3</sup> <i>J</i> =7.6 Hz), 7.32 (d, 1H, <sup>3</sup> <i>J</i> =8.9 Hz), 7.65 (d, 1H, <sup>3</sup> <i>J</i> =8.9 Hz), 7.74 (dd, 1H, <sup>3</sup> <i>J</i> =8.75 Hz, <sup>4</sup> <i>J</i> =1.6 Hz), 7.97 (d, 1H, <sup>4</sup> <i>J</i> =1.6 Hz), 8.18 (d, 1H, <sup>3</sup> <i>J</i> =8.75 Hz)	55.9 (CH <sub>3</sub> ), 56.9 (CH <sub>3</sub> ), 60.5 (CH <sub>3</sub> ), 61.1 (CH <sub>3</sub> ), 111.5 (CH), 115.4 (CH), 120.9 (CH), 122.8 (CH), 124.1 (CH), 124.5 (CH), 127.7 (CH), 128.0 (CH), 128.1 (C), 129.7 (C), 134.1 (C), 135.8 (C), 143.0 (C), 146.8 (C), 148.4 (C), 153.2 (C)
<b>3b</b>	2.92 (d, 2H, <sup>2</sup> <i>J</i> =16.6 Hz), 3.29 (dd, 2H, <sup>2</sup> <i>J</i> =16.6 Hz, <sup>3</sup> <i>J</i> =5.9 Hz), 3.74 (s, 6H), 3.79 (s, 6H), 5.29 (d, 2H, <sup>3</sup> <i>J</i> =5.9 Hz), 6.74 (d, 2H, <sup>3</sup> <i>J</i> =8.3 Hz), 6.83 (d, 2H, <sup>3</sup> <i>J</i> =8.3 Hz)	31.4 (2CH <sub>2</sub> ), 55.7 (2CH <sub>3</sub> ), 59.9 (2CH <sub>3</sub> ), 68.5 (2CH), 110.5 (2CH), 120.7 (2CH), 126.0 (2C), 131.0 (2C), 146.3 (2C), 150.9 (2C)
<b>2c<sup>a</sup></b>	3.96 (s, 3H), 4.01 (s, 3H), 4.038 (s, 3H), 4.045 (s, 3H), 6.99 (d, 1H, <sup>3</sup> <i>J</i> =8.6 Hz), 7.16 (s, 1H), 7.21 (s, 1H), 7.26 (d, 1H, <sup>4</sup> <i>J</i> =1.6 Hz), 7.27 (dd, 1H, <sup>3</sup> <i>J</i> =8.6 Hz, <sup>4</sup> <i>J</i> =1.6 Hz), 7.60 (dd, 1H, <sup>3</sup> <i>J</i> =8.3 Hz, <sup>4</sup> <i>J</i> =1.9 Hz), 7.76 (d, 1H, <sup>3</sup> <i>J</i> =8.3 Hz), 7.79 (d, 1H, <sup>4</sup> <i>J</i> =1.9 Hz)	55.9 (2CH <sub>3</sub> ), 56.05 (CH <sub>3</sub> ), 56.08 (CH <sub>3</sub> ), 106.2 (CH), 106.6 (CH), 110.6 (CH), 111.7 (CH), 119.5 (CH), 123.8 (CH), 123.9 (CH), 126.8 (CH), 128.2 (C), 129.6 (C), 134.5 (C), 136.9 (C), 148.6 (C), 149.3 (C), 149.5 (C), 149.9 (C)
<b>3c<sup>b</sup></b>	2.67 (d, 2H, <sup>2</sup> <i>J</i> =15.9 Hz), 3.46 (dd, 2H, <sup>2</sup> <i>J</i> =15.9 Hz, <sup>3</sup> <i>J</i> =5.9 Hz), 3.78 (s, 6H), 3.84 (s, 6H), 5.20 (d, 2H, <sup>3</sup> <i>J</i> =5.9 Hz), 6.48 (s, 2H), 6.57 (s, 2H)	35.5 (2CH <sub>2</sub> ), 55.7 (2CH <sub>3</sub> ), 56.0 (2CH <sub>3</sub> ), 69.2 (2CH), 108.0 (2CH), 111.5 (2CH), 123.4 (2C), 129.5 (2C), 147.4 (2C), 148.0 (2C)
<b>2d</b>	3.76 (s, 3H), 3.84 (s, 3H), 3.96 (s, 3H), 3.97 (s, 3H), 6.71 (s, 2H), 6.89 (dd, 1H, <sup>3</sup> <i>J</i> =9.0 Hz, <sup>4</sup> <i>J</i> =2.9 Hz), 6.96 (d, 1H, <sup>3</sup> <i>J</i> =9.0 Hz), 7.06 (d, 1H, <sup>4</sup> <i>J</i> =2.9 Hz), 7.75 (dd, 1H, <sup>3</sup> <i>J</i> =8.8 Hz, <sup>4</sup> <i>J</i> =1.8 Hz), 8.25 (d, 1H, <sup>3</sup> <i>J</i> =8.8 Hz), 8.36 (d, 1H, <sup>4</sup> <i>J</i> =1.8 Hz)	55.78 (CH <sub>3</sub> ), 55.80 (CH <sub>3</sub> ), 55.9 (CH <sub>3</sub> ), 56.5 (CH <sub>3</sub> ), 103.4 (CH), 103.5 (CH), 113.0 (CH), 113.2 (CH), 117.1 (CH), 121.3 (CH), 122.1 (CH), 125.3 (C), 126.4 (C), 127.9 (CH), 132.1 (C), 136.2 (C), 149.5 (C), 149.8 (C), 151.1 (C), 153.9 (C)
<b>2e</b>	3.66 (s, 3H), 3.91 (s, 3H), 3.96 (s, 3H), 3.97 (s, 3H), 3.98 (s, 3H), 4.07 (s, 3H), 6.77 (d, 1H, <sup>3</sup> <i>J</i> =8.6 Hz), 6.99 (s, 1H), 7.12 (d, 1H, <sup>3</sup> <i>J</i> =8.6 Hz), 7.54 (dd, 1H, <sup>3</sup> <i>J</i> =8.6 Hz, <sup>4</sup> <i>J</i> =1.6 Hz), 7.82 (d, 1H, <sup>4</sup> <i>J</i> =1.6 Hz), 8.06 (d, 1H, <sup>3</sup> <i>J</i> =8.6 Hz)	55.9 (CH <sub>3</sub> ), 56.1 (CH <sub>3</sub> ), 61.0 (CH <sub>3</sub> ), 61.1 (CH <sub>3</sub> ), 61.2 (CH <sub>3</sub> ), 61.5 (CH <sub>3</sub> ), 102.6 (CH), 107.6 (CH), 121.3 (CH), 123.2 (C), 125.0 (CH), 125.6 (CH), 126.3 (CH), 128.7 (C), 130.8 (C), 135.7 (C), 140.8 (C), 142.6 (C), 147.9 (C), 151.6 (C), 152.1 (C), 153.2 (C)
<b>2f</b>	3.92 (s, 3H), 3.97 (s, 3H), 3.997 (s, 3H), 4.000 (s, 3H), 4.08 (s, 3H), 6.90 (s, 2H), 6.98 (s, 1H), 7.61 (dd, 1H, <sup>3</sup> <i>J</i> =8.5 Hz, <sup>4</sup> <i>J</i> =1.9 Hz), 7.76 (d, 1H, <sup>3</sup> <i>J</i> =8.5 Hz), 8.19 (d, 1H, <sup>4</sup> <i>J</i> =1.9 Hz)	55.8 (CH <sub>3</sub> ), 56.2 (2CH <sub>3</sub> ), 60.9 (CH <sub>3</sub> ), 61.1 (CH <sub>3</sub> ), 61.5 (CH <sub>3</sub> ), 102.1 (CH), 104.7 (2CH), 119.4 (CH), 124.4 (C), 125.4 (CH), 127.0 (CH), 129.9 (C), 136.7 (C), 137.52 (C), 137.55 (C), 141.2 (C), 148.0 (C), 153.1 (C), 153.5 (2C)
<b>3f</b>	2.76 (d, 2H, <sup>2</sup> <i>J</i> =16.5 Hz), 3.39 (dd, 2H, <sup>2</sup> <i>J</i> =16.5 Hz, <sup>3</sup> <i>J</i> =6.2 Hz), 3.81 (s, 6H), 3.85 (s, 6H), 4.00 (s, 6H), 5.34 (d, 2H, <sup>3</sup> <i>J</i> =6.2 Hz), 6.35 (s, 2H)	34.1 (2CH <sub>2</sub> ), 55.8 (2CH <sub>3</sub> ), 60.6 (2CH <sub>3</sub> ), 60.7 (2CH <sub>3</sub> ), 65.8 (2CH), 107.3 (2CH), 122.9 (2C), 128.0 (2C), 139.8 (2C), 149.2 (2C), 152.7 (2C)

<sup>a</sup> IR (cm<sup>-1</sup>): 2934w; 2836w; 1606m; 1506s; 1462m; 1256s; 1241s; 1166s; 1138s; 1023m; 857m.<sup>b</sup> IR (cm<sup>-1</sup>): 2995w; 2919m; 2833w; 1610m; 1517s; 1465m; 1358m; 1249s; 1120s; 1016m; 848m.

**Table 3.** Physical, analytical and mass spectroscopic data for compounds **2a–f**, **3a–b** and **3f**<sup>a</sup>

Product	Mp (°C)	Elemental analyses	MS (IE)
<b>3a</b>	115–118	Anal. Calcd for C <sub>18</sub> H <sub>18</sub> O <sub>3</sub> (282.33): C, 76.57; H, 6.43. Found C, 76.86%; H, 6.31%	<i>m/z</i> (%)=283 (26), 282 ([M <sup>+</sup> ], 100), 267 (27), 254 (45), 253 (42), 251 (28), 249 (29), 239 (45), 224 (22), 223 (32), 208 (25), 179 (30), 165 (38), 151 (27), 122 (82)
<b>3b</b>	159–161	Anal. Calcd for C <sub>20</sub> H <sub>22</sub> O <sub>5</sub> (342.39): C, 70.16; H, 6.48. Found: C, 69.98; H, 6.39	<i>m/z</i> (%)=342 ([M <sup>+</sup> ], 100), 314 (45), 313 (29), 311 (43), 299 (62), 284 (28), 283 (59), 280 (27), 268 (28), 252 (22), 165 (23), 152 (74), 137 (25)
<b>2e</b>	102–104	Anal. Calcd for C <sub>22</sub> H <sub>24</sub> O <sub>6</sub> (384.42): C, 68.74; H, 6.29. Found: C, 68.42; H, 6.47	<i>m/z</i> (%)=385 (36), 384 ([M <sup>+</sup> ], 100)
<b>3f</b>	181–182	Anal. Calcd for C <sub>22</sub> H <sub>26</sub> O <sub>7</sub> (402.44): C, 65.66; H, 6.51. Found: C, 65.95; H, 6.39	<i>m/z</i> (%)=402 ([M <sup>+</sup> ], 100), 374 (12), 373 (15), 359 (10), 343 (10), 182 (19)

<sup>a</sup> Known products: **2a**, yellow powder, mp 90–92 °C (lit.<sup>16</sup> mp 92 °C); **2b**, white powder, mp 63–65 °C (lit.<sup>16</sup> mp 68–69 °C); **2c**, yellow powder, mp 177–179 °C (lit.<sup>17</sup> mp 179–180 °C); **3c**, yellow powder, mp 162–164 °C (lit.<sup>6</sup> mp 163–164 °C); **2d**, white powder, mp 97–99 °C (lit.<sup>16</sup> mp 99 °C); **2f** white powder, mp 164–166 °C (lit.<sup>24</sup> mp 165.5–166 °C).

Whatever the number and the position of the methoxy groups, a pronounced preference for the C-condensation and the formation of **2** was observed attested by the relative proportions of **2** and **3** calculated from the <sup>1</sup>H NMR spectra of the crude product. Higher proportions in **3** were observed when a hydrogen atom substituted the position 2 (Tables 2 and 3).

As a conclusion, we reported in this paper the facile synthesis and isolation of six methoxylated 2-phenylnaphthalenes and four 1,2,9,10-tetrahydro-1,9-epoxydibenzo[*a,e*]cyclooctenes. The yields in 2-phenylnaphthalenes are quite good and suffer the comparison with the literature<sup>16</sup> except for the serendipitously synthesis of **2c**.<sup>17</sup> Amongst the four 1,2,9,10-tetrahydro-1,9-epoxydibenzo[*a,e*]cyclooctenes, only **3c** has been previously obtained from **1c** and trimethylsilyl iodide in high yield.<sup>6</sup>

### 3. Experimental

#### 3.1. General

Arylethanals **1** were synthesized according to a known procedure.<sup>15</sup> Arylethanals **1a–d** and **1f** were previously described.<sup>18–23</sup> Mps were determined on a Reichert Thermopan apparatus, equipped with a microscope and are uncorrected. NMR spectra were obtained on an AC 300 Bruker spectrometer in CDCl<sub>3</sub> with TMS as internal reference. Mass spectra were recorded on a Thermo-Finnigan PolarisQ mass spectrometer (70 eV, Electronic Impact). Elemental analyses were performed by CNRS laboratories (Vernaison). Infra-red spectra were obtained on a Perkin-Elmer 881 spectrometer on KBr paths.

**3.1.1. 2,3,4-Trimethoxyphenylethanal 1e.** Yellow oil, 85% yield, <sup>1</sup>H NMR (CDCl<sub>3</sub>, 300 MHz): 3.57 (d, 2H, <sup>3</sup>J=2.0 Hz), 3.82 (s, 3H), 3.84 (s, 3H), 3.84 (s, 3H), 6.62 (d, 1H, <sup>3</sup>J=8.3 Hz), 6.79 (d, 1H, <sup>3</sup>J=8.3 Hz), 9.66 (t, 1H, <sup>3</sup>J=2.0 Hz).

**3.1.2. Reaction of 1 in HCl/dioxane—General procedure.** **1** (5 mmol) was dissolved in freshly distilled 1,4-dioxane (10 mL) and HCl 12 M (15 mL) was added. The mixture was stirred for 1 h and water (10 mL) was added. When a precipitate was obtained, it was filtered and washed with water and then with diethyl ether. Otherwise, the aqueous

dioxane mixture was extracted with diethyl ether. The combined organic layers were dried over Na<sub>2</sub>SO<sub>4</sub> and evaporated in vacuum.

**Purification of 2a and 3a.** The crude product was purified by column chromatography on silica gel using a mixture of hexane/ethyl acetate 80:20 as eluent to give **2a** and **3a** in 32 and 10% yield, respectively.

**Purification of 2b and 3b.** The crude product was purified by column chromatography on silica gel using a mixture of hexane/ethyl acetate 70:30 as eluent to give **2b** and **3b** in 62 and 12% yield, respectively.

**Purification of 2c and 3c.** In this case, a precipitate was obtained. Its spectroscopic data were in accordance with the structure of **2c** (87% yield). The crude product obtained by extraction was purified by column chromatography on silica gel using a mixture of hexane/ethyl acetate 70:30 as eluant. **3c** was obtained in 3% yield.

**Purification of 2d.** The crude product was purified by column chromatography on silica gel using a mixture of hexane/ethyl acetate 70:30 as eluant to give **2d** in 54% yield.

**Purification of 2e.** The crude product was purified by column chromatography on silica gel using a mixture of dichloromethane/methanol 97:3 as eluant to give **2e** in 65% yield. Whereas **3e** has been identified on the <sup>1</sup>H NMR spectrum, it could not be isolated in a pure form.

**Purification of 2f and 3f.** Compounds **2f** and **3f** were precipitated by addition of water. The yield was almost quantitative. The solid mixture was triturated twice in hot diethyl ether and rapidly filtered to give pure **2f** (53% yield). The filtrate was maintained at 0 °C during 2 h and **3f** crystallized. It was obtained in 15% yield.

#### Acknowledgements

This work was financially supported by grants from le Centre National de la Recherche Scientifique (CNRS) and l'Agence Nationale de la Recherche contre le SIDA (ANRS).

## References and notes

1. Kagan, J.; Chen, S. Y.; Agdeppa, D. A.; Watson, W. H.; Zabel, V. *Tetrahedron Lett.* **1977**, *51*, 4469–4470.
2. Kagan, J.; Agdeppa, D. A.; Chang, A. I.; Chen, S. A.; Harmata, M. A.; Melnick, B.; Patel, G.; Poorker, C.; Singh, S. P.; Watson, W. H.; Chen, J. S.; Zabel, V. *J. Org. Chem.* **1981**, *46*, 2916–2930.
3. Carter, H. E.; Van Loon, E. J. *J. Am. Chem. Soc.* **1938**, *60*, 1077–1080.
4. Dupont, R.; Cotellet, P. *Tetrahedron Lett.* **1998**, *39*, 8457–8460.
5. Jung, M. E.; Mossman, A. B.; Lyster, M. A. *J. Org. Chem.* **1978**, *43*, 3698–3701.
6. Jung, M. E.; Miller, S. J. *J. Am. Chem. Soc.* **1981**, *103*, 1984–1992.
7. Cort, L. A.; Manders, R. G.; Parlett, G. R. *J. Chem. Soc.* **1964**, 2844.
8. Cotellet, P.; Catteau, J. P. *Tetrahedron Lett.* **1997**, *38*, 2969–2972.
9. Dupont, R.; Cotellet, P. *Synthesis* **1999**, 1651–1655.
10. Dupont, R.; Jeanson, L.; Mouscadet, J. F.; Cotellet, P. *Bioorg. Med. Chem. Lett.* **2001**, *11*, 3175–3178.
11. Maurin, C.; Bailly, F.; Cotellet, P. *Curr. Med. Chem.* **2003**, *10*, 1795–1810.
12. Maurin, C.; Bailly, F.; Cotellet, P. *Tetrahedron* **2004**, *60*, 6479–6486.
13. Maurin, C.; Bailly, F.; Mbemba, G.; Buisine, E.; Vezin, H.; Mouscadet, J. F.; Cotellet, P. *J. Med. Chem.* **2004**, *47*, 5583–5586.
14. Weinges, K.; Nagel, D. *Chem. Ber.* **1968**, *101*, 3018–3021.
15. Coote, S. J.; Davies, S. G.; Middlemiss, D.; Naylor, A. *Tetrahedron: Asymmetry* **1990**, *1*, 33–56.
16. Gopinath, K. W.; Govindachari, T. R.; Nagarajan, K.; Purushothaman, K. K. *J. Chem. Soc.* **1957**, 1144–1148.
17. Massingill, J. L., Jr.; Reinecke, M. G.; Hodgkins, J. E. *J. Org. Chem.* **1970**, *35*, 823–825.
18. Nelson, N. A.; Wollensak, J. C. *J. Am. Chem. Soc.* **1958**, *80*, 6626–6630.
19. Kaufman, T. S. *J. Chem. Soc., Perkin Trans. 1* **1996**, 2497–2505.
20. Oka, Y.; Motohashi, M.; Sugihara, H.; Miyashita, O.; Itoh, K.; Nishikawa, M.; Yurugi, S. *Chem. Pharm. Bull.* **1977**, *25*, 632–639.
21. Hendrickson, J. B.; Silva, R. A. *J. Am. Chem. Soc.* **1962**, *84*, 643–650.
22. Billman, J. H.; Tonnis, J. A. *J. Pharm. Sci.* **1971**, *60*, 1188–1192.
23. Watanabe, K.; Kayano, Y.; Matsunaga, T.; Yamamoto, I.; Yoshimura, H. *Biol. Pharm. Bull.* **1995**, *18*, 696–699.
24. Scott, A. I.; McCapra, F.; Buchanan, R. L.; Day, A. C.; Young, D. W. *Tetrahedron* **1965**, *21*, 3605–3631.